6th U.S. NAVY SYMPOSIUM OF MILITARY OCEANOGRAPHY

THE PROCEEDINGS OF THE SYMPOSIUM

26-28 May 1969

VOLUME I

APPLIED PHYSICS LABORATORY
UNIVERSITY OF WASHINGTON
SEATTLE, WASHINGTON

6th U. S. NAVY SYMPOSIUM ON MILITARY OCEANOGRAPHY

26-28 MAY, 1969 SEATTLE, WASHINGTON

THE PROCEEDINGS OF THE SYMPOSIUM

VOLUME I

SPONSORED BY

OCEANOGRAPHER OF THE NAVY

APPLIED PHYSICS LABORATORY
UNIVERSITY OF WASHINGTON
SEATTLE, WASHINGTON

DEPARTMENT OF THE NAVY
OFFICE OF THE OCEANOGRAPHER OF THE NAVY
THE MADISON BUILDING
732 N. WASHINGTON STREET
ALEXANDRIA, VA. 22314

IN REPLY REFER TO

The publication of these Proceedings of the Sixth U. S. Navy Symposium on Military Oceanography provides a valuable reference work for all who attended the Symposium. For those who were unable to attend but who maintain a strong interest in matters relating to oceanographic technology, the theme of the 1969 Symposium, this volume will also be very useful.

Many fine papers submitted by some of the best people in the oceanographic community could not be presented in Seattle because of time restrictions. But we now have access to these papers since these Proceedings contain everything passed by the referee committee.

The Seattle Symposium was most successful and I would again like to thank everyone who took time from their busy schedules to attend. I would particularly like to express my gratitude to Dr. Joseph E. Henderson and his staff at the Applied Physics Laboratory of the University of Washington for their superb organization of the three day session, and to Dr. J. B. Hersey of the Office of Naval Research for his excellent guidance as the General Chairman of the 1969 Symposium.

O. D. WATERS, JR.
Rear Admiral, U. S. Navy
Oceanographer of the Navy

CONTENTS

STATE OF THE NAVY IN OCEANOGRAPHY

Opening Remarks by
Rear Admiral O.D. Waters, Jr.
Oceanographer of the Navy

Mr. Chairman:

It is a pleasure, though somewhat astounding, to see this many eminent oceanographers gathered at one time in one place for a three day brain-picking session.

Oceanographers as a class are surely the world's greatest travelers and meeting attenders. But as trained environmentalists they have a tendency to be pretty selective about their traveling. Except where duty assignments are involved you are not likely to find an oceanographer in the Arctic Circle in the winter time or in Florida in the middle of the summer. Too smart for that.

Take our host, Dr. Henderson, for example. Last I heard of him he was in La Spezia, Italy. An excellent spring-time selection.

But come to think of it, Seattle is also noted as a very pleasant place to visit and I am sure that everyone of you will enjoy your short stay here.

If you do, give the lion's share of the credit to Joe Henderson and his staff at the Applied Physics Laboratory of the University of Washington. They have worked hard and well to organize both our working sessions and our leisure time activities.

I am going to put in a reference here to Seattle as the Oceanographic Capital of the Country. Truth is, I'm afraid my remarks might get back to friends of mine in San Diego, or Honolulu, or Norfolk or Miami. They all claim the same title.

Now since the subject assigned to me is "The State of the Navy in Oceanography" I will start with a few words on the State of the Nation.

A while back as you know the National Council on Marine Resources and Engineering Development was established by Congress to provide an organizational framework and increased momentum to marine science activities. The Council's Chairman is the Vice President.

In addition, the Commission on Marine Science, Engineering and Resources was established to make a study and recommend a permanent organization and a national marine science program. Their report is now before the Congress.

Let me read a short quotation from the report --

> "Because instabilities in the world situation cannot be remedied quickly, military power will continue to be a central factor in world affairs. As naval technology increases, the depth and variety of undersea operations require detection systems of ever increasing power and complexity. Today's advances in military undersea technology forecast an increasingly important role for U.S. defense and deterrence capabilities in the global sea. As the uses of the sea multiply, the Navy's defense mission will be complicated by the presence of structures, vehicles, and men. The resulting problems can be resolved only by the closest cooperation between civil and military users of the sea. Furthermore, military and civil science and technology for undersea operations can and should be mutually supporting, emphasizing the need for cooperative action."

> "The Commission believes strongly that the Nation's stake in the uses of the sea requires a U.S. Navy capable of carrying out its national defense missions anywhere in the oceans, at any desired depth, at any time."

These two paragraphs and others I could quote indicate that the Commission had a clear understanding not only of the role of naval oceanography in national defense but of the importance of close cooperation between the Defense Department and whatever central civilian agency Congress might set up as a result of the report.

Additional effort by another agency would be welcome. But the important thing is that the programs be constructed to complement each other and so avoid duplication of effort at the taxpayer's expense. As recognized by the Commission, we cannot of course abdicate our responsibilities, for the sea is our natural operating environment and the nation will accept no excuse if we fail to maintain an adequate security posture.

To us, oceanography is merely a means to an end. Our efforts in this field account for more than one-half of the entire Federal program. The budget we have submitted for Fiscal Year 1970, which starts a few days from now comes to $278 million dollars.

When I mention dollar figures I should say that these are not just handed to us by people who think oceanography is a great thing. Every program fights its way through the budget cycles in competition with all other Navy efforts.

As the Navy's Oceanographer, I have three double-hatted assistants whose authority in their primary jobs extends into wide areas of the naval establishment. These assistants are the Chief of Naval

Research, the Deputy Chief of Naval Material for Development and the Commander of the Naval Weather Service.

Under these three Assistant Oceanographers plus myself as my own deputy for operations, we have divided our program into three broad areas for management purposes. These areas are Ocean Science, Ocean Engineering and Development and Oceanographic Operations.

Under the Ocean Science Program, our goal is to advance our knowledge of the physical, chemical, biological and geological nature of the world's oceans and their bottom and surface boundaries. The program, which is requested at $60 million dollars this year, concentrates on reaserch projects in support of high priority operational requirements. So there is considerable emphasis on underwater acoustics, oceanographic prediction and geophysics as they are related to submarine, and antisubmarine and amphibious warfare.

We are developing methods of predicting sound behavior and thermal structure changes in the ocean by studying physical, chemical and biological processes. The effort includes the study of ocean circulation, air-sea interactions and internal waves.

Geophysics research is concentrated mainly on understanding the bottom and the sediment and rock below it as they related to sound reflection, hence to the operation of our sonar systems.

In Marine Biology our work is directed toward understanding the habits of various types of marine life which can degrade the performance of our equipment. A major concern is the deep scattering layer which masks submarine echoes.

The Ocean Science Program is carried out by academic and nonprofit institutions, industrial plants and our own Navy laboratories throughout the country. The University of Washington is a major performer in this program.

There are about a thousand scientists and a great variety of facilities involved in the program. Facilities include thirty-four ships, a variety of deep submersibles, stable platforms for work in deep water, monster buoys, airplanes, satellites and even ice islands.

Now a few words about Ocean Engineering and Development, which is in the Fiscal 1970 budget at $102 million. This is our newest and fastest growing program and it is being developed in seven major areas:

1. Undersea search and location
2. Submarine rescue and escape
3. Salvage and recovery

4. Diving
5. Survey
6. Environmental prediction
7. Underwater construction

We are having to build a broad base of new technology to provide these expanded capabilities. The technology base has been divided, for administrative purposes, into functional areas such as energy sources, materials and structural analysis, environmental support, sea floor engineering and so on.

The efforts involved in this Engineering program are well known to most of you here. The underwater search and location program involves a 20,000 foot vehicle in addition to unmanned devices.

Work on a fuel cell power plant is underway.

In Submarine Escape and Rescue we are putting our chips on a Deep Submergence Rescue Vehicle-DSRV for short. The contractor will deliver the first of these vehicles for testing late this summer. It will be transportable by air, surface vessel or submarine. These systems will permit us to respond quickly to the need to rescue personnel from any submarine bottomed above its crush depth.

Another remarkable vehicle in this program is the recently launched NR-1. This is a small nuclear powered submersible capable of sustained operations; we expect it to be a very valuable platform for undersea research. It will not go as deep as the DSSV I mentioned, but it will stay down till the crew tires out.

Our Salvage and Recovery efforts are aimed at developing the ability to raise objects the size of a submarine hull from depths down to 850 feet.

The Salvage program, in turn, is dependent on our Man-in-The-Sea program which includes the development of improved deep diving techniques. The Navy has pioneered in diving and developed the technique of saturation diving. As you know we have had recent difficulties. However we cannot give up on this. It is too important both to the Navy and to the private sector of our country. We intend to pursue Man-in-The-Sea to completion in order to give our operating forces the hardware and techniques they require for accomplishing useful work by divers to depths of 1,000 feet or more. Biomedical knowledge is critical here, and we are working hard at it.

Underwater construction also is dependent to a great extent on the work being done in the diving and vehicle areas, and these programs are all being pushed along together.

The broad base of support for the Engineering program comes from Navy laboratories, industry and universities. Seventy percent of the money goes to private industry.

The overall objective of the program is to give us the ability to operate at any place and at any time within the oceans in support of our defense mission.

Our third and largest program area is Oceanographic Operations. It is at the $116 million level in Fiscal 1970. The work is carried out through the Oceanographer's largest field activity, the Naval Oceanographic Office and through the Commander of the Naval Weather Service Command acting as Assistant Oceanographer for Environmental Prediction Services.

This program consists of oceanographic and hydrographic surveys in all ocean areas and the dissemination of date to provide environmental information, forecasts, charts and publications to support such operations as Vietnam, POLARIS, ASW, Mine Warfare, Amphibious operations and fleet activities in general. Our charts and other publications are also supplied to the merchant marine, statutory responsibility we have held since the early 1800's.

There is not time to even highlight Navy's efforts here. There are our coastal surveys in Far East waters and in the Mediterranean. Our deep ocean surveys result in the collection of hundreds of thousands of track miles of precise bathymetry, gravity, geomagnetic, and sub-bottom seismic data annually.

Since our last Symposium, a year ago, we have, to mention first a few items:

-- Completed our hydrographic surveys along the coast of South Vietnam.

-- Conducted almost one-half million miles of deep ocean bathymetry and geophysical data collection.

-- Conducted a major underwater acoustic experiment in the Pacific called PARKA I. This was part of a continuing and broader project designed to establish the environmental factors which control long range sound transmission.

-- Flown 200,000 miles of geomagnetic surveys.

-- Launched the NR-1, the nuclear propelled submersible I mentioned earlier.

-- Launched the Sea Cliff and Turtle, two new LAVIN-type deep research vehicles with 6,500 foot depth capabilities.

-- Let the contract for our first catamaran hull research ship, to Todd Shipyard here in Seattle.

-- Taken delivery on two new survey and two new research ships.

Looking ahead to Fiscal Year 1970 I can think of these items:

-- We will have two new ships ready to turn over to universities in support of Navy's science program, and our four ships delivered in 1969 will commence operational surveys and support of Navy Laboratory research here on the West Coast.

-- Our nuclear submersible will commence its shakedown, which will include scientific cruises, and we will launch our first two DSRV's.

-- If all goes well with our funding request to the Congress, we will procure a new aircraft to replace our two old ones engaged in airborne magnetic surveys.

-- And we will receive our first funding for our newly established National Oceanographic Instrumentation Center. This center will use an existing Navy facility and will expand to provide instrument development and reliability reference services, test and evaluation data and calibration facilities for industry and non-military Federal agencies.

-- Our newly developed unmanned recovery vehicle CURV III, a 7,000' version of the device which recovered the unarmed nuclear weapon off Palomaris, will become operational.

In the present financial climate we can hope for only a minimum of new starts. In fact the only significant increase in program dollars will go to the development of a DSSV, a deep submergence vehicle designed to do many useful tasks down to a depth of 20,000 feet.

In general our emphasis in the coming year will be on Deep Submergence, Biomedicine and Deep Ocean Technology.

This is about all I can tell you in the time allotted me. The rest you can get from the experts assembled here.

I will conclude by inviting you all to the 7th Symposium on Military Oceanography to be held at the U.S. Naval Academy on 12, 13 and 14 May 1970. Your host will be the Naval Ship Research and Development Center.

Annapolis can also be a pleasant place in the Spring.

OCEANOGRAPHIC EDUCATION OF THE NAVAL OFFICER

Rear Admiral Robert W. McNitt, U. S. Navy
Superintendent, Naval Postgraduate School

ABSTRACT

The undergraduate education of candidates for a commission in the line of the Regular Navy does not provide for instruction in oceanography either in the required curriculum of the NROTC, or in the core curriculum at the Naval Academy, although majors in oceanography and ocean engineering are available. This is acceptable if the functional service schools treat environmental support adequately, and if we have a subspecialist in oceanography aboard certain fleet units such as each destroyer type ship, submarine, and ASW aircraft squadron, and the staffs which support them. A suggestion is offered that the Oceanographer of the Navy's proposal of October 1966 concerning P-coding of fleet billets be reconsidered by the Commanders-in-Chief, U. S. Atlantic and Pacific Fleets, in light of the revision of OPNAV Instruction 1211.6B which now permits P-coding billets for which it is highly desirable to have incumbents with graduate education.

Graduate education in oceanography in the Navy today treats specialists and subspecialists alike, both at the Naval Postgraduate School and in the civilian universities. Some ideas to revise the curriculum to accommodate the different requirements of these two categories of officers are discussed.

OCEANOGRAPHIC EDUCATION OF THE NAVAL OFFICER

In this discussion we will be talking about three general areas of oceanographic education for Naval officers. First we will discuss the undergraduate preparation of young men who seek a commission in the line of the regular Navy. Secondly we will discuss the graduate education of our specialists - the officers in the newly created Special Duty Officer category in Oceanography/Hydrography. Thirdly we will discuss the graduate education of our subspecialists in oceanography. The subspecialists are officers who must maintain expertise in their primary specialty of naval warfare and command at sea by operational tours of duty at sea. These officers are needed in billets that are closely associated with the specialty, but which may not require the degree of technical expertise possessed by special duty officers.

Two innovations will be proposed as we go along - not new ideas necessarily, but ideas which now seem ready for adoption. The first of these is the not very startling notion that specialists and subspecialists may each need a different kind of graduate education.

The second is the somewhat more bold proposal that the Navy will benefit by identifying billets in operating units of the Fleet for the oceanographic subspecialist.

Let us first look therefore at the undergraduate education of our line officers today. The two principal sources are the Naval ROTC and the Naval Academy.

The Regular Naval ROTC student is required to complete one year of college mathematics (calculus level), one year of college physics or chemistry, and a course in computer science, all of which are useful but minimum prerequisites for later work in oceanography. He does not study oceanography as a part of the required curriculum, although he may take a major in this field.

At the Naval Academy, oceanography is no longer part of the core curriculum for the midshipmen. However a science major in oceanography, and an engineering major in ocean engineering are offered among the 27 majors approved for the class graduating in 1972, with the oceanography major available beginning with the class of 1971.

The oceanography major is built on a good background of science, mathematics and engineering, and offers courses which introduce the student to physical, chemical, geological and biological oceanography, along with three electives which allow a student to continue this flexible

program, or to concentrate in one of these major fields of oceanography. Except for the management major, this is at present the most popular of all the majors offered to the midshipmen.

Since oceanography was first introduced as a minor/major curriculum, it has grown from 20 midshipmen in the class of 1969 to 150 in the class of 1972, leveling off at a planned enrollment of 160 per year. The objective of the oceanography major curriculum is to provide a program for in-depth study of oceanography at the undergraduate level, to produce better naval officers by providing an understanding and appreciation of the naval environment, and to prepare midshipmen for graduate study in the field of oceanography.

In the Spring of 1969 an ocean engineering curriculum, offering basic courses in oceanography, was approved. This major will develop for the students an appreciation of the marine environment, as for an example, the effect of waves on structures. To date, 17 students have enrolled for next year's courses.

The Committee on Ocean Engineering of the National Academy of Engineering reviewed the Naval Academy program in June of 1968 and observed that meteorology and oceanography are foundation blocks in the Academy's engineering curricula.[1] The Committee recommended that the Naval Academy in all of its engineering curricula, should "strive for excellence in - and reputation for - interaction with the naval environment, which is the ocean." They recommended this in preference to developing a specially identified major in ocean engineering. The Committee recommended that all basic engineering courses at the Naval Academy should be rewritten or modified to present maximum emphasis on the ocean environment, and that areas of concentration rather than formal minors be considered.

Although in theory this is an attractive approach it isn't surprising that the Naval Academy found it nearly impossible to implement. Rewriting a course to reflect an emphasis on the ocean environment isn't much help unless the teacher himself has been schooled in oceanography, or has been a practicing ocean engineer. Staffing every basic engineering course with such talent would be extremely difficult, and organizationally would be hard to sustain. Viability and strength develop only when departmental, or at least curricular major status is granted. Diffusion throughout the existing organization usually is an invitation to ineffectiveness.

Until recently, oceanography and ocean engineering were not widely offered in undergraduate curricula. However, some of the basic courses in oceanography can now reasonably be taught at the

undergraduate level. The risk always is that, in so doing, a portion of the fundamental preparation in mathematics, science and engineering will be displaced, and will need to be presented during the graduate program, instead of being a tool already in hand and ready for use. Since the Navy provides a continuum of experience in oceanography, it is fortunate that the Naval Academy major and the Postgraduate School advanced degree programs are being developed with close cooperation between the two schools, so that the maximum education including the desired amount of basic science and engineering is provided in the minimum time.

An interesting question might be raised at this point. Should every officer during his undergraduate education be given an introduction to oceanography - a survey course perhaps - to familiarize him with the marine environment? Or is it sufficient to interest enough undergraduates in taking a major in oceanography or ocean engineering, so that the specialist and subspecialist needs of the Navy will later be met by these officers completing a graduate program?

I think that the latter process is preferable at this point in the Navy's development, providing two things are done. First, we must recognize the need for subspecialists in oceanography at sea by identifying the billets they should occupy, so that each ASW operating unit and the supporting staffs do in fact have one subspecialist aboard; and secondly we should insure that the training courses in the functional schools teach environmental support in an adequate manner. We will return to the use of subspecialists in the Fleet a little later.

Now let us move along to the graduate education of naval officers. This year the Navy has 28 officers in graduate studies in oceanography at 11 universities, half of whom are in doctoral degree programs. In addition there are 80 officers enrolled at the Naval Postgraduate School in programs leading to a Master of Science in Oceanography. Both specialists and subspecialists are eligible for any of these courses.

The Naval Postgraduate School oceanography curriculum provides a broad base in physical oceanography. Options within the program encourage studies in the structure of the environment, the prediction of acoustical propagation, and the geophysics of the ocean. A newly adopted option surveys the applications of engineering technology in the ocean environment, and studies the design of underwater platforms, submerged vehicles, and buoys. It also examines the geophysical, chemical and biological effects of the sea on naval hardware, marine equipment and instruments.

There are three unique features in the Naval Postgraduate School oceanography curriculum. First is the strong emphasis on physical

oceanography for all students. Second is the intimate working relationship with the Department of Meteorology, and third is the availability of the Fleet Numerical Weather Central for student and faculty research and practice-oriented experience.

The graduates of all these programs can elect either to remain line officers of the Navy with an 8703 P-code, or to apply for selection as special duty officers with the new designator 1820 (Oceanographer/ Hydrographer). The P-code is a number which indicates the field of graduate study (subspecialty) of the line officer who alternates between shore and sea assignments, and the designator is a number which indicates the specialty of an officer whose assignments would be within the area of specialization.

The question now should be raised as to whether it is sensible to provide the same curricular programs, to the same degree level, for both specialists and subspecialists in oceanography, as we are now doing.

I think probably not, and we are in the midst of reviewing this question at Monterey in preparation for discussions with the curriculum sponsor.

In the future it seems likely that there will be three general interests represented among the officers enrolling in the oceanographic curricula. One will be the officer who is already a specialist, or hopes to be selected for the specialist category. Another is the line officer who is interested in a subspecialty in oceanography. The third is an officer whose major and primary subspecialty is in another area such as meteorology, but who wants a second subspecialty or a minor in oceanography.

First let's take a look at the specialist and see what trends will affect the education he should get. An example is in one of the rapidly developing aspects of oceanography - prediction. Two significant recent reports - The Effective Use of the Sea in 1966[2] and the Stratton Report of 1969[3] stressed the unity of the environmental sciences of meteorology and physical oceanography. These sciences are not in balance now, because synoptic analysis and prediction of the ocean variables is just becoming a significant effort, while meteorological forecasts have been issued for decades.

In the analysis and prediction of the ocean variables of pressure, temperature, salinity and water motion the same basic equations are used as in predicting the corresponding variables of pressure, temperature, moisture, and motion in the atmosphere. Captain Paul M.

Wolff, USN, of the Fleet Numerical Weather Central predicts that all practical operational analyses in both fields will soon be done by computer, requiring specialists educated to a high academic level with a sound preparation in mathematical and synoptic meteorology, and descriptive and predictive oceanography, viewed always as an inseparable system.

If, in the future, we find ourselves depending to a greater extent on deep mounted, high powered, active sonar systems, we will require specialists with a broad oceanographic education in the physical variables and their prediction; and in climatology, computer mathematics, and physics supporting probability analysis of detection; geology relating to bottom boundary effects; and some biology and chemistry. It also seems likely that an understanding of high speed communications and signal processing theory will be needed.

Now let's look at the subspecialist. What is his function in the Navy? Commander Don Walsh who has earned a Ph. D. in oceanography and has given this a good deal of thought since his deep dive in Trieste, says that the subspecialist should be an enlightened manager, able to hold his own in a roomful of oceanographers, and capable of deciding which proposals or projects to encourage, which to hold back and which to initiate. This judgment of course must be based on a clear understanding of operational need combined with sound technical competence.

Commander Walsh sees two broad areas of employment for subspecialist officers. One would be in the applications area, through performance in fleet operational billets such as a staff specialist, or in a shipboard billet requiring this subspecialty. The other would be in the management area through assignment to R&D programs at either the headquarters or laboratory level. He regards the subspecialist as the "bridge" between the fleet and the R&D establishment, representing the ultimate customer, the operator in the Fleet. Particularly pertinent in this regard is the operations option in oceanography at the Naval Postgraduate School. The oceanography subspecialist should be the one who inspires the ship's company or the air crew to get the most out of equipment and the environment, and who proposes the improvements to gear and tactics which in the long run are the quickest route to enhanced operational readiness.

Commander Walsh is also certain that the demand for both specialists and subspecialists in oceanography will grow rapidly because the Navy is faced with pioneering much of the scientific exploration and technological development of inner space which will lead to the civil efforts in ocean exploitation.

A good example of a particularly effective subspecialist is Captain Earle W. Sapp, USN. As Commanding Officer of the destroyer USS EUGENE A. GREENE (DD-711) he showed his enlisted men and officers how to measure and predict the characteristics of the air-ocean environment in the operating area, and to lay out surveillance, screens, zigzag plans, and aircraft search plans to take best advantage of the conditions. He identified a design deficiency in the audio response of his sonar, and developed a simple modification which removed distortion and greatly improved the detection and classification capability of the system. He analyzed the relationship of minimum pulse length to reverberation limitations in the visual display, determined the optimum minimum pulse length and recommended its adoption. He devised a weapons utilization doctrine based on environmental conditions which was practical and effective. These improvements were adopted for use in all destroyers, and the USS EUGENE A. GREENE was awarded the Atlantic Fleet ASW Trophy.

In his present shore duty assignment he is holding down a key assignment in the Department of Defense, with responsibility for reviewing proposals for funding of sea warfare projects. This is the subspecialist ashore - immensely influential because he combines an intimate knowledge of operational need and sound technical judgment.

Now, how can we arrange the graduate educational experience to prepare officers for all these functions?

One way to accomplish these goals at the Naval Postgraduate School might be to provide a common core curriculum in basic oceanography, called an "ocean package", for all three officers - the specialist, the subspecialist, and the subspecialist seeking a minor in oceanography. The ocean package would have a strong offering in physical oceanography, and a good introduction to chemical, biological and geophysical oceanography. It would include several courses in dynamics, and field experience.

The specialist then could proceed either to advanced work at a civilian university, or to a program of high quality and depth in one of the major fields of oceanography at the Naval Postgraduate School. The subspecialist where qualified, could proceed either to a civilian university, or to a program of additional courses in oceanography at the Naval Postgraduate School. The subspecialist in another major program would terminate his oceanographic education with the completion of the ocean package. A flexible program in oceanography, assuming a common core of basic oceanography, is the key to meeting the needs of the Navy and the interests of the Naval officer.

At the same time, some thought must be given to the possibilities of interdisciplinary offerings, further combining meteorology and oceanography, or acoustics and oceanography, for example.

Now one last point. It was pointed out earlier in this paper that the Navy will benefit by identifying billets in ships and aircraft squadrons for the subspecialist in oceanography. Let's look at the history of this problem.

In October 1966 the Oceanographer of the Navy submitted a list of billets to the Commanders-in-Chief, U. S. Atlantic and Pacific Fleets, which appeared to be appropriate for P-coding and asked for concurrence or nonconcurrence. The response of both Commanders-in-Chief in January 1967, based on comments from Type, Fleet and other Commanders, said in effect that Fleet requirements can be fulfilled in most cases by P-coding key billets within staffs and wider use of oceanographic S-coding. S-coded billets are those filled by officers who have gained their expertise through experience rather than through formal graduate education. The Commander-in-Chief, U. S. Atlantic Fleet, said that the requirement for understanding of the naval warfare environment does not constitute valid justification for P-code billets in oceanography or hydrography because oceanographic operational services are provided to ships, staffs and aircraft squadrons by meteorological units.

Although I recognize the practical problems involved at that time, I do not agree at all with this reasoning. Expertise in staffs, and superb environmental support from meteorological units, will be useful only to the extent that some one in the ship, submarine or ASW aircraft squadron is interested and well enough educated to apply these services intelligently in operating the ASW weapon systems. Use of S-coded officers also is no solution. A recent analysis by the Career Planning Board of the Bureau of Naval Personnel has shown that there are practically no billets to which an officer can be sent to gain the experience needed for obtaining an S-code. As a result, no reliance can be placed on this source of talent in the future.

There was some sympathy for the Oceanographer's proposal among a few commands, but some practical problems killed it. No destroyer, submarine or aircraft force commander was willing to say that graduate education in oceanography/hydrography was essential for duty in the proposed billets in ships and ASW aircraft. To do so would exclude many fine officers from these billets, who had not had graduate education, and would set up very restrictive detailing practices. There were those, such as Commander Cruiser-Destroyer Force, Atlantic Fleet, who agreed that oceanography might be included as a very desirable qualification to be considered in assigning officers to these billets.

The key to this puzzle then is the word essential in the instruction governing P-coding, and fortunately a very significant step was taken by the Navy Department on 13 May 1969 when this wording was revised in OPNAV Instruction 1211.6B[4]. It now reads "highly desirable". This opens up the opportunity to expand the number of P-coded billets in ships and ASW aircraft squadrons.

There is another reason why I think this step must be taken. In the past we have always assumed that the P-coded billets at sea were far fewer in number than those ashore, and that those at sea would easily be filled by qualified subspecialists in the normal rotation of officers. This is not the case in oceanography. At present there are 83 subspecialist billets for oceanographers and 21 for hydrographers, only 3 of which are in fleet operating units (ASW groups). The number proposed by the oceanographer for units of the fleet is much greater than this. In other words, the seagoing requirements exceed those ashore, and inventory planning for the career community should be based on this number.

Furthermore the officer who accepts oceanography as a subspecialty likes to think that his education and experience will also make a direct contribution to his specialty of naval warfare and command at sea, and he is anxious to practice his trade at sea, and should be permitted and encouraged to do so.

I suggest therefore that the Fleet Commanders-in-Chief be asked to review again the Oceanographer's previous proposal. Two new notions might be introduced. It might be quite useful to double P-code certain billets to ease the restriction on detailing. The billet of Operations Officer of a destroyer for example could be filled by an officer with either an oceanography or operations analysis P-code. As an interim measure, guidance could be given to the placement officers in the Bureau of Naval Personnel, so that at least one officer in each of certain Fleet units such as submarines, destroyers, and ASW aircraft squadrons would have an oceanographic P-code.

I am convinced that these steps will simultaneously strengthen the performance and readiness of our ships and aircraft, and enhance the career opportunities of the fine officers who have committed themselves to the oceanographic specialty and subspecialty in our Navy.

BIBLIOGRAPHY

1. Comments and Judgment on an Ocean Engineering Curriculum in the U. S. Naval Academy, June 1968. Committee on Ocean Engineering, National Academy of Engineering.

2. Effective Use of the Sea. Report of the Panel on Oceanography of the President's Science Advisory Committee, June 1966.

3. Our Nation and the Sea. A plan for national action. Report of the Commission on Marine Science, Engineering and Resources, January 1969.

4. OPNAV Instruction 1211.6B dated 13 May 1969. Identification of Unrestricted Line Subspecialty Billets and Restricted Line and Staff Corps Officer Billets Requiring Graduate Level or Other Special Education.

THE U.S. NAVAL WEATHER SERVICE

by
Captain Edwin T. Harding, USN
Commander, Naval Weather Service Command

ABSTRACT

The Naval Weather Service is described as to composition organization, functions, and methods of operation. Meteorological and oceanographic products used in support of Fleet operations are discussed, with emphasis given to those which show the Navy's technical treatment of the oceans and atmosphere as an indivisible, coupled environmental system. Trends in development of future environmental service products are discussed.

. . . .

Many must have raised the question when they saw the program, "Why a talk on the Naval Weather Service at a symposium on military oceanography?" The answer lies in the fact that the Naval Weather Service, from the operational standpoint, is military oceanography. The scene of our activity lies over water. Nearly half of our prediction products are concerned with the ocean surface or subsurface. We probably should change our name to the Naval Environmental Prediction Service.

The Naval Weather Service is now the Navy's operational arm in both the meteorological and oceanographic disciplines. For years our emphasis was on aviation forecasting, but in the last fifteen years, we have taken over more and more oceanographic forecasting. Research and development in the oceanographic area have been done mostly by other activities, such as the Oceanographic Office, and as techniques and accompanying products have reached the point of having potential operational use to the Fleet, the Naval Weather Service has taken them over. The reasons for our takeover are that the atmosphere and the oceans are treated as one environment, and our customers require simultaneous forecasts for both media. Further considerations are that we have communications, our weather units are located with the Fleet, and our people have the scientific capability to forecast in the oceans as well as in the air.

The reason for this Naval Weather Service talk, then, is to show you -- the engineers, researchers, and industrialists -- how we work and how we mesh with the oceanographic community.

The Navy has recognized the need for a Weather Service for over 100 years, dating back to the days of Lt. Matthew Fontaine Maury in the 1840's. An organization called the Marine Meteorological Service actually existed in the 1800's; from this, we

have matured in the bureaucratic womb, in many queer and unusual shapes and forms, until, in July 1967, the Secretary of the Navy established the Naval Weather Service Command with a mission: "To provide meteorological services in support of sub-surface, surface, and air operations of the Navy, and to provide oceanographic forecasts of the Armed Forces in support of military plans and operations."

This mission sounds simple, but it conceals a support service of tremendous complexity. The Navy is nearly 200 years old, and never have its problems been so complicated. It maintains fleets around the world. It must be capable of landing an amphibious force at any point in the world on short notice. The enemy submarine threat grows by the day. Polaris submarines must be maintained on-station half a world away from our shores. Every Fleet job, and there are many more than those mentioned, requires environmental support. It is hard to find any environmental parameter which does not affect Naval operations, often to the degree of creating a no-go situation. These parameters include those under the ocean surface such as temperature, layer depth, sound propagation; at the surface, those such as sea state, tides, currents, surf, ice; and finally, in the atmosphere, density, wind, icing, stability, contrails, refractive index. The requirement to forecast such a wide variety of parameters and do it on a world-wide basis (Fig. 2) makes the Naval Weather Service unique in its complex forecasting responsibilities.

How are we organized to do the work I have just outlined? We are a line organization, stemming from the Naval Weather Service Command, headquartered in Washington, D.C. Four Fleet Weather Centrals -- Guam, Pearl Harbor, Norfolk, and Rota -- have huge areas ff responsibility (Fig. 2), within which they perform the functions of data collection, computer processing, and dissemination of analyses, forecasts, and warnings. A fifth Weather Central is located in Alameda.

Within the Weather Centrals' areas of responsibility are ten Fleet Weather Facilities, located at Yokosuka, Sangley Point, Kodiak, Quonset Point, San Diego, Pensacola, Jacksonville, Suitland, Keflavik, and London. The Fleet Weather Facilities assist the Weather Centrals in accomplishing their missions, and, in most cases, have a specialized function. For example, Suitland has forecasting responsibility for the entire Arctic Basin, Kodiak concentrates on ice forecasting (Fig. 3), Alameda is heavily engaged in Optimum Track Ship Routing (Fig. 4), Keflavik and Quonset Point provide detailed support for antisubmarine warfare aircraft operations (Fig. 5) and Jacksonville deals with hurricanes (Fig. 6).

Naval Weather Service Environmental Detachments are assigned to each of the Fleet Weather Centrals and Fleet Weather Facilities. The primary function of these 53 detachments is to support aviation operations.

Because it became evident about 10 years ago that the sheer volume of data involved in global environmental analysis and forecasting and the inevitable advances in related techniques could only be handled by numerical methods, the Navy established the Fleet Numerical Weather Central, Monterey (Fig. 7), to move the Navy into the era of computerized environmental products. Today, as the hub of our Weather Central System, it is one of the world's largest scientific computer complexes, with hemispheric meteorological and oceanographic responsibilities -- producing analyses and forecasts for direct operational use and in support of all units of the Naval Weather Service Command.

Completing the organizational picture requires one more concept -- The Naval Weather Service System. The System is a term used to describe all commands and units in the Navy to which environmental personnel are attached, either for making observations or for providing professional or technical support to Naval Force Commanders. The System is composed of the Naval Weather Service Command -- The Centrals, Facilities, and Environmental Detachments -- plus elements of other naval commands (Fig. 8). Roughly 100 major ships, major force and fleet staffs, and several shore commands have environmental groups of varying sizes attached to provide local and special interpretations of the basic products furnished by Monterey and the Centrals and Facilities. The Marine Corps has similar environmental terms to support aviation and artillery operations. The Naval Weather Service Command furnishes technical guidance to the entire System.

How it all works is shown in Figures 9 and 10. Environmental observations are collected world-wide, including observations made by Naval Weather Service units. The observations are transmitted to Fleet Numerical Weather Central at Monterey where they are quality-checked, sorted, and edited by ADP programs. Then, the analysis and prognosis programs take over, and the analyzed fields are transmitted back to the Fleet Weather Centrals, computer-to-computer at the equivalent of 4,000 teletype words per minute. Here, the data fields of interest are automatically extracted, supplemented with local data, and then disseminated by radioteletype, radio facsimile, or data link to other Naval Weather Service Command units and ultimately to the Fleet and Marine Corps units.

Most of the analysis and dissemination processes are completely automatic, utilizing modern computer and ancillary equipment, coupled with a highly efficient three-continent, high-speed communication system called the Naval Environmental Data Network (NEDN). The main trunks emanate from Monterey, connecting with computers at Guam, Pearl, Norfolk, and Rota (Fig. 11). From Norfolk and Alameda, the trunks fan out along the East and West Coast tie lines to the locations shown in Figure 12. The terminal stations are concerned basically with antisubmarine warfare or fontrol of operational forces,

but we have some non-Navy customers, too. The terminals shown are all connected to digitally controlled automatic X-Y plotters, which provide hard-copy map analyses and prognoses.

The NEDN is interconnected with the U.S. Air Force automated weather network (Fig. 13). Meteorological data is collected in England and Japan and sent at high speeds to Tinker Air Force Base and subsequently to Monterey. Over 90% of the data used in Monterey's analyses comes via the AWN circuit.

I move now from organization, mission, and method of operations to some of our products and services. First, let's examine things relating primarily to meteorology.

A variety of analyses and prognostic weather charts is constantly generated to provide the operating forces with a three-dimensional hemisphere picture of the atmosphere from surface to 100,000 feet. These basic charts are used in the conventional way by forecasters to provide necessary services to the Fleet.

Supplementing the basic material are a number of specifically tailored products and services; the Naval Weather Service moves more and more in the direction of providing tailored services. Among others, these tailored services include:

High winds and high seas warnings
Hurricane and typhoon forecasts
Short-term ice forecasts
Enroute weather forecasts for individual ships and forces
Surf forecasts for amphibious operations (Fig. 14)
    These include a variety of parameters--height, type, and period of breakers; width of surf zone; littoral currents.
Aviation forecasts--route winds at flight altitude and ditch headings (Fig. 15). FLEWEACEN Pearl runs a tropical program, covering the whole Pacific, from which 100,000 military and civilian clearances a month are made.
Ballistic winds and density--for accurate firing of guns and missiles (Fig. 16).
Refractive index--for determination of radar propagation conditions in the atmosphere.
Underway replenishment forecasts--these forecasts provide a measure of the anticipated difficulty of replenishing one ship from another while underway (Fig. 17).
Optimum track ship routing
    This service, developed by the Naval Oceanographic Office, integrates anticipated sea and weather conditions with ship characteristics and operating constraints to select a safe least-time track for a given ship voyage. FLEWEACEN Alameda routed 3328 ships in 1968.

All of the services discussed are provided on a global basis. Other meteorological services are provided as requirements of the operating forces dictate.

Let us move now to oceanographic services and products.

Our approach is to treat the oceans and atmosphere as two fluids in a single, coupled system with significant transfers of mass and energy across the interface. It follows that we deal mainly with physical oceanography--temperature, sound velocity, motion, and other characteristics of the ocean which can change the operating environment. Our mission is to forecast these changes before they occur. Since most of the driving forces are atmospheric in origin, it is possible to predict changes in such ocean state variables as temperature, sea state, and currents by integrating the total exchange of heat and momentum occurring at the interface.

The operational programs which comprise most of our oceanographic services and which include the interface exchange concepts just described, are:

Sea surface temperature
Sea state
Layer depth products
Currents (stream and transport)
Sub-surface temperature structure
Underwater sound mapping
Sonic range predictions

Our synoptic analysis of all these products is limited by lack of data; only sea surface temperature analysis can be prepared synoptically, where "synoptic" means using today's data to prepare today's analysis. In Figure 18 we see the coverage of sea surface temperature reports. Contrast this with the bathythermograph report coverage in Figure 19. Obviously, the models used for oceanographic forecasting, other than SST, must rely upon composite data sets and accurate analysis of the atmospheric driving forces.

To illustrate the method by which we treat the oceans and air as a coupled system, I shall describe the analysis method used for sea surface temperature (Fig. 20). Forecasting is based upon physical cause and effect principles. The forecast driving forces are taken from numerical meteorological forecasts. Heat advection is computed from sea surface temperature gradients and forecast surface current components. Heating or cooling is computed from the heat exchange forecast, utilizing wave mixing as one input. Forced mixing by wave action is computed from wave forecasts. Forecasting accuracy depends largely on the accuracy of the initial analysis and the accuracy of the meteorological forecast.

The preparation of other oceanographic products is as intimately related to the atmosphere as is the sea surface temperature analysis.

Sea state, surf, tide and current predictions are invaluable to many naval operations, such as amphibious landings, replenishment at sea, carrier operations, or just moving ships from one part of the ocean to another. However, our interest in the past few years has been directed more and more to underwater operations, both defensive and offensive (Fig. 21). The rapid growth of the Soviet submarine fleet has forced upon us the necessity of being able to detect, track, and if need be, destroy these boats. We have made an intensive effort to become proficient at forecasting underwater sound propagation, and to adapting our forecasts to the existing defensive vehicles and their sound gear. As you know, the Navy uses the greatest possible mix of search vehicles in order to exploit the peculiar advantages of each--ships, fixed wing aircraft, helicopters, and submarines all of which carry a variety of sound sensors.

To provide Fleet units with unending volumes of sea surface temperature, layer depth predictions, temperature profiles, and sea states is to miss the mark slightly. These parameters are important not in themselves, but to the extent that they influence or affect the sound ray path and propagation loss. Fleet operators really are only concerned with the question, "At what range will my sonar system acquire a target in my immediate area today?" So, the Naval Weather Service has devised a system for providing forecast detection ranges for each of the several sonar systems now in use. The approach is to combine a full array of oceanographic analysis field into composite propagation loss profiles for a series of point locations which are representative of predetermined acoustical regimes. Each regime is an area reasonably homogenous as to water mass, bathymetry, and bottom bounce acoustical loss. Both power-limited (Fig. 22) and ray path-limited ranges are predicted; the selection depends upon the spatial relationship of the transducer and target, whether they are in the same layer, lie across a layer boundary or are both in a duct. Range variability which might be expected with each regime is also calculated. The system is adaptable to both active and passive detection systems.

To present the acoustic ranges in the most useable form, we have divided our system into two parts (Fig. 23). Acoustic Sensor Range Prediction (ASRAP) is for the support of fixed wing aircraft, the P2/P3/S2 squadrons. Ship Helicopter Acoustic Range Prediction System (SHARPS) is for the support of other Fleet users. Both ASRAP and SHARPS are simple to use. The user knows what sonar ranges are possible in the area in whish he is operating, or in which he is about to go. The operator is freed of most computational work. He knows the range variability for his area. For the first time bottom

reverberation loss calculations are provided for Fleet use (Fig. 24). Convergence zone and bottom bounce ranges and recommended dip depths and tilt angles are provided so that ships can select the optimum mode of operation. Ranges are presented for in-layer and below-layer targets and various ship speeds, based on a 50% detection probability of a random aspect target by an unalerted operator. And the range calculations are based on noise limited performance figures corresponding to sonar type and ship speed.

What now of the future? Are there new products of a revolutionary nature just over the hill which might equal the breakthroughs we have had in recent years? The consensus among Naval Weather Service people is that the period just ahead of us will not be one of exciting discoveries, with an exception to be discussed, but one of smoothing the rough edges off existing models to get improved forecast accuracy.

As I have pointed out, the poor data base with which we work limits the efficiency of the models. There are a few possibilities for increasing our data base. Satellites would be the most likely contributor in the near future. The newest weather satellite appears to be able to define sea surface temperature and vertical temperature structure of the atmosphere. If this is so, and reasonably accurate soundings can be obtained over most of the earth's surface, our numerical atmospheric analyses will be greatly improved, with an assured by-product of improved oceanographic forecasts. Other data sources which could help, if they ever come into being, are buoys and an expanded observational program in merchant ships.

There is work being done at Monterey on a new product which could have tremendous impact upon both meteorological and oceanographic forecasting. This is a new analog system which can provide forecasts for periods of from one hour up to ten days. An analog is selected by computer-search through hemispheric historical data to find that day when the state of the atmosphere matched or nearly matched that existing today. Once found, it is assumed that the atmosphere will behave in the future just as it did following the historical day we selected for our analog. The idea is not new at all, but the complicated method of selecting the analog by computer is. The analog system is being tested right now, and has shown skill. With improvement and refinement, we may soon be able to provide prognostic charts out to ten days which have enough accuracy to be used for forecasting any atmospheric and many oceanographic parameters.

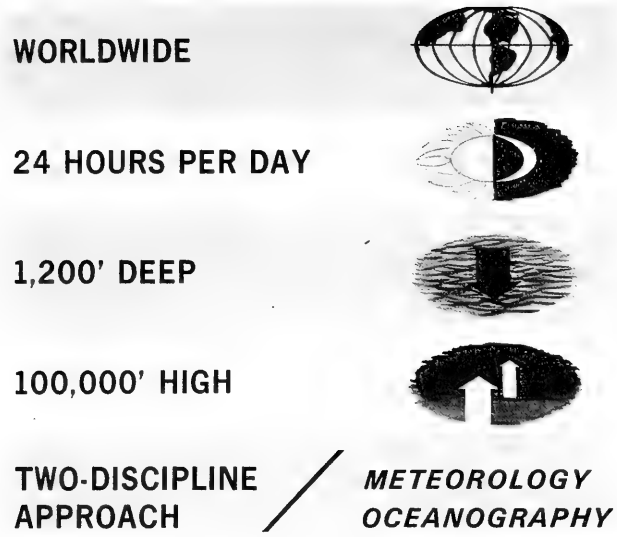

Figure 1

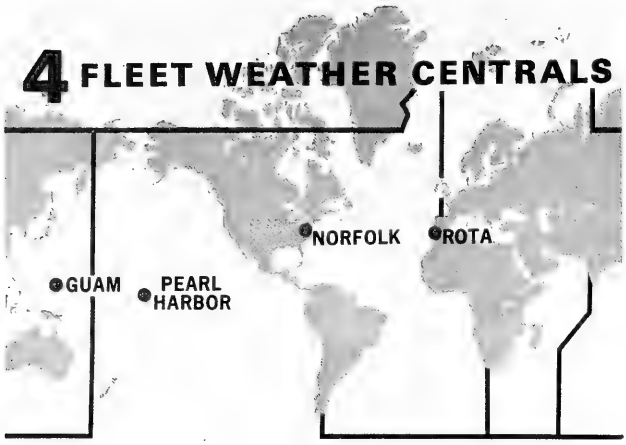

Figure 2

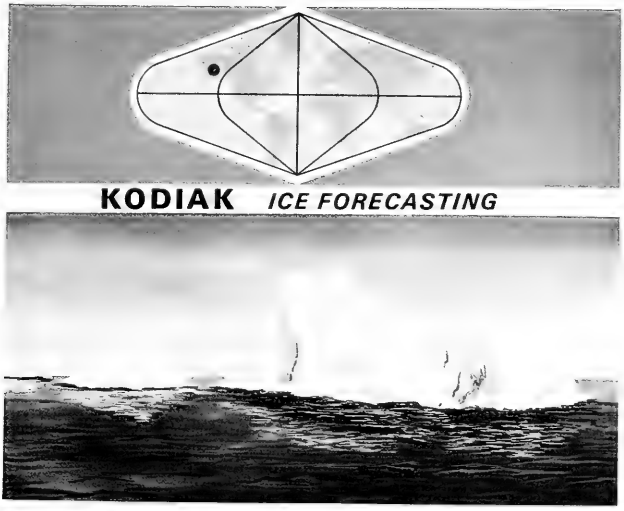

Figure 3

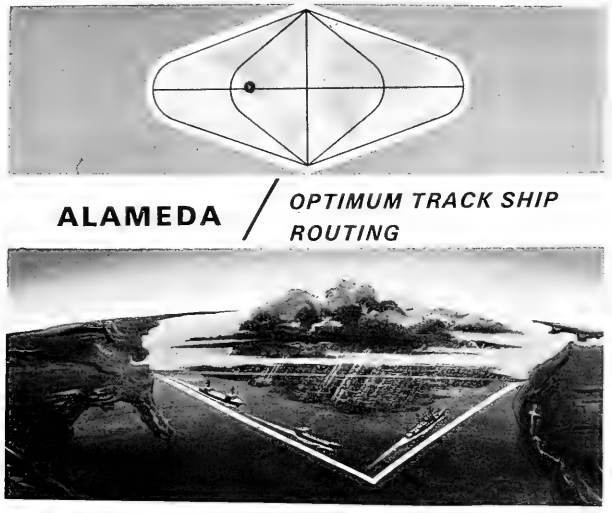

Figure 4

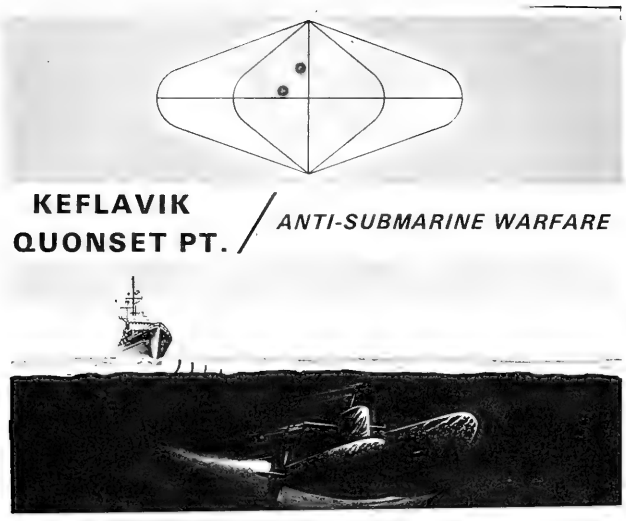

Figure 5

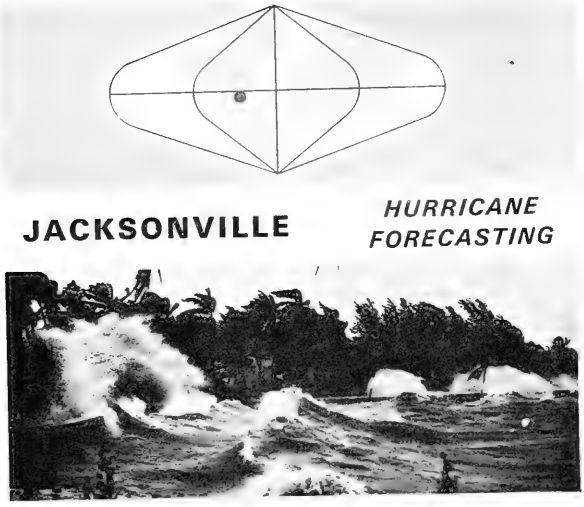

Figure 6

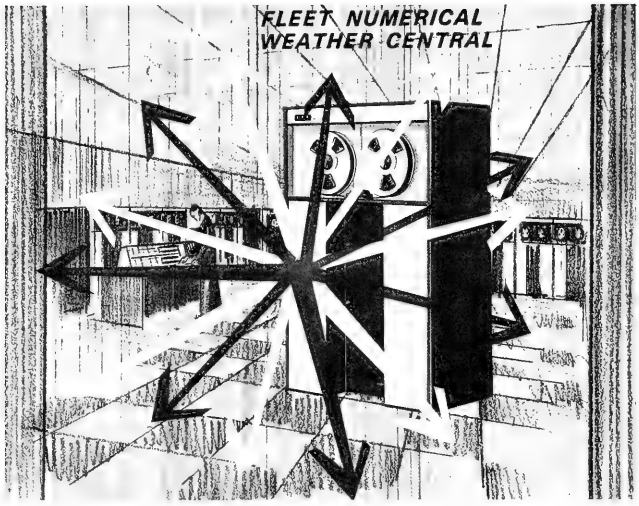

Figure 7

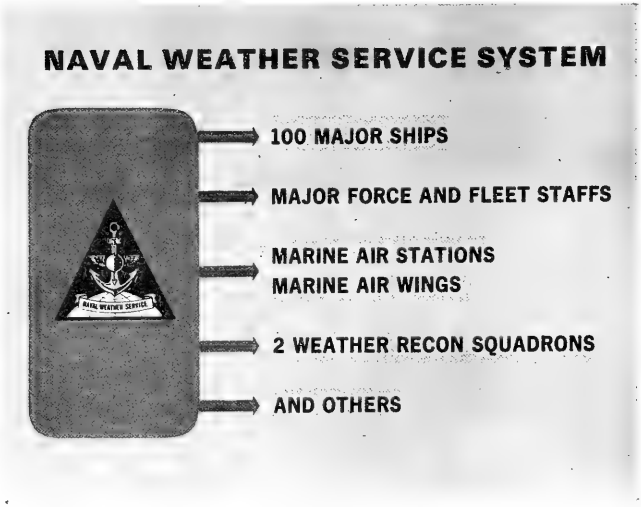

Figure 8

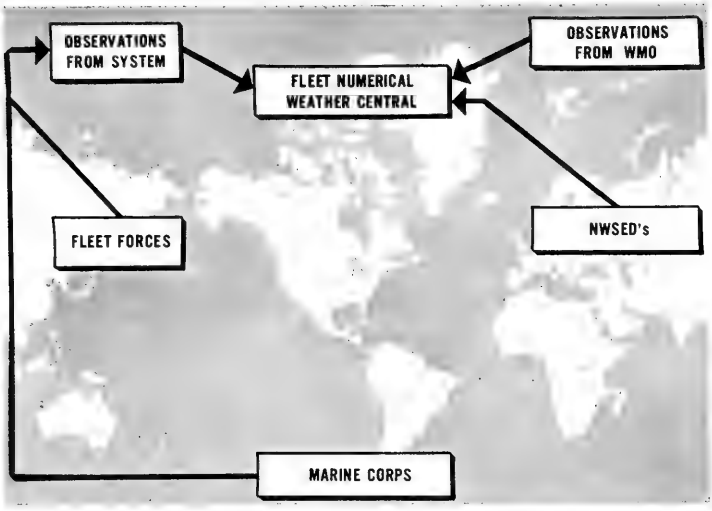

Figure 9

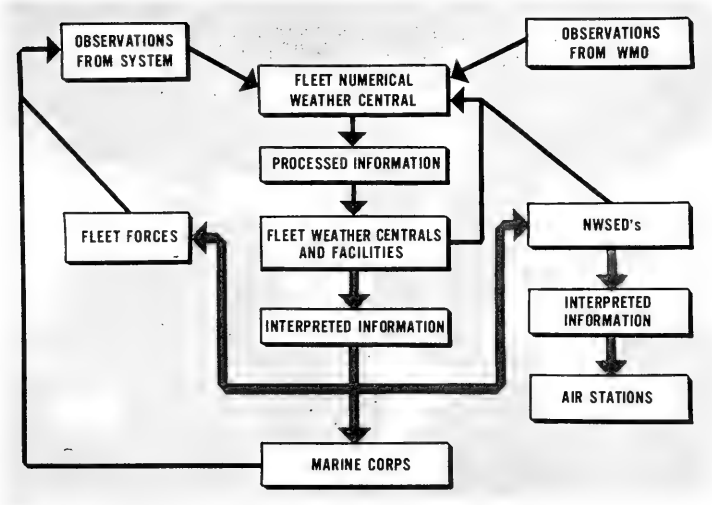

Figure 10

Figure 11

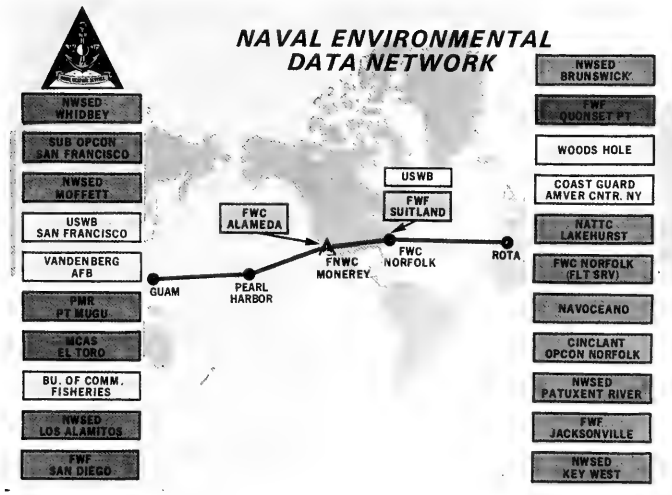

Figure 12

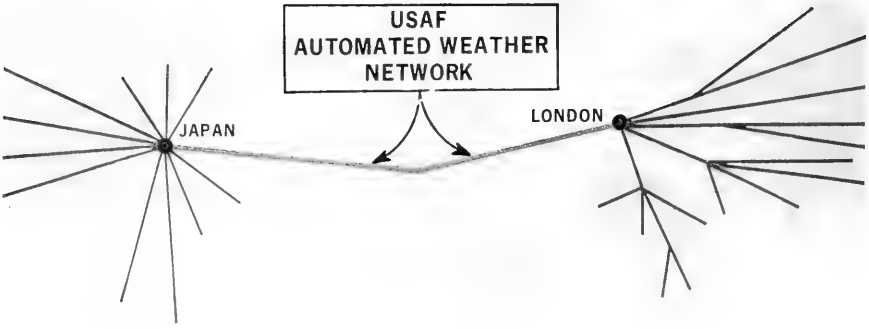

Figure 13

AMPHIBIOUS OPERATIONS

Figure 14

Figure 15

Figure 16

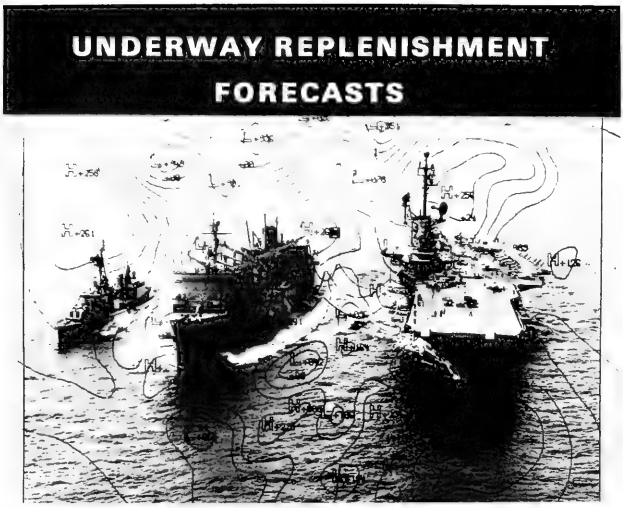

Figure 17

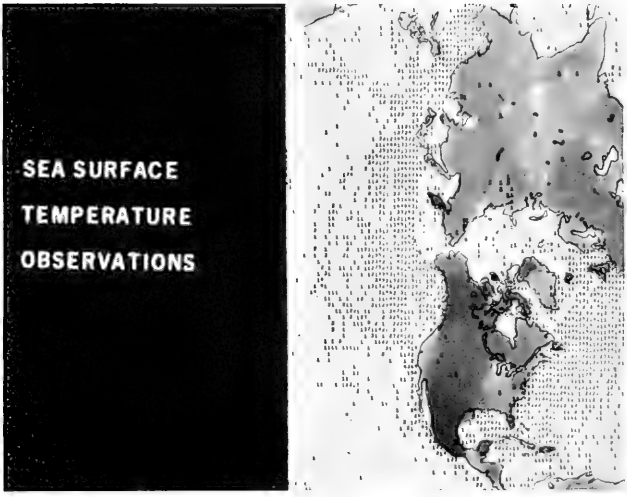

Figure 18

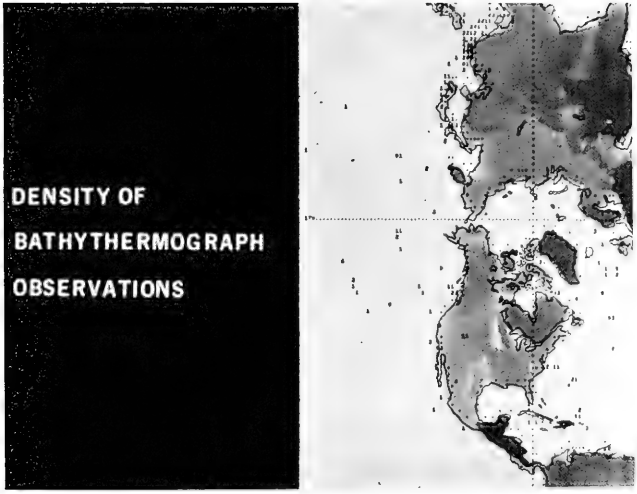

Figure 19

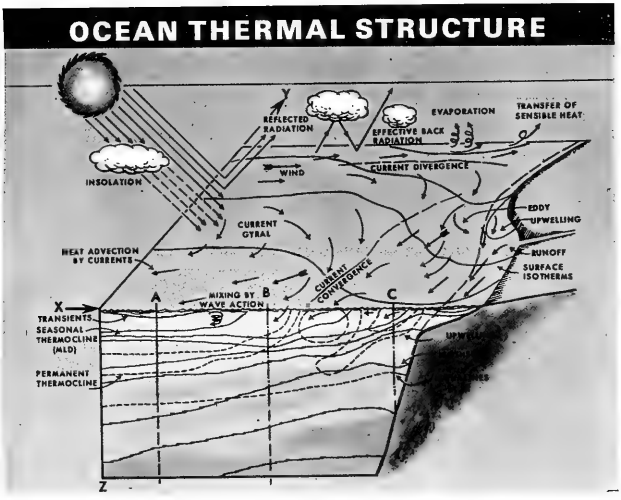

Figure 20

Figure 21

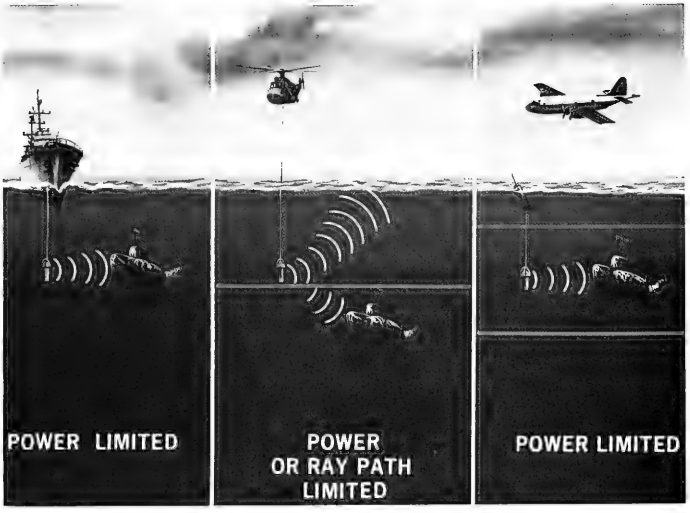

Figure 22

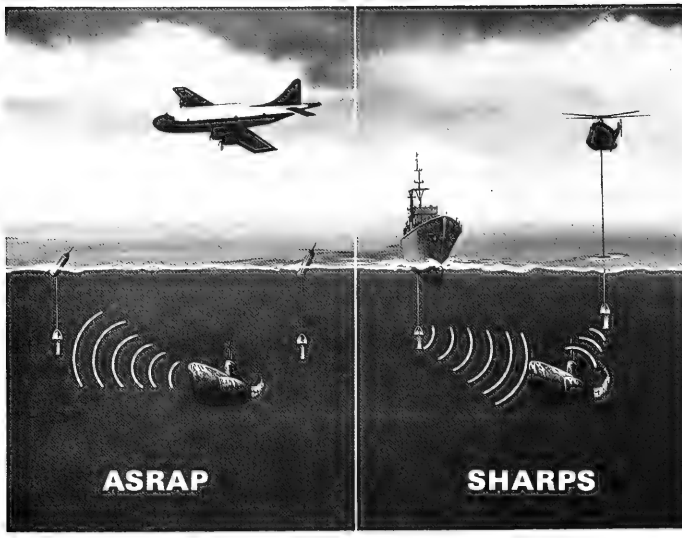

Figure 23

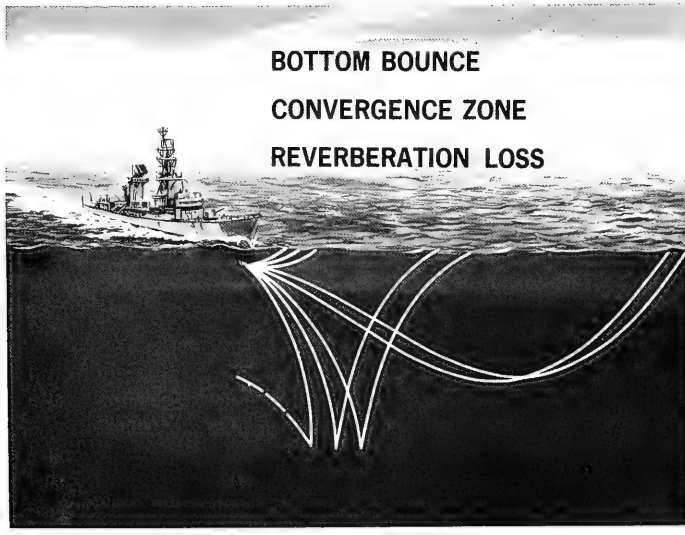

Figure 24

AN EXAMINATION OF SEAGOING COMPUTERS

(Opening Remarks to Panel Discussion on Seagoing Computers)

T. E. Ewart
Applied Physics Laboratory
University of Washington

INTRODUCTION

The digital computer has had almost as profound an effect on science and scientists as the transistor has had on electronics and electronic designers. The computer has had a very major impact on scientific budgets and on the allocation of scientific manpower. The computer is not just a gadget but is an important adjunct to scientific research and practical development.

We scientists who participate in ocean research have been slow in acquiring computing skills, especially in the "at sea" phase of our research. Other fields such as physics have incorporated computers into the research as fast as computer technology developed, and many state-of-the-art developments in computers have been produced by research programs.

Throughout the remainder of this talk I shall attempt to present economic and scientific arguments for selecting the proper computers for "at sea" usage. Much of the information I have used in preparing this talk has been gained through operation of our seagoing computer and data acquisition system since February 1966. This computer system is described in detail in the "Proceedings of the Marine Technology Society's Symposium on Seagoing Computers" held in January 1969.

PHILOSOPHY

Seagoing computers can be divided into three operational categories. The first is small computers, costing $8000 to $20,000, directly connected to specific scientific apparatus. Examples of this type of system are found in satellite navigation; salinity, temperature and depth data acquisition; gravity and magnetic data acquisition and many others. These applications are characterized by the fact that shoreside programs are written to take data in a particular fashion and perform a particular analysis or data handling operation. Such computers have been called "dedicated" computers.

The second type or medium-sized computer combines the ability to interconnect with scientific apparatus and yet provide the seagoing scientist with a general-purpose analysis facility. Such computers cost between $20,000 and $100,000 depending on the flexibility of the input-output. Such computers are easily programmed by scientists. Applications of this kind of computer include those cases where data analysis techniques will vary depending on the outcome of the experiments or where sophisticated computations are required before one can proceed with further experimentation.

The third type is a general-purpose, time-shared system capable of data acquisition simultaneously with scientific analysis and program compilation. Such systems generally cost in excess of $100,000. Some of these systems can even include the capability of partial operation of the ship. Such systems represent a computer center facility at sea.

The dedicated computer is basically integrated with one or more problems to which the attention of the computer is devoted entirely. The scientist and a programmer write in basic machine language a program dedicated to their specific task. On a particular cruise many scientists can use the same computer, but only in their turn. This type of computer is poorly suited to data analysis problems requiring large storage, sophisticated analysis or large volume input-output.

The medium-sized computer generally has a more advanced compiler. Its connection to the scientific apparatus can be more easily programmed if systems are developed in the secondary language. Usually one systems programmer and one technician are required for operation. Scientists can more easily incorporate this type of system in their experiments, and with this greater flexibility in input-output the scientist can easily change the operation at sea.

The computer center facility requires a highly trained staff of two or three to operate and perform system maintenance. It can, of course, perform any of the functions of the other two types.

Administratively, the first type should be considered quite separately from the last two. The cost of a dedicated computer is small in relation to the cost of experiments and ship time. No more justification should be required for this type of computer than for any other scientific apparatus which is incorporated into experiments. Compare, for example, the cost of an STD probe or a PGR to that of a small computer.

A medium-sized computer requires considerable justification with particular attention to the number of users and the types of problems encountered. Great care must be exercised in long range plans which incorporate the computer into future research. Considerable effort must be spent in making this type of computer system accessible to the scientist.

The computer center facility can be justified only if the long range plans of several scientific groups can project 5 to 10 years of full-utilization of the facility. Careful thought must be given to the fact that many smaller computers might outperform the giant. Such large computer systems might be better on the shore with only dedicated or medium-sized computers participating in the "at sea" phase of operation.

We must be very careful in allocation of our seagoing scientific manpower. Survey jobs are probably more effectively analyzed on shore with a seagoing computer performing data manipulation and consistency checks. The temptation in this area is to obtain a computer center facility and do all the processing at sea. This would be a mistake, since survey experiments can be well planned in advance and data checks can be made with simple computers on a routine basis. Our costly computer science specialists at sea should be allocated to problems requiring creativity and careful co-ordination of computer and experiment. Most creative people will simply not spend significant fractions of their life at sea.

The decision on whether to do on-line or off-line processing hinges on the requirements of a particular experiment. Programming languages should be developed which allow the maximum flexibility to the scientist. The scientist using an on-line facility should be able to bring cables from his sensor apparatus to the computer and proceed from there to data acquisition and analysis via simple programming steps. This programming is preferably written in a secondary language such as FORTRAN or ALGOL. Thus the scientist wishing to make changes in his experiment does not have to resort to rewiring electronics but to altering a computer program.

The medium-sized computer is best suited to this flexible on-line operation because it can combine the interface capability of the dedicated computer with a more easily operated compiler. The medium-sized computer generally has punched card input-output and a printer to facilitate programming. There are many who feel that eliminating paper tapes and typewriters justifies the additional cost of the medium-sized computer.

EXAMPLE OF A MEDIUM-SIZED SYSTEM

The Ocean Physics Group of the Applied Physics Laboratory, University of Washington has operated a medium-sized computer system on five major cruises since February 1966. The computer is an IBM 1130 with card, paper tape, printer, plotter and magnetic disc input-output. To its interface channels are attached devices for reading and writing voltages, frequencies, switches, magnetic tape and a complete shipboard acoustic tracking system. The system has been used on-line with acoustic propagation experiments, sound velocity, salinity, temperature and depth measurement and tracking of many types of in-water apparatus such as our self-propelled underwater research vehicle.

A complete set of programs has been written for our system to allow us direct access via the FORTRAN language to our experiment sensors. This has resulted in significant flexibility to alter experiments in progress via simple program changes. The programming allows us to read volts, frequencies or whatever by easily understood program steps. This eliminates the necessity of having each of us be a computer expert as is the case for the dedicated computer.

An example of this flexibility can be seen in an experiment performed by the Ocean Physics Group to measure vertical acoustic transmission fluctuations. It was decided while on a cruise that it would be interesting to examine vertical acoustic transmission fluctuations and correlate these with temperature data taken to examine internal wave spectra. The experiment was designed, the equipment was attached to the computer, two very simple programs were written, the data were taken and some analysis was done - all during a three-day period at sea. The computer system in this case replaced a great deal of black box electronics which would have been required to perform such an experiment.

Another example of the on-line use of a computer is the Ocean Physics Group's sound velocity, salinity, temperature and depth system. The frequency output from the sensors is directly connected to the frequency-to-digital converters attached to the computer. The data can be taken under program control by time increments or depth increments. Taking data by depth increments, which is possible only with a computer, requires a computer algorithm which will take data while the SVSTD probe is traveling one direction. This procedure eliminates differential flushing errors and produces a clean data file monotonic in depth. Further analysis of SVSTD data is performed to produce results available almost immediately for planning our other experiments. This rapid turn-around time is essential to us in planning acoustic, microstructure or diffusion experiments.

ECONOMICS

The economics of computers used in ocean research is very complex. One has to match the increased cost of technology against the nebulous notion of progress in science. Suppose we break up a scientific experiment into three parts: the planning phase, the experimental phase and the analysis phase. Before the seagoing computer, one planned an experiment, set up a cruise plan, took the data and then returned to the laboratory for the analysis phase. Now it is possible to plan an experiment, plan a cruise and then undergo cycles of experiment and analysis on the same cruise.

The computer is used in all three phases of the experiment. In the planning phase the computer is used for modelling and prediction and the analysis methods are developed in advance. Experiment modelling can save ship time by eliminating some of the cut and try. The second phase operation requires the computer to be used in on-line or off-line processing or data acquisition. The third phase analysis confirms or modifies the results of the planning phase and in certain experiments one can make changes in the experiment and go through phases two and three again.

CONCLUSIONS

From a cost effective basis it appears that a carefully planned medium-sized computer can accomplish most of the tasks undertaken by ocean scientists. However, such a system should be attached to the scientific laboratories and not to the research ships. This last statement is justified by an observation of long standing that bureaucracies carefully engineer creativity out of scientists by the imposition of simplistic rules and arbitrary regulations.

The philosophy of a shipboard computer must be that of service to the scientist and not control of the scientist. In this light dedicated computers have the edge since they most directly connect scientist and computer. Medium-sized computers can generate this connection provided they are not assigned too many permanent tasks. The computer center facility is inevitably hopelessly far away from the scientist since the computer entity is larger than most experiments. The fear I have of the computer center and possibly the medium-sized systems is that they will be used primarily for data gathering and graph plotting. The ability to print thousands of pages and plot hundreds of graphs at sea can be a millstone to science if improperly used. Computer technology changes rapidly and we must be prepared for this change. We must not burden our research ships with any more inflexible, often inoperable and often out-of-date equipment. If

we do, the day will come when the creative scientist will bring his own black box aboard and step over the out-of-date monster bequeathed by a well-meaning bureaucracy. Ocean scientists have far too often tried to define the ultimate instrument and use it confidently forever. Please let us avoid this with the digital computer. Let us define carefully the priorities, the expenditure of money and the even more precious manpower.

THE SEARCH FOR SCORPION: PHOTOGRAPHIC AND OTHER SENSORS

R. B. Patterson

Naval Research Laboratory
Washington, D. C. 20390

ABSTRACT

A multi-sensored instrument vehicle towed by the USNS MIZAR (T-AGOR-11) located the USS SCORPION (SSN 589) as it had located the USS THRESHER (SSN 593) approximately four years earlier. In both searches, the magnetometer was the most useful non-photographic sensor, though the presence of natural magnetic anomalies reduced the effectiveness of this equipment in the SCORPION area. Two side looking sonar systems were used in the search, but they lacked the ability to discriminate between natural bottom discontinuities and artifacts. A radiation detector was also used with negative results. No non-optical sensor presently available has the ability to classify bottom contacts, and until such a sensor is developed, towed camera systems will remain the best tools for ocean floor search. Since the loss of THRESHER, the search effectiveness of underwater camera systems has been greatly improved. The use of wide angle lenses with hemispherical windows has resulted in a better utilization of the short ranges inherent in present photographic systems. During the five months of the SCORPION search, the Naval Research Laboratory camera system took 142,000 photographs and logged about 1,000 hours of bottom time.

INTRODUCTION

The lost submarine THRESHER (SSN 593) was relocated on 26 June 1964 with a multi-sensored instrument vehicle towed by the Naval Research Laboratory's ship, the USNS MIZAR (T-AGOR-11). The lost submarine SCORPION (SSN 589) was relocated on 28 October 1968 with a multi-sensored instrument towed by NRL's ship, the MIZAR. If these two statements do not indicate progress during the intervening 52 months, the indications are misleading. There has been enough progress to make possible a five month search for SCORPION which would have required five years using the equipment and techniques which found THRESHER. It is the purpose of this paper to describe some of these improvements while reporting on the effectiveness of various sensors used in the search.

TOWED VEHICLE

The towed vehicle, commonly called the "fish", is shown in Figure 1. This view was obtained before all the equipment

was installed on the vehicle and is shown to illustrate the type of construction. The structural members are all of 6061-T6 aluminum. The round stock is 1-1/2" solid bar. The rest is 2" x 2" x 3/8" angle except for the 8" channel belt at the tow point. An electronic light source is mounted at each end with two cameras just aft the tow point, approximately half way between the two lights. The telemetry system, battery, transponder, and other equipment are mounted in the space between the cameras and the two lights. Not shown in the figure are the boom which supports the magnetometer head approximately four feet behind the rear light source, and the side-looking sonar transducers which are mounted on the sides of the vehicle. The open construction is used to allow modification of the sensor package in order to fit the job at hand. Since the unit is towed at speeds of about one knot, the added drag resulting from this type of construction is not significant when compared to the drag of the cable.

MAGNETOMETER

As in the THRESHER search, the magnetometer was the most useful non-optical sensor used in locating the SCORPION. The NRL designed proton precession type unit has a toroidal head. This head reduces noise due to stray electrical fields and eliminates the null that results when the polarized field is parallel to the ambient field. The problem of winding a hollow toroidal coil was solved by using a wax form. After the head was wound, it was impregnated with epoxy and then heated so the melted wax could be poured out. Recently, we have found an easier method which uses hollow plastic cores obtained from an inexpensive infant's toy called "Rock-a-stack".

During most of the search, the magnetometer head was mounted on a boom approximately four feet aft of the rear electronic light source. The pressure housings for the flash and most of the other instruments are made of 17-4PH stainless steel. This material is very strong but also ferromagnetic. The bottles therefore distort the earth's magnetic field. As a result variations in the "fish" heading introduce fluctuations in magnetic intensity. The level of these fluctuations varied considerably as a function of heading, speed, and other variables. Levels higher than 100 gamma were measured, a small portion of the time. Since the size of the centerwell precludes lengthening the boom, we experimented with towing the head below the "fish", and this significantly reduced the fluctuations.

Unlike the THRESHER area which was fairly uniform as far as magnetic measurements were concerned, the SCORPION area contained a large number of natural magnetic anomalies.

Many of these anomalies were of small area and high magnetic intensity, not unlike a submarine. An example is shown in Figure 2. This anomaly has a peak level of almost 2000 gamma which lasts for about 2 minutes or 200 feet assuming the tow speed was one knot. Both the leading and trailing edges are several hundred gamma above ambient more than 5 minutes or 500 feet from the peak. This is the type of anomaly one would expect from a very large piece of metal, but it was measured miles from SCORPION and identified as a pile of rocks.

While an anomaly like that shown tends to raise hopes after hours of fruitless search, it is really small compared to the anomalies produced by the SCORPION. These were of such a high level that the head stopped ringing. At the time the first photographs of the submarine were obtained, three photographs similar to Figure 3 were obtained in one minute. There was no precession signal for a period of five minutes and the measured magnetic intensity was well above ambient for a much longer period. Though the run lasted for many more hours, the magnetic measurement made the crew confident that they had found the stricken submarine. Once SCORPION had been located, the magnetometer proved useful in maneuvering the "fish" so as to obtain more photographs.

SONAR

Two quite different side-looking sonar systems were used in the SCORPION area with very little success. The Westinghouse OBSS operated at a frequency of about 200 kHz, while the NRL modified Hudson Laboratory system used a frequency of about 30 kHz. Bottom contacts were made with both systems. The example shown in Figure 4 was obtained with the OBSS. The time 0510 corresponds to the peak of the magnetic anomaly shown in Figure 2. Photographs taken at this time show rocks. The figure shows a number of contacts and that is the difficulty. There are too many contacts, and present day systems have neither sufficient resolution to determine the shape of the contact nor the ability to differentiate between a steel plate and a bottom discontinuity. This is unfortunate because in an underwater environment sound provides greater ranges than other types of radiation. In the past, most sonar systems have been developed to either find the distances to the bottom or to locate a submarine within the ocean volume. In order to develop a sonar system which will be a useful tool for searching the ocean floor, it will be necessary to find ways of obtaining greater resolution and what might be called "contrast"; that is, the ability to differentiate between different solid materials.

NUCLEAR RADIATION

A gamma detector was used to make readings in the vicinity of the hulk. When lowering such a sensor, a definite rise in the background level is observed as the sensor approaches the bottom. This is due to the natural radiation level of the bottom sediments and is a handy check on the operation of the equipment. Measurements were made simultaneously with photographs so there can be no doubt when the sensor was in close proximity to the hulk. No radiation above the normal background was detected. Since water is a pretty good shield for gamma rays, this unit has very little range.

PHOTOGRAPHY

While the non-optical sensors were helpful, they all lacked the ability to classify bottom contacts. For this reason, the underwater cameras were the prime search tool in this operation as they were in the THRESHER search. Improved cameras and techniques made it possible to conduct a successful search in a time which would have been impossible a few years ago.

During the THRESHER search, EG&G model 204 cameras, like the one shown in Figure 5, were used first in stereo pairs and later as part of a three camera array. The angular field of view of these cameras is 46 by 33 degrees. In order to increase the coverage, a three camera array was developed which had an angular coverage of 110 by 46 degrees. This array provided better coverage and three times as many photographs to look at. This latter factor was a significant problem.

In order to overcome this problem, the camera shown in Figure 6 was developed. This is an EG&G model 204 modified by the addition of a wide angle lens system developed at NRL. This lens, which has been reported by Patterson[1], has a 114 degree field of view. This camera was first used in the search for the H-bomb off Palomares, Spain and took over half of the photographs taken in the SCORPION search.

The amount of improvement this camera represents is seen in Table 1. The table compares the search capability of three different camera systems: the single model 204, the three camera array, and the wide angle camera. The search widths are based on an operating height of 25 feet, which could be increased to 30 feet in clear water such as that in the SCORPION area. The number of photographs per minute assumes a tow speed of one knot and provides reasonable overlap. The number of photographs required to search a square mile is the number to photograph two square miles.

If one takes this number of photographs, randomly, within a square mile, he will photograph about 90% of the area. While two miles of cable does have some effect on the control which can be exercised on the "fish", our techniques are certainly better than random. Also, the SCORPION is quite large, so these figures can be reduced for this particular search. They must all be reduced by the same factor, so the wide angle camera still requires significantly less photographs. Film costs about 5 cents a foot, so the film costs in all cases are insignificant compared to operating expenses. However, the time required to expose, process, and view the film is an important consideration. The single camera is inferior in all these aspects. The photographing time is the same for the three camera array and the wide angle camera since they have the same search width. If processing time were the only consideration, the values shown could be decreased by use of high speed processors, but the viewing time provides the real test. It is necessary to view film for a few hours in order to appreciate what 130 hours of viewing time really means. Viewing film effectively for many hours is not difficult -- it is impossible! The 15 hours of viewing time spread over 150 hours of bottom time is much more practical.

The wide angle camera shown in Figure 6 is handicapped by a low film capacity. To overcome this difficulty the camera shown in Figure 7 was developed. This is an EG&G model 207A survey camera modified to use the NRL developed wide angle lens system. The camera holds 500 feet of film and will take about 4000 photographs per lowering. Taking two exposures per minute, the camera will photograph approximately one half a square mile and a run will last over 33 hours. Difficulty with the hemispherical windows on this camera precluded its use until the latter part of the search. It was used for 8 of the 80 lowerings and made nearly 25% of the photographs taken during the operation, including the first photographs of SCORPION.

For most of the search, EG&G model 208 Electronic Light sources were used. These are certainly an improvement over the equipment available at the time of the THRESHER search. They are more efficient, produce more light, are more dependable and are much quieter from an electrical interference viewpoint.

During the five months of the SCORPION search, the MIZAR made 80 camera runs and took approximately 142,000 photographs. On some of these runs, two or three cameras were used. If the resulting redundancies are eliminated, approximately 119,000 photographs remain. The total area photographed was about 13 square miles. Comparing these figures with the 84,000 photographs of less than one square mile obtained during two years

of the THRESHER search yields some indication of the progress made in the intervening years.

The Naval Reconnaissance and Technical Support Center fitted approximately 925 of the THRESHER photographs into a photo mosaic which includes most of the wreckage and the surrounding area. It is too small to see much detail, so a portion of it is shown in Figure 8. This portion, which contains about 25 individual photographs, shows the sail, high pressure air bottle, and other small debris.

A similar mosaic was also made with the SCORPION photographs. The use of the wide angle cameras made it possible to obtain similar coverage with about 20% of the number of photographs needed for the THRESHER mosaic. This gain is illustrated by a comparison of Figure 9 with Figure 8. Figure 9 is a single photograph of SCORPION's sail. No attempt has been made to use equal scales for the two figures, but the areas shown are certainly comparable and the reduction in the number of required photographs is a significant improvement in the search capability. On the other hand, the THRESHER mosaic certainly contains more detail than the SCORPION photograph. On a given film size, a narrow angle lens will generally produce a more detailed image than a wide angle lens.

While the wide angle camera was an ideal search camera, the standard model 204 cameras were used to obtain more detailed photographs once the submarine had been located. For this portion of the operation, three cameras were used one wide angle camera and two standard units. One of the narrow angle cameras was loaded with color film while the other two cameras were loaded with black and white. The color film really did not provide any additional information. With the "fish" 30 feet off the bottom, the light must travel through a 60 foot water path. This long light path is a narrow band blue filter. If blue photographs are desired, better ones can be obtained by viewing black and white photographs through a blue filter. The black and white film is less grainy than the blue layer of high-speed color film.

A number of different films were used during the search. Kodak Tri-X on a 4 mil. Estar base was used for the first part of the search. This was later replaced by Kodak Linograph Shellburst which has a number of advantages. Though it is a bit slower, it has finer grain, higher resolution and higher acutance. It is more readily available and is designed for high temperature processing. The color film used was Kodak Ektachrome EF. This film was returned to this country for processing, but the black and white film was processed

aboard MIZAR using a system previously described by Patterson[2].

Underwater optical sensors are the only presently available devices with the ability to classify bottom contacts, and therefore they remain the prime tool for ocean floor search. As a result of the short ranges inherent in such sensors, the search of any large area will entail many hours spent close to the bottom. The MIZAR left Norfolk on 2 June 1968 and completed the search on 7 November 1968. This is about 3800 hours of which 2500 were spent in the search area. The towed camera system was close to the bottom, taking photographs, for 1000 hours or 40% of this time. This percentage could have been increased if the time in the area had been spent solely for photographic operations.

Observers in a manned submersible can see no farther than the camera. No presently available submersible can even approach a 40% duty cycle. The cost of building and operating a deep submersible is sufficient to pay for a number of towed systems such as that on MIZAR. For these reasons, a towed camera system is and will remain the optimum ocean floor search system for years to come.

SUMMARY

This paper has demonstrated that the successful search for the SCORPION represents a significant improvement of techniques and equipment over those used to locate the THRESHER in 1964. The magnetometer was the most useful of the non-optical sensors. The acoustic systems were of little use and this is unfortunate as they have greater range potential than other types of underwater sensors. The wide angle lens systems and large capacity cameras developed since the end of the THRESHER search have been proven to be ideal search tools. However, these cameras lack necessary resolution, so that after the submarine is located it is necessary to supplement them with narrow angle cameras. In the future it may be possible to use larger film sizes in order to obtain the required resolution without sacrificing angular coverage. Finally, it is shown that towed systems are economical and can be operated at high duty cycles which gives them some advantage over manned submersibles as deep ocean floor search tools.

REFERENCES

1. Patterson, R. B., "A Wide Angle Camera for Photographic Search of the Ocean Bottom", Society of Photo-Optical Instrumentation Engineers, Underwater Photo-Optics Seminar Proceedings, 1966.

2. Patterson, R. B., "Photographic Techniques for Ocean Floor Search and Research", Plenum Press, Marine Sciences Instrumentation 1968.

Table 1
Comparison of Photographic Search System's Ability to Search One Square Mile with 1 Knot Tow Speed and 25 Foot Operating Height

	Single Camera	3 Camera Array	Wide Angle Camera
Search Width	14 ft	80 ft	80 ft
Photographs Per Minute	6	18	2
Number of Photographs Required	310,000	160,000	18,000
Film Required	58,000 ft	30,000 ft	2,300 ft
Photographing Time	860 hrs	150 hrs	150 hrs
Processing Time	950 hrs	500 hrs	38 hrs
Viewing Time	260 hrs	130 hrs	15 hrs

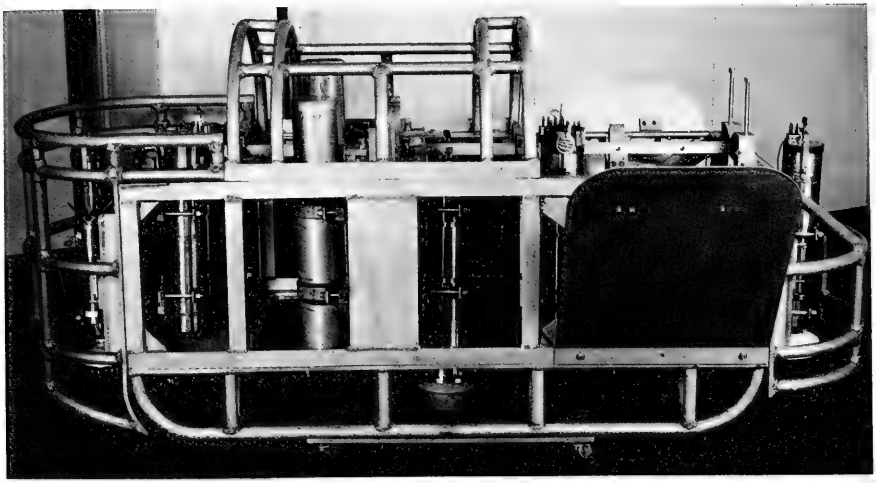

Figure 1. Towed Instrument Vehicle

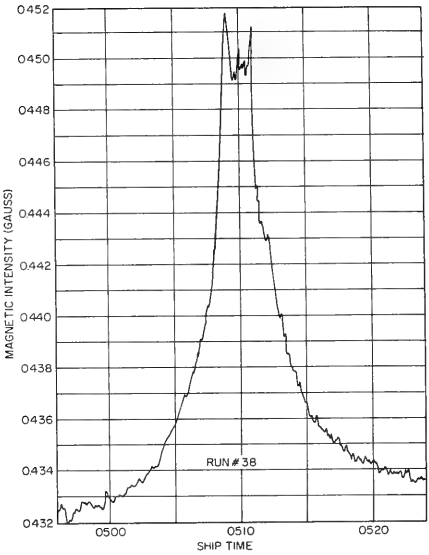

Figure 2. Magnetic Anomaly

Figure 3. First Photograph of SCORPION

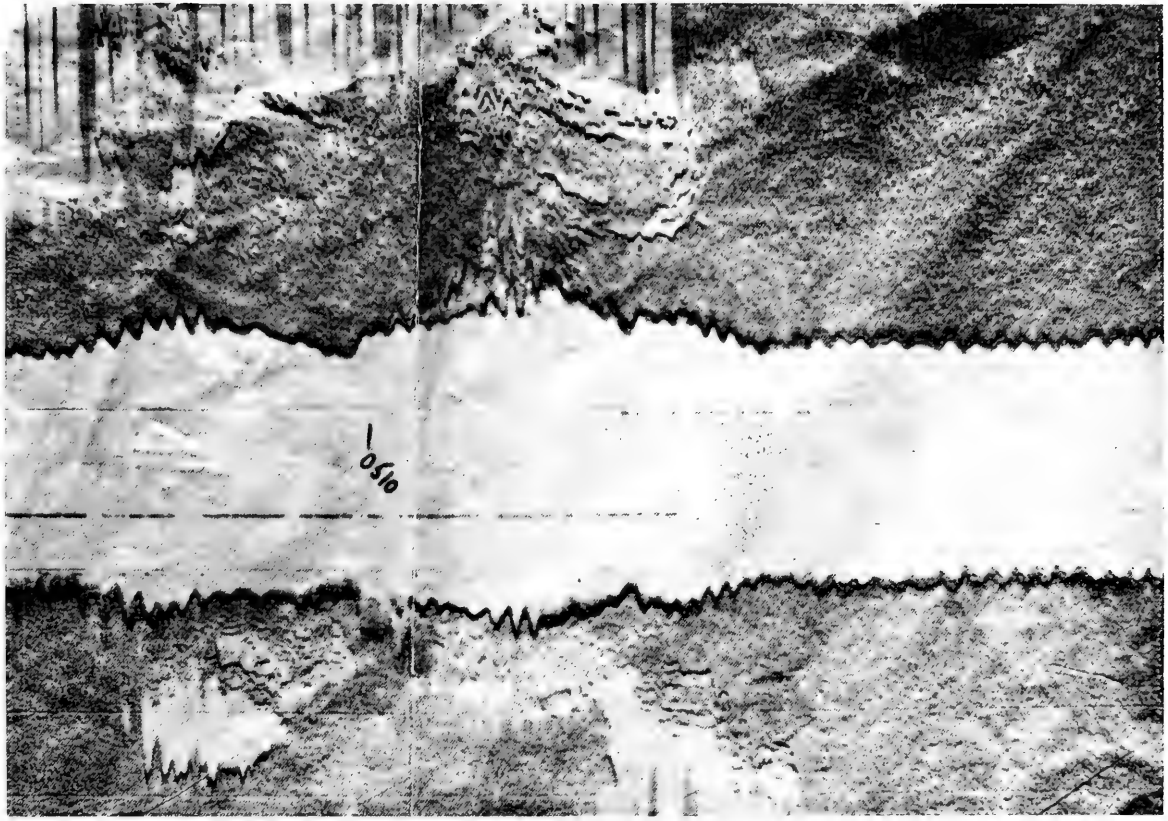

Figure 4. Side Looking Sonar Record

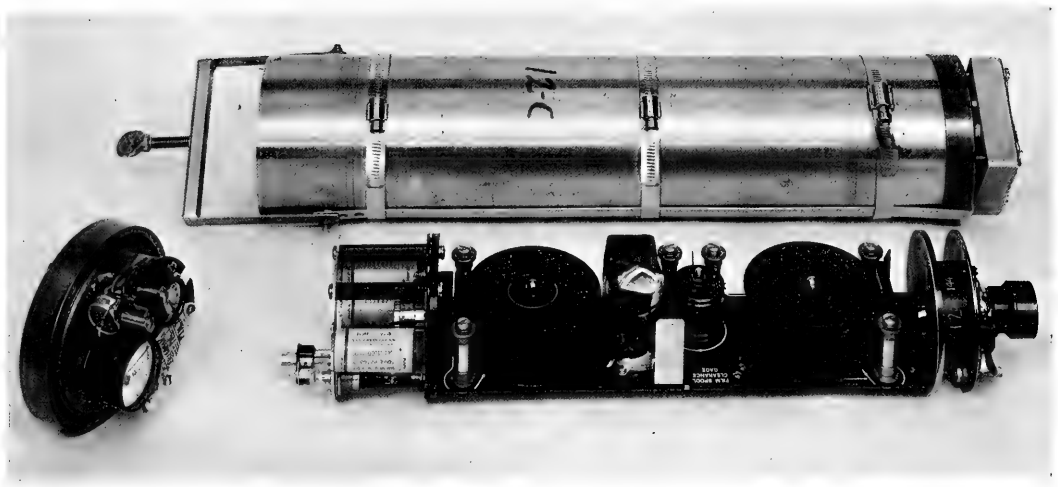

Figure 5. EG&G Model 204 Camera

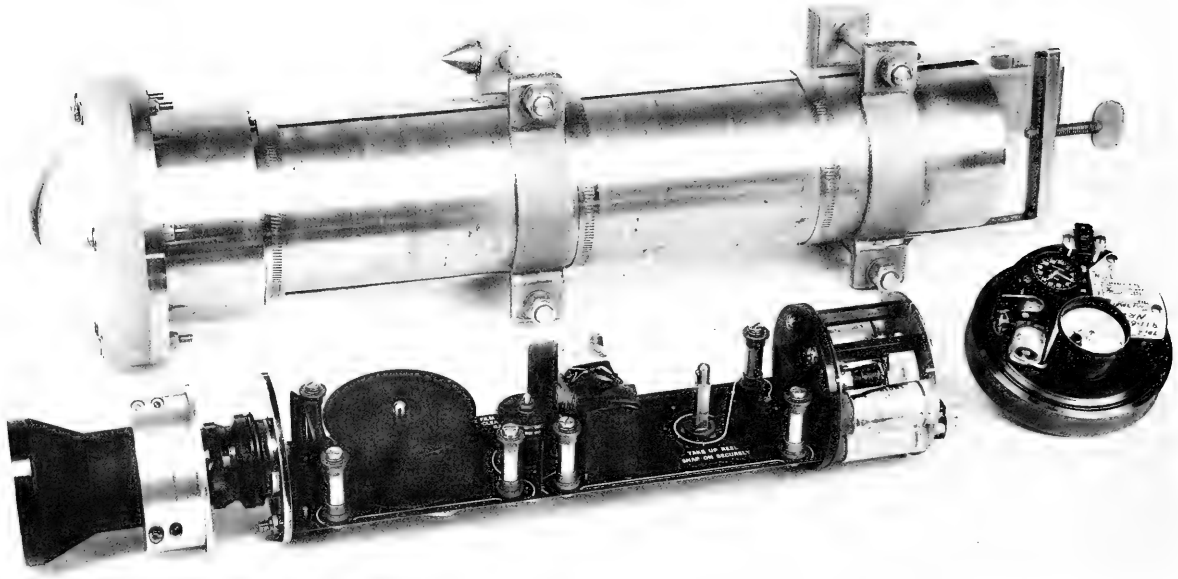

Figure 6. Wide Angle Lens Modification of EG&G Model 204 Camera

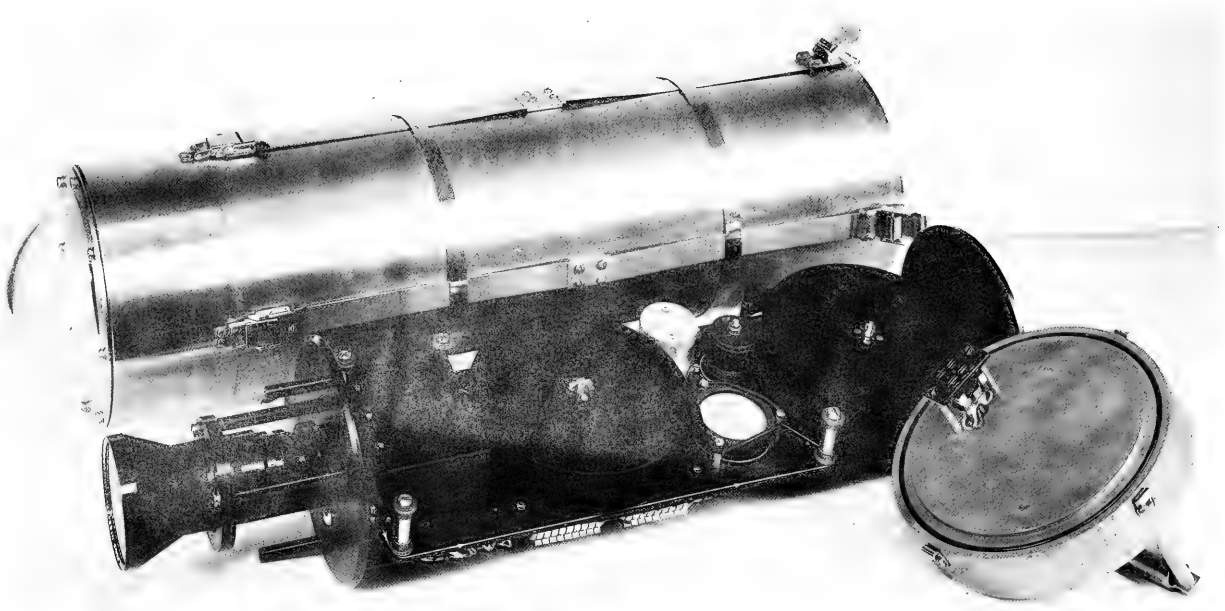

Figure 7. Wide Angle Lens Modification of EG&G Model 207A

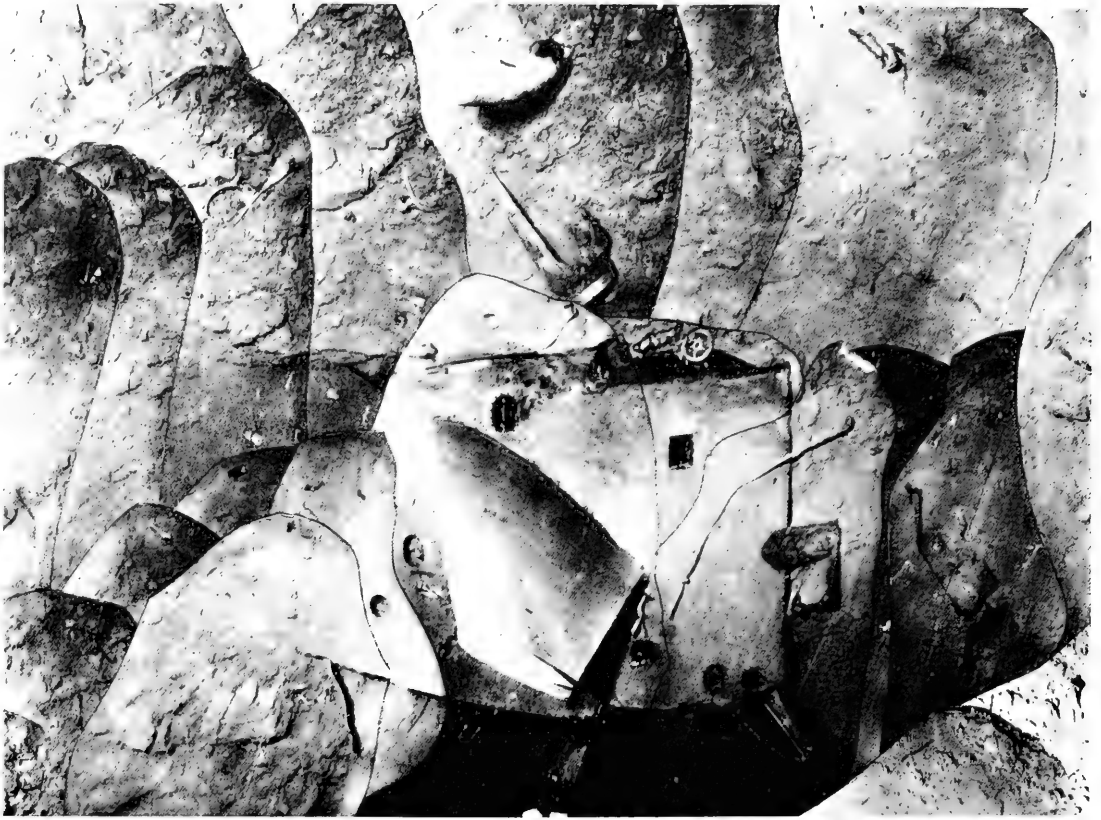

Figure 8. Enlarged Portion of THRESHER Mosaic

Figure 9. SCORPION's Sail

SEARCH FOR SCORPION:
ORGANIZATION AND SHIP FACILITIES

C. L. Buchanan

Naval Research Laboratory
Washington, D.C. 20390

ABSTRACT

The operational Navy is lacking in vehicles, personnel and procedures for conducting a deep ocean inspection such as the search for SCORPION. For this reason an ad hoc organization consisting of operating Naval units, research ships and personnel and an advisory group of technically qualified personnel were assembled. This organization proved to be very effective and should serve as a model in future emergencies which may involve research facilities in fleet operations.

The USNS MIZAR (T-AGOR-11) which was chosen as the primary search vessel, has a special center well for launching towed vehicles and a built-in Underwater Tracking System. A special telemetry system permitted rapid expansion of the normal instrument complement to accommodate new requirements.

This is a two part presentation of information of importance to the Military Oceanographic Community. The first portion will cover the organization, the special shipboard equipment, and the navigation systems. The second part will cover the towed sensors and their performance.

This information is presented with the thought in mind that other research organizations might find themselves involved in a fleet operation. It is important that research organizations with special capabilities recognize the possibility of an emergency preempting their time and facilities, and consider contingency plans for such an event.

ORGANIZATION

When SCORPION failed to arrive at her destination, the standard SUBMISS search plan was put into action. Immediately thereafter planning was initiated to organize a task force for deep ocean search if this should prove necessary. The Chief of Naval Operations assigned primary responsibility for this task force to OP33, Admiral Donaldson. Admiral Schade, Commander of Submarine Atlantic, was assigned as Task Force Commander.

The primary vessel chosen for the deep ocean search was USNS MIZAR (T-AGOR-11) operated by the Military Sea Transportation Service for the Naval Research Laboratory. This was the third time in her four years as an oceanographic research vessel that MIZAR was operated as a unit of a Navy task group. The special oceanographic equipment for deep ocean research aboard MIZAR was operated by personnel from the Naval Research Laboratory, with some special support from the Navy Oceanographic Office and, on some occasions, by personnel from commercial contractors.

Funding and commercial contract assistance functions were handled by the Office of the Supervisor of Salvage, Captain W. Searle in the Naval Ships System Command.

The unusual nature of the task assigned indicated the desirability of a pool of technical advisors. The Honorable R. A. Frosch, Assistant Secretary of the Navy for Research and Development, assigned Dr. John Craven, Chief Scientist for the Deep Submergence Systems Project, as Chairman of this group, which was to report as an advisory panel to Admiral Donaldson. The membership of this group was drawn from various operational and research activities having special facilities or knowledge required in deep ocean search operations.

This ad hoc organization worked exceedingly well. The Task Group Commander of Captain rank was on the scene, usually aboard MIZAR. There was excellent liaison between the chairman of the Technical Advisory Group, the Chief of Naval Operations, and the Task Force Commander, resulting in an efficient decision making organization with the ability to act very quickly.

USNS MIZAR CHARACTERISTICS

MIZAR is a 3700 ton ice strengthened freighter (see Figure 1) modified for deep sea research. She displaces 3700 tons and is 268 feet long and 51 feet wide with a draft of 18 feet six inches.

Centerwell

The most unusual feature of the ship is a centerwell (see Figure 2) 22 feet fore and aft and 10 feet wide in the center of the ship. An elevator like structure operating on guide rails within the well permits lowering towed instruments through the center of the ship. This configuration has many advantages: (1) It permits launching in rough seas, (2) It permits maneuvering the ship without restriction, (3) It removes the accelerations due to roll and pitch from the tow

point, and (4) It permits housing the towed vehicle in an enclosed space where maintenance and equipment installation and removal can be carried out regardless of weather conditions.

Underwater Tracking Equipment

The second unusual feature in MIZAR is the Underwater Tracking Equipment (UTE). (See Figure 3) Three hydrophones are mounted on the ship's hull in the form of a 90 degree isocoles right triangle with 50 foot like sides. The triangle has its hypotenuse approximately parallel to the centerline and the other two sides roughly at 45 degrees to the centerline. A small digital computer controls the system automatically.

A sonar transponder is planted on the ocean floor in the area to be searched, and a second transponder is mounted on the submerged vehicle. In operation the fixed reference transponder is interrogated by a coded signal. The reply is received at each of the three hydrophones and from these arrival times the location of the transponder relative to the ship in three dimensions is computed and printed out by the computer (See Figure 4). Next, the submerged vehicle transponder is interrogated and its location relative to the ship is computed. A simple subtraction of these two numbers yields the location of the submerged vehicle relative to the bottom reference transponder. This entire process is repeated about twice each minute.

Some difficulty was experienced due to the narrow-beam pattern of the available hull mounted hydrophones in the first portions of the search. Later, a new hydrophone with a hemispherical beam pattern was obtained and used to replace the original units. After this change operations were satisfactorily carried out at ranges to about 3-1/2 miles in water over 10,000 feet deep. The position data under these conditions showed a scatter with a standard deviation of about 250 feet.

Satellite Navigation

The Underwater Tracking Equipment is a "relative" system. The SRN-9 Satellite Navigation System was used to obtain geodetic coordinates for the submerged reference.

The satellite system was the most accurate navigation system available in this area. It suffers from the fact that location data are available only during the passage of a satellite at an appropriate elevation. For this reason passes may be as much as six hours apart. The method used was to obtain the ship's position on each appropriate satellite pass and record the position of the ship relative to

the bottom transponder at that time. The final location of the bottom reference transponder was based on a total of 86 satellite passes. The scatter of these passes had a standard deviation of 1500 feet in the east-west direction and 1000 feet in the north-south direction.

Telemetry

During the search for THRESHER in 1963 and 1964 the operation of multiple sensors was difficult and ineffective due to telemetry difficulties. The long cable telemetry system reported at the Fifth Symposium on Military Oceanography by Buchanan and Isaacson was available for the SCORPION search. This system used a special filter design in a frequency division multiplex system and permitted simultaneous operation of all sensors and control function with a minimum of interference. Without this system the search time requirement would have been much greater.

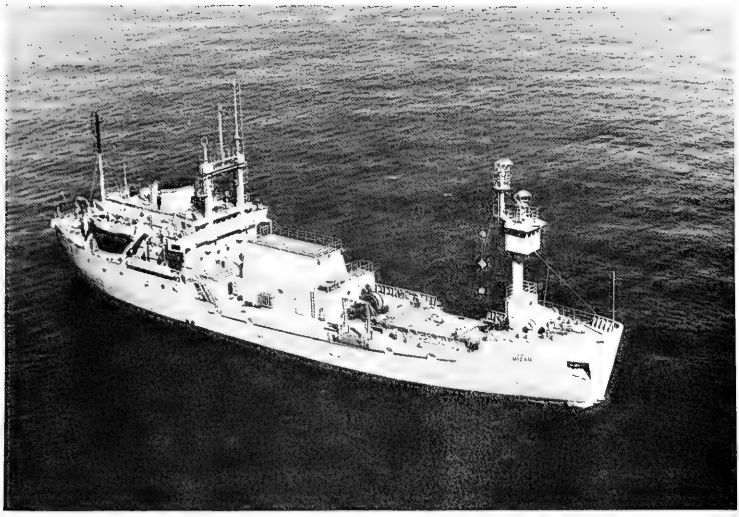

Figure 1. USNS MIZAR (T-AGOR-11)

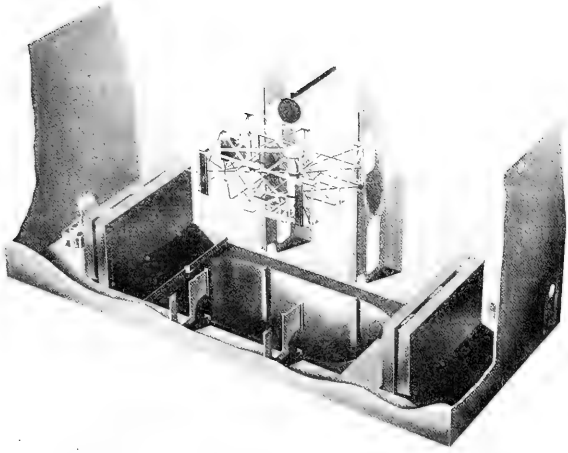

Figure 2. Center Well Launching Arrangement in MIZAR

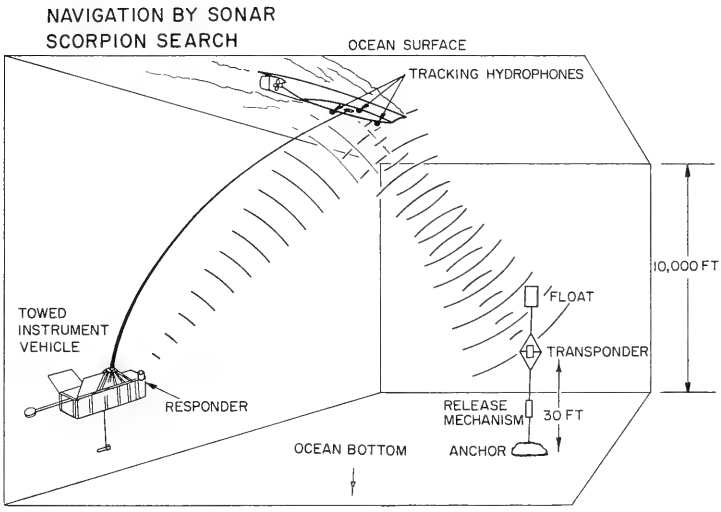

Figure 3. Underwater Tracking System in Mizar

TIME	DIST(N-S)	DIST(E-W)	DEPTH	IDEN
10 36 29	1059 N	416 E	8229	F
10 36 45	515 S	188 E	8260	T
	1574 N	228 E	- 31	F-T
10 37 21	1626 N	698 E	8121	F
10 37 37	386 S	7 E	8253	T
	2011 N	691 E	- 132	F-T
10 37 58	1395 N	525 E	8182	F
10 38 14	476 N	468 W	8181	T
	918 N	993 E	0	F-T
10 38 35	1353 N	403 E	8201	F
10 38 51	437 S	35 E	8262	T
	1790 N	368 E	- 62	F-T
10 39 12	1332 N	478 E	8207	F
10 39 28	301 S	59 E	8250	T
	1633 N	419 E	- 43	F-T
10 39 49	1635 N	349 E	8166	F
10 40 05	283 S	46 W	8249	T
	1918 N	395 E	- 84	F-T
10 40 58	1583 N	435 E	8182	F
10 41 13	163 S	128 W	8288	T
	1745 N	563 E	- 105	F-T

Figure 4. Underwater Tracking System Printout

A BRIEF SURVEY OF MILITARY OCEANOGRAPHY AT THE NATO SACLANT ASW RESEARCH CENTRE

Dr. Melbourne Briscoe
NATO SACLANT ASW Research Centre
La Spezia, Italy

The NATO SACLANT ASW Research Centre is located in La Spezia, Italy, on the coast of the Mediterranean about 120 km south of Genova. The staff is international, there now being scientists from 13 of the 15 NATO countries, totalling about 50 scientists with about 150 support personnel; this does not include the crew of our research vessel the MARIA PAOLINA G., a converted 2000 gross ton merchant ship. There are normally nine U.S. scientists attached to SACLANTCEN, the quota being established by the U.S.; they are distributed throughout the working groups of Oceanography, Sound Propagation, Target Classification, Operations Research, and Theoretical Studies. We all live and work in relative harmony, enthusiasm, and co-operation, especially considering the two languages of Italian and English that are normally used, plus the German, French, and especially American that seems to get everyone so confused!

Our assignment is to provide scientific assistance to the ASW efforts of the NATO countries. It is sometimes difficult to find an appropriate operating slot in the middle of the multiple-overlapping of the programs of the various countries, but this has been our goal. This paper is not a report on all the work of the Centre*, nor even on all the work of the Oceanography Group, but an attempt to tell you what we have done and what we are thinking of doing in the context of multiship, military oceanography. We call cruises to this end MILOC surveys.

In 1964 we planned and participated in a cruise involving several ships and airplanes between ocean stations KILO and JULIET in the eastern Atlantic just west of Ireland. The bathythermograph data from the cruise and much of the BT data on our later cruises have been subjected [Ref. 3] to what we call a three-line analysis [Fig. 1]. This simply means that the BT trace

* More complete information is available in References 1 and 2.

has undergone a least-squares fit of three straight lines in an attempt to define the temperature structure of the surface-layer, thermocline, and lower waters in a mechanized and unambiguous way.

During a traverse from KILO to JULIET, we took BT's each thirty minutes and performed the three-line analysis of each BT trace. Figure 1 shows the traverse in "BT space". The results were plotted [Fig. 2] in Ref. 4 versus an ASWEPS-type forecast of the area, and versus a simple climatological forecast from H.O. Pub. 761. The results in Fig. 2 for layer depth show that the climatological forecast is as good, or better, than the ASWEPS-type forecast. I must emphasize that these results were for the cooling season (the cruise was in September) and cannot be extrapolated or particularly interpreted in terms of other seasons without a much better basic understanding of the mechanisms involved.

One phase of MILOC 64 consisted of two ships, side-by-side, twelve nautical miles apart, traversing from KILO to JULIET and taking synoptic sea-surface temperature and BT's each thirty minutes [Fig. 3]. The SST's were plotted against each other to establish the coherence of the two sets of measurements and the coherence was, indeed, quite good. The two sets of BT's were put through our three-line-analyses, and the layer depth was plotted [Fig. 4] again to establish the coherence. The results were not encouraging in the least; it appears that, although a sideways extrapolation of SST for twelve nautical miles is appropriate, it would not be prudent to expect a twelve-mile extrapolation of layer depth to be too meaningful. If we want to use airborne measurements of SST to infer layer depth, it appears that the correlation of SST and layer depth is not certain. Again, I must emphasize that these conclusions apply to this region (KILO to JULIET) in this season (September).

The MILOC's in 1965 and 1966 were at the same location and were similar to that in 1964, but were in the heating season and with the addition of much more meteorology and a more sophisticated approach to the problem of spatial variability. In MILOC 65 we again traversed KILO to JULIET and subjected the BT's obtained to the three-line analyses. The resulting layer depths and first-layer gradients were plotted [Fig. 5] on a typical range-prediction chart in a frequency-of-

occurrence presentation*. Although MILOC 65 was in the heating season (July), the strong winds that prevailed should have caused strong mixing and, hence, nearly isothermal water. We certainly expected a lot of data to yield a sound-velocity gradient indicative of isothermal water (the points on the right of Fig. 5), but we did not expect so much data to be indicative of non-isothermal water (the rest of the points). We are forced to conclude — for this location, in this season — that the variability of gradients is higher than expected and that the ranges of hull-mounted sonars — particularly those with high range capability — are very sensitive to the sound velocity gradient, always assuming that the underlying model for the propagation of sound in water is correct.

The MILOC 66 data have not yet been thought about enough for us to be able to deliver any conclusions. One of the interesting differences between MILOC 64 and MILOC 66 is that the traverse of two ships side-by-side from KILO to JULIET was repeated, but not at a constant lateral separation; the ships started 1.5 n.miles apart and gradually increased their separation. We are now looking at the data to discover if a horizontal coherence length exists for layer depth and layer gradient. We know from MILOC 64 that 12 n.miles is greater than the coherence length of layer depth and less than the coherence length of SST. We hope to find these coherence lengths more exactly with this new approach. Perhaps the presence of internal waves makes the hope for coherence a small hope**.

MILOC 67 was held in the Baltic Sea and was the start of our present air-sea interaction efforts. The cruise was organized by the Germans and the Danes and we have not yet seen any reduction of the general data. Our own meteorological experiments have been processed and reported [Ref. 5]; a somewhat dishearting result [Fig. 6] was that the wind profile measured on the ship and that measured simultaneously 100 m away on a buoy were not in good agreement. It is entirely possible that the air we

---

* No report on this work has been released.

** Note added in press: Preliminary analysis of these data indicates that 1 n.mile is greater than the coherence length for individual layer depth measurements, but that the mean values of layer depth at two points are coherent over much larger distances, e.g. 15 n.miles.

measured at the ship was air that was closer to the sea surface at the buoy location and had risen to pass over the ship. If this is so — and we have no reason to think otherwise — then to obtain accurate wind profiles we must use data measured only on buoys and preferably with sensors at three heights; two heights yield the typical logarithmic profile and the third height yields a check point on the curvature.

From this experience in MILOC 67, we designed a new meteorological buoy [Fig. 7] for use in the Ionian Sea in MILOC 68 [Fig. 8]. The meteorological buoy was built with sensors for wind speed and dry and wet-bulb temperatures at 2 m, 4 m and 8 m above the nominal-mean sea-surface.

A major part of MILOC 68 was an experiment to measure the turbulent diffusion processes in the surface waters. For this we built six large drogues [Fig. 9] which were installed in the water and allowed to drift freely for several weeks. It is supposed that their motion is determined almost exclusively by the surface currents since their size below the surface was 16 m^2 and only a radar reflector showed above surface. They were tracked by the several ships involved in MILOC 68 and hourly reports on the position of everything were transmitted to the MARIA PAOLINA G. A picture of the motion of two of the drogues [Fig. 10] shows the very random and turbulent motion during a six-day period; if one knew only that a certain mass of water at the starting position had arrived at the recovery position six days later, very likely the inference as to water-mass speed, location, and direction at any one of the intervening days would be in error.

Attached to four of the drogues were 60-m long thermistor chains containing 21 thermistors spaced along the length. A typical output [Fig. 11] from the meteorological equipment on the MARIA PAOLINA G. gives wind and radiation data "synoptically" with the distribution of subsurface temperatures from one of the drogues; the ship was near to, but not coincident with, the drogue. One can observe the thermocline moving about in response to changes in wind stress and solar radiation. There is also an internal-wave structure that appears to end a day or so after a period of high winds has ended. We will continue this type of work.

Perhaps I should mention that there is ART data available to cover the drogue locations during the period of their drifting, so that we can estimate whether the surface temperatures were drifting in the same way as were the surface velocities.

We have some other data on internal waves [Refs. 6 and 7] that were taken in the Strait of Gibraltar [Fig. 12]. A thermistor chain and recording system [Fig. 13] were hung from an anchored sub-surface buoy, instead of from a surface buoy, in an attempt to eliminate the effects of surface waves. The very nice data obtained [Fig. 14] shows a very clear thermocline that is destroyed by internal waves and more or less re-established at a new depth only 100 minutes later. These quickly starting and quickly stopping internal waves do not exactly fit the classical picture of progressive waves! Just what picture they <u>do</u> fit is not yet clear, but at least the data necessary to provide the picture are beginning to accumulate*.

Looking backwards at these five MILOC's, we feel that much information and experience has been obtained, particularly when the cruise was designed with a specific or operational goal in mind, and it seems to us that the scientific goals have inspired more interest, co-operation, preplanning, and postprocessing speed than have the operational goals. (In this context an operational goal might be, for example, the hydrographic surveying of a particular region for classic purposes and by classic methods).

We want our MILOC's to be relevant to our mission as a research center and to our multinational sponsorship, and we want our MILOC's to be successful — that is, we wish to plan a MILOC with a specific goal as its reason for being, and we want that goal to be relevant to the ASW problems that are the reason for our existence.

To further this end, the Director of SACLANTCEN has initiated a study exercise that is designed to re-assess the nature of the environmental problems related to sonar performance, to up-date our philosophics if need be, and

---

* See also Ref. 8 for some interesting looks at sound velocity profiles and ray tracing diagrams through internal waves.

specifically to relate oceanographic research projects to the potential gain in the performance of sonar systems, both present and future.

If one were to try to draw up a list [Fig. 15] of all possible sonar systems, one possible approach would be to define a "system" as a combination of platform and sound channel. For example, in deep water a submarine using a convergence-zone mode would be a feasible system, but the same system would be unlikely in shallow water. Using this classification scheme — not a unique approach, only convenient — one obtains for active* sonar 75 possible systems, of which thirty are likely to exist.

We also divided the possible environmental factors [Fig. 16] into those related to Transmission, Reverberation, and Ambient Noise. A more-or-less natural subdivision then occurs, for example, in breaking reverberation into boundary-caused, volume-caused, etc. Finally, a sub-subdivision into the oceanographic factors that one might study reveals enough factors to spend one's life pondering.

From the list of 30 sonar systems and 24 environmental factors we chose the prominent candidates and were then faced with having to define the "payoff" of this game — we decided to assess the importance of a particular environmental parameter on a particular sonar system in terms of the potential benefit to the system likely to be provided by increased knowledge of that parameter.

For existing sonar systems, the potential benefits are primarily in helping us to understand the various causes of signal degradation, but for future systems improved knowledge of the environment might help us to optimize the design characteristics. For a simple example, improved knowledge of absorption will not help us with our present systems, but if there were some "closed door" of strong absorption at, say, a particular frequency, then we could possibly design a new sonar to ignore that "closed door".

Note that the presentation here does not use any weighting factors to reflect the relative effectiveness or popularity of the various sonar systems. This is, instead, an attempt to look at the effect of environmental studies on the whole sonar complex and not to tie

---

* Note the following discussion is only for active systems.

ourselves to one kind of concept.

The picture that emerges for our current sonar systems [Fig. 17] is the importance of the sound velocity structure (including microstructure), the sea surface, and the deep scattering layer. Next in importance — and in first place if you are a shallow-water person — is the sea bottom. For future systems [Fig. 18] the sea surface becomes prominent, with sound velocity structure and the DSL still ranking. Once again the sea bottom assumes a greater role in shallow water.

These results are not surprising, but they are not obvious either. One tends to think of the sea surface as something rather awkward and distasteful, but the sum of these two pictures (present and future) reveals that an increased knowledge of the surface characteristics should be one of our major research projects.

In the context of the importance of sound velocity structure, it is felt that a major problem aside from the microstructure is the spatial variability: what are the space scales over which an on-the-spot profile can be considered representative? During MILOC 68 we took many temperature-depth-salinity* profiles with our quick-response electronic profiler and were overwhelmed with the time and space variations observed.

The medium we are studying and the reasons for doing it are complex. MILOC surveys and the program of the SACLANTCEN Oceanography Group are an attempt to match priorities to projects and thereby more effectively study the environment.

---

* Parenthetically, it is interesting to explain why we refer to a "TDS" system instead of the more common "STD" terminology: for the non-English speaking tongue, TDS is easier to say. In fact, it is easier to say for the English-speaking person also, once you get started on it.

REFERENCES

1. "The SACLANT ASW Research Centre". A brochure on SACLANTCEN available on request from the Director SACLANT ASW Research Centre, APO 09019, New York, N.Y.

2. "Bibliography of Unclassified Technical Reports and Technical Memoranda" (with abstracts). Available on request from SACLANT ASW Research Centre, APO 09019, New York, N.Y.

3. J. Caperon, B. Schipmolder, and W. Harwood, "Three-line Analysis of Bathythermographs" SACLANTCEN Technical Report 107, March 1968, NATO UNCLASSIFIED.

4. A. Dahme, "Study of the Oceanography of the Upper Layer in the N.E. Atlantic: MILOC 64 Data - Phase A" SACLANTCEN Technical Report 52, November 1965, NATO UNCLASSIFIED

5. R. Pesaresi, "Meteorological Data of the MILOC-BALTIC 1967 Cruise", SACLANTCEN Technical Report 125, October 1968, NATO UNCLASSIFIED.

6. J. Ziegenbein, "A Study of Internal Waves in the Strait of Gibraltar during October-November 1967", SACLANTCEN Technical Report 127, November 1968, NATO UNCLASSIFIED.

7. J. Ziegenbein, "Spatial Observations of Internal Waves in the Strait of Gibraltar", SACLANTCEN Technical Report 147, June 1969, NATO UNCLASSIFIED.

8. T.D. Allan, "Observed Sound Velocity and Temperature Profiles in the Strait of Gibraltar during the Passage of an Internal Wave", SACLANTCEN Technical Report 66, October 1966, NATO UNCLASSIFIED

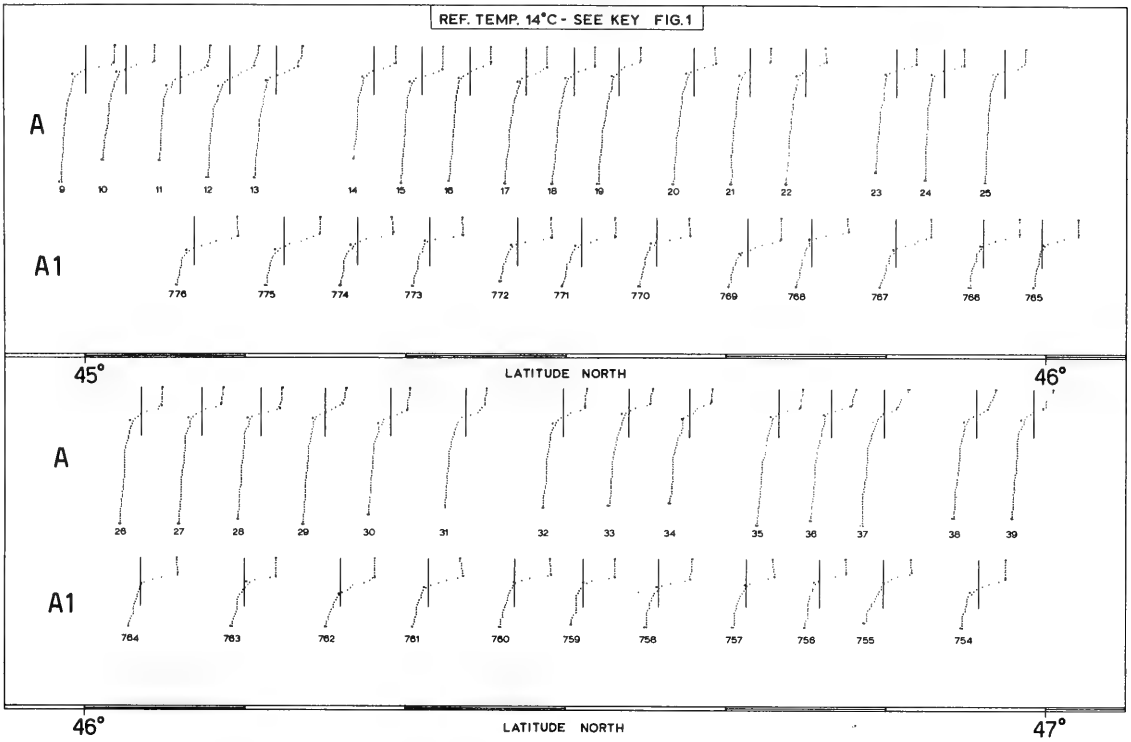
REF. TEMP. 14°C - SEE KEY FIG.1
A
9 10 11 12 13 14 15 16 17 18 19 20 21 22 23 24 25
A1
776 775 774 773 772 771 770 769 768 767 766 765
45°
LATITUDE NORTH
46°
A
26 27 28 29 30 31 32 33 34 35 36 37 38 39
A1
764 763 762 761 760 759 758 757 756 755 754
46°
LATITUDE NORTH
47°

Figure 1.

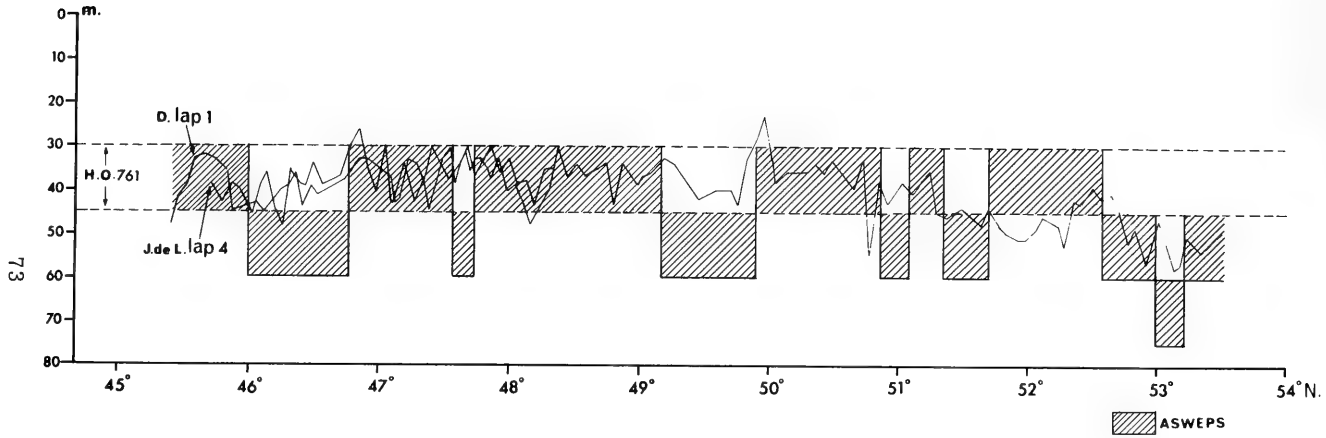

COMPARISON OF LAYER DEPTH AS STATED BY PASWEPS AND H.O.761, AND AS MEASURED BY DALRYMPLE (LAP 1) AND J. DE LISBOA (LAP 4)

Figure 2.

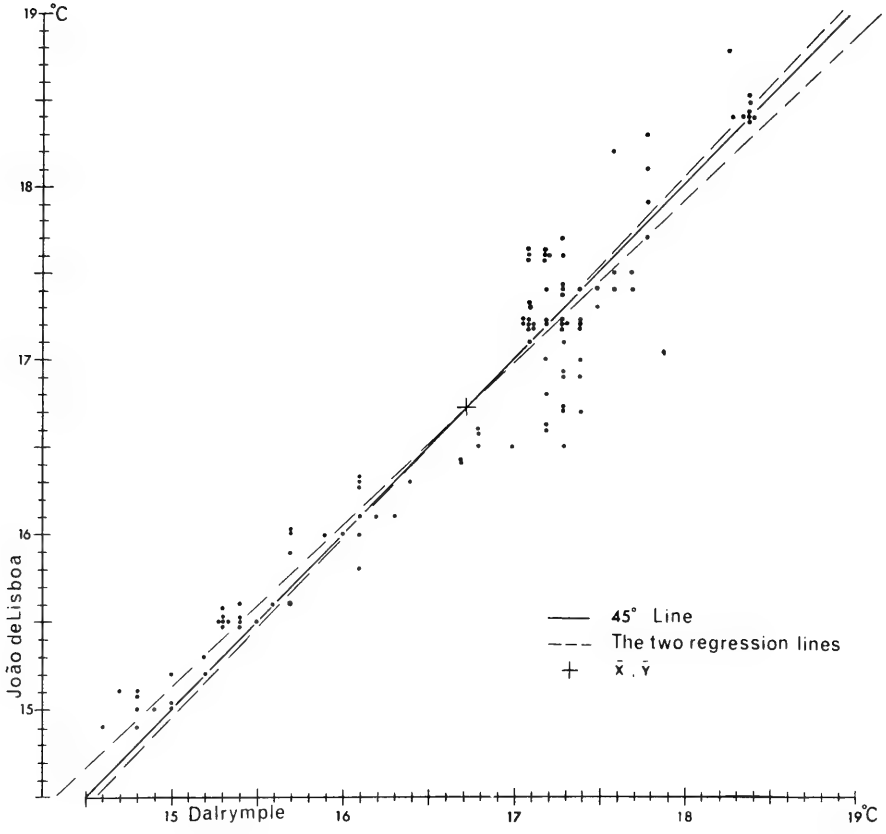
19 °C
18
17
16
15
João de Lisboa
15 Dalrymple
16
17
18
19°C
45° Line
The two regression lines
x̄ , ȳ

Figure 3.

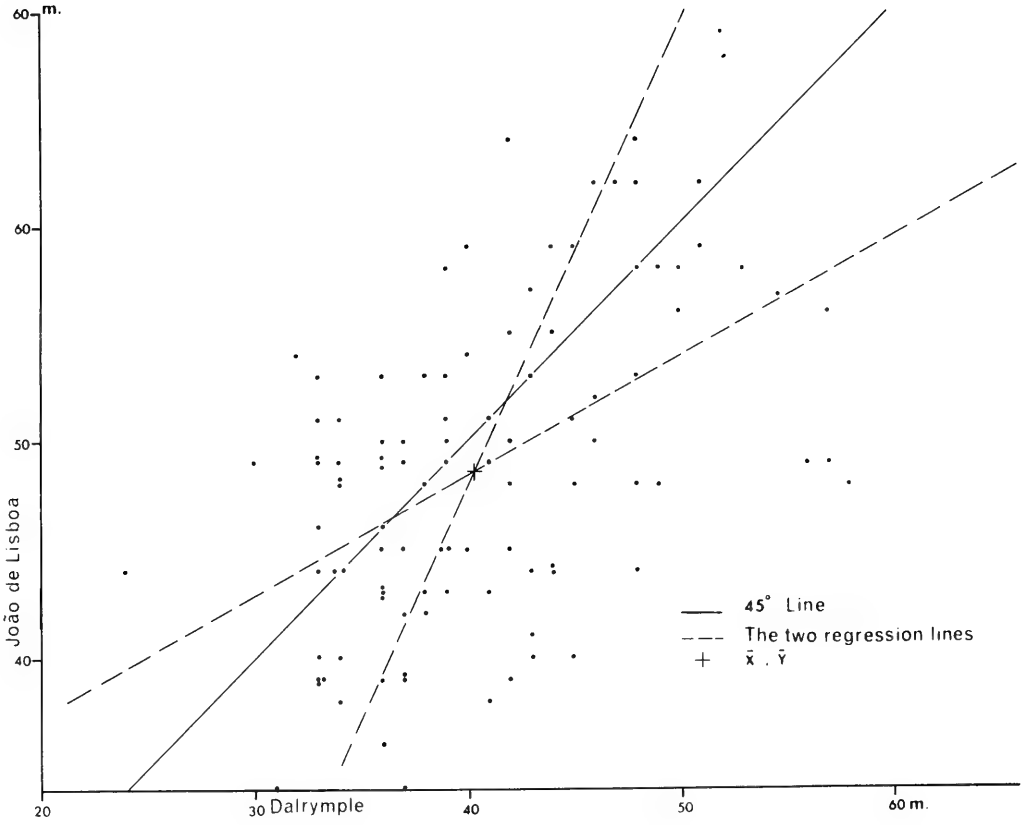
m.
60
60
50
40
João de Lisboa
20
30 Dalrymple
40
50
60 m.
45° Line
The two regression lines
x̄ . ȳ

Figure 4.

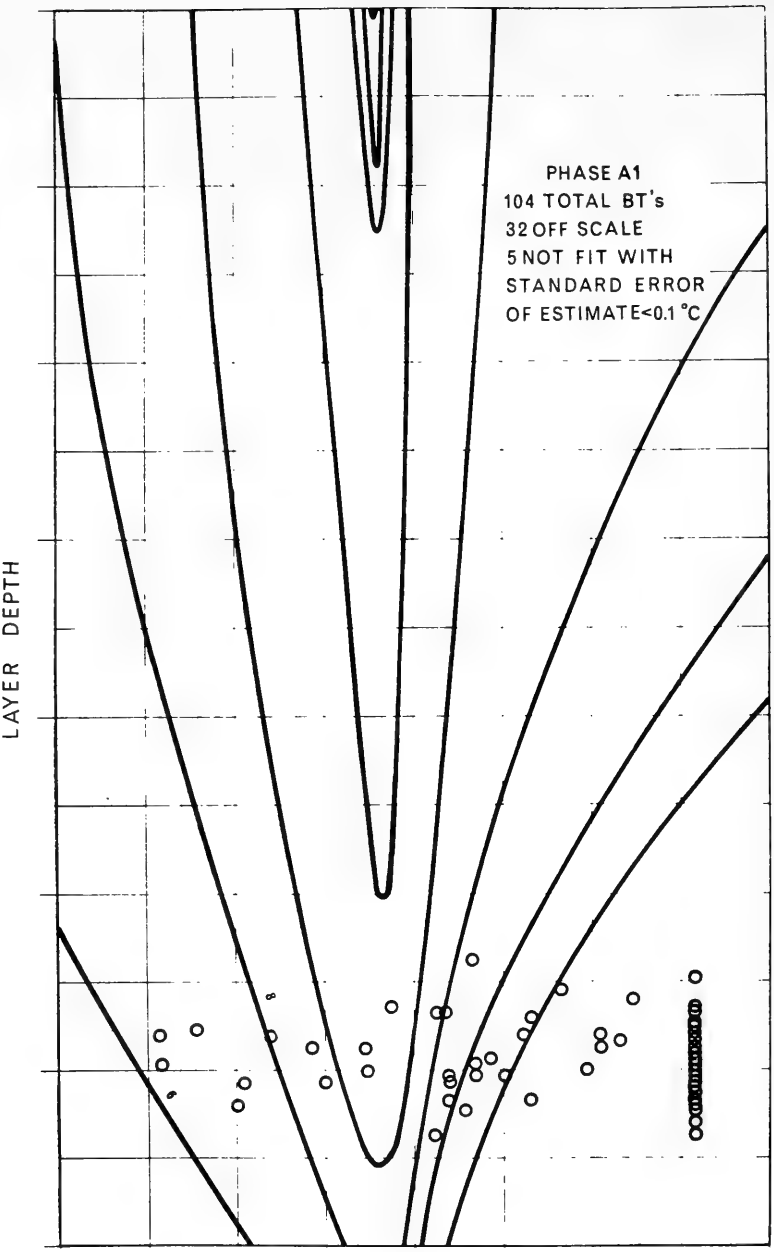
PHASE A1
104 TOTAL BT's
32 OFF SCALE
5 NOT FIT WITH
STANDARD ERROR
OF ESTIMATE<0.1 °C
LAYER DEPTH
SOUND VELOCITY GRADIENT

Figure 5.

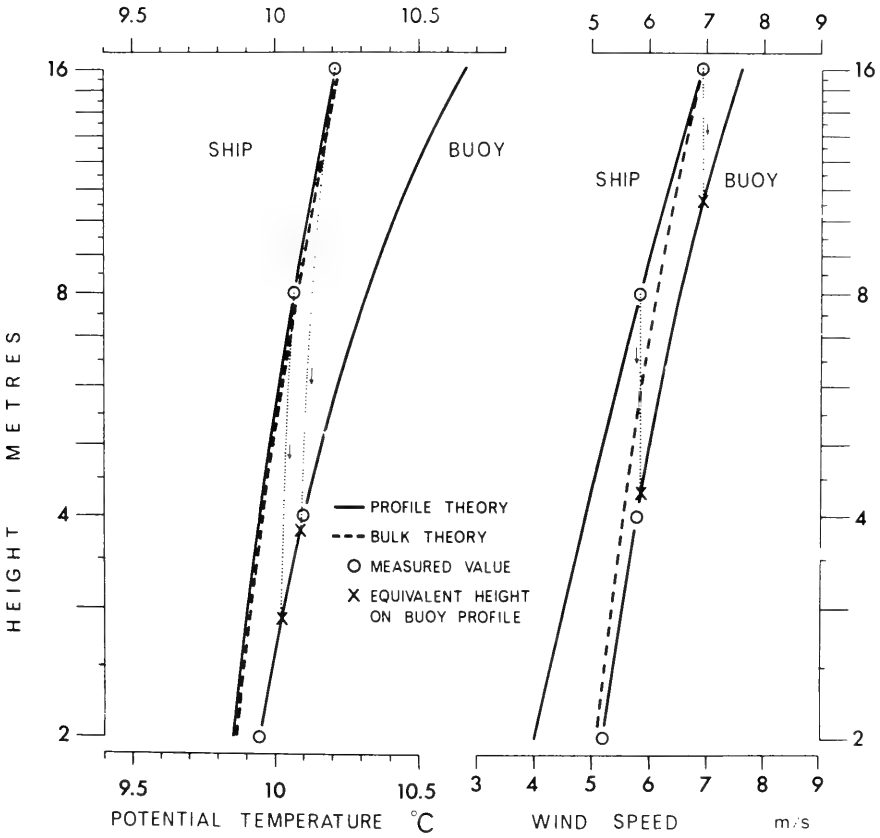
9.5
10
10.5
16
8
4
2
SHIP
BUOY
PROFILE THEORY
BULK THEORY
MEASURED VALUE
EQUIVALENT HEIGHT ON BUOY PROFILE
HEIGHT METRES
9.5
10
10.5
POTENTIAL TEMPERATURE °C
5
6
7
8
9
SHIP
BUOY
3
4
5
6
7
8
9
WIND SPEED m/s

Figure 6.

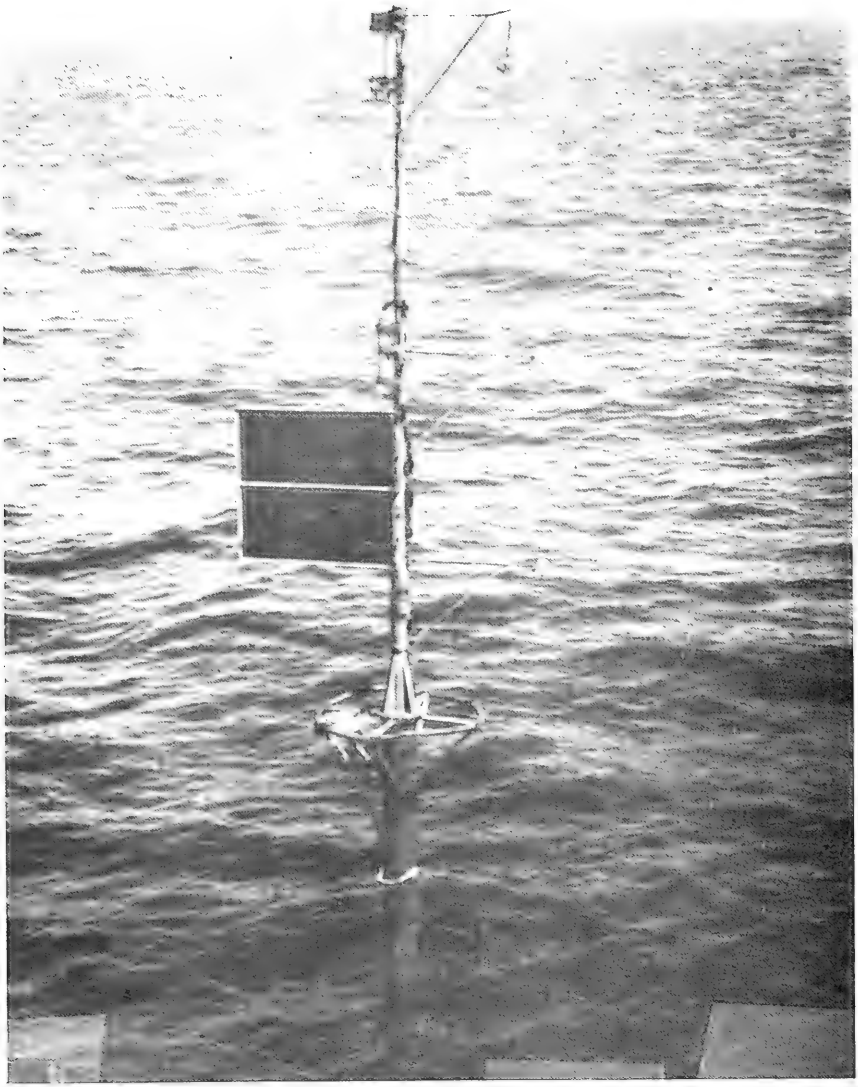

Figure 7.

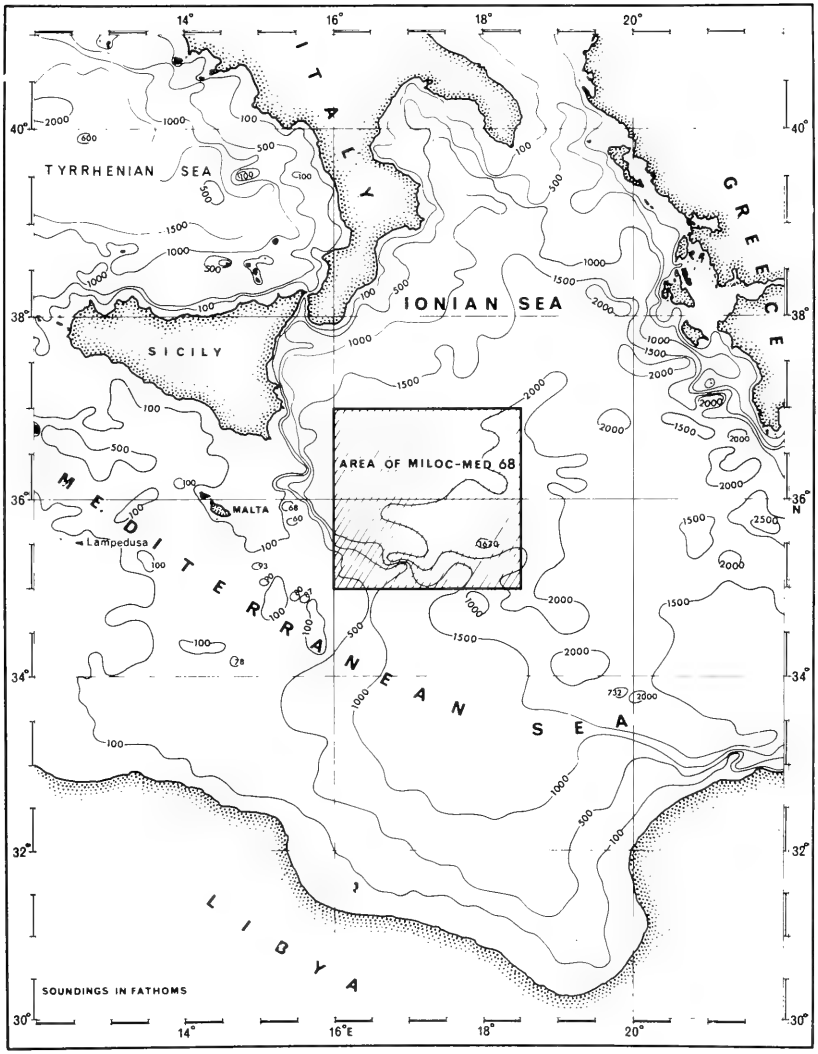
14°
16°
18°
20°
40°
38°
36°
34°
32°
30°
ITALY
GREECE
TYRRHENIAN SEA
IONIAN SEA
SICILY
AREA OF MILOC-MED 68
MALTA
Lampedusa
MEDITERRANEAN SEA
LIBYA
SOUNDINGS IN FATHOMS
16°E

Figure 8.

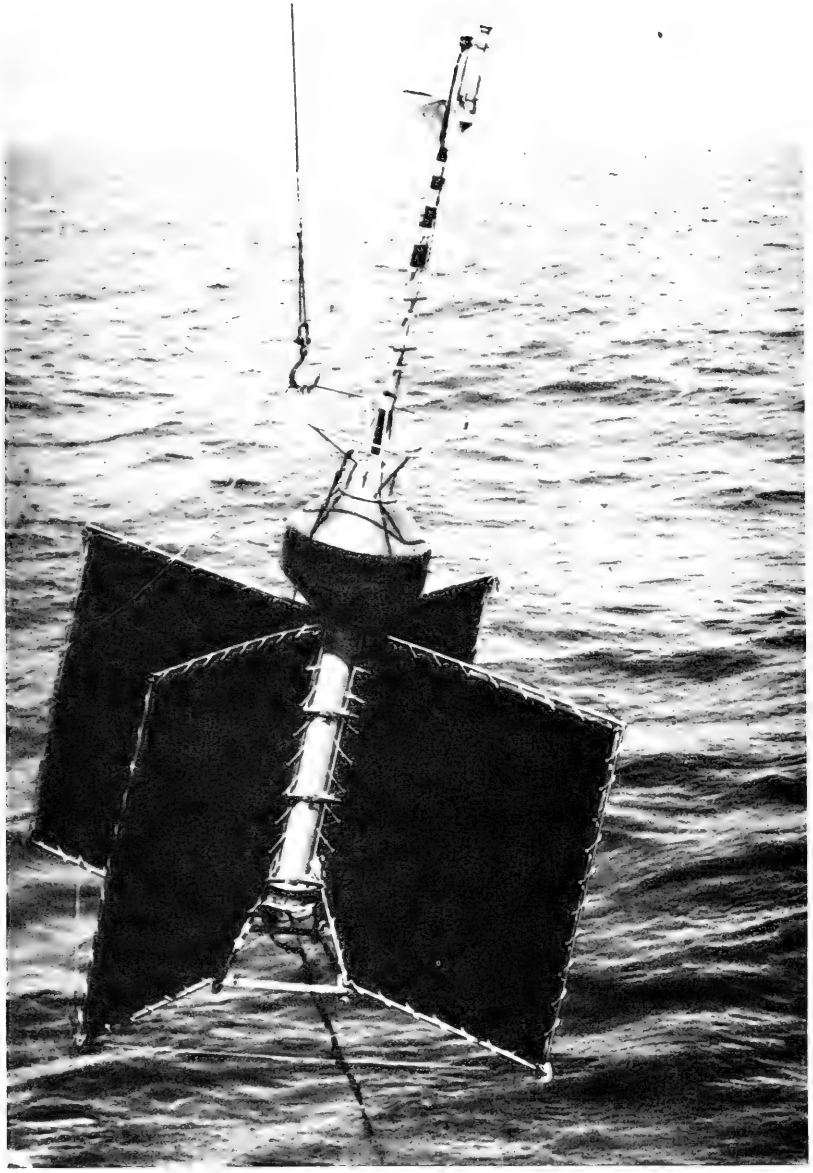

Figure 9.

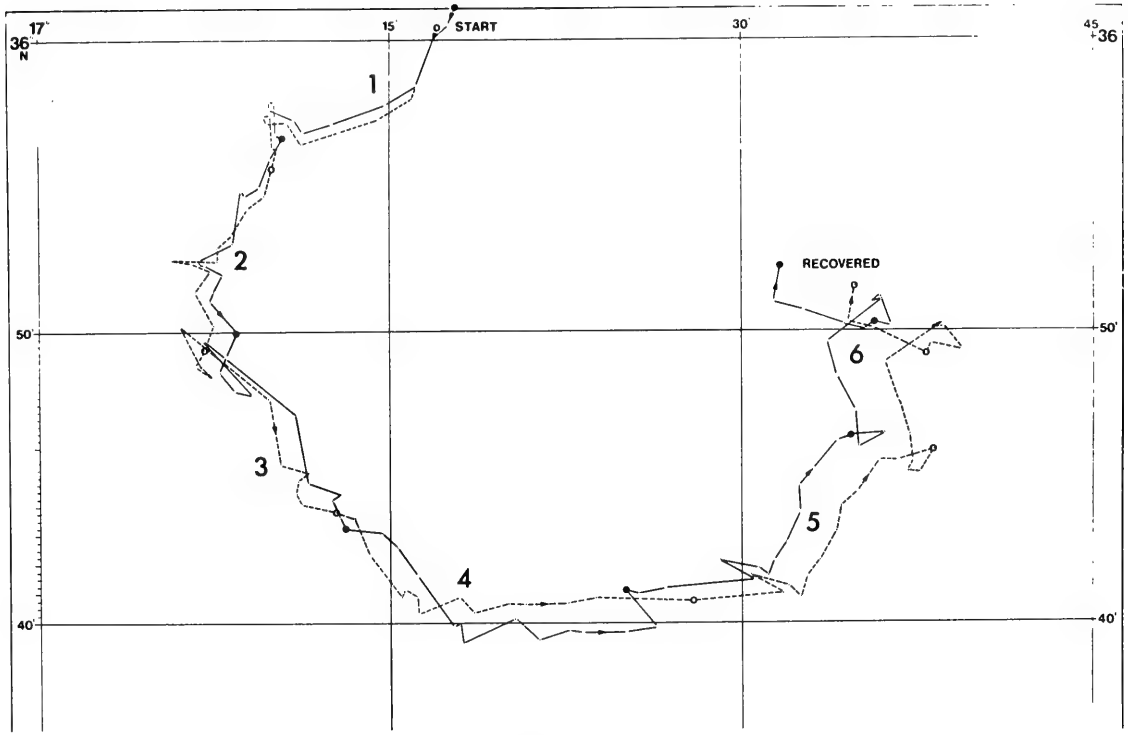

Figure 10.

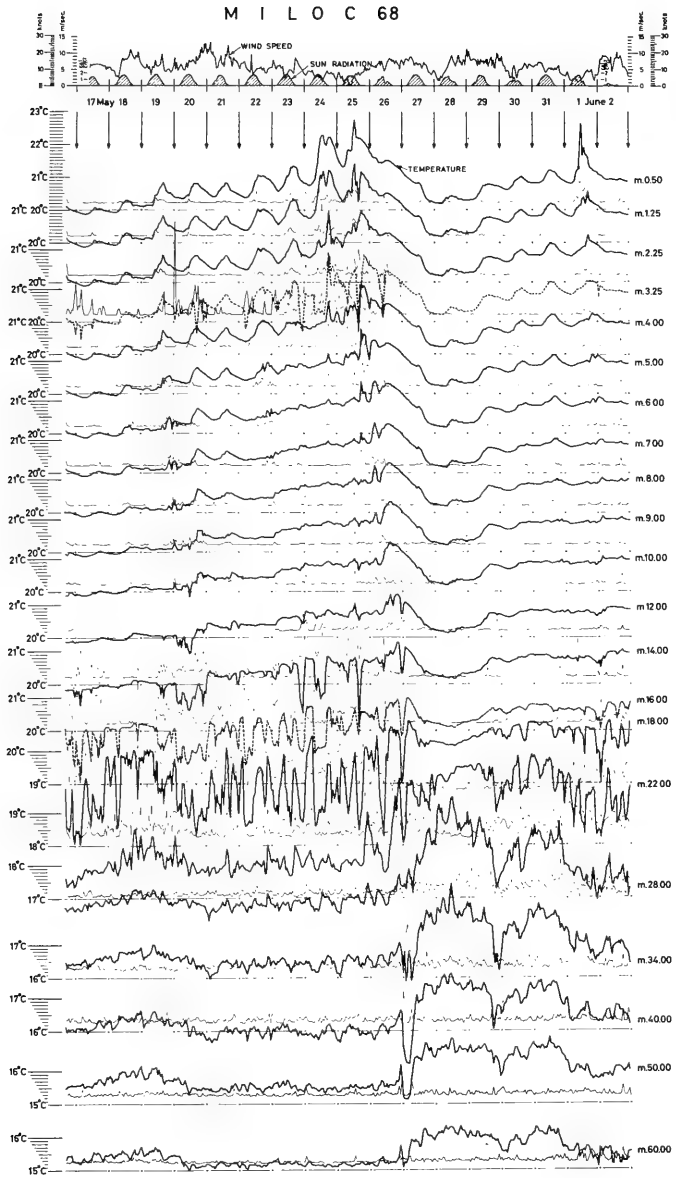
M I L O C 68
WIND SPEED
SUN RADIATION
17 May 18 19 20 21 22 23 24 25 26 27 28 29 30 31 1 June 2
TEMPERATURE
m.0.50
m.1.25
m.2.25
m.3.25
m.4.00
m.5.00
m.6.00
m.7.00
m.8.00
m.9.00
m.10.00
m.12.00
m.14.00
m.16.00
m.18.00
m.22.00
m.28.00
m.34.00
m.40.00
m.50.00
m.60.00

Figure 11.

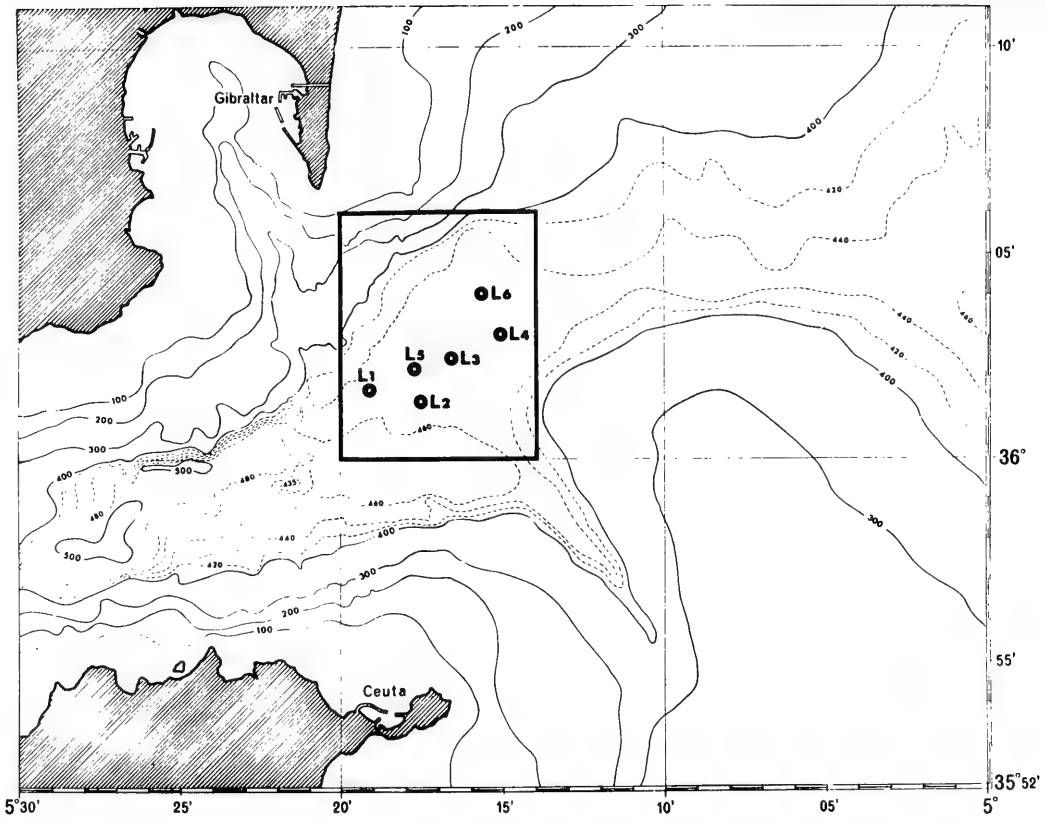
Gibraltar
Ceuta
L1
L2
L3
L4
L5
L6
100
200
300
400
420
440
460
480
500
10'
05'
36°
55'
35°52'
5°30'
25'
20'
15'
10'
05'
5°

Figure 12.

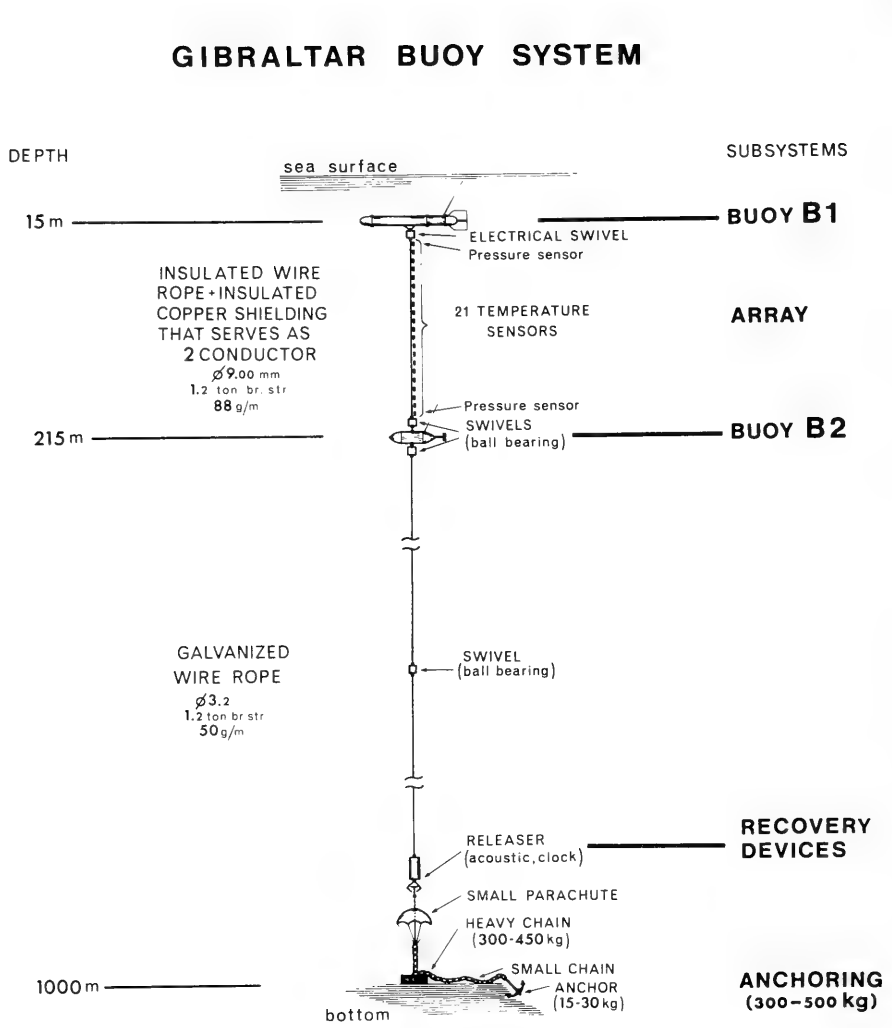
GIBRALTAR BUOY SYSTEM
DEPTH
SUBSYSTEMS
sea surface
15 m
BUOY B1
ELECTRICAL SWIVEL
Pressure sensor
INSULATED WIRE ROPE+INSULATED COPPER SHIELDING THAT SERVES AS 2 CONDUCTOR
ø9.00 mm
1.2 ton br. str
88 g/m
21 TEMPERATURE SENSORS
ARRAY
Pressure sensor
215 m
SWIVELS (ball bearing)
BUOY B2
GALVANIZED WIRE ROPE
ø3.2
1.2 ton br str
50 g/m
SWIVEL (ball bearing)
RELEASER (acoustic, clock)
RECOVERY DEVICES
SMALL PARACHUTE
HEAVY CHAIN (300-450 kg)
SMALL CHAIN
1000 m
ANCHOR (15-30 kg)
ANCHORING (300-500 kg)
bottom

Figure 13.

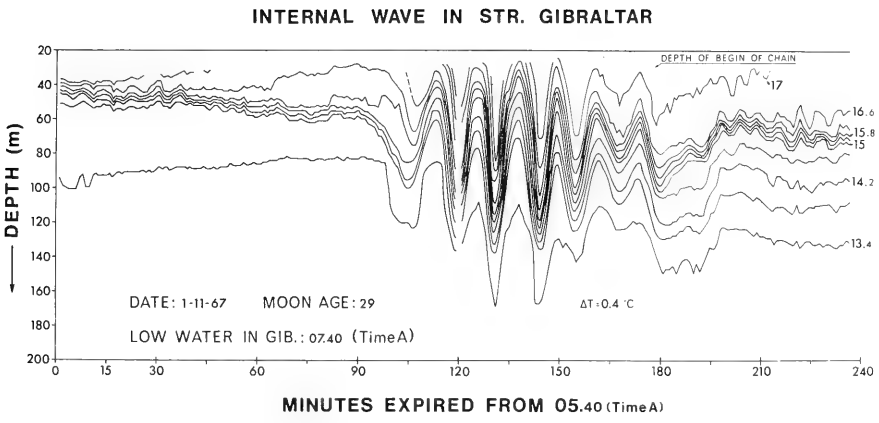

Figure 14.

A C T I V E

PROVINCE	DEEP WATER					CONTINENTAL SLOPE					SHALLOW WATER				
PLATFORM / CHANNEL	SHIP	SUB	HEL	BUOY	BOTTOM ARRAY	SHIP	SUB	HEL	BUOY	BOTTOM ARRAY	SHIP	SUB	HEL	BUOY	BOTTOM ARRAY
SURFACE DUCT	1	1	1	1	0	1	1	1	1	0	1	1	1	1	0
BELOW LAYER	1	1	1	1	0	1	1	1	1	0	1	1	1	1	1
BOTTOM BOUNCE	1	1	0	0	0	0	0	0	0	0	0	0	0	0	0
CONVERGENCE	1	1	0	0	0	0	0	0	0	0	0	0	0	0	0
RAP	1	0	0	?	0	0	0	0	0	0	0	0	0	0	0

30 from 75

Figure 15.

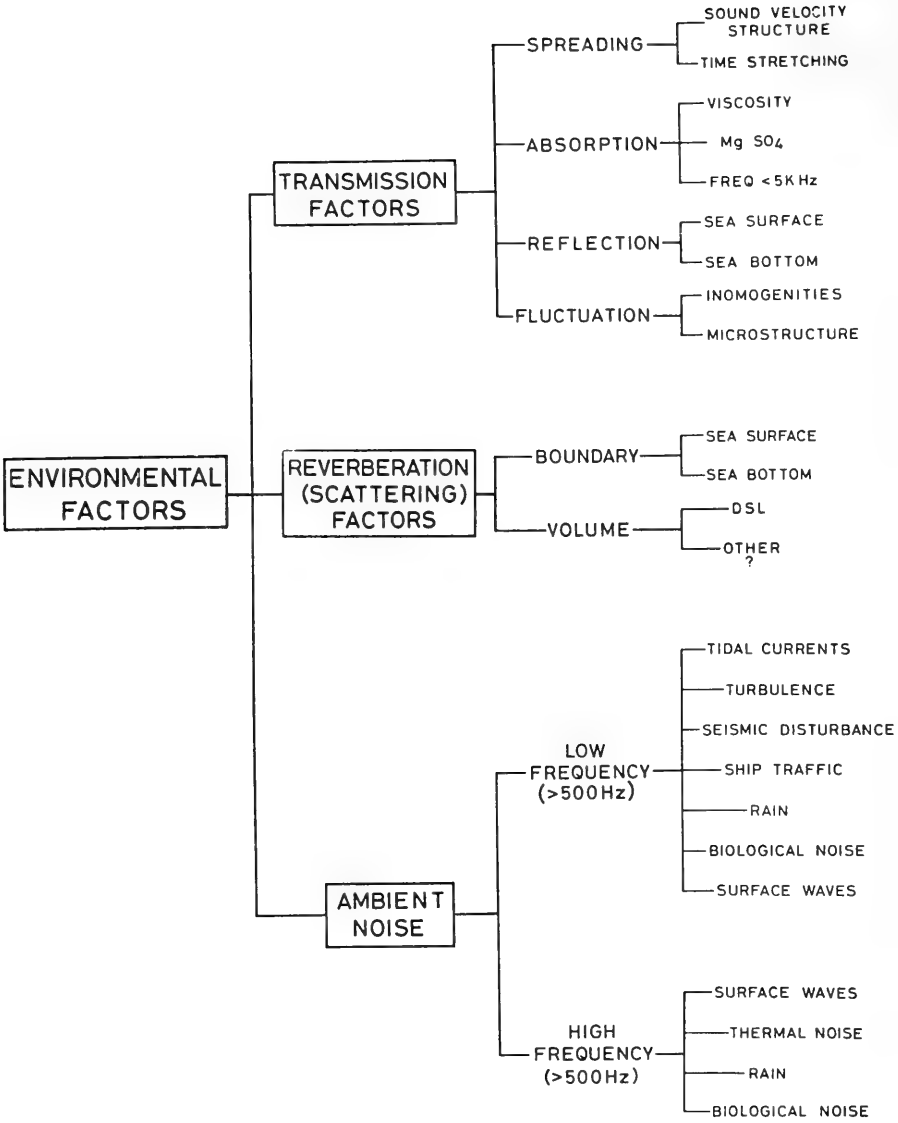
ENVIRONMENTAL FACTORS
TRANSMISSION FACTORS
SPREADING
SOUND VELOCITY STRUCTURE
TIME STRETCHING
ABSORPTION
VISCOSITY
Mg SO4
FREQ < 5K Hz
REFLECTION
SEA SURFACE
SEA BOTTOM
FLUCTUATION
INOMOGENITIES
MICROSTRUCTURE
REVERBERATION (SCATTERING) FACTORS
BOUNDARY
SEA SURFACE
SEA BOTTOM
VOLUME
DSL
OTHER ?
AMBIENT NOISE
LOW FREQUENCY (>500Hz)
TIDAL CURRENTS
TURBULENCE
SEISMIC DISTURBANCE
SHIP TRAFFIC
RAIN
BIOLOGICAL NOISE
SURFACE WAVES
HIGH FREQUENCY (>500Hz)
SURFACE WAVES
THERMAL NOISE
RAIN
BIOLOGICAL NOISE

Figure 16.

POTENTIAL BENEFITS OF IMPROVED KNOWLEDGE

PRESENT

SONAR SYSTEM								
ENVIRON. FACTOR	BB	RAP	CZ	DEEP WATER			SHALLOW	TOTAL
				ABOVE THERMOCLINE	IN THERMOCLINE	BELOW THERMOCLINE		
ABSORPTION	0	0	0	0	0	0	0	0
AMBIENT NOISE	0	0 2	0	0	0	0	0	0* 2
SEA SURFACE	1	1	1	1	1	1	1	7
SEA BOTTOM	2	0	0	0	0	0	2	4
DSL	1	2	1	1	1	1	1	8
SOUND VEL. STRUCTURE	0	1	1	2	2	2	1	9

0 - Little
1 - Moderate
2 - Great

*Only if platform moving, otherwise 2

Figure 17.

POTENTIAL BENEFITS OF IMPROVED KNOWLEDGE

FUTURE

SONAR SYSTEM								
ENVIRON. FACTOR	BB	RAP	CZ	DEEP WATER			SHALLOW	TOTAL
				ABOVE THERMOCLINE	IN THERMOCLINE	BELOW THERMOCLINE		
ABSORPTION	1	2	2	0	0	0	0	5
AMBIENT NOISE	0	0 2	0	0	0	0 2	0 1	0* 5
SEA SURFACE	2	2	2	2	2	2	2	14
SEA BOTTOM	2	1	0	0	0	0	2	5
DSL	1	2	2	1	2	2	1	11
SOUND VEL. STRUCTURE	1	1	1	2	2	2	2	11

0 - Little
1 - Moderate
2 - Great

*Only if platform moving otherwise the higher figure.

Figure 18.

OCEAN TECHNOLOGY DEFICIENCIES

Duane U. Beving, LCDR, USN
Project Officer for Non-Combatant Vehicles and Safety Certification

Neil T. Monney, LCDR, USN
Project Officer for Sea Floor Engineering and
Deep Ocean Test Facilities

Ocean Engineering Branch
H.Q. Naval Material Command
Washington, D.C.

It is well recognized that, in order to provide the required ocean engineering capabilities such as search, rescue, salvage and seafloor construction, the first step in the capability development cycle is to build a broad base of effective technologies. A program to advance fundamental technology is necessary for developing elements and processes that can be combined into useful ocean components, subsystems and systems. The Advanced Sea-Based Deterrence Study of 1964 recommended programs of research and development which were considered necessary to guarantee the availability of technology options for the acquisition of future deterrence systems. The 10 broad functional areas immediately following are primarily an outgrowth of the Seabed and earlier strategic studies which identified the need for a technology base to support future Navy missions. Deficiencies in these areas have been identified in the Navy's Deep Ocean Technology (DOT) Project and are recognized throughout the Navy and in industry.

10 Functional Areas

1. Energy Sources and Conversion (Power)
2. Materials and Structural Analysis
3. Electrical, Mechanical and Fluid Systems (Auxiliary Systems)
4. Oceonics
5. Swimmer/Diver Systems
6. Bio-Medicine
7. Sea Floor Engineering
8. Environmental Support
9. Test Facilities
10. Non-Combatant Vehicles

Also, studies conducted by the National Academy of Engineers (NAE) and the National Academy of Science (NAS) and the recent report of the Commission on Marine Science, Engineering and Resources, entitled Our Nation and The Sea, reflect the need for a sound technology base. Elimination of technology deficiencies within these 10 broad functional areas is not only required for putting a vehicle at 20,000 ft. or man at 2,000 ft., but is also necessary to make work in the ocean at much lesser depths more effective.

Even though technical deficiencies in these areas are well recognized, the Navy programs to eliminate them and to improve our technology base are not entirely adequate. The reasons why our R&D programs are not adequately addressing these functional areas are many. Perhaps more often than is actually the case we hear the words "funding limitations" and "budget cuts" given as the reasons for not pursuing development more vigorously in certain areas. However, programs to improve and advance our technology base often suffer because technology development by itself offers little visibility to the developing agency. For this reason, laboratories have a tendency to put their resources toward a system or even a capability development without first mastering the technologies that are required to build an effective capability. The laboratory may also put emphasis on a project because it is intriguing and offers visibility, but may result in limited benefit to the Navy when compared to other problems that require solving.

Efforts to eliminate these technical deficiencies are being carried out in Exploratory Development programs, the Bio-Medical program, the DOT project, and in cases where the deficiencies limit hardware development, in the projects which are developing systems capability. Technology deficiencies in each of the 10 functional areas will briefly be discussed in the following text.

Power

Power has been identified as one of the critical restraints in deep ocean systems. In the area of power sources endurance, reliability and high energy per unit weight and volume are primary requisites for a wide variety of undersea applications. At present, the lead acid and the silver zinc batteries represent the only available proved power sources for the near term submersible design. Batteries have been a primary energy source because of their relatively low cost, reliability and adaptability to submerged operations. However, they are more frequently recognized by the severe weight, space and endurance penalties they impose on small vehicles.

In small power sources we have a very low level of effort. We are evaluating existing radioisotope thermoelectric generators in coordination with the AEC. Attempts to increase the cyclic efficiency of silver zinc batteries are also being investigated.

In the medium power source range, the fuel cell appears essential to efficient undersea operations. The major effort just recently initiated is development of a fuel cell for the 20,000 foot Deep Submergence Search Vehicle. It is planned that this fuel cell will be modular and have the potential for wider application. A conservative estimate for the DSSV fuel cell development is about $10 million. Although this is not a small figure, it should be recognized that it would be much greater had it not been for the aerospace power needs. The impetus of the space race and the expenditure of over $100M has provided the Navy with a technology base from which fuel cell development for undersea power systems can proceed at lower costs and in a shorter time period than would otherwise be possible.

The potential of the thermal dynamic and chemical dynamic systems were recognized in the early 1950's. However, development efforts stopped about 1955 when the nuclear reactor development replaced this power concept. The thermal dynamic and chemical dynamic systems appear to have sufficient advantages and warrant renewed consideration as primary energy sources for medium range endurance (up to 30 days). At present, there is essentially no Navy development effort underway for such a system. It is considered that a development effort for this system should parallel that of the fuel cell. After about 2 years sufficient information should be available to compare it with the fuel cell and to justify further development and qualification as a primary energy source.

Recent studies conducted by the NAS concluded that undersea power cable technology is relatively well developed and available to the Navy. Therefore, to achieve a land link capability, no additional development effort appears warranted in this area except for efforts leading to improved and reliable cable connectors.

In nuclear power and radioisotope thermoelectric sources we should continue to provide our requirements to the AEC and coordinate development efforts in this area. The present program is small, but should grow to become a major development in the next few years.

No single power source candidate is preferable over the entire spectrum in which submersibles, habitats, and other systems

may operate. Excluding Navy submarines, only batteries have been employed for main power in manned submersibles. Until fuel cells, thermal dynamic systems, small nuclear plants and other power sources can be developed for deep ocean service our undersea activities will be limited.

Materials

Material developments for hydrospace structures and equipment are basic to advances in most other technological areas and are essential for advances in ocean engineering capability. Improvements are necessary in strength-to-weight ratio, corrosion resistance and manufacturability. Because of the necessity to use materials with a low strength/weight ratio, our pressure hull structures have a weight displacement ratio too high for penetrating deep depths unless auxiliary buoyancy is utilized. Development of high strength-to-weight ratio pressure-hull material is necessary. HY 180 steel, the best material available today, still produces a pressure hull heavier than the water it displaces for depths greater than approximately 24,000 feet.

In the field of metals our major developments have been in high strength steels and titanium. When developing a new material, like the HY 130 presently being certified as a Class I steel for submarine construction, the Navy must not only look at the base metal and its properties, but also must consider the problems associated with fabrication, manufacturing, welding, fatigue strength, corrosion resistance, and non-destructive testing. Thus, it is important to develop a new material as a system. Our work presently underway in the HY 130/150 steel is an illustration of material being developed as a system, and of work previously carried out under exploratory development and being picked up and continued under advanced development. The development of HY 130 as a Class I material will be about a 4-year program costing $16 million. This does not include the exploratory development effort on HY-130 or account for the knowledge gained and carried over from other steel developments, such as HY-80.

The DSRV tri-sphere pressure hulls, made from HY-140 steel, are examples of the progress that has been made in applying high strength steels to relatively small structures.

Titanium shows great potential for deep submergence applications in the area of pressure hulls, buoyancy spheres and outer hull structural members. This fiscal year the Navy is starting construction of a titanium (100,000 psi yield strength) replacement hull

for the SEACLIFF or TURTLE vehicle. The hull is scheduled for completion and installation early in FY 71. When completed, and with other modifications to the vehicle, this hull will provide a 12,000 foot operating depth capability with a 2,300 pound payload. Also, this type of titanium will be qualified as a Class I material for small structures. With the present HY-100 steel hulls the SEACLIFF and TURTLE vehicles have a 6,500' operating depth and approximately a 350 pound payload.

In the area of non-metals, development should continue in structural glass, fiber reinforced plastics, acrylics, ceramics, syntactic foam and concrete. These materials have been identified within the Navy and by the NAE and the Marine Council as having an important role in ocean engineering. Of all the non-metals considered, glass is the one material where there is an abundance of claims but a conspicuous lack of available technical information. Fabrication, joining techniques, and non-destructive test procedures do not yet permit reliable exploitation of the theoretically achievable strength obtainable with glass. To date, the Navy's program in glass has been splintered and fragmented. Efforts are being formulated for a comprehensive program in development of structural glass. We are only at the point of investigating the chemical, physical and mechanical properties of glass. Establishment of specifications, fabrication technology, and non-destructive test methods and standards are later objectives. The end goal is a certified manned glass pressure-hull for 20,000' within 8 years at a total estimated program cost of $16 million.

Concrete, long used for ocean surface and near surface installations in and around harbors, is an interesting candidate material for future deep water work such as mobile and fixed underwater stations. Ease of fabrication and low cost make concrete attractive as a primary building material for ocean bottom installations at the continental shelf depth levels of 600'. It has not, however, been properly investigated for these new ocean applications and therefore requires considerable development.

Today's buoyancy material provides too little buoyancy (about 1/2 pound per pound of material) and its resistance to high pressures is not satisfactory. State-of-the-art syntactic foam weighs 42 lbs/ft^3 for a 20,000 ft. application. We need 34 lb/ft^3 foam or less to keep vehicle size within reasonable limits and to provide an increased payload capability.

The importance of materials technology development must be re-emphaiszed. Upon it the economy and effectiveness of undersea activities depends. If the pressure hull cannot provide needed buoyancy, supplemental material must be added,increasing vehicle weight, size and cost and reducing maneuverability and overall effectiveness. It is a program which the Navy must pursue primarily because of its requirements for submarines.

Auxiliary Systems

The most obviously deficient areas of ocean technology are the mechanical, electrical, and fluid systems for deep submergence. Vehicle operators are invariably beset with failures and constrained capability in current operations due to inadequacies in these systems. Improvements are needed in seals, bearings, alloys, compensating fluids, electric hull penetrators, cables and connectors, and machinery components.

High on the list of deficiencies is the matter of reliability and simplicity. High bulk and weight of systems and equipment and slow response of dynamic systems are other principal deficiencies.

Navy submarines operate at relatively shallow depths with most machinery systems inside the pressure hull and a minimum of equipment exposed to the ocean environment. However, the small submersible hull generally encloses only the man and the electronic equipment. Also, in unmanned systems, it is desirable to utilize as little heavy pressure-resistant structure as possible. As a result an efficient design requires the use of components and subsystems exposed directly to the ocean environment. The attempt to use off-the-shelf or slightly modified equipment in the ocean environment because of cost has in many cases proved unwise. Few items have worked as planned and modifications are usually extensive. The use of off-the-shelf equipment, in effect, has led to in-situ testing during operations -- a costly and wasteful procedure.

In the area of electric motors, associated controllers, inverters, and in particular electrical penetrators, cables and connectors, we have been, and are, continually plagued with problems. Development and operational failures in these components for the NR-1, Deep Submergence Rescue Vehicle, the MK II Deep Dive System, and the SEALAB III Habitat have contributed to program delay and cost problems. Often failures of cables, connectors,

etc., are resolved by a high degree of quality control. Early and detailed attention to the basic material and dimensional tolerances during fabrication and assembly are essential if improved reliability is to be achieved. Development efforts should be continued to provide a reliable electric drive system including high pin density electrical penetrators, light weight cabling, void and flaw free encapsulation and cable jackets and fluid for pressure compensated switching circuits.

In variable ballast and trim systems there is a need for a high head salt water pump of small size and low power requirements.

Small, light weight hydraulic systems capable of reliable operations at 20,000' are not available today. Hydraulic power is frequently more reliable and more easily controlled than electric power and therefore is a popular choice for more subsystems. For conventional systems, greater reliability at lower size and weight must be investigated. In addition, a breakthrough is needed to develop ways for using seawater itself as a hydraulic fluid.

Improved high capacity and lighter weight constant-tension winches are required for deep ocean towing of sensors and for the safe launching and recovery of instrumentation and vehicles.

Whatever the mission requirements may be, the auxiliary systems must be optimized in terms of reliability, simplicity, maintainability, weight and volume. Development has not received the attention given materials and power sources, although of equal importance.

Oceonics

Sensors, navigation, and command and control, termed "oceonics", are also areas requiring major development. Much of our present effort in this area should be devoted to improving performance and reliability of equipment and reducing bulk and weight of existing equipment.

A need exists for equipments capable of detecting, locating and inspecting man-made objects or installations on the ocean floor. At-sea search operations depend primarily on the search rate and the vehicle's navigational accuracy. Our present search sensors, whether towed or mounted on submersibles, provide a

low search rate (on the order of 0.1 sq. mi./hr.) A search rate which permits large area inspection at an acceptable cost is required.

In practical applications, such as the THRESHER, H-Bomb, and SCORPION search operations, the magnetometer and camera produced the most useful results. These systems, however, are inherently short range systems. In these same search operations the poor performance of the sonar, a relatively long range system by comparison, is of particular concern and requires further investigation.

Present lighting and photographic systems are limited by backscattering and high power requirements. Considerable development effort is required in volume scanning, light gating, and polarization techniques, all of which have the capability of reducing the backscatter phenomenon. Also needed is instrumentation for measuring backscatter in meaningful terms. Likewise, improved TV and acoustic imaging systems require further development and evaluation in the environment.

Navigational improvements are required along two routes – one is refinement and miniaturization of inertial systems, and means for updating, and correcting, these systems on or near the bottom through application of doppler sonar. The other navigational development requirement is brought about by the need for sonic reference points on the ocean floor and interrogation/ranging systems. These sonic reference and interrogation systems require standardized, small, easily deployable, and long life transponders.

The combination of human operator, sensors, navigation, communication, propulsion devices and manipulators make up the total command and ship control system. In present day systems, such as found in DEEP QUEST, DSRV and NR-1, performance requirements exceed human response and analytical capabilities. Therefore, to permit effective slow speed operations near the bottom or in proximity to other submarines, an automatic sensing and control system is necessary. Such a system must be reliable and simple to operate and maintain, and must provide for an emergency backup mode of operation.

Although the ability to get to the depths of the sea requires development of power sources and material, the ability to do effective work once we arrive is almost entirely dependent on our advances in oceonics and auxiliary systems.

Diver Technology

Navy developments in diving are focused on providing the capability to perform useful work on the continental shelf. With today's operational hardware, the Navy hard hat diver is limited to a depth of 300 feet for 30 minutes in an inflated suit of rubberized canvas, a heavy copper helmet, weighted belt and shoes, and inefficient tools. For depths greater than about 200 feet he breathes a mixture of helium and oxygen. At shallow depths he wears a lighter weight dress and breathes compressed air. Hard hat diving is conducted in a "non-saturated" mode which requires extensive decompression time (approximately 3 hours for a 30-minute dive at 300 ft.) following each trip to the bottom work site. While decompressing, the diver is suspended in the water beneath the support ship exposed to environmental hazards and discomforts. The support ship is effectively immobilized until decompression is complete and the diver hoisted aboard. The scuba diver has increased mobility, but is limited to about 200 feet on mixed gas and 135 feet on compressed air.

Saturated diving systems are undergoing test and evaluation. In this mode the diver remains under pressure until his blood and tissues become saturated with the breathing gas at the ambient pressure. He lives in a pressure chamber and is sheltered from the ocean environment while resting between work shifts and during decompression. After the diver becomes saturated, at a certain pressure, his decompression time remains constant regardless of the time he remains at that pressure. Thus, the ratio of working time to decompression time, and hence the diver's effectiveness, increase with mission duration. The diving systems consist essentially of personnel transfer capsules which act as elevators to and from the worksite, and deck decompression chambers which house the diver in relative comfort aboard the support ship.

Regardless of the diving mode, there are critical technical deficiencies in diving equipment which currently restrict diver effectiveness. These deficiencies generally become more serious as diving depths increase. For example, the problem of maintaining body heat increases as greater pressure collapses and helium

permeates insulating material in the diver's dress. Development is proceeding with electrically heated underwear worn beneath a conventional wet suit. Another approach is to improve the insulating qualities of the suit material. Developments thus far, such as filling the voids of the suit material with microspheres, have restricted diver mobility. Other deficiency areas are communications, visibility, tools, gas monitoring and control, and diver transport and navigation. Extensive development is necessary in these areas before divers can perform useful work at pressures up to limits imposed by physiological considerations.

Bio-Medical Development

Coincident with diver equipment development must be biomedical research to determine the physiological and psychological aspects of working in an environment of high pressure, cold, and darkness. Advances are required in treatment of decompression sickness, determination of optimum gas mixtures, toxicological and microbiological control, and hyperbaric medical treatment. In addition, the physiological aspects of audio-visual aids, thermal protection, and communication must be fully understood and made available to designers of diver equipment.

Man's physiologic depth limitations have not yet been determined. During a recent experiment at Duke University, divers completed a very successful simulated dive in a pressure chamber where they stayed at a pressure equivalent to 1000 feet of water for 78 hours. Projections of man's eventual depth capability breathing mixed gases range from about 1,500 feet to as high as 3,000 feet. Hydrogen, and other inert gases, are being evaluated as a replacement gas for helium at depths beyond the limit imposed by helium narcosis. For extreme depths, perhaps as great as 12,000 feet, liquid breathing is a promising development. Experiments with animals have proved that mammals can live under pressure equivalent to several thousand feet of water while breathing an isotonic saline solution which has been charged with dissolved oxygen. The critical unresolved limitation in breathing an oxygenated liquid is elimination of carbon dioxide. The removal of carbon dioxide from the lungs by liquid breathing would require a greater respiratory rate than that required by air breathing; but since water is about 40 times more viscous than air, the lungs can only exchange water at about 2.5% of the rate at which air can be exchanged. Until this problem can be solved, the idea of divers working beyond the continental margin is rather fanciful. Principal

efforts must be directed toward solving the primary near-term problems; which are decompression, communications, and thermal protection.

Seafloor Engineering

This technology area involves the design, construction, and maintenance of fixed ocean installations. The long term goal is the capability of performing any construction task on or in the ocean floor which the Navy may require. Major technology deficiencies may be divided into three areas: Site Selection; Site Preparation and Construction; and Structures and Structural Subsystems. For site selection we need to be able to determine bottom topography, sediment strength, sediment stability, turbidity potential, seismic activity, current and wave forces, environmental corrosion potential, and biological fouling potential. Site preparation and construction require development in power source and transmission capability, foundation design criteria, bottom stabilization equipment, earth moving equipment, drilling and excavating equipment, lifting and positioning systems, and underwater construction tools. For structures and structural subsystems we require structural design criteria, ingress/egress systems, inexpensive high strength structural materials which are easy to fabricate and resist corrosion, and massive operational power. It must be emphasized that seafloor engineering represents a major void in our technical knowledge which will require major resource application.

An intermediate and long-term objective of the Navy is developing technology for undersea habitats. Although there is no specified Navy requirement for a habitat, this will be an inherent part of any mission which requires long term seafloor operations. As part of an effort to identify engineering constraints where further R&D will be required, the Navy has evaluated several concepts for manned habitats at a depth of 6000 feet. The "rocksite" habitat concept has also been evaluated, which would utilize caverns hollowed out of the ocean floor. This is a promising idea for future, large habitats, and development effort has been initiated which will lead to this capability. Under a Navy contract, industry recently completed a study of one-atmosphere, manned underwater stations; the study compared concepts and provided production cost estimates for different habitats at different depths. The study also identified technical areas which require further R&D, and this, in general, confirmed

deficiencies already identified by the Navy. As an example, the study has shown which direction to take in habitat power development. It indicated that an umbilical power link from shore will be most cost effective for habitats less than about 100 miles from shore. For other habitats nuclear power will be required. It also identified knowledge of the behavior of marine sediments as a critical technology restraint.

For several years we have been conducting research to bridge the gap between terrestrial soil mechanics and what can be termed "mechanics of marine sediments". An example of one of the questions we have answered through laboratory research is that hydrostatic pressure appears to have only a minor effect on the strength of marine sediments. In-situ measurements are necessary to validate laboratory measurements. Sediments forming in a seawater environment tend to have a flocculated grain structure which exhibits large changes in strength when disturbed. Besides the disturbance inherent in sampling, a sample undergoes a large change in pressure (which may affect interparticle bonds as porewater and gas expand) and transport disturbance before strength tests are performed in the laboratory. A deep-ocean sediment test system has recently been developed which may be used to make in-situ measurements of the engineering properties of marine sediments to depths of 6000 feet. Initially it has been equipped with a vane shear device, cone penetrometer and other simple work systems. Developments underway for this system include a 30-foot coring capability and instrumentation for determining seismic activity and turbidity potential.

Although progress is being made in seafloor engineering, many deficiencies, such as sediment stability, seismic response, excavation, ingress, and remote power have only recently been addressed. Because of the limited development in seafloor engineering and the eventual requirement for this capability for any effective ocean resource utilization, this is one of the most challenging and potentially rewarding technology areas in ocean engineering.

Environmental Support

Objectives in environmental support of ocean engineering are to develop feasible solutions to the problems of measuring the undersea, atmosphere, and interface environment, predicting it, and influencing it. In order to effectively plan and execute any

ocean engineering operation, predictions of environmental parameters are extremely important. Predictions are only as good as the observations on which they are based. Deficiencies in this area require the development of new and improved instrumentation, prediction techniques, and application of the products to planning operations. The general areas of interest are weather, waves, currents, temperature, salinity, pressure, sound velocity, gravity and magnetic field data. Developments are proceeding on expendable instruments, multiple sensors, high-speed data collecting platforms, satellite utilization, buoys, and data processing.

Expendable instruments are desirable to eliminate the costly, time consuming task of stopping a ship and lowering and retrieving oceanographic instrumentation by winch. This is a particularly important factor in determining whether use of "ships of opportunity" will be successful.

Use of multiple sensors and high-speed vehicles (such as air cushion, captured air bubble, or hydrofoils) from a mother ship, promises to increase data acquisition speed by several times.

Even more promising for rapid determination of many environmental parameters are remote sensing techniques using aircraft or satellites. It appears feasible that satellites may eventually collect virtually all required environmental data. Oceanographic data beyond the theoretical reach of satellites can be relayed to the satellite from a buoy system and be available for readout by users on shore or at sea.

Test Facilities

Ocean engineering test facilities, particularly pressure test chambers and undersea test ranges, are necessary to provide the means for developing technology. Requirements for test facilities must be established by projecting RDT&E and operational programs and determining necessary testing. Technical deficiencies in this area are primarily the lack of design and certification criteria for large, high-pressure test facilities. Cost estimates for required future facilities range from $10 to $30 million dollars each, using conventional materials. Fabrication techniques required for these pressure chambers are currently beyond the state-of-the-art. New materials for chamber construction such as concrete or

filament-wound fiberglas need further development, but promise to significantly reduce the cost of future pressure test facilities.

A major problem facing the nation's pressure test chambers is that they wear out. The low cycle fatigue curve for typical large high pressure (20-30 ksi) chambers shows that cyclic pressure capability is only about 1/3 of the static capability. For a chamber which is planned to be constructed at NSRDC Annapolis in 1970, this curve shows that each time the full static pressure is reached, the chamber deteriorates in value by about $700. Each cycle at cyclic pressure reduces the value of the chamber by 70¢. Typical tests on deep ocean submersible equipment require on the order of 50,000 cycles. Many experimenters don't realize that the life of each pressure facility is limited. Of 269 major chambers catalogued in a recent nation-wide survey conducted by the Navy, only a few of the owners had any idea of the remaining life of their chambers. Design standards are virtually non-existent, so choice of materials and designs varied radically among the chambers surveyed. There have been 2 explosions of pressure chambers recently, and based on this analysis we can expect more.

One problem which will necessitate new design concepts for larger pressure chambers is steel billet size. The largest steel billet size in the U.S. is approximately 100 tons, and the fabrication of a chamber which will be operational this year at NSRDC Annapolis approached this limit. Welding sections of this chamber together also presented major difficulties. Filament-wound fiberglas is a promising development for overcoming this limitation. A small pressure chamber using this concept has already been cycled over 100,000 times. This technology may permit very large pressure chambers to be constructed on site at much lower costs than are now possible.

Non-Combatant Vehicles

The weaknesses in our non-combatant vehicles stem primarily from the shortcomings in the technological areas just reviewed. Our efforts range from surface ships to deep submergence vehicles to unmanned deep recovery systems. Design of support ships with associated handling equipment which must handle submersibles in the dynamic air-sea interface is a major problem. For manned and unmanned vehicles, improved and new developments in material, power, and vehicle auxiliary systems will lead to optimization in terms of weight, volume, simplicity, reliability and maintainability.

Summary

The objective of the Navy program in ocean engineering is to permit full utilization of the ocean environment in support of national security. The capabilities required to achieve this objective can only be developed with a broad base of proven technologies. Elimination of the deficiencies mentioned in each of the functional areas discussed is necessary to provide this sound and effective base of technology. Development programs must be closely coordinated and continually reviewed to ensure that within the resources available we are putting forth a maximum effort to eliminate these deficiencies.

AN INVESTIGATION OF THE FEASIBILITY OF HOT PRESSING A HEAVY WALLED HEMISPHERIC HEAD FROM WELDED TITANIUM ALLOY PLATE

H. Nagler, Welding Engineer
F.J. Lengenfelder, Physical Metallurgist
R.J. Wolfe, Head, Titanium Program

Naval Applied Science Laboratory
Brooklyn, New York 11251

ABSTRACT

Thick plate alloy titanium is being considered by the Navy as a potential material for deep diving submersible pressure hulls. The production of very large titanium plates (160" or more in diameter and 4" or greater in thickness) that may be required for such applications approaches the limit of mill capacity in this country.

To provide an alternative method for the production of very large plates, a feasibility study was undertaken to determine if small plates, joined by welding to produce a large plate, could be hot formed into a hemispheric head of the type that might be used for the construction of a pressure hull.

Out-of-chamber welding techniques developed at NASL were used to join two 3" thick by 24" wide by 48" long Ti-721 alloy titanium plates to produce a 4' square weldment. A 2-11/16" thick by 42" diameter disc was machined from the weldment and then hot press formed to make a 24" diameter head. Non-destructive tests and mechanical property evaluations were conducted on the formed head to determine the effects of forming on the quality and properties of the finished head.

The results of this investigation indicate that it is feasible to hot press form a heavy walled hemispheric head from welded alloy titanium plate. However, the head produced during the course of this investigation was not of acceptable quality because of fissuring in certain areas of the weld deposit during the forming operation.

Successful hot forming of welded alloy titanium plate would appear to require that weld properties at least match those of the base plate at the forming temperature, either by appropriate selection of weld filler wire or by design of the weld joint. In addition, the welding process used to join the plates should be one that is not prone to lack-of-fusion type defects.

INTRODUCTION

Thick plate alloy titanium is being considered by the U.S. Navy as potential material for the fabrication of pressure hulls for very deep diving submersibles. Under the sponsorship of the Naval Ship Systems Command and the Deep Submergence Systems Project Office of the U.S. Navy, the U.S. Naval Applied Science Laboratory is developing forming, welding and nondestructive testing techniques for the fabrication of alloy titanium pressure hulls.

The very large plate sizes that may be required for the fabrication of spherical hulls (150" or more in diameter and 4" or greater in thickness) have yet to be produced and, in addition, approach the limit of mill capacity in the United States for the production of alloy titanium plate.

In order to provide an alternative method for the production of very large plates, a feasibility study was undertaken to determine whether small plates, joined by welding to produce a large plate, could be hot formed to produce a hemispheric head of the type that might be required for the construction of a pressure hull.

Earlier work at the Laboratory[1] had shown that thick plate alloy titanium could be welded, out-of-chamber, using gas metal arc welding techniques, both in the spray and short-circuit transfer modes, with appropriate trailing and backing shields. The gas tungsten arc technique had also been used at the Laboratory and by others[2,3] for welding thick titanium plate. All three welding techniques were used in the work reported herein.

MATERIAL

Material for the study consisted of a rolled plate of Ti-721 alloy, 24" wide by 96" long by 3" thick, and 41 pounds of welding wire of two sizes, 0.030 and 0.062 inch diameter, of similar composition to that of the plate. Ti-721 is a near alpha alloy of the composition Ti-7Al-2Cb-1Ta with superior fracture toughness (in air) to that of any titanium alloy of comparable strength. Mechanical properties of the plate and chemical composition of the plate and welding wire are given in Tables 1 and 2.

(1) Superscript numbers refer to references at end of report.

WELDING

The plate was saw cut into two pieces, each 24" wide by 48" long, and one long edge of each plate was machine beveled in preparation for welding, as shown in Figure 1. The bevels were machined to provide a 60° included angle, sharp nosed, double "V" weld joint. The two plates were then joined by welding to form an assembly 48" square. Weld run-on and run-off tabs were attached to the plates prior to joining in order to avoid the effects of arc starting and stopping in the main weld and also to provide sample weld material for test and evaluation.

Welding was performed in three separate stages, as depicted in Figures 2, 3 and 4. A balanced welding sequence was used in each stage with weld metal deposited first on one side of the joint and then on the other, to avoid excessive distortion and weld cracking. The first stage, welding the root passes, was performed by gas metal arc (GMA) short-circuit welding in the vertical welding position as shown in Figure 2. The second stage, during which the large bulk of the weld was deposited, was performed by the gas metal arc (GMA) spray welding process, in the flat welding position, Figure 3. The final stage was performed by gas tungsten arc (GTA) welding in the flat position to provide the capping passes as shown in Figure 4. A total of fifty-seven weld passes were required to complete the joint.

Welding conditions for each of the three stages are listed in Table 3.

The completed,four foot square weld assembly, weighing approximately 1300 pounds, is shown in Figure 5.

FORMING

In order to provide the appropriate shape for the forming operation, the weldment was machined to a 42" diameter disc, 2-11/16" thick, with both surfaces flat and parallel, as shown in Figure 6.

The disc was then shipped to a contractor, the Lukens Steel Company, for the press forming operation. In view of the experimental nature of the work and because of the high cost of special dies, available dies were used to press-form the disc. Since the dies had been designed for use with 4" thick plate, it was necessary to use a 1-1/4" thick, carbon-steel liner plate as a spacer, in combination with the 2-11/16" thick titanium disc, to fill the die.

The titanium disc was centered on the liner plate and charged, as a pack, into a gas-fired oxidizing atmosphere furnace at 1850°F. The furnace and charge were stabilized at 1750°F and held at this temperature, until the pack reached a uniform temperature throughout. Furnace temperature was then raised to 1960°F and the pack heated until the outer edges had reached 1950°F and the center was at 1925°F. This differential was considered desirable to allow for the more rapid cooling at the edges during transfer to the press. The pack was removed from the furnace, transferred to the 2000 ton capacity forming press, and centered on the lower platen as shown in Figure 7. The pack was then pressed through the bottom ring die with one steady stroke of the upper ram and male die. The estimated pressure required to form the pack was less than 1000 tons. Temperature of the pack at the time of contact with the male die was 1750°F, uniform within 10°F from edge to center; the finishing temperature, measured on the steel liner was 1710°F. Quenching effects were reduced by preheating male and female dies to approximately 500°F. The formed titanium head, encased in the steel spacer plate, was allowed to cool in still air. A view of the head within the spacer plate is shown in Figure 8. After return of the jacketed head to the Laboratory, the steel jacket was removed by oxy-acetylene flame cutting. Figure 9 shows the head after removal of the spacer plate and Figure 10 shows the head after machining.

QUALITY ASSURANCE

At every stage in the fabrication of the head, nondestructive inspection techniques were used to monitor the quality of the product. The original plate was dye penetrant and ultrasonically inspected. During the welding operation every weld pass was monitored by visual examination and ultrasonic hardness-inspection tests. Dye penetrant, X-ray radiography and ultrasonic inspection techniques were used to assess the quality of the as-welded assembly, the machined disc, the as-formed head and the head after machining.

In addition to the nondestructive tests, specimens were machined from the original plate, from run-off tabs on the welded assembly and from the formed head in both the weld and base plate areas of the straight flange section to provide mechanical property data for assessment of the effects of forming on properties. A section, oxy-acetylene cut from the machined head to provide test material from the curved portion of the head, is shown in Figure 11. Specimens prepared for test included: tensile, side bend, Charpy V-notch, and sections for macro and microexamination.

FABRICATION ANALYSIS

No unusual problems were encountered in welding the assembly. Nondestructive tests on the as-welded assembly showed no indications of surface or internal discontinuities. Visual and dye penetrant inspection of the machined disc, prior to forming, showed no evidence of surface discontinuities. Radiographic examination of the disc, however, revealed evidence of widely scattered porosity and a small lack of fusion defect in the weld, the latter approximately 10 inches from the edge of the disc. Ultrasonic examination of the disc confirmed the lack of fusion defect observed by radiography and also disclosed three additional small discontinuities along the weld/base metal fusion line. All of the discontinuities appeared to be located on one side of the weld,and this side was selected to be the inside of the formed head.

Although the hot pressing operation was the first of its kind to be performed on welded titanium plate, careful attention to detail resulted in successfully forming the head without unusual difficulties. It was noted, however, that localized bulging had occurred at the weld joint on the inner surface of the formed head for a distance of about 10 inches from the open end, as may be seen by close examination of Figure 9 in the bracketed area. After the steel jacket was removed, several minor fissures were found on the outer surface in the weld area near the apex of the head. There were no indications, however, that these fissures were associated with the internal discontinuities that had been detected in the weld during examination of the disc prior to forming. It was noted that the thickness of the weld, in the region where fissuring was observed, was less than that of the surrounding base plate, indicating that this region of the weld had undergone a reduction in area as a result of the forming operation.

Dye penetrant examination of the head after machining revealed three small fissures in the weld, on the outer surface of the head, in a region extending from about 6 to 9 inches from the apex. X-ray radiography and ultrasonic examination indicated that there were numerous internal fissures in the weld, extending from 3/4 to 12 inches from the apex, on both sides. Radiographic prints of a 5 inch long section of the weld in this region, before and after forming, are shown in Figure 12. The extensive fissuring in the weld area, after forming, may be noted in these prints. There were no indications of similar defects in the area of the weld that had bulged during forming nor in any areas of the formed base metal.

The wall thickness of the head after machining was not uniform and varied from 1.85 inches at the apex to 2.45 inches at the edge.

This variation in thickness was not due to thinning during forming but to a malfunction in the tracer unit of the vertical boring mill on which the head was machined.

EVALUATION OF PROPERTIES

Average properties of weld and base plate specimens, before and after forming, rounded out to the nearest whole number for ready comparison, are shown in Table 4.

The data shown in Table 4 indicates that although the numerical values of tensile yield and ultimate strength were not changed significantly as a result of forming there was a trend in the way the values changed. There was a slight loss of strength in the weld metal and a slight increase in base-plate strength. The same trend is evident in ductility as measured by elongation and reduction in area. Ductility of the weld was reduced after forming, while that of the base plate improved slightly. Charpy energy values were generally lower in the weld after forming as compared with little or no change in the base metal. The reduction in weld properties after forming may be attributed, at least in part, to the presence of the fissures previously noted, since many of the weld test specimens contained these discontinuities. It is somewhat surprising, however, to find that these discontinuities had such little effect on the weld properties.

A greater effect was observed in side bend tests performed on weld specimens before and after forming. Three side bend specimens of the weld, before forming, satisfactorily withstood 180° bends over a 4T radius mandrel without rupture. Only one of two side bend specimens removed from the formed weld satisfactorily withstood a 180° bend without rupture; the second specimen ruptured after bending to only 104°.

MACRO-AND MICRO-SECTION ANALYSIS

Typical macro-sections of the weld joint, before and after forming, are shown in Figure 13. The clearly delineated weld passes of the section before forming are no longer evident in the section of the formed weld. This is to be expected since the forming operation was carried out above the beta transus temperature and homogenization of the cast structure has taken place in the weld area. The outline of the cast weld metal, however, is still visible in the formed section. An outline of the formed macro-section has been superimposed on the as-welded section and it is evident that, for

the section chosen, some expansion of the weld has occurred during the forming operation.

Although not evident in the photographs of the macro-sections, a significantly greater number of discontinuities were observed in sections of the GMA short circuit weld deposit than in either the GMA spray weld or GTA weld deposits. This was true both before and after forming for the GMA welds. The GTA weld had been removed when the disc was machined, so that this area of the weld was not involved in the forming operation. Despite the numerous fissures observed in the GMA short circuit weld after forming, they did not cause catastrophic failure of the head during the forming operation. It is believed that the high quality of the GMA spray weld deposit may have acted to contain these discontinuities during forming.

Microscopic examination of weld and base metal areas in the flange and curved sections of the head showed that no fissures had occurred either in the weld or in the base metal in the region extending up to 10 inches from the edge of the head. Typical fissures found in the weld between 10 inches from the edge and the apex are shown in the photomicrograph in Figure 14. These fissures appeared to have formed by growth and joining of pores and other discontinuities in the weld. The majority of the fissures were found in the short circuit weld deposit where the greatest incidence of discontinuities had been observed before forming. Despite indications of porosity in the weld near the skirt of the head, these pores did not grow into fissures. This result may be attributed to the state of stress in the skirt area; longitudinal tension/lateral compression as compared with biaxial tension in areas of the weld nearer the apex of the head where minor discontinuities grew into fissures.

ELEVATED TEMPERATURE TESTS

Although weld properties overmatched those of the base plate at room temperature, the performance of the weld during the hot pressing operation suggested that the strength of the weld, at the forming temperature of 1750°F, was lower than that of the base plate at that temperature, causing the weld to undergo considerably greater plastic strain than the base metal. In order to confirm this hypothesis, elevated temperature tests were conducted on samples of weld and base metal obtained from the run-off tabs of the as-welded plate. The results of these tests are shown in Table 5 along with data on room temperature properties for purposes of comparison.

The data indicate that although weld strength exceeded that of the base plate at 70°F, the reverse was true at 1750°F, the forming

temperature of the head. In addition, the weld was more ductile than the base metal at 70°F but less ductile at 1750°F. The combination of lower strength and ductility at 1750°F would appear to account for the localized bulging of the weld in the laterally compressed skirt area of the head, and thinning and fissuring in the biaxial tension strained curved area during forming.

CONCLUSIONS

The results of this investigation indicate that it is feasible to hot press a heavy walled hemispheric head from welded titanium alloy plate. However, the head produced during the course of this investigation was not of acceptable quality because of fissuring in certain areas of the weld deposit during the forming operation. The fissuring appeared to be attributable to: (a) the presence of minor lack-of-fusion defects, primarily in the short-circuit weld, which opened up during hot forming; and (b) undermatching of weld strength and ductility with corresponding base plate properties at the forming temperature of 1750°F (even though the weld overmatched the base plate at room temperature).

Successful hot forming of welded titanium alloy plate would appear to require that weld properties at least match those of the base plate at the forming temperature, either by appropriate selection of weld filler wire or by design of the weld joint. In addition, the welding process used to join the plates should be one that is not prone to lack of fusion type defects.

FUTURE PLANS

A weldment in 4-inch-thick alloy titanium plate, similar to the assembly described in this paper, is being fabricated and will be used for further hot-press forming studies. This weldment will be formed with the weld reinforcement intact, to reduce plastic flow in the weld during the forming operation. An opportunity will thereby be afforded to examine the effect of weld joint design on performance during hot forming.

REFERENCES

1. Wolfe, R.J., Nagler, H., Crisci, J.R., and Frank, A.L., "Out-of-chamber Welding of Ti-7Al-2Cb-1Ta Alloy Titanium Plate", Welding Journal, 44(10), 443-457, (1965)

2. "Titanium Welding Techniques", Bulletin No. 6, Titanium Metals Corporation of American, New York 7, New York

3. Savas, J., "Development of Fusion Welding Techniques for Two-Inch Thick Titanium Plates", Final Report, Republic Steel Corp., Canton, Ohio, Contract No. NOas 60-6091-F (May 1961) (RSIC 0794)

Table 1 - Mechanical Properties of 3" Thick Ti-721 Alloy Plate

Direction	UTS ksi	TYS ksi	CYS ksi	Elong. 4D, %	RA %	Charpy V-Notch, ft-lbs -80°F	Charpy V-Notch, ft-lbs +32°F
Longitudinal	122.7	101.1	117.7	12.5	21.8	32	41
Transverse	120.7	100.8	113.6	13.0	22.9	31	43

Table 2 - Chemical Composition of Plate and Wire, %

	C	O_2	H_2 (ppm)	N_2	Fe	Al	Cb	Ta
Plate	0.02	0.064	56	0.01	0.12	7.3	2.2	0.7
Wire, 0.030" dia.	0.04	0.083	38	0.008	0.08	6.4	2.13	0.94
0.062" dia.	0.023	0.08	68/90	0.006	0.053	6.26	2.09	1.14

Table 3 - Welding Conditions

Welding Condition	Stage 1 GMA Short-Circuit	Stage 2 GMA Spray	Stage 3 GTA
Number of Layers/Passes Side 1 Side 2	3/5 3/5	4/13 3/10	1/8 2/16
Filler Wire Dia., in.	0.030	0.062	0.062
Volts, avg.	18	33	16
Amperes, avg.	155	330	290
Polarity	DCSP	DCRP	DCSP
Heat Input, Kilo-joules/in., avg.	13.1	52.6	22.0
Preheat and Interpass Temp. °F, avg.	170	150	170
Shielding Gas, SCFH, avg.	A-Argon	H-Helium	
a. Torch	35(3A,1H)	15(A)	35(3A,1H)
b. Trailing Shield	250(A)	200(A)	230(A)
c. Backing Shield	200(A)	-	-

Table 4 - Average Properties of Weld and Plate

Item	Condition	UTS, ksi	TYS, ksi	Elong. 4D, %	RA %	Charpy V-Notch, ft-lbs -80°F	Charpy V-Notch, ft-lbs +32°F
Weld	As-Welded	121	110	14	32	33	38
	Formed, Flange	117	103	9	19	27	29
	Formed, Curved	118	109	11	23	27	35
Plate	As-Received	115	103	13	22	33	42
	Formed, Flange	120	106	13	24	29	42
	Formed, Curved	118	108	15	27	29	39

Table 5 - Room and Elevated Temperature Properties Before Forming

Condition and Test Temperature	Item	UTS, ksi	TYS, ksi	Elongation 4D, %	RA %
Before Forming 70°F	Weld Metal, W	121.0	109.5	13.9	31.7
	Base Metal, B	114.9	102.9	13.0	22.4
	Ratio*	+5.3	+6.4	+6.9	+41.3
Before Forming 1750°F	Weld Metal, W	4.6	4.0	60.0	100
	Base Metal, B	4.8	4.3	71.1	100
	Ratio *	-4.2	-7.0	-15.5	0

* W-B/B x 100%

FIG. 1 PLATES BEFORE WELDING

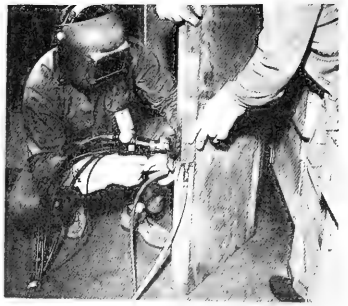

FIG. 2 GMA SHORT CIRCUIT WELDING

FIG. 3 GMA SPRAY WELDING

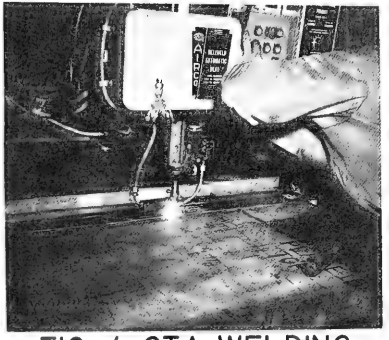

FIG. 4 GTA WELDING

FIG. 5 COMPLETED ASSEMBLY

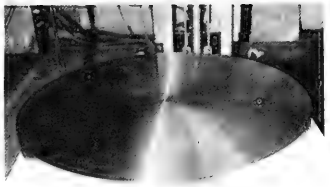

FIG. 6 MACHINED DISC

FIG. 7 DISC IN PRESS

FIG. 8 FORMED HEAD AND SPACER

FIG. 9 SPACER PLATE REMOVED

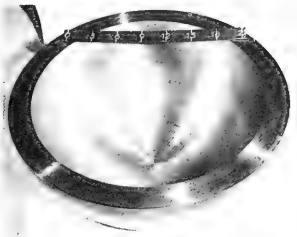

FIG. 10 MACHINED HEAD

FIG. 11 SECTION REMOVED FROM HEAD

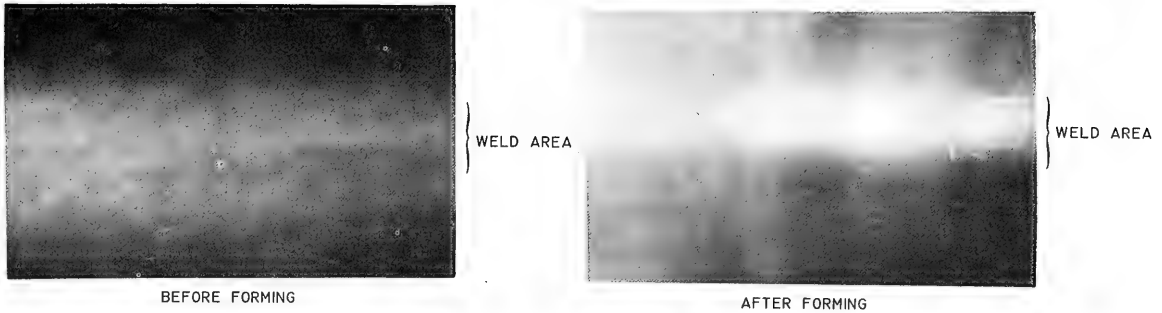

Fig. 12 Radiographic Prints of Weld Joint

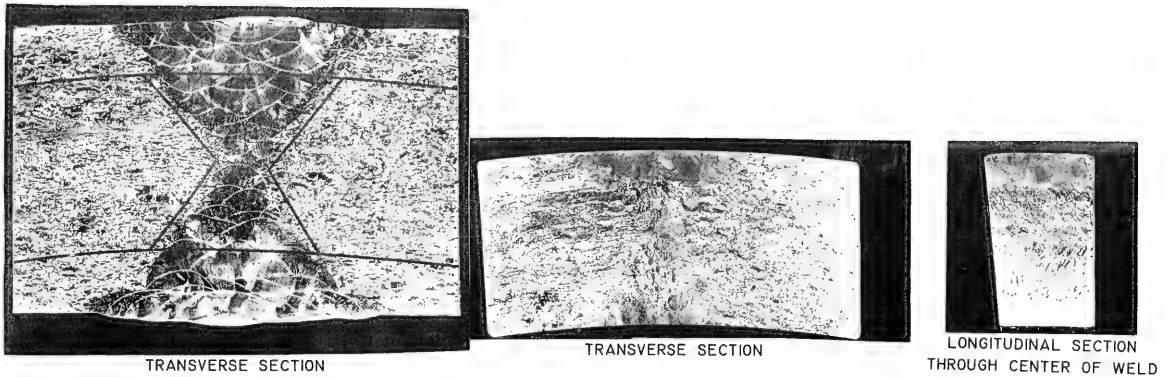

Fig. 13 Macro Sections of Weld Joint

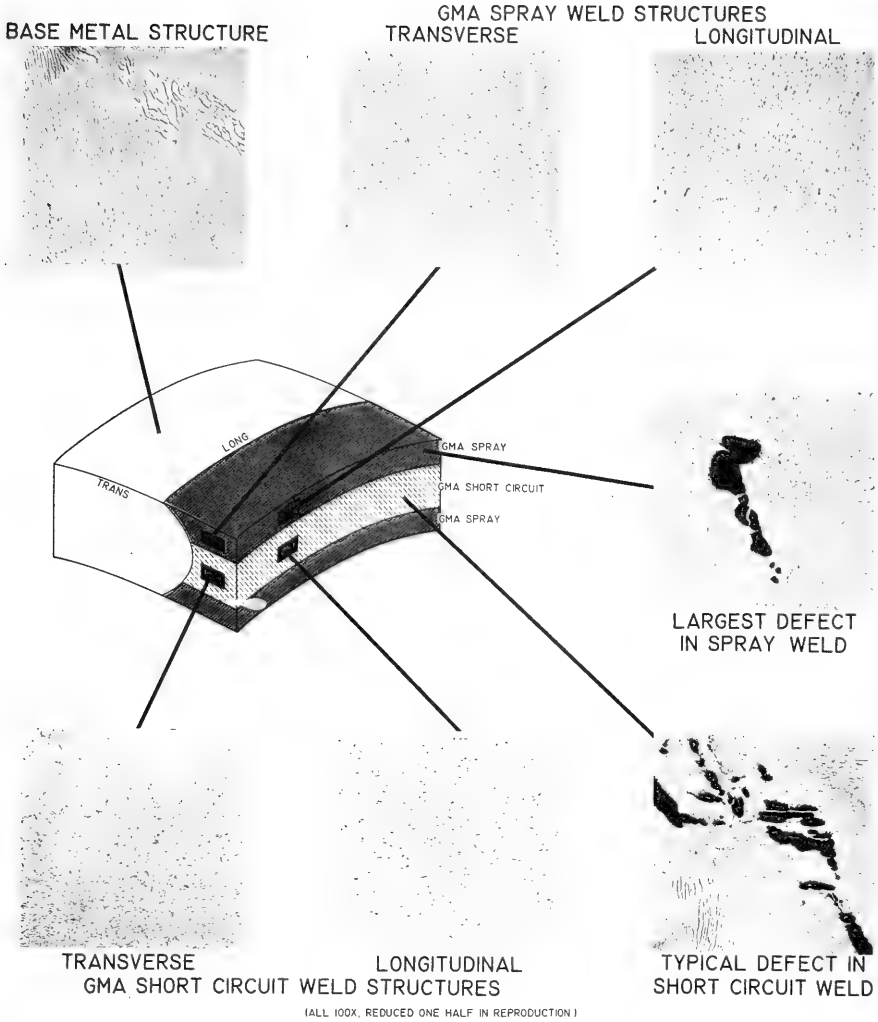

Fig. 14 Photomicrographs of Weld Joint Material After Forming

UNDERWATER TOOLS

Charles Young, Jr.
Project Manager

Swimmer Weapons System
U. S. Naval Ordnance Laboratory

ABSTRACT: Tools being developed at the U. S. Naval Ordnance Laboratory, White Oak, for use by underwater swimmers are discussed. Particular emphasis is placed on stud drivers, cable cutters, and fastening devices for use in raising sunken articles from the Continental Shelf. The presentation includes pictures of tools and a discussion of function and intended use and development status for each.

INTRODUCTION

Over the years, new tools have improved the capability of man to do work. In his normal environment today, he uses a large number and variety of tools to do an incredible number of tasks. However, with few exceptions, these tools are not suitable for use under water. Some of the reasons for this are quite obvious, while others are not.

First, effective electrical or pneumatic tools must be supplied by relatively large power sources through well-insulated cabling. Cabling is heavy and difficult to move about under water. Operating depths are limited when surface power supplies are used. Second, bottom time for a working diver or vehicle is precious and at times may be measured in seconds. Rapid cutting or drilling operations are essential. Third, unless he is well anchored, a diver reacts to the output forces of a power tool. A power tool providing rotary motion may be as likely to spin him as to perform its work function.

Less obvious underwater tool problems exist because the user is operating in a hostile environment. Underwater currents, poor visibility, and generally a neutrally buoyant condition all tend to disorient the working diver. The object of his work may be tilted awkwardly and he may be unable to brace himself properly. Moreover, he may be cold and fatigued. His hands may be soft and unfeeling after long underwater exposure. Tasks requiring more than a few simple operations will be in jeopardy unless the man has been well rehearsed. Even then, the working diver, suddenly confronted with a large chunk of kelp in his face, may react involuntarily and unpredictably. He may not always recover quickly enough from momentary distractions such as these. An underwater power tool may become a lethal instrument, or the sequence of an

operation may be forgotten indefinitely under these conditions. Finally, extreme effort and expense may have gone into placing a diver or vehicle on a work target under water. Under these circumstances, a tool must perform as expected. Cost effectiveness parameters differ considerably between tools developed for use on land, and those developed for use under water.

The operating limitations described above dictate three primary considerations in the performance of underwater tools, safety, reliability and simplicity of operation. In response to requirements for underwater tools, the Naval Ordnance Laboratory (NOL), White Oak, has placed these considerations first in every design approach. Historically, propellant-driven actuators have been proven safe, reliable, and simple to operate in man's normal environment. Moreover, for underwater applications, tools powered by propellant-driven actuators appear to have a natural design advantage. A propellant-drive actuator normally develops large pressures within a tool when fired. Therefore, as a general rule, these tools also will withstand considerable external hydrostatic pressures.

In light of these considerations, a family of first-generation, propellant-actuated tools has emerged as the mainstay of the underwater tools development effort at NOL. This paper documents that effort, and in addition, touches on other allied projects including an interesting and promising new approach in the development of underwater tools. Each of the items described may be used on land. Each is being considered for possible use with underwater vehicle manipulators, although this has not been a design requirement to date.

UNDERWATER TOOLS DEVELOPMENTS

Primary support for the development of underwater tools at NOL has come from three sources: Under Specific Operational Requirement 38-01, the Swimmer Weapons System has produced the small Driver Mk 22 Mod 0 and the Cable Cutter Mk 20 Mod 0. Under the combined support of the Deep Submergence Systems Project and the Supervisor of Salvage, two additional stud drivers are being developed for relatively heavy duty work. In addition, a Salvage-Lift PADEYE is under development.

DRIVER MK 22 MOD 0. The Driver Mk 22 Mod 0 is shown in Figure 1. This driver was designed for use in nailing light objects to wood or thin steel plating. Prior to use, the driver is completely sealed against water leakage. Therefore, when firing occurs, the stud is able to build up maximum kinetic energy for penetration of the target upon emerging through the barrel cap of the driver. The stud is pushed along inside of the driver, from right to left in Figure 1, by expanding gases from a burning propellant. The propellant is ignited by triggering of a spring-loaded striker

into a primer. Table I lists some of the physical characteristics of this driver and other tools discussed in this paper. The Driver Mk 22 cannot be reloaded and is discarded once used. The same propellant and stud weights are used for each target. This driver is in production and in the Fleet.

SALVAGE DRIVER (LIGHT-DUTY). This driver is shown in Figure 2. It is 17 inches long and is used for fastening underwater patch plates over holes in ship hulls during salvage operations. The driver breaks open at the breech to accept an actuator (or cartridge) which may be inserted under water. Unlike the Driver Mk 22, this driver may be fired repeatedly. However, the barrel of the driver is open to water and, as a result, the kinetic energy of the stud, and underwater operating depth, are limited (see Table I). Because of variations in the hardness and thickness of ships' plate, there also are variations in propellant and stud weights in actuators for this driver. On the working site, the diver selects actuators which match the plate being patched. A heavy stud, driven by a heavy propellant load, will go right through thin plating. Figures in Table I show the largest of the available propellant and stud weights for this driver. The Light-Duty Driver originally was designed by the Mine Safety Appliances Co. of Pittsburgh, Pa., and in this form has been in the Fleet since World War II. Because of the age of the drivers in the Fleet and the addition of tighter specifications on navy gun-type mechanisms, these drivers all were reworked during 1968. Then, a development program for a replacement driver was undertaken and is planned for completion in April 1970.

SALVAGE DRIVER (HEAVY-DUTY). Figure 3 shows the Heavy-Duty Driver being used during a test shot. This driver is 20 inches long and has much greater penetrating power and operational depth characteristics than the Light-Duty Driver. The increased power comes from having a sealed barrel and heavier propellant and stud weights (see Table I). As is the case for the Light-Duty Driver, this driver has a variety of propellant and stud weights available. Table I shows the heaviest of these. The Heavy-Duty Driver has a greater operating depth than the Light-Duty Driver due to the sealed barrel. The diver carries the basic driver mechanism and loaded sealed barrels to the underwater work site. After each shot, the expended barrel is replaced by a loaded barrel. Expended barrels are reloaded with propellant and a new stud and are resealed in a surface support area. In addition to normal stud driving, this driver has the capability to punch a hole in ships' plate using an especially configured 5/8-inch diameter ram in place of the normal bullet-shaped stud. The Heavy-Duty Driver also is a product of the Mine Safety Appliances Co. A program of rework and redesign has been undertaken similar to that for the Light-Duty Driver. This work is scheduled for completion in May 1970.

SALVAGE-LIFT PADEYE. On occasion, it is desired to lift heavy objects from the sea floor. The capability to provide a lift point from which 25 long-tons of steel may be raised will be provided by the Salvage-Life PADEYE, Figure 4. The dimension across the diagonal of the PADEYE is 18 inches. Initially, the PADEYE is attached with 4 magnets to the plate to be lifted. Four stud driver barrels similar to, but heavier than, the barrels of the Heavy-Duty Driver are screwed into place. Figure 4 shows one of these in firing position. The 4 studs are fired into the plate to be raised. Next, the expended barrels are removed. The swiveled attachment bar remains in the center of the PADEYE. A hole in the attachment bar will accept a 2-inch diameter line, the other end of which is secured to a pontoon or other lifting device. Development of the PADEYE is scheduled for completion in February 1970.

CABLE CUTTER MK 20 MOD 0. The Cable Cutter Mk 20 Mod 0 is shown in Figure 5. This cutter is approximately 10 inches long. A guillotine-type blade in the cutter easily severes 1-inch diameter plough steel cable. The propellant and cutter blade are located in the midsection of the tool. As shown in Figure 5, the Cable Cutter Mk 20 has a shipping bar in place. The shipping bar is retained in place until the cable cutter is to be used. If the cutter is fired accidently, the shipping bar will be severed, but in this circumstance, the hardened cutter blade will not shatter upon impact with the anvil. In air, fragments from a shattered cutter blade could injure personnel in the immediate vicinity of the cutter. Figure 6 shows the cable cutter with the shipping bar removed and a 1-inch diameter cable in place. The Cable Cutter Mk 20 is discarded after use. This cutter has been recommended for release to production by NOL and a fleet operational evaluation is about to begin.

PYRONOL Cutter. A new and interesting method of cutting recently has been revealed by NOL. Cutting is accomplished by electrically igniting a metal slurry called PYRONOL. Figure 7 shows a view of a PYRONOL Cutter which has severed a 2-inch cable under water. When loaded, this cutter assembly weighed 8 pounds which is approximately half the expected weight of a mechanical cutter that could do the same job. PYRONOL is an exothermic mixture of powdered nickel, aluminum, and ferric-oxide. When ignited, this mixture achieves temperatures approaching 2400°C. A little fluorocarbon added to the metal slurry causes a pressure buildup within the cylindrical section of the tool and forces the burning slurry mix to be ejected down through an especially configured nozzle onto the cable. The cable is completely severed in less than a second. To date, cutting work using PYRONOL has been exploratory. An underwater electrical firing system and a convenient arrangement for fastening the tool to the cable under water are yet to be developed. In addition, more test firings and side effects studies will be required at various underwater

depths before the system has proven itself. PYRONOL promises a new and somewhat revolutionary power source for underwater tools design. Full exploitation of this new capability is intended for the future.

NITINOL. There are requirements for especially designed, hand-held, unpowered tools. In particular, Explosive Ordnance Disposal (EOD) divers need knives and other items which are nonmagnetic. An underwater diver's knife made from an NOL developed nickel-titanium alloy (NITINOL) has proved superior to present divers' knives during recent tests performed at EOD Facility, Indian Head, Md. Its edge holding qualities were so good that the NITINOL knife took only one-third of the strokes necessary to cut through a 3-inch manila rope than the knife now used. From this favorable evaluation, it is expected that other NITINOL nonmagnetic tools such as chisels, wrenches, etc., will become available where strength, hardness, corrosion-resistance and edge holding characteristics are required. Work will continue on this type of tool in the future.

SUMMARY

The tools described in this paper all perform relatively simple functions under water. All are hand-held or hand-emplaced, and were designed originally for use at 1000-ft. depths or less. Each satisfies a particular, well defined need. From this beginning, what may be anticipated in the future? First, it is expected that variations of these tools will be required to satisfy additional requirements. Remote handling from a vehicle may be needed. This might generate the need for electrical firing systems, modifications necessary to interface with manipulators, and deeper operating depth capabilities. In that connection, most tools described in this paper have been subjected to tests at underwater depths that exceed design depths. Table I includes maximum test depths at which successful shots have been fired. No data exist for depths at which failures might occur due to excessive external pressures. It should not be concluded from data on maximum test depths, that a design could successfully be achieved for that depth although there is every indication of it. Second, more tools to satisfy other relatively simple requirements may be needed. An example is the rapid cutting of metal plates at any depth. Third, fixed tools to perform routine functions on a set time schedule or in response to coded acoustic signals may be required. In fact, remotely controlled valves on underwater oil wells are a reality today. It appears that the list of possible requirements for underwater tools in the future is dependent only on one's imagination. However, it must be concluded that, because of the expenses involved, development efforts should be expended only on those tools for which definite requirements exist.

TABLE I - CHARACTERISTICS OF PROPELLANT DRIVEN TOOLS

	DRIVER MK 22	LIGHT DUTY DRIVER	HEAVY DUTY DRIVER	SALVAGE LIFT PADEYE	CABLE CUTTER MK 20
DESIGN DEPTH	200 ft	300 ft	850 ft	1000 ft	200 ft
MAXIMUM TEST DEPTH	800 ft	300 ft	1000 ft	10,000 ft	650 ft
STUD WEIGHT	175 GRAINS	32 GRAMS *	131 GRAMS *	280 GRAMS	170 GRAMS
PROPELLANT WEIGHT	2.9 GRAINS	15 GRAINS *	3 GRAMS *	22 GRAMS	1 GRAM
TARGET	3/4" wood to 1/2" steel	TWO 1/2" * steel plates	1" HY-80 steel plate * *	2 5/8" HY-80 steel plate	1" PLOUGH STEEL CABLE
OVERALL TOOL WEIGHT (AIR)	3/4 LBS	6 LBS	17 LBS	160 LBS TOTAL 75 LBS WITHOUT BARRELS	5 LBS

* MAXIMUM LOADS — MAXIMUM CAPABILITY

* * PUNCHING RAM WILL PUT 5/8" DIA HOLE IN 1/2" STEEL PLATE.

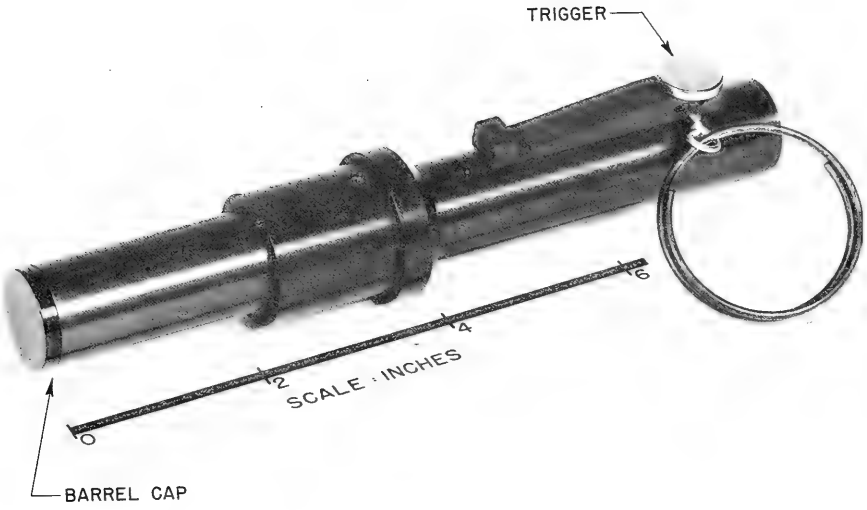

Figure 1. Driver Mk 22 Mod 0

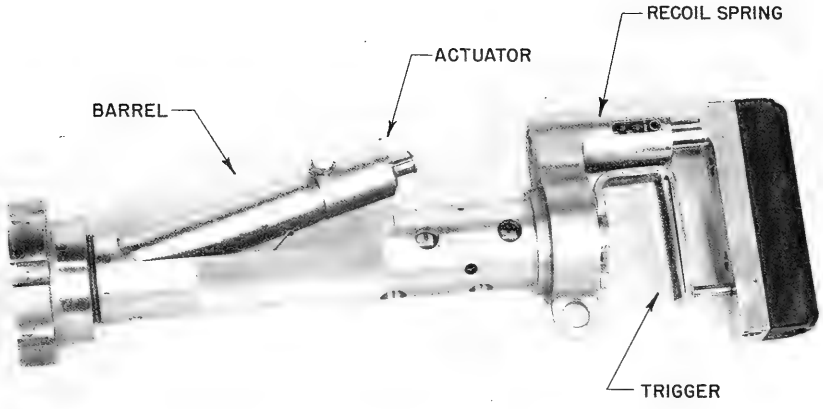

Figure 2. Salvage Driver (Light Duty)

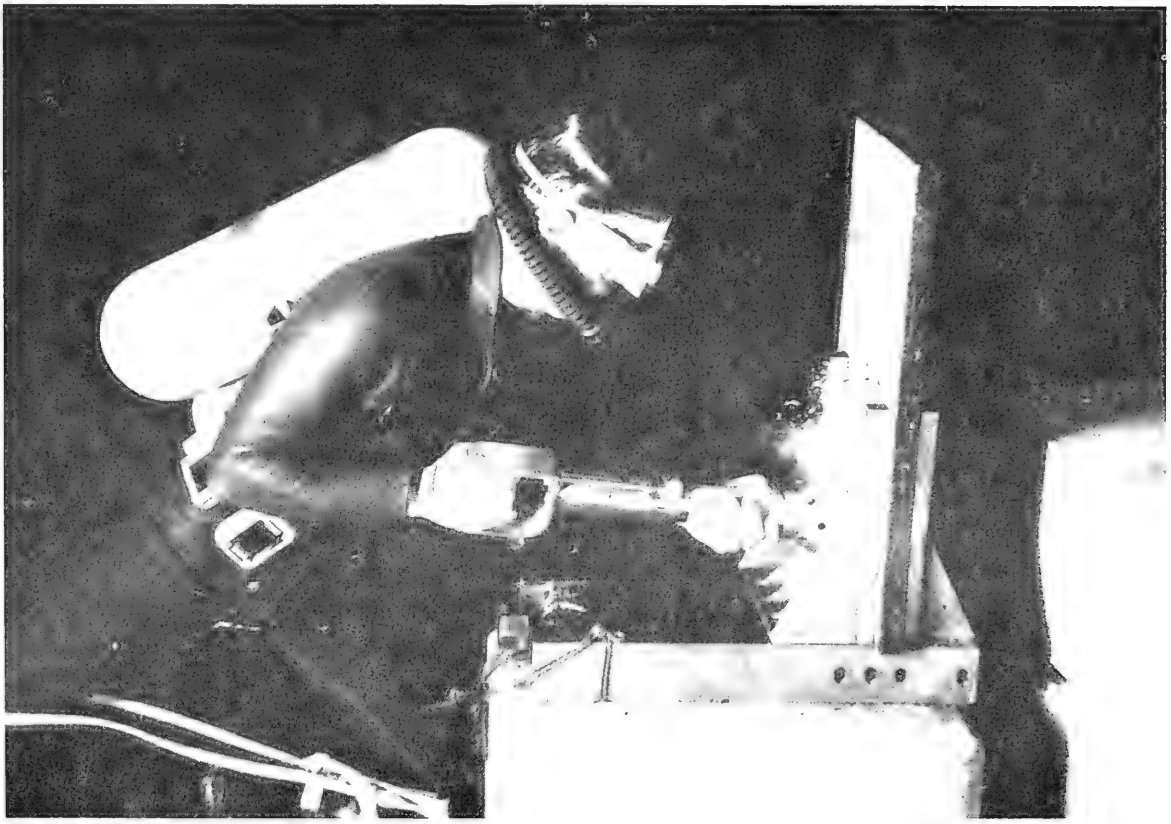

Figure 3. Salvage Driver (Heavy Duty)

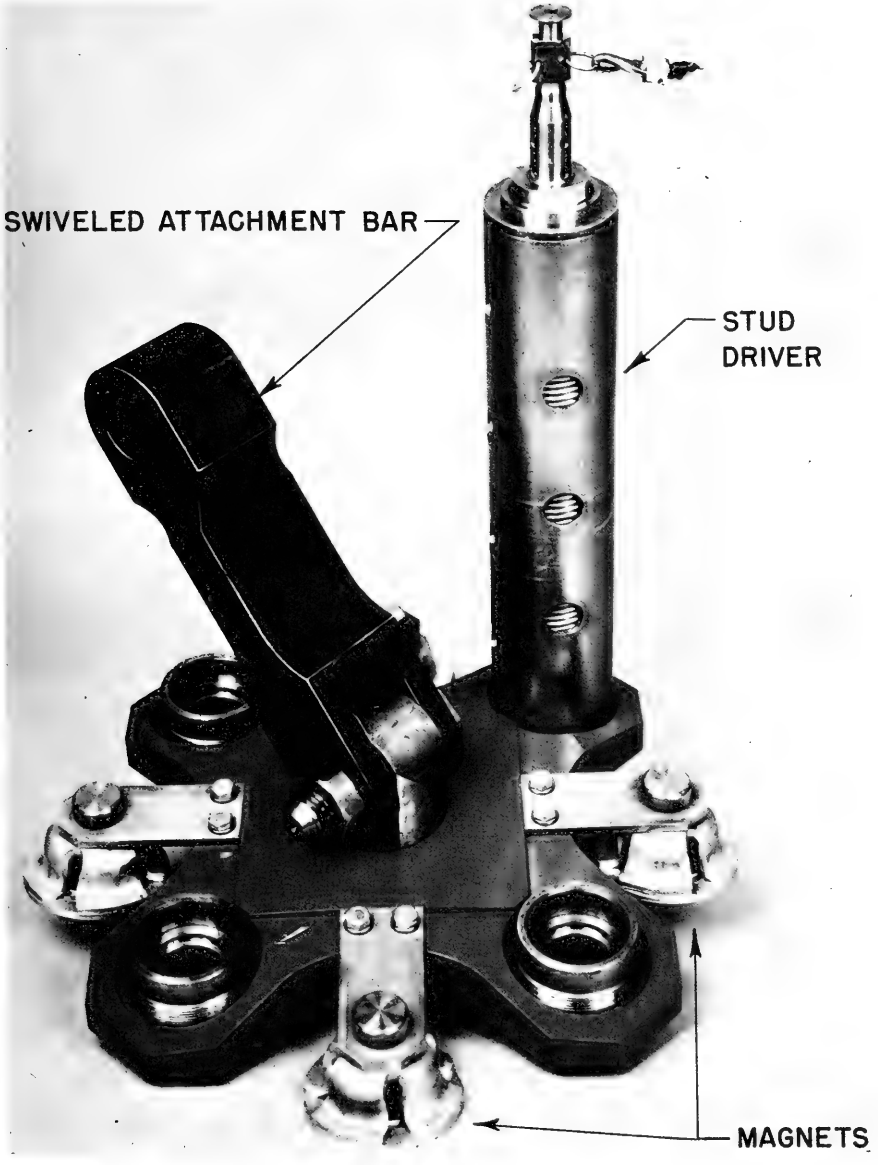

Figure 4. Salvage-Lift Padeye

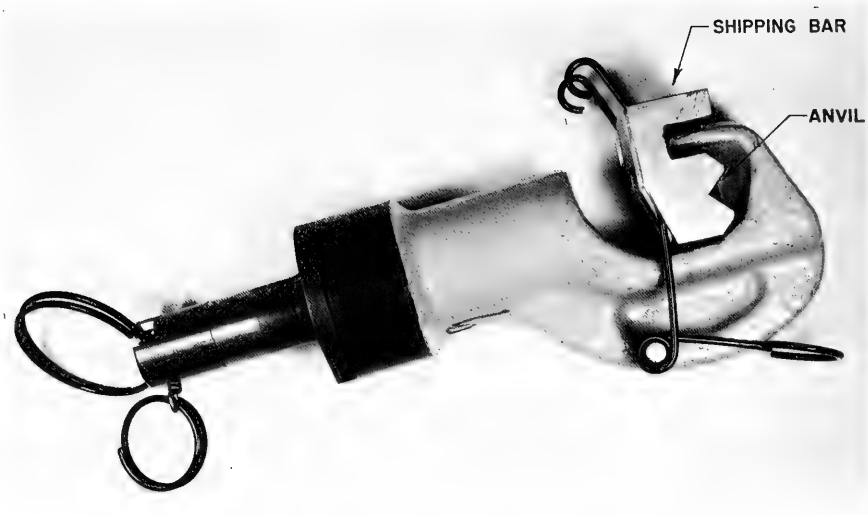

Figure 5. Cable Cutter Mk 20 Mod 0 with Shipping Bar in Place

Figure 6. Cable Cutter Mk 20 Mod 0 with 1-inch Cable in Place

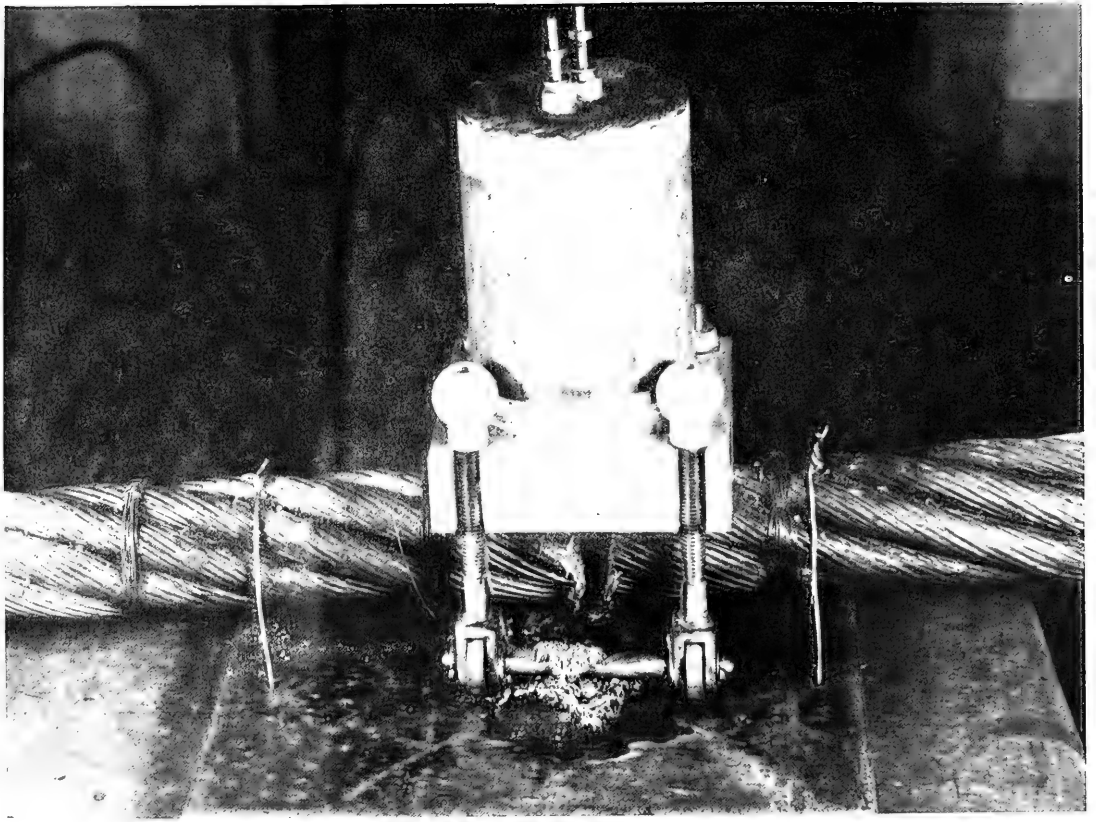

Figure 7. Pyronol Cutter with 2-inch Severed Cable

NATIONAL DATA BUOY DEVELOPMENT PROJECT
A STATUS REPORT

Captain J. A. Hodgman, U. S. Coast Guard

National Data Buoy Development Project
U. S. Coast Guard Headquarters
Washington, D. C. 20591

Abstract

In 1967 the U. S. Coast Guard was selected by the National Council to undertake the RDT&E necessary to develop the capability to implement National Data Buoy Systems. The development is based upon the composite Federal agencies' requirements, both military and civilian, for marine environmental data to the greatest degree practical.

The development of National Data Buoy Systems is predicated upon a "systems effectiveness concept" focused on the capability output - the product of the total system: data buoys, servicing ships, shore station support, telecommunications and sensors. System planning embraces the "user-producer" dialogue and the concept formulation/engineering development philosophy of the RDT&E process as a guide. The Preliminary Concept Formulation Summary document provides an outline of initial progress and plans.

The Fiscal Year 1969 program encompassed project management and systems planning and investigations associated with Concept Formulation. The in-house, contractual and cooperative activities are described. These efforts are being used as inputs to formulation of Proposed Technical Approaches (PTA) with contractual assistance as part of a long-range development plan. The systems engineering and management support teams will also contribute towards formulation of the Concept Formulation Plan (CFP) down to the work statement level, and a detailed test and evaluation program.

The development program consists of a three-pronged attack: (1) laboratory and in-situ test and evaluation program for sensors, buoys and subsystem components, (2) Pilot Buoy Network development, the concept formulation and engineering development of RDT&E networks, and (3) an exploratory development program - improvements

---

The opinions and assertions expressed in this paper are those of the author, and do not necessarily represent the views of the Commandant or the Coast Guard at large.

beyond the near-term state-of-the-art for high risk or low performance components and materials. In addition, national requirements for the U. S. Great Lakes, estuaries and Arctic will be investigated.

INTRODUCTION

In 1967 the U. S. Coast Guard was selected by the National Council on Marine Resources and Engineering Development to undertake the research, development, test and evaluation (RDT&E) necessary to develop the capability to implement National Data Buoy (NDB) Systems.

There is an urgent need for marine environmental data to further improve our scientific knowledge of the atmosphere and the oceans, depict their present state more accurately, and improve predictions of their future state. Data buoys have been shown to be cost effective and have a significant capacity to acquire the volume and quality of data required, within a variety of platforms [References 1, 2, 3]. More recently, other national and international planning activities have stressed the need for a coordinated data collection system utilizing buoys and other appropriate platforms [References 4-9]. Another recent study, the Report of the President's Commission on Marine Science, Engineering and Resources, highlights a "pilot buoy network" as a national project meriting "consideration for early implementation" [Reference 10]. It identifies the Coast Guard as the agency to develop buoy technology, develop and evaluate systems requirements, and take the necessary technical and analytical steps leading to a national capability to deploy NDB Systems. This paper summarizes the NDB Development Project's planned program and first year of progress. It should be emphasized that the program is in the conceptual stage and is working with other Federal agencies, the scientific community, interagency groups, users and the Congress to develop a course of action that will meet national needs at the least cost.

PLANNED PROGRAM

A fundamental development goal of the NDB Development Project is to deploy pilot-buoy networks by 1975. The pilot buoy networks will:

...be deployed along the continental shelf and deep oceans adjacent to the United States.

...be used to assess the reliability and effectiveness of the prototype development.

...provide data that will permit a better scientific understanding of the marine environment.

...demonstrate the economic, military, scientific and social benefits that may be derived from operational NDB Systems.

The development program is based generally on a three-pronged plan of attack (Figure 1):

(1) First, a thorough assessment of buoy and sensor technology. Concurrent laboratory and in situ testing and evaluation of sensors and support hardware will be conducted. Platforms in the oceans, together with mobile communications equipment, will be used for in situ testing of components such as sensors, moorings, telemetry, and buoy platforms. This effort will provide performance information for correlation with laboratory test results.

(2) Second, a program of applied research and exploratory investigations. This phase will be directed at achieving improvements beyond the near-term state-of-the-art for high risk or low performance components and materials. Investigations will cover items such as sensors with a minimum number of moving parts, improved protective coatings to prevent marine fouling, new materials for mooring cables, and improved power supplies. The requirements for observations in the Great Lakes, estuarial, and polar regions will also be studied. Development of biological and chemical sensors which would expand buoy system capability may also be undertaken.

(3) Finally, concept formulation and engineering development of pilot buoy networks. The objective of concept formulation is to provide the technical and economic bases for a decision to initiate engineering development. During concept formulation, cost, performance, and schedule estimates of system alternatives needed for adequate tradeoff and risk analyses will be undertaken. Design factors of major components such as sensors, moorings, power supplies, telemetry, buoy platforms, servicing ships and shore stations will be investigated along with operational and maintenance concepts. Mission and environmental variability analyses and refined requirements will be integrated with the technical development to yield realistic performance characteristics, and the technical feasibility of the systems proposed will be demonstrated. The activities of concept formulation will result in firm requirements and baseline characteristics for data buoy systems with competitive cost-effectiveness values. During engineering development, design specifications will be developed and pilot buoy networks designed and manufactured.

YEAR OF PLANS AND PROGRESS

The project has now been in existence over a year. For the first few months, the Project Office was supported by available reprogrammed funds within the Coast Guard. The primary activities centered around organization, staffing, development of system planning, programming and budgeting, and continuation of follow-on studies to amplify the initial Feasibility Study [Reference 1].

As you remember, the general Federal budget reduction in Fiscal Year 1969 precluded a full-scale start of the development program. Funds in the amount of $580,000 were reprogrammed from within the Coast Guard Research and Development appropriation to sustain the project after Congress deferred funding of the project without prejudice. With these resources we were able to perform selected activities incident to concept formulation in Fiscal Year 1969. Needless to say, the budgetary situation for Fiscal Year 1970 is still uncertain. The portion of the planned program the project will be able to execute the coming year will be determined by the present budgetary decisions and subsequent congressional action.

Despite the relatively low-level project funding to date, however, significant steps have been taken this past year. They encompass systems planning and investigations through in-house, contractual and cooperative efforts. I will briefly touch on twelve of these activities.

(1) System planning embracing the "user-producer" dialogue of the RDT&E process has been initiated. The Preliminary Concept Formulation Summary document [Reference 11] issued by the Project Office outlines the factors involved in the development task, an approach to the problem and general plans for concept formulation. It also promulgated a Tentative Specific Operational Requirement TSOR.

(2) Under contract to the Project Office, the Travelers Research Corporation has completed additional work consisting of:

...Refined national marine environmental data requirements [Reference 12].

...Computer programs for simulation and cost models [Reference 13].

...Simulation models of the operations involved in the deployment and maintenance of buoy networks [Reference 14].

...Investigations of the natural variability of pertinent marine environmental parameters and the impact on data use and performance characteristics [Reference 15].

...Cost effectiveness sensitivity studies of alternative data buoy systems, alone and in various combinations with other platforms [Reference 13].

(3) The opportunity was used to add a real-time satellite relay capability to one buoy being deployed as part of the joint Scripps Institution of Oceanography-Office of Naval Research (ONR)-Coast Guard North Pacific experiment. One of ONR's large discus buoys was fitted with VHF communications equipment to permit the relay of measured data via the NASA ATS-1 synchronous satellite. This added capability will provide side-by-side comparison of data transmitted directly by HF with data transmitted by satellite link communications.

(4) In sensor development, the efforts of the Project Office have focused on a survey of oceanographic and meteorological sensor technology. Similar review of other system components is underway. In cooperation with other Coast Guard activities interested in oceanographic sensor development, and in coordination with the National Oceanographic Instrumentation Center and the National Oceanographic Data Center, the project is currently reviewing proposals for a study to:

...Assess the state-of-the-art of oceanographic sensors.

...Formulate test and calibration standards and procedures for Coast Guard sensors.

...Establish standard specifications for hardware.

(5) A limited mooring test and evaluation program is in the planning stage; tests in the oceans will commence in the fall of 1969.

(6) Quantification of the potential benefits to users which will be achieved from improved marine environmental information is recognized as a difficult task. Not only must one determine and relate the necessary increased volume and quality of data, with appropriate spatial coverage, to improved levels of environmental prediction, but a second step is also necessary--that of relating the net worth of the improved environmental predictions and data to benefits to the users. And finally, the appropriate mix of sensors and platforms for the optimum environmental system must be determined. Much of this work is beyond the scope of the Project Office. However, initial efforts impinging upon NDB Systems development have been undertaken. For

example, in-house efforts have resulted in survey and documentation, in a preliminary fashion, of the extensive need for and use of improved environmental information by the construction, offshore oil, and gas industries and by marine military (naval) activities. Similar efforts are also being directed toward the fisheries industry. In addition, the Project Office has recently contracted with the Resource Management Corporation of Bethesda, Maryland, to assess the benefits to transportation (air, land and sea) that will accrue from improved environmental prediction. Similar in-depth quantitive studies are needed for all major functional users of improved environmental information.

(7) Six high-frequency radio bands have been set aside for oceanographic use on an international basis. The Project Office is funding and coordinating a study effort by the Environmental Science Services Administration's (ESSA) Institute of Telecommunication Sciences to recommend the optimum utilization and allocation of this limited resource.

(8) Earlier this month the Project Office sponsored a Scientific Advisory Meeting at the Coast Guard Academy, New London, Connecticut. Attendance included more than 30 leading scientists working in the field of the marine environment. The experience and guidance of this knowledgeable group will provide an important contribution to the development and use of NDB systems. Their interest in integrating scientific experiments into pilot buoy networks and operational systems is particularly noteworthy.

(9) Ship support for the major Federal government data buoy programs has provided valuable experience and information on buoy handling and servicing problems.

(10) As in any other major development effort, extensive coordination with potential users, the scientific community and industry is considered necessary and is being effected on a continuing basis. In addition, the Project Office is working with other Federal agencies in developing United States' positions for implementing "ocean stations" for data acquisition, and in international sharing of the data and resulting products. These activities are coordinated internationally through the Integrated Global Ocean Station System (IGOSS) Working Group of the Intergovernmental Oceanographic Commission (IOC) and the World Weather (Watch) Program (WWW) of the World Meteorological Organization (WMO).

(11) In the areas of alternative technical approaches and cost-effectiveness analyses, two major in-house studies have been undertaken. The first contains substantial elements of a proposed technical approach (PTA) for data buoy network development in the deep ocean and coastal areas, considering only data

buoys with an optimum capability. The second study compared alternate levels (vertical) of sensing capability with costs associated with achieving the postulated capability. The latter results indicate that systems incorporating advanced technology are significantly more cost effective than systems based on existing capability. The extent of systems implementation should not alter this relationship. However, there does not appear to be a clear cut differentiation among the various levels of capability based on cost-effectiveness alone. Therefore, systems planning should incorporate flexibility during the early development phases. These study efforts will be used, in conjunction with contractual support, to develop a proposed technical approach.

(12) Through competitive selection, the Project Office has contracted with the Systems Management Division, Sperry Rand Inc., for system engineering and project management support. Sperry Rand is now assisting the Project Office in documenting the proposed technical approaches as part of a long-range development plan. The work will include, in more detail, a concept formulation plan down to the work statement level and a test and evaluation program.

FUTURE PLANS

The scope of future plans will depend upon the level of funding authorized. It is anticipated that the Fiscal Year 1970 program will continue mission and systems engineering analyses, initiate a program of sensor tests and development, and investigate and test design factors for buoy hulls and moorings. Additional important work, however, needs to be accomplished. System performance requirements must be defined more accurately to permit improved system engineering analyses, and reliability and maintenance concepts must be investigated in detail as part of the systems engineering effort. The initiation of sensor development and a testing program are critical first steps in pilot-buoy network development. Buoy hull and mooring design factors are needed now, due to the extensive interaction of these two components with other segments of the system. The efforts of Fiscal Year 1969 will form the basis for selection of the critical activities to be carried out in 1970.

CONCLUSION

The development of NDB Systems is difficult, time consuming and costly, even using the experience of related programs. Yet all initial analyses indicate that the benefits which should be derived from improved understanding and prediction of the global environment will exceed costs by a large margin. Near real-time synoptic information from the ocean areas of the world is essential to improved understanding and prediction of the environment, and buoys are a cost-effective approach to obtaining that

information. For this reason, the Coast Guard project to develop the capability to implement national buoy networks is an important part of the United States' marine sciences program. The demonstration of the ability to operate limited networks in the oceans, to solve scientific problems and derive economic, military and social benefits from them, is a major development goal. I anticipate buoys of more than one class or capability. It is probable that following the development program operational systems will be deployed in oceans adjacent to the United States where national benefits will be greatest and in nationally sponsored environmental experiments. It is clear, however, that each step in development and implementation must be justified, and the potential benefits defined, to assure that limited national resources are effectively utilized.

The development program requires coordination with similar programs involving data communications, processing and archiving systems, as well as compatibility with international systems. Through such coordination and a systematic approach to development, the Coast Guard will assure that NDB Systems will be developed that are responsive to the composite national requirements.

REFERENCES

1. Aubert, E. J., "A Summary of the Study of the Feasibility of National Data Buoy Systems", TRC Report 7485-286, USCG Contract TCG-16790-A, The Travelers Research Center, February 1968 (AD 665314).

2. Jenkins, C. F., E. J. Aubert, W. R. B. Caruth, L. H. Clem and R. G. Walden, "A Cost Effectiveness Evaluation of Buoy and Non-Buoy Systems to Meet the National Requirements for Marine Data", TRC Report 7485-274, USCG Contract TCG-16790-A, The Travelers Research Center, September 1967 (AD 664619).

3. Jenkins, C. F., A. Thomasell, Jr., D. B. Spiegler and G. M. Northrop, "Cost Effectiveness Sensitivity of National Data Buoy Systems: An Essay", TRC Report 7493-336, USCG Contract DOT-CG-82504-A, The Travelers Research Center, December 1968(AD 682516).

4. "Federal Plan for Marine Meteorological Services" (MARMET), Office of the Federal Coordinator for Meteorological Services and Supporting Research, U. S. Department of Commerce/Environmental Science Services Administration, Report OFCM 68-4, May 1968.

5. "Federal Planning Guide for Marine Environmental Prediction (MAREP)", Ad Hoc Task Group, Committee on Oceanographic Exploration and Environmental Services, National Council on Marine Resources and Engineering Development, January 1969.

6. "World Weather (Watch) Program Plan for Fiscal Year 1970" (WWW), President's Report to Congress, March 1969.

7. "Integrated Global Ocean Station System (IGOSS)", The Plan and Implementation Programme-Phase I, United Nations Educational Scientific and Cultural Organization, Intergovernmental Oceanographic Commission, Working Paper (Unpublished), January 1969.

8. "Summary Report, Working Committee for an Integrated Global Ocean Station System (IGOSS)", 2nd Meeting, World Meteorological Organization, Geneva, 24 February 1969, United Nations Educational Scientific and Cultural Organization, Intergovernmental Oceanographic Commission (Unpublished), March 1969.

9. "An Oceanic Quest", The International Decade of Ocean Exploration (IDOE), Joint Study by the National Academy of Sciences and National Academy of Engineering for the National Council on Marine Resources and Engineering Development, February 1969.

10. "Our Nation and the Sea", A Plan for National Action, Report of the Commission on Marine Science, Engineering and Resources, January, 1969.

11. "Preliminary Concept Formulation Summary for National Data Buoy Systems", National Data Buoy Development Project, U. S. Coast Guard Headquarters, Wash. D. C., October 1968 (AD 678696).

12. Clem, L. H. and G. M. Northrop, "Applicability of National Data Buoy Systems to Refined National Requirements for Marine Meteorological and Oceanographic Data", Vol. I & II, TRC Reports 7493-332a & b, USCG Contract DOT-CG-82504-A, The Travelers Research Center, October 1968 (AD 682512 & AD 682513).

13. Davis, E. L., B. J. Erickson and E. R. Sweeten, "Computer Programs for National Data Buoy Systems Simulation and Cost Models", TRC Report 7493-333, USCG Contract DOT-CG-82504-A, The Travelers Research Center, October 1968 (AD 682514).

14. Northrop, G. M., "An Analysis of Cruise Strategies and Costs for Deployment of National Data Buoy Systems", TRC Report 7493-337, USCG Contract DOT-CG-82504-A, The Travelers Research Center, November 1968 (AD 682517).

15. Jacobs, C. A. and J. P. Pandolfo, "Characteristics of National Data Buoy Systems: Their Impact on Data Use and Measurement of Natural Phenomena", TRC Report 7493-334, USCG Contract DOT-CG-82504-A, The Travelers Research Center, December 1968 (AD 682515).

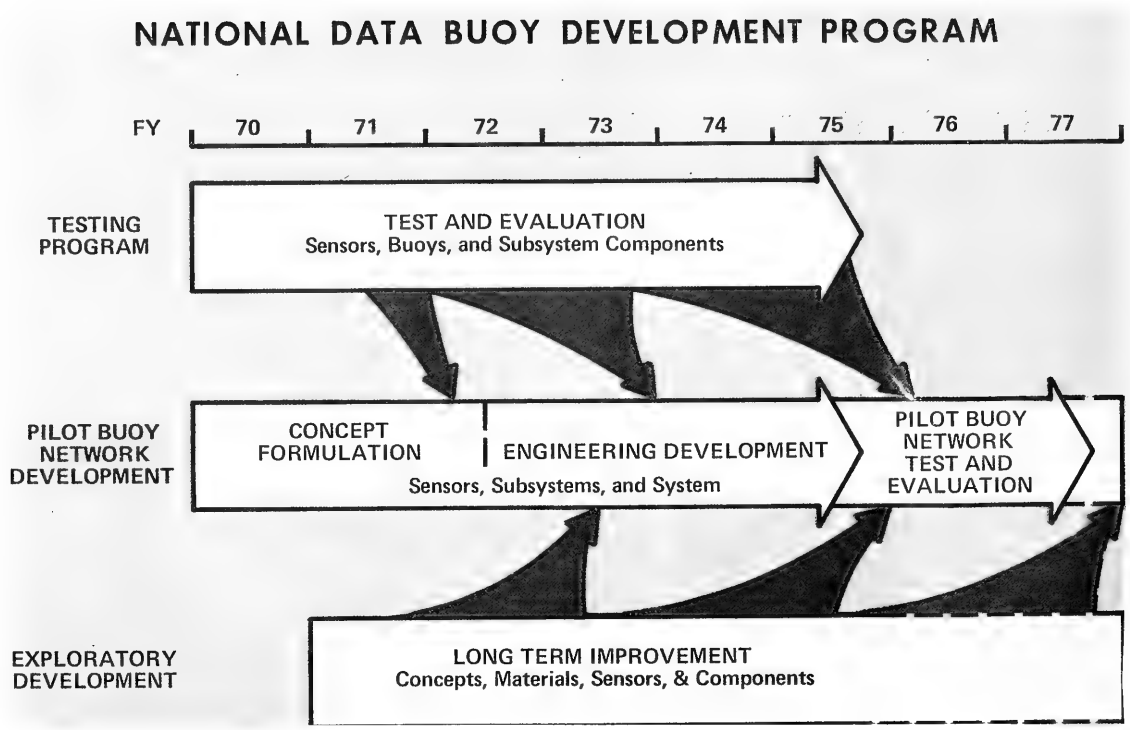
NATIONAL DATA BUOY DEVELOPMENT PROGRAM
FY
70
71
72
73
74
75
76
77
TESTING PROGRAM
TEST AND EVALUATION
Sensors, Buoys, and Subsystem Components
PILOT BUOY NETWORK DEVELOPMENT
CONCEPT FORMULATION
ENGINEERING DEVELOPMENT
Sensors, Subsystems, and System
PILOT BUOY NETWORK TEST AND EVALUATION
EXPLORATORY DEVELOPMENT
LONG TERM IMPROVEMENT
Concepts, Materials, Sensors, & Components

Figure 1

OCEAN ENGINEERING RANGE, CAPABILITIES AND LIMITATIONS

Howard R. Talkington
Head, Ocean Engineering Department
Naval Undersea Research and Development Center

The Naval Undersea Research and Development Center's NUC mission is "to conduct a program of warfare analysis, RDT&E systems integration, and fleet engineering support in underseas warfare and ocean technology." One of the Center's functions under this mission, to "conduct...development and operation of instrumented ocean RDT&E ranges," involves the following tasks:

a. Provide simulation, test and evaluation facilities for ocean technology and ASW systems, as appropriate, including support for government, university, and industry ocean-technology programs.

b. Conduct research, development, test and evaluation on specific items contributing to ocean technology and underseas warfare.

However, with the increase in developments in the field of ocean engineering (defined as noncombatant undersea systems), sea test facilities and instrumentation requirements have multiplied. The sea off Southern California, near the Navy owned San Clemente Island (SCI), has been developed into an Ocean Engineering Range by the Naval Undersea Research and Development Center. Thus, the mission of the Range, which was developed and is continually used for underwater weapons development tests, has been expanded to include support for research, development, test, and evaluation operations of noncombatant ocean engineering systems (search, rescue, salvage, and man-in-the-sea, for example).

This paper deals with the Ocean Engineering Range's past and present objectives (including instrumentation and special test equipment), its use in the past, its current capabilities and limitations, and near-term and long-range plans for its further development.

The Island, 21 miles long and 1.0 to 4.5 miles wide, lies approximately 55 nautical miles south of Long Beach, California (Fig. 1). It has relatively smooth terrain with steep cliffs along the eastern shore (mainland side) rising sharply to a main ridge and tapering off in terraces to beaches on the western shore

(Fig. 2), the seaward side. The maximum elevation on the island is 1962 ft at Mount Thirst.

The San Clemente Island area offers an environment, climatic and underwater, totally amenable to a wide variety of ocean science and engineering experimentation. There, equable temperatures (~80°F high and ~45°F low) and calm waters prevail approximately 300 days a year. As a result test programs which require surface support ships and good visibility can be accomplished with a minimum of lost time.

The water surrounding SCI is relatively clear, with good underwater visibility to a distance of 75 ft at 100 ft depths from January through March. Increased marine life and other suspended material during warmer months generally limit visibility to approximately 30 ft. The ocean floor near the Island is composed of smooth gray sand, primarily, with occasional rock outcrops along the underwater ridges. Water depths increase rapidly on the east side, averaging 1,800- to 2,000-ft one mile from shore, with depths to 4,200 ft available within three miles from shore, and 6,000 ft and 12,000 ft depths nearby. The slope of the ocean floor on the west side, where the depth averages only 300 ft. one mile from shore, is much more gentle.

The Ocean Engineering Range has been used for missile and torpedo programs. One missile program, SUBROC, involved the developmental and technical evaluation tests of live SUBROC missiles. These tests required extensive communications, photometric data coverage, telemetered data-recording capabilities, radio-destruct precautions (Command Flight Interruption), and numerous launch site, range length, and target condition configurations. The Antisubmarine Rocket (ASROC) weapon system was conceived, developed and tested by NUC. Firings are conducted at SCI either from shipboard within range of instrumentation sites, or from one of two permanent launch pads, depending on the type of target site. The Mk 46, Mk 44, Mk 43 Mod 0, and Mk 43 Mod 1 torpedoes have been tested at the Island. These tests were captive warshot runs, airdrops, or ASROC flights delivering free-running torpedo payloads to the target area.

Airdropping instrumented test packages into waters off the Island is a major activity involving all types of aircraft. Some programs are for the evaluation of aircraft and release mechanisms rather than the hardware being dropped. Past tests have included JATO-boosted units, free-fall units, parachuted units, torpedoes and depth bombs. Nearly all drops must be supported by photometric and telemetric data-acquisition systems.

The early emphasis at SCI on air and underwater launched missiles produced a need for facilities capable of supporting air and underwater launch programs through the research, test, and initial evaluation phases. Thus the numerous test facilities at the Ocean Engineering Range incorporate a wide variety of instrumentation to ensure full documentation for any test series. This consists of electronic, photometric, communications, oceanographic, and weather instrumentation.

The electronic instrumentation at the Island includes radar, telemetry, radio command control (destruct), correlation timing, closed-circuit television, and meteorological units. All electronic facilities, except the main telemetry station and the meteorological station, are housed in vans or trailers. This feature enables range configurations to be altered to suit any test requirement.

Telemetry (TLM) capabilities consist of RF-link receiving-demodulation-recording facilities compatible with standard Inter-Range Instrumentation Group (IRIG) carrier-subcarrier assignments. The main TLM station is situated at an elevation of 600 ft and overlooks Area "A." Closed-Circuit Television (CCTV) is used to provide range-control personnel surveillance of several functions at one time or to enable observation of events in hazardous areas. In addition, many underwater television systems (both shallow and deep submergence) have been developed by NUC and are used by various projects.

Photometric facilities at the Island are capable of recording external data and documentary coverage of any test, either underwater or above. More than 200 concrete camera pads have been constructed on the Island to accommodate any of the wide variety of photometric instruments in use. Photometric data provides a timed record of visible events, including space position versus time, as well as attitude, velocity, and acceleration of flight-test vehicles. The nucleus of the data package (space-position) is supplied by askania cinetheodolite instruments. These tracking cameras are fitted with relatively long-focal-length lens systems and operate at low exposure rates up to five frames per second (fps). Bowen cameras are preoriented to a specific point in the missile trajectory and provide highly accurate acceleration velocity and attitude data because of their greater exposure rate, 30-180 fps. Typical events covered by the Bowen cameras would include launch sequence, stage separation, and impact. Additional photometric coverage throughout a missile trajectory is provided by several types of high-speed 16-, 35-, and 70-mm cameras. The high-speed data cameras may be used as tripod-mounted, fixed instruments or may be placed on M-45 tracking mounts coupled to a variety of lenses (up to 200 in.). Underwater photometric requirements are fulfilled

by a complement of motion picture camera bells and deep-water still-photography systems. There are also facilities for same day film processing on the Island for a quick look at black and white or color films.

The communications system has several radio frequencies which are assigned for use at SCI and at companion facilities on the mainland. These frequencies are so distributed that they provide reliable long-range and short-range communications under all atmospheric conditions. On-Island communication occupies a main transmitter-receiver building at Station Peak with a backup utilized by several stations through a direct-wire link.

Available oceanographic instrumentation can provide pertinent information for any underwater test program. Among the primary equipments ready for use are Roberts' electric current meters, Savonius-type direction and velocity and recording meters, a portable precise echo-sounder, sound velocity and salimetry meters, optimal transmission meters, electronic thermistors, and oceanographic winches. Supplemental equipment includes items such as a Phleger-sediment corer and bathythermographs. Also, the SCI meteorological station is equipped for complete surface and upper air weather observation.

Now, the human element of the Ocean Engineering Range is introduced. Underwater projects at SCI that require diving service may draw upon a contingent of three officers and 24 Navy divers (including a medical diving officer and four hospitalmen) assigned to NUC. This group is based at the Long Beach Naval Station and serves requirements at Morris Dam, Long Beach Sea Range, and San Clemente Island. Personnel are rotated between the four areas as the work load requires. Military diving activities at the Island began in 1958 with the inception of Pop-Up Facility installation and have expanded ever since. Nearly 200 man-hours of underwater work are performed weekly by NUC divers in one of the largest Navy diving efforts in the United States. Diving requirements at the Island include numerous trade skills. Routine work includes periodic inspection and maintenance of sea-cable installations, inspection and replacement of underwater winch cables, maintenance of the underwater launcher complex, installation and final adjustment of underwater instrumentation, photographic work, welding and salvage, hardware search and recovery, heavy-equipment rigging, and observation of experimental submerged equipment for proper functioning. Both scuba and helmet diving capabilities and shore-based and ship-based recompression chambers are available.

Among the utility floating equipment stationed at the Island are various work barges equipped with cranes and winches and propelled by one or more diesel outboard "sea mules." Personnel transport craft and outboard work boats are also available (Table 1). Several activity vessels are based at the Long Beach Naval Station and provide range patrol and surveillance, recovery service, and other specialized functions on all NUC ranges (Table 2).

The YFU-53 is a modified LCU with a 15- by 32-ft well through the main deck equipped to handle different tasks. One task was the conducting of underwater test launchings from a submersible torpedo tube. The tube was lowered through the well to the ocean floor where the launching took place. Deep water search and recovery operations have also been conducted. A frame fitted with a mercury vapor lamp, a television camera, and recovery snare is lowered through the well to search the ocean floor. Deck compartments house electronic equipment and data recorders. Other modifications included a 6-ton capacity traveling bridge crane, four hoisting winches, and a four-point self-mooring capability.

The Acoustics Research Vessel, YFU-44, is specially equipped for underwater research. Power generators and special compartments were added to house electronic equipment. An 8- by 36-ft well, cut through the center of the main deck, permits the ship instrumentation platform which carries selected underwater equipment to be lowered to depths of 600 ft. The vessel having fore and aft winches with Danforth anchors has a two-point self-mooring capability.

All of the facilities described are still operational, but as the Naval Undersea Research and Development Center's mission indicated above there is a new and additional interest. Whereas the early emphasis at San Clemente Island was on research, test, and initial evaluation of ordnance, the present concern with ocean engineering and all its related technologies in the deep ocean environment represents a more diversified challenge.

The Ocean Engineering Range is expanding in order to provide a test range for experiments on ocean engineering components and systems for such projects as the Deep Submergence Systems Project (DSSP) and the Deep Ocean Technology (DOT) Project.

DSSP requested NUC to establish and operate additional ocean engineering test capabilities as part of the Ocean Engineering Range. These capabilities are designed to support testing required by the various systems of the DSSP Submersible Vehicles, Man-In-The-Sea (MITS), Large Object Salvage System (LOSS), now under the Naval Ships Systems Command, and Sensors and Controls.

Because of the increase in size and complexity of the underwater operations at SCI, a larger (than the YFU-53) primary range operation ship was needed. The "Elk River" (IX-501), having been recently converted from a LSMR, is capable of supporting all the test operations previously assigned to the YFU-53 in addition to some specific DSSP requirements:

1. Deep (Saturation) Diving for SEALAB and LOSS
2. Deep Submergence Rescue Vehicle (DSRV) test and evaluation
3. Deep Submergence Search Vehicle (DSSV) test and evaluation
4. LOSS test and evaluation
5. Component testing for above systems
6. Deep tethered operations

The "Elk River" (Fig. 3) is 225 ft long, 50 ft across the beam, and displaces 1,100 tons. It cruises at 7 knots and has a maximum speed of 11 knots. Maximum for range and endurance are 3,000 miles and 20 days, respectively. The crew complement is 45 (25 Navy and 20 civilian). Instrumentation and facilities will be comprehensive, including items such as tape recorders, underwater television and still cameras, and darkroom and maintenance facilities. Moreover, it has a 55- by 19-ft centerwell with sliding bottom-closure doors. The diving support compartments are equipped with the Mk II deep diving system, including two large, 4-man, deck decompression chambers (DDC), two 4-man personnel transport capsules (PTC), mixed gas stowage, diver's ready room, a station for shallow diving, and auxiliary equipment. A gantry crane is available for handling the PTC's. There is main deck space for four 8- by 35-ft instrumentation and control vans. There is lift equipment capable of hoisting the DSRV and DSSV over the stern or through the centerwell. A fully equipped frame may be lowered through the centerwell for deep search and recovery and component testing. Instrumentation cabling for depths to 6,000 ft and two traction winches with 20,000 ft capabilities are available. A dynamic positioning system is installed on the ship. The ship has a capability for a 5-point moor in depths to 2,000 ft with remote controlled mooring winches. And, finally, it has its own navigation and communications systems and maintenance facilities such as an electric shop, diver's shop, and work shop.

To conduct the ocean engineering test programs properly, certain dummy units are required for use as practice or demonstration items. These will be used when the real unit is not available or if unproven techniques make it wise not to risk the real items.

The Simulated Distressed Submarine (SDS) is a mockup of the escape trunk portion of a submarine hull and structure providing a portable mating platform for DSRV trials. The mockup includes hatches of the flush and extended types. In addition the hatch arrangements will permit DSRV mating exercises in various positions to simulate distressed submarine roll angles up to 45° from the vertical attitude.

The SDS is portable to enable positioning at various slopes and depths to 300 ft. The hatch installed on the mockup opens into a small sealed escape trunk. Most of the mockup shape is sheet metal over a light skeleton, and the surfaces near the mating hatches will be steel plate of sufficient strength to withstand loads imposed by the DSRV during mating exercises. The mockup will incorporate mounting points for the installation of television and photo cameras to observe and record DSRV mating exercises.

The Dummy Hatch (false seat) will be a weighted mating hatch from a submarine for use with sensor evaluation and other tests requiring only a hatch. The hatch will be much lighter and more portable than the simulated submarine mating surface and is intended for test and training applications to submarine collapse depth.

The Dummy DSRV, designated Handling and Training Vehicle (HTV), is an inexpensively fabricated hull that simulates the outer configuration, weight, center of gravity, and moment of inertia of the DSRV. The unit will be utilized to check out handling procedures, train rigging crews, and practice emergency recovery procedures.

A complete submarine hull will be available for placement at various depths for salvage experiments and technical tests. This will be a surveyed hull still capable of water-tight integrity and with operable ballast tanks. In addition, some parts of submarine hulls will be provided for experiments in cutting and explosive-driven devices.

Additional instrumentation is also ready at SCI. An electronic positioning system serving all of the Ocean Engineering Range operating areas will be in operation soon. LORAC Mod B development of the LORAN (Long Range Navigation) System, is a phase comparison, hyperbolic radio location system, equipped with "Course-Medium" networks for lane

identification. The system operates with a geographical accuracy ranging from ±15 ft near the base lines to approximately ±400 ft at the maximum range of 300 nautical miles. The repeatability of the system is reliable; that is, the user may relocate a previously used position with accuracy better than that stated above for geographical accuracy.

SCI and the primary Ocean Engineering Range areas are within the plot of the theoretical 25 ft accuracy, i.e., the geographical accuracy of position determination in the area east of SCI averages 15- to 20-ft (Fig. 1).

The Cable-controlled Underwater Research Vehicle (CURV) is an unmanned, tethered vehicle developed to locate and recover expended torpedoes from depths to 2,500 ft (Fig. 4). This vehicle has an acoustic location system, active and passive sonar, underwater television, photographic cameras with lights, and a hydraulic claw. This vehicle has also proved to be valuable as an underwater inspection tool, site survey instrument, and sensor test bed. As evidenced at Palomares, Spain, it can be "jury-rigged" to go deeper and to perform additional tasks such as recovering stray nuclear weapons. CURV III has a capability of operating at depths of 7,000 ft and is scheduled to be operational on the Ocean Engineering Range by the end of 1969.

Most of the DSSP test activities will be conducted in either of two test areas within the COMNUC Range. The greater number of operations will be executed along the northeastern shore of the Island. Depths vary from shoreline shallows with a smooth hard-sand bottom, to 4,000 ft and soft sedimentary bottom at the seaward edge of the area. This area will have a bottom-mounted, two-dimensional underwater positioning system, navigational transponders, and miscellaneous objects in known locations to check the accuracies of vehicle sensors. All underwater television, photometric equipment, and other instrumentation are to be portable installations to ensure maximum range versatility. The area will also contain a submarine hull and smaller salvageable objects for the Large Object Salvage System (LOSS) tests and evaluation, a complex to accommodate Man-In-The-Sea (MITS, principally SEALAB) experiments, and the Poseidon test complex. Most remaining test needs can be fulfilled by another area, a noninstrumented region to the west of the Island.

Testing of four major systems development programs (MITS, LOSS, DSRV, and DSSV) at the Ocean Engineering Range began in 1968 and will extend well into the 1970's. Each program will be able to contribute additional support for one or more of the other programs. In this way, through coordination, cooperation, and joint use

of instrumentation and support equipment the programs will make greater progress.

This year will be the first year of substantial ocean engineering testing, with particular emphasis on SEALAB III. The "Elk River" (IX-501) will be the MITS support vessel. Operations at 850- to 1,000-ft depths are relatively certain in the near future. The Man-In-The-Sea Program is a continuing effort, and one in which final capability will be dictated by the physiological and psychological limits of man himself.

The LOSS program will utilize new range installations such as the complete submarine hull and other submarine parts in the early 1970's.

Initially, the tests of the DSRV will be of the basic vehicles, but once the DSRV becomes operational it will be integrated with other elements in the rescue system. To evaluate whether the vehicle can mate in unfavorable conditions, tests will be conducted first with the new simulated hardware and finally with actual submarines configured as "mother" submarines and simulating distressed conditions. The first phase of the DSRV 1 technical evaluation tests is scheduled to begin at SCI in October, 1969, and last about 18 months. Approximately 6 months after the beginning of the DSRV 1 tests, the phase 1 tests for the DSRV 2 will start. About the time tests on the last of the six presently scheduled rescue vehicles and associated support elements are completed, the search vehicle (DSSV) testing is scheduled to begin.

By the mid-1970's elements of the Deep Ocean Technology (DOT) Project such as the Remote Unmanned Work Systems (RUWS) * and II will be ready for environmental testing at the Ocean Engineering Range.

Additionally sites are available at other U.S. Navy underwater ranges. The primary function of each of the following ranges is to measure accurately the performance of ASW systems: the Atlantic Undersea Test and Evaluation Center (AUTEC) in the Bahamas, the BARSTAR range in the Hawaiian Islands, and the Naval Torpedo Station (NTS) Keyport ranges in the northwest. Each one has an instrumented sea test area that complements the Ocean Engineering Range by offering different environmental conditions and access to many widespread Navy, industrial, and educational centers.

The requirements for the Ocean Engineering Range at SCI have expanded over the years and even greater development is seen for the future. The Range is limited by the state-of-the-art in operations instrumentation and total areas instrumented. The following are specific requirements that must be implemented in the near future:

1. Deep instrumented areas, to depths to 20,000 ft
2. Detailed bottom surveys at all depths from 100 ft to 1,000 ft and at the 5,000 ft and 12,000 ft depths for sea floor operations
3. Surface support platforms with good stabilization and position keeping capabilities for long-term deep sea operations
4. All weather surface handling for submersible vehicles
5. Precise underwater navigation systems to locate accurately bottom and in-volume instrumentation sites
6. High resolution underwater imaging systems to monitor tests
7. Additional shore support for sea operations
8. A mobile instrumented saturation diving R&D test facility
9. Additional man-rated pressure/temperature tanks for physiological and diver's equipment testing
10. Additional and larger equipment pressure/temperature cycling test tanks

To keep pace with the demands of the burgeoning field of ocean technology, a development program planned for the next 10 to 15 years covers a number of items. There is a need for a protected harbor and docking facility where technical and support craft can safely berth during inclement weather. This project includes a protective breakwater, wharf, and small craft piers. Close to the causeway-supporting preparation, maintenance, and repair of systems being tested will be constructed. In order to give proper support to the divers on the Range whose diving depths must at times exceed the limitations for natural air breathing, a mixed gas recompression chamber and equipment preparation facility must be made available. A concept to fulfill other future requirements is an underwater marine railway. This test facility

would consist of a three-rail underwater track beginning above high water and following the slope of the ocean floor to the depth of 1,000 ft. Project elements could then be tested at any depth on the continental shelf while being prepared and supported by a shore-based facility. An underwater optical bench would enable optical sources, targets, and receivers to be researched, tested, calibrated, and evaluated under controlled and monitored conditions in the ocean environment. A necessary element of the Range is the capability to track moving targets precisely in specific areas and to monitor large (10 miles by 20 miles) ocean areas. Thus, 3-D underwater tracking systems for precise coverage in a limited area and broad area coverage are planned. Also a nuclear plant for providing fresh water and electrical power has been suggested. The rest of the development program consists of supplementing, modifying, and updating existing facilities in order to handle the variety of test programs at the Ocean Engineering Range at San Clemente Island.

The development of ocean technology is now well underway. Ocean test facilities are a vital and important element in this technology. Now, these facilities are predominantly used by the Navy, but they are available to industry and the rest of the scientific community. It is not unlikely that the San Clemente Island area will prove to be the outstanding national ocean engineering test range of the future.

TABLE 1. Work Boats and Barges

TYPE	OVER-ALL DIMENSION, ft.	REMARKS	QUAN.
YD barge	142 x 58	60-ton crane, three diesel outboards, capable of moving in any direction and turning in its own length	1
YSD barge	130 x 34	20-ton crane, 2-120 HP diesel twin screw, main propulsions; compartmentized 2nd deck	1
CB barge	55 x 20	10-ton crane, 15-ton double-drum winch, and two diesel outboards	2
Pontoon work barge	35 x 15	15-ton double-drum winch with A-frame, and one diesel outboard	1
LCPL boats	36	Personnel transportation	3
Work boat	17	10-hp outboard motors	10

TABLE 2. NUC Activity Vessels

TYPE	OVER-ALL LENGTH, ft.	REMARKS	QUAN.
TRB[a]	63 and 72	Speed: 16 kt and 20 kt	3 3
AVR[b]	63	Speed: 20 kt, equipped with instrumentation vans	1
YTM 759	107	Steel tugboat, 1,200 hp, speed: 12 kt (normally used for CURV support)	1
LCM	56	TYPE 6, speed: 12 kt, equipped for Helmet Diving operations	1
LCM	50	TYPE 3, speed: 12 kt, equipped with acoustic instrumentation	1

[a]All TRB's are equipped with UHF and VHF radios, radar, fathometers, recovery booms, and winches.

[b]Similar to TRB's but not fitted with torpedo ramp or winches.

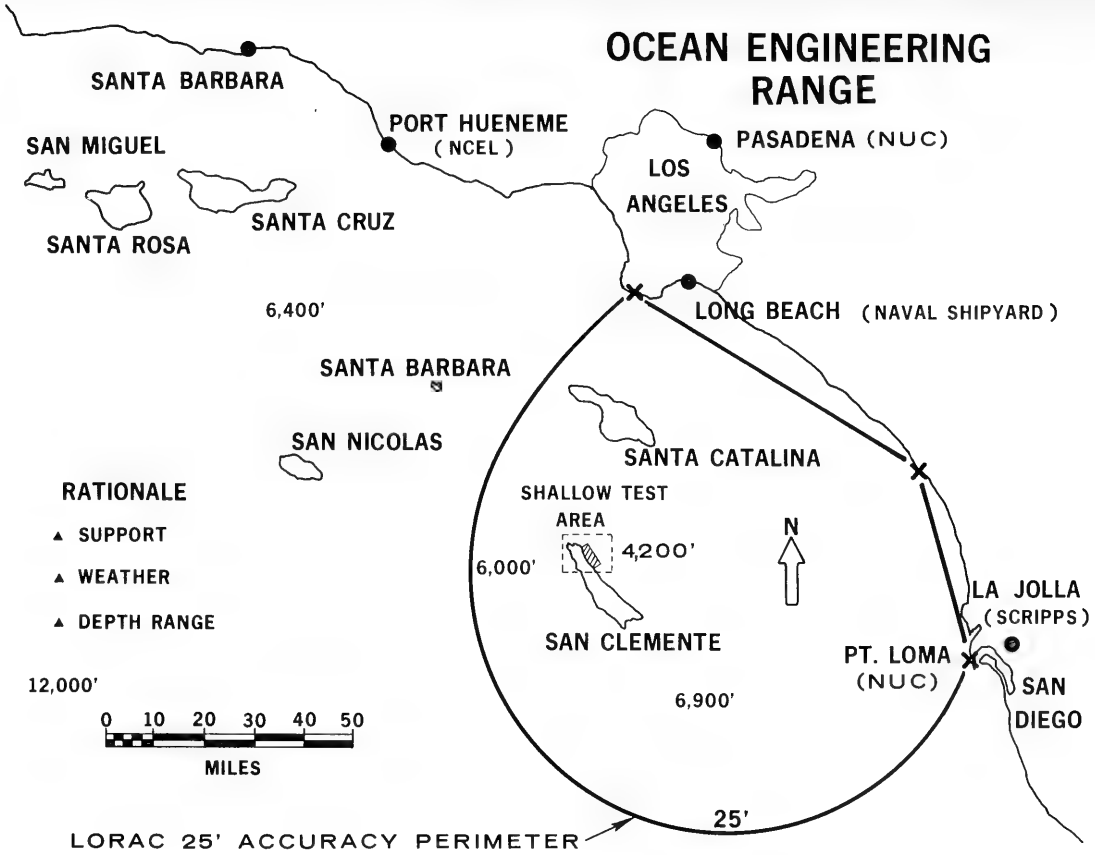

Figure 1. Location of the Ocean Engineering Range Near San Clemente Island

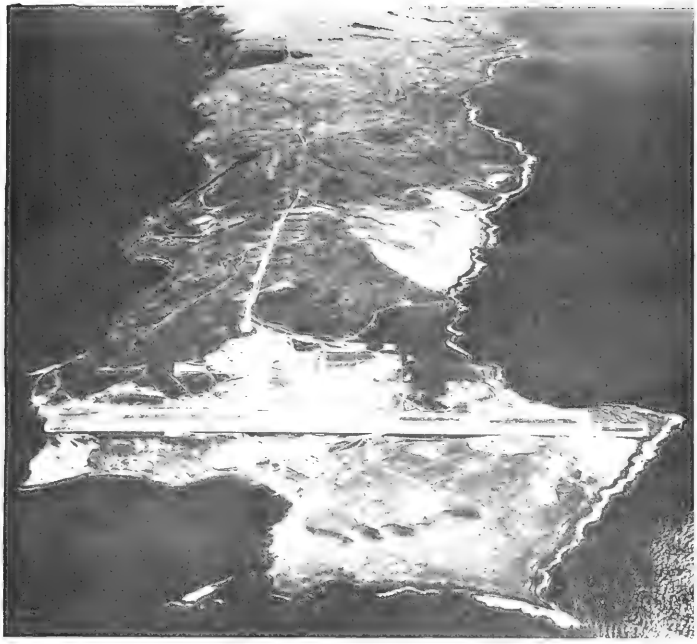

Figure 2. San Clemente Island (looking from the Northwest toward the Southeast).

Figure 3. The "Elk River" (IX 501), Primary Range Operations Ship of the Ocean Engineering Range, SCI.

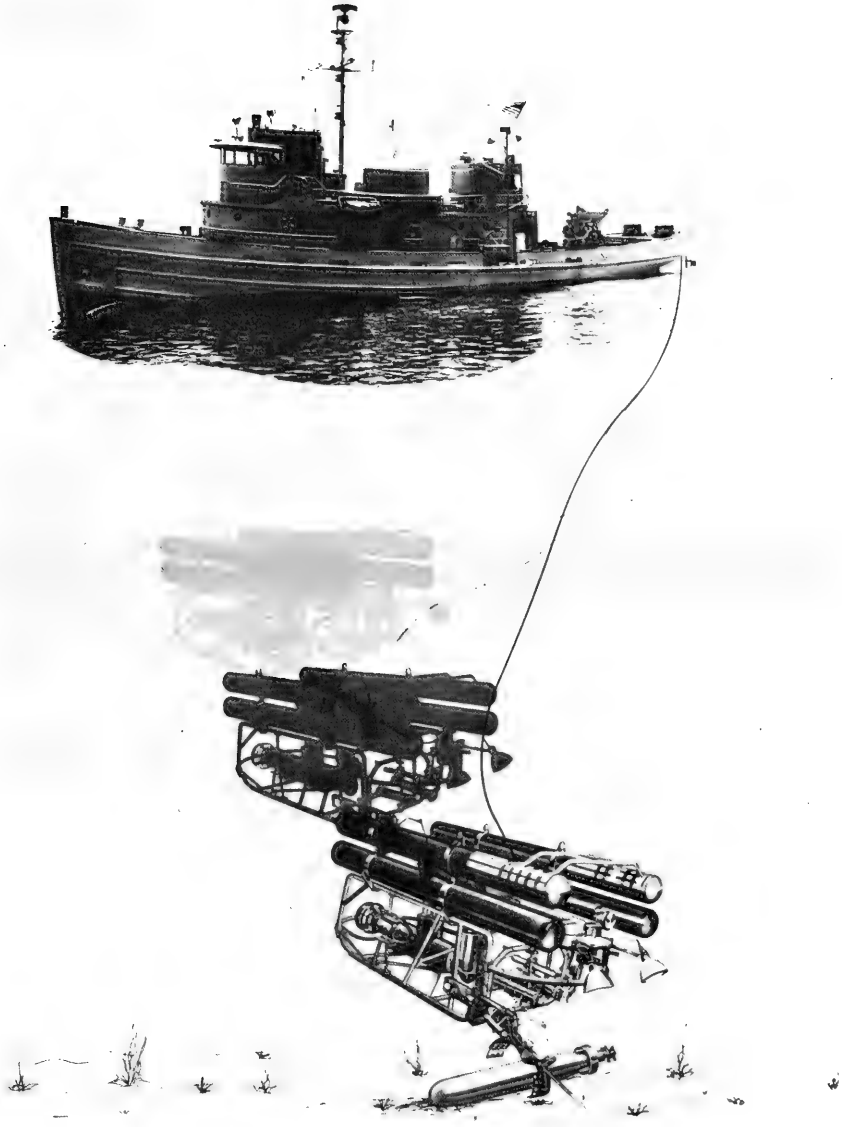

Figure 4. CURV and Support Vessel

TECHNICAL BARRIERS TO DEEP APPLICATIONS OF UNMANNED SYSTEMS

H. D. Smith
CURV Program Manager
Ocean Technology Department
Naval Undersea Research & Development Center

ABSTRACT

The Naval Undersea Research & Development Center, Pasadena Laboratory's Cable-controlled Unmanned Research Vehicle (CURV) Systems have conducted small-object recovery and other underwater work tasks to 2,500-foot depths. A 7,000-foot CURV capability will be established in FY 70. The CURV capability will be established in FY 70. The CURV capability is desired to depths of 20,000 feet. CURV vehicles, main control cable and surface support equipment all require development to enable 20,000-foot operations. Most problems are resolvable within the state-of-the-art, but there are two technical barriers to be overcome: (1) control cable development including transmission of adequate TV and control signals over a cable of acceptable size and weight, and techniques for cable support, handling, and maneuvering; and (2) vehicle bottom navigation. Approaches to overcoming these barriers such as the investigation of TV and control transmission techniques that minimize the size and weight of the cable, are discussed.

TECHNICAL BARRIERS TO DEEP APPLICATIONS OF UNMANNED SYSTEMS

INTRODUCTION

In approaching the technical barriers to deep applications of unmanned systems the problem will be discussed in terms of the most successful and advanced unmanned systems - the CURV Systems developed by the Naval Undersea Research & Development Center, Pasadena Laboratory (NUC) which have been successfully performing underwater recovery and many other work tasks for over 5 years.

The CURV systems provide a safe, reliable, and versatile underwater work capability by extending man's eyes, ears, hands, and feet to the ocean floor without placing him in the dangerous underwater environment, thus providing a useful and necessary complement to manned systems in ocean technology.

CURV SYSTEMS

Four CURV systems have been developed to date. CURV I, the system that recovered the unarmed nuclear weapon off Palomares, Spain in April 1966 from a depth of 2,850 feet, had a design depth of 2,000 feet. It has since been retired. CURV II, an improved version of CURV I with a design depth of 2,500 feet, is the operational NUC system at present. A CURV III system for 7,000-foot depths is in the initial checkout stage at NUC ranges. The last system is the NTS CURV for 2,500-foot depths which was developed by NUC for the Naval Torpedo Station, Keyport, Washington and is conducting ordnance recovery on their ranges.

SYSTEM DESCRIPTION

A CURV system consists of the vehicle, control cable, control van, support and handling equipment, and the support vessel. A CURV vehicle includes sensors, propulsion, controls, and actuators mounted on an open frame for easy maintenance access. The sensors include active and passive sonar, television (TV) and lights, 35 mm still camera and strobe lights, compass, altimeter, depthometer, and vehicle locator. The

vehicle propulsion is supplied by three 10 Hp, 440 VAC, three-phase induction motors. The hydraulically-operated actuators include pan-and-tilt units on which are mounted the TV, 35 mm camera, strobe, and spotlight; and a tool arm assembly with six motions in which a claw, hook, grapnel, snare, scoop, or other tool can be used.

A CURV system control cable assembly includes the power and instrumentation cable, a nylon support line, and cable floats. The portable control van houses the control console and topside electronics. The console has TV, sonar, locator, compass, altimeter, and depthometer displays and vehicle controls. Support and handling equipment on-board the support vessel includes a trainable over-the-side tracking hydrophone, 100 KVA generators, power conversion equipment, and handling gear such as the articulating vehicle crane and support line winch. The support vessel currently used for the CURV II system operations is the Navy Yard Tug Medium (YTM)-759.

A new support vessel has been developed for CURV III operations. This vessel, the YFNX-30, is equipped with cycloidal propulsion units and is larger and more seaworthy than the YTM-759 in order to meet the harsher requirements of 7,000-foot operations.

TYPICAL CURV III OPERATION

The CURV III system will utilize the same basic operational procedures as CURV II when it becomes operational in FY 70. In typical operations CURV III will be seeking to recover an object or perform work in the vicinity of a cooperative target; i.e., a target equipped with a pinger or beacon. The YFNX-30 will hold position over the target. The CURV III vehicle, which is approximately 10 pounds positively buoyant, will be swung over the side using the crane and powered to the bottom. As the vehicle descends, the cable will be payed out and the nylon support line tied to it by hand. The first 1,000 feet of the cable will be made neutrally buoyant with floats to enable vehicle maneuvering freedom. The vehicle's passive sonar will be used to home the vehicle in on a pinger-equipped target. The support ship will be moved toward the target if the buoyed portion of the cable is not long enough to reach the target area.

During the final 300 feet of horizontal approach, the active sonar will be used to determine the location, attitude, and configuration of the target. At close range TV will be used to classify the target and conduct the work task at hand. In the case of recovery this will involve maneuvering the vehicle close to the target and attaching the claw or another tool. Then,

if the object is more than 150 lbs, the vehicle will swim to the surface with the target in the claw. If the object is more than 150 lbs, vehicle ascent will be aided by pull on the nylon support line. If the target is more than 500 lbs, the claw will be ejected and recovery of the target and claw made from the surface by a winch using a separate line previously attached to the claw.

OTHER OPERATIONS

While CURV systems have been used primarily for ordnance recovery, many other types of operations have been performed that illustrate the potential that exists for CURV systems to attain the goal of performing many types of useful underwater work at 20,000 feet. Other operations have included bottom surveys, biological and bottom sampling, underwater installation inspections, monitoring of bottom coring and drilling operations, and small area searches. CURV II and CURV III are expected to add other capabilities in the near future, including in-situ oceanographic measurements, bottom mapping, and bottom coring operations.

CURV GOALS

The goal of the CURV program system development has always been twofold: (1) to conduct CURV operations at 20,000 feet, and (2) to advance underwater work technology as much as possible in the achievement of that 20,000-foot capability.

The immediate goals of the CURV program are to continue to operate CURV II to develop CURV capabilities, to demonstrate a CURV III recovery capability in December 1969, and to have CURV III fully operational by July 1970. The next step is the development of a CURV system for 20,000-foot depths, to be known as CURV IV, which will be based on CURV III.

TECHNICAL BARRIERS TO 20,000-FOOT OPERATIONS

At this point in CURV systems development, the technical barriers to extending the CURV capability to 20,000 feet can not be precisely defined until CURV III is operational, some operational experience has been acquired, any new problems isolated, and a firm CURV IV concept generated. Some of the major problems, however, have been determined in the course of CURV development because of the ultimate goal of 20,000-foot operations. Many CURV III components are already designed to operate at

20,000 feet; and some of them including the main cable connector, tool drive assembly and claw, altimeter, compass, sonar, and 35 mm still camera are appropriate for use on CURV IV. Other CURV III components such as the buoyancy unit, hydraulic power package, and propulsion system are presently designed to operate at 20,000 feet, but may be altered or replaced to improve reliability or increase versatility in the CURV IV system.

The other components which are needed to make up a CURV system are not, in their present form on CURV III, designed for operation at 20,000 feet. Some of these such as the small cables and connectors, pressurized electronics, pressure housings, frame, and lights require development, but they will probably not constitute technical barriers, since state-of-the-art equipment and techniques exist that can be adapted to CURV IV requirements.

After eliminating the components which are good to 20,000 feet, and those which can be developed within the current state-of-the-art, we find there are two major technical barriers to CURV IV presently anticipated: (1) the main cable including transmission, support, handling, and storage and (2) vehicle bottom navigation.

The technical barriers that the cable and bottom navigation developments present to the deep application of unmanned systems will be described below in detail to delineate problems and interfaces of development, to give anticipated approaches, and to postulate the chances of overcoming the technical barriers.

TECHNICAL BARRIER: CABLE TRANSMISSION, SUPPORT, HANDLING, AND STORAGE

To establish the CURV capability at 20,000 feet, the control cable must house the conductors necessary to transmit approximately 30 KVA power to the vehicle, receive TV signals from the vehicle, transmit control signals to the vehicle, and transmit and receive other miscellaneous power and sensor signals. In addition the cable must have the proper insulation, be nonhosing (water-blocked) and have a tough yet flexible outer jacket. This can be accomplished in the present state-of-the-art only with a cable that is larger in diameter and heavier than on CURV III. The size and weight of the cable are crucial to system performance because of their effect on support, handling and storage. At this point it is not certain how large nor how heavy the cable can become, but it is obvious that a significant change has taken place between the 2,500-foot CURV II cable and the 7,000-foot CURV III cable. The diameter has grown from 1-1/4

inch to 1-1/2 inch, the in-water weight has increased from 0.5 lbs per foot to 0.6 lbs per foot, and the handling, support, and storage problems have been compounded by the substantial increase in length. This increase in diameter is important not only because of the support, handling and storage problems, but also because of drag considerations during operations. During a typical operation the support vessel must move the entire length of cable through the water; as the cable becomes larger and heavier the drag problem grows exponentially. This is due not only to the increase in cross-sectional area of the cable but also to the increased diameter of support members.

Since the CURV IV cable will be three to four times as long as the CURV III cable, the problem grows even more acute and the size and weight must be kept to absolute minimums.

Based on past CURV experience, it is assumed that the size and weight of this cable required for CURV transmissions and the interfaces in support, handling and storage will establish a technical barrier. A more detailed discussion of each aspect, the problem and the expected results is given below.

TRANSMISSION CONSIDERATION

As was pointed out earlier there are several aspects to the cable transmission problem, namely Power Transmission, TV Transmission, and Control Signal Transmission.

Power Transmission

The first problem is the transmission of approximately 30 KVA of power to the vehicle. It is desirable to separate the main power from the instrumentation power; therefore, approximately 27 KVA needs to be transmitted separately from the 3 KVA instrumentation power. In order to transmit the 27 KVA of main power and the 3 KVA of instrumentation power, it is necessary to utilize several large conductors. A preliminary study on optimizing power utilization for CURV IV indicated that if a transmission voltage of 1300 V were used to minimize line loss and provide adequate regulation, and a central vehicle power source were developed to take advantage of all available power, it would take nine #9 wires to transmit the 30 KVA.

TV Transmission

The second aspect of the transmission problem is the necessity to transmit near-real time TV pictures from the vehicle to the surface. This problem is the hardest to solve and the most difficult to assess of the cable problems. The number and size of coaxes required to transmit the TV can significantly affect the size and weight of the cable.

CURV III has three RG-59-type coaxes (0.2 inch in diameter) to transmit signals from the two TV's over 8,000 feet of cable. To transmit without signal attenuation, two comparable TV signals over 26,000 feet of cable will require a significant increase in size of the coaxes used. This increase in turn would radically increase the size of the control cable. The ways of minimizing the size of the coax are to accept slow-scan TV, accept less picture quality, or develop new TV transmission techniques. A near real-time picture is needed; the 20,000-foot goal includes the capability to do real-time work, making slow-scan techniques unacceptable. It is not obvious what quality of picture is needed. The first step, then, is to define the magnitude of the problem by determining what picture quality is required and what attenuation and interference will be encountered in various coaxes.

The quality of picture that is acceptable is important because it determines the amount of attenuation that can be accepted. Since attenuation is a direct function of the size of the coax, if less picture quality is acceptable, smaller coaxes can be used. For example, in all coaxes the high frequencies are attenuated more rapidly than the low frequencies. Attenuation of the high frequencies results in less resolution, the picture becomes blurry and the outline of objects is lost. To get 600 line resolution requires a bandwidth of 8 MHz; whereas if only 400 line resolution is needed, the bandwidth is only 5 MHz. If 400 line resolution is acceptable, it might therefore be possible to use a coax that provides only 5 MHz of usable signal after attenuation, rather than going to a larger coax that provides the full 8 MHz after attenuation.

How much effect reduced picture quality will have on the cable design, of course, depends on the amount of attenuation. To get a feel for the magnitude of the attenuation problems, an analysis was conducted assuming transmission over a RG-11/U coax, which is approximately 0.4 inch in diameter. It was found that regardless of equalization techniques (amplification of signal directly proportional to frequency) the maximum amplitude of the received signal at the surface was too far below the main power voltage (approximately 120 db below) to prevent main power interference. Both pre-equalization and post-equalization of the signal were studied. It

was also discovered that with pre-equalization, the lower frequencies are lost when an attempt is made to recover them at the surface. When post-equalization is used, the amplifier input noise is too close to the received signal level (amplitudes are equal at approximately 3 MHz).

Using the results of the analysis and assuming that some degradation of picture quality is acceptable, it appears that it might be possible to get an acceptable TV picture with a 0.4 inch coaxial cable, if optimized equalization techniques are used; but it is quite unlikely that the proper power voltage-isolation can be attained.

The TV portion of the cable transmission aspect of the cable technical barrier will be more precisely defined by (1) conducting a more thorough analysis of different conductors and various equalization techniques, (2) conducting empirical tests on cable segments to adequately define attenuation characteristics and power line interference, and (3) conducting empirical tests to define an acceptable picture for CURV type operation. It is anticipated that once this is done an acceptable transmission system can be specified using state-of-the-art hardware; however, it is possible that new TV techniques will have to be developed to solve this transmission problem.

Control and Sensor Signal Transmission

The third aspect of the transmission problem is the necessity to transmit control signals to the vehicle and receive the signals from the sensors on the vehicle other than the TV. This is presently accomplished by using a myriad of small conductors. Since these small conductors are normally used instead of fillers when making up the control cable, it is difficult to assess the need of combining these signals into a few larger conductors until the power and TV conductors have been defined; but it is highly probable that combining these signals will result in an optimum weight and size of the cable. Making these improvements also has the desired advantage of increasing the system capability, since more control functions can be made available and more signals from the vehicle can be transmitted.

TRANSMISSION SUMMARY

When the requirements of insulation, ruggedness, strength, flexibility, and nonhosing characteristics are added to the transmission needs for nine power leads, three TV coaxes, and a number of control conductors, the possible growth of the cable size and weight becomes a distinct possibility.

This technical barrier is not unlike technical barriers which have been overcome in past CURV programs. NUC's approach will be to conduct analytical studies, empirical tests, and hardware evaluation programs to adequately define this barrier and obtain a minimum size and weight for a cable to meet all CURV transmission needs. Results from these studies will be integrated into the results from the cable support, handling, and storage studies, and the technical barrier will be solved.

SUPPORT, HANDLING, AND STORAGE CONSIDERATIONS

The second aspect of the cable technical barrier is defining just how large and heavy the cable can become without seriously hampering support, handling and storage.

Support

All CURV cables to date have had both inner strength members and the nylon support line. Factors such as the stretch of nylon under weight, diameter of nylon line required, and the weight and size of a sufficient inner strength member make these methods undesirable at 20,000 feet. It is important to note that even if the cable for the 20,000 foot system were to be the same size and weight as the present CURV III cable, the system could be unacceptable from a support standpoint. For example, the CURV III cable weighs 0.6 pounds per foot in water and, if it is assumed that approximately 26,000 feet of cable is needed for the 20,000-ft system, then the cable net weight would be 15,500 lbs. The support member would actually have to support a load considerably in excess of 15,500 lbs, since it must also withstand the dynamic forces built up by the action of the sea and support vessel. If nylon line were to be used, the line would be larger than the 1 inch diameter line used on CURV III, which has a working capability of approximately 10,000 pounds. An adequate nylon support member could be designed, but it would be large and cumbersome. The support member could also be wire rope, intermittent buoyancy could be provided along the cable with adequate internal support, or a combination of all these techniques could be used.

Regardless of the method of support used, dynamic analyses will be performed to determine the forces caused by the sea and the effect on entire system performance when the cable is moved from one location to another with the cable out.

Handling and Storage

The cable and its support system must also be handled and stored. CURV systems cable handling in the past has been done manually, including feeding the cable, tying the nylon line to the cable, retrieving it, and storing it. This was possible because the size, weight, and length of cable and time involved was not excessive; however, because of these considerations, handling and storage methods may even have to be modified for CURV III operations to 7,000 feet. For CURV IV, as the cable size grows and support systems other than nylon are considered, the handling and storage problems grow. Sophisticated hardware may have to be developed just to maintain deployment and retrieval rates similar to CURV III. And, for a 20,000-foot CURV IV system, these deployment and retreival rates may not be adequate. In any case, it is probable that some type of semi-automatic or automatic system will have to be employed. The approach NUC is taking now is to develop cable and support line winches, brakes, and storage reels. While some of these items exist in the state-of-the-art, an integrated operational handling system of this type is not available.

SUPPORT, HANDLING, AND STORAGE APPROACH

To adequately define the technical barrier and eventually solve it, both support and dynamic studies and handling and storage studies will be conducted. The various means of supporting the cable and possible specialized equipment will be included in the studies. The outcome of the investigation will be tradeoffs in equipment pointed at defining the practical and maximum cable size limit. The cable support, dynamics, and handling and storage requirements for different sizes and weights of cables will be studied, and the cable size and weight tradeoffs will be defined.

The results will be integrated with the transmission consideration and the technical barrier will be defined. These studies will also help solve the technical barrier by indicating proper approaches, defining equipment capabilities, determining system tradeoffs, and establishing necessary performance criteria.

TECHNICAL BARRIER: VEHICLE BOTTOM NAVIGATION

The vehicle botton navigation technical barrier has two parts: Operational Navigation and Precision Bottom Navigation.

OPERATIONAL NAVIGATION

Operational Navigation is knowing the location of the CURV vehicle with respect to the support vessel accurately enough to allow the vehicle to operate within the radius of the buoyed portion of the cable or "whip." If the vehicle attempts to move beyond the length of the whip cable, it begins to pull a catenary in the main cable, which hangs vertically from the support vessel. The vehicle does not have enough power to do this, and the vehicle loses all maneuverability. In fact, if the support vessel happens to be drifting in the other direction, the vehicle will be pulled off the bottom and out of the work area. To prevent this, the location of the vehicle with respect to the support ship must be known, so if the vehicle begins to utilize all of the whip cable, it can be determined how far and in what direction to move the support vessel to give the vehicle added cable for maneuvering.

Present CURV systems utilize a directional hydrophone which is lowered over the side of the support vessel to track the vehicle. This hydrophone can be trained in azimuth or tilted. The hydrophone listens for a 37.5 kc pulse which is being emitted from the vehicle.

This technique for determining vehicle location is definitely limited to shallow water work since the angle between the support ship vertical reference and the vehicle becomes very small as the depth increases. For example, at 20,000 feet with a 600-foot whip, the angle is only 1.5°.

It is anticipated that an operational navigation system can be installed on the CURV IV support vessel, but at present no system is in operation which meets the CURV needs. There are, however, equipments which probably could be modified, installed, and evaluated to meet the 20,000-foot CURV needs. A short base-line system, one in which several hydrophones are mounted on the support vessel, as opposed to a long base-line system, one consisting of transponders or beacons forming a grid on the bottom, appears most desirable for a CURV operational navigation system, since it is undesirable to have to drop, calibrate, and recover bottom-mounted equipment during typical CURV operations. There are three basic types of short base line systems which may be used

independently or in combination for CURV IV: (1) a pulse positioning measurement system, (2) a phase-comparison system, and (3) a phase correlation system.

NUC's approach to overcoming the technical barrier will be to evaluate the short base-line system and to develop a system based upon this evaluation. The system will be used at 20,000 feet and tested at-sea with CURV III.

Precision Bottom Navigation

Precision bottom navigation is knowing the position of the vehicle with respect to the bottom accurately enough to enable the vehicle to do a systematic small area search or to enable the vehicle to return repeatedly to a work site. The accuracy needed is estimated to be approximately ±20 feet. At the 20,000-foot depths, this represents an accuracy of 0.1%.

CURV II has used its sonar and compass in conjunction with a bottom beacon to accomplish some small area searches. This technique is time consuming (sonar range is only 300 feet) and accuracies of only about ±50 feet are obtained.

A long base line system looks promising in overcoming this technical barrier. Long base line systems are currently in use but not in a CURV application, and CURV operations present some unique problems: (1) CURV has to operate on the bottom thereby decreasing the effective range of the bottom beacons and magnifying the interference due to bottom terrain, and (2) the CURV vehicle generates acoustic noise which could interfere with the long base line systems operation. In overcoming this technical barrier, navigation systems will be studied for application to CURV operations, navigation equipment will be modified and evaluated, the acoustic noise interference will be defined, and development approaches delineated.

CONCLUSION

It should be reiterated that the type of problems which appear pre-eminent now are based on assumptions that certain CURV techniques and equipment will suffice or fail. Much of the initial CURV IV development work will be to define the exact performance at 20,000 feet of CURV III components, which could alter the

critical problem. New advances in various state-of-the-art techniques also could eliminate what are now considered barriers, and of course new problems could arise.

The experience of NUC CURV program development indicates that the technical barriers to the development of a deep operating unmanned system are not insurmountable. The cable problems are basically a matter of trading off desired system capabilities and cable size to reach the optimum configuration. Bottom navigation is a question of making the search time and navigational accuracies involved reasonable. Therefore the matter of eventually developing a 20,000-foot unmanned system is not seriously in question at this time.

TUNED SPAR BUOY SYSTEM

L. O. Olson
Ocean Physics Group
Applied Physics Laboratory
University of Washington

ABSTRACT

The Ocean Physics Group of the Applied Physics Laboratory, University of Washington, has developed a portable, tuned spar-buoy system as a stable support for oceanographic instrumentation packages in the ocean. This system can be disassembled, shipped on conventional transportation and reassembled on station. Tuning is accomplished by a captured water mass that fixes the natural period of oscillation many times longer than the expected driving wave period. With the spar system free-floating on station, the payload package can be checked or changed from a ship easily. All the buoyancy elements of the system are compartmentalized; seal failure in any area will not cause loss of the spar or equipment. Should the spar system sink or be towed under, a pressure-releasable ballast will return the spar to the surface for recovery.

Operations in rough seas off the Washington coast on the USNS CHARLES H. DAVIS have shown that this half-ton system is capable of supporting self-contained packages to depths of several thousand feet in the ocean while coupling less than 10% of the vertical, surface-wave motion to the payload.

INTRODUCTION

A portable spar buoy system was developed by the Applied Physics Laboratory, University of Washington during 1968 to serve as a stable support for an array that records temperature structure at various depths in the ocean.

Originally, the temperature array[1] was hung on a coaxial cable from the fantail of the research ship. This scheme imposed amplified ship motion on the temperature data and necessitated an independent support platform that would isolate the array from surface wave motion. An initial spar system constructed from snap-together sections of foam-filled, plastic pipe was easy to launch and helped reduce vertical motion, but proved too fragile. Even in mild seas, ship maneuvering could not keep the data-linking umbilical cord between the ship and the spar slack, and eventually the spar was towed under the surface and collapsed.

The objectives for the tuned spar system were: a) support a

160 lb (in water) array to depths of 500 m in the ocean with a maximum vertical excursion of ±1 m in the wave period spectrum (5 to 20 sec) up to Sea State 6, b) all equipment had to be portable and capable of being launched from the deck of an AGOR class research vessel at sea, and c) the array had to be self-contained with internal recording because, owing to drift, a small spar can not function properly with an umbilical data cable to the ship.

Literature on spar systems showed that these objectives required a cross between a FLIP style vessel and a wave pole. The FLIP has enough buoyancy to safely support submerged packages and has enough draft to obtain a natural period of oscillation much longer than the expected wave periods. Wave poles are built with portability in mind, but have little excess buoyancy.

The resulting spar configuration is shown in Fig. 1. This spar is 106 ft long with a main diameter of 5½ in. The surface piercing section is reduced to about 3 in. diameter. Two flooded 55 gal drums are connected beneath the spar for virtual mass. Weight in air for the total system, including the captured water and the array, is 2327 lb. This ratio of weight-to-surface cross-sectional area tunes the natural period of the system to about 31.4 sec. A pressure-releasable ballast is suspended from the bottom of the virtual mass containers. This additional buoyancy will return the spar to the surface in the event of a structural failure or a seal failure in any spar section. Mounted on the top of the spar are navigational aids for station-keeping by the mother ship.

This spar system has evolved as a small part of a Navy-funded project to measure ocean temperature structure. Prime concern on this project was to obtain a seaworthy, stable support for the array by isolating the system from surface wave energy as much as possible. No attempt has been made to instrument the spar for actual motion analysis. All measurements obtained have been recorded as pressure fluctuations at the thermistor array or by visual observations. Mathematical analyses of spar buoy motions have been developed by several investigators, but are beyond the scope of this paper.

THE BUOY SYSTEM

Spar Tuning

The basic principle of the spar float is to tune the natural period of oscillation outside the spectrum of the expected wave period. This spectrum for wave energy is normally accepted to be from 5 to 20 sec. A reasonable "ballpark" period of 30 sec was used. The system response can be approximated by the equation for

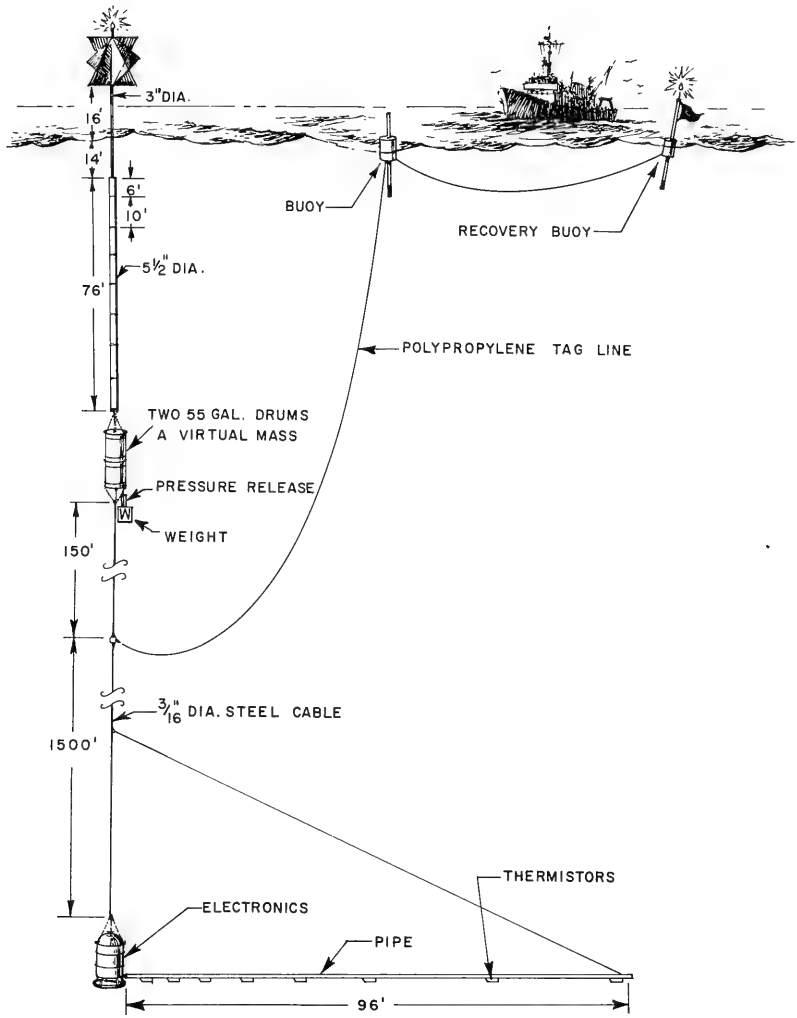

Figure 1. Spar System with Array

the natural period of oscillation of a single degree of freedom, spring-mass system without damping:[2]

$$T = 2\pi\left(\frac{M}{K}\right)^{\frac{1}{2}}$$

or (1)

$$T = 2\pi\left(\frac{W}{Kg}\right)^{\frac{1}{2}},$$

where T is the natural period of oscillation in seconds, W is the total system weight in air*, g is 32.2 ft/sec^2 and K is the spring rate in pounds buoyancy per foot of the surface-piercing section.

Practical experience has shown that a cross section with a K of 3 lb/ft gives adequate reserve buoyancy to a spar for seaworthiness and a section modulus capable of withstanding the bending stresses encountered in handling. By solving Eq. (1) for required system weight, using 30 sec for natural period and 3 lb/ft for K, a guideline parameter for the spar can be determined. With these values, and the limitations of maximum spar length and weight capable of being launched from the ship, the final spar dimensions were determined. The exact spar buoyancy constant, K, and system weight put back into Eq. (1) give a natural period of 31.4 sec. (W = 2327 lb and K = 2.89 lb/ft.)

A rough check of these calculations was made in Lake Washington on a very calm day with the full-scale spar. The array was simulated by an equivalent weight, adjusted to compensate for the difference in density between fresh and salt water. The spar was marked every 3 in. for a distance of several feet on either side of the neutral position. Observations of the magnitude and elapsed time of excursions both positive and negative, caused by releasing the spar from an initial vertical displacement, were recorded. Fig. 2 shows a curve of displacement versus time for the oscillatory motion resulting from an initial displacement of 5 ft. Three complete cycles can be easily distinguished before motion damps beyond recognition. These tests showed an average period of 33 to 34 sec for initial displacements up to 5 ft. Displacements over 5 ft showed longer initial periods as would be expected with nonlinear damping, but the periods always ended the same. Varying the system mass gave changes in period corresponding to calculated values, thereby increasing confidence in the testing scheme.

*includes array weight and weight of captured water

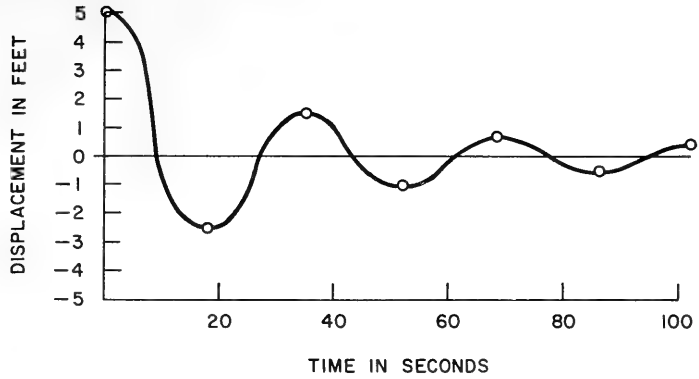

Figure 2. Plot of Free Spar Oscillations From Initial Displacement

Spar Specifications

The spar pole is assembled from the following components:

1. 76 ft of 5 in. nominal diam, schedule 40, 6061-T6 aluminum pipe.
2. 10 ft of 3 in. diam, 7075-T6 aluminum tube with 0.250 in. thick wall.
3. 20 ft of 2½ in. nominal diam, schedule 40, 6061-T6 aluminum pipe.
4. 10 couplings and 2 caps specially made from 6061-T6 aluminum, with straight continuous threads, O-ring seals and bulkhead partitions. (Fig. 3)

All components of the spar are capable of withstanding the pressure of submersion to at least 1000 ft as well as the bending stresses as a result of handling. Couplings with straight, continuous threads are required for the stress level created by bending, even though they take considerable time to assemble. A length of 7075-T6 tube was used for the reduced portion immediately above the spar step because this area is highly stressed by the flexing action when the spar is partially erected. (The 7075-T6 tube is roughly twice as strong as 6061-T6 but is harder to obtain and is not as corrosion resistant.) To facilitate handling on board ship, the top 30 ft of the spar can be removed quickly by separating the reducing coupling at the transition zone. That coupling is held together by four studs. Overall length of the spar pole is 106 ft with a normal trim of 16 ft above the neutral water line. Gross weight is 480 lb with a net buoyancy of 430 lb.

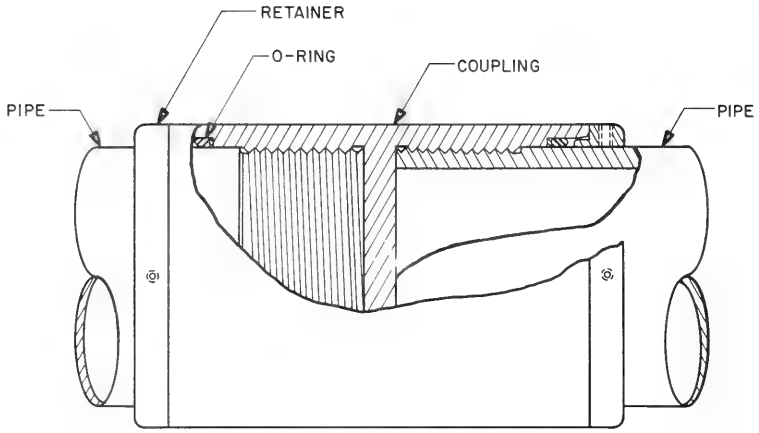

Figure 3. Spar Coupling

Virtual Mass

Two flooded 55 gal drums, which serve as virtual mass, are connected below the spar by a chain. The weight of the releasable ballast and of the array hanging from the bottom of the drums forces them to move vertically with the system almost as well as if they were rigidly fixed to the spar. Swell-surge action during launch and recovery does not allow a rigid connection, although that would be the best. Each drum has about 15 1-inch diameter holes punched in the sides near their bottoms, and smaller vent holes in the tops to allow for rapid flooding upon launch. This scheme of captured mass raises the natural period tuning-weight by 1040 lb, yet requires only 100 lb of additional buoyancy to support the drum weight.

Reserve Buoyancy

As a backup, in case any part of the buoyancy system fails, a pressure releasable ballast weight was added. This is a 100 lb, cast-iron weight suspended beneath the virtual mass containers by a Benthos Corporation model 1790A-PH pressure-actuated, pelican release. If for some reason the spar sinks, water pressure at approximately 75 m will trip the release and drop the ballast. This additional buoyancy will more than compensate for flooding of a 10 ft length of large spar pipe, flooding of all 30 ft of reduced spar section, or the complete loss of the top 30 ft of spar.

Navigational Aids

Two radar reflectors were mounted on top of the spar for station-keeping purposes. One was a portable lifeboat reflector and the other was a small, stainless steel, "Sea Me" reflector manufactured by C. M. Murray Instrument Company. To facilitate visual observation during the day, the top 30 ft of the spar was painted with high visibility orange paint. For night observation, two fishnet, marker type, flashing lights were used, one on top of the spar and the other on the recovery buoy.

Excitation Forces

The interaction of a multitude of forces, which change with every different sea state and internal current structure, will have many varied effects on the spar system. Usually, in an attempt to understand basic reactions, many of the forces are either assumed linear or are neglected because of relative magnitude. The number of components added to the system described in this report greatly complicate an analysis for an ordinary spar; therefore, an attempt has been made to isolate the major driving force. Experience with the spar tends to indicate that this main driving force is due to the pressure fluctuation against the step area.

If a spar is of constant diameter a passing wave will create a change in buoyancy proportional to the attenuated pressure variation on the spar bottom. This pressure fluctuation can be estimated for different sea states by the equation:[3]

$$P = P_o e^{-2\pi Z/L}, \tag{2}$$

where P = attenuated pressure fluctuation at depth Z
P_o = pressure fluctuation at the mean surface
L = length of surface wave.
e = spar draft

Using a sample Sea State 6:

Significant wave height = 13 ft
Average wave length = 164 ft
Spar draft Z = 90 ft
Sea water pressure per foot of depth = 0.444 lb/in.^{2}

$$P = \frac{13}{2}(0.444)e^{-2\pi(90)/164}$$

$$= 0.093 \text{ lb/in.}^2$$

This pressure fluctuation, P, multiplied by the area of the

spar bottom, A, gives an approximation of the force created by the change in buoyancy due to the wave.

$$F = PA$$
$$= 0.093(24.4) \qquad (3)$$
$$= 2.27 \text{ lb.} + \text{friction}$$

The magnitude of this force is not large enough to validate neglecting drag and friction forces. However, the same calculation made for the pressure change against the step area, on the spar dealt with in this paper, gives a much larger force for the same wave.

$$P = P_o e^{-2\pi Z/L}$$
$$= (2.89)e^{-2\pi(14)/164}$$
$$= 1.69 \text{ lb/in.}^2$$

$$F = P(A_{Bottom} - A_{Top})$$
$$= 1.69(24.4 - 7.1)$$
$$= 29.2 \text{ lb.}$$

The motion caused by this downward force is of course resisted by increased buoyancy: $4.9 \text{ in}^2 \times 0.444 \text{ lb/in}^2\text{/ft} = 2.18 \text{ lb/ft}$. This force opposes most of the neglected forces in direction, and the magnitude is large enough so that one can assume this to be the main driving force. One must remember that this force is approximate and it is difficult to evaluate how much the spar motion would be reduced by a smaller step area without testing. The best approach would probably be to design with a smaller step area and have it much deeper at possibly half the draft. This would allow the spar to operate in a null zone for waves of expected sea state where downward force on the step would be nearly balanced by the upward force on the bottom.

FIELD EXPERIENCE

Shipping and Assembly

The volume of the spar system, including pipes, pipe fittings, virtual mass containers, ballast weights, cable, chain and navigation aids is about 35^3 ft. All of the disassembled lengths of the spar are less than $10\frac{1}{2}$ ft long, so that shipment by most conventional means is possible. The total shipping weight is roughly 730 lb. From the shipping configuration two men can

inadequate for station-keeping and were nearly useless for locating the spar when visual contact was lost during storms.

SUMMARY

This system withstood the test of being handled and operated at sea under severe weather conditons (to Sea State 7) with no failures. Deployment of the spar from an AGOR class research ship by scientists has become a routine task. The objective of supporting the thermistor array system to within ± 1 m depth at several hundred meters has easily been met with only the shear currents affecting absolute depth outside of this range. Changes to the system in the near future include better navigation aids and some hardware refinements for easier handling.

ACKNOWLEDGEMENTS

The author wishes to thank Messrs. James O. P. Schultz for mechanical design on the project, Charles O. Hill for the rigging at sea and all members of the Ocean Physics Group, Applied Physics Laboratory, University of Washington, for their contributions to this project.

This work was supported by the Naval Ordnance Systems Command, U. S. Navy, under contract NOw 65-0207-d.

REFERENCES

1. A. M. Pederson, "Ocean Temperature Structure Array Electronics," presented at the IEEE Geoscience Conference, April 1969.

2. Owen H. Oakley, "Vehicles and Mobile Structures," Ocean Engineering, John F. Brahtz, ed., John Wiley & Sons, New York, 1968, 368-370.

3. F. N. Spiess, "Oceanographic and Experimental Platforms," Ocean Engineering, John F. Brahtz, ed., John Wiley & Sons, New York, 1968, 560-561.

4. C. L. Bretschneider, "Wave Forecasting," Handbook of Ocean and Underwater Engineering, John J. Myers, Carl H. Holm and R. F. McAllister, ed., McGraw-Hill, New York, 1969, 11-97 to 11-99.

assemble the system by hand in about 5 hours and disassemble it in about 3 hours.

Launch and Recovery

The assembled spar has been stowed, with the top end aft, outboard of the starboard rail on the AGOR ship, USNS CHARLES H. DAVIS, during transit. Owing to some flexibility, the spar can be hogged tightly against the rail with the bottom end at the oceanographic platforms, amidships to starboard. When the system is to be launched the spar is supported by four hand cranked winches clamped to the rail about 25 ft apart. These winches have adequate line to reach into the water and are equipped with special hooks in which the spar is cradled. By simultaneous actuation of the winches the spar is lowered into the water (see Fig. 4). As soon as the spar is floating the hooks are cleared and retrieved. Next, the virtual mass containers and the reserve buoyancy ballast are lowered into the water. These are connected to the spar by a length of chain. The ballast causes the containers to fill rapidly and the load is eased down onto the spar by a 3/16 in. wire rope which is connected to the bottom of the containers. At this time the spar is partially righted and is most vulnerable because wave action flexes it severely.

Launching the instrument array onto the spar cable by a polypropylene tag-line tilts the spar to vertical and leaves about 16 ft of spar above the water line. The other end of the polypropylene tag-line is terminated with a lighted float and is cast free of the ship. This configuration allows the array to be recovered or changed without having to recover the spar. Spar recovery is the reverse of the launch procedure and requires about half an hour with six men.

Spar Motion

Accurate information on actual sea conditions during the October 1968 cruise aboard the USNS CHARLES H. DAVIS, off the Washington coast, was hard to obtain. No wave instrumentation was available; therefore wave heights were estimated by observation of excursion against the side of the ship and on the spar pole. Wave periods were noted by timing crests passing the spar. These values, in combination with wind speed, gave approximate Sea States 4 - 7 on a scale of 9.[4]

Records of vertical spar motion were obtained by reading the pressure fluctuations of a Vibrotron (pressure sensor) located on the array. Pressure variations with periods of less than a few minutes were assumed to be caused by spar motion. In this range most of the motion occurred with periods between 5 and 20 sec. This matches the expected spectrum of surface wave and swell periods.

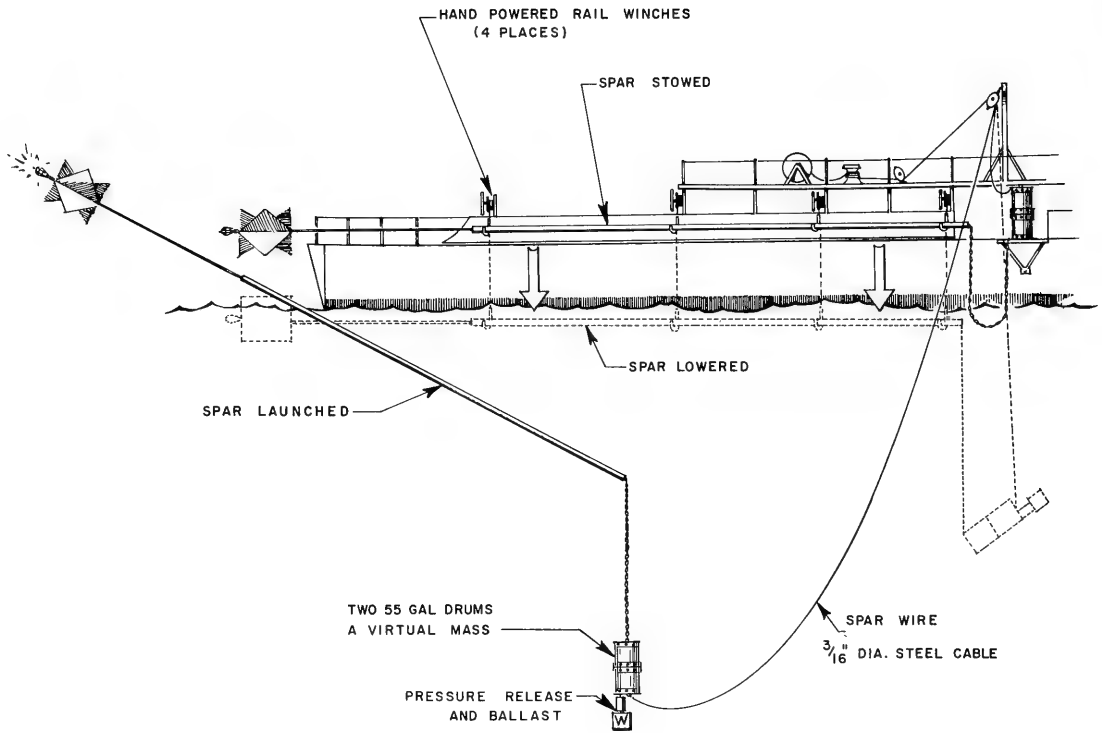

Figure 4. Spar Launch

A sample of the array depth excursion data recorded from the Vibrotron* pressure sensor is shown in Fig. 5. The average peak-to-peak fluctuation in depth on the trace is about ½ m with a 10 to 12 sec period. At the time of this plot, the sea state was about 7, with steady 30 kn winds gusting to 40 kn, and waves 10 to 16 ft in height. Gradual, random excursions of up to 4 m with periods in hours were recorded. These were attributed to horizontal drag forces created by shear currents, because rapid changes in array orientation had direct effects on maximum depth. Satellite fixes showed that the drift rate of the spar was about 0.2 kn.

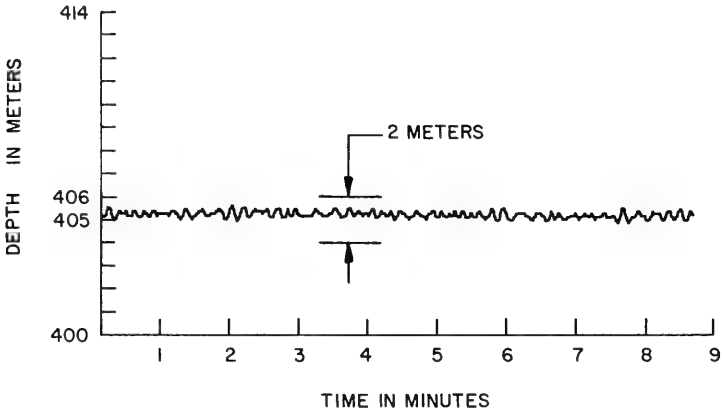

Figure 5. Vibrotron Depth Trace

Station-Keeping

Maintaining station on the spar in rough weather proved to be very difficult. On a dark night the spar light was easy to see for 2 miles or better, but was of little use in breaking seas with bright moonlight, in heavy rain or in fog. Neither of the radar reflectors used could be seen reliably on the ship's radar in breaking seas because of the backscatter. Also, the portable lifeboat reflector was too fragile to reliably withstand being dunked during spar launch. These navigation aids were very

*The Vibrotron output is digitized for recording pressure once per second, and the resolution in depth is better than ±0.1 m.[1]

SEAFLOOR CONSTRUCTION EXPERIMENTS (SEACON)

Robert A. Breckenridge
Program Manager, Ocean Engineering Department
Naval Civil Engineering Laboratory (NCEL), Port Hueneme, California

ABSTRACT

Implicit in many planned applications of oceanography to naval development, operations, and warfare is the capability to construct installations of various types in the ocean. SEACON is a number of interrelated SEAfloor CONstruction experiments. It will force technological integration of recently developed construction equipment and techniques and identify deficiencies or gaps in existing seafloor construction technology. The ultimate goal is to achieve a demonstrated capability for the construction of bottom installations.

SEACON will be conducted near Port Hueneme, California at a depth of 600 feet. Preliminary site selection experiments have begun and will consist of an acquisition of data on the seafloor sediment and oceanographic environment as well as an evaluation of the equipment used to obtain the data. Site preparation is scheduled to commence in 1970. Methods for constructing foundation systems will be evaluated, and their structural response will be determined. Although a complete habitable structure is not proposed, one or more precast concrete spherical or cylindrical hull structures will be emplaced to evaluate long-term effects on structural response as well as to develop methods for constructing one-atmosphere concrete structures. In addition, these structures will be used to support experiments on newly developed windows, antifouling agents, seals, and gaskets.

To conduct these construction experiments, there will be requirements for power, lighting, load-handling equipment, and anchors and moorings. Where appropriate the systems providing this support will be evaluated as part of the program.

PURPOSE

The purpose of SEACON is to:

(a) Provide visible benchmarks for the achievement of discrete technological milestones, where such achievements will ultimately lead to a demonstrated capability for seafloor construction.

(b) Force technological advancement of the various components of ocean engineering that will tie together current achievements and capabilities into operating systems.

(c) Identify deficiencies in existing technology and enable the efficient selection of research and development tasks to achieve desired technological levels.

BACKGROUND

SEACON is in agreement with the Technical Development Plan for Deep Ocean Technological Project (DOT)[1] and provides for the development and demonstration of several of the technologies required for implementation of the Navy's plans. Those plans are expressed in the Plan for Definition of the (NAVFAC/NCF) Role in Ocean Engineering,[2] the Navy Deep Submergence/Ocean Engineering Program (Proposed) 1970-1980[3] and the Navy's role in the Exploitation of the Ocean (Proj. BLUE WATER).[4]

The Deep Ocean Technology Project will be in its third year in FY-70. Some construction equipment and techniques will have advanced to the stage where they will be ready for, and in need of, field (i.e., ocean) testing and evaluation. Many of these experiments would have been performed independently in the due course of hardware development, but SEACON brings all the individual experiments together into one large experiment and integrates them.

In addition to the programs noted above, SEACON will make use of equipment and capabilities developed at NCEL and other Navy laboratories and activities in R&D program which are not under DOT Project sponsorship. For example, NCEL is conducting studies on bottom stabilization, embedment anchors, and materials which will be evaluated as a part of SEACON.

There are a number of other seafloor projects related to SEACON. They include Atlantis,[5] Project SEA USE,[6] and TEKTITE.[7] The Atlantis program, which proposes a test and evaluation facility on the continental shelf off the east coast of Florida, will attempt to satisfy a wide range of mission requirements. Project SEA USE proposes a test installation at shallow depth on the Cobb Seamount in the Pacific Northwest. The installation will be used for exploration of the seamount and the ocean. TEKTITE was a shallow-water (50 feet) installation for biological, biomedical, and geological studies.

The Bay Area Rapid Transit (BART) project involves construction of large concrete conduits on the floor of San Francisco Bay. This project has served to establish, to a certain extent, underwater construction techniques at shallow depths (160 feet).

APPROACH

The SEACON experiments are to be carefully chosen, integrated and time phased. Where feasible the major developments will be tied together so that they provide visibility of total capability and allow integration of different technologies. However, in cases where this is not feasible, separate experiments are planned.

A number of experiments which will push the state-of-the-art are described. While interrelated to the extent that they would or could all contribute to placing a complex installation on the ocean bottom at great depth, they are designed and implemented in such a way that failure of one experiment will not jeopardize the overall experiment. Their independence will also provide the necessary program flexibility to allow expansion or reduction of the SEACON experimental program with availability of project support.

The NAVFAC portion of the DOT project is primarily directed toward developing seafloor construction technology at depths greater than diver capability. Therefore, the main emphasis in SEACON is on developing non-diver-assisted techniques.

At the conclusion of major portions of the experiment, a report will be prepared evaluating the overall program. Where appropriate, individual reports will be prepared in detail on the results of specific experiments.

PLAN

Depth and Location

SEACON will be at a depth of about 600 feet. Shallower depths would not adequately push the state-of-the-art, but greater depths would preclude the effective assistance of saturated divers if required. The 600-foot depth is also generally considered about the edge of the continental shelf, and any capability demonstrated for that depth would be applicable for most of the shelf.

SEACON will be located near Port Heuneme, California, close to most of the ocean engineers and scientists involved and to its primary source of logistic support. Costs should thereby be reduced and time saved. The choice of the exact site will have to take into account its potential availability and the conflicting requirements

of the various experiments. For example, topographic surveying experiments could best be performed on a rock bottom where the water is very clear, whereas foundation experiments need a soft cohesive bottom material to be meaningful. It might be possible, however, to find a site where both experiments could be performed.

Description of Possible Experiments

In SEACON the emphasis is on the construction experiments themselves and what these experiments will do to advance deep ocean technology. The end item (i.e., what is constructed) is of much less importance. Equipment or hardware to be used at sea in SEACON may include the following:

Surface support ships
Warping tug
Submersible workboat
Tethered work systems (e.g., Cable-Controlled Underwater Recovery Vehicle)
Manipulators
Manipulator tools
Load-handling lines
Long Range Accuracy (LORAC) location system
Depth-measuring devices
Coring devices
Deep Ocean Test Instrumentation Placement and Observation System
In-situ plate bearing device
In-situ vane shear device
Automatic topographic plotting system
Oceanographic instruments
System for placing plastic overlays
Sub-bottom profiling equipment
Navy Experimental Manned Observatory

Items to be emplaced or constructed at the SEACON site may include the following:

Current meters
Electrical power connectors
Power generator
Power transmission system
Footings and foundations
Anchoring and mooring systems
Overlays (plastic)
Concrete cylinders (dry one-atmosphere interior)
Seals and gaskets
Windows
Benchmarks
Release devices

Pingers
Radioisotope power device and batteries
Lights and visual beacons
Sonar beacons
Oceanographic instruments
Antifouling devices
Guide lines
LOBSTER

The experiments are outlined under the following technological work breakdowns established by the 1968 issue of the DOT TDP.[1]

I. Site Selection Subsystem (WBS 2.1100)

A. Instruments (WBS 3.1110)

1. Sediment Properties. A comprehensive sediment sampling and testing program will be performed on the soils of the proposed SEACON sites. The results of these experiments and tests will be used to select the most suitable site for SEACON and provide design data on the chosen site in support of other SEACON experiments.

Shallow coring using hydroplastic or Ewing gravity corers will be performed at the proposed sites. The DOTIPOS mounted corer will also be used to obtain 10-foot long samples. A complete series of laboratory tests will be performed on these cores. The various corer systems will be evaluated for use in site surveys for structural systems of the kind required for SEACON.

In addition to coring and laboratory testing, various types of in-place tests will be performed. In-situ plate bearing tests will be run in order to determine the allowable bearing capacity for the spread footings used in SEACON. In-situ vane shear and cone penetrometer tests will be performed to a depth of 10 feet into the sediment at the sites, using DOTIPOS as the support platform. This information will be evaluated with relation to the comparable data obtained from cores. Also, interrelationships between the various types of in-situ test results will be examined. An in-situ test of the long-term behavior of sediments using the LOBSTER system will be performed at the selected SEACON site.

2. Oceanographic Properties. Information on the oceanographic properties is required for choosing a suitable site, designing many of the SEACON experiments and for interpreting

the results of experiments, such as scour and fill around structures, radioisotope-generator performance, material corrosion and deterioration, fouling and turbidity suppression tests.

Short-term bottom current measurements will be obtained at the proposed SEACON sites using the DOTIPOS-mounted current meter. Long-term bottom current measurements may be made from an oceanographic mooring system or from gages mounted on the structure. Temperature measurements will also be made using various systems. Water sampling will be performed at the proposed sites using both the DOTIPOS and a submersible. Some transmissibility measurements will be made from a ship, and others using DOTIPOS for short-term measurements and an oceanographic mooring system for long-term data collection.

3. Seafloor Topography. Topographic surveys using an acoustic profiling system will be performed at the proposed SEACON sites to provide information on the gross topographic features of the sites. Topographic charts of the areas will be generated by a computer using the data collection and processing system currently being developed by NCEL.

   Information on the detailed topography and micro-relief at the selected SEACON site will be obtained by use of a tethered photographic camera as well as by cameras on DOTIPOS and/or a submersible. Side-scan sonar and stereo-photographic techniques may also be used to obtain data on the small scale topography at the chosen SEACON site. It is anticipated that this will be a joint effort with the Naval Oceanographic Office.

   An evaluation will be made of the various techniques used for determining seafloor microrelief. The information on microrelief will be used in choosing the precise location for SEACON and in the detailed design of some of the other experiments for SEACON.

   The topographic characteristics of the site will be evaluated relative to the variation of sediment properties at the site.

4. Sub-Bottom Sediment Profiling. Sub-bottom surveys of the proposed SEACON sites will be performed in order to provide information on site geology, depth of sediment overlying rock and sediment layering. A comparison of the profiles determined by sub-bottom sounding and those

provided by laboratory tests on cores will be made. Attempts will also be made to determine the applicability of sub-bottom sounding techniques to the indirect determination of in-situ sediment properties.

5. Lights, Beacons, and Benchmarks.

a. Work Area Illumination: Fixed lighting units, portable moored (buoyant) lights, and lighting units for use with mobile equipment will be designed, fabricated, tested, and installed as appropriate.

b. Benchmarks: A suitable benchmark device will be developed. Benchmarks or beacons which can be detected from surface vessels and submersibles will be placed to adequately mark the site. They will be placed by a submersible which will position them as closely as possible on a geographic reference and relative to one another to accurate ranges and bearings.

II. Site Preparation and Construction Subsystem (WBS 2.1300)

A. Deep Ocean Energy/Power Generation, Transmission, and Conversion (WBS 3.1320)

1. Power Transfer from Surface Ship. As separate experiments or as part of any other experiment, power will be transferred at one stage of SEACON from the surface. A protected cable system running from the surface to the bottom work unit will furnish electrical power. The system may have connectors suitable for manipulation by small submersibles or for being remotely joined. Hydraulic devices will be utilized. The serviceability of such a system will be tested under these severe conditions.

2. Radioisotope Power Devices. RPD's in the 1- to 35-watt power range may be used for charging batteries on the seafloor. The batteries will be supplying power to instruments, recorders, acoustic pingers or flashing beacons. Both the pingers and the beacons will be useful in site surveying, local navigation, orienting to the surface, and for returning to the seafloor installation. The light would be visible to a few hundred feet and the sonar pulse over large distances.

B. Bottom Stabilization Subsystems (WBS 3.1340)

1. Foundations.

a. Foundation designs: Several foundation designs

(pile, footing and hybrid) may be investigated. A portion of the foundation system will probably be precast reinforced concrete slabs.

b. Experimental Results: The performance of the foundations will be evaluated with respect to stability, total and differential settlements, initial penetrations, and lateral movements. The observed and predicted performance of the foundations will be compared in order to obtain measurements of safety, and to determine the adequacy of the design procedure. In addition, an evaluation will be made of the scour and fill effects on the various foundation configurations.

2. Moorings and Anchors.

a. Moorings: Explosive anchors with 10 kip and 50 kip capacity and newly developed expendable vibratory anchors will probably be used to moor the surface support vessels utilized in SEACON and to moor any oceanographic data equipment. When the primary mission of these anchors is completed and their performance recorded, tests will be conducted to determine their pullout resistance. The results of these tests will be used to investigate the relationship of ultimate holding power to the anchor configuration, penetration depth, and sediment engineering properties.

b. Anchors for Seafloor Structures: Vibratory anchors may be emplaced to provide uplift resistance for some of the buoyant SEACON structures. Various systems for connecting the structures to the emplaced anchor will be investigated. The performance of the anchors and connecting devices will be evaluated.

3. Turbidity Control. To suppress turbidity, a plastic overlay may be laid at the site from a submersible or tethered vehicle.

C. Lifting, Transporting and Positioning (WBS 3.1370)

1. Flexible System with Constant Tension Winch.

a. Without guidelines: A constant-tension device (to be purchased in early FY70) may be used to lower or raise SEACON materials and equipment as required. The vessel motion, line force and load motion will be monitored during emplacement and retrieval. The result will serve as a basis to evaluate the winch and the handling techniques.

b. With two guidelines: The guidelines will be used to restrict the path of the load and improve the accuracy of the landing of the load. Possible use includes the assembling of prefabricated parts of a structure. The experiment will also evaluate the possibility of line entanglement for a multiline load handling system. Various types of embedded anchors may be included in the experiment for evaluation.

2. Buoyancy Control Systems for Near Bottom Operations. Collapsible pontoons (8 tons or 25 tons capacity) may be used as subsurface short-range lifting and lowering devices. The air supply will be provided by a surface vessel. The purpose of the experiment would be to study the feasibility of using a buoyancy controlled system for local lifting chores. To facilitate control, moorings may be employed.

III. Structural Subsystems (WBS 2.1500)

A. Pressure-Resistant Structures (WBS 3.1510). The objectives of these experiments are: to evaluate the technology for the modular construction of permanent-type, one-atmosphere structures on the ocean floor; to study the long-term effects of the ocean environment on concrete structures, and to evaluate window and connector hardware components and techniques for installing them. A one-atmosphere concrete structural system will be assembled and will consist of one or more 5- to 10-foot diameter concrete cylinders. The cylinders will be about 20 feet long and will be capped at each end with concrete hemispheres. Each of the one-atmosphere hulls will be lowered to the ocean bottom with a dry one-atmosphere interior. Particular experimental areas are described below:

1. Concrete Cylinders and Spheres. The one-atmosphere concrete structural system will be left in place after completion of the construction phase in order to study certain long-term effects of the ocean environment on the integrity of concrete structures.

a. Moisture Penetration: The long-time effectiveness of various waterproofing techniques will be evaluated.

b. Creep Experiments: Deformations in the structures will be monitored periodically to determine whether significant changes take place.

c. Deterioration Experiments: The condition of the concrete will be examined periodically from a submersible or a tethered vehicle.

2. Windows and Antifouling Devices. Spherical acrylic windows, 38 inches in diameter and 4 inches thick, will be installed in the hemispherical end-closures of each cylinder. Each of the windows will have a different operational system for keeping the fouling of the windows to a minimum. These large windows will permit the observation of the interior of lighted concrete hulls without entering the structure.

IV. Work/Test Subsystem (WBS 2.2500)

A. Submersible Work Boat. The services of an available underwater work vehicle are required to assist in the construction experiments. The submersible may be used in site survey operations, establishing benchmarks, in-situ soil sampling and tests, in-situ water analysis, site clearing and leveling, turbidity suppression, emplacing and recovering loads, controlling other work units, and making structural and mechanical connections.

B. NEMO. NEMO is a tethered underwater system with a spherical acrylic hull that provides panoramic vision. It has a one-atmosphere environment and will function as an in-situ observation, documentation, communication, and control center.

C. Manipulator Systems. The capabilities and limitations of manipulator systems utilized will be evaluated. One or more manipulators and several tools will be utilized to operate instruments, carry or maneuver loads, operate survey and construction equipment, take samples, make connections and operate valves.

Surface Support Vessels

A variety of ships will be required to support SEACON from the early site selection phase through the final performance monitoring phase.

The AGOR (Auxillary General Oceanographic Research) type oceanographic research vessel will be suitable for supporting much of the site survey work. This class of ship is periodically available for use by NCEL.

Ships of the Ocean Tng.Fleet (ATF) or similar class available from the Fleet would be adequate for performing such operations as establishing moorings, performing load-handling experiments and site surveys, and placing relatively small pieces of equipment such as location markers. The USNS GEAR ARS which is operated under the cognizance of the Navy Supervisor of Salvage should be considered as the possible support ship to use during the SEACON construction phase. It is capable of handling relatively large loads and has a fair amount of deck space available for test equipment.

All of the above-mentioned vessels or classes of vessels are available to SEACON without cost except for overtime operation in some cases. The salaries of NCEL personnel would, of course, have to be funded. Though the cost to SEACON of using the ships in relatively low, the scheduling may be very difficult because they are sometimes on call for some other primary mission. For this and other reasons it may be necessary to obtain another type of vessel from Navy sources or to lease a vessel for the peak use period when a schedule must be rigidly followed. An oil-well service boat would probably be a good choice if leasing ship-time is required.

The new NCEL Warping Tug may be suitable for performing some of the tasks which were mentioned under the capabilities of ATF or ARS vessels.

Participants

Joint participation or assistance will be obtained from other Navy Laboratories that have competence in ocean engineering and from NAVFAC consultants. Other Navy Laboratories, government activities, industry, and universities will be invited to participate in SEACON.

Upon approval and funding of SEACON, other potential participants will be contacted and their experiments incorporated as appropriate.

Schedule

The major portion of SEACON is scheduled to be performed in FY70, with most of the experiments conducted about April 1970. This should provide sufficient time for site selection, foundation investigation, design and fabrication. Also, the weather and seas should be fairly good at that time of year. For SEACON to be conducted in FY70, however, it is assential that preliminary work be started in FY69.

In FY71 long range experiments are scheduled to be continued, reports completed, and plans made for SEACON II. The major milestones for SEACON are planned as follows:

FY69

Nov 1968	Preliminary plans completed
Jan 1969	Formulation of initial concepts completed
Feb 1969	Preliminary site survey started
Jun 1969	Initial detailed plans completed

FY70

Jul 1969	Preliminary site survey completed
Aug 1969	Critical procurement specifications and contract scopes written

Dec 1969	Major procurements completed
Apr 1970	Site work for SEACON started
Jun 1970	Construction of SEACON completed

FY71

Nov 1970	Results available (except for long-term tests)
Apr 1971	Major plans complete for SEACON II

REFERENCES

1. Deputy Chief of Naval Material (Development). TDP 46-36X: Deep Ocean Technology Project Technical Development Plan. Washington, D.C., 1 May 1968. CONFIDENTIAL.

2. Naval Facilities Engineering Command. Study Topic 68-1: Plan for Definition of NAVFAC/NCF Role in Ocean Engineering. Washington, D.C., September 1968. SECRET.

3. Navy Deep Submergence/Ocean Engineering Program Planning Group. U. S. Navy Deep Submergence/Ocean Engineering Program (Proposed) 1970-1980. Washington, D.C., June 1968. CONFIDENTIAL.

4. U. S. Navy Chief of Naval Operations, Center for Naval Analyses. The Navy's Role in the Exploitation of the Ocean (Proj. BLUE WATER), Phase I. Washington, D.C., June 1968.

5. Chrysler Corporation Space Division. Atlantis, Industrial Contractors Mid-Term Report (Phase B). New Orleans, La., 26 August 1968.

6. Battelle Memorial Institute, et al. Project SEA USE, Proposed Exploration of Cobb Seamount. 24 April 1968.

7. General Electric Missile & Space Division. TEK-MIS-001, TEKTITE I, Scientific Mission Requirements Plan. TEK-01-5002, Technical Description of the TEKTITE Habitat. TEK-OP-102, TEKTITE I Emplacement Plan. Philadelphia, Pa. July and August 1968.

8. Naval Civil Engineering Laboratory. NCEL Ocean Engineering Program, March 1967 - March 1968. Port Hueneme, Calif., June 1968.

MIT/ONR OCEANIC TELESCOPE

John M. Dahlen
Division of Sponsored Research Staff
Mass. Institute of Technology

ABSTRACT

The Oceanic Telescope is a very stable array of temperature, pressure, and tension sensors located on a taut, horizontal cable at 700 meters depth pointing toward the deep South Atlantic on a bearing 155° true from St. Davids Lighthouse, Bermuda. The purpose of this array is to observe internal waves in the main thermocline, and to obtain engineering data required for the design of a larger scale, longer-lived future array. The taut, horizontal cable is nearly two miles long and holds three sensor stations 1000 meters apart. The sensor outputs are measured, digitized and stored on magnetic tape by a shore-based automatic Data Acquisition System connected to the array by a bottom cable. A schematic drawing is given in Figure 1-1.

Installation of the Oceanic Telescope was completed successfully on 9 October, 1968. Since 2009 hours on that data a continuous record of scientific and engineering data has been obtained.

This paper describes the design of the Telescope, the testing programs accomplished, the installation techniques employed at sea, and some characteristics of the data analyzed to date. Reference 10 presents a complete report on the engineering program.

Design criteria, configuration, analyses, and hardware components are treated in sufficient detail to give the reader a description of system performance and hardware design, and an appreciation for the design compromises and trade-offs involved. The test program description should be of general interest as it sheds some light on the quality and reliability of many components and techniques which are widely used in oceanographic applications. The discussion of sea installation attempts to show the relationships between the design and the installation techniques, and the precautions taken to avoid the many pitfalls which can lead to loss or damage of the hardware at sea.

This paper should be of general interest because:

(a) It describes the full scope of activities that were involved in transforming the Oceanic Telescope from

a feasibility study to a functioning oceanographic instrumentation system.

(b) It treats a system whose large-scale, taut-cable hydro-structure is similar to the Sea Spider and other systems which provide a very stable base for oceanographic mid-ocean sensors.

The Oceanic Telescope Program has been sponsored by the Office of Naval Research, Ocean Science and Technology Division. The Departments of Geology & Geophysics*, Meteorology*, Naval Architecture & Marine Engineering, and the Instrumentation Laboratory of the Massachusetts Institute of Technology have collaborated in this experiment which, it is hoped, will contribute to the science of physical oceanography and the technology of ocean engineering.

* Now Dept. of Earth & Planetary Physics

1.0 INTRODUCTION

Installation of the Oceanic Telescope was completed successfully on October 9, 1968, and since 2009 hours on that date a continuous record of scientific and engineering data has been obtained.

The Oceanic Telescope is a very stable array of temperature, pressure, and tension sensors located on a taut, horizontal cable at 700 meters depth pointing toward the deep South Atlantic on a bearing 155° true from St. David's Lighthouse, Bermuda. The purpose of this array is to observe internal waves in the main thermocline and to obtain engineering data required for the design of a larger scale, longer-lived future array. The taut, horizontal cable is nearly two miles long and holds three sensor stations 1000 meters apart. The sensor outputs are measured, digitized, and stored on magnetic tape by a shore-based automatic Data Acquisition System connected to the array by a bottom cable. A schematic drawing of the telescope is given in Fig. 1-1. Preliminary analysis of the data indicates thermal fluctuations over a $2^{\circ}C$ range and a broad frequency spectrum. Pressure fluctuations indicate vertical movements nominally under 1.5 meters, but occasionally as large as ten meters and constant for many hours.

Five weeks of intensive effort at Bermuda were required for system assembly and test, ship loading and sea deployment. The MIT group was supported in assembly, test and loading activities by the shop and other facilities at Navy Operating Base, Bermuda under the supervision of the ONR representative. Our vessel loading and sea operations were supported by vessels and crew attached to the Navy Sofar Station (Columbia University Geophysical Field Station) and the Bermuda Biological Station. The principal vessels used were the tug boat, T-426; the cable laying barge, YC-1378; the R/V Panulirus; and a pontoon barge.

The project was initiated in June 1967 with the objective to attempt installation before winter. We succeeded in this effort but were thwarted at the final stage of installation. On 24 November, 1967, when the inner mooring was within 90 fathoms of the bottom, a faulty armored cable junction parted at 25% rated ultimate load. The array was immediately recovered and subsequently repaired by the manufacturer at no cost to the government. Project activity remained at a slow pace characterized primarily by hardware testing until June 1968 when the cable repairs were completed. Preparations

for the Bermuda operations and final system testing were accomplished during July and August, 1968.

An appraisal of the design and test activities documented in this report and Ref. 10 will reveal that a number of compromises have been made between the sometimes conflicting dictates of sound development engineering, the need for early scientific data, and the limited resources available. While these conflicts exist in most oceanographic projects today, we feel that some mention, if not apology, for our course should be made. First of all it seems abundantly clear that the technology is not available to support the design of an oceanic telescope which will survive the many years desired to meet the ultimate scientific goals. This is particularly true in the areas of cables, floats, electrical connectors, and biological factors. To an extent this shortcoming can be overcome by the use of safety margins which are excessive in our circumstance. On the other hand evaluation of available hardware and techniques, and new developments where necessary, also had to be compromised because of schedule and funding limitations. Secondly, our knowledge of the environment, particularly the water velocity, topographical, and biological factors is very inadequate. In this area, the desired information can be had, but the necessary surveys would have been prohibitively expensive and time-consuming. Finally, it was not feasible to implement the vessel modifications and repairs required for acceptable levels of risk to the hardware during installation. As a consequence of these three basic limitations,the engineering program has been characterized by a degree of risk which prompts us to be prudently guarded in our expectations for continued successful operation of the hardware.

At this point it should be clear why the Oceanic Telescope is labeled a Pilot Project. Considering the need for internal wave data, the state-of-the-art in ocean engineering technology, and the current funding environment, we feel that we have steered the proper course.

2.0 THE SCIENTIFIC EXPERIMENT

A large theoretical literature exists on the possible thermal oscillations of the ocean. In principle, thermal oscillations exist with periods ranging from seconds to eons. A detailed knowledge of the precise behavior of the deep ocean temperature structure is fundamental to questions as diverse as baroclinic instability, air-sea interaction, and the energy dissipation of the moon in the ocean.

A handful of observations have been made of temperature fluctuations in other than coastal waters. A useful summary is contained in Ichiye (Ref. 2). Most of these observations were made from ships, and of necessity were of short duration. It has been assumed that the observed oscillations were due to internal gravity waves.

On the continental slopes, observations of relatively long durations have been obtained (e.g., from the NEL tower). It seems unlikely that these are representative of deep ocean conditions.

Array configurations are required for long-term, large-scale thermal observations, since internal waves constitute a 3-dimensional field phenomenon, propagating with specific wave numbers and frequencies through a time-dependent propagation medium. Measurements then must be made from 3-dimensional arrays sufficiently dense to maintain coherence across the array and occupying a sufficient volume of space to have directional resolution. The quasi-random nature of the temperature field demands long-time series of measurements to obtain meaningful statistics.

The design criteria for sensor stability rule out buoy techniques. We have used instead a modification of a method due to Stommel, who maintained a cable on the Bermuda slope for 9 months in 1954. Two thermistors were placed on the cable at a depth of 50 and 500 m., on the bottom, about 1 mile apart. The results, reported by Haurwitz, Stommel and Munk (Ref. 8), are the longest deep-ocean measurements that have been made.

From an array designer's point of view, the results from the cable are discouraging, showing relatively featureless spectra and nearly-zero coherence between the two sensors. In an effort to understand the significance of these results, and to determine the distance over which 2 sensors would be coherent, another experiment at Bermuda was performed in September, 1966, by Wunsch of MIT and Parker of Woods Hole.

Small arrays of sensors were set on buoys off Castle Harbor and maintained for 2 days each. The sensors were primitive strip chart recorders and metal thermometers. Instruments were placed on the bottom and several higher up in the water column. The details were reported elsewhere (Refs. 3, 9), but in summary, a high degree of coherence was found at horizontal distances up to 2 miles, for waves of period about 5 hours. The higher frequency motion (all results are qualitative) are coherent at 300 meters in the horizontal. The fluctuations of temperature were greatest at the bottom, and there is a suggestion that the slope (20 degrees) not only amplifies the motion, but also degrades the incoming energy into higher frequencies, thus accounting for the low coherence found by Haurwitz, Stommel and Munk. Some theoretical work has been done on the effects of bottom slope (Refs. 4, 7).

The results of the buoy measurements were considered encouraging enough to warrant proceeding to the actual construction of an array. Our design uses Stommel's cable technique, but suitably modified to avoid the limitation of a bottom mounting. Argus I., Bermuda was originally chosen as the site for installation because the bottom drops away so steeply that comparatively deep water is reached quickly. However, logistic considerations dictated the use of the slope off St. Davids, Bermuda. The array is confined to one dimension (horizontal and perpendicular to the contours). We later added more dimensions using short-term buoys. A long-term buoy is planned to extend the aperture. For greatest directionality of the linear array (i.e., the main lobe of the antenna function) the sensor cable points toward the deep South Atlantic. The center of the main thermocline is at approximately 800 m. near Bermuda, and this is the optimum experiment depth. A working depth of 700 m. was used, however, in order to increase the safety margin of the floats.

The optimum configuration of the sensors is the subject of considerable guesswork. The sampling interval is dictated by the time-constant of the instrument, which in turn is dictated by the phenomena of interest. In principle, there is no propagation of gravity wave disturbances with frequencies greater than the maximum of the Brunt-Vaisala frequency. Using hydrographic data (and there is 15 years of twice-a-month Panulirus data) estimates can be made of the high-frequency cut-off. These estimates are somewhat crude due to the nature of water-bottle sampling. However, it appears that the high-frequency cut-off is in the neighborhood of 15 minutes, dictating samples of not less than one every 5 minutes.

At any frequency between the Brunt-Vaisala frequency, and the low-frequency cut-off at the inertial period, there are an infinite number of gravity modes, each having a different vertical structure and a different horizontal wavelength. It can be shown that the horizontal wave number k, in the case of no rotation, is very nearly

$$K \sim \frac{\sigma n \pi}{\sqrt{N^2 - \sigma^2}\, d} \qquad (1)$$

where N is the Brunt-Vaisala frequency, d is the depth, σ the wave frequency, and n the vertical mode number. The horizontal wavelength goes to zero as $\sigma \rightarrow N$, and grows rapidly away from this limit.

With a limited aperture array, we are thus restricted to high frequencies, or high vertical mode numbers if the array is to have an antenna property. Very high wave numbers, above the Nyquist wave number, will be aliased, but this can be suppressed by rapid time sampling. High wave numbers at low-frequencies will cause an alias, but its magnitude is unknown. The use of the array depends upon concepts that are now very familiar from seismology, radar, and a few oceanographic applications.

Consider a simple example. With a pilot project aperture of 2000 m., we have a theoretical wave number resolution of:

$$\Delta K = \frac{2\pi}{2 \times 10^3} = 10^{-3}\pi \quad m^{-1}$$

where the wavenumber is that component lying along the array. (See Figure 2-1). We have no direct resolution perpendicular to the array. With 3 instruments equally spaced out along the line, we have a wave-number alias frequency of

$$K_N = 10^{-3}\pi$$

also. In principle, therefore, we can unambiguously observe only one wave-length. However, there is considerable additional information available to us from the dispersion relation for internal waves.

Consider a plane-wave:

$$w(x, y, t) = A e^{i(Kx + \ell y - \sigma t)}$$

approaching the array lying along the x-axis, and let the 3 sensors be at the points (x_i, y_i), $i = 1, 2, 3$. Then at each sensor we measure:

$$w(x_i, y_i, t) = A e^{i(k x_i + \ell y_i - \sigma t)}$$

At each sensor we can get a Fourier transform:

$$\hat{w}(x_i, y_i, \omega) = A e^{i(k x_i + \ell y_i)} \delta(\omega - \sigma)$$

From a coherence computation we obtain a phase between each pair (ambiguous up to multiples of 2π):

$$\eta_{ij} = k(x_i - x_j) + \ell(y_i - y_j), \quad i, j = 1, 2, 3 \quad i \neq j,$$

only 2 of which are independent. If the sensors are restricted to the y = 0 line, and if the mean x positions are known, then we can unambiguously solve for k. In practice neither the y_i nor the x_i and precisely known, and the phases are

$$\eta_{ij} = k(x_i - x_j) + \ell \delta_{ij} + k \epsilon_{ij}$$

where ϵ_{ij} and δ_{ij} represent positioning errors. There will then be a relative wave-number error of:

$$\epsilon = \frac{\epsilon_{ij} + \ell/k \ \delta_{ij}}{x_i - x_j}$$

Ignoring the y-variation for simplicity, this is:

$$\epsilon = \frac{\epsilon_{ij}}{x_i - x_j}$$

and is directly proportional to the uncertainty in the mean position values. To bring the wave-number uncertainty down to the 1% level, the position differences cannot exceed 10 m. out of 10^3 m.

If the sensors oscillate at the frequency σ and are decoupled, then the phase estimates will be uncertain (the coherence will be reduced due to the lack of phase lock) so that we have constraints upon both the absolute uncertainty of sensor position and the frequency of change. The out-of-line movement (y-displacement) is less severely constrained than the x, since the determination of the x wave-numbers is relatively insensitive to this motion, assuming the waves come in dominantly along the array (a topographic consideration we will not go into here).

With a one-dimensional array, even with sensors in perfectly known positions, we obviously cannot fully determine the modal distribution of the waves present. Other information is required, and this is obtained from knowledge of the mean vertical structure. Knowing both σ and k, we can obtain the x-phase speed as

$$c_x = \frac{\sigma}{K} = \frac{c_p}{(x_i - x_j)\sin\theta}$$

where c_p is the wave-phase speed and θ is the angle between the wave number vector and the normal to the array axis (see Fig. 2-1). Clearly c_x will always be greater than or equal to c_p. Using theoretical knowledge of c_p (from the computer program written for this purpose) it is possible to deduce the modal structure for a small number of modes.

We are helped in the determination of modes by relationship (1) which says that at a given frequency, the modal wave-lengths will differ by ratios of integers. Thus if mode 1 has a wavelength of 2 km. (which is true at about 14 minute periods) then mode 2 will have a wavelength of only 1 km., and a correspondingly smaller phase speed.

With 3 sensors we can perhaps distinguish 2 modes at any given frequency. If, however, a few modes are dominant, we can make use of the so-called "group-delay"

$$T_g = d\eta_{ij} / d\sigma$$

which is related to the theoretical group velocity, and gives additional information from adjoining frequencies.

In the Bermuda area at a depth of 700 m., a 1 degree temperature change corresponds to 100 m. of water displacement. We have set a maximum permissible vertical excursion of 3 m. (.03 degree) or about 3 times the stipulated sensor sensitivity. The pressure transducers will detect vertical motion greater than 1.5 m. which will permit us to partially compensate the temperature records.

We will continue to rely on the availability of Panulirus station data to provide sufficient information about the vertical to compute the normal mode decomposition.

There are many difficulties involved in this project, and the utility of these methods and the hardware design have to be proven. The

pilot project is intended to permit us to master the technology, and to prove the array concepts. If the internal wave propagation characteristics are highly structured, then some of the hardware constraints can be relaxed; if, as seems more likely, there are many modes with a more-or-less isotropic dependence, then the technical specification must be tightened.

3.0 PILOT PROJECT DESIGN

The internal waves to be observed are expected to have a minimum period of 15 minutes and a minimum half amplitude of 10 meters. Of primary importance is the accurate, continuous measurement of water temperature.

The pilot project has the dual objective of obtaining internal wave and engineering data which are both of immediate value and essential for successful design of a future larger scale experiment. A long-lived system providing both spectral and synoptic data for not less than two years and hopefully for five years is our ultimate goal.

The balance of this section is divided according to the three distinct aspects of the telescope design: Structure, Sensors, and Data Acquisition. A general arrangement drawing is given in Figure 3-1.

3.1 Telescope Structure

The structure illustrated in Figures 1-1 and 3-1 is designed to hold the sensors on a horizontal line with the great stability required for proper data interpretation, which is 3 meters displacement in the vertical and sensor line directions and 12 meters in the cross-sensor line direction. Examination of available current data has led us to believe that the magnitude of the current at 700 meters and deeper is usually less than 0.3 knots, and this value was therefore used in sizing the structure to meet the stability requirement. The major parameters determining stability are excess buoyancy, which pre-stresses the array, and cable drag. The current data and local legend also indicated that the structure should be strong enough to withstand a 1.5 knot current. The effect of a strong current is both a large scale deflection and greatly increased cable tensions. These factors are of primary importance in the design of moorings, chafing gear, float depth rating and cable strength. Finally, the failure mode resulting from an extreme current condition should be cable parting rather than float implosion, in order to permit recovery and examination of the array.

The chosen design meets the stated requirements for minimum cost and minimum difficulty of installation. Installation was accomplished by first implanting the outer moorings and joining them to form the "inverted V". The Signal Cable/Sensor Array was then attached and paid out from a barge on the sea surface toward shore. The inner mooring was next attached and lowered from another barge while the first barge hauled the signal cable inshore, pulling down the entire array.

Tables 3-1 and 3-2 provide summaries of calculated stresses and deflections at critical locations for various assumed currents. These data were derived from a digital computer program, SEASNAKE, which is described in detail along with a more complete tabulation of analytical results in Reference 6.

The following sections briefly describe each portion of the telescope structure. Further details may be obtained by reference to the engineering drawings.

3.1.1 Signal Cable/Sensor Array

The array is made up of four shots of armored electrical cable interconnected and terminated by metal junctions which serve to transmit loads and contain the sensors. Referring to Figure 3-1, we see that the shore end is terminated in a splice box which connects the system to a heavy P115 cable carrying the signals to shore. The first shot is 11,200 feet long and is laid slack on the bottom down to Station 1. At Station 1 (see photo in Figure 3-4) the signal cable is held by a bridle to the Inner Mooring Assembly which anchors the shore end of the taut array. The Inner Mooring Assembly also prevents rotation of the cable at Station 1 and holds it about 80 feet off the bottom to avoid topographical hazards. See Figure 3-2 and description of the Inner Mooring Assembly below. Six hundred feet of signal cable on the shore side of Station 1 is wrapped with polyurethane tape to provide extra abrasion protection where the cable makes the transition from the bottom to the floating Station 1. Some 90 floats are also attached to this section of cable near Station 1 to hold the cable clear of the mooring. Station 1 is articulated to permit relative pitching motion between the cables on either side of the Station. This feature prevents bending of the cable at the terminations and is especially important during deployment and retrieval.

The second shot runs taut horizontally 3698 feet from Station 1 to Station 2, which contains temperature and pressure sensors. Station 2 (see photo in Figure 3-5) is required to be at least 200 meters off the bottom to avoid sensing shoaling effects on the wave characteristics. This cable shot, like the entire taut array from Station 1 to Station 4, is floated to slightly positive buoyancy with 5.15 lb. buoyancy floats on 16 foot centers.

The third shot runs taut horizontally 3292 feet from Station 2 to Station 3 (see Figure 3-6), which contains a temperature sensor.

The fourth shot runs taut horizontally 3200 feet from Station 3 to Station 4, which contains temperature, pressure, and tension sensors. Station 4 (see photo in Figure 3-7) is secured to the Head Frame (see photo in Figure 3-8), which transmits the signal cable tension to the outer mooring cables and which prevents rotation of the ends of the signal and mooring cables.

3.1.2 Inner Mooring Assembly

The Inner Mooring Assembly is designed to anchor the shore end of the taut array and to prevent rotation and chafing of the signal cable. A schematic is given in Figure 3-2. Table 3-3 provides a summary of the calculated loads on the inner mooring and the clearance of Station 1 above the coral bottom for critical current conditions. It is seen that the mooring must resist dragging loads up to 6400 lbs. and lifting loads of nearly 1000 lbs. These numbers and the bottom material which may be encountered govern the mooring design. The worst bottom material likely to be found in the area is hard, smooth coral and dictates a very heavy coral-penetrating anchor preceded by enough heavy chain to isolate the anchor from lifting forces. This anchor, which we call a Coral Hook, has been fabricated by cutting and welding together scrap I-beams available at the Bermuda Naval Station. The Coral Hook should also serve well in the event it is implanted on clay, sand, or in a region of irregular topography. With proper respect for nautical traditions, a 90H Hi-Strength Danforth anchor is provided. The width and height of the Coral Hook were minimized to lessen water drag and virtual mass forces while the mooring is being lowered to the bottom. The inner mooring Coral Hook is shown in Figure 3-9b. The heavy chain wrapped around the structure was added to build up the weight.

The 250-foot, high-strength alloy Chain Leader resists abrasion by topographic features such as coral heads, boulders, cliffs, etc., while transmitting the tension in the array to the anchor. Its length in conjunction with the lift from the 4 foot diameter buoy (O.R.E.SS-48) above Station 1 provides clearance for the taut array cable. The 1804 feet of wire rope between the buoy and Station 1 also serves to support the anchor during deployment and retrieval. The Bridle straps are one foot long and the tension in the wire rope at the attachment to the Bridle is 1050 lbs. Thus the upper straps of the Bridle provide 18 foot-pounds of restraining torque per degree of cable rotation. The lower straps provide additional restraint of nearly the same stiffness. Knowledge of cable torque indicates that no more than 10 degrees of cable rotation will occur.

3.1.3 Outer Mooring Assemblies

The Outer Mooring Assemblies are designed to anchor the seaward end of the taut array and, in conjunction with the Head Frame, to prevent rotation at the seaward end. Figure 1-1 and the schematic drawing given in Figure 3-3 illustrate the layout and function of these moorings. Tables 3-4 and 3-5 provide summaries of the calculated loads on the outer moorings and the clearances provided to the wire rope by the Chain Leaders at critical currents. We see that the outer moorings must resist dragging loads up to 7300 lbs. and lifting loads of nearly 1800 lbs. The same factors mentioned above with respect to the inner mooring apply here. We have selected 1900 lbs. (wet) of heavy chain to isolate the Coral Hook from lifting loads. In order to remain within safe cable loads during deployment the Coral Hook is limited to 700 lbs. (wet). Clearly, we are depending upon an effective friction coefficient of 10 if the Coral Hooks are not to drag in the 1.5 knot current. This does not seem unreasonable, especially since some dragging of the outer anchors would be tolerable. The inner mooring coral hook must not drag, however, or tensioning of the bottom cable would result. Note that the inner mooring coral hook requires only an effective friction coefficient of 2. Each outer mooring also has a 60H Hi-Strength Danforth anchor. The Coral Hooks are fabricated of scrap I-beams. One is shown in Figure 3-9. The roll bar prevents the structure from laying on its side. Again, as in the case of the inner mooring coral hook, the width and height of the structure is minimized to lessen drag and virtual mass forces during lowering. Since the static load during lowering is about one third of the cable's breaking strength, we were more concerned that

these forces would slacken the cable to a dangerous extent than over-stress it. We therefore imposed a safe "G" limit at the stern chute of the cable-laying barge. The 200 foot chain leader is included to clear the wire rope from topographical hazards.

The upper ends of the mooring cables are floated to support the cable and chain leader and provide excess buoyancy to pre-stress the entire array. The 228 floats on 18 inch centers provide 1300 lbs. of sub-surface buoyancy to hold the mooring system taut and vertical after initial implantment. They are closely spaced to minimize the depth of the deepest floats in the final telescope configuration. The remaining floats are appropriately spaced over the available cable length up to the Head Frame. Small floats were used primarily because they were the only economical deep sea floats available. They also smooth tension gradients and provide damping of cable oscillations. After the moorings are joined at the Head Frame, the "inverted V" remains about 30 feet below the sea surface, thus minimizing the risk of damage due to shipping or storms while awaiting attachment to the Signal Cable/Sensor Array.

In the original design, 840 lbs. of buoyancy for each mooring was uniformly distributed above the cluster of 228 floats. All the stress and deflection data tabulated in this paper have been calculated from this original design. We subsequently learned that, because of cold flow or creep, a significant fraction of the floats in the cluster of 228 may fail during the first year's service. To compensate for this, an additional 650 lbs. of buoyancy was added to the upper 820 ft. of each outer mooring. The effect of this additional buoyancy is to increase the initial nominal stress levels by about 20%, to increase the stability, and to increase the stress levels at the extreme 1.5 knot current condition by only 2%. Float performance is discussed further in Sections 3.1.9 and 4.1.4.

3.1.4 Signal Cable (Vector Cable Co. Dwg. A-5051)

The signal cable is a double-armored, eight conductor neoprene cable of a design which has been used in many oceanographic applications. The center conductor is #16 AWG stranded copper wire. The remaining seven conductors are #20 AWG stranded copper wire. Insulation is a .021" wall propylene copolymer. These conductors are wrapped with fiberglass yarn and imbedded in neoprene of .062" minimum wall thickness to form the watertight electrical cable. The

armor wires are pre-formed and twisted around the center electrical cable. They provide the necessary tensile strength (15,000 lbs. ultimate) and protection against abrasion and fish bite. The inner layer is made up of thirty-two .035" galvanized high strength steel wires in right lay. The outer layer has thirty-two .042" galvanized high strength steel wires in left lay. This construction has much less torque than single lay construction. For additional corrosion protection the armor is imbedded in an outer polyethylene jacket of .050" wall thickness. Total cable diameter is .615". Weight in air is 440 lbs/1000 ft. Weight in water is 310 lbs/1000 ft. Cable stretch was measured to be 0.64 ft. per 1000 ft. length per 1000 lbs. tension.

3.1.5 Signal Cable Terminations (Vector Cable Co. Dwg. 13030)

The electromechanical cable termination is designed to hold the armor wires and make a pressure-tight electrical connection to the instrument housing. These functions are accomplished by encapsulating the armor wires in an epoxy plug while connecting the electrical cable to a pressure-tight electrical feed-through. An assembly drawing is given in Figure 3-10. The conductors are sealed even if the space inside the DAT (Double-Armored Termination) shell is flooded due to a break in the outer cable jacket or a leak past the neoprene boot. Tests have proven that this termination will develop nearly the full strength of the armor (failure of armor strands will occur just outside the DAT shell). Tensile failures below 15,000 lbs. that have occurred at this termination were due to improper epoxy encapsulation. The armor wires were not adequately hooked or sand-blasted to remove the zinc plating, or the epoxy was not properly filled or formulated. It is believed that such failures can readily be avoided by careful manufacture. We have found that X-ray photographs are a useful final inspection tool. Proof testing to 50-60% of ultimate strength is also recommended.

3.1.6 Instrument Housings

The instrument housings provide a one-atmosphere air environment for the back side of the sensors and for the electrical wiring. This technique was used for convenience in assembly, economy, and to evaluate such housings for use on a future telescope which might require the use of electronic decoding and switching circuits at the sensor stations. The housings are bolted to the DAT shells using flange joints with double O-ring seals. If a housing should flood due to seal

failure, the electrical connectors, having their own O-ring seals, would continue to function. Thus flooding of one housing would not affect the transmission of data which originated at another station.

The combination of a sensor housing with sensors and adjacent DAT shells is referred to as a Station. Station 4 is fabricated from 6A14V Titanium and contains one thermistor, one pressure transducer, and one tensiometer. Station 3 is fabricated of Hard-Anodized 6061-T6 Aluminum and contains one thermistor. Station 2 uses 6A14V Titanium and contains a thermistor and a pressure transducer. Station 1 is fabricated of 316 Stainless Steel. The different materials were used in order to obtain engineering data applicable to future design problems. Certain design changes to save weight and to permit faster assembly and leak checking would be incorporated in a later design.

3.1.7 Outer Mooring Cable (Vector Cable Co., Dwg. B-3540)

The outer mooring cable is a polyethylene-jacketed torque-balanced wire rope which has been used in many oceanographic applications. It is laid up using 41 galvanized high-strength steel wires in three layers around a .045" core wire. The first and second layers are right lay, with six .040" and twelve .040" wires, respectively. The outer layer is left-hand lay, with twenty-two .031" wires. The wire rope diameter is .265". The .050" wall polyethylene builds up the outside diameter to .365". Cable weights per 1000 feet are 160 lbs. in air and 114 lbs. in water. Ultimate strength is nearly 10,000 lbs. Cable stretch was measured to be 1.16 feet per 1000 feet per 1000 lbs. tension.

Torque-balanced wire rope was chosen to minimize rotation during lowering of the anchor. Rotation might induce hockling at implantment or whenever tension might slacken due to dynamic conditions. Synthetic lines were avoided to prevent potential fish bite damage. It remains to be seen whether or not the torque balanced construction has adequate strength for the oscillatory fatigue loads.

Rope terminations are swaged 304 Stainless Steel clevis fittings (ACCO P/N MS-20667-9) except at the bottom where the cable must interface with chain. There a swaged drop-forged steel eye fitting is used (MACWHYTE P/N RA 152-9). A neoprene boot is molded to the fitting and sealed over the polyethylene jacket with internal O-rings. This boot provides strain relief and seals the wire rope/swaged fitting interface against sea water penetration. To minimize

bending moments at the terminations, a modified Hooke's Joint coupling is used between the clevis fittings. A hole is drilled through the center of each coupling for attachment of stopper hardware. A photograph of a typical wire rope connection is given in Figure 3-11. Various length shots were used to fit the deployment procedure and to accommodate errors in depth and mooring location.

3.1.8 Inner Mooring Cable (Vector Cable Co., Dwg. B-3695)

The inner mooring cable is also a polyethylene-jacketed torque-balanced wire rope. It is laid up using 58 galvanized high strength steel wires in four layers around a .045" core wire. The first three layers are right lay, with six .040", twelve .040", and fifteen .049" wires. The outer layer is left hand lay, with twenty-four .039" wires. The wire rope diameter is .380". The .050" wall polyethylene builds up the outside diameter to .480". Cable weights per 1000 feet are 297 lbs. in air and 217 lbs. in water. Ultimate strength is 16,000 lbs. Cable stretch was measured to be 0.59 feet per 1000 feet per 1000 lbs. tension.

The underlying reasons for selecting this rope are the same as those mentioned above for the outer mooring cable. Rope terminations and couplings are of the same type used on the outer mooring cables, (clevis fittings: ACCO P/N MS-20667-12, eye fittings: MACWHYTE P/N RA 152-12.

3.1.9 Cable Floatation

The development of a suitable cable floatation scheme has been a difficult task, primarily because of schedule and funds limitations.

Approximately 8000 lbs. of net buoyancy is required. The price for reliable glass spheres was about $3.00 per lb, plus hardware to capture the spheres. Glass buoyancy would therefore have cost in excess of $30,000. More exotic techniques (using syntactic foam, for example) were not only too expensive but were also ruled out for the pilot project because of the tight schedule. Since the available glass spheres are so expensive and apparently over-strengthed for our application, we were prompted to search the market for a more suitable float. Only two commercially available designs having adequate specifications were found: A cast aluminum alloy sphere

(Figure 3-12) manufactured by Phillips Trawl Products Ltd. of England and a molded polystyrene sphere (Figure 3-13) manufactured by Plasticos De Galicia, S. A. of Vigo, Spain. Both of these spheres are manufactured primarily for use on trawl fish nets. The former, designated the FE-18, is rated for 1000 meters; the latter, called the Marola 200, is rated for 1300 meters. Each cost about $2.25 for a 6 lb. buoyancy sphere, thus promising to reduce the total floatation cost to less than $3500. The order-of-magnitude price saving over glass, and the ready availability of large quantities were very attractive. About 100 floats of each type were immediately procured for evaluation tests. It was quickly found that the FE-18 float did not have sufficient depth capability and the Marola 200 exhibited excessive cold flow resulting in short life at depth. Refer to the next chapter for a summary of test results.

Each manufacturer promptly improved his float to meet our specifications. Phillips increased the wall thickness to provide the "XX" float which can withstand the pressure at 1250 meters and Plasticos De Galicia molded a "Special" Marola 200 using a "high grade" non-impact-resistant polystyrene for much reduced cold flow. It should be noted that the Marola float is encased in a waffled outer polyethylene jacket to cushion the inner polystyrene sphere against impact loads. The space between the inner sphere and outer jacket is free-flooding.

The principal parameters affecting float life are pressure difference from maximum rated pressure and water temperature. A large number of test points have been correlated with available creep failure laws. At this time it does not appear that one should hope for an average float life much in excess of one year at 1000 meters. For this reason excess buoyancy was used, and other materials and float designs must be evaluated for the future long-lived telescope. Thermal-setting plastics appear worthy of further investigation in this regard.

3.2.0 Float Attachment Device

Development of a suitable float attachment device was a vexing problem. This device had to meet the following requirements:

..hold the float at a fixed location on the cable
..permit rotation of the float around the cable
..protect the cable jacket from implosion shrapnel
..avoid point loading and cable jacket wear
..be capable of rapid attachment
..permit spooling the cable under tension
..cost under $2.00 per float
..be available in very short lead time

The solution is shown in the photographs in Figure 3-14. It is in two parts. The float sleeve is attached to the cable before spooling on the barge. A short piece of polyethylene tubing, sawed helically, is spread and slipped over the cable jacket. Two PVC threaded couplings (standard pipe-fitting hardware) are then threaded over the ends of the tubing, one from each end. The couplings cut their own thread in the soft tubing and clamp it and themselves firmly in place. A molded urethane float clamp is later folded over the float sleeve and clamped to the float handle. This technique has worked very well, is nearly indestructable, and meets all requirements admirably. It has two disadvantages: The PVC nuts must be slipped over the cable before the terminations are applied and later translated to their proper positions (one can imagine the activity required to locate the nuts on 16 foot centers on the three signal cable shots!). The other disadvantage is that a cable so encumbered with float attachments cannot be spooled under tension without some damage to the cable jacket. These difficulties were worked around satisfactorily, however, as described later. We have a design concept for a combination sleeve/float clamp which can be clamped in place in one rapid operation and avoid the above mentioned disadvantages, but further work on this improved device is not justified at the present time.

3.2 Sensors

The task of determining the presence of internal waves is accomplished by monitoring the temperature of the water at fixed points. As the internal wave passes the measuring stations, the surrounding water is displaced by water at a different temperature; hence, the time history of the internal wave.

As indicated earlier, the measuring stations are restricted in their motion by the taut array. However, since the stations cannot be held absolutely rigid in one position, the vertical motion of Stations 2 and 4 are measured by pressure transducers in order to monitor deflection and permit application of a correction factor in the data reduction.

In order to monitor the structural integrity of the array and provide engineering data, a tensiometer is placed in Station 4.

The sampling rate for data storage is adjustable commensurate with the experiment. The data may also be monitored continuously with auxilary equipment. All sensors have performed extremely well throughout testing and since the October 1968 deployment.

3.2.1 Transducer Circuitry

The pressure, tension, and temperature transducers, as discussed in this section, manifest a change in resistance proportional to the magnitude of the quantity that they sense. This change in resistance is a very small quantity and, therefore, cannot be measured with conventional ohmmeters or voltmeters with sufficient precision. Consequently, each transducer is made part of a bridge circuit that is capable of measuring resistance to the required accuracy. The bridge circuit is described in Section 3.3 as an element of the Data Acquisition System. The wiring schematic is given in Figure 3-15. A standard two-wire technique is adequate because of the small size of lead wire resistance errors relative to sensor resistance variations. A disadvantage of the system used is that even high impedance shorts due to water penetrations cannot be tolerated.

3.2.2 Temperature Sensors

At the depth of the measuring station, the transducers are exposed to small temperature changes. Thus, in measuring the temperature of the water to determine the presence of an internal wave, the resolution and time of response of the transducer are the critical design parameters, with the overall absolute accuracy and stability with time requirements being somewhat relaxed. Many electrical-type temperature sensing devices are available, including the thermistor, thermocouple, and various metallic sensor elements. However, because of the design parameter requirements, the thermistor is most suitable and is most compatible with a Wheatstone Bridge circuit.

The thermistor we are using is the Fenwal Electronics, Inc., Type D-10 Oceanographic Sub-Mini-Probe, encapsulated 100K at $25^{o}C$ Iso-curve Thermistor. This particular thermistor meets all design requirements. It is designed to have an accuracy predictable

to $\pm$ 0.1°C over the temperature range on a standardized R-T curve. Furthermore, it has a stability of 0.05°C per year maximum change, and extremely fast time of response. In order to permit a low sampling and data storage rate, the temperature sensing time constant is increased to 60 seconds by insulating the sensor from the sea water and thermally coupling it to the relatively massive sensor housing. At the nominal operating temperature of 11°C, the thermistor resistance is 200 K ohms and its scale factor is 10 K ohms per °C. Since the bridge resolution at 200 K ohms is 80 ohms, we have no difficulty in achieving the desired temperature resolution of .01°C.

3.2.3 Pressure Sensors

At the 700 meter array depth the pressure is approximately 700 decibars, or 1040 PSI.

The pressure transducer selected is manufactured by Sparton Southwest, Inc. as Type 890-A-200-450 which employs a Bourdon tube connected to a potentiometer. It has a pressure range of 0-2000 PSI and a resolution of 2 PSI. Absolute accuracy is approximately 1%. The scale factor is approximately 20 ohms/PSI. The time constant is approximately 0.1 second.

3.2.4 Tensiometer

Because a suitable off-the-shelf tensiometer could not be obtained for the available funds, we built our own. Figure 3-16 contains an incomplete but adequate drawing of the unit. The tension sensing element is the end plate of Station 4 which deforms as a diaphram under load. A hydraulic amplification of diaphram displacement is accomplished by the trapped fluid and bellows arrangement. The bellows in turn is connected to a linear potentiometer which provides a resistance output compatible with the over-all dc bridge measurement scheme. The unit is clearly temperature and pressure sensitive, so that its output must be combined with the pressure and temperature outputs at Station 4 to determine tension from the formula

$$R = K_o + K_1 T + K_2 W + K_3 P$$

where

R = Resistance output

T = Temperature in ^{o}F

W = Tension in lbs.

P = Pressure in PSI

K_o = 21,500 ohms

K_1 = 388.6 ohms/^{o}F.

K_2 = -3.33 ohms/lb.

K_3 = 32.5 ohms / PSI

The time constant is approximately .05 sec. Resolution is about 20 ohms.

3.3 Data Acquisition System

The basic function of the Data Acquisition System is to extract and record information from individual sensors on the Signal Cable/ Sensor Array at regular intervals in time. This information is reduced to numerical form and written (recorded) onto a 7-track IBM-format digital magnetic tape. This tape is referred to as the Primary Data Tape.

All of the sensors on the Array translate what they measure - temperature, pressure, etc., - into a variable electrical resistance. The information actually recorded on the Primary Data Tape is the electrical resistance of each sensor (plus the resistance of the intervening cable). During computer analysis of information from the tape, the resistance of the cable between each sensor and the System's input connections is subtracted from the measured resistance to recover the resistance of the sensor itself. This cable resistance has been previously measured to the desired accuracy and can be compensated for temperature and other effects by comparison with the measured resistance of a calibration wire in the array.

The Data Acquistion system uses both epoxy-encapsulated semiconductors and Flat-Pack style micrologic elements. The tape is produced by a Digi-Data model DSR-1400 incremental tape recorder with a recording density of 556 characters per inch of tape. At the fastest data-acquisition speed of one measurement per second, a 2400 foot reel of tape will therefore hold about 20 days worth of data. At slower data-acquisition speeds, the tape will last proportionately longer.

3.3.1 Functional Operation

The Data Acquisition System makes a complete measurement, which includes the recording of electrical resistance as well as of identification numbers every N seconds. This Measurement Interval may be any integral number of seconds from 1 to 64 seconds. The Measurement Interval is set by switches on the front panel of the System. Each time the System takes a Measurement, it indexes to a new sensor. It thus cycles through all of the sensors on the array in a regular sequence. Seven electrical resistance measurements are taken on the Signal Cable. Each sensor is therefore measured every 7N seconds.

Every resistance measurement has associated with it two identification numbers, called the Sensor Number and the Measurement Number. These two numbers are held in binary form in registers within the Data Acquisition System, and both are incremented by 1 during each Measurement Cycle (the sequence of operations involved in recording on tape a single Measurement - data plus identification numbers - is called a Measurement Cycle). The Sensor Number ranges from 0 to 6 and indicates which of the seven inputs from the array is being measured. After measuring input 6, the Sensor Number register resets to input 0. The Measurement Number ranges from 000 to 251, and simply numbers each of the 252 Measurements in a Block of data on the Primary Data Tape. The actual manner in which these operations are carried out may be seen from Figure 3-17, which is a flow diagram of system operations. Figure 3-18 shows the actual format of data as recorded on the Primary Data Tape.

If desired, the resistance measurement may be replaced during a single Measurement Cycle by a 16-bit External Data Word, which is entered from the front panel. This is accomplished simply by

pressing the External Data Button on the front panel.

Data on the Primary Data Tape is organized into Blocks of 252 Measurements plus a Block Number at the beginning of each Block. Blocks are simply numbered sequentially from the beginning of the tape. The block number register is not reset until the tape is changed. Blocking of the data is necessary to allow a computer to read the tape. The Primary Data Tape is written one character at a time (asynchronously); the computer, however, reads it back at fixed speed, one block at a time. Each block on the tape must be transferred at one time, as it is read, into the computer's primary memory (core storage). The Block length used in the Primary Data Tape amounts to 1766 characters (252 7-character Measurements plus a 2-character Block Number). The input buffer in the computer's core storage must therefore be 1766 6-bit characters in length (or 1766 8-bit bytes in the IBM System/360). This choice of block length requires a buffer which could be accommodated in the core storage of most any computer which might be used to process data from the Oceanic Telescope.

Before final data reduction and analysis, the Primary Data Tape is examined by a set of preprocessing programs. These programs check for consistency of identification numbers, location of delimiter characters, and the like. From a knowledge of the starting time of the Primary Data Tape and of the Measurement Interval, the preprocessing programs construct an array containing real time versus measured resistance for each of the seven inputs from the Sensor Cable. Any inconsistencies in the Primary Data Tape are flagged in the array. This array forms the input to the Data Analysis and Reduction Programs.

3.3.2 The Measurement Bridge

Wherever it is necessary to make very accurate measurements, it is desirable to have the accuracy of the measurement depend on the accuracy of as few "standards" as possible. In most commercial digital ohmmeters, a constant current is forced through the resistor being measured, and the resulting voltage is measured by a digital voltmeter. This scheme has the disadvantage that the accuracy of the measurement relies on the accuracy of both the current source and the digital voltmeter.

A bridge configuration was therefore selected for making resistance

measurements. Figure 3-19 shows a simple bridge of the sort initially considered for this project. A null will be obtained when $R_1R_3 = R_2R_4$. Because we have specified R_2 and R_3 as matched resistors, a null will be obtained when the variable (switch-settable) resistor network designated R_4 is set to equal the resistance of the sensor switched in as R_1. The bridge configuration has the advantage that only the network R_4 must be known precisely; R_2 and R_3 need only be matched, because their absolute values do not affect the measurement. The conditions for null across the bridge are independent of the voltage placed across the bridge. Dependence on resistors as standard elements also reduces the amount of long-term drift, because resistors are very stable circuit elements.

The error-detecting amplifier will affect bridge stability only if its null-sensing point (the point where it recognizes its two inputs as equal) drifts. In fact, this amplifier's drift is less than the input created by a change (in either R_1 or R_4) of 10 ohms, which is the smallest resistance change we are trying to resolve. The operation of setting the resistors in the network R_4 does not require the error-sensing amplifier to be linear; the amplifier is always driven to preset limits, indicating whether R_4 is set too large or too small. It should also be noted in passing that the switching elements used are mercury-wetted-contact relays, which have a life expectancy of over one billion operations.

The bridge of Figure 3-19 has the disadvantage that it allows the voltage across a sensor to vary. Each time a sensor is switched in or out of the bridge, a voltage transient is created on the signal cable. These voltage changes would not be a problem if the measurement interval were much longer than the cable time constant. The actual installation, however, places several miles of cable between the sensors and the Data Acquisition System. This cable introduces over 1.0 μf of capacitance. As a result of this capacitance, any voltage transient will take several seconds to settle out.

The problem of capacitive coupling among the lines is solved by providing an individual amplifier for each sensor line. These amplifiers by means of feedback,. hold the voltage across each input line nearly constant for all time, whether or not the sensor is being measured. Through this feedback scheme, the voltage variations on each line are reduced to about 0.02% of the value they would have using the scheme of Figure 3-19.

Figure 3-20 illustrates the measurement bridge, revised to include

the amplifiers discussed above. The operation of this system can be more readily understood from Figure 3-21, which shows only one sensor channel. The inverting (-) input of the bridge-voltage amplifier has an input resistance on the order of 10^{10} ohms so as not to load the bridge. The effective input resistance, however, is reduced by feedback to a value equal to R_2 divided by the gain of the bridge voltage amplifier, thus holding the voltage across each sensor line virtually constant. Although this method causes the voltage across the bridge to vary as sensor resistance varies, recall that the conditions for null are independent of the supply voltage across the bridge. In fact, it can readily be verified that the conditions for d.c. balance of the bridge of Figure 3-21 are identical to those for the bridge of Figure 3-19.

The provisions of individual sensor amplifiers also yields other advantages. Two advantages result from the fact that capacitor C_2 (Figure 3-21) allows us to set the high-frequency response of each channel. We could thus increase the effective time-constant of any sensor channel at will by suitable choice of C_2. Although we do not, at present, plan to use this option, it could be advantageous in avoiding aliasing if extremely long measurement intervals were ever to be used. The main advantage of the high-frequency roll-off is simply that, even when the shortest Measurement Interval is used, the time constant provided by C_2 can still be set so that 60-Hz noise (and other electrical interference likely to be floating around any substantial installation of electronic equipment) will be considerably reduced.

The inclusion of individual sensor amplifiers provides, for each channel, a voltage signal representing instantaneous sensor resistance (after low-pass filtering performed by the bridge voltage amplifier with C_2). This voltage is available at point P in Figure 3-21. It is therefore possible to monitor any (or all) of the seven signals from the Sensor Cable with an analog device, such as a stripchart recorder, without disturbing normal operation of the Data Acquisition System. If, for example, significant mechanical oscillations were to develop in the cable, it would be possible to accomplish continuous, analog recording of pressure (i.e., depth) and tension data without sacrificing normal digital measurement of all seven inputs. A photograph of the digital measurement bridge is given in Figure 3-22. The complete Data Acquisition System is shown in Figure 3-23.

4.0 TEST PROGRAM

It is the intention of this section to describe the pre-deployment testing performed and summarize the results obtained. The nature of the test program has been dictated by the schedule and funding environment. As a result we have emphasized demonstrations of component adequacy. Little testing has been done with the objective of developing improved components.

4.1 Structural Testing

Structural testing consisted of:

a. sample testing to determine yield and rupture

b. proof testing of critical in-line components

c. radiographic and other inspections of shackles, couplings, terminations, and other fittings

Experience has demonstrated the need for proof testing all critical components since quality control procedures are rarely known to be adequate. This is not to say that proof testing is a satisfactory substitute for quality control. It is the only means at our disposal to minimize the probability of a structural failure during installation and during the first few weeks of operation. It will be seen that all tensioned components of the telescope were proof loaded except wire rope couplings, head frame, Station 1 bridle, sensor stations, and anchors. These components (except anchors) require only radiographic and dye-penetrant inspection since they are inherently structurally reliable and much overstrengthed.

4.1.1 Testing of Wire Rope Shots

Table 4-1 outlines the tensile yield and ultimate strength tests performed on sample wire rope shots, including swaged terminations.

The swaged stainless steel terminations on the B-3540 wire rope slipped off because standard terminations and swaging dies for 9/32" wire rope were mistakenly used (the B-3540 wire rope diameter is .016" less than 9/32"). Both the first and second orders (October 1967 and June 1968) exhibited this error. In each case the problem was fixed under schedule duress by re-swaging the terminations using special dies. The correct procedure is to use terminations specially bored for the .265" rope diameter. Re-swaging introduced a small curvature to the terminations and cold-worked the material more than desired. As a result the life expectancy of the terminations and wire rope may have been reduced. Fig. 4-1 contains photographs of a failed termination pulled off during testing at NOB, Bermuda.

The B-3695 wire rope order exhibited no such problem because the wire rope diameter is .380" (.005" larger than the standard 3/8" wire rope), and standard 3/8" terminations and dies may be used with good results. Cyclic tension tests are considered necessary to support development of a long-lived mooring system. These will be carried out if funds become available.

Subsequent to the re-working and sample testing, wire rope junctions on the 1967 Eastern Outer Mooring System were proof tested to 6500 lb. tension while loading on the barge.

Table 4-2 outlines the inspection and proof test procedures performed on all wire rope shots used on the telescope installed last October. Tensioning long shots of wire rope is a hazardous, expensive, and, in many cases unnecessary, procedure. However, it was considered appropriate in our case because the test facility was already required for tensioning signal cable shots, the cost was borne by the manufacturer, and the test provided more data and higher confidence than would be provided by simply proofing the cable terminations.

4.1.2 Testing of Signal Cable Shots

Prior to the November 1967 installation attempt a reasonably high level of confidence was held in the signal cable terminations. This confidence was based on the extensive experience of the manufacturer in this area, backed up by good experience with potted epoxy terminations had by other users. This confidence coupled with the high cost of each termination led us to forego building special articles for qualification testing and to restrict ourselves to proof testing all the in-line terminations. Also, in order to conserve funds and avoid a lengthy proof-test procedure which would have slipped the schedule into an even worse weather period, it was decided to proof test the terminations while loading the signal cable under tension on the barge drum. When it came time to do this, an unexpected difficulty developed. The signal cable on either side of Station 1 was covered by 3/4" ID polyethylene tubing for extra abrasion protection. As the high-level tension (6400 lbs.) required for proof testing was approached, the cable moved inside the polyethylene tubing resulting in slipping and grabbing motion and related large tension transients. We therefore suspended this test, resumed loading, and decided to proof-load subsequent stations which were unencumbered by the polyethylene tubing. This proved to be a fatal decision, since termination 1B on the seaward side of Station 1 failed at approximately 4000 lbs. tension during the final stage of installation! The bitter end is shown in Fig. 4-2.

After recovery it was decided to test termination 4A to destruction. We constructed a tensile test machine using scrap I-beams and a hydraulic ram. The termination was pulled in 500 lb. tension increments, and held for at least 4 hours at each level. X-rays were taken at the start, after the 8000 lb. proof test level, and after destruction. The 8000 lb. proof test level was applied at both room temperature and at 40° F. Failure occurred at 15,000 lbs. tension (Fig. 4-3) since the armor was designed for 15,000 lbs. ultimate strength, the test proved conclusively the adequacy of the epoxy-potted termination for static loads. A cyclic load test is considered necessary to support development of a long-lived system, and will be conducted if funds become available.

Also subsequent to recovery, the manufacturer attempted an 8000 lbs. proof test of Shot 2B-3A. In this test, termination 3A failed at 6800 lbs. Station 3 had been proof tensioned to 6400 lbs. during loading on the barge in November! The mode of failure was identical to that experienced at termination 1B i.e., the armor strands slipped out of the epoxy plug due to inadequate potting or improper preparation of the armor strands. Fig. 4-2 illustrates this failure mode. During subsequent proof testing, the armor slipped out of termination 3B at 6500 lbs!

Clearly the failures during installation and subsequent proof tests could be traced to inadequate quality control. The manufacturer took steps to remedy the problem, and we devised a procedure to inspect and proof test all signal cable shots at delivery. It was decided to pull the complete length of all shots to prevent damage to the cable during testing and to provide confidence that no serious damage had been sustained during deployment, retrieval, or shipping; or because of subsequent corrosion. The procedure and results obtained are given in Table 4-3. The test "facility" used for pulling the long shots of cable consisted of two Schlumberger well-logging winch trucks at either end of a straight stretch of road. Some testing was done on a stretch of new, unopened highway in Houston, and the balance was conducted on a dirt farm road Northwest and outside the city limits of Houston. Photographs are shown in Fig. 4-4.

4.1.3 Testing of Standard Hardware and Special Fittings

In this section we shall review the testing of standard hardware such as shackles, chain, and synthetic rope, and special fittings such as couplings, bridle, head frame, etc. The standard articles are produced under somewhat uncertain quality-control procedures for a competitive market and are generally recommended for use with safety margins larger than we can permit. Consequently we have adopted a

conservative testing policy toward them. The special fittings are less suspect.

In preparation for the November 1967 installation, all standard hardware components were proof tested at the Bermuda Naval Operating Base. A crane and large dead weights such as Navy Anchors were used to static load the test articles. In some instances the articles failed well below advertised yield. Some photographs are given in Figs. 4-5 and 4-6. Table 4-4 summarizes the results obtained. The Bridle for Station 1 was proof loaded to 15,000 lbs. at MIT before shipment. In addition all carbon steel shackles were radiographed and magnetic-particle inspected with the result that 3% were rejected because of internal cracks. All stainless steel shackles and a sample of stainless steel couplings were radiographed and dye-penetrant inspected with the result that no flaws were found.

In preparation for last October's operation, all standard hardware components were proof tested at MIT. Table 4-6 summarizes the results obtained. Radiographic inspection was performed on all steel shackles after proof loading. Stainless steel fittings were radiograph and dye-penetrant inspected. Twelve percent of the carbon steel shackles were rejected. Stainless steel fittings exhibited no flaws. Before proof testing, yield point and ultimate tensile strength were obtained on samples. Table 4-5 summarizes the yield and ultimate strength tests.

4.1.4 Testing of Cable Floats

As described in Section 3, our interest has been centered on the Phillips XX and the Plasticos de Galicia Special Marola 200 floats. Neither float can be expected to survive five years at the depth of the deepest outer mooring float, which is nominally 870 meters (1290 PSI) and which increases to 1130 meters (1680 PSI) at the maximum current condition. However, the pilot project has gone ahead with a modification of the original design. The dense arrays of 228 Special Marolas used on each outer mooring cable are expected to suffer a significant number of casualties during the first year because they have been pulled down to a depth in excess of 800 meters. Since they are slightly buoyant after collapse, the Marolas will not weigh down the system. These losses are compensated by the attachment of about 125 extra XX floats on each outer mooring cable near the Head Frame.

Our float testing efforts have been directed to evaluate:

a. time to failure as a function of pressure and temperature

b. corrosion characteristics

c. leakage

Until increased support is available we have postponed efforts to evaluate the effects of pressure cycling and to develop a new float which is both structurally and economically satisfactory. In regard to the development of a new float, we have stimulated some company-funded effort in a local manufacturing concern and have some ideas of our own which merit exploitation. Corrosion and protective coatings are discussed in a later division of this section. Leakage is not a problem with any float tested. Sympathetic implosion in the ocean has not been observed when the floats are spaced more than one foot apart, except when the depth is much greater than nominal.

Our principal concern has been with the problem of creep or plastic flow. Test data obtained on a large number of XX, Special Marola 200 (1967 small lot), and Special Marola 200 (1968 large lot) are tabulated in Ref. 10. It is immediately evident that the 1968 large lot of Marolas is grossly inferior to the 1967 small lot, even though the supplier attempted to manufacture the 1968 lot using the same materials and processes as had been used on the 1967 lot. The reason for the discrepancy has not as yet been found, and probably will not be found until the precise mode of failure has been determined. Test results for the 1967 lot had been very favorable, indicating that the Special Marola was probably superior to the XX. At this writing it appears that the Marola is superior only at pressures above about 1100 PSI whereas the reverse is true below 1100 PSI.

It is believed that the XX float failure mode has been found. After a period of constant pressure a flat spot develops on the surface of the sphere, usually 135° (but on two occasions 45°) from the float handle. This flat progresses to a depresssion of the surface and consequent high stresses around the depression. Finally the material ruptures around the depression and a massive collapse occurs. The flat or depression corresponds to an anode for the first buckling mode shape. Its location 45° or 135° from the handle is expected when one considers that the float handle provides stiffening and should therefore be located at a node where no change of curvature occurs. Growth of the depression appears to be a creep or plastic flow process. It is felt that the Marolas also fail by a creep process. Consequently we have attempted to correlate our data with the Larson-Miller chemical-mechanical equation of state which expresses the equivalence of temperature and time in the creep process:

$$K = T(\log_{10} t + 20)/(1 - T/T_o)$$

T = temperature in ^{o}F Absolute

T_o = temperature in ^{o}F Absolute at which strength~0

t = time to failure in hours

The stress level at which failure occurs at temperature, T, and after a time, t, is reported to be a function of K. Thus by testing at high temperature, we should be able to observe failures in reasonable testing periods. The data so obtained should then permit determination of time-to-failure at normal temperature by using the factor, K. It is also approximately true that failure stress is a linear function of K. Hence, the logarithm of life may be a linear function of stress for the time and stress levels of interest. Life data have therefore also been plotted vs. stress on a semi-log graph. Life has necessarily been estimated by extrapolation to operating pressures from test data so plotted. These plots are given in Figs. 4-7 through 4-10. There is much scatter in the data due to the lack of uniformity within any batch. Note that we estimate the following life expectancies at 11°C:

XX 1000 PSI, $10^6 <$ life $< 10^9$ hrs., avg. life $\sim 10^7$ hrs.

Marola, 1500 PSI, $10^1 <$ life $< 10^8$ hrs., avg. life $\sim 10^5$ hrs.

Marola, 1000 PSI, $10^2 <$ life $< 10^{10}$ hrs., avg. life $\sim 10^7$ hrs.

Figs. 4-11 and 4-12 contain photographs of collapsed floats.

4.2 Sensor Calibration and Environment Testing

It is the intention of this section to describe simply the tests performed prior to installation. It is not felt that detailed information is of general interest.

4.2.1 Thermistors

a. Standard R-T curve: property of semiconductor material checked for each lot at factory.

b. Individual thermistor bias from standard curve determined at MIT/IL in ice water bath, August and April 1968. No change of bias resistance was detected.

c. Time constant as installed in sensor housing: continuous resistance record after immersion in ice water bath at MIT/IL, September 1967.

d. Gross check in pressure environment: comparison with crude indicator during SRI pressure tank test up to 1300 PSI, 6, 7 October 1967; reasonableness check during SRI pressure tank test up to 1200 PSI, 29, 30 July 1968; proper operation during deployment to 600 meters depth, 24 November 1967.

4.2.2 Pressure Transducers

a. R-P curve: factory calibration using dead weight tester, August 1967. Repeat at MIT/IL in hydraulic pressure chamber, September 1967 and in air pressure chamber June 1968. Repeat at SRI during hydrostatic tank test to 1300 PSI, 6, 7 October 1967, and to 1200 PSI, 29, 30 July 1968.

b. Time constant: not checked, factory data accepted.

c. Resolution check: continuous resistance record during bleed off in air pressure chamber, at MIT/IL, June 1968.

d. Gross check during deployment to 600 meters, 24 November 1967: agreement with Station depth determined by geometrical construction.

4.2.3 Tensiometer

a. R-Tension curve: calibration up to 12,000 lbs tension on MIT Instron Test Machine, September 1967; repeat June 1968.

b. R-Temperature curve: calibration over temperature range in oven and during cool-down in ice water bath at MIT/IL, September 1967; repeat in ice bath and room temperature, June 1968.

c. R-Press curve: calibration during SRI hydrostatic tank test to 1300 PSI, 6, 7 October 1967, and to 1200 PSI, 29, 30 July 1968.

d. Time constant: continuous resistance record after step function tension load, July 1968.

e. Gross check during deployment, 24 November 1967: indicated tension agreed with prior estimates for geometry attained.

4.3 System Checkout

The Data Acquistion System and Signal Cable/Sensor Array were married for the first time at Bermuda. Before this marriage the DAS had undergone extensive checkout at MIT/IL including an end-to-end functional demonstration that sets of known resistances can be sampled, precisely measured, and properly formatted on magnetic tape. The IBM 360/75 Assembly Language and Fortran programs for reading the tape and filing the data for analysis programs were verified and ready for use

before the system was operating at Bermuda. Dynamic coupling between cable impedance and the bridge electronics was measured using the actual cable and an error sensing amplifier October 1967 at the cable plant. Thus, no dynamic problems were expected. The complete Signal Cable/Sensor Array was checked out for short-term water pressure integrity and sensor calibration at the 90-inch diameter hydrostatic pressure tank at Southwest Research Institute, San Antonio, Texas. This test was carried out at 100 PSI pressure increments up to 1300 PSI, including a 10 hour hold at 1300 PSI on 6, 7 October 1967. This test was repeated on the repaired array to 1200 PSI, on 29, 30 July 1968. As reported earlier, structural integrity for tension loads was demonstrated by proof tensioning all load-carrying members.

4.4 Corrosion and Protective Coatings

The only telescope components which have been exposed to the ocean environment for a significant period of time and which have been recovered for examination are as follows:

a. Upper ends of the outer moorings attached to form the "inverted v" on 18 November 1967 and removed on 6 February 1968 after nearly 3 months at depths less than 120 meters.

b. Array of floats attached to the WHOI experimental mooring at a depth of 1100 meters at Station D from 23 April to 7 June 1968.

Significant results are as follows:

a. 316 and 304 Stainless Steel fittings suffered no deterioration except for slight deposits of iron oxide on surface scratches.

b. Bare Aluminum floats developed a dull grey surface color and suffered no significant deterioration.

c. A very successful protective coating for the aluminum floats was obtained using IRIDITE primer and three cover coats of Neoprene paint (3MEC1706). Polyurethane paint over various primers (MIL- P-15328R, and 856-28D) proved to be very unsuccessful because the primers did not adhere to the metal surface.

d. Materials in the shallow depth off Bermuda accumulated a thin coating of a slimy and fibrous biological growth. Materials at 1100 meters at Station D accumulated no biological growth.

4.5 Design Support Tests

In the near future it is planned to lay two wire ropes on the bottom from the shallow area just beyond the reef line to a depth of 1000 meters or more. Attached to these ropes will be samples of ocean telescope hardware identical to components already on the telescope or under evaluation for future use. It is hoped that these ropes can be readily recovered six months to one year after installation and that they will provide valuable information to support future design efforts and possible failure analysis. Some particularly interesting articles which would be attached to this array are:

a. XX and Marola Floats.

b. Glass, Syntactic Foam, and other existing floats.

c. New prototype floats and float retainers.

d. Samples of various metals and metallic interfaces with and without protective coatings.

e. Samples of armored cables for evaluation of their resistance to wear on the coral bottom.

f. Electrical connector and splice water-pressure seals and non-wicking electrical cables for evaluation of long-term resistance to leakage.

g. Wire rope terminations for evaluation of corrosion at the bi-metallic interface.

5.0 BERMUDA INSTALLATION

The installation procedure was as follows: The Outer Moorings were first placed on site in the taut, vertical configuration. Later, additional floated wire rope shots were attached at the top ends and winched together to form the inverted "v", which remained below the sea surface. Next the Signal Cable/Sensor Array was attached to the Head Frame at the apex of the "v" and played out on the sea surface while steaming for shore. When Station 1 was put over the stern, a small barge moved in to connect the Inner Mooring Assembly to Station 1 and lower the Inner Coral Hook. The main barge continued toward shore paying out signal cable. When the main barge was approximately one mile inshore from the small barge, the Inner Coral Hook was implanted using a carefully coordinated procedure in which the main barge held sufficient tension to pull down the entire array while the small barge lowered the Inner Coral Hook to the bottom. Once this was accomplished, the remaining signal cable was laid on the bottom to a point just outside the reefs where its bitter end was sealed and left on the bottom in 14 fathoms. Later the tug boat came out with a heavy cable which was connected to the smaller signal cable in a splice box and laid in through the reefs to shore.

5.1 Depth Determination

Because of the steep slope and irregular bottom topography in the installation area, we did not trust the wide beam, sound echo depth information available. We therefore sounded the depth and several profiles at each anchor site by lowering a weighted, metered wire from the R/V Panulirus I (see Fig. 5-1).

5.2 Navigation

Position information during all sea operations was obtained in the form of ship bearings radioed from the Mt. Hill and Paynters Hill optical tracking stations on shore (see Fig. 5-2). Position fixes could be obtained once per minute when necessary, and the error was generally less than 20 ft. These fixes were plotted manually on specially constructed plotting charts from which steering instructions could be readily determined if required. The helmsman was usually able to maintain station without steering instructions by simply monitoring the radioed bearing data.

5.3 Cable Barges and Loading Procedure

The Outer Moorings and Signal Cable/Sensor Array were installed off the YC-1378, a 120 ft. barge whose cable handling equipment had been specially designed for the COLOSSUS ARRAY. This barge had generous working space and winching power, but the large, vertical axis cable drums were not suited for winding small diameter cable.

The Inner Mooring was lowered from the Pontoon Barge, an 80 ft. assemblage of 6 bridge pontoons upon which we installed a mammoth braked drum which had been laying idle at Navy Operating Base (NOB). This drum is capable of paying out a tremendous weight (never measured) when braked, but can winch in only a 1000 lb load; hence the Inner Mooring could not be hauled up except by the YC-1378. Signal cable and wire rope were loaded on the YC-1378 under tension at NOB (approximately 1/3 pay-out tension). The barges and loading rig are illustrated in Fig. 5-3. The YC-1378 drum winched the cable in at the desired tension against the drag provided by the braked drum on the Pontoon Barge. The cable or wire rope was fed manually onto the braked drum, passed four turns around the drum, then around a 36-inch block (tied down to the deck of a YD crane 200 ft. away), and run back to the cable drum on the YC-1378 which was tied up out board of the Pontoon Barge. Tension was measured by a Dillon Gauge in series with the 36 inch block tie-down line. (This tie-down line was sized to be the weak link in the system.)

5.4 Outer Mooring Implantment

The Outer Moorings were lowered in place anchor first from the YC-1378 barge under tow from the tug boat, T-426 (see Fig. 5-4). The taut configuration of these moorings after initial implantment is illustrated in Fig. 5-6. After the Coral Hook and Chain were slipped off, the full weight of the system was taken on the wire rope mooring line. Tension reached a maximum of about 3500 lbs. just before the floats were submerged. In order to minimize the danger of slackening or overstressing the cable due to wave-induced dynamic motions, we calculated a GO-NO-GO limit for acceleration of the barge stern. Because we stayed in port during rough weather, this limit, 0.50 "g", was never reached at sea. If it had been reached, we would have returned to port before slipping off an anchor.

Because of the aforementioned unsuitability of the vertical axis drums, we experienced much difficulty with dropped turns of the Western Outer Mooring line wound last on the drum. Several times this necessitated stopping the wire rope with Cline grips, re-winding many turns, and the repairing of the polyethylene wire rope jacket where the grip had been applied. Fig. 5-5 illustrates the dropped turns encountered when the signal cable was loaded on the drum. When the top of the 101 ft. shot reached the stern roller, the port drum was braked and the load taken up on a synthetic line which had been wound on the starboard drum. This synthetic line was 8-strand, plaited, 1-inch diameter POLY PLUS (Wall Rope Works), nearly torque-balanced to minimize the danger of putting turns into the mooring line.

The 985 ft. shot,which had been flaked out on the cat walk with all floats attached before we left port (Fig. 5-7),was now passed to the Buoy Boat (Fig. 5-8) which pulled the top end straight astern. We then attached the bottom end to the 101 ft. shot (with some difficulty because of inadequate provision for stoppering), and resumed lowering on the synthetic line while the Buoy Boat maintained approximately 500 lbs. strain on the top end. This phase of the operation is illustrated in Fig. 5-9. When the Coral Hook was estimated to be 200 ft. off the bottom we stopped lowering until the path of the barge was directed toward the Station 4 site. We then resumed lowering knowing that the coral hook and chain would lay down in the proper direction. When the synthetic line went slack we cut it free,knowing the anchor had bottomed. The Buoy Boat then set the top end free with Marker Buoy (Fig. 5-10) attached. Periodic visual surveillance of the Marker Buoys was maintained from the tracking towers.

Because of the problem with dropped turns, 7 hours were required to set the Western Outer Mooring, and the final phase involving the Buoy Boat had to be carried out in darkness. The Eastern Outer Mooring was set in 3 hours without serious difficulty.

When the first outer moorings were set in November 1967, turns were developed in the 985 ft. shots because they were lowered from the YC-1378 and the synthetic tag line was not torque-balanced. Even so, these moorings survived five months in the taut, vertical configuration until April, 1968 when they were deliberately sunk to remove a hazard to submarine navigation.

5.5 Formation of the Inverted "v"

Fig. 5-12 attempts to illustrate this operation. On the day we went out to form the inverted "v" the current was setting the surface lines and Marker Buoys toward the East. We had loaded all the necessary wire rope with floats attached on the T-426. We then attached one end of a 1400 ft. float string to the top of the Eastern Outer Mooring and passed the other end (attached to the Head Frame) to the Buoy Boat which dragged the line up-current as we payed it out from the T-Boat. Once this was completed, we left the Buoy Boat to hold the float string toward the West and steamed to the Western Outer Mooring.

There we attached a 1471 ft. float string to the top end of the mooring and fell back toward the Buoy Boat while paying it out. When the end of the 1471 ft. of wire rope was reached, we attached a 5/8 inch diameter polyproylene line and continued to fall back. This synthetic line was 8 strand plaited and therefore nearly torque balanced to avoid putting turns into the mooring cable. When we reached the Buoy Boat she passed the Head Frame to us and we lashed it to the gunwale.

At this point we passed the synthetic line through a set of snatch blocks, rigged with a Dillon gauge to monitor tension, and winched the line in to pull the float strings together. When the end of the 1471 ft. float string came aboard we made it fast to the Head Frame and removed the synthetic line. The Head Frame, now under 1500 lbs. tension, was lowered into the water and tagged off with a floated shot of wire rope to a Marker Buoy. The Head Frame settled about 20 ft. below the surface.

Periodically during this operation we used a small boat, the MIC MAC, to inspect the float strings on the surface and watch for any abnormality such as a back turn. Also, while we were winching in the synthetic line the Buoy Boat assisted by holding the T-Boat on a line between the two moorings, a task which would only be essential in very high winds to prevent overstressing the polypro line. The operation, as described above, was completed successfully in about 5 hours.

5.6 Installation of the Signal Cable/Sensor Array

We waited for a calm day and favorable 24 hour forecast before starting on this most difficult phase of the installation. The YC-1378 barge, under tow by the T-426, was on station over the inverted "v" at 0920, 4 October 1968. We winched the Head Frame up to the stern chute of the barge, attached Station 4, and had it back in the water at 1030. The T-Boat then simply headed for shore along the telescope back azimuth. It was easy to maintain a slow speed with the barge aligned with the cable since the course was directly into the wind. The 100 ft. long cable trough was well suited for the float attachment task. We would simply stop the cable drum permitting each of seven men to attach a float. We would then engage the drum, pay out 100 ft. of cable, stop the drum again, and repeat the procedure. By 1540 we reached Station 1, having payed out over 10,000 ft. of cable and attached almost 700 floats. This activity is illustrated in Figs. 5-11 and 5-13. Even though many turns had dropped (see Fig. 5-5), the cable pulled off the drum without much difficulty since the tension was not excessive (1000 lbs.) and no turns became captured.

We attached the Bridle to Station 1 (see Fig. 5-14) and passed a tag line from the Bridle to the Pontoon Barge which was ready on Station under tow from the R/V Panulirus II (see Fig. 5-15). When Station 1 was several hundred feet aft and clear of the main barge, the Pontoon Barge was backed down to bring the Station close aboard for attachment of the Inner Mooring Assembly. Even though the wind and sea conditions were favorable the maneuvering of two barges in concert proved very difficult, mainly because

there had been no opportunity to practice. The T-426 was struggling to hold the YC-1378 on station while the Panulirus was attempting to hold the Pontoon Barge stern to the signal cable at Station 1. Once the Inner Mooring Assembly was attached to the bridle and the Inner Coral Hook was slipped off, it was possible to pay out some cable from the large braked drum to get the signal cable well below the surface where it could not be damaged. We achieved this situation at 1700 hours.

Fig. 5-16 is a scale drawing which shows the sequence of operations involved in laying the Signal Cable/Sensor Array and setting the Inner Mooring. The geometric situation at 1700 hours, just described, is shown as Stage 1 in the drawing. Both barges moved inshore while paying out cable until Station 1 was 1200 ft. from the Pontoon Barge and 4100 ft. from the YC-1378. At this time (1835 hours, Stage 2) the cable drums were stopped and a geometry check was made. At this and later stages the geometry check was made on a large scale plot of the cable geometry as determined from two sources: (1) a graphical construction based upon the known positions of the barges and Outer Coral Hooks and the known cable lengths, and (2) a determination of Station 2 and Station 4 depth from their pressure transducer signals. The tension transducer provided an overall reasonableness check and a warning of potential overstress. Note that all the array sensors were interrogated and recorded during the entire operation by means of the Backup Data Acquisition System. This System, shown in Fig. 5-17, consisted of a digital ohmmeter, printer, and sequencing electronics.

Next the barges moved up to Stage 3 and another geometry check was made. From this point on the YC-1378 merely held station and braked the cable drum with 4100 ft. of cable out to Station 1. The Pontoon Barge was then required to hold station only approximately by visual reference to the angle of the Inner Mooring Cable and the line between the YC-1378 and St. Davids Lighthouse. The Pontoon Barge then lowered the Inner Coral Hook another 600 ft. to achieve Stage 4.

At Stage 4 the Inner Coral Hook was known to be within 200 ft. of the bottom. The YC-1378 position had been chosen so that, after Stage 4, the array between Stations 1 and 4 would translate parallel to itself while the Inner Coral Hook was lowered to the bottom. In this way, whenever the Inner Coral Hook grounded, establishing Stage 5, the array would pitch up to the horizontal attitude (Stage 6) as the tensile load was transferred from the YC-1378 barge to the Inner Coral Hook. At 2137 hours the coral hook grounded. We immediately reduced throttle on the T-426, permitting the YC-1378 to slip seaward while transferring the load

to the coral hook. After allowing nearly an hour for the coral hook to settle in and Stage 6 to stablize, the remaining signal cable was laid on the bottom up to the pre-arranged splice area outside the reefs. At 0100, 5 October, the bitter end was sealed and left on the bottom in 14 fathoms. At 0300 we were on our harbor moorings.

The principal difficulties experienced in the Signal Cable/Sensor Array installation were associated with control of the vessels. The problems we encountered while attaching the Inner Mooring to Station 1 have already been described. Another problem was encountered in holding the YC-1378 barge on station after Stage 4. The required thrust was slightly over 7000 lbs. whereas we had already measured that the T-426 could only pull 6000 lbs. We had therefore planned to use assistance from the R/V Erline during the final stages after she was no longer needed for patrol duty. In order to minimize the control problem we requested a constant pull from Erline while the T-Boat regulated her throttle below 100% to hold station. It was not possible to adhere to this plan exactly due to a lack of experience in this mode of operation. To avoid overstressing the cable, we requested a throttle hold and accepted some backsliding during the final minutes before the coral hook grounded, missing its target by a few hundred feet.

On October 9, after delays due to weather and other difficulties, we spliced the signal cable to a heavy 115P cable, which we then laid 8000 ft. through the reefs to Ruth's Bay. In a beach box at Ruth's Bay,the 115P cable was connected to a land line we had previously run to the SOFAR Station recording room. Thus ended the five-week continuous field operation.

ACKNOWLEDGEMENT

This paper was prepared under DSR Project 53-30200, sponsored by the Ocean Science and Technology Division of the Office of Naval Research through Contract Nonr-3963 (31) with the Massachusetts Institute of Technology, Cambridge, Massachusetts.

For their assistance in the engineering program, the following persons merit the Institute's appreciation:

Feenan Jennings and Worth Nowlin of the Ocean Science and Technology Division at ONR for their steadfast support and encouragement, particularly throughout our most trying experience.

Prof. Godfrey Savage of the University of New Hampshire; Robert Heinmiller of the Woods Hole Oceanographic Institution; Dan Clark, president of Scientific Marine, Inc.; and Walter Whitaker of USN Underwater Sound Lab for their contributions to the design and installation concepts.

LCDR Warren Fischer and other personnel at the ONR Bermuda detachment; William Adams, Charles Trumbull and many others at the Navy Sofar Station; and to George Taggart, his crew, and Margaret Emmot at the Biological Station; for their many efforts, often strenuous, that contributed to the success of the Bermuda operations.

At MIT, particular credit must be given to Profs. Henry Stommel and Carl Wunsch, Principal Investigator, for their initial concepts and experiment design. Many engineers at the Instrumentation Lab collaborated in the telescope design and exerted great efforts to install it in the ocean. At the risk of dragging this on excessively or of forgetting to mention some deserving individual, I must list Phil Bowditch, Art Grossman, John Lawson, Forbes Little, Ron Morey, Ed Scioli, Frank Siraco, Matti Soikkeli, Jack Suomala, Ken Theriault, Bill Toth, Bill Vachon, Bob Werner, and Peter Wolfe.

Carl Wunsch contributed Section 2 and Peter Wolfe contributed Section 3.3. Many thanks are due Mrs. Hall for her diligence in typing this paper.

The publication of this paper does not constitute approval by the U.S. Navy of the findings or the conclusions contained therein. It is published only for the exchange and stimulation of ideas.

REFERENCES

1. Oceanic Telescope, Mass. Inst. of Tech., Depts. of Meteorology, Geology & Geophysics, and Instrumentation Laboratory, 31 May 1967. Unpublished manuscript containing original feasibility study and proposal to ONR.

2. Ichiye, T., 1966, J. Oceanographic Society of Japan, 22, No. 5.

3. Upper Thermocline Internal Wave Measurements (Abstract Only), Parker, C., and Wunsch, C., Trans. of the American Geophysical Union, 48, p. 140, 1968.

4. On the Propagation of Internal Waves Up a Slope, Wunsch, C., Deep Sea Research, June 1968.

5. Calculation of the Gravity Fall Motion of a Mooring System, Froidevaux, M., and Scholten, R., MIT Instrumentation Lab Report E-2319, July 1968.

6. A Stress and Stability Analysis of the Pilot Project Oceanic Telescope, Little, H. F., MIT Instrumentation Lab Report E-2321, August 1968.

7. Progressive Internal Waves on Slopes, Wunsch, C., Jour. of Fluid Mechanics, in press, 1968.

8. On the Thermal Unrest in the Ocean, Haurwitz, B., Stommel, H., and Munk W., Rossby Memorial Volume, Rockefeller University Press, 1959.

9. Observations of Thermal Fluctuations on the Bermuda Slope, Parker, C. and Wunsch, C., unpublished manuscript, 1967.

10. Oceanic Telescope Engineering Program - Report on Pilot Project Design, Testing, and Progress through October 1968, Dahlen, J.M., MIT Instrumentation Laboratory Report E-2320.

11. An Experimental Study of the Unsteady Forces Causing Vortex-Excited Oscillations of a Circular Cylinder, Pearce, B.R., MIT Instrumentation Laboratory Report T-518, May 1969.

Table 3-1
Stresses at Critical Locations

Current (Kts.) → / Tension (Lbs.) ↓		Zero Current V = 0	Northerly Onshore Current V_x = -1.5 Kts.	Westerly Coastal Current V_z = 1.5 Kts.
TENSION	T_x	3648	1098	6415
PULL ON	T_y	0	-4	-515
STATION 1	T_z	0	0	2448
	$\|T\|$	3648	1098	6885
TENSION	T_x	-1824	-2323	-1095
PULL ON	T_y	1268	1268	493
WESTERN	T_z	-1246	-1197	28
OUTER MOOR	$\|T\|$	2547	2905	1201
TENSION	T_x	-1824	-2323	-5320
PULL ON	T_y	1268	1268	2554
EASTERN	T_z	1246	1197	4704
OUTER MOOR	$\|T\|$	2547	2905	7547

Table 3-2

Deflections at Critical Locations

Deflection (Meters)→ Current (Kts.) ↓	Station 4 Position Changes (Meters) Δx	Δy	Δz	Station 2 Position Changes (Meters) Δx	Δy	Δz	Depth of Deepest Float On Outer Mooring Cable (Meters)
Zero Current V = 0	0	0	0	0	0	0	871
Northerly Onshore Current V_x = -0.3 Kts.	-0.1	+0.2	0	0	+0.1	0	872
Northerly Onshore Current V_x = -1.5 Kts.	-2.7	-8.5	0	~0	-3.3	0	875
Westerly Coastal Current V_z = 0.3 Kts.	-0.3	-1.2	8.6	~0	-0.3	19.8	879
Westerly Coastal Current V_z = 1.5 Kts.	-65	-246	174	-43	-86	288	1127

Table 3-3

Inner Mooring Loads and Clearance of Station 1

Current (Kts.) → / Loads and Deflections	Zero Current V = 0	Northerly Onshore Current V_x = -1.5	Westerly Coastal Current V_z = 1.5	Easterly Coastal Current V_z = -1.5
Azimuth of Array at Station 1 (Deg. True)	155	155	176	134
Bottom Slope under Array at Station 1 (Deg.)	7.4	7.4	8.8	5.2
Clearance of Station 1 above Bottom (Ft.)	77	154	44	28
Lifting Force on Mooring (normal to bottom) at lower End of 250 Ft. Chain Leader (Lbs.)	953	540	955	554
Dragging Force on Mooring (Parallel to Bottom) at Lower End of 250 Ft. Chain Leader (Lbs.)	3547	1040	6336	6387

Table 3-4

Western Outer Mooring - Loads and Clearance of Wire Rope

Current (Kts.) → / Loads and Deflections ↓	Zero Current V = 0	Northerly Onshore Current V_x = -1.5	Westerly Coastal Current V_z = 1.5	Easterly Coastal Current V_z = -1.5
Azimuth of Cable at Mooring (Deg. True)	189	182	153	197
Bottom Slope under Cable at Mooring (Deg.)	7.0	6.9	6.4	6.7
Clearance of Cable above Bottom (Ft.)	69	54	40	41
Lifting Force on Mooring (normal to bottom) at Lower End of 200 Ft. Chain Leader (Lbs.)	668	630	47	1376
Dragging Force on Mooring (parallel to bottom) at Lower End of 200 Ft. Chain Leader (Lbs.)	2310	2700	1105	7312

Table 3-5

Eastern Outer Mooring - Loads and Clearance of Wire Rope

Current (Kts.) → / Loads and Deflections ↓	Zero Current V = 0	Northerly Onshore Current $V_x = -1.5$	Westerly Coastal Current $V_z = 1.5$	Easterly Coastal Current $V_z = -1.5$
Azimuth of Cable at Mooring (Deg. True)	121	128	113	157
Bottom Slope under Cable at Mooring (Deg.)	5.8	7.5	3.7	13.2
Clearance of Cable above Bottom (Ft.)	73	52	52	16
Lifting Force on Mooring (normal to bottom) at Lower End of 200 Ft. Chain Leader (Lbs.)	716	600	1765	0
Dragging Force on Mooring (parallel to bottom) at Lower End of 200 Ft. Chain Leader (Lbs.)	2297	2710	7219	1103

TABLE 4-1

Tensile Yield and Ultimate Strength Tests of Wire Rope Shots

(Short Lengths with Swaged Terminations)

Component	Result
B-3540* - two samples from first delivered order	Swaged SS fork terminations slipped off: 100' shot with SS fork ends: 7200 lbs., 24 October 1967 (see Fig. 4-1) 1' shot with SS fork and Galvanized Eye ends: 7000 lbs., early October 1967
B-3540* - three samples from re-worked first delivered order	Wire rope parted: 6' shot with SS fork ends: 8600 lbs., 25 October 1967 shot with SS fork ends: 9800 lbs., 24 October 1967 shot with Galvanized eye ends: 8900 lbs. 24 October 1967
B-3695** - two samples from first delivered order	Wire rope parted: shot: 13250 lbs. 1' shot with SS fork and Galvanized eye ends: 12,800 lbs., 12 October 1967
B-3540* - two samples from second delivered order	Swaged SS fork terminations slipped off: 5' shots with SS fork and Galvanized eye ends: SS forks slipped 1/8" at 7500 lbs. and slipped off completely at 9000 lbs., 26 June 1968
B-3540* - two samples from re-worked second delivered order	Wire rope parted: 5' shots with SS fork and Galvanized eye ends: SS fork started slipping at 8500 lbs., slip increased to 1/16" at 9000 lbs. Wire rope parted at 9400 lbs., 27 June 1968
B-3695** - sample from second delivered order	Wire rope parted: 5' shot with SS fork and Galvanized eye ends: Ends started slipping at 13500 lbs., slip increased to 1/8" at 17000 lbs. Wire rope parted at 17400 lbs., 26 June 1968

* Rated ultimate strength of B-3540 wire rope is 10,000 lbs

** Rated ultimate strength of B-3695 wire rope is 16,000 lbs.

TABLE 4-2

Inspection and Proof Tests of Wire Rope Shots

(26-29 June 1968)

Procedure

1. Measure swaged fitting diameters for proper dimensions before and after swaging.

2. Apply reference mark to cable near swage termination.

3. Conduct the following tension proof tests for 10 minutes on each shot:

    a. B-3540 wire rope shots to 7000 lbs.

    b. B-3695 wire rope shots to 12, 000 lbs.

4. Measure length of each shot at 50% and 25% of proof load after successful completion of proof load test.

5. After completion of proof test inspect location of reference mark for evidence of pull-out from swaged termination.

6. X-ray and Zyglo all terminations and examine for evidence of damage or faults.

7. Complete molding of boots over terminations.

Results

1. All shots completed procedure successfully.

2. Elastic stretch of wire rope:

    a. B-3540: 1.16×10^{-6} ft./ft.-lb.

    b. B-3695: 0.585×10^{-6} ft./ft.-lb.

3. Measured lengths given elsewhere in this report.

TABLE 4-3

Inspection and Proof Tests of Signal Cable Shots

Procedure

1. X-ray all DAT Shells at 0^{o} and 90^{o} orientation
2. Tension proof test:
   a. Shot 4A-3B to 8000 lbs. for 1 3/4 hrs., 25July, 1968
   b. Shot 3A-2B to 7500 lbs. for 2 hrs., 27 June, 1968
   c. Shot 2A-1B to 8000 lbs. for 1 1/2 hrs., 24 July, 1968
   d. Shot 1A-5116 ft. mark to 9000 lbs., for 3 hrs., 29 June, 1968
   e. Shot 1A-MS2L splice to 5000 lbs. for 1/2 hr., 24 July, 1968
3. Measure electrical resistance and leakage of all shots before slacking off from proof tension.
4. Measure length of each shot at 50% and 25% of proof load after successful completion of proof load test.
5. X-ray all DAT Shells at 0^{o} and 90^{o} orientation and inspect for damage.

Results

1. Above procedure completed successfully (See Fig. 4-4).
2. Initial proof test of shot 3A-2B in April 1968 resulted in pull-out of armor from termination 3A at 6800 lbs.
3. Initial proof test of shot 4A-3B on 29 June 1968 resulted in pull-out of armor from termination 3B at 6500 lbs.
4. Initial proof test of shot 2A-1B took place on 30 June 1968 to 8500 lbs. for 2 hours. Subsequently, termination 1B was re-done because of suspected electrical leakage. Proof test was therefore repeated.
5. Elastic stretch of A-5051 signal cable is 0.64×10^{-6} ft./ft.-lb.
6. Measured lengths given elsewhere in this report.

TABLE 4-4

Summary of Proof Loading Tests on Standard Hardware at Bermuda NOB

(October, November 1967)

Component	Result
Both 100' Outer Mooring Chain Leaders (3/8" Proof Coil)	Loaded with 5800 lbs. for five minutes, O.K.
150' Inner Mooring Chain Leader (7/16" Proof Coil)	Broke weak link at 7800 lbs. tension. Repaired with 1/2" shackles and re-tested at 7800 lbs. for five minutes, O.K. (See Fig. 4-6).
Critical 7/16" Galvanized Steel Shackles (Crosby-Laughlin G-215)	Loaded with 5800 lbs. for five minutes, O.K.
Critical 1/2" Galvanized Steel Shackles (Crosby-Laughlin G-2150)	Loaded with 7800 lbs. for five minutes, O.K.
Four 3/8" Stainless Steel Shackles (Type A)	Fractured with 10,000 lbs. load. Discarded this type shackle, (See Fig. 4-5).
Critical 7/16" Stainless Steel "D" Shackles (Type B, Norwegian)	Loaded with 10,000 lbs. for five minutes, O.K.
Eye Splice on 3/4" 3-strand Nylon Rope	Loaded with 7800 lbs. for five minutes, O.K.
Eye Splice on 1 1/4" 3-strand Nylon Rope	Loaded with 12,000 lbs. for five minutes, O.K.

TABLE 4-5

Tensile Yield and Ultimate Strength Tests of Standard Hardware and Special Fittings

Item	Yield Point (lbs.)	Ultimate Load (lbs.)
5 ft. length of 3/8" "Cam Alloy" Chain	Loaded specimen to 17,500 lbs. between grab eye and 7/16" shackle. No yield evident except at grab eye. Yield is 13,200 lbs. and ultimate strength is 26,000 lbs. according to Campbell Chain Co.	
Coupling for B-3540 WR	-	>16,000
3/8" G-215 Shackle	>6000	-
7/16" G-215 Shackle	~8000	19,000
1/2" G-2150 Shackle	9000	>21,000
Coupling for B-3695 WR	-	>18,500
Stopper for B-3540 WR	5500	16,000 1/2" Al Pin Sheared
Stopper for B-3695 WR	10,000	>18,500 5/8" Al Pin yielded badly at this load
Grab Eye for 3/8" Chain	10,000	17,500 eye opened up
7/16" 3/6 SS Shackles	7000 (improper pin loading)	>10,000

TABLE 4-6

Proof Tests at MIT/IL of Standard Hardware and Special Fittings in Preparation for Deployment, Summer 1968

	Item	Proof Load (lbs.)
34	7/16" G-215 Shackles	9,000
19	1/2" G-2150 Shackles	10,000
18	5/8" G-2150 Shackles	15,000
6	3/4" G-2150 Shackles	20,000
4	3/8" G-215 Shackles	6,000
7	Stopper Shackles for B-3540 WR	5,500
5	3/8" Grab Eyes	13,000
2	Miller's Swivels (Type 3, Model BB)	1,500
3	Stopper Shackles for B-3695 WR	10,000
4	7/16" 316 SS Shackles	6,000
2	Eye Splices on ends of 1600' length of 1" Rope (Wall Rope Co., Plaited POLY-PLUS)	7,000
1	Eye Splice on end of 600' length of 1 1/4" Rope (Wall Rope Co. Plaited POLY-PRO)	10,000
2	Eye Splices on ends of 5000' length of 5/8" Rope (Wall Rope Co., Plaited POLY-PRO)	3,000
	3/8" CAM ALLOY Chain	13,200 (at factory)

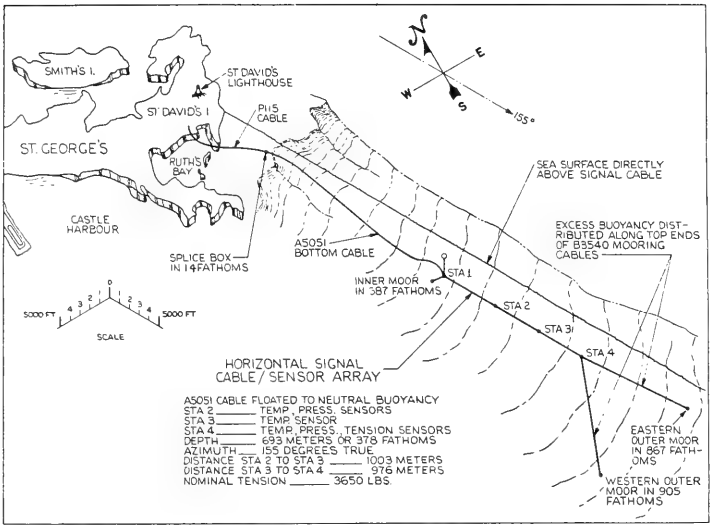

Figure 1-1. Oceanic Telescope Schematic

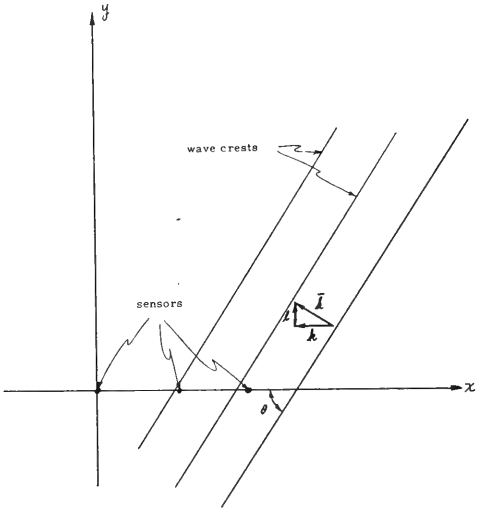

Figure 2-1. Wave/Array Geometry

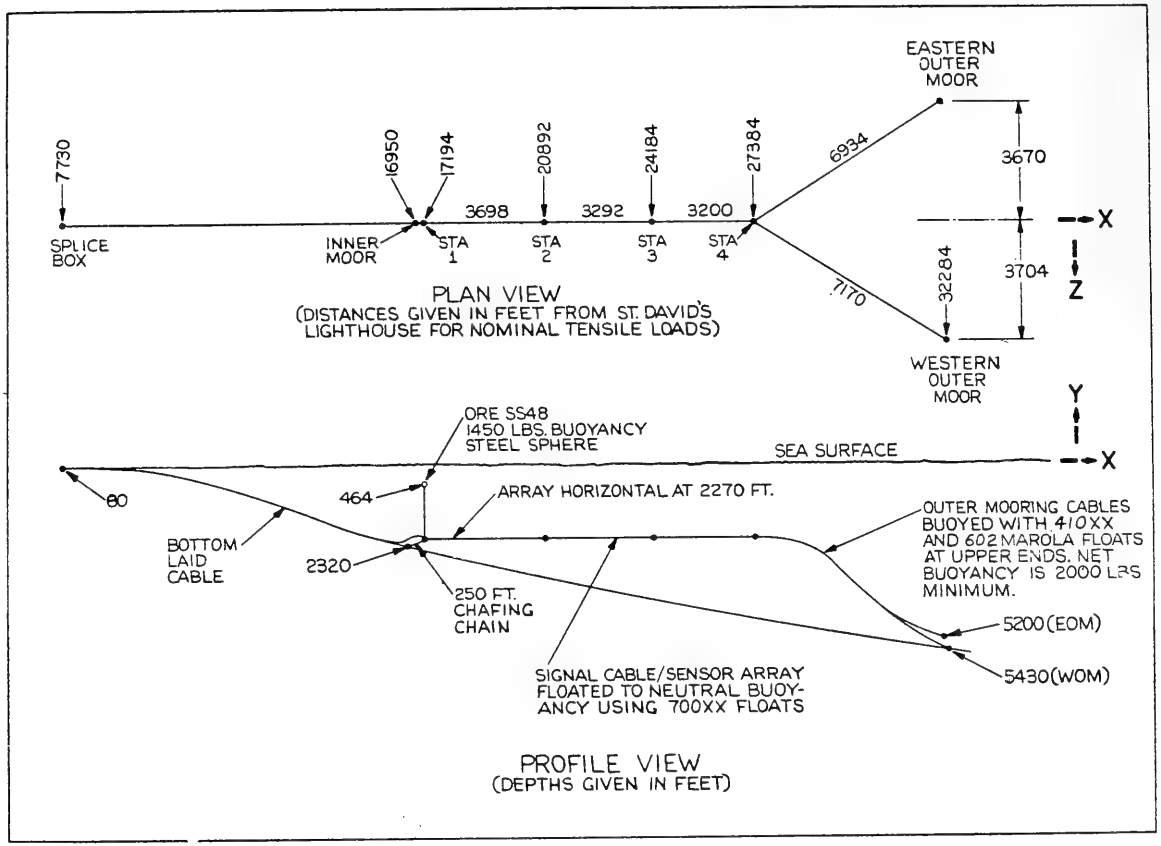

Fig. 3-1 Oceanic Telescope General Arrangement

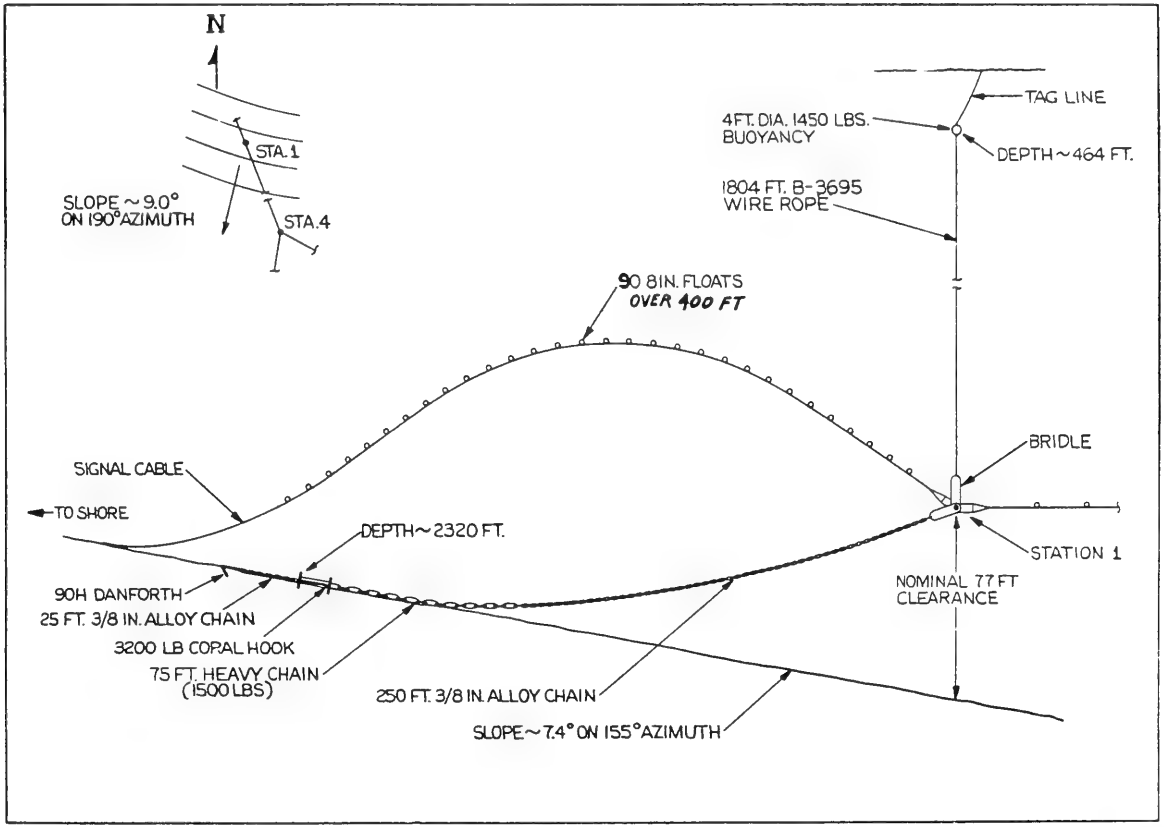

Fig. 3-2 Inner Mooring Assembly Schematic

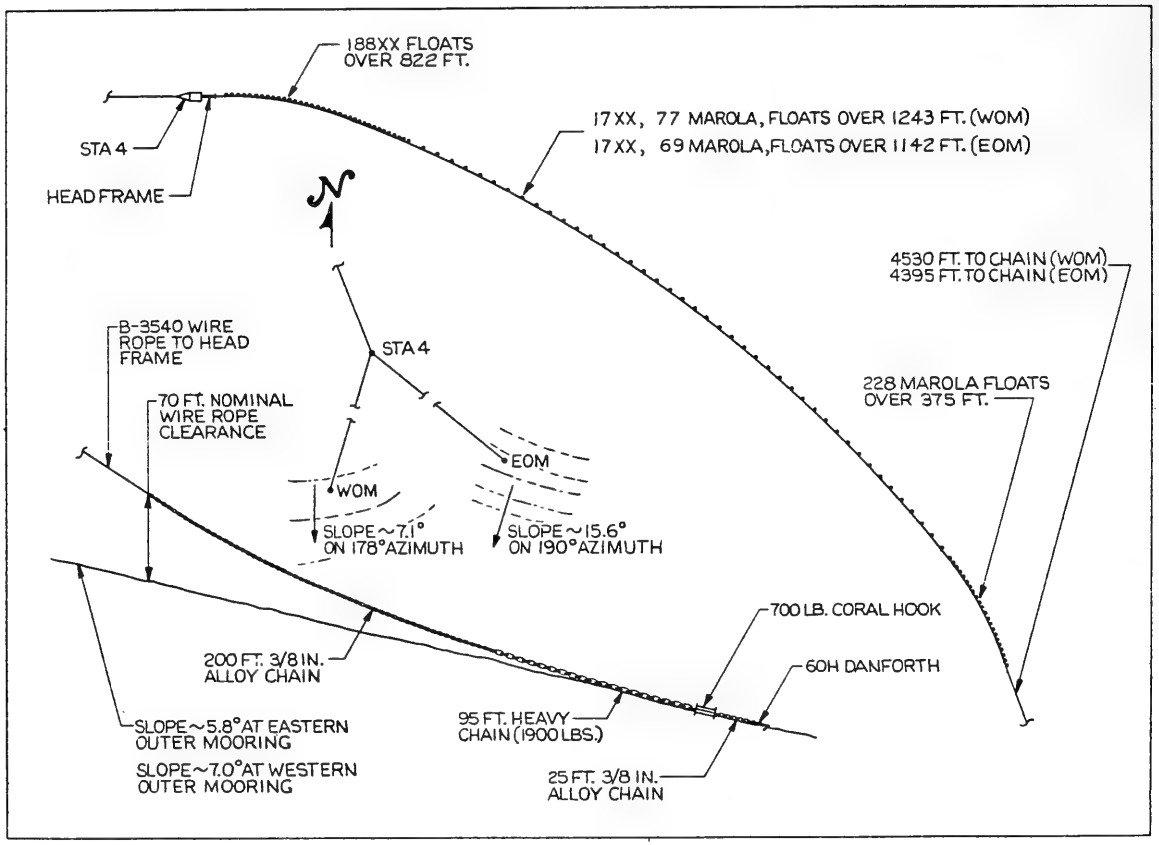

Fig. 3-3 Outer Mooring Assembly Schematic

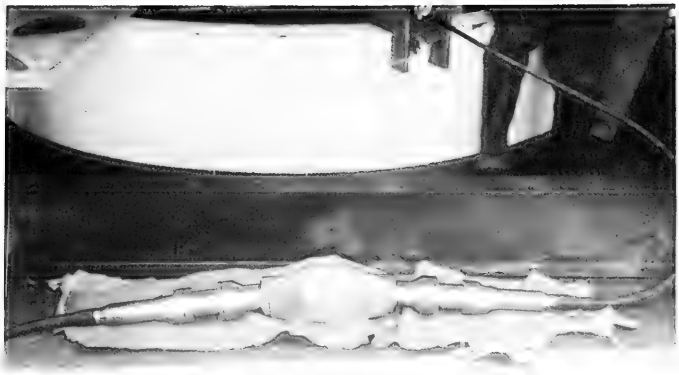

Figure 3-4. Station 1 at Hydrostatic Pressure Test Facility

Figure 3-5. Station 2 at Hydrostatic Pressure Test Facility

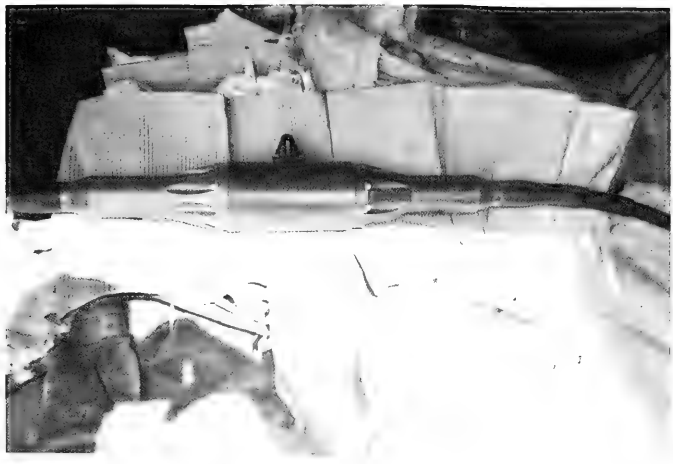

Figure 3-6. Station 3 at Hydrostatic Pressure Test Facility

Figure 3-7. Station 4 at Hydrostatic Pressure Test Facility

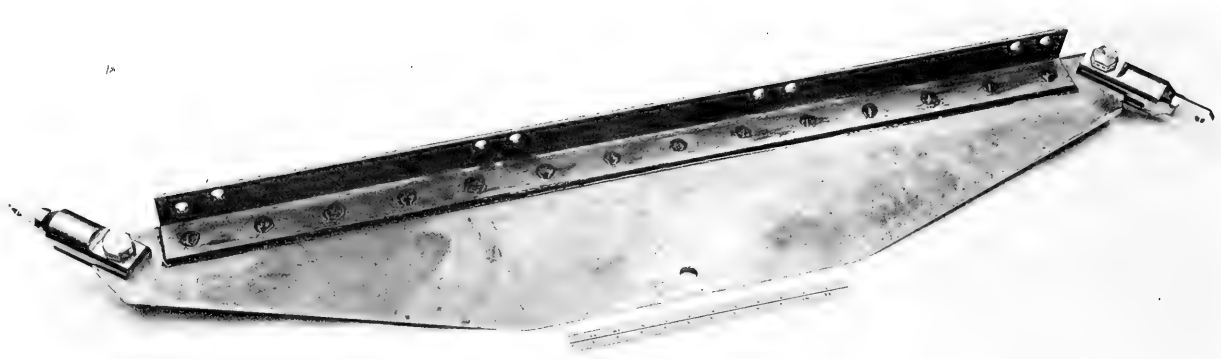

Figure 3-8. Head Frame, Coupling for Station 4 Not Shown
(Refer to Figure 3-7)

Figure 3-9a. Outer Mooring Coral Hook Slung Over Side of Cable Laying Barge

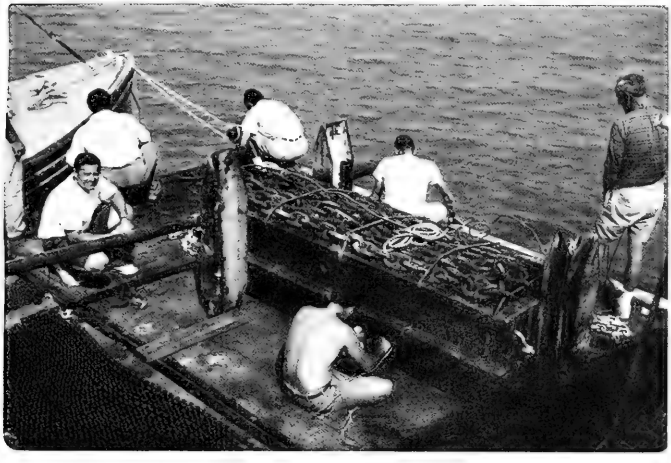

Figure 3-9b. Inner Mooring Coral Hook on Deck of Pontoon Barge

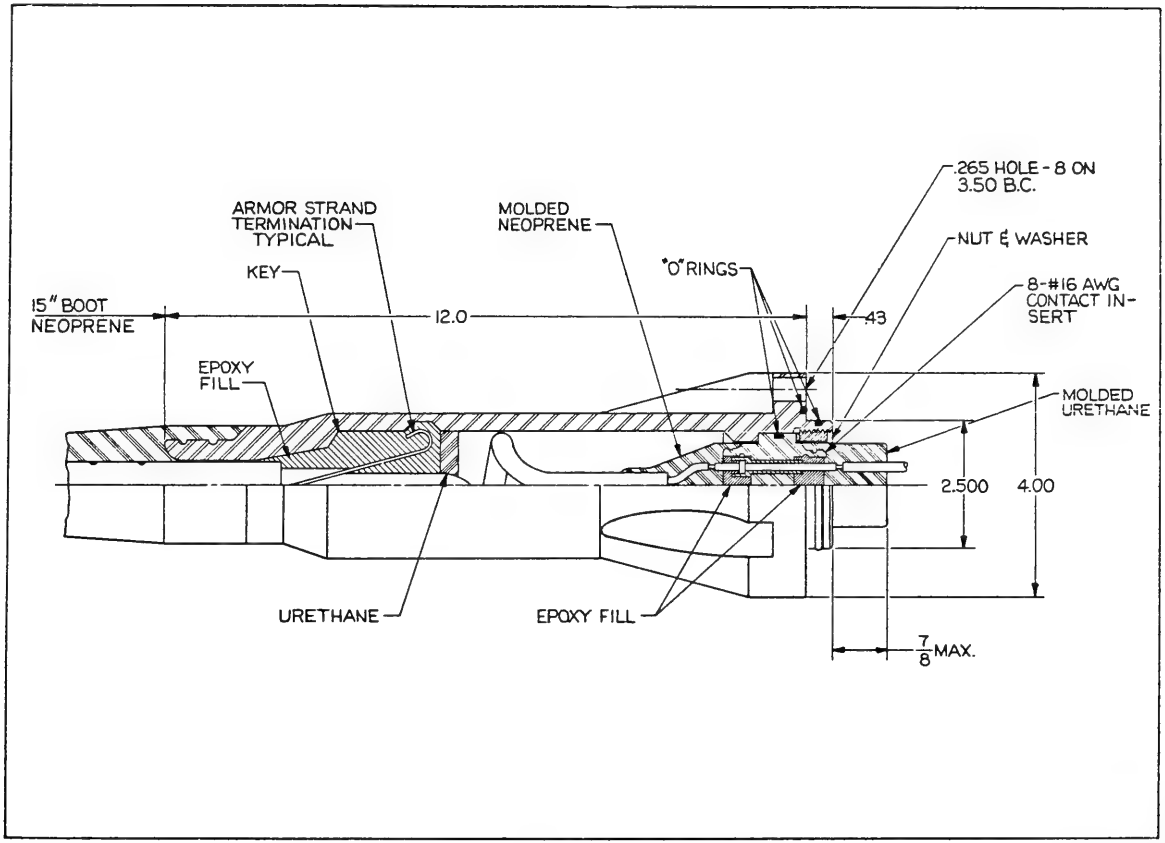

Fig. 3-10 Signal Cable Termination

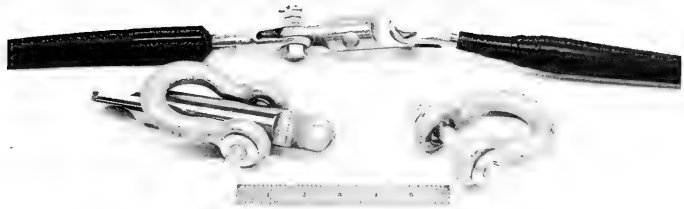

Figure 3-11a. Typical Wire Rope Connection, Rope-Rope, including Stopper Hardware

Figure 3-11b. Typical Wire Rope Connection, Rope-Chain, including Stopper Grab Eye

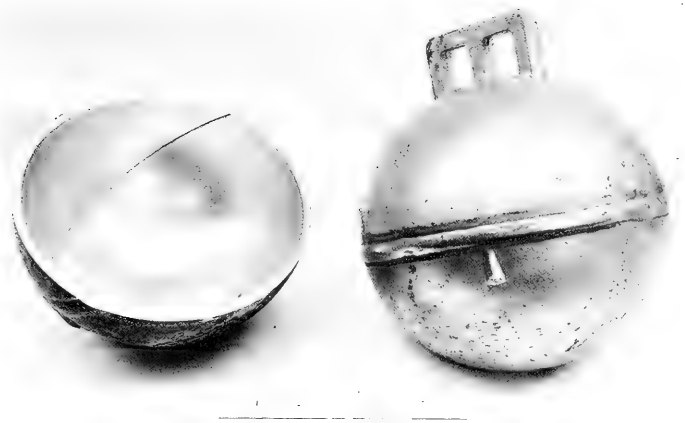

Figure 3-12. Phillips Cast Aluminum XX Float

Figure 3-13. Plasticos De Galicia's Marola 200 Float

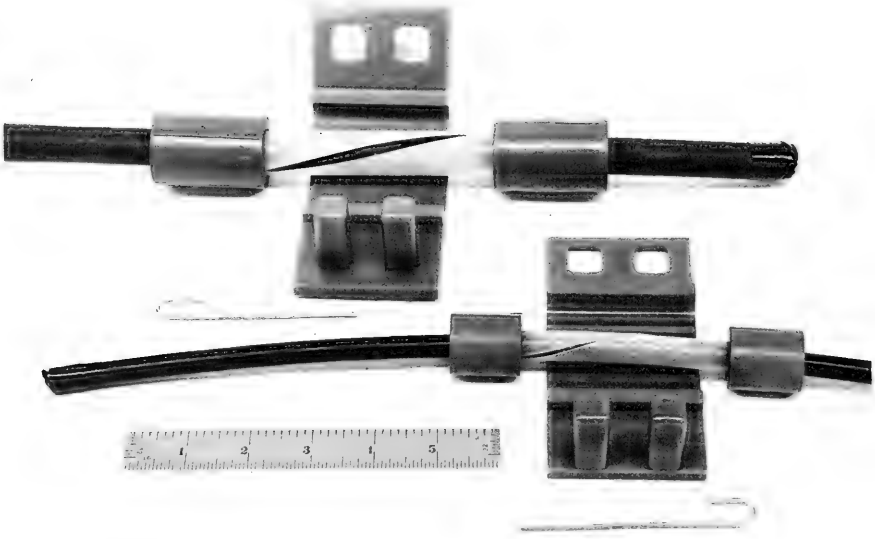

Figure 3-14a. Float Attachment Device Parts

Figure 3-14b. Float Attachment Device Assembled

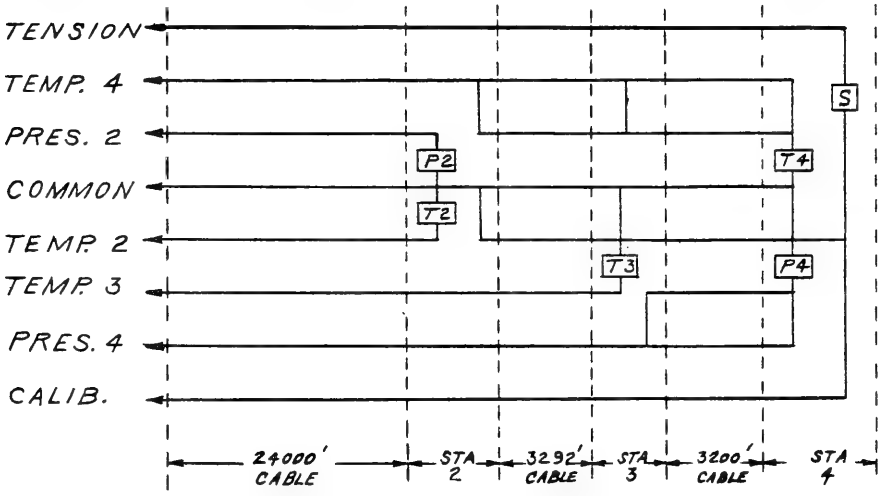

Figure 3-15. Sensor Wiring Schematic

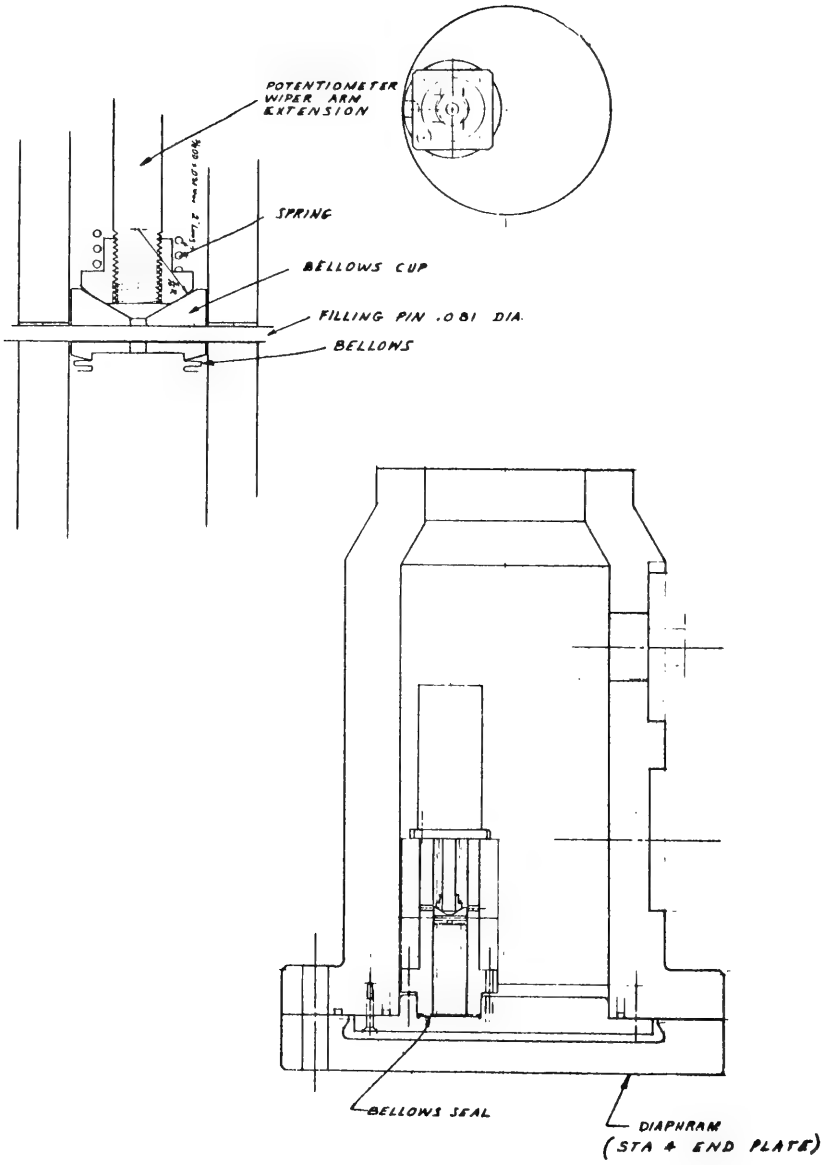

Fig. 3-16 Tensiometer Layout (incomplete)

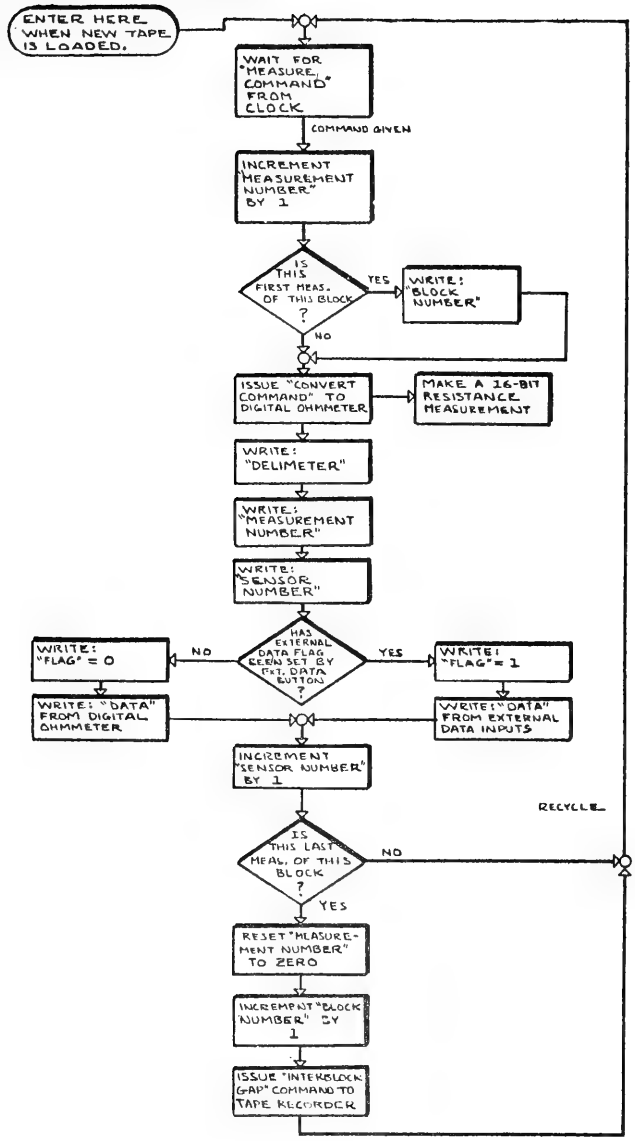

Fig. 3-17 Flow Diagram of Operations within the Data Acquisition System

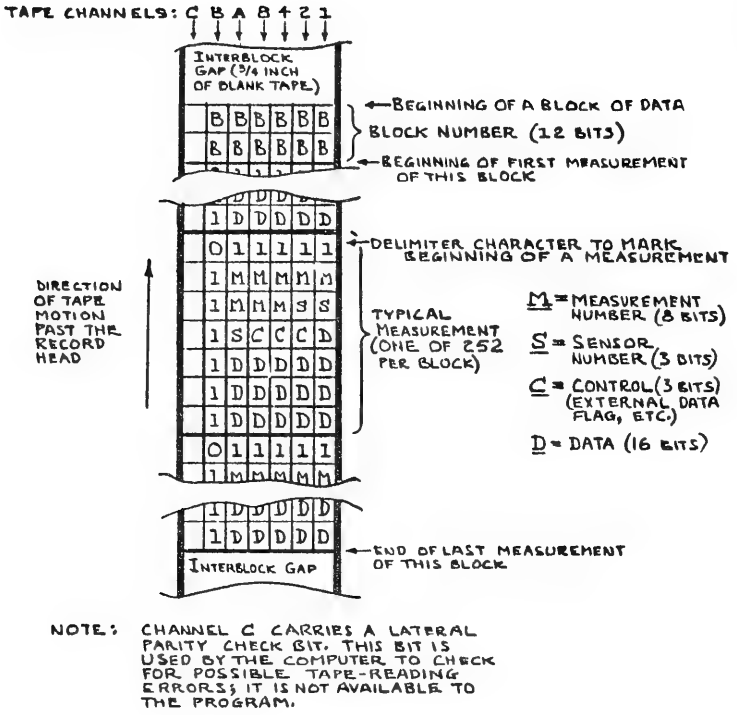

Fig. 3-18 Primary Data Tape Format

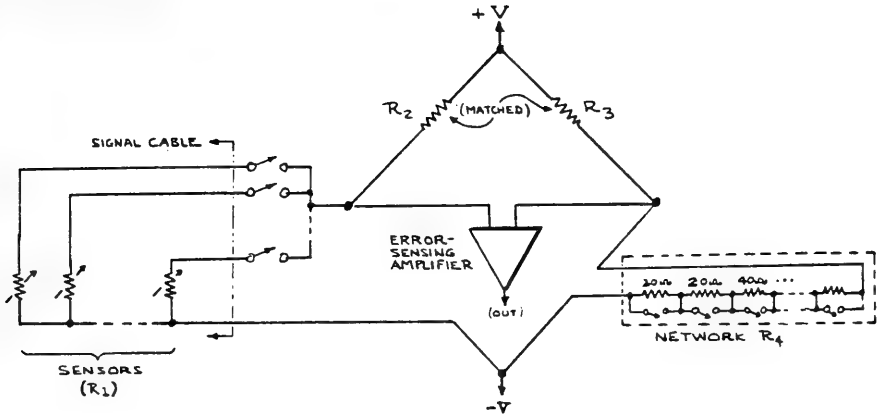

Fig. 3-19. A Simple Digital Measuring Bridge

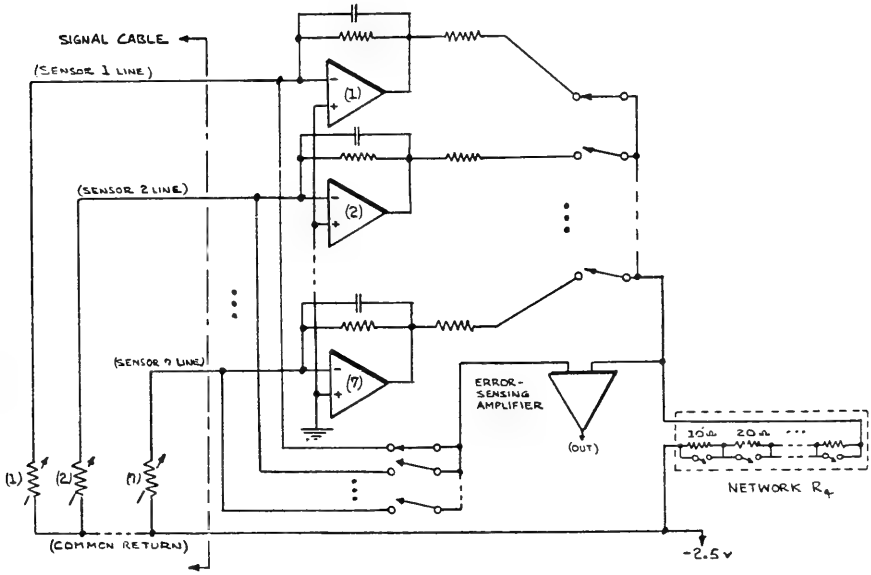

Fig. 3-20. Simplified Diagram of Revised Bridge with One Amplifier per Sensor

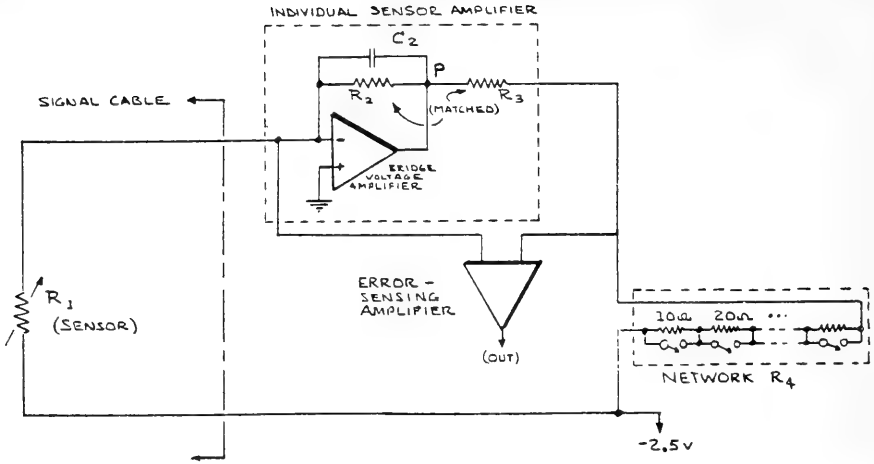

Fig. 3-21. Revised Bridge with only One Sensor Amplifier Shown

Figure 3-22. Digital Measurement Bridge

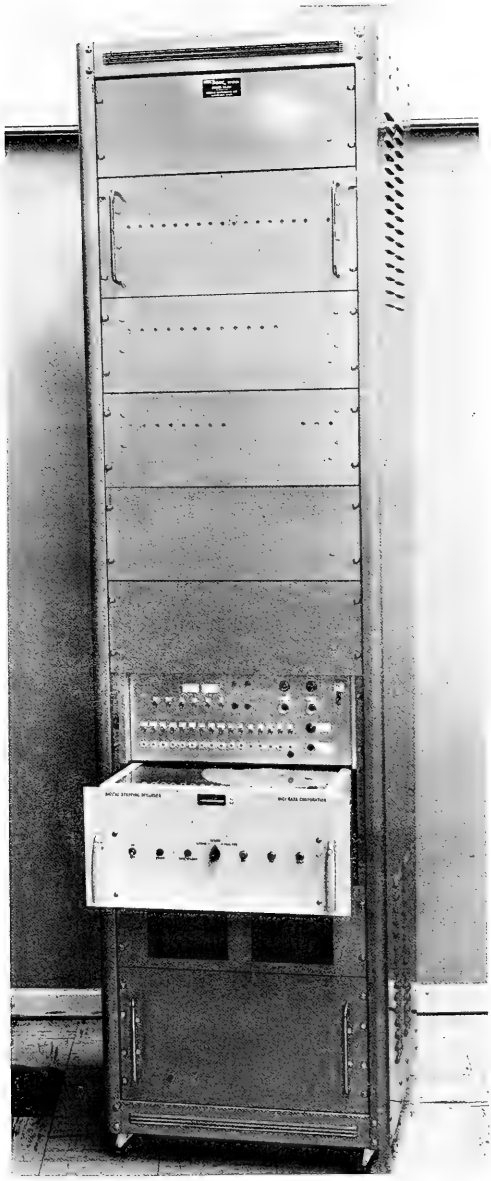

Figure 3-23. Data Acquisition System

Figure 4-1. Failure of B-3540 Wire Rope Termination during Strength Test

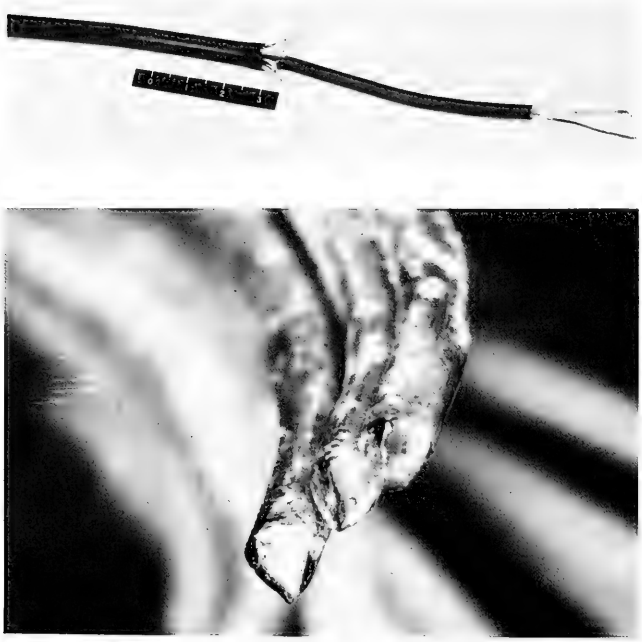

Figure 4-2. Bitter End of Signal Cable Slipped out of Termination 1B

Figure 4-3. Armor Strands at Termination 4A. Parted at 15, 000 lbs. Tension

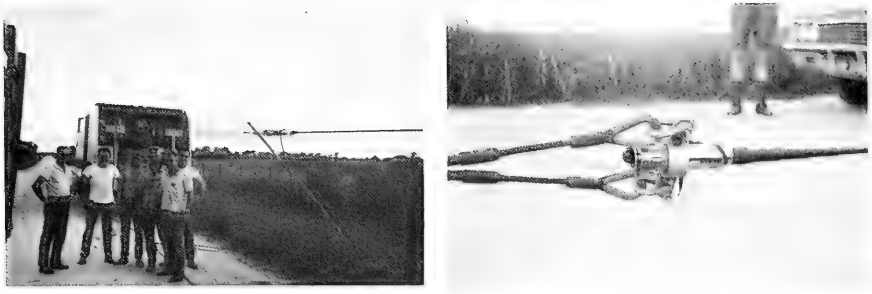

Figure 4-4. Proof Tensioning Long Shots of Cable

Figure 4-5. Failure of Stainless Steel Anchor Shackle at NOB, Bermuda

Figure 4-6. Proof Tensioning of Inner Mooring Components at NOB, Bermuda

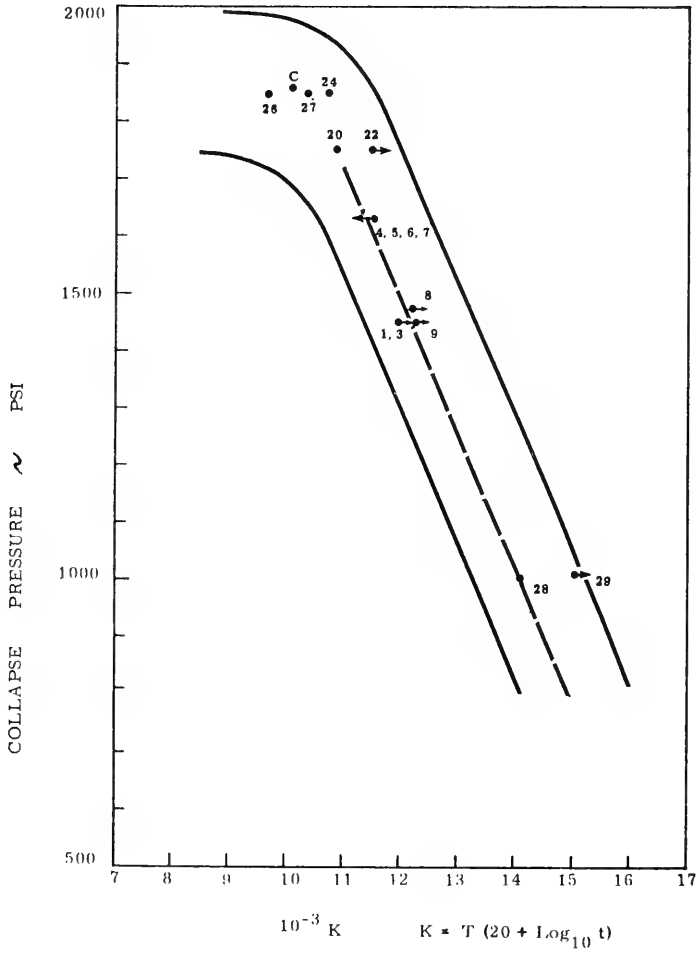

Fig. 4-7 Pressure vs K for XX Floats

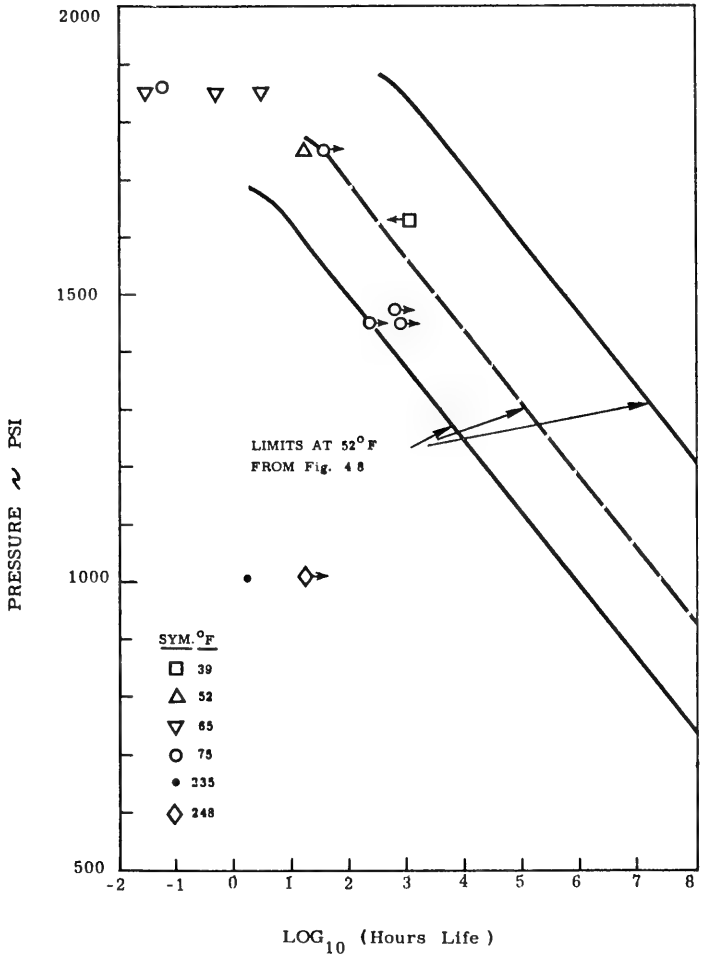

Fig. 4-8 Pressure vs Life for XX Floats

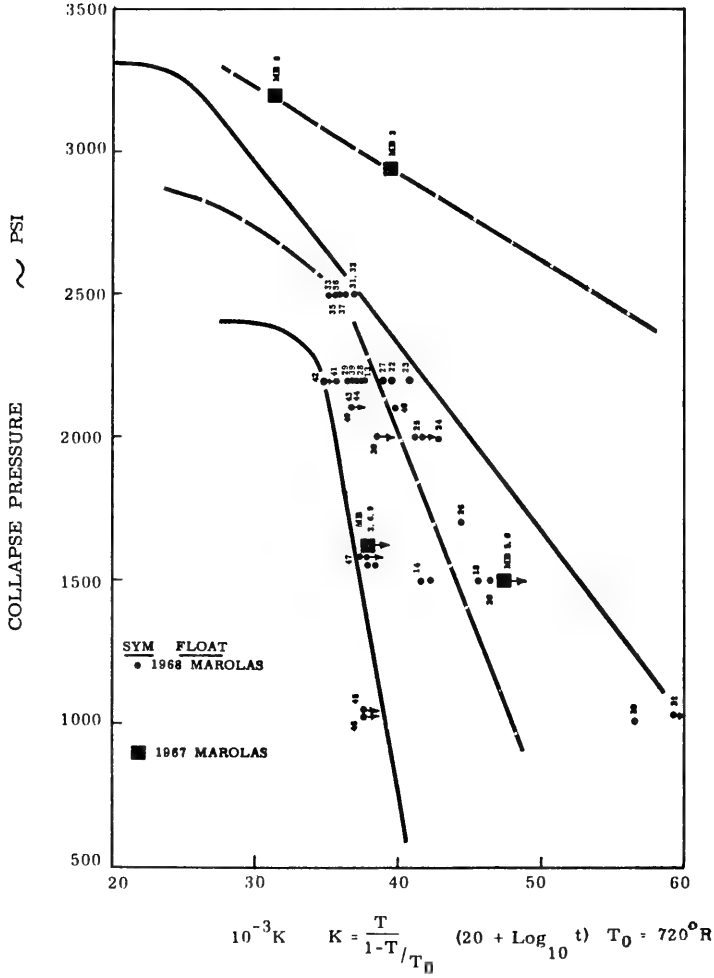

Fig. 4-9 Pressure vs K for Marola Floats

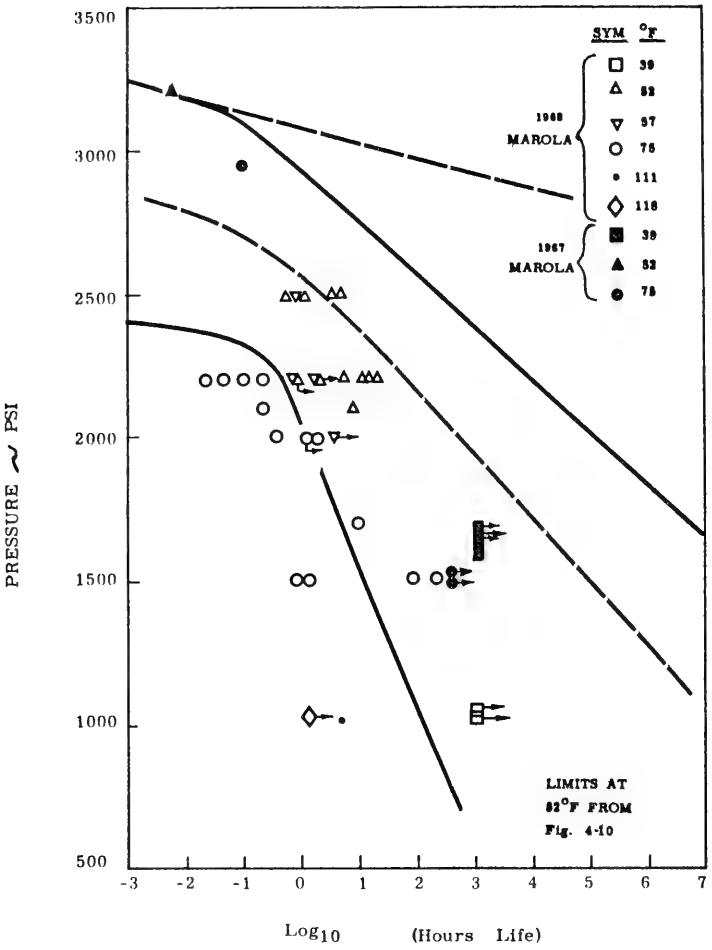

4-10 Pressure vs Life for Marola Floats

Figure 4-11. Collapsed XX Floats

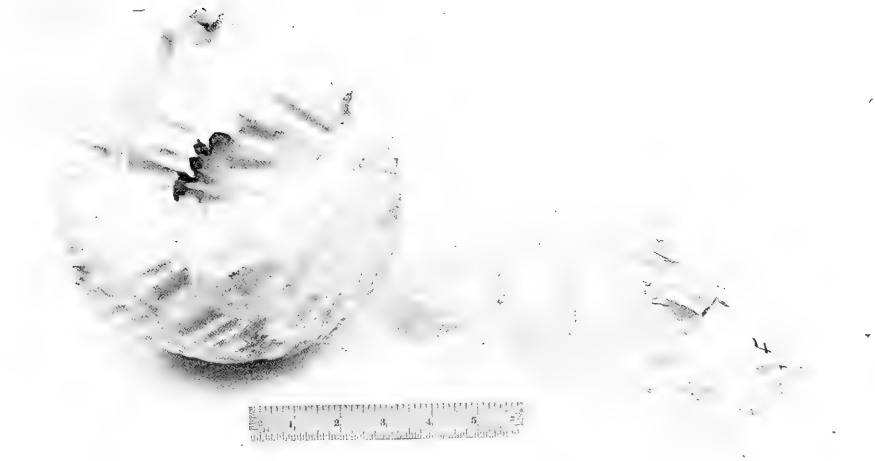

Figure 4-12. Collapsed Special Marola Floats

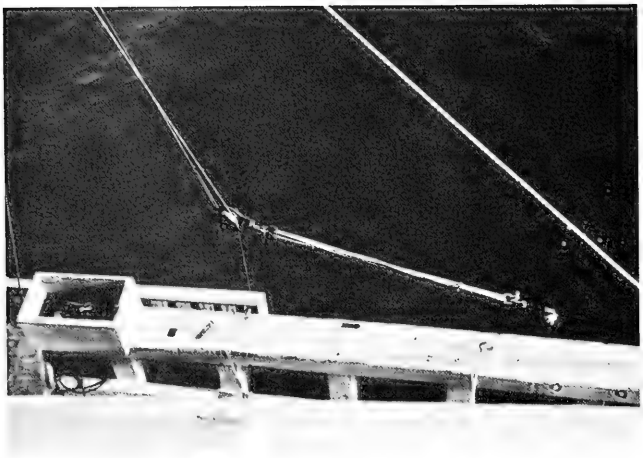

Figure 5-1a. R/V Panulirus I Wire Sounding Rig

Figure 5-1b. Metered Sheave Used in Wire Sounding

Figure 5-2a. Paynters Hill Tracking Station

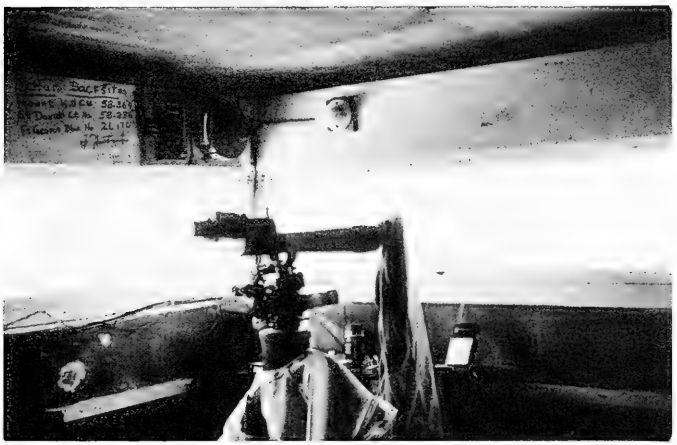

Figure 5-2b. Tracking Telescope

Figure 5-3a. YC-1378 Outboard of Pontoon Barge Loading Cable under Tension

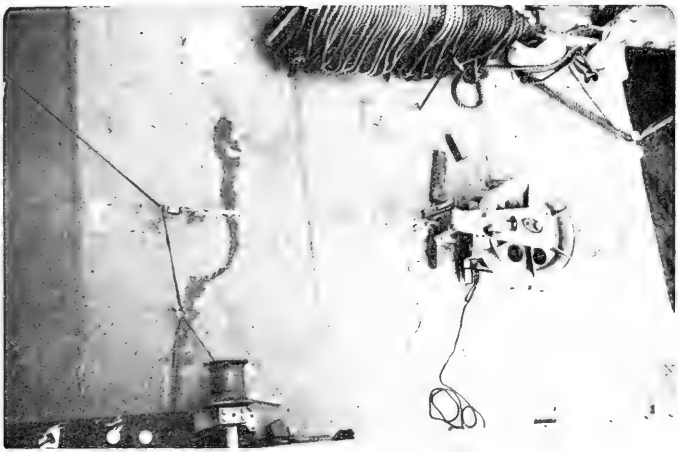

Figure 5-3b. 36-inch Diameter Block Rigged for Cable Loading

Figure 5-4. T-426 Towing YC-1378

Figure 5-5. Dropped Turns from Signal Cable/Sensor Array Wound on YC-1378 Vertical Axis Drum

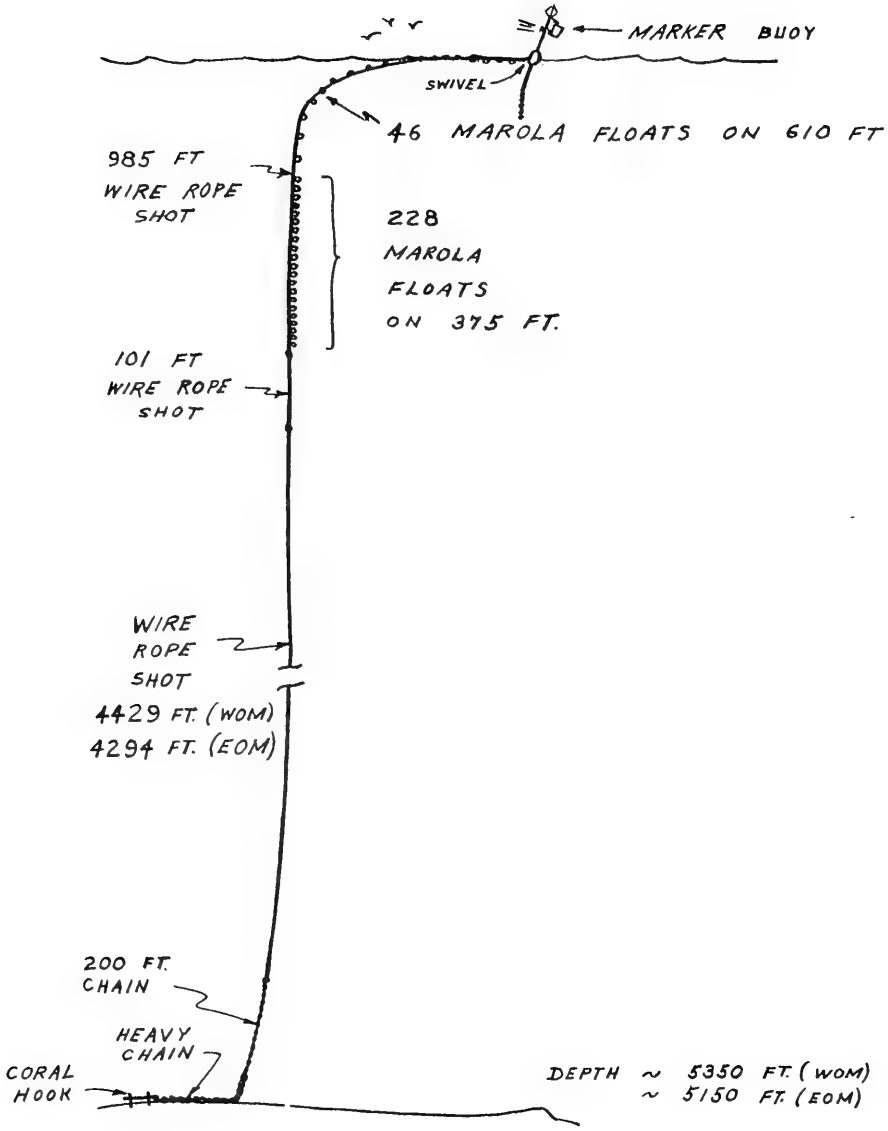

FIG. 5-6 OUTER MOORINGS AFTER INITIAL IMPLANTMENT

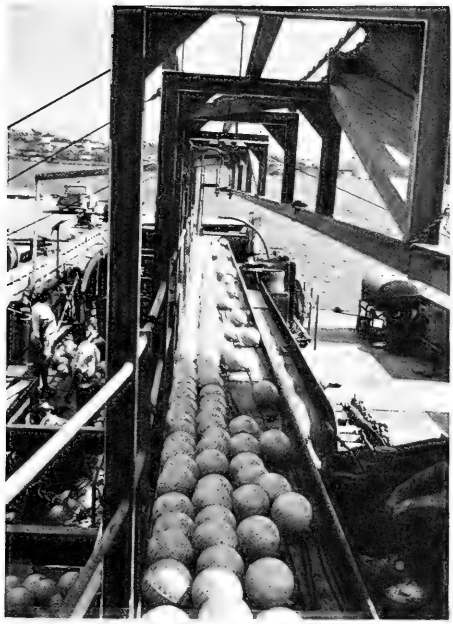

Figure 5-7. 985 Ft. Float String for Western Outer Mooring Flaked Out on YC-1378 Catwalk

Figure 5-8. Buoy Boat

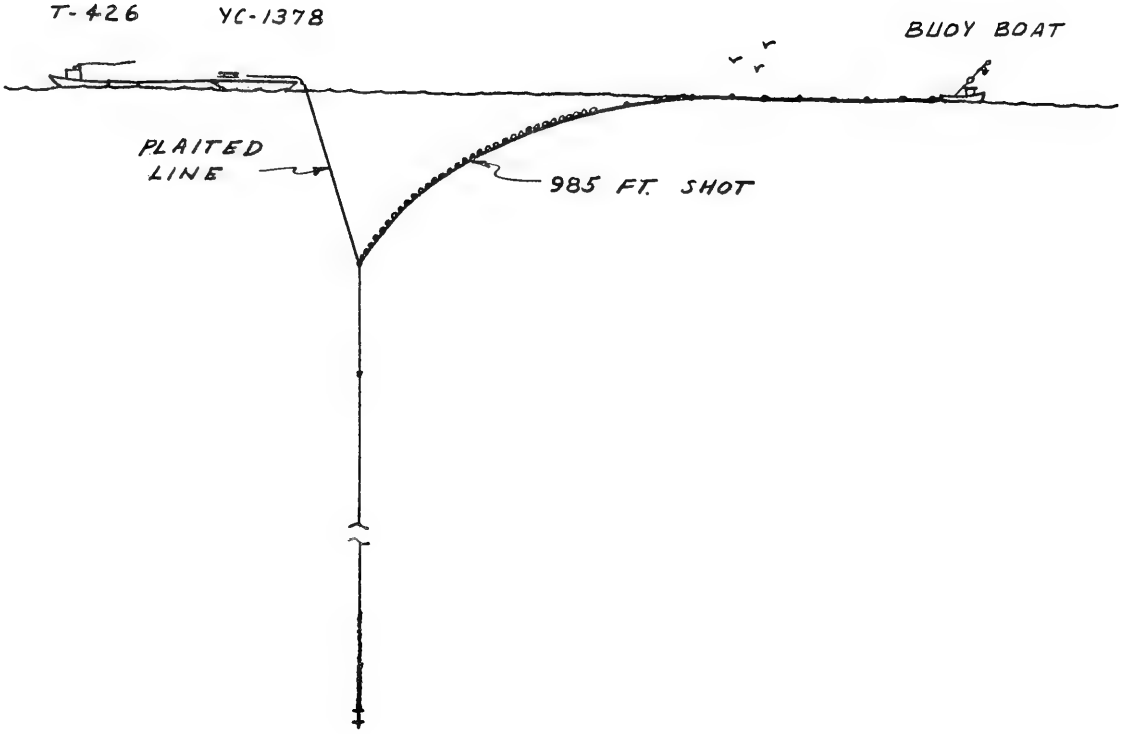

FIG. 5-9 FINAL PHASE OF OUTER MOORING IMPLANTMENT

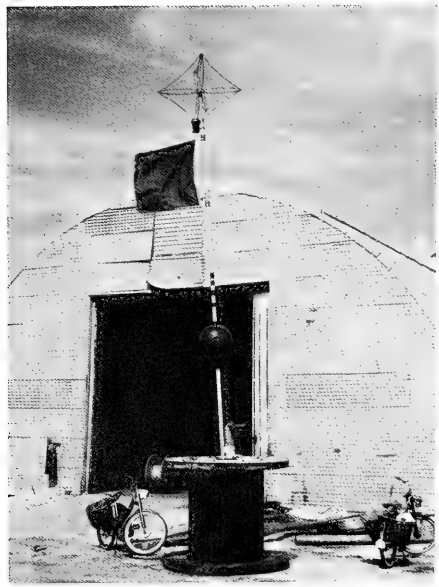

Figure 5-10. Marker Buoy Assembled in Front of Storage Hut at Navy Operating Base

Figure 5-11. Attaching XX Float to Signal Cable

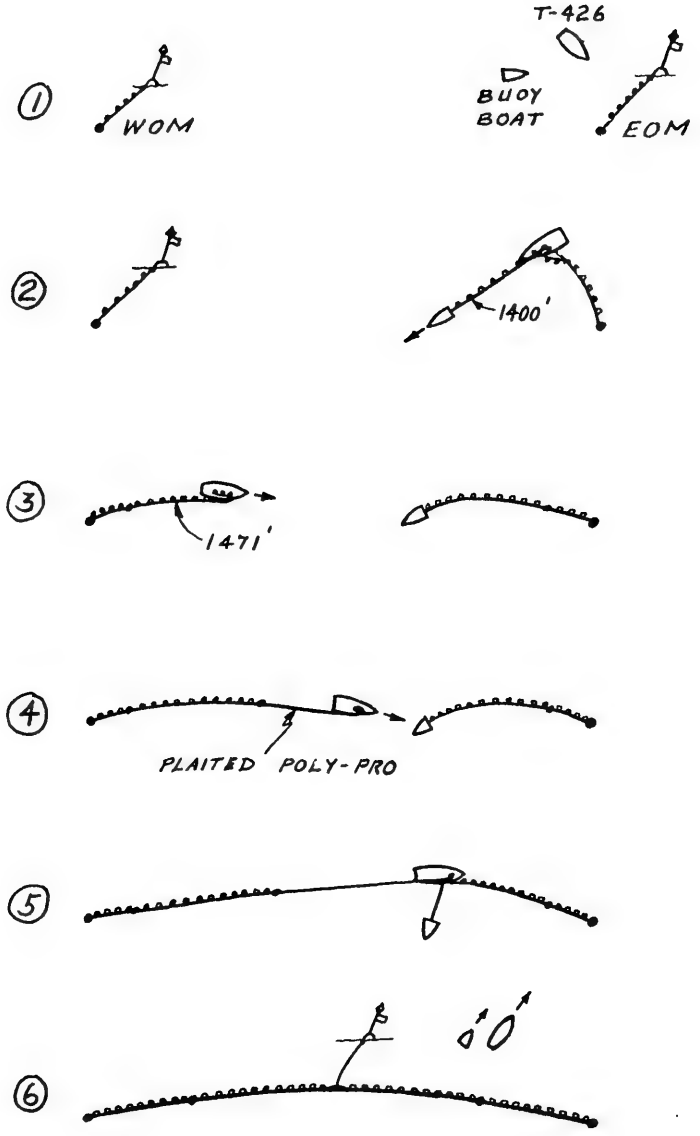

FIG. 5-12 FORMATION OF INVERTED "V"

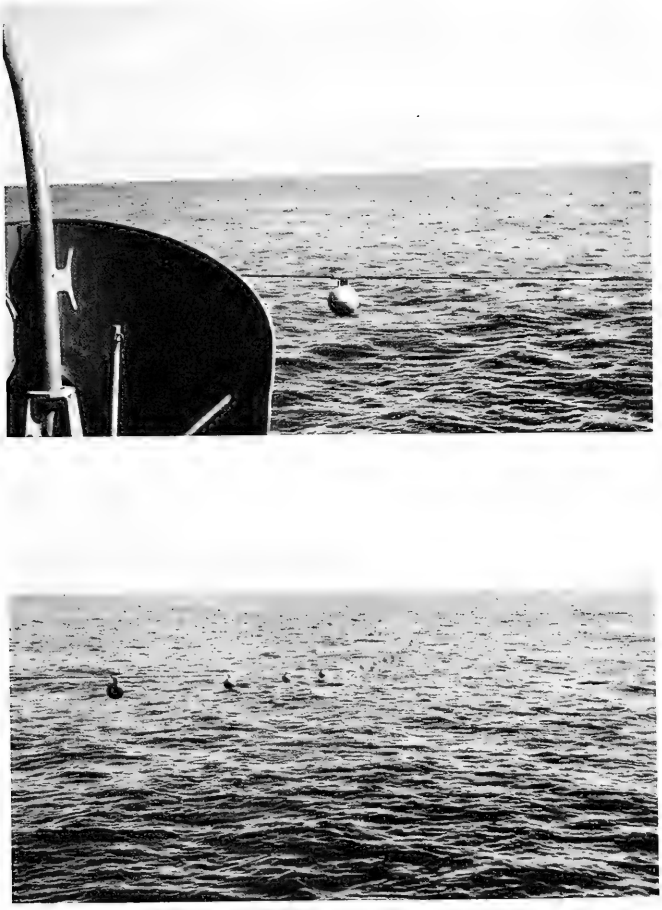

Figure 5-13. Paying Out Signal Cable from YC-1378 Barge

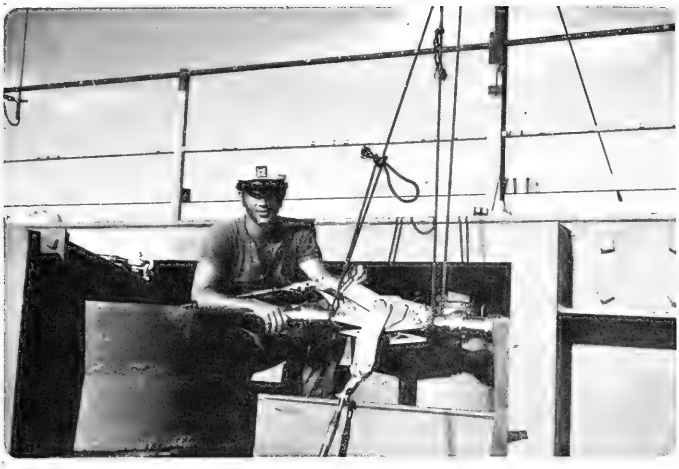

Figure 5-14. Station 1 with Inner Mooring Bridle Ready to be Payed Out from the YC-1378 Barge

Figure 5-15. R/V Panulirus II Towing Pontoon Barge

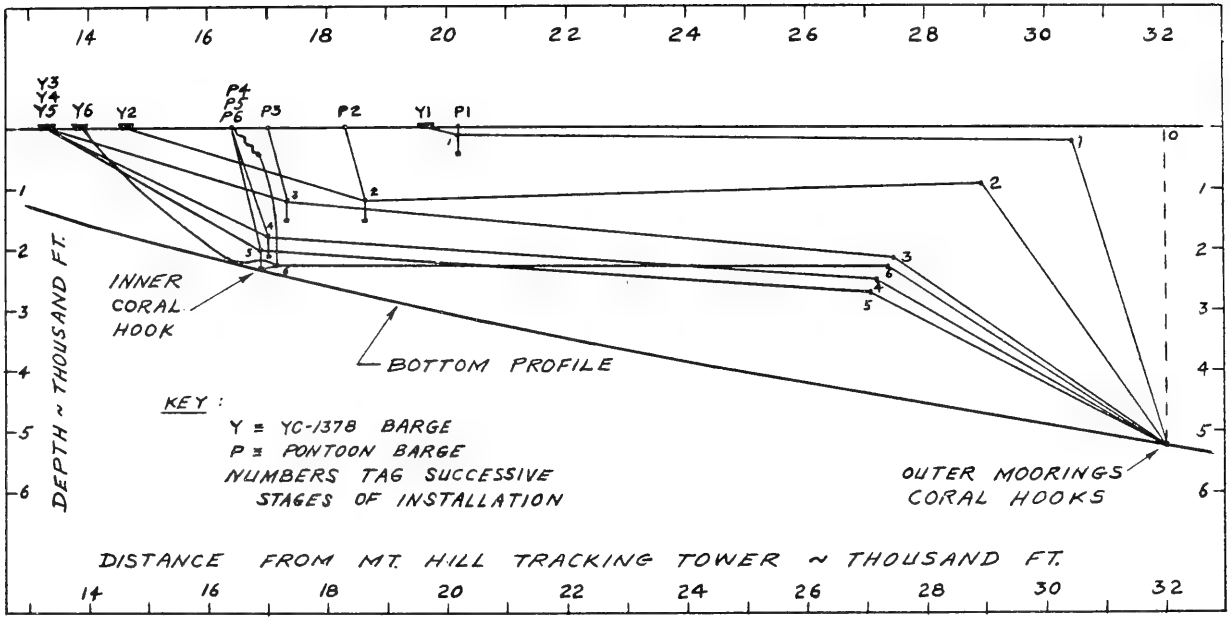

FIG. 5-16 INSTALLATION OF SIGNAL CABLE/ SENSOR ARRAY

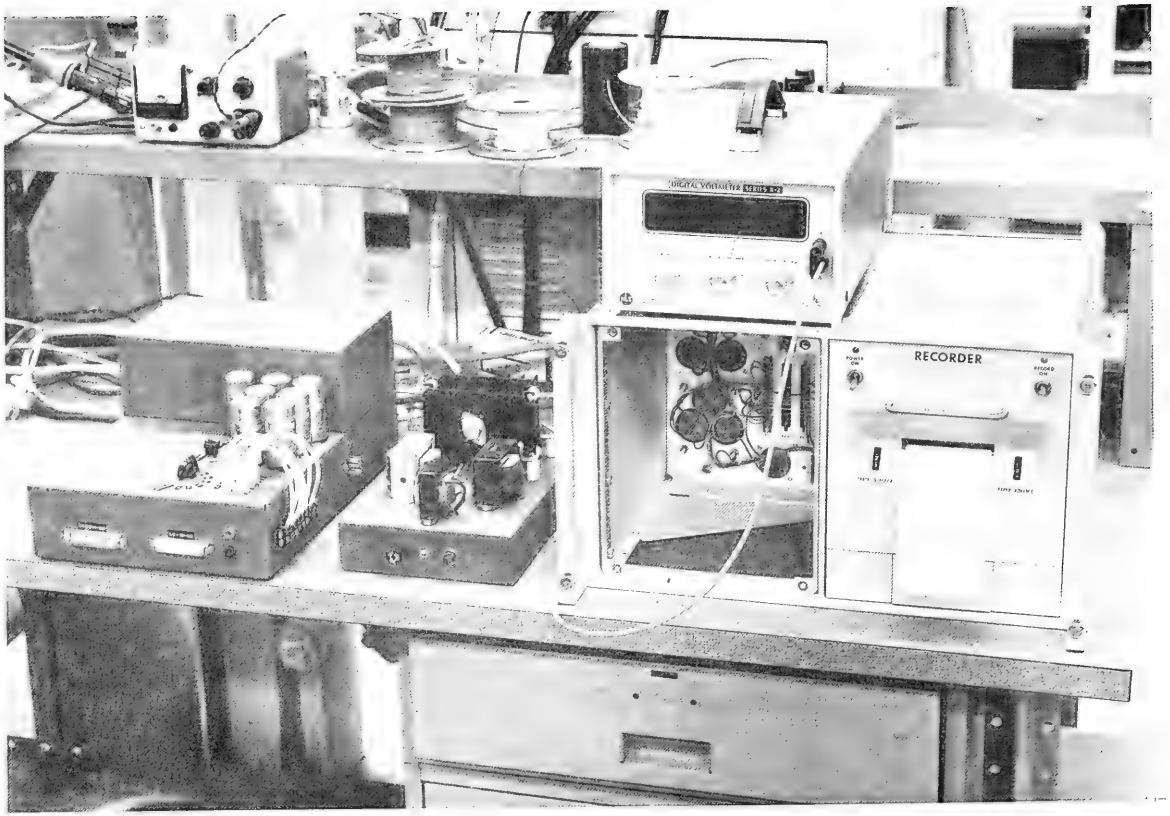

Figure 5-17. Backup Data Acquisition System Used at Sea

EXPERIMENTAL DETERMINATION OF THE TRANSLATIONAL STABILITY OF A TETHERED BUOY IN DEEP WATER

P. R. Wessel
Research Physicist

and

E. S. Dayhoff
Supervisory Physicist

A submerged instrument platform, with a high degree of stability is required for many oceanographic and military programs which are conducted in deep water. We have conducted a test of a submerged buoyant system in the underwater tracking range in the Virgin Islands. The buoy was a sphere four feet in diameter tethered by a single mooring line at a depth of 600 ft. in 1900 ft. of water. A self-contained pinger unit attached to the buoy was monitored by the tracking range for a period of 42 hours and its position accurately determined.

Preliminary estimates of the motion to be expected, based on very limited deep water current measurements in the area, are compared with the experimental results. The motion of the buoy was primarily in response to tidal currents. The results can be readily extrapolated to systems of a similar nature when the physical dimensions of the system and the approximate magnitude of the current are known.

I. INTRODUCTION

It is sometimes necessary to install an instrument package in the ocean at a prescribed depth between the surface and the bottom and to maintain the location of the package within prescribed limits even in the presence of tidal and other currents. The instrument package is commonly installed in a buoyant housing (a buoy) tethered to the bottom by means of cables. A high degree of locational stability in the presence of water currents can be obtained by use of three tether lines fastened to three widely spread anchors on the ocean bottom. This type of mounting often presents great difficulty and expense in installation, especially at larger depths. An alternate mounting is obtained by use of a single tether line with a buoy of large buoyancy and a very heavy anchor. The high tension in the tether line helps prevent the currents from moving the buoy sidewise. We have found that the latter approach is applicable to a situation where the lateral motion of a subsurface buoy in deep water had to be limited to ten feet and subsurface currents were estimated to be 0.2 knot.

II. EXPERIMENTAL DETERMINATION OF STABILITY

In order to accurately calculate the stability of a buoyant system one must first know the vertical current profile over a given period of time. Since this information was not available in sufficient detail, an experimental approach to the problem was made. A spherical steel buoy, four feet in diameter, was anchored in 1900 ft. of water with 1300 ft. of one-inch diameter nylon line and a 3500 lb. concrete block. The net buoyancy of the sphere was 1300 lbs. A self-contained pinger unit (SCUPU) was attached to the sphere to allow acoustic tracking by the 3-D tracking range.

With the anchor tied alongside and the sphere streaming aft the support vessel maneuvered up to the release point. On command the anchor was released and the SCUPU was tracked as the anchor dragged the buoy along the surface and then down into position. The tracking data is shown in Fig. 1. Analysis of the buoy track indicates that the anchor struck the bottom, with the buoy at a depth of 530 ft.,and then slid westward down a steep incline dragging the buoy to a depth of 590 ft. The buoy then slowly stabilized its position above the anchor.

The SCUPU was tracked continuously for thirty minutes after the buoy was in place to be certain that its position had stabilized. After that a series of twenty readings (1.31 seconds apart) was taken at the end of each five minute interval for a period of 42 hours. The variation within each 20 bit grouping was generally three feet or less. The averages of the group taken in successive five minute intervals occasionally varied by as much as six feet.

To obtain a reasonably smooth curve it became necessary to consider the average of the tracking data obtained in a thirty minute interval (seven groups of 20). This data is plotted in Fig. 2. Pertinent tide information is also given in the figure.

The data shows a clear pattern related to the tidal cycle, with the maximum deviation of the buoy occurring during the peak ebb tide. In the first two hours after planting the system exhibited an unusually large amount of drift as shown by the irregular track at that time. Twelve hours after planting the computer suddenly dropped out of synchronization with the SCUPU with a resultant error in the track position. The data for the four hours following this event was given a constant correction on each axis to account for the shift in the time base. At that point (approximately 0730 local time) a correction was entered into the range computer to correct for the shift and the tracking was continued for 25 more hours. An abrupt shift of 4 feet in depth at 0200 of the second day indicates that a small shift in the synchronous relation of the SCUPU and the computer may have occurred at that time.

Continuous tracking was discontinued at 0900 in preparation for the recovery of the buoy. An acoustic release mechanism near the anchor was triggered on command from the surface and the buoy and anchor line allowed to float freely to the surface. The tracking data obtained during ascent indicates that the terminal velocity during ascent was about 10 ft./sec. compared to the maximum during descent of less than seven. This is reasonable since the net (negative) buoyancy of all components was 1000 lbs. in descent and 1100 lbs. (positive) in ascent with the drag contribution of the anchor removed.

Data from the 42 hours that the buoy was on the bottom indicates that the maximum shift of position is about ten feet, occurring primarily along a north-south line at the time of maximum ebb tide. It is apparent that the tidal effect is not uniform in the opposing parts of the cycle. It should be noted that tides in this area are weak, the rise and fall being less than one foot, and that a few current measurements made at mid-depths indicated a maximum tidal velocity of about 0.2 knot. The water deepens to the northward going to over 2000 fathoms. We can only speculate that this influences the currents to produce the observed effect.

III. CALCULATION ON TRANSLATIONAL MOTION

In this section we undertake to calculate the shape of the tether line, the tension in the line, and the offset of the buoy. The calculation explicitly includes the drag forces on the buoy and, in distributed form, on the anchor line. It also includes the buoyancy of the anchor line. It is assumed that the drag forces will not change due to non-vertical slope of the cable, but an extension can be made for this, if necessary. The cable form can deviate substantially from the vertical in our basic equations but we have chosen to use a small angle approximation for cable slope in carrying out their solutions. Although extensive tables of buoy cable parameters found in Taylor Model Basin report 687 by Pode obviate the above calculation, we found it simpler to calculate than to interpolate with the tables.

Figure 3 illustrates the geometry of the problem. The buoy has a buoyancy force B_b and a drag D_b, which must be determined independently. The resultant force of these two is F_b and is collinear with the tether line at the point of attachment. At a depth X below the buoy the tether line has an offset distance of Y.

Figure 4 shows a short section of the line of length dx, in the x direction. It is acted on by the four forces: T(x) pulling generally upward, T+dT pulling downward, Ddx the drag on the line segment, and Wdx the buoyant weight. The latter two have a resultant which we call Fdx in a direction ϕ as shown. We can immediately write the equations for static equilibrium of this line segment.

$$\begin{aligned} &\text{Vertical: } (T+dT)\cos(\Theta+d\Theta) - T\cos\Theta = -Wdx \\ &\text{Horizontal: } (T+dT)\sin(\Theta+d\Theta) - T\sin\Theta = Ddx \end{aligned} \tag{1}$$

On expanding the trigonometric quantities and dropping products of two infinitesimals we obtain:

$$\begin{aligned} \frac{dT}{dx}\cos\Theta - T\sin\Theta\frac{d\Theta}{dx} &= -W \\ \frac{dT}{dx}\sin\Theta + T\cos\Theta\frac{d\Theta}{dx} &= D \end{aligned} \tag{2}$$

Two alternate forms may be obtained by first multiplying the upper by cos Θ and the lower by sin Θ and adding, thus

$$\frac{dT}{dx} = D\sin\Theta - W\cos\Theta \tag{3a}$$

or, on combining in the reverse manner we obtain

$$\frac{d\Theta}{dx} = \frac{D}{T}\cos\Theta + \frac{W}{T}\sin\Theta \quad . \tag{3b}$$

The form can be simplified by putting:

$$F = \sqrt{D^2 + W^2}$$

$$\sin \phi = W/F \tag{4}$$

$$\cos \phi = D/F \ .$$

Then

$$\frac{dT}{dx} = D \frac{\sin(\theta - \phi)}{\cos \phi} \ , \tag{5a}$$

$$\frac{d\theta}{dx} = \frac{D}{T} \frac{\cos(\theta - \phi)}{\cos \phi} \ . \tag{5b}$$

This is a pair of non-linear simultaneous differential equations for the two variables T and θ with the fixed parameters D and ϕ. The boundary conditions to be met are that $T(0)$ is to have a value $T_o = F_b$ and $\theta(0)$ is to have a value $\theta_o = \tan^{-1}(D_b/B_b)$. The offset Y can then be determined from

$$Y = \int_o^X \tan \theta \, dx = \int_o^X \theta \, dx \tag{6}$$

where we have introduced the small angle approximation for $\tan \theta$.

The above equations can be solved by numerical computation if desired, but some rather good simplifying approximations can be made which enable analytical expressions to be obtained. Before doing this we introduce the numerical values of the constants typical of our experimental test conditions. Assuming a uniform current velocity of 0.2 knot we can calculate the pressure drag for the buoy and line. Surface drag is neglected.

B_b = 1300 lb.

D_b = 0.53 lb.

X = 1300 ft.

D = 11 lb./1300 ft. = .0085 lb./ft.

W = 0.35 lb/ft. x (1.14-1.03) = .039 lb./ft.

Hence F_b = 1300 lb.

θ_o = .00041 radians

ϕ = 77.7° = 1.35 radians.

Consider now equation (5a). The tension in the cable will vary from T_o at the upper end to something of the order of $T_o \pm D \sin\Theta$ at the other end. This drag contribution is less than 1 lb. in 1300 lb. In the case of neutrally buoyant cable $\phi = 0$, and the tension will increase with depth in proportion to Θ, but the whole increase will be only a pound or so. For the value given above for ϕ we can neglect Θ, so dT/dx becomes a constant; and the tension increase with depth is now linear with depth and still very small. Thus on passing to equation (5b) a good first approximation to the factor T is to make it a constant T_o.

Consider now equation (5b) with $T = T_o$. It can now be directly integrated, but first we discuss it qualitatively. If ϕ is positive (as for non-buoyant cable) the cosine ratio has a maximum value greater than one for $\Theta = \phi$. All values of Θ occurring in our problem will be small compared to ϕ, and the cosine ratio will be greater than one for all Θ. Therefore, the total offset Y will always be greater than for the case of weightless cable. In the case of buoyant cable (ϕ negative) the opposite is true. To find the numerical amount, we put equation (5b) in the form

$$\frac{\cos\phi \, d(\Theta-\phi)}{\cos(\Theta-\phi)} = \frac{D}{T_o} \, dx + d(\ell n \, c)$$

where c is an arbitrary constant.

Then

$$\frac{\cos\phi}{2} \, \ell n \left(\frac{1+\sin(\Theta-\phi)}{1-\sin(\Theta-\phi)}\right) = \frac{D}{T_o} \, x + \ell n \, c \ .$$

Hence

$$\frac{1+\sin(\Theta-\phi)}{1-\sin(\Theta-\phi)} = c \, e^{\frac{2D \, x}{T_o \cos\phi}} \ .$$

The constant is to be determined from the condition that $\Theta=\Theta_o$ for $x=0$, thus

$$c = \frac{1+\sin(\Theta_o-\phi)}{1-\sin(\Theta_o-\phi)} \ .$$

Then

$$\sin(\Theta-\phi) = - \frac{1-c \, e^{2Dx/T_o\cos\phi}}{1+c \, e^{2Dx/T_o\cos\phi}} \ .$$

The exponents are small compared to unity and can be expanded

$$\sin(\Theta-\phi) = \frac{1 - c - 2cDx/T_o\cos\phi - \ldots}{1 + c + 2cDx/T_o\cos\phi + \ldots}$$

$$= \frac{1-c}{1+c}(1 - 4cDx/(1-c^2)T_o \cos\phi \ldots .$$

Using a first order expression for $\sin(\Theta-\phi)$ we have

$$\sin\phi = \frac{1-c}{1+c}$$

and

$$\Theta = 4cDx/T_o(1+c)^2 \cos^2\phi \quad .$$

The ϕ dependence comes through the factor $c/(1+c)^2\cos^2\phi$ which can be reduced, on assuming that Θ_o is small but ϕ is not, to the value $(1+\sin\phi)/4$; hence:

$$\Theta = Dx(1+\sin\phi)/T_o$$

is the equation defining the shape of the cable. Since ϕ is 77.7° in our chosen example we see that the total cable offset is nearly doubled when the cable weight is included in the calculation. The predicted offset is now:

$$Y = DX^2(1+\sin\phi)/2T_o = 11 \text{ ft. in the example.}$$

The angle of drag on the anchor is about one degree from the vertical.

IV. DISCUSSION

The rather strong dependence of the shape of the anchor line on the relatively small buoyancy/weight forces acting on the cable itself appears surprising. Evidently, the shape of the cable must be viewed as rather weakly enforced by the cable tension and side thrust forces acting alone. It is apparent that minimization of the offset can be accomplished by use of self-buoyant cable or cable with many small buoyant bodies attached (provided they do not increase the drag appreciably). Weighting the cable by attaching, for example, heavy electrical cables would greatly increase the offset distances.

Another interesting feature can be seen in the tension equation (3) which suggests that the tension in the line stops increasing with depth for the depth where $\Theta=\phi$. Since the cable is sloping, the drag forces resolved along the cable direction balance the weight forces also resolved along the cable direction and dT/dx becomes zero. In practice it must be possible to reach such a condition, although it is doubtful that the use of constant values for the drag will accurately predict the location of this point.

In view of the weak currents encountered in this location it is apparent that a single moor will provide adequate stability for most purposes. The calculation can be extended to higher current values. For a current of 0.6 knot the displacement will be about 80 feet for the same conditions used in the experiment. This is still a fairly small deviation and could be reduced through use of greater buoyancy or by use of faired anchor lines or other materials which will give lower cross-sections and drag values.

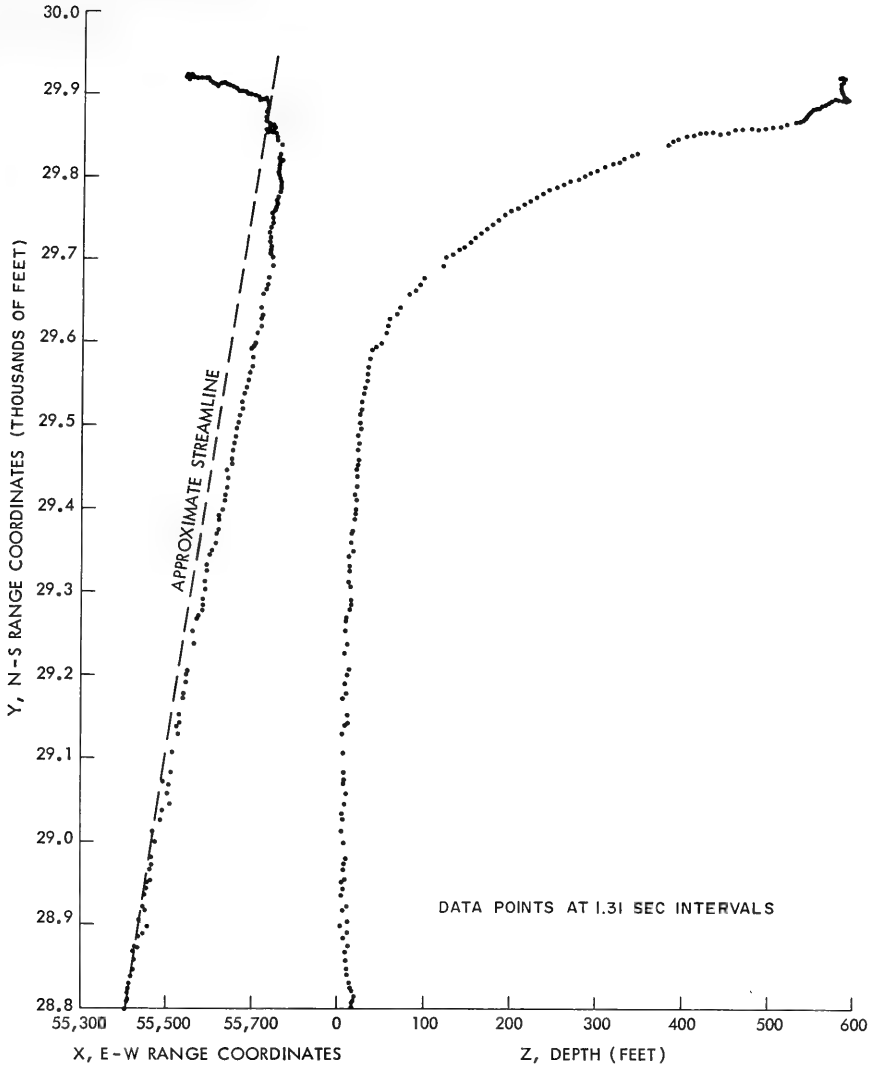

Figure 1. Tracking Data Obtained during Installation of Subsurface Buoy

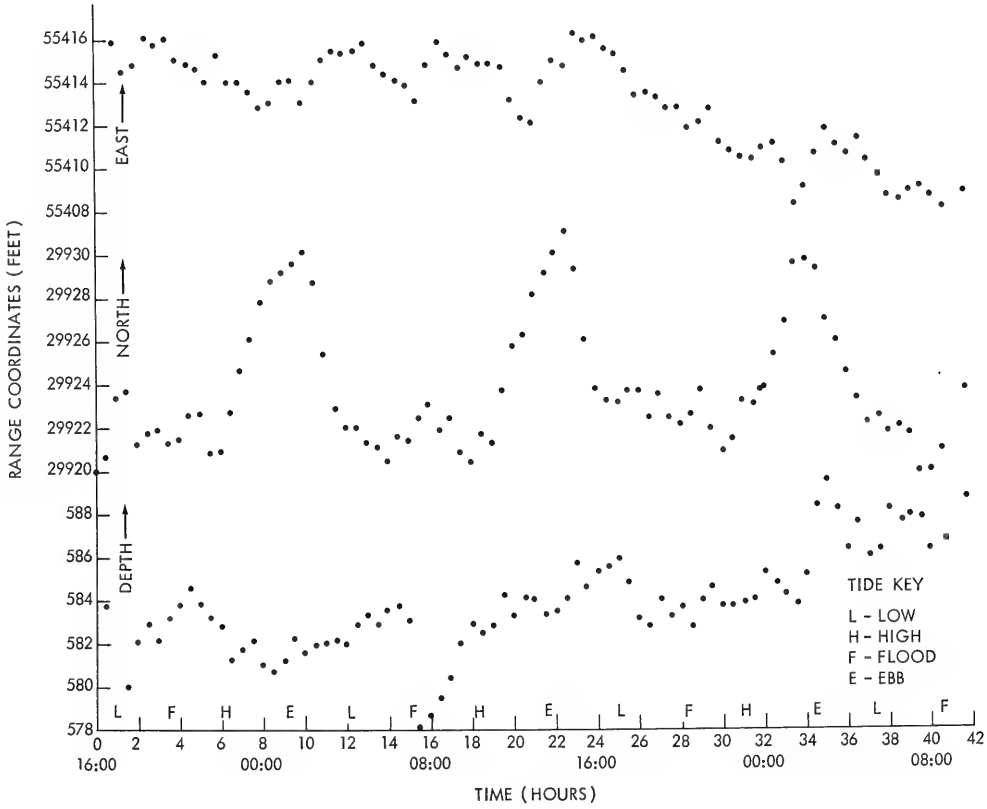

Figure 2. Buoy Position as a Function of Time and Tide Cycle

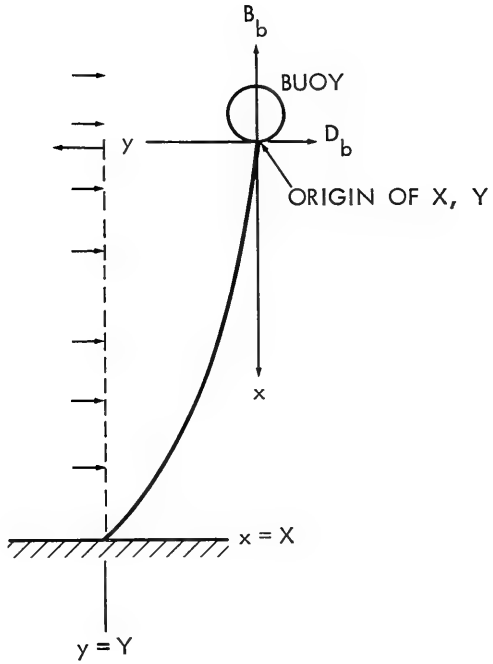

Figure 3. Geometry of the Anchored Buoy Problem

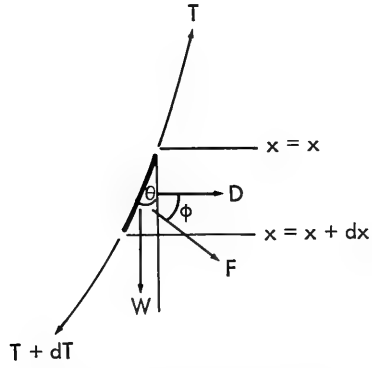

Figure 4. Forces Acting on a Section of Anchor Line

RESIDUAL STRESS IN HIGH STRENGTH STEEL WELDMENTS APPLICATION OF X-RAY DIFFRACTION TECHNIQUE

Giulio DiGiacomo
Research Physicist

Irving Canner
Physicist

Joseph R. Crisci
Physical Metallurgist

Naval Applied Science Laboratory
Flushing and Washington Avenues
Brooklyn, New York 11251

ABSTRACT

Residual stresses develop in weldments during fabrication. Their presence may be detrimental to the fatigue life and strength of the structures during service. In the past few years, the need for residual stress measurements by nondestructive means has paralleled the need for material of higher strength and durability. On the basis of the works published in the literature, the only proven nondestructive method for stress analysis is X-ray diffraction; however, it has not had appreciable application in actual structures and weldments. This paper deals with the determination of residual stresses in the weld and/or heat affected zone of high strength steel weldments by the X-ray diffraction method. The study included tee and butt weldments, tested in the as-welded and stress relieved conditions. The residual stresses were measured in the directions parallel and transverse to the weld, on the surface and two mils below the surface following electropolishing. Both film and diffractometer techniques were utilized in the investigation. Results show that residual stresses at the surface of both weldments studied are generally compressive in both directions. The as-welded specimens show residual stresses as high as the yield strength, while the residual stresses in the stress relieved specimens are reduced by more than 50%.

INTRODUCTION

Structural materials such as steel and titanium alloys must possess high strength and fatigue life if they are to endure ocean environment. The higher the strength and fatigue requirements, however, the greater the need to ascertain the integrity of the structure during fabrication and in service by nondestructive methods. X-ray diffraction is one method which is used to determine residual stresses in metal structures nondestructively.

The determination of residual stresses in metals by X-ray diffraction is based on the measurement of residual lattice strain of favorably oriented crystallographic planes of suitable Miller indices. Residual stresses develop in metal components and weldments during fabrication as a result of thermal gradients and metallurgical reactions. The presence of residual stresses in metal structures may weaken their strength and shorten their service life. As higher strength materials are required in the construction of naval vessels, residual stresses become of greater concern, especially in the presence of surface discontinuities as well as alloy heterogeneities. High tensile residual stresses, for example, in the presence of notches and cracks may lead to brittle fracture at relatively low temperatures. Fatigue properties and dimensional stability of the structure may also seriously suffer from the residual stresses.

X-ray diffraction is the only practical nondestructive method for the determination of residual stresses in metal structures. X-ray stress analysis has been useful in many fundamental and applied research studies, including quality control and maintenance of structural components in the aircraft, railroad and ball-bearing industries. As already mentioned, residual stresses are calculated from residual strains, assuming that the material behaves elastically. When the material is a weld deposit, the residual strain may not be entirely elastic, and, therefore, the calculated stresses may contain considerable errors. It has been shown[1] that residual stresses in butt-welds determined by X-ray diffraction agree, within experimental error, with the residual stress values obtained by layer removal technique despite the fact that some plastic deformation may have been present. On this basis, plastic deformation in welds does not appear to be a serious factor; therefore, no consideration was given to its possible effects on the results of this investigation. Stress analysis by X-rays is by no means an easy task, even when the material is ideally suitable for the analysis. The analysis involves linear measurements of the diffraction line position, and those measurements require a reproducibility of at least a tenth of a millimeter if the method is to be useful for the determination of low and intermediate residual stress values. Measurements of diffraction line shift and distance between film and specimen are most important; they therefore must be effected with great precision.

1. DiGiacomo, G. "Residual Stresses in High Strength Steel Weldments and Their Dimensional Instability During Welding and Stress Relieving"; MS Thesis (Physics) 1968, Polytechnic Institute of Brooklyn.

2. Ibid.

The most generally accepted X-ray method at the present time is the $\sin^2\psi$ - method which involves four or more X-ray exposures at different angles of incidence whereby lattice strain components are measured at such angles. This method has been proven by recent investigations[2] to be more accurate and reliable than the classical methods (one or two exposures), especially if the material is anisotropic and contains plastic deformation. This report deals with the application of the $\sin^2\psi$ X-ray method for the determination of residual stresses in tee and circular weldments.

OBJECTIVE

The objective of this work was to determine residual stresses in tee and circular weldments by X-ray diffraction film technique, employing the $\sin^2\psi$ method, and to evaluate the effectiveness of stress relief by heat treatment.

PROCEDURE

The study involved two types of HY-130/150 steel weldments: a circular fillet weld-test specimen (weldability specimen) and a tee welded plate. The circular weldment consisted of a steel disc, 6 inches in diameter and 2 inches thick, welded on a 15x15x2 inch steel plate along the disc circumference, as shown in Figure 1. The tee weldment, shown in Figure 2, consisted of a 15x15x1$\frac{1}{2}$ inch basal plate on which a stiffener, 2x1$\frac{1}{2}$ inch cross section, was welded along the middle of the plate. The two types of specimens were welded by the Gas Metal Arc process, using an M3 McKay filler wire. The tee weldment was saw-cut into 2 one-inch wide sections perpendicular to the weld to provide specimens for different heat treatments.

Three sections were selected for stress analysis studies. One section was left in the as-welded condition, another section was stress relieved at 1025°F and water quenched, and the third was furnace cooled after being stress relieved at the above temperature. The residual stresses were determined at the toes of the welds in three azimuthal directions: parallel to the weld; perpendicular to the weld; and 45° to the weld. Each specimen was analyzed in three areas, equally spaced and aligned parallel to the weld, as shown in Figure 3. The analysis consisted of four X-ray exposures for each azimuthal direction, at incident angles (ψ) 0°, 15°, 30°, 45° from the normal to the specimen surface. The lattice strains were calculated from the equation

$$(1) \qquad \text{Strain} = \frac{\Delta S}{2R\tan\theta}$$

where ΔS is the diffraction line-shift due to the presence of

residual strain in the lattice, R is the film-to-specimen distance, and Θ is the Bragg angle. The strains were plotted versus $\sin^2\psi$ for each azimuthal direction, as shown in Figure 4, a typical plot.

From the theory of elasticity, the slope of the line is related to the residual stress and elastic constants by the equation

$$(2) \qquad \text{Slope} = \frac{1+\nu}{E_{hkl}} \sigma_\phi$$

where ν is the Poisson's ratio, E_{hkl} is Young's modulus in the direction of the Miller indices hkl, and σ_ϕ is the stress in the azimuthal direction, ϕ .

The circular weldment was analyzed similarly, but only after removing a surface weld layer by the electropolishing process. Residual stresses were determined on two areas of the weld in two azimuthal directions: parallel and perpendicular to the weld, as shown in Figure 5. Figure 6 is a typical plot of the strain values versus $\sin^2\psi$.

RESULTS AND DISCUSSION

Measured residual strains obtained from one area at the toe of the tee weld and one area on the circular weld (for the azimuthal directions indicated) are plotted versus $\sin^2\psi$ in Figures 4 and 6, respectively. The slope of each least-mean-square line through the points is proportional to the residual stress averaged over the four ψ -directions at angles 0°, 15°, 30°, 45° from the normal to the specimen surface. It is evident from the graphs that the strain values obtained from the circular weld are scattered more than those obtained from the toe of the tee weld. This may be explained by the possible presence of some anisotropic plastic deformation in the weld material.

Despite the scatter and poor reproducibility of individual strain values, as illustrated in Figure 6, the slope of the line, which characterizes the state of residual stress, remains rather constant with new sets of experimental strain values. This is an important aspect of the $\sin^2\psi$ method since it allows the determination of residual stress on the basis of a statistical strain distribution over a range of four directions, rather than on the basis of an assumed distribution (one- or two-exposure methods). It is to be noted that a positive slope means that the residual stress is tensile.

The residual stresses were calculated from the strain data using equation 2. The results for the three tee-welded sections are shown in Table 1. The results in Table 1 indicate that the

surface residual stresses in the heat affected zone are highly compressive, about 100 ksi for the as-welded specimen, and are fairly uniform along the weld for the three azimuthal directions. The two stress relieved specimens contain much lower compressive stresses, about one third the magnitude of the as-welded. These results are in good agreement with those of DiGiacomo[3], although, in that work, the weld was of a different type. It shows the existence of a steep stress gradient at the surface layer, changing from compression to tension through shallow depths. A complete study of the state of residual stresses in three directions (triaxial stresses) would entail the combination of X-ray diffraction and layer removal techniques.

Residual stress values obtained from the surface of the circular weld are listed in Table 2. These stresses are moderately compressive in both of the directions studied. The surface of the weld was electropolished prior to the X-ray stress analysis to a depth of 0.003 inch to rid the weld surface of scale and contaminations. Inevitably, this operation removed base metal which may have had much higher compressive stresses than that obtained from the underlying surface exposed after the removal. This may account for the low compressive stresses obtained from the circular weld.

The X-ray diffraction method is also applicable to titanium alloys, provided that modifications are made in the technique to satisfy more stringent requirements.

CONCLUSIONS

Based on the results of this investigation it may be concluded that residual stresses at the surface of welds and adjacent base metal of tee and circular fillet HY-130/150 weldments are highly compressive, and that a stress-relief heat treatment reduces the residual stresses by a factor of three.

FUTURE WORK

Stress gradients in the direction normal to the surface of additional high strength steel weldments will be studied. The study will require the removal of thin metal layers by the electropolishing technique and the determination of the residual stresses by X-ray diffraction at the surface exposed by each removal.

ACKNOWLEDGMENT

The work reported herein was accomplished under the overall

3. Ibid.

direction of Mr. M. L. Foster, former Head of the Metallurgy Branch. The work was sponsored by the Naval Ship Systems Command, in connection with the "Fabrication of Ferrous Structural Alloys" program. The program managers for this work are Messrs. G. Sorkin and B. Rosenbaum, Naval Ship Systems Command (Code 0342). Acknowledgment is due to Mr. W. J. Jones for his assistance in acquisition of the data and to J. Gabriel in the fabrication of the tee weld specimens.

TABLE 1 – RESIDUAL STRESSES IN THE HEAT AFFECTED ZONE OF HY-130 TEE WELD SPECIMENS

Specimen Condition	Spot Location	Azimuth Angle (ϕ), Degrees	Residual Stress (σ), ksi
AS WELDED	A	0	−98
		45	−86
		90	−86
	B	0	−84
		45	−123
		90	−110
	C	0	−75
		45	−167*
		90	−120
STRESS RELIEVED AND WATER-QUENCHED	A	0	−34
		45	−46
		90	−52
	B	0	−35
		45	−33
		90	−36
	C	0	−18
		45	−19
		90	−46
STRESS RELIEVED	A	0	−16
		45	−18
		90	−14
	B	0	−24
		45	−41
		90	−32
	C	0	−43
		45	−35
		90	−32

*It is not known whether this anomaly of stress above the yield point is due to the state of the material or the experimental procedure.

TABLE 2 – RESIDUAL STRESSES ON THE WELD OF THE CIRCULAR FILLET WELDABILITY SPECIMEN

Specimen Location	Azimuth Angle (ϕ), Degrees	Residual Stress (σ), ksi
1	90	−40
1	0	−43
2	90	−51
2	0	−4

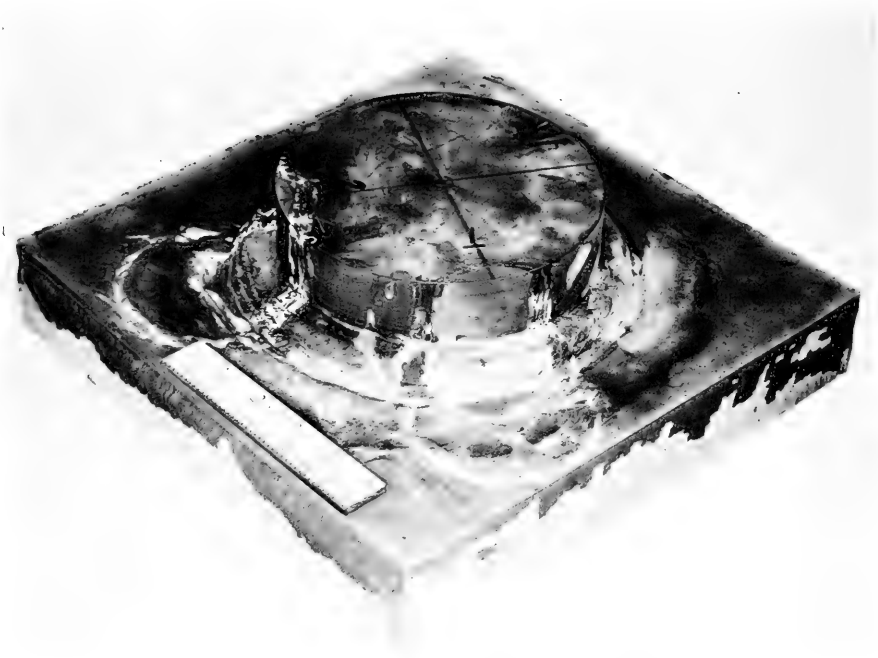

Figure 1. Circular Fillet Weldability Specimen

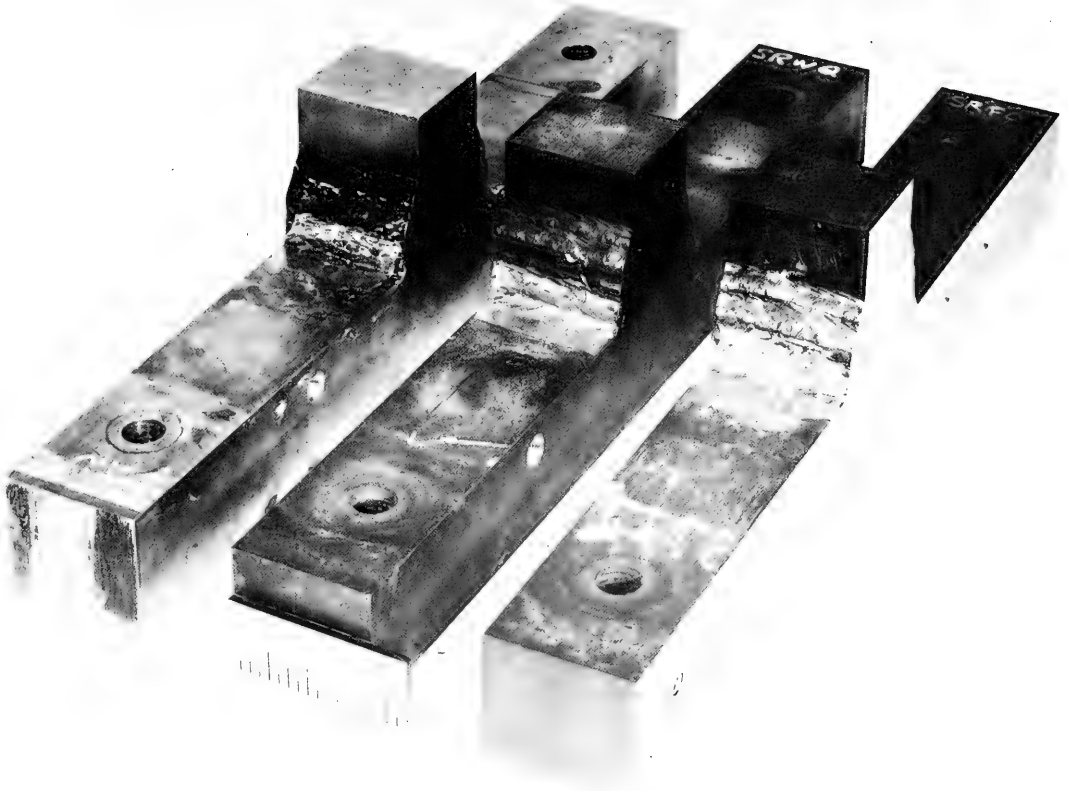

Figure 2. Tee Welded Plate Specimen

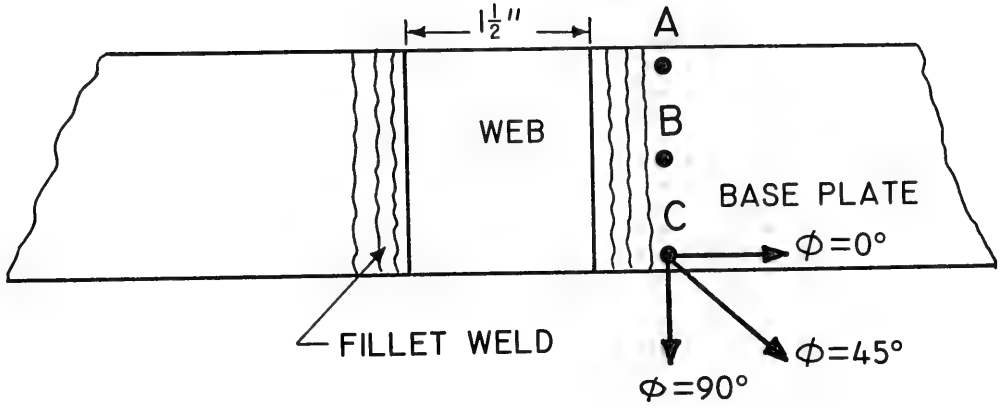

Figure 3. Tee Welded Specimen Showing Locations and Directions of Residual Stresses Determined (Plan View)

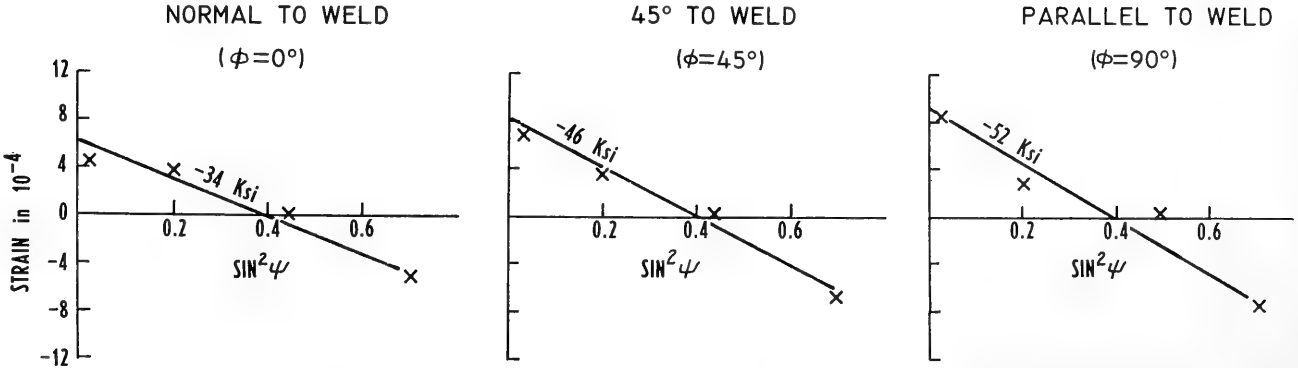

Figure 4. Strain versus $\sin^2\psi$ for the Stress Relieved and Water Quenched Tee Welded Specimen (Area C)

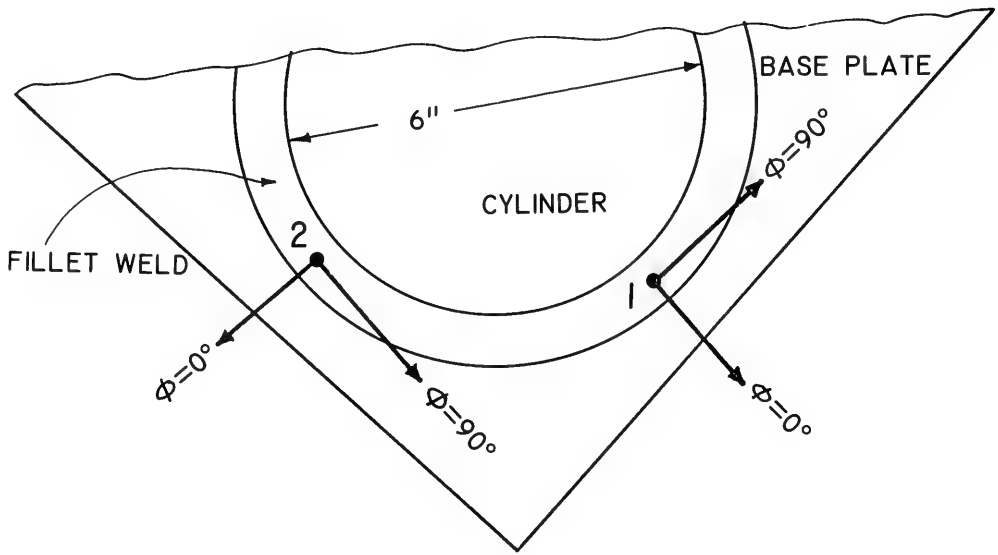

Figure 5. NASL Circular Fillet Weldability Specimen Showing Location and Directions (ϕ) of Residual Stresses Determined (Plan View)

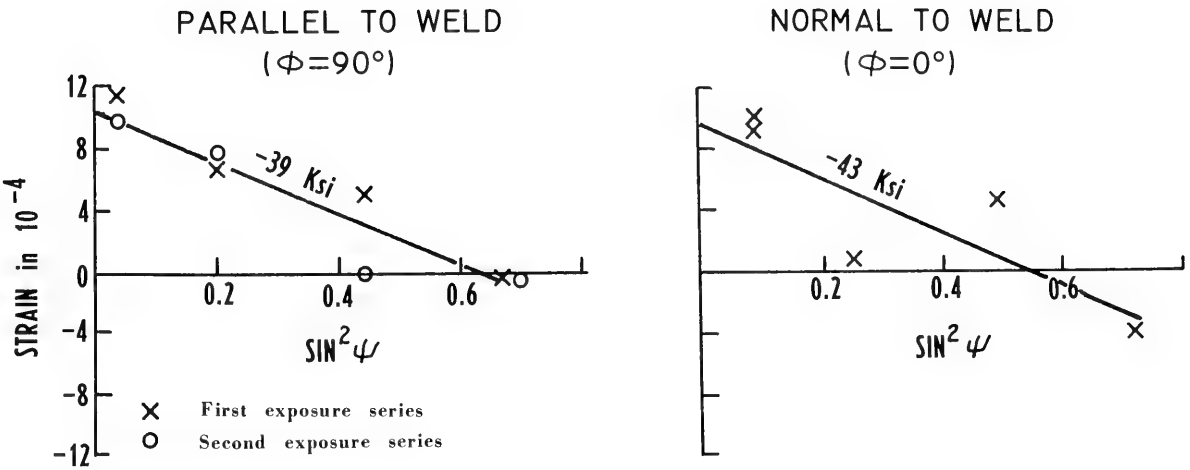

Figure 6. Strain versus $Sin^2\psi$ for the Weld Metal of NASL Circular Fillet Weldability Specimen

MILITARY APPLICATIONS OF AN OCEANOGRAPHIC LIVE ATLAS

Robert A. Peloquin, Richard A. Bolton, Walter E. Yergen
Naval Oceanographic Office
Washington, D. C. 20390

Anthony R. Picciolo
National Oceanographic Data Center
Washington, D. C. 20360

I. ABSTRACT

The rate at which oceanographic data are being accumulated has stimulated considerable thought in the improvement of data storage and handling capabilities. The realization of the need for new hardware and computerized techniques to contend with the large data volumes which are anticipated in the future has left its mark. In-house programs at NAVOCEANO and NODC have, for this reason, been oriented toward the attainment of these goals. Specifically, a joint program for the development of a "live atlas" has been initiated. This atlas, as conceived, is a computerized system which consists of efficiently formulated data files, computer software to access these files, and a cathode-ray tube display console which enables its operator to display data summaries, such as contoured horizontal and vertical sections of a data distribution, and manipulate programs for generating summaries and displays through console selectable instructions in real-time. The compression of oceanographic files to ratios exceeding eight to one are discussed. Details concerning the display speeds are presented. Experimental results of preliminary displays are shown. Specific military applications, such as command and control displays, automated atlas, compilation, and quality control operations for data archival, are discussed.

II. INTRODUCTION

A critical look at oceanographic data files, their management and accessibility has been afforded under the live atlas project which has been undertaken jointly by the Research and Development Department of the Naval Oceanographic Office and the National Oceanographic Data Center (NODC). This developmental effort has utilized existing computer facilities within the Navy and at the Goddard Space Flight Center.

The live atlas is a dynamic display capability intended for use in data analysis and/or information retrieval and presentation. It differs from a static display in that it allows the user to interact

with the display in real-time. Thus, given a real-time data display capability, an individual could modify and refine a desired product in response to a particular requirement or objective. The atlas provides access to large data bases, such as the NODC global ocean station and bathythermograph files. Basically, this display consists of a large data base structured for rapid retrieval, a display integrated program library which allows for great flexibility and a wide spectrum of use applications, and computer hardware which includes a computer driven cathode-ray tube display unit, a sufficiently large data storage device. The accomplishments to date include restructured ocean station and bathythermograph files. A number of real benefits have already been realized as a consequence of these accomplishments: (1) the Undersea Surveillance Oceanographic Center (USOC) is making use of a sound velocity file extracted from the North Atlantic Ocean station file, (2) NODC has used the files to satisfy data requests with substantial savings in cost and time, (3) the Fleet Numerical Weather Central, Monterey (FLTNUMWEACEN) has used the file to extract data which were not previously included in their data bank.

III. DESCRIPTION OF THE LIVE ATLAS

As mentioned earlier, the live atlas consists of a compact data base, a computerized visual display, and a computer software package which enables accessing, displaying, and/or manipulating the data in real-time. A schematic representation of the live atlas hardware is shown in figure 1.

A. Ocean Station Files

The North Atlantic Ocean station file has been restructured from a binary coded decimal line image format to a variable length free field binary format. This technique, along with high density storage, has allowed the reduction in the physical size of the file from 22 to less than a single reel of magnetic tape. As a result, the file scanning time has been reduced from approximately 24 hours to 4 minutes. The NODC global ocean station file has been similarly reduced in size without the omission of data. Data representing approximately 350,000 ocean stations will be contained on a single reel of magnetic tape.

B. Bathythermograph

A global file containing all current digitized mechanical BT traces is contained on 1.25 reels of magnetic tape. Each BT is fitted with a series of least square regression lines. The temperature and depth at the points of intersection are stored. In addition, the temperature gradient between successive points and a goodness of fit indicator of the line of regression are provided as is shown in a printout of the data (figure 2).

C. Bathymetric File

The bathymetry file compaction program treats a cruise as a string of successive ship positions versus depths. Differences between successive ship positions rather than ship coordinates are recorded to limit storage memory requirements. The string of ship positions is cut at critical points to yield minimum cumulative positional differences. The substrings are then recorded using free field format methods. Memory compaction ratios exceeding five or six to one over the source data are effected in this way.

D. Sound Velocity

A sound velocity file for the North Atlantic is now available; a global sound velocity file which will be contained on less than a reel of magnetic tape will soon be completed. The data contained in these files are extracted from the ocean station files.

IV. THE LIVE ATLAS DISPLAY

The live atlas, in its present form, has been developed using the NASA Goddard Space Flight Center IBM 360/95 and a Model 3 2250 display station. The data can be accessed directly by the console operator from magnetic tape, data cell, or a disc storage unit. Station data of any area in the North Atlantic at any standard depth can be retrieved and displayed. For example, a 4° square centered at 39°N latitude and 70°W longitude can, on request, be displayed on the CRT at any standard depth (figure 3). Using mean values which are determined for each grid containing data (figure 4), a 2° square is filled. This is accomplished by searching in all directions from each empty grid cell and computing a mean value which is inversely proportional to the radius of search (figure 4). Horizontal contours of the data, such as shown in figure 5, can also be displayed. The estimated processing time required to generate and display a contoured surface is 1.5 seconds. An effort is underway to incorporate the software package in the projected NODC computer. In addition, hardware procurement is contemplated to support the live atlas within the Oceanographic Office.

The scientist sits at the 2250 display station and specifies any area in the North Atlantic and any time boundaries he wishes to impose on a retrieved data set. He then asks the system to retrieve that data set through the function keyboard of the 2250. All station data in the North Atlantic that falls within the specified geographic-time boundaries is then extracted from the file and put in temporary memory of data cell, magnetic tape, or disc.

At this point, a sort task is attached which allows the data that were requested to be sorted into depth planes while control is returned back to the scientist. The scientist may then display other data sets or change program parameters while the sort is taking place. At any time, the scientist can interrogate the system and see if his latest data set has been completely retrieved and sorted. When the sort is complete then the oceanographer may request that the data be pre-processed. The data elements of interest are then selected from the whole retrieved data set and stored on disc memory in a format quickly accessed for display. In most cases, this will take less than a second. The scientist can then call for a scattergram plot, a grid display, or a contour chart of the variable in question. To make the grid and contour displays, a grid must first be developed. This is done with an objective analysis. This is an analysis that evaluates all data falling within a certain range of a grid point and assigning a computed value to that grid point. This grid is then processed to generate a contour chart or grid plot, if desired.

During this whole process the 2250 operator can request that: (1) the stations involved in a retrieval be pointed out in their entirety, (2) retrieved data sets be saved on magnetic tape, data cell, or disc, (3) contour analyses be refined and produced in hard copy.

V. MILITARY APPLICATIONS

Applications of the live atlas to military needs and fleet requirements are numerous. Furthermore, there are many non-military uses which would come to light as a result of military developments. Realizing a capability which consists of an extensive but compact data file, a means of rapid access of these data, and displaying them almost instantaneously on a CRT in any form desired, it is likely that each and every one of us could come up with an extensive list of possible applications. That is not necessary, however, since there are existing requirements which have a need for a live atlas.

The tabulation and preparation of data for release in the form of atlasses, such as the National Intelligence Survey, has been a long and laborious task which consisted of searching through large quantities of data. Through improved technology, the updating of such documents may become physically impossible in the future unless new techniques are employed. The CRT has one feature which undoubtedly will prove indispensable; i.e., the scientist has a means of looking at large quantities of data in rapid order. As an example, a request to update an atlas would involve loading a magnetic tape data file on a computer and editing these data by physically scanning and displaying them on the CRT. The operator would have the capability of selecting and storing all or that part of the data which he has judged epresentative of an area or best suited to meet the study which he

is conducting. Through the use of computer programs (to be written in FORTRAN), the operator can present the data in any graphical form he chooses; this includes an ability to perform complex mathematical calculations through the use of the computer processor. The graphical presentation can then be studied for accuracy and edited and photographed for permanent retention on microfilm or converted for atlassing from film to printing plate. Graphic displays could also be stored in digital form on magnetic tape or punched cards, printed in numeric or plotted using calcomp plotters.

The live atlas can be used in engineering applications to study large quantities of data in order to establish design criteria for ocean instruments and platforms. The energy spectrum of ocean surface waves is of great significance in the study of ship motions and resulting stresses enacted by these motions. To date, these stresses have been calculated, in part, using spectral information calculated from time-series wave measurements; however, additional stress data are required, particularly at the higher sea states. It is not enough to select representative spectra derived from theoretical curves; however, a wave hindcast climatology of the North Atlantic contains a total of 900,000 spectra calculated at 519 points at 6-hour intervals over a 15-month period. Obviously, there are more data contained in this file than is humanly possible to study using conventional techniques. The use of the live atlas and its graphical presentation features would allow the scientist or engineer to selectively study these large quantities and select the wave spectra which are characteristic of the physical environment. Thus, greater reliability and improved confidence would be assured in the design and development of ships and ocean platforms.

Possibly the greatest single potentially significant military application lies in shipboard display. The compaction of data files shows that it is conceivable in the near future to maintain a meaningful shipboard environmental data base. All fleet surface ships and submarines could carry environmental files or magnetic tape atlasses which, when updated using on-site data, could serve to produce a complete three-dimensional picture of the ocean environment within a specified radius of the ship. For example, sound velocity could be stored directly or could be computed from salinity and temperature data. Bathymetry could also be stored in a compact form, along with these data, in sufficient detail to give a description of surrounding bottom terrain. Furthermore, acoustic characteristics of the bottom could also be included. In addition, by combining this environmental data as part of a computerized sonar system, detection probabilities could be displayed on a continuous basis or on command. Such features as selectable target and transducer depths, would be possible.

A surveillance problem which has already been addressed is that of tracking distant ship targets with sonar (figure 6). The live atlas file has been used to retrieve sound velocity profiles along a great circle route connecting a transmitter and target. The USOC has, on repeated occasions, utilized the retrieval software to extract information of this type from the North Atlantic sound velocity file.

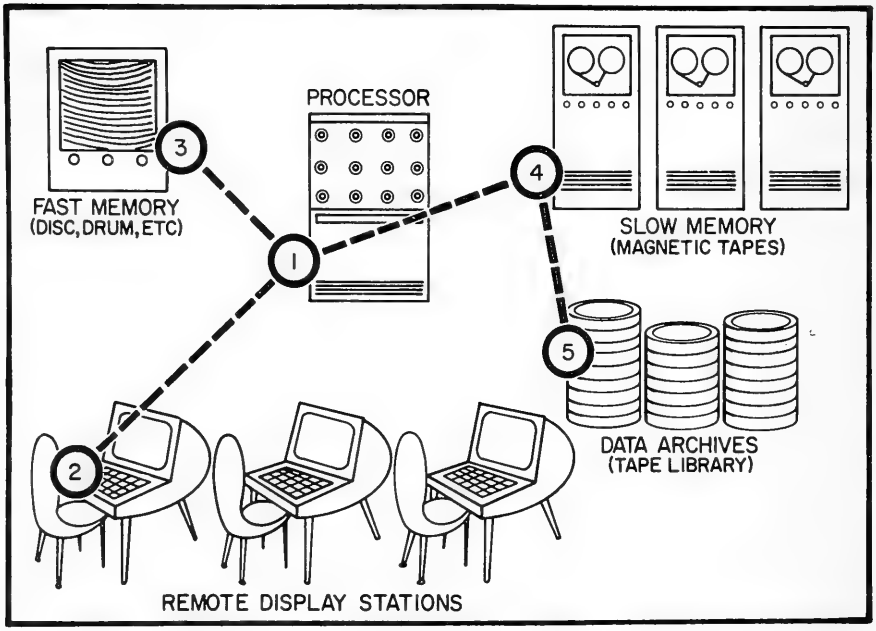

Figure 1. A Projected Live Atlas Hardware Scheme

BT PROFILES

NODC DATA * YERGENS FORMAT *

MSQR DEG MO

042 47 APR 19 1961 TIME 0300

REF 04156 14 37 N 057 59 W
CSC 887 QUAL 2

BOTTOM DEPTH 4572 M
WIND 18 KNOTS, E
WAVES 3
TD=26.7 TW=23.3
P=1015 MB
CUMULUS COVER 2

	DEPTH M	TEMP C	GRAD C/M	RMS C
1	0	26.9		
2	19	26.7	-0.01	0.06
3	43	26.3	-0.02	0.06
4	81	26.1	-0.00	0.06
5	97	26.4	0.02	0.06
6	118	24.9	-0.07	0.13
7	128	23.9	-0.09	0.13
8	131	23.8	-0.06	0.06
9	166	20.9	-0.08	0.13
10	177	19.8	-0.10	0.06
11	220	17.6	-0.05	0.06
12	240	17.1	-0.03	0.06

Figure 2. BT File Format

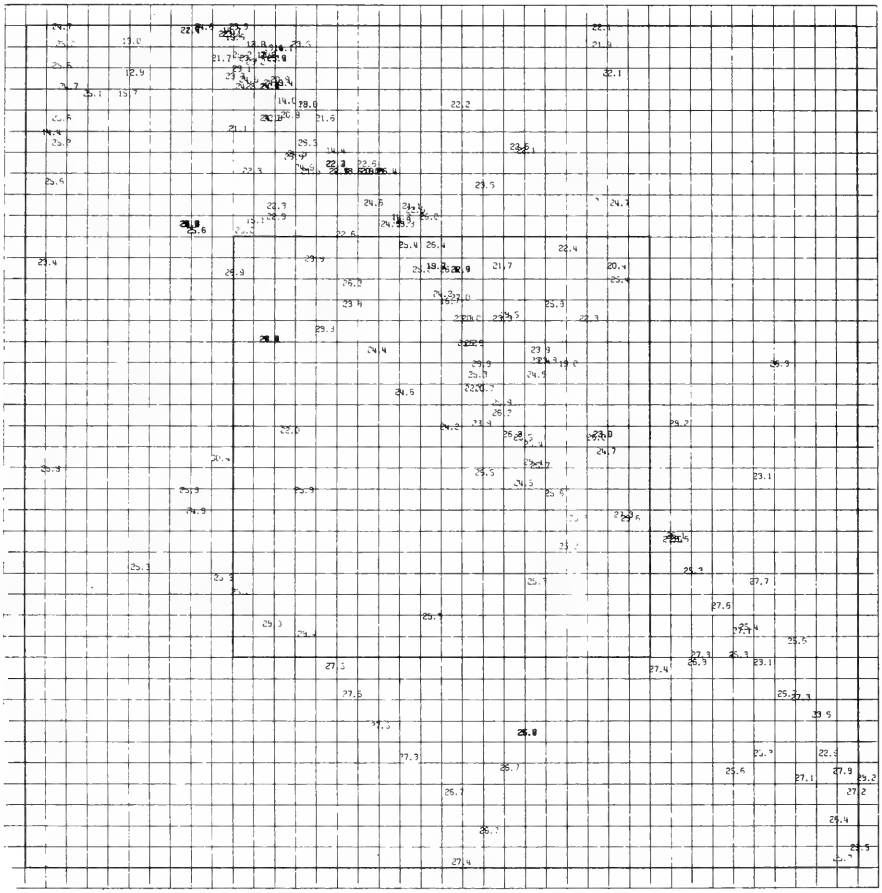

Figure 3. Plot of Input Surface Temperature Data

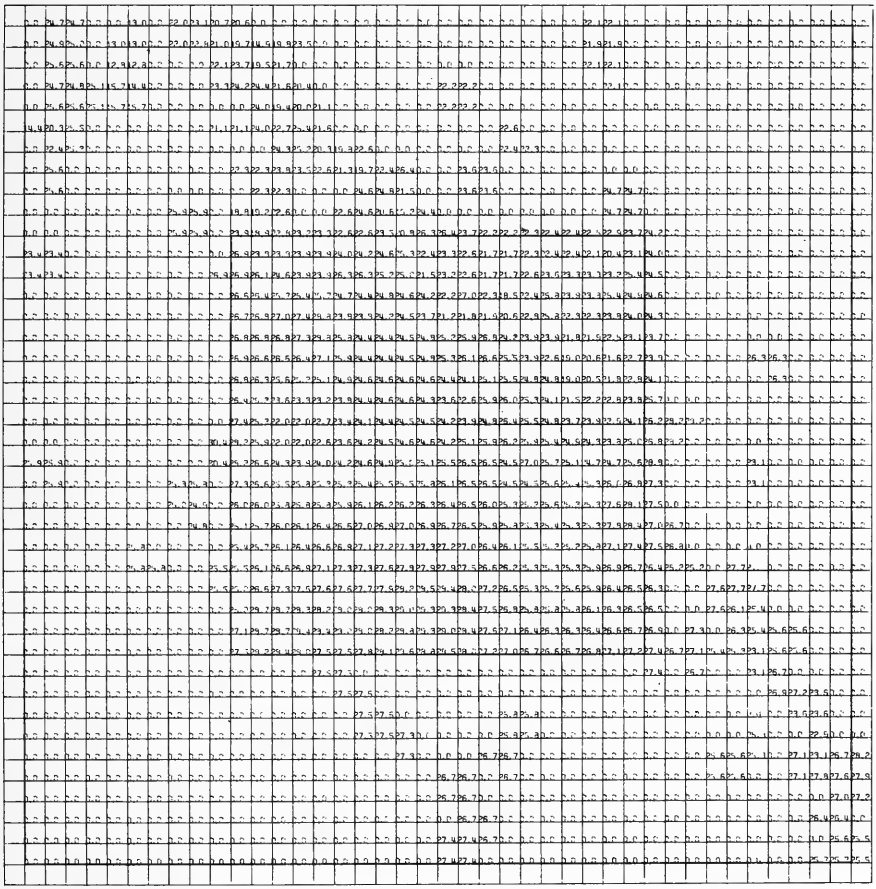

Figure 4. Plot of Filled Grid-Surface Temperature

Figure 5. Plot of Contours Surface Temperature

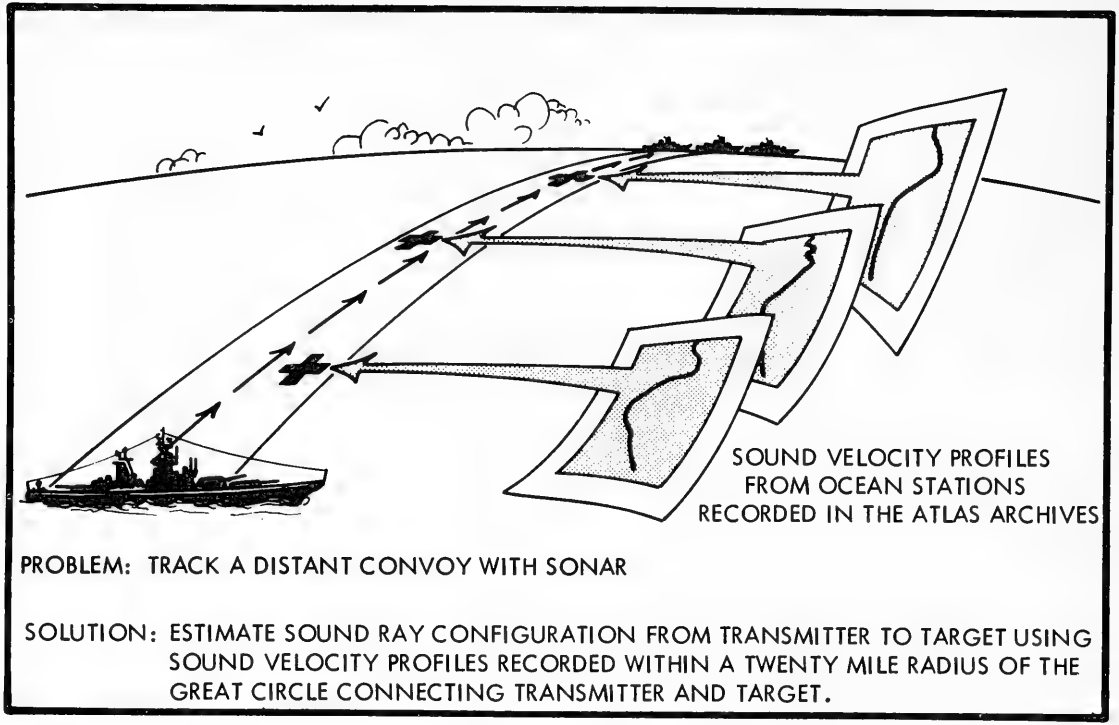

Figure 6. A Typical "Real Time" Problem

AN OCEANOGRAPHIC OPERATION CONDUCTED THROUGH AN ICE COVERED EMBAYMENT

by
Dr. Lloyd R. Breslau
Leo J. Fisher
F. M. Daugherty, Jr.
James P. Welsh

ABSTRACT

An oceanographic environmental survey was conducted in the vicinity of Thule, Greenland, during March-April 1968 to determine the direction of movement of the ice at spring thaw. Operations were conducted during extremely adverse weather conditions. Air temperatures dropped to as low as -45°F and wind speeds averaged about 15 knots.

Standard oceanographic instruments and techniques were adapted for use through a thick ice cover. Current measurements, sea floor photographs, ice thickness measurements, and through-ice echo soundings were obtained.

The measured currents are predominantly tidal and will result in an oscillatory motion of the water in the area with a slow net transport seaward through the channel between Wolstenholme Island and the mainland. These currents are not strong enough to have any significant effect on the break-up and movement of the ice, and consequently, the dominant factor affecting break-up and ice movement are wind direction and speed.

Introduction

In January 1968, an Air Force B-52 jet aircraft crashed on fast ice approximately 10 miles southwest of Thule Air Force Base, Greenland. The aircraft fragments were scattered over the surface of the ice on impact. Intense heat generated by fire associated with the crash melted the surface layer of the ice. As the ice melt refroze, some of the fragmented material became imbedded in the ice. To determine the direction of movement of the ice and imbedded material at spring thaw, a knowledge of the surface currents in the vicinity of the crash site was required. The U.S. Naval Oceanographic Office (NAVOCEANO) was requested by the Air Force in February 1968 to obtain the required surface current information. During the planning of the operation, spot photographs of the sea floor were requested to obtain information on the nature of the bottom in the vicinity of the crash site. In addition, a non-interference research experiment was incorporated into the operational field survey to investigate the feasibility of through-the-ice echo sounding.

NAVOCEANO responded to the Air Force's request for assistance by forming an ad hoc field party composed of personnel from its Coastal Oceanography Branch, Sea Ice Branch, and Ocean Dynamics Branch of its Research and Development Department. The field operation was planned and prepared for under a quick-fix time schedule; however, cleanup operations at the crash site delayed the NAVOCEANO field survey until late March. The NAVOCEANO field party (authors of this paper) arrived at Thule AFB on March 25, 1968 and departed on April 11, 1968, after obtaining current measurements and sea floor photographs, and proving the feasibility of through-the-ice echo sounding. We found that conducting an oceanographic operation over an ice-covered area was very different from working over open water. The remainder of this paper will discuss both the methods employed in the field operation and the data obtained.

Field Operation

The crash site was located approximately 10 miles southwest of Thule AFB, Greenland, midway between Saunder Island and the mainland. The general area (Figure 1) is a semi-enclosed basin bounded on the north and east by the mainland, and on the west by Saunder and Wolstenholme Islands.

The deepest water in the area is located in a southwest-northeast oriented channel which extends from Kap Atholl on the southwestern end and terminates in Wolstenholme Fjord on the northeastern end. Another relatively deep water channel trends westward from Wolstenholme Fjord between the northern tip of Saunder Island and the mainland. Shoal water exists in the channel between Saunder and Wolstenholme Islands. Maximum water depth in the general area of the crash site is approximately 135 fathoms (247 meters). All water depths shown on the chart in Figure 1 are in fathoms.

The geography of the area indicates four possible paths through which water might flow out of the general area of the crash site:

1. Between the northern tip of Saunder Island and Kap Abernathy on the mainland. 2. Between Saunder and Wolstenholme Island, 3. Between Wolstenholme Island and Kap Atholl on the mainland, or 4. Into Wolstenholme Fjord. To determine the direction and speed of the current through each of these passages, current measurements were to be made at mid-channel in each of the four passages. In addition, current measurements were to be made at each of three stations extending across the general area of the crash site on a line from Nasarssuak, on Saunder Island, to Nungavarssuk on the mainland. The planned current measurement sites (Figure 2) were precisely located by a USAF geodetic survey team prior to the beginning of the NAVOCEANO field operations.

The field operation was conducted during extremely adverse weather conditions. Air temperatures dropped to as low as -45°F, and wind speeds averaged 15 knots. At times, zero visibility ("whiteout") conditions prevented personnel movement over the ice. Twice, the tracked vehicle started to break through the ice, but was carried across the fractured area ("wet cracks") by the forward momentum of the vehicle. Needless to say, special precautions and procedures were adhered to during the operation. The Air Force assigned a survival expert, Sergeant JOHN KERSHNER to work with the scientific party for the duration of the field operation. Sergeant KERSHNER not only assured personnel safety but also contributed to the success of the mission by suggesting arctic procedures and actively participating in the field work.

Original plans specified 24 hours surface and bottom current measurements at each of the seven sites shown in Figure 2. In addition, a string of five current meters was to be installed at Site 1 at the beginning of the operation for continual data recording until retrieval of the meters at the completion of the operation. Bottom photographs also were to be taken at each of the sites upon completion of the current measurements. The current meters and camera were to be lowered and raised with a winch mounted in a specially constructed mobile laboratory.

Rapid deterioration of the ice in the vicinity of Sites 4, 5, 6, and 7 necessitated relocation of the originally selected sites. The positions of the relocated sites are shown in Figure 2. Figure 3 shows the approximate ice limits observed by aerial reconnaissance on 7 April 1968. Dangerous ice conditions prevented moving the heavy mobile laboratory to sites 3, 4, 5, 6, and 7. As a result, operations at these sites were limited to surface current measurements obtained by lowering and raising the current meters by hand. Bottom photographs were obtained only at Sites 1 and 2.

The mobile laboratory was designed by us at Thule using available material. A large flat-bed truck was located in the surplus lot of the motor pool, and its flat-bed section was used as a rolling platform. We had brought along a gasoline powered winch and derrick for use on the operation. The Air Force Base support group under Lt. Colonel T.W. Evans mounted the winch and derrick on the flat-bed section and constructed an enclosing shed. Since this was an oceanographic operation, we commissioned the mobile laboratory "the Research Vessel THULE."

The R/V THULE is shown in Figures 4A, 4B, and 4C. Figure 4A shows the R/V THULE being towed to its station by an Air Force trucked vehicle (TRACKMASTER). The reason that we used a rolling bed rather than a sledded bed was the towing capability of available tracked vehicles. This arrangement was adequate for the type of ice cover present, which was first-year plate ice with occasional embedded icebergs. Figure 4B shows the R/V THULE on station. The winch mounted inside the shed is

a SASGEN SINGLE DRUM LIGHT DUTY HOIST loaded with 2,000 feet of 3/16 inch wire rope, and capable of pulling 2,000 pounds. The shed was constructed to overhang the rear of the flat-bed truck section. A trap door was located in the overhung section for lowering and raising oceanographic instruments. A canvas skirt pegged to the ice surrounding the ice hole made it possible for a kerosene stove to maintain normal room temperature inside the shed. Figure 4C shows personnel working around the ice hole under the overhang. They are tieing off a lowered current meter strung to a wooden cross-piece support, preparatory to moving the R/V THULE off station.

While drilling a hole through the ice might sound like a rather mundane task, it is both a necessary and difficult part of an oceanographic operation carried out on an ice covered area. This phase of the field operation is shown in Figures 5A and 5B. A small diameter, hand-powered ice auger used for making ice thickness measurement holes is shown in Figure 5A. A large diameter gasoline-powered ice auger used for making instrument access holes is shown in Figure 5B.

Oceanographic measurements made through sea ice require drilling a relatively large hole in the ice. The dimensions of the hole depend on the size of the equipment to be passed through the ice and the type of measurement to be made. The technique described was used to make holes large enough to pass through the ice, the Hydroproducts and Geodyne current meters and the modified E., G., and G. sea floor camera. The size of the hole required was 24" by 24". Eight holes were prepared, varying in size from 19" by 31" to 27" by 31", all of which were adequate. The time for preparation varied from 15 minutes to 1.5 hours.

The following equipment was used to make the holes:

(a) Ice thickness kit, (b) an ice auger, 32" long and 7" in diameter, powered by a 3HP Tecumsh, 2 cycle engine (c) a shovel and (d) an ice spud.

The procedure, in outline form, follows:

1. Measure the ice thickness.

2. Clear an area of 20 square feet.

3. Drill 10 overlapping 7" diameter holes in the ice to within 4" of the sea water. This configuration leases an "island" in the center of the hole.

4. Depending on the thickness of the ice, the "island" may be broken up and cleared from the hole or may be removed in one piece. Forty inch thick ice left an "island" that could be removed by 2 men.

5. Drill through each of the 10 holes to the sea water and free the "island," with an ice spud if necessary.

6. Remove the ice "island" and clear the slush.

The ice auger used would drill a 32" hole, 7" in diameter in 20 seconds. The engine operated at temperatures to -27°F with slight choke adjustments. When extensions were used to drill a hole greater than 32" deep, the auger became difficult to manage. The technique was successful in ice varying in thickness from 21" to 44". The auger was also used to make single 7" diameter holes in 65" of ice.

The current data was obtained with two types of current meters: the Hydroproducts Model 501B, and the Geodyne Model A-101.

The Hydroproducts Model 501B meter is a self contained system with an integral recorder capable of unattended recording of current speed, current direction, and temperature for periods up to 30 days. The record is a permanent and easy to read analog plot that can be analyzed immediately after recovery of the meter. The Hydroproducts meters were used to obtain a 24 hour current record at each site. The records were analyzed as soon as possible after recovery of the meters to provide the on-site SAC Disaster Control Team with immediate information on the surface currents in the vicinity of the crash site. Surface current measurements with the Hydroproducts meters were made at sites inaccessible to the R/V THULE. Figure 6 shows this phase of the field operation. The Hydroproducts meter is in the foreground.

The Geodyne Model A-101 is a self contained system capable of recording up to 200 days of current speed and direction data. The data are recorded as a digital coded dot matrix on photographic film. The Geodyne meters were used to obtain a seven-day current record from five different depths at Site 1. These data were not processed until the field team returned to NAVOCEANO where the necessary data processing facilities were available. The Geodyne current meter array is shown in Figure 7. Since the array was to be emplaced for seven days and since the Geodyne meters are rather delicate, they were transported to Site 1 by a helicopter which happened to be available (Figure 8).

Both the Hydroproducts and Geodyne current meters use a magnetic compass in determining current direction. The crash site was located close to the earth's north magnetic pole where the horizontal component of the earth's magnetic field is very weak, and the vertical magnetic force is relatively strong. The weak horizontal and strong vertical magnetic forces acting on the compasses in the current meters suggested difficulty in measuring current directions. To overcome this difficulty, one Hydroproducts meter was modified to measure current direction by referencing the compass to an artificial

magnetic north. This was accomplished by attaching a bar magnet to the frame of the current meter near the housing for the compass (Figure 9). The compass in the current meter now used the bar magnet as a north reference. The bar magnet and the current meter were aligned to a true north reference (provided by the Air Force Geodetic Survey Team) by means of sections of rigid pipe attached to the current meter as it was lowered into the water.

The underwater camera and electronic flash combination that was used to obtain the sea-floor photographs was a model-205 camera and model-206 light source (Figure 10), manufactured by E.G.& G. International, Inc. These units were mounted in a steel protective framework which was designed to fit through a two-foot diameter hole. A bottom sensing trigger weight was used to activate the camera and flash combination at the proper distance (8 feet) above the sea floor.

The camera utilizes an F/4.5 lens especially designed for underwater use. It was mounted on the frame so as to point at the sea floor at a 40 degree angle with the vertical. The angular dimensions covered by the optical system in the camera itself are such as to provide 38 degree coverage on the short side of the rectangular photograph and 51 degree coverage on the long side of the rectangular photograph.

The camera is loaded with standard 35mm film in a 36 exposure cassette. Twenty two exposures can be obtained during a lowering. The film used during this survey was Kodak plus X. The flash uses a Xenon light; therefore, the spectrum produced is similar to that of sunlight.

Operation of the camera and light source is accomplished by the closing of the bottom sensing switch. Momentary actuation of this switch causes the shutter to open, triggering the light source. Immediately after the exposure has been made, the film is automatically advanced to the next frame in about 2 to 4 seconds, depending on the condition of the battery.

During this survey, the camera and flash combination was lowered until the trigger weight touched the sea floor. It was then repeatedly raised and lowered a distance of approximately 20 feet off the sea floor, allowing 30 seconds between lowerings to double insure that the flash capacitors were charged to maximum energy.

The feasibility of through-the-ice echo sounding was investigated using an E.G.& G. Model-254 Continuous Seismic Profiling System, which NAVOCEANO happened to have on hand. The system operates at an acoustic frequency of 12 kilocycles and has a high peak power output (about 105 db//1 dyne /cm^2), short pulse length (about 0.1 millisecond), and high repetition rate (10 or 20 pulses per second). The entire system consists of three separate physical components: (1) a recorder/driver console, (2) a transmitter/receiver transducer,

(3) a gasoline-powered electric generator. This non-interference research operation is shown in Figures 11A and 11B. Figure 11A shows the tracked vehicle with the recorder/driver mounted inside its cabin, and trailing power cables to the gasoline-powered generator and recorder/driver transducer on the ice. Figure 11B shows the recorder/driver transducer coupled to the ice. The snow cover was shoveled away, and the transducer was set in a water filled pot (borrowed from the galley) which rested on the ice.

DISCUSSION OF DATA

Currents

The current meter data for all of the seven sites shown in Figure 2 indicates that the currents in the area are predominantly tidal. Tidal currents are the horizontal movements of water that accompany the rise and fall of the tide. The horizontal movement of the tidal current, and the vertical movement of the tide, are intimately related parts of the same phenomenon induced by the tide-producing forces of the sun and moon. Tidal currents, like the tides, are periodic; it is the periodicity of the tidal current that distinguishes it from other types of currents, which are generally called non-tidal currents. Non-tidal currents are generated by causes that are independent of the tide, such as winds, fresh water run-off, and differences in water density and temperature. Currents of this class do not exhibit the periodicity of tidal currents.

The tidal currents in a restricted area, such as the study area, are generally of the reversing type; i.e., the current flows in one direction for a period of about six hours, then reverses and flows in the opposite direction for approximately the same period of time. The current flowing towards land is generally referred to as the flood current, and the current flowing seaward is called the ebb current. The reversal in current direction gives rise to a period of slack water during which the speed of the current is zero. An example of these features is shown in Figure 12, which denotes a section of the current meter data obtained at 228 meters depth at Site 1. The tidal current in the study area is semi-diurnal; therefore, the current will reverse direction twice daily with two floods and two ebbs. The figure shows the reversal in current direction, and the change in speed from zero to a maximum during each flood and ebb at Site 1. The current floods towards 20° (north-northeasterly) and ebbs towards 225° (southwesterly). The shift in direction from ebb to flood is gradual, whereas the shift from flood to ebb is relatively abrupt.

The strongest currents occur with the spring tides at full and new moon, and the weakest currents with the neap tides during the moon's first and third quarters. The change in strength of the measured tidal current at Site 1 and its relation to the predicted

tides in North Star Bay are shown in Figure 13. The shape of the tidal current curve is similar to that of the predicted tide curve. The maximum current speeds occurred at the beginning of the period in conjunction with the maximum tide range generated by the new moon on 28 March. The weakest currents and minimum tide range occurred on 6 April in association with the moon's first quarter. The relationship between the changes in current velocity and the tide at North Star Bay is information that can be used to predict the strength of the tidal currents in the study area.

The current direction rises for Site 1 indicate the reversing nature of the tidal current at all depths, and the current speed plots indicate the changes in speed of the tidal current caused by the direction reversal and change in tide range. Figure 14 is a summary of all the current data. The cones extending from the site locations indicate the most frequently observed current directions at each site. The numerals indicate the maximum current speed in knots recorded for each range of directions.

Sea Floor Photographs

Sea floor photographs were obtained at Sites 1 and 2. A representative photograph taken at Site 1 is presented in Figure 15, and some representative photographs taken at Site 2 are presented as Figures 16-18. Annotated sketches of bottom flora and fauna present in the photographs are presented below the photographs to serve as an identification key.

Site 1, at a depth of 240 meters, is almost devoid of marine life and indicates a soft bottom typical of an area of fine sediment deposite.

Site 2, at a depth of 135 meters, shows an abundance of marine life and rocky bottom typical of an area scoured by currents. The area appears to be a common Macoma calcarea benthic community which is characteristic of relatively shallow water. Many of the indicator species of the Macoma calcarea community are quite tolerant of variations in both water and bottom conditions, and are consequently circumpolar. The identification of the marine life in the photographs is tentative and mostly an educated guess, since positive identification of invertebrates is impossible without the animal. The following tentative identifications have been made:

Phylum Coelenteratea - Sea anemone (Class Anthozoa, probably Order Antinaria, possibly Anthopleura spp. or Epiactis spp.), Hydroid (Class Hydrozoa) - small jelly-like masses.

Phylum Echinodermata -

Starfish (Class Asteroidea)

Brittle star (Class Ophiuroidea, probably Ophiura sp., possibly Ophiura sarsi, plus others)

Sea urchin (Class Echiuroidea, probably Strongy-locentrotus droebachiensis)

Sea cucumber (Class Holothuroidea, burrowing type with reversible respiratory tree (gills) extended above mud)

Sea lily (Class Crinoidea, probably Helimoctra glacialis)

Phylum Mollusca

Macoma calcarea, white shells on mud (Class Lamellibranchiata)
Pecten sp., possibly p. islandicus (Class Lamellibranchiata)

Through-Ice Echo Sounding

The through-ice echo sounding experiment demonstrated that it is possible to 12 kilocycle echo sound through a 4-foot thick first-year plate-ice cover in a shallow water area. A photograph of an annotated section of echo sounding record is presented as Figure 19. A crisp echo from the sea floor is present on the record and indicates a depth of 440 feet. (Note: full sweep is 240 feet, and the sea floor echo is arriving during the second sweep.) A diffuse long-drawn-out echo return is present on the left hand side of the record. This is reverberation caused by the out-going ping passing through the ice cover. The reverberation appears on the first recording sweep only and can be phased out by not recording on the sweep associated with the out-going ping. This has been done on the top-most section of the record in Figure 19.

Ice Thickness Measurements

The thickness of the ice was measured at 50 random locations throughout the study area. Ice thickness ranged from a minimum of 20 inches to a maximum of 46 inches. A representative areal distribution of the ice thickness during the beginning of the survey is shown in Figure 20. Additional measurements were made at Sites 1 and 2 to determine the homogeneity of the ice thickness over a small area. The thickness measurements were made systematically at 10 and 20 foot spacings along two intersecting lines, each 100 feet long. The results of the measurements at Site 1 indicated a mean thickness of 32 inches, a maximum of 37 inches, and a minimum of 29 inches. Measurements at Site 2 indicated a mean thickness of 42 inches, a maximum of 44 inches, and a minimum of 39 inches. These measurements indicate a relatively uniform ice thickness over the small areas sampled.

Conclusions

1. An oceanographic operation was successfully conducted through an ice covered embayment during extremely adverse weather conditions. The procedures and techniques utilized and data obtained are contained in the preceding sections of this report.

2. The currents in the area observed are predominantly tidal, and will result in an oscillatory motion of the water in the area, with a slow net transport seaward through the channel between Wolstenholme Island and the mainland. The analysis of the data indicates that the currents measured during this operation are not strong enough to have any significant effect on the break-up and movement of the ice, and that the dominant factor affecting the break-up and movement of the ice is the wind direction and speed.

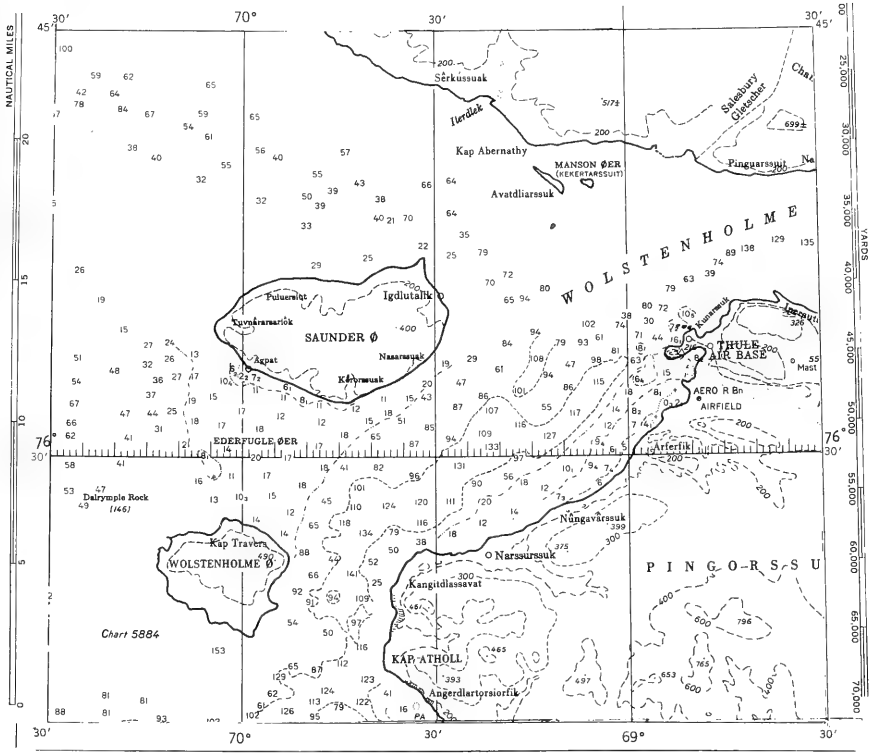

Figure 1. General Operational Locale

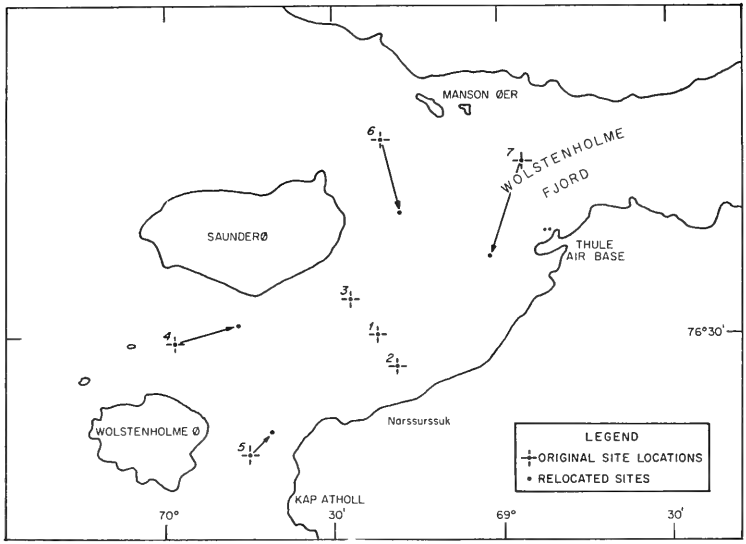

Figure 2. Site Location

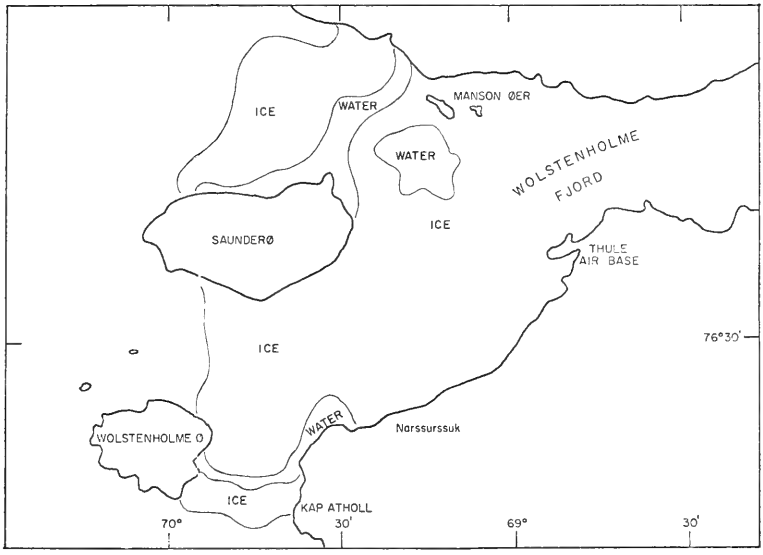

Figure 3. Approximate Ice Limits - 7 April 19

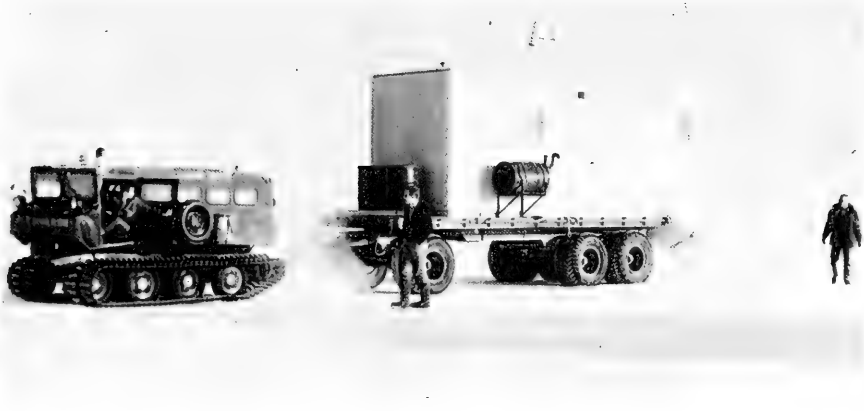

Figure 4.a. Tracked Vehicle Pulling "R/V Thule"

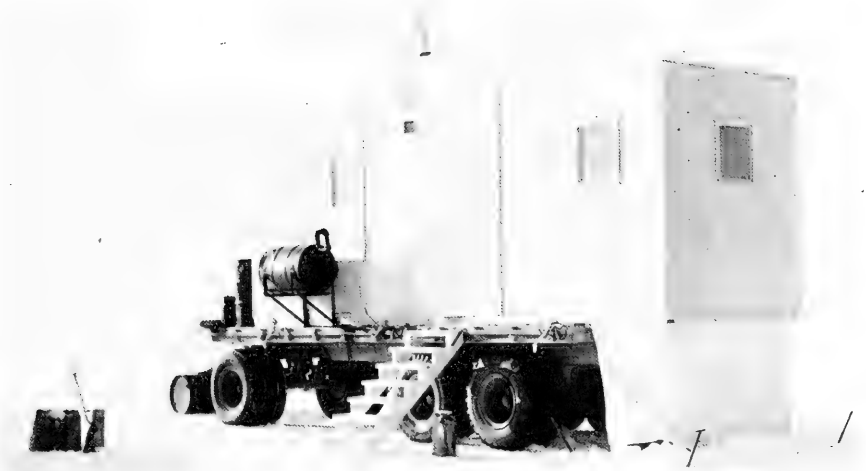

Figure 4.b. "R/V Thule" on Station

Figure 4.c. Stern Section of "R/V Thule"

Figure 5.a. Drilling Ice-Thickness-Measurement Hole

Figure 5.b. Drilling Instrument-Access Hole

Figure 6. Current Meter Station Using Tracked Vehicle

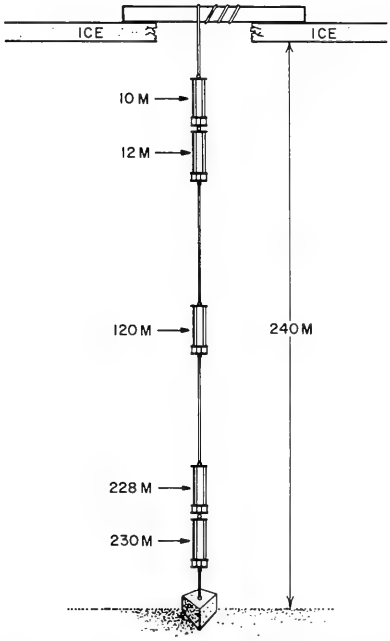

Figure 7. Geodyne Current Meter Array

Figure 8. Helicopter Transport of Current Meters

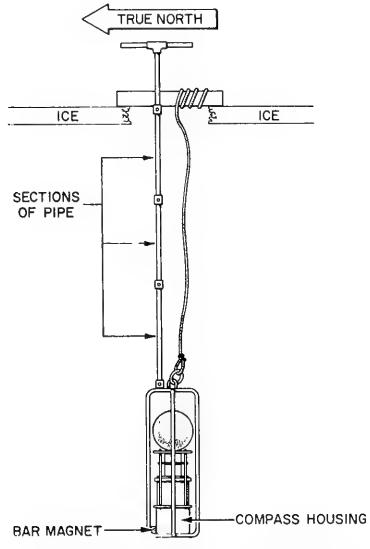

Figure 9. Modified Hydroproducts Current Meter

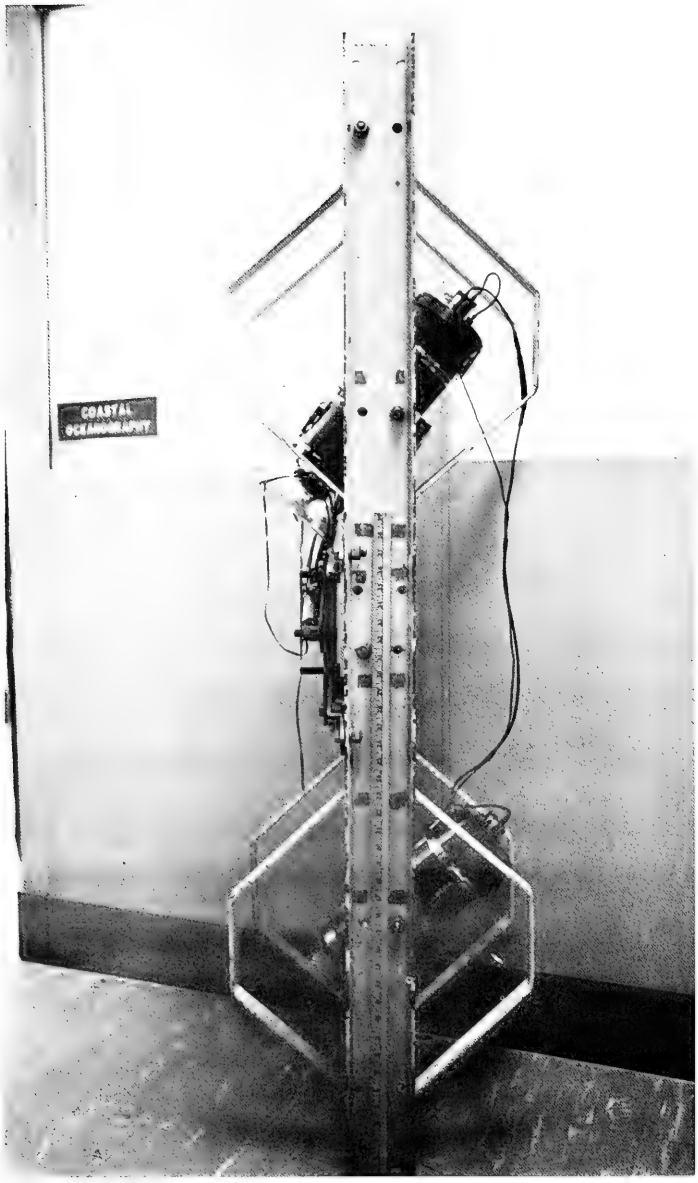

Figure 10. Modified Deep Sea Camera

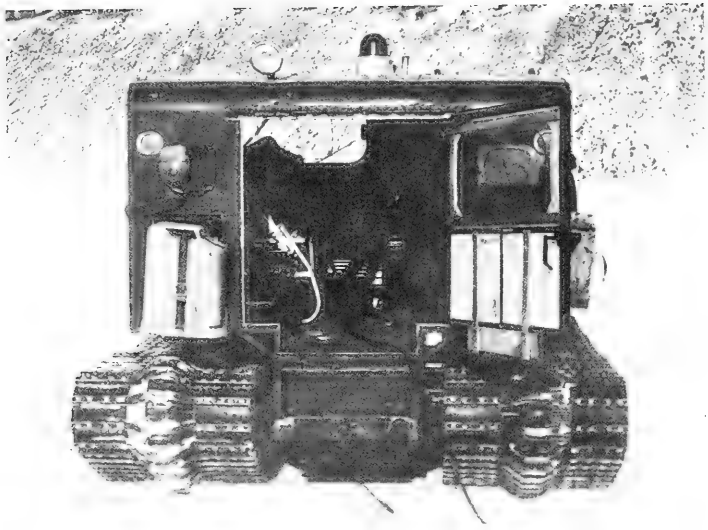

Figure 11.a. Seismic Station Using Tracked Vehicle

Figure 11.b. Seismic Transducer Coupled to the Ice

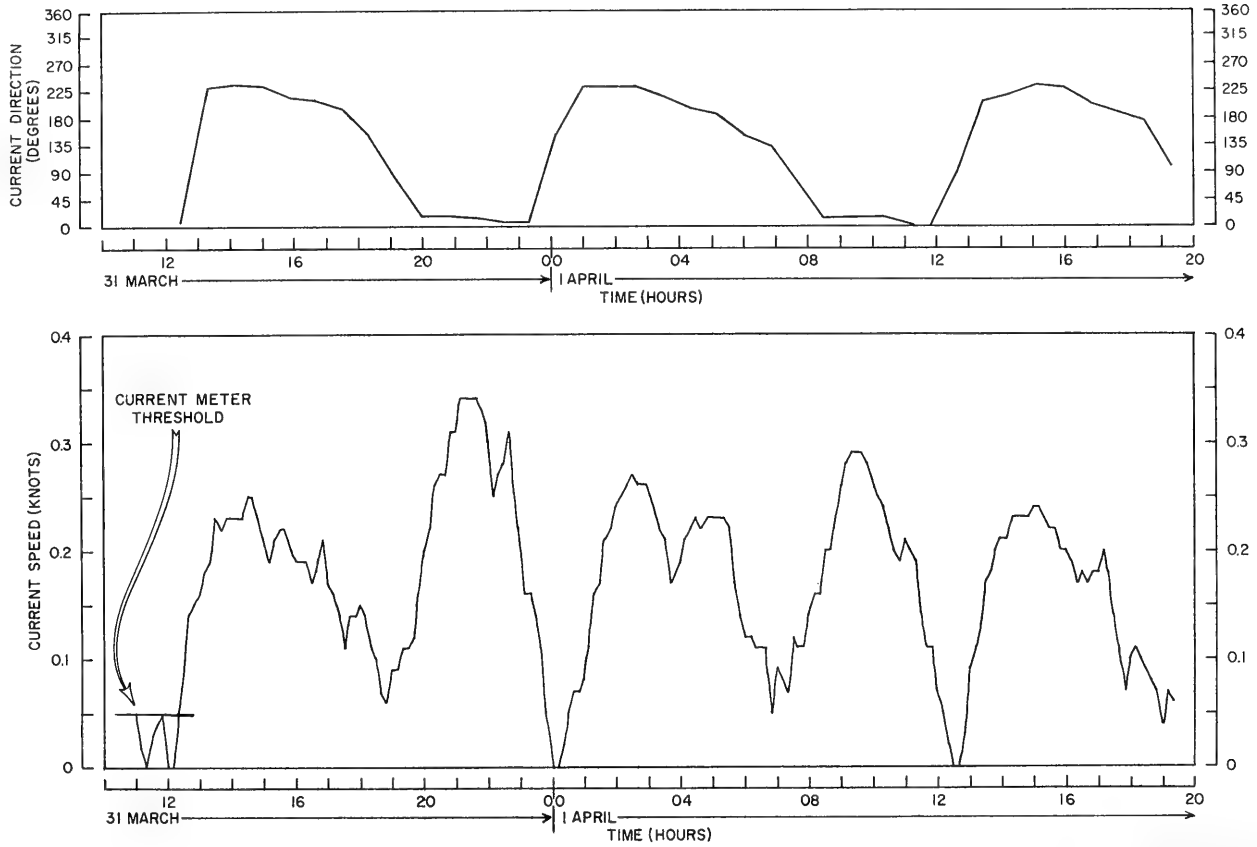

Figure 12. Relationship between Tidal Current Direction and Speed

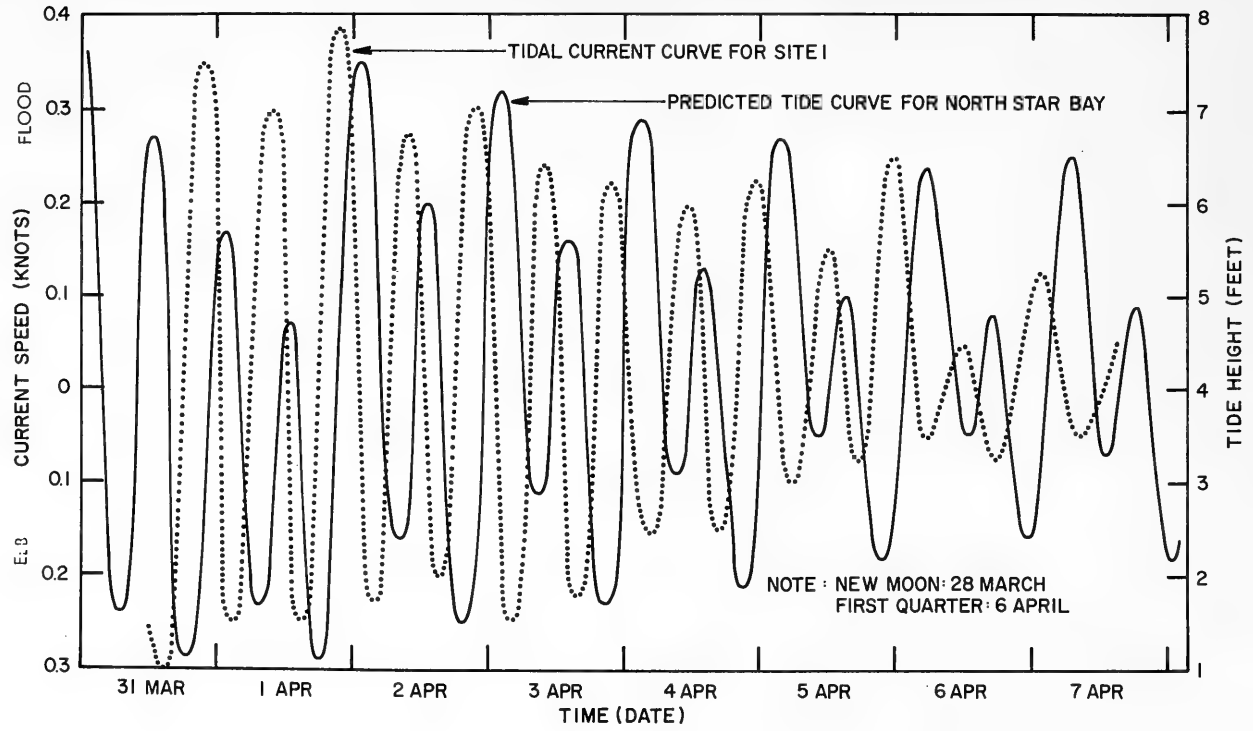

Figure 13. Relationship between Tidal Currents and the Tide

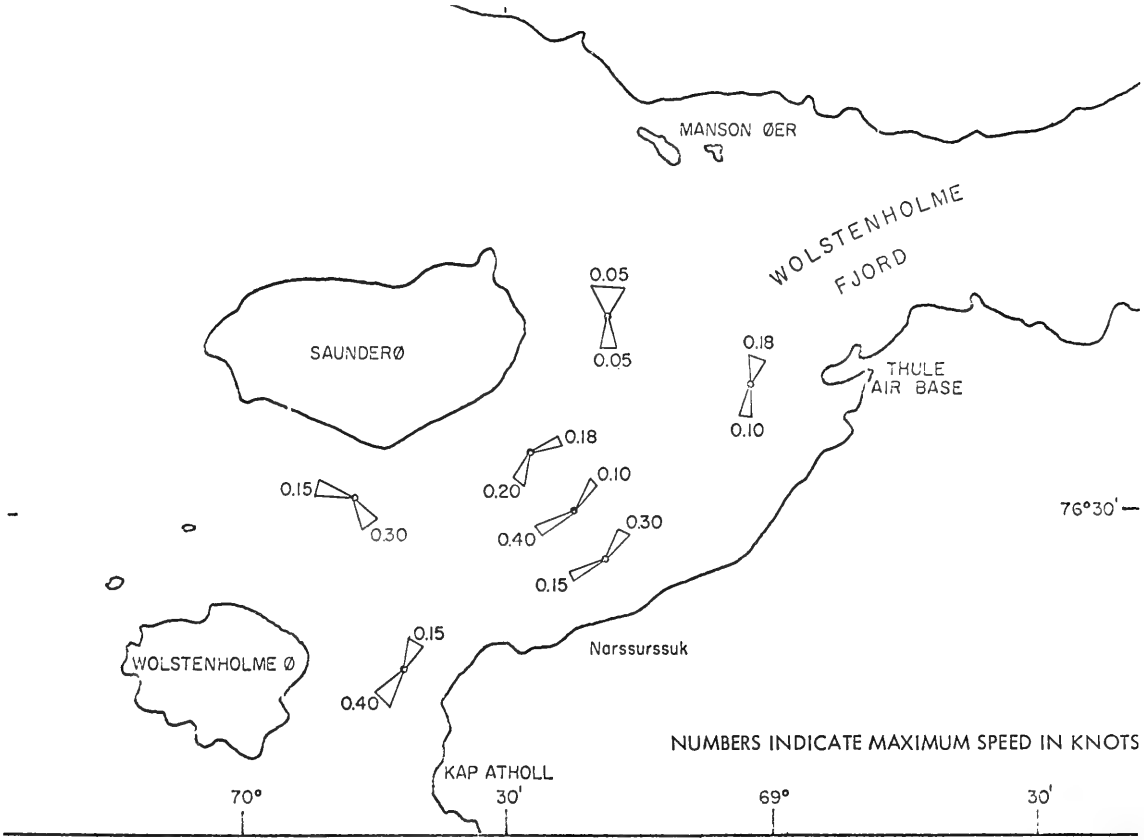

Figure 14. Summary of Current Data

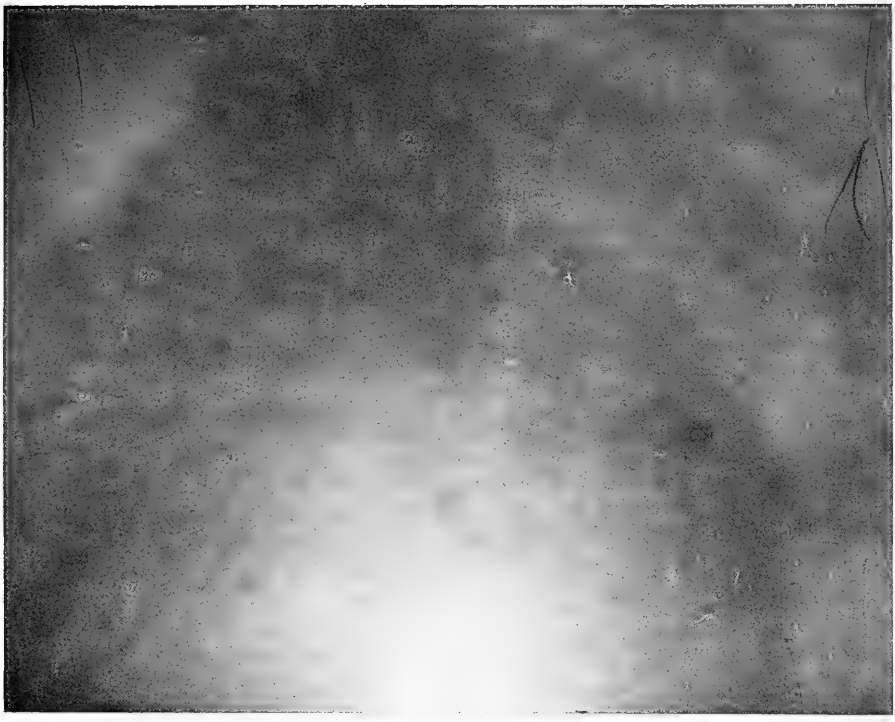

Figure 15. Bottom Photograph - Site 1

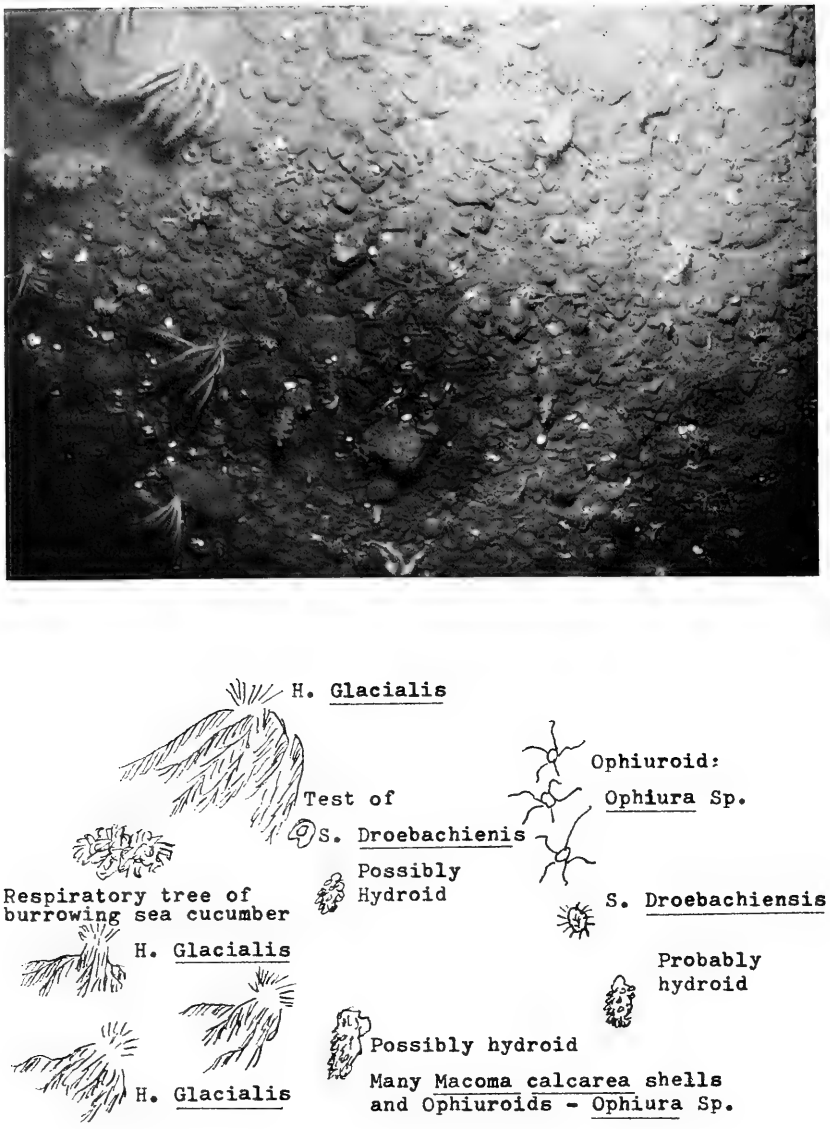

Figure 16. Bottom Photograph - Site 2

Figure 17. Bottom Photograph - Site 2

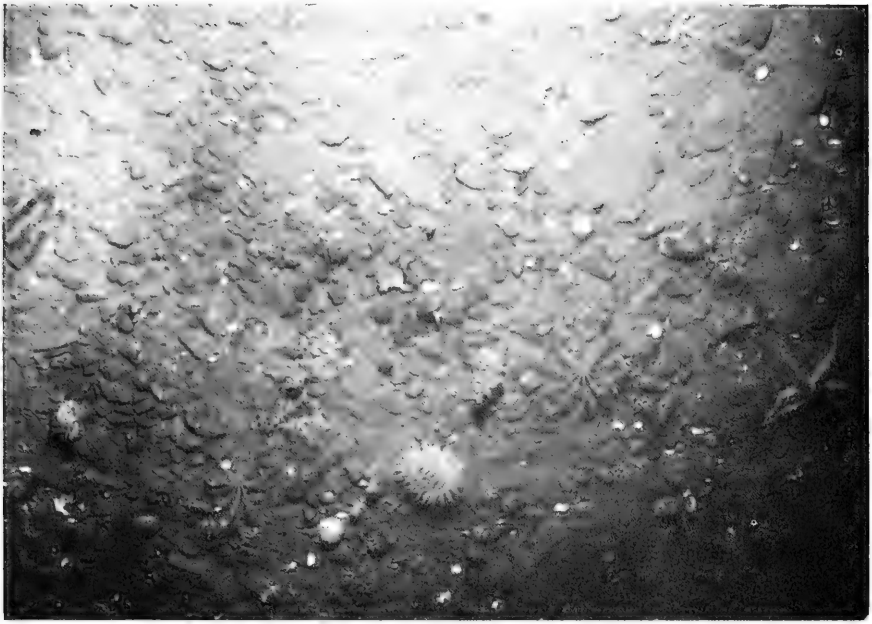

Figure 18. Bottom Photograph - Site 2

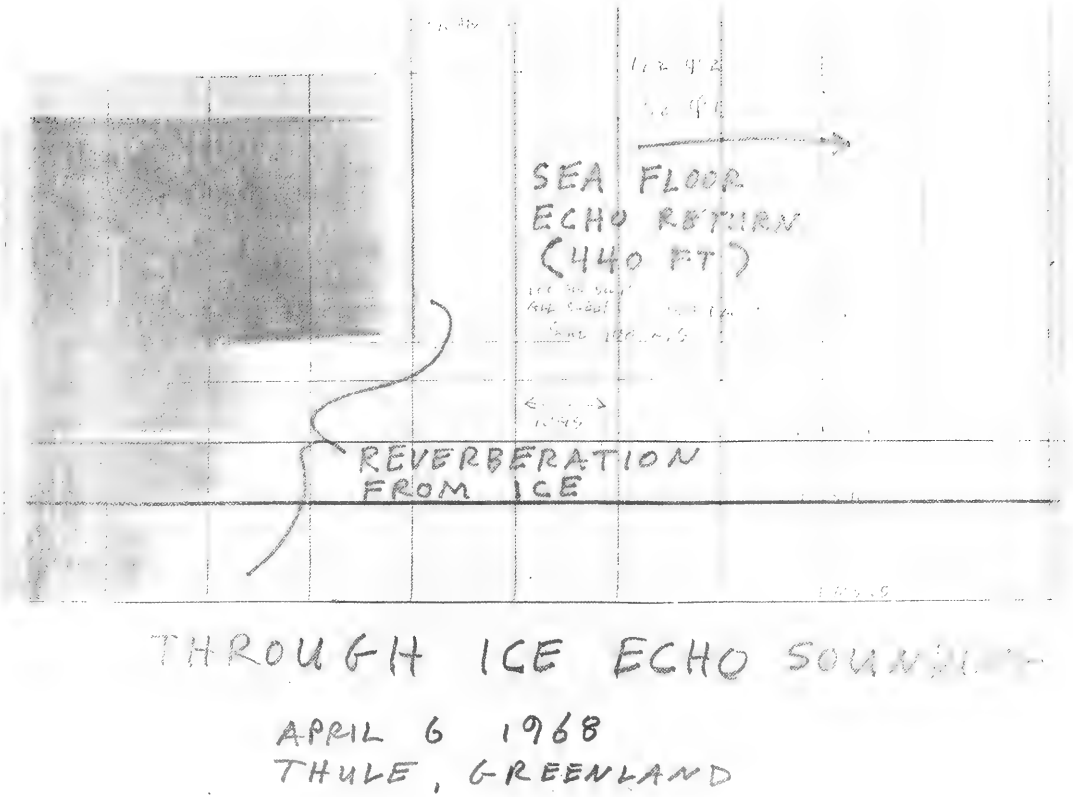

Figure 19. Bathymetric Record Obtained through-the-ice Echo Sounding

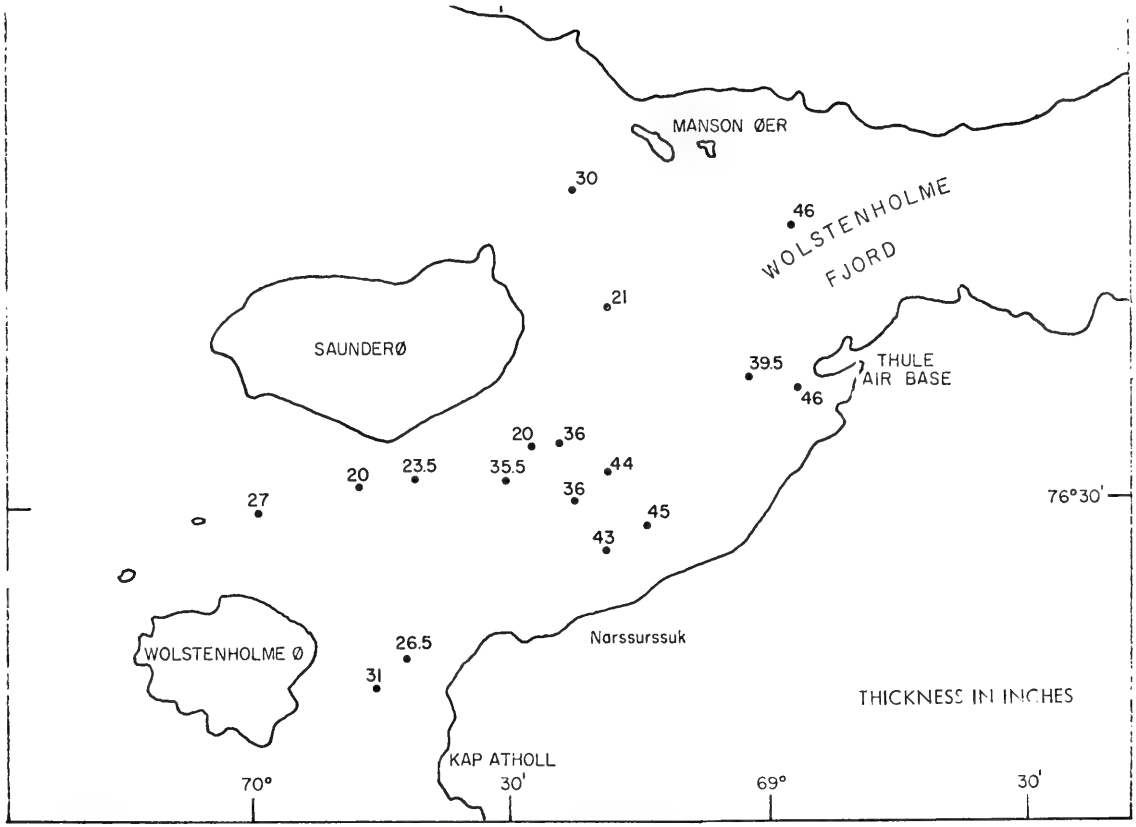

Figure 20. Ice Thickness

MAPPING THE NORTH PACIFIC OCEAN SEA FLOOR

T. E. Chase
Associate Specialist in Marine Geology

S. M. Smith
Associate Specialist in Submarine Geology

Scripps Institution of Oceanography

Abstract: A series of sea floor topographic and physiographic charts of the North Pacific Ocean are being prepared for the Undersea Surveillance Oceanographic Center (NAVOCEANO). In addition, reliable bathymetric and magnetic data throughout the Pacific are being put into digital storage.

Divided into three areas, the coverage consists of 160 topographic charts originally prepared at approximately 1:1,000,000 scale, then reduced to about 1:2,500,000 for printing into three atlases; 10 composite contour charts, and 10 physiographic diagrams will be prepared for distribution throughout the scientific and naval communities. 49 charts between latitudes 0° to 60°N and longitudes 100°E to 160°E are completed and published in an atlas form. Three composite charts covering the area are also completed and undergoing color separation and printing.

Computer programs have been developed to aid in processing data, and to date 392,000 miles of bathymetry and 206,000 miles of magnetics plus navigational tracks have been digitized.

On July 1, 1967, the Scripps Institution of Oceanography began a contract with the Undersea Surveillance Oceanographic Center of NAVOCEANO to prepare a series of charts and a digital tape of bathymetric soundings of the North Pacific Ocean.

The purposes of these efforts are many, and two are of immediate importance.

Increased studies of the origin and history of the Pacific basin are important to the fields of Marine Geology and Geophysics. Detailed bathymetric sea floor charts are critically needed in such studies.

Within many research organizations, studies of sound transmission in water along selected paths are often interrupted by topographic features. Here, reliable charts are also important. The majority of existing sea-floor contour charts, however, have been found to be of a smaller scale, contour interval, or too old to aid in these studies.

Four series of charts are being produced: physiographic charts (10 sheets); bathymetric contour charts (10 sheets); bathymetric contour charts at approximately 1:1,000,000 scale (160 sheets); and 3 atlases of bathymetric contour charts.

The charts are a compilation and interpretation of the best bathymetric contours and sounding data available, and they present a complete series of topographic and physiographic charts for ease in referencing the floor of the North Pacific Ocean. They are designed for use by interested persons or groups working in the marine sciences as a quick reference to bathymetric contours and physiographic provinces.

Figure 1 shows the distribution of and numbering system for location of the charts. The heavy borders are small-scale regional contour and physiographic charts. Areas I, II, and III are boundaries of the three atlases. Area I is contoured, and 49 charts are published in the Bathymetric Atlas of the Northwestern Pacific Ocean. Figure 2 shows a page from that atlas. (H. O. Pub. 1301.)

The atlas of area I contains 49 bathymetric charts covering nearly 7-1/2 million square miles of the North Pacific Ocean between 4°S and 60°N latitude and between 100°E and 160°E longitude, including the South and East China, Yellow, Japan and Okhotsk Seas.

SOURCES OF DATA

Figure 3 shows the different sources of data used. The most useful were original echograms or soundings with high navigational quality.

J. C. Sylvester, Bathymetry Division (NAVOCEANO), supplied random soundings for each chart plus microfilm copies of original echograms and ships' navigational tracks.

Marine Geophysical Surveys, NAVOCEANO, supplied original echograms of detailed cruises in the North Philippine Sea. The ASW/USW Project, NAVOCEANO, under Mr. W. T. Hammond, supplied soundings of extensive surveys in the Sea of Japan. Published charts from the Maritime Safety Agency, Japan and the USSR gave detail in areas where soundings were sparse.

Echo sounding equipment used to gather data for the charts included the Edo Corporation Sonar Sounding Set AN/UQN-1B, Westrex Corporation Mark V, X, and XV Precision Depth Recorders (PDR), Thomas Gifft Company Depth Recorder (GDR), Alden Electronic and Impulse Recording Equipment Company, Inc., Precision Graphic Recorder (PGR), Alpine Geophysical Associates, Inc., Precision Echo Sounder Recorder (PESR), and Kelvin-Hughes Echo Sounder.

EVALUATION OF DATA

All data was evaluated for its importance in preparing the contour charts and for digitizing into the data bank. Unfortunately, many of the random soundings were of value in predicting topographic trends but lacked enough precise navigational information to warrant inclusion in the digital data collection.

A large segment of the data was shown on charts and sounding sheets contoured in meters, both corrected and uncorrected for sound velocity. These were converted to "uncorrected" fathoms by use of Matthew's Tables of the Velocity of Sound in Pure Water and Sea Water.

Initially, efforts were made to use digital (computer) output for the chart preparation. However, the random spacing of precision sounding information with precise navigation was insufficient. Therefore, it was necessary to prepare a data tape separately and to develop the charts by visual interpretation and manual cartographic methods with extensive use of stable base materials.

DIGITIZING OPERATION

Data from smoothed navigation plots were digitized onto IBM cards using the Benson-Lehner OSCAR S-2 XY Reader. After the cards are run through data checking programs and errors removed, they are input to a program which produces a magnetic tape containing time in accumulated minutes and positions at these times. A parallel series of operations are carried out on the echograms and magnetic records, using a CALMA 480 in addition to the B-L OSCAR, the final product being another magnetic tape having time in accumulated minutes and the depth or magnetic field values at these times. Most of the depth data were digitized on the OSCAR at 3 to 5 minute intervals of ship time (1/2 to 1 mile apart), the remainder being done on the CALMA at 1 minute intervals. The interval for magnetic data was 6 minutes. The navigation and depth on magnetic value tapes are used in turn as input to another program which merges the navigation and depth or navigation and magnetics onto another tape that becomes the primary storage for the expedition. The merged data can then be used for profiles at various scales and vertical exaggerations (Figure 4), sounding plots of single expeditions, sounding compilations of many cruises within a given area (Figure 5), statistical analyses, and transmission to other agencies. Additional programs are being developed for producing computer plotted index track charts of digitized data as well as bathymetric and magnetic profiles plotted along tracks on Mercator projection. As of March 1969, 392,000 miles of bathymetry and 206,000 miles of magnetics have been processed.

CONCLUSIONS

The efforts expended during the chart preparation has resulted in contours of many previously uncharted seamounts, trend determinations of other primary structural features like trenches and ridges, plus limits of large physiographic provinces.

Basic knowledge of structural and tectonic conditions were used throughout the chart preparations. Where sounding data was not sufficient to give detailed portrayal, interpolation was extended to gain the most accurate configuration.

The charts presented here do not represent the final configuration of the sea floor, for many precise and detailed surveys are needed to give complete coverage. It is felt, however, that the different scales, contour interval, and physiographic interpretation used is sufficient to give as complete a sea-floor portrayal as possible with the present data available and knowledge of geologic features.

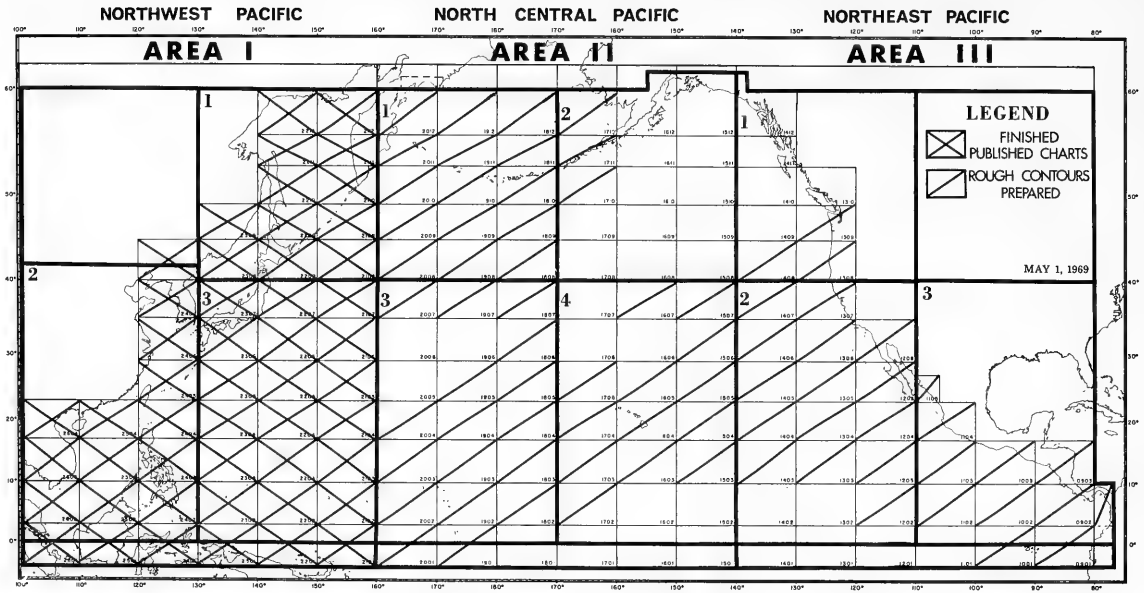

Figure 1. Index chart of the North Pacific showing location of charts and atlases

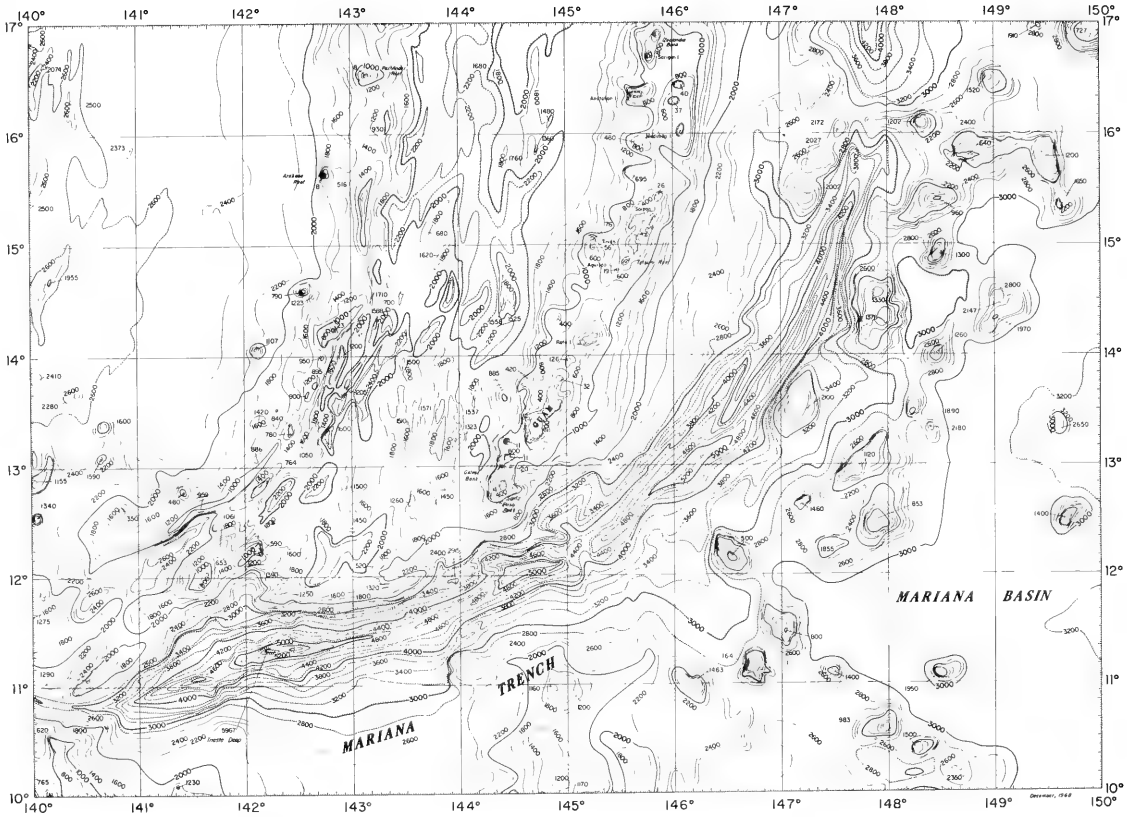

Figure 2. Page from atlas of Northwest Pacific showing contour interval and format used in preparation of the contour charts

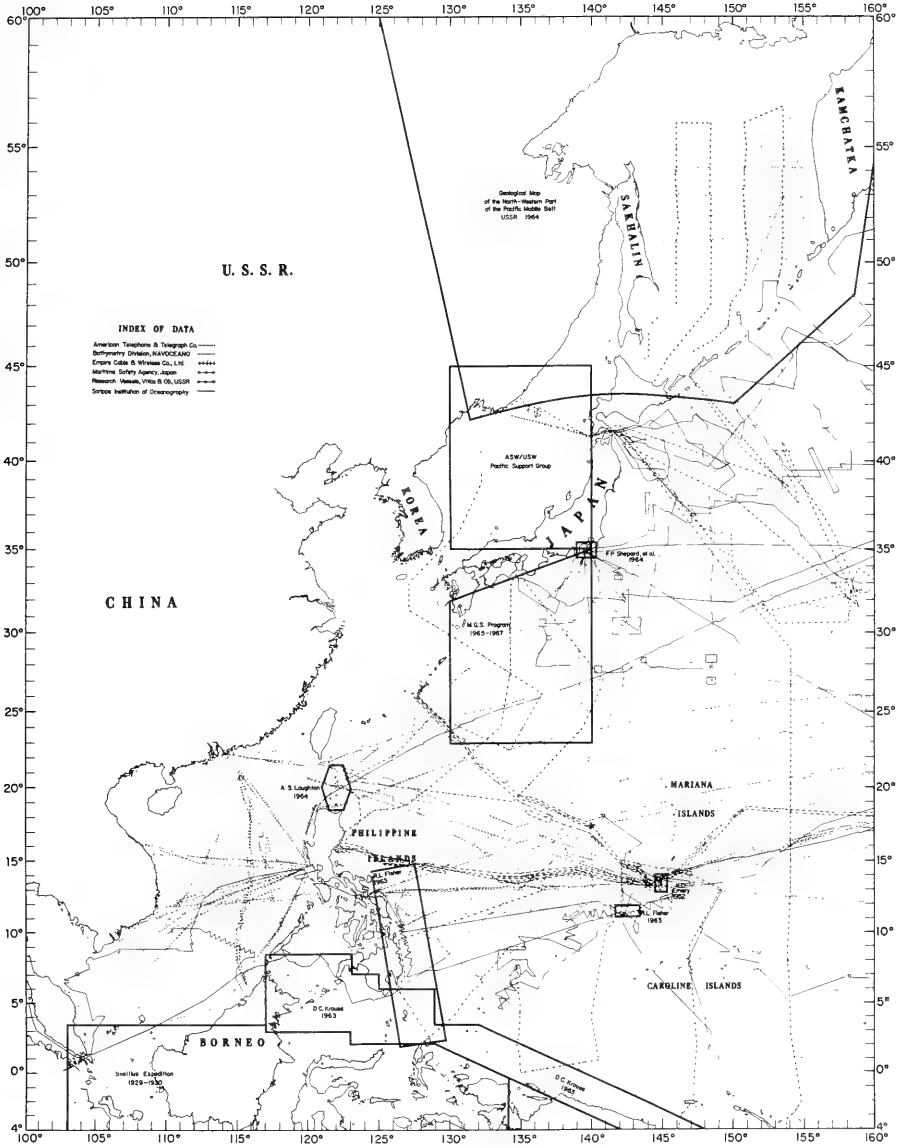

Figure 3. Index chart of data used for preparation of contour charts

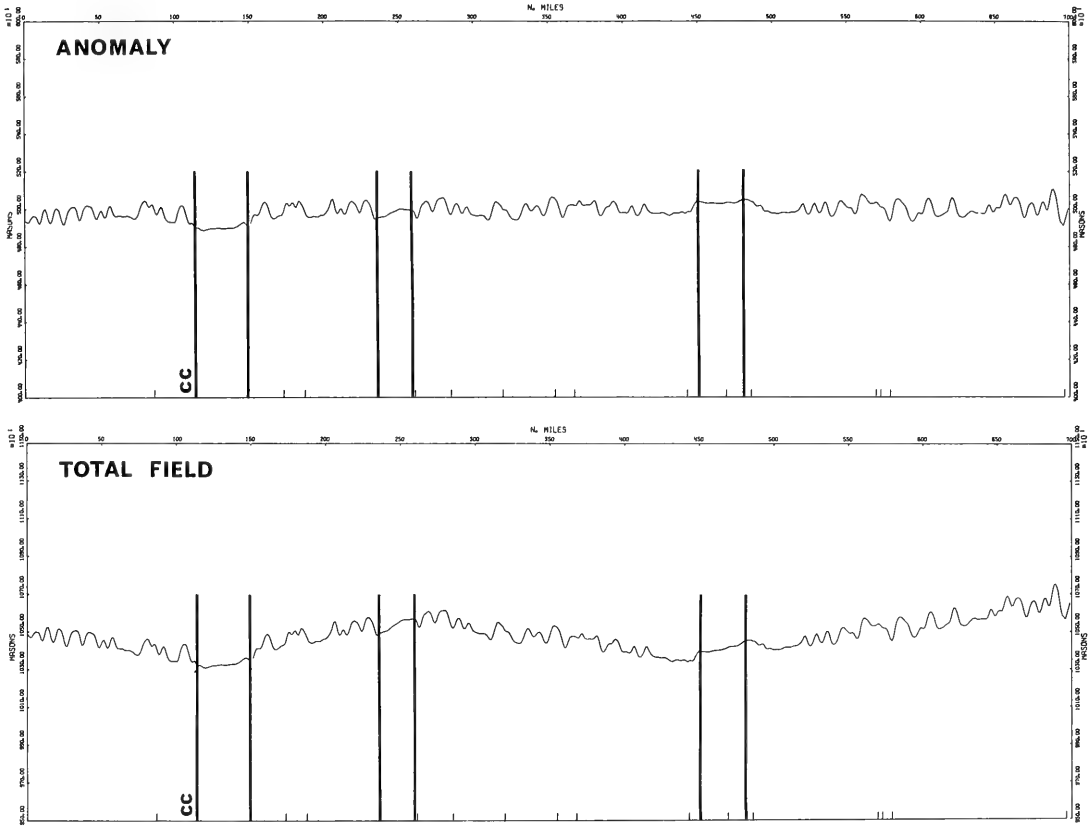

Figure 4. Example of computer plot of magnetic profiles with and without the total field

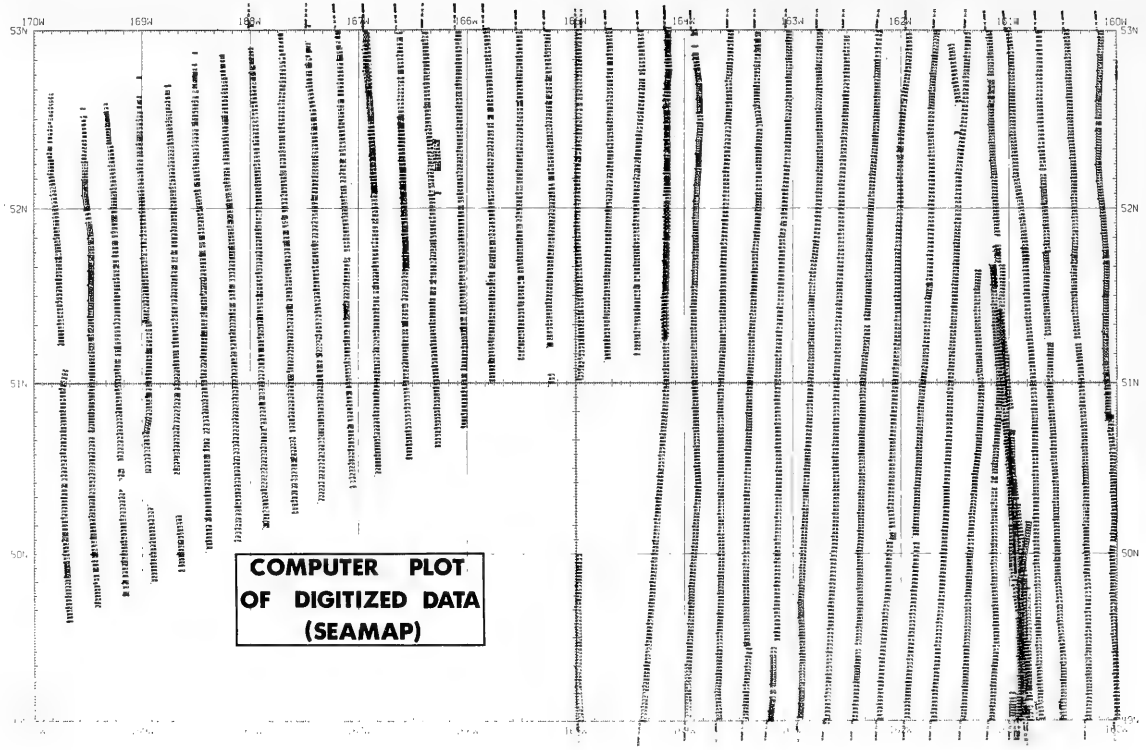

Figure 5. Computer plot of soundings at 1:1, 000, 000 scale. Data is from ESSA's SEAMAP cruises in North Pacific

A TECHNIQUE FOR GRAPHIC PRESENTATION OF WATER LEVEL FORECASTS USING A TOPOGRAPHIC CONTOUR CHART FORMAT

Don Burns, Dennis Clark and Pat Martin
Oceanographers
U. S. Naval Oceanographic Office
Washington, D. C. 20390

ABSTRACT: A contoured graphic format has been adapted for the presentation of water-level forecasts such that heights for any time can easily be read from monthly charts for each station. An entire year's forecast can be generated by an on-line plotter in 50 minutes. The charts will be useful in day-to-day and long-range planning of naval operations in tidal waters.

INTRODUCTION

During 1968, the Coastal Oceanography Branch, NAVOCEANO, provided COMNAVFORV with limited water-level forecasts for Nha Be, RVN. The forecasts were presented in tabular form similar to standard "tide tables" and were evaluated informally by the NAVOCEANO representative, NRDU-V (Naval Research and Development Unit, Vietnam) (Figure 1, Coast and Geodetic Survey, 1969). The tabular format was especially difficult to use in conjunction with other data such as moonrise and moonset for nighttime operational planning. Based upon this in-field evaluation, it was decided to change the format, if possible, from a tabular to a contoured display (Suthons, 1959). A graphic, chart type format is considered to have an advantage over tabular listings because a chart presents a complete picture of water-level fluctuations for an entire month and can be rapidly interpreted by visual inspection (O'Conner, 1964).

A prediction program (Pore and Cummings, 1967) is now operational and is run on a high-speed digital computer, including the contouring of the data with an on-line plotter (Branstetter, 1966). Machine contouring insures that the

interpretation and drawing of all contour lines will be unbiased for all charts. For the purpose of this report, machine plots were traced for better reproduction and readability. Each month requires about four minutes of plotter time or about fifty minutes per location per year.

DISCUSSION

This graphic display of water level data can be described as a plan view of monthly water level fluctuations contoured in time-space. Consider the common portrayal of water-level fluctuations in graphic form where height is usually taken as the ordinate and time forms the absicca. A simple water-level curve so constructed might look something like a sine curve (Figure 2).

If sequential daily water level curves are placed adjacent to one another in three dimensions so that the zero hour for each falls along a third axis, then that third axis represents day numbers. The three dimensions of this coordinate system are then hours, days and height. The adjacent daily water-level fluctuations now form a surface (Figure 3). This surface represents the time variations in water level, and we need only to find a useful way of looking at the surface. Lines drawn through points of equal height are contours of water level and may be interpreted in plan view (Figure 4).

The water level for any time throughout the month can be found by linear interpolation of either the hour scale or between contours. Detailed examples are presented in Appendix A. Interpolation between days is not meaningful. A regular trend in water levels is apparent and reflects the difference between the lunar and solar days. Since tides more closely follow the moon, a lag of about one hour per day in similar water levels is observed.

As an example of the utility of this display, note how quickly the highest and lowest water levels for a month can be found and their date and time determined. Similarly, the natural technique of visual comparison allows easy detection of sustained high or low water levels by locating relatively widely spaced contours along the day lines.

Since the charts represent monthly time histories of water level fluctuations, important natural parameters affecting operations may be shown on the contour charts. For example, hours of darkness may be shaded in according to sunrise and sunset tables (Figure 5). An operation requiring a combination of minimum visible light and maximum water depth can be scheduled by examining the monthly chart for periods of dark hours and times of extended high water (Figure 6).

Field use of water level predictions might be enhanced by providing booklets with monthly predictions contoured for a full year for stations of interest. Contoured water level predictions could be printed in fluorescent inks for increased visual security in nighttime operations.

CONCLUSIONS

Response to a field need has led to an improved format for presentation of water-level predictions. Contoured water-level predictions are useful in operational planning and should permit wider use of water level predictions in the field. It should be remembered that the display technique is only as accurate as the hourly predictions on which it is based.

REFERENCES

Branstetter, E. C., 1966, Contour, A Fortran Subroutine for Producing Contour Maps, Oak Ridge National Laboratory, Contract No. W-7405-eng-26.

O'Conner, Paul, 1964, Short-Term Sea-Level Anomalies at Monterey, California, U.S.N. Postgraduate School Thesis.

Pore, N. A. and R. A. Cummings, 1967, A Fortran Program for the Calculation of Hourly Values of Astronomical Tide and Time and Height of High and Low Water, Technical Memorandum WBTM. TDL-6, U. S. Department of Commerce/Environmental Science Services Administration.

Suthons, Commander C. T., R. N. (Ret.), 1959, The Admirality Semi-Graphic Method of Harmonic Tidal Analysis (over a period of one month), Admirality Tidal Handbook No. 1, H.D. 505.

U. S. Coast and Geodetic Survey, 1969, Tide Tables, High and Low Water Predictions, Central and Western Pacific Ocean and Indian Ocean.

APRIL						MAY						JUNE					
DAY	TIME H.M.	HT. FT.	DAY	TIME H.M.	HT. FT.	DAY	TIME H.M.	HT. FT.	DAY	TIME H.M.	HT. FT.	DAY	TIME H.M.	HT. FT.	DAY	TIME H.M.	HT. FT.
1	0113	10.5	16	0224	11.6	1	0200	11.2	16	0316	11.3	1	0344	11.6	16	0444	10.7
TU	0758	3.8	W	0840	4.6	TH	0804	5.2	F	0846	6.9	SU	0856	7.7	M	0928	8.4
	1424	11.3		1433	11.5		1346	11.6		1356	11.5		1349	12.1		1358	11.0
	2027	5.9		2056	3.3		2024	2.8		2103	1.1		2117	-0.8		2146	0.2
2	0203	11.3	17	0314	12.0	2	0249	11.8	17	0401	11.5	2	0437	11.8	17	0522	10.7
W	0838	3.8	TH	0914	5.2	F	0844	5.7	SA	0917	7.4	M	0938	8.2	TU	1001	8.4
	1445	11.6		1453	11.6		1409	12.0		1417	11.5		1423	12.3		1426	10.8
	2054	4.8		2128	2.5		2058	1.5		2135	0.7		2159	-1.3		2217	0.3
3	0250	12.0	18	0359	12.1	3	0337	12.3	18	0442	11.3	3	0532	11.6	18	0601	10.7
TH	0913	4.1	F	0946	5.9	SA	0921	6.4	SU	0947	7.9	TU	1019	8.7	W	1037	8.5
	1506	11.8		1512	11.6		1435	12.1		1438	11.5		1457	12.1		1453	10.7
	2124	3.6		2159	1.8		2135	0.5		2206	0.7		2243	-1.0		2251	0.8
4	0335	12.5	19	0442	11.8	4	0427	12.3	19	0524	11.2	4	0631	11.5	19	0638	10.5
F	0948	4.6	SA	1013	6.7	SU	0957	7.1	M	1015	8.2	W	1105	8.9	TH	1115	8.5
	1527	12.0		1530	11.6		1500	12.3		1456	11.3		1535	11.6		1525	10.3
	2157	2.5		2231	1.6		2212	-0.2		2237	0.8		2329	-0.3		2326	1.3
5	0422	12.5	20	0525	11.5	5	0521	12.1	20	0610	10.8	5	0730	11.2	20	0714	10.5
SA	1021	5.4	SU	1041	7.4	M	1033	7.9	TU	1046	8.7	TH	1202	9.0	F	1202	8.4
	1549	12.1		1545	11.6		1527	12.3		1515	11.2		1616	11.0		1602	9.8
	2233	1.8		2302	1.6		2254	-0.2		2309	1.3						
6	0513	12.3	21	0612	11.0	6	0623	11.6	21	0658	10.7	6	0019	0.7	21	0003	2.0
SU	1054	6.6	M	1106	8.0	TU	1110	8.7	W	1119	9.0	F	0826	11.0	SA	0751	10.3
	1611	12.1		1559	11.5		1554	12.1		1535	10.8		1313	8.7		1257	8.0
	2312	1.3		2336	2.0		2340	0.2		2344	1.8		1711	10.0		1650	9.4
7	0611	11.6	22	0704	10.5	7	0734	11.2	22	0751	10.3	7	0114	2.0	22	0046	2.8
M	1128	7.7	TU	1133	8.7	W	1156	9.4	TH	1204	9.2	SA	0920	10.8	SU	0825	10.3
	1634	12.1		1612	11.2		1623	11.6		1556	10.5		1439	8.0		1358	7.4
	2356	1.3											1851	9.0		1804	8.7

Figure 1. "Tide Tables" the Standard Digital Presentation of Tide Predictions as Times and Heights of High and Low Waters

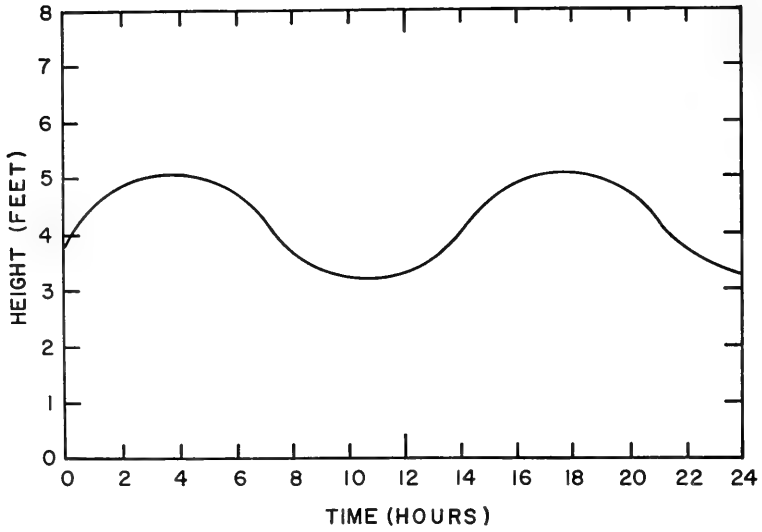

Figure 2. Time Series Water Level Information for One Day

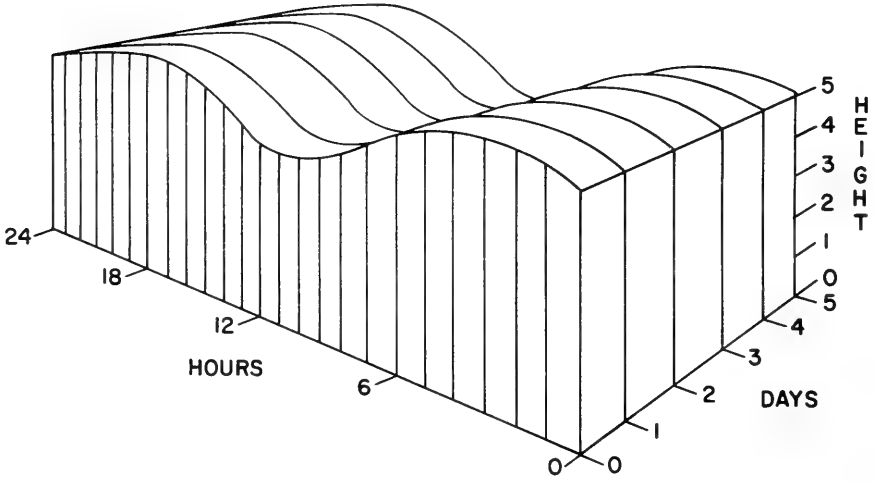

Figure 3. Adjacent Daily Water Levels Form a Surface in "Time Space"

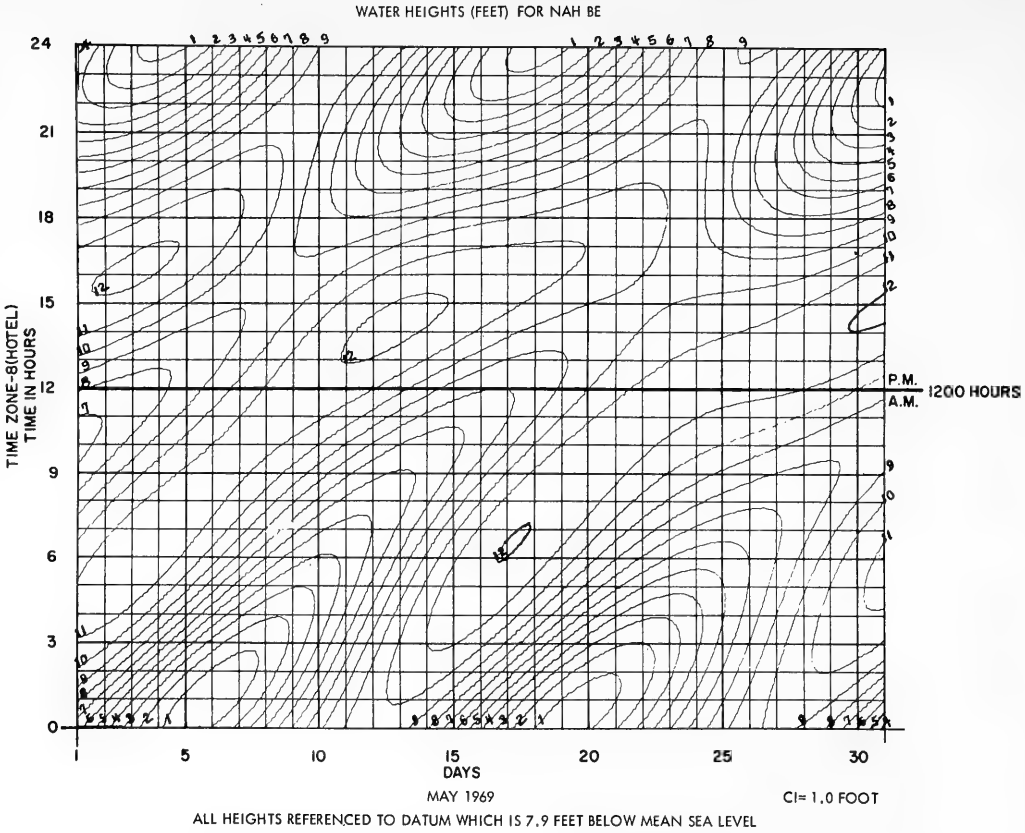

Figure 4. Plan View of Monthly Water Level Surface with Heights Contoured

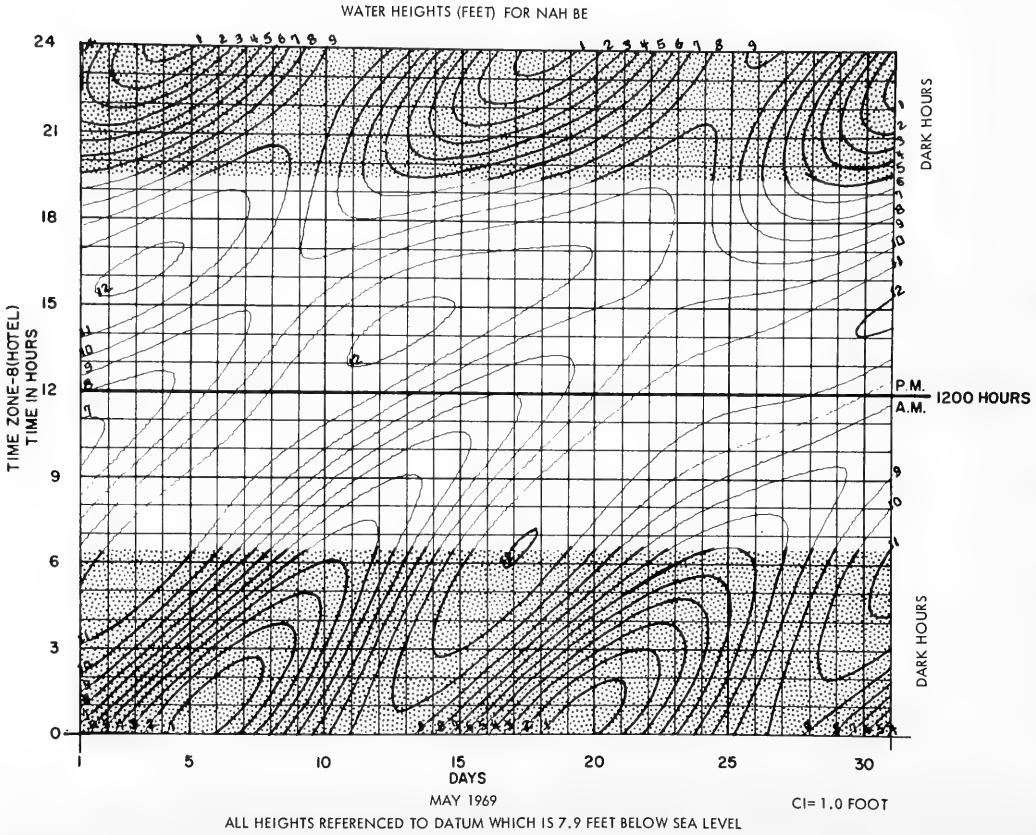

Figure 5. Dark Hours Represented on Monthly Water Level Chart

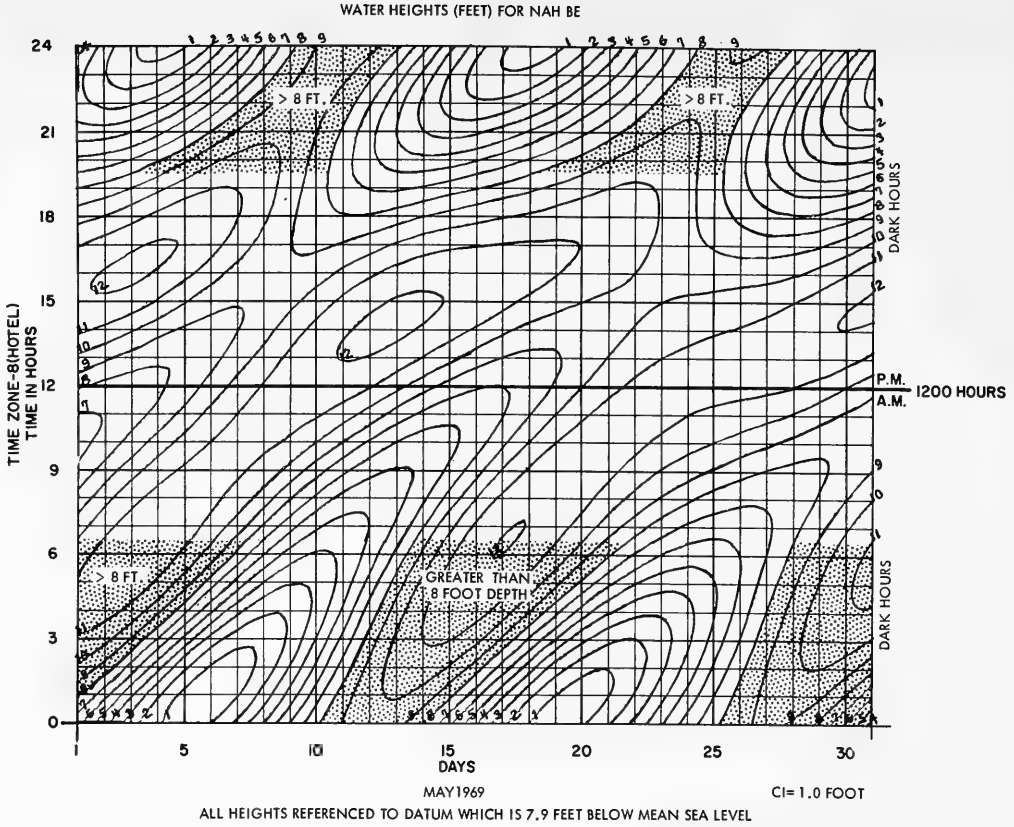

Figure 6. All Monthly Water Levels Greater than Eight Feet that Occur During Dark Hours

APPENDIX A

EXPLANATION OF USE OF WATER-LEVEL CONTOUR CHART

Figure A-1 contains predicted hourly water-level heights for this station for July 1969. When these values are added to the chart depth for this station (or near this station), the total water depth for any time will be known.

a. To find the total water depth at or near this station during any hour of July 1969, proceed as follows:

1. From appropriate chart determine charted depth in feet. This value is the depth below datum (depth below zero of Figure A-1).

2. From Figure A-1 read the additional height due to tide and discharge at the intersection of the hour and day lines; interpolate between time or height lines as necessary.

3. Add values obtained in (1) and (2) above to obtain correct water depth. If the value from (2) above is negative (-), subtract this amount from (1).

4. *Example: What additional heights should be added to charted depth for the following times during July; problems (a) through (c)?

   a. Hour 06, day 5

   b. Hour 19, day 12

   c. Hour 0930, day 21

   Solution: Find intersection of hour and day lines for examples (a) and (b). Read answers (1) + 9.0 feet; (2) +4.0 feet.

*All five lettered problems are shown on Figure A-1 by a small circle and sample letter. If the same number appears more than once, it is being used to indicate a time period.

For example, (c) interpolates halfway between 0900 and 1000. Read up day 21 to this point and note that the value lies between two 11 contour lines, but less than 12. Read answer as +11.

b. Other uses of chart

1. Boat clearances under low bridges.

Example: boat passing under bridge.

Problem (d): A small craft is passing under a low bridge, at or near this station, at 0400 on 21 July. The boat captain visually estimates his vertical clearance between bottom of bridge and top of craft as 3 feet. During what hours of the day will the craft not be able to pass back under the bridge?

Solution: At the intersection of the 4-hour line and 21-day line read height as +6 feet. Add vertical clearance (+3 feet) to this value giving +9 feet. This means that any time during the day when the height is +9 or more the craft will not be able to go under the bridge. The dashed arrows point towards the times when passage under the bridge would be restricted. These times are:

Day	Hours
21	0600-1230
	1815-2245

Example: Boat waiting to pass under bridge.

Problem (e): A small craft is unable to pass under a low bridge because of insufficient vertical clearance, at or near this station, at 0800, 13 July. The boat captain visually estimates he needs 3 feet less water to clear bridge. How long must he wait?

Solution: At the intersection of the 8-hour lines and 13-day line read height as +10.5 feet. The water must fall 3 feet or to +7.5 feet before craft can

clear bridge. The two solid arrows point towards the times during which the craft cannot pass. Earliest passage would be at time 1730.

2. Boat movements in shallow streams or canals near this station.

   Maximum use of shallow waterways at or near this station depends upon maximum water depth available. Times of these occurrences may be determined by examining the monthly water-level chart and noting times of extended minimum and maximum heights.

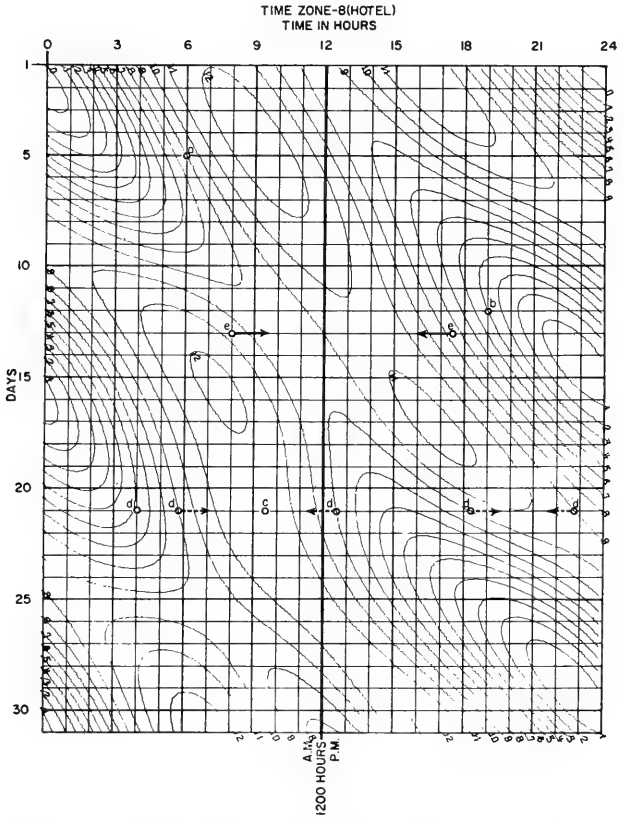

Figure A-1. Example of Hourly Water Level Contour Chart

POTENTIAL IMPACT OF SATELLITE DATA ON SEA SURFACE TEMPERATURE ANALYSIS

John C. Wilkerson
Project Manager

&

Dr. Vincent E. Noble
Project Physicist
Airborne Remote Sensing Oceanography Project
Naval Oceanographic Office
Washington, D. C. 20390

ABSTRACT

The sea surface temperature field of a 10 x 20 degree area of the North Atlantic is constructed from synoptic temperatures of the ocean surface obtained from High Resolution Infrared Radiometer (HRIR) data from NIMBUS II meteorological satellite. The computer analysis of these satellite data is compared with the computer analysis of three and one half days of conventional ship data produced for the same time period by the Fleet Numerical Weather Central (FNWC), Monterey, California, with a manual analysis of the same ship data prepared by the Fleet Weather Central, Norfolk, Virginia, and with an experimental numerical analysis done by NAVOCEANO. Significant features in the surface temperature field, as revealed by the satellite data and confirmed by independent ship and aircraft observations, are absent in the analysis of the conventional ship data. The HRIR radiation temperature data are biased 2.4°C warmer than the "ground truth" Airborne Radiation Thermometer (ART) data, with a residual mean absolute error of 2.0°C. The magnitude of the sea surface temperature gradients associated with the Gulf Stream boundary range from a maximum of 6°C/600 meters from the analog ART data, to 5°C/11 kilometers from the digitized HRIR data, to 4°C/110 kilometers from the FNWC ZOOM analysis. The differences between these analyses provide a measure of sea surface temperature analysis improvement potentially available through the increased synoptic data coverage afforded by satellite.

INTRODUCTION

A study is now in progress by industry under a contract with the Naval Oceanographic Office (NAVOCEANO) to determine the impact of an improved environmental prediction capability, afforded by a satellite data collection system, upon naval mission effectiveness. As the first step of this study, a particular case of sea surface temperature (SST) measurements obtained from the National Aeronautics and Space Administration's (NASA) NIMBUS II meteorological satellite has been compared with independent surface data and with SST analysis products to assess the capability of current satellite data for characterization of the true sea surface temperature structure.

Synoptic measurements of the SST field of a 10 x 20 degree area of the North Atlantic by Airborne Radiation Thermometer (ART) and shipboard bathythermographs (BT's) have been used to provide ground truth for the interpretation of NIMBUS II High Resolution Infrared Radiometer (HRIR) radiation temperature observations. The composite SST field, derived from HRIR, ART, and BT data, is used as a basis of comparison with SST analysis products to determine data base requirements for adequate characterization of sea surface temperature patterns for the Gulf Stream area for 22 June 1966.

The SST analysis products were derived from standard ship observations by the Fleet Numerical Weather Central (FNWC), Monterey, (using a ZOOM analysis program), the Fleet Weather Central (FWC), Norfolk, (using a numerical technique) and by the Anti-Submarine Warfare Environmental Prediction Services (ASWEPS), NAVOCEANO, (using a large-scale numerical technique). The comparison data base was independent data from ASWEPS ART flights, a Gulf Stream tracking cruise conducted by the Environmental Science Services Administration (ESSA) aboard the USCGSS WHITING, and HRIR data from NIMBUS II.

GULF STREAM GROUND TRUTH DATA

Gulf Stream ground truth data were provided by ASWEPS ART flights of 21 and 23 June 1966 and the ESSA ship surveys of 15-21 June 1966. The flights were designed to map the sea surface temperature patterns in the Gulf Stream area and to delineate the Gulf Stream boundary. The cruise of the WHITING, 15-21 June 1966, mapped the Gulf Stream boundary by tracking the 15° isotherm at 200-meter depth with BT casts taken at 15-minute intervals, after the technique of Fuglister and Voorhis (1965). Figure 1 depicts the Gulf Stream boundary defined by the ship cruise of 15-21 June 1966 and the ASWEPS flight tracks of 21 and 23 June 1966.

NIMBUS II HRIR DATA

Figure 2 is an analog display of the NIMBUS II HRIR data from day and night orbits of 22 June 1966. Local times were approximately 0100 and 1300. The data were obtained on orbits 504 and 509/510 (composite). Both the day and night coverage show a bright cloud bank lying just to the east of the Gulf Stream boundary. The warm edge of the Gulf Stream water indicated by arrows appears as the dark feature at the western edge of the cloud bank. The western protrusion of the meander of the Stream as shown in the ship survey in Figure 1 can be seen in the central portion of both displays. The colder Slope Water appears as a grey scale intermediate between the warm Gulf Stream water and the cold cloud bank.

For analysis, the HRIR data were digitized and rectified for display at a scale of 1 : 1,000,000. The data were filtered to remove system noise, and the basic 8km x 9km resolution elements were combined to provide radiation temperature data points in a 10 x 8 grid within each 1° latitude-longitude square. The radiation temperature data from the grid-print map were manually contoured for surface temperature values. The SST analysis from the HRIR data is depicted in Figure 3.

Five ranges of radiation temperature are indicated in Figure 3. Within the Gulf Stream/Slope Water mass bounded by the east coast and the cloud bank, radiation temperatures between 18°C and 22°C are unshaded, temperatures between 22°C and 24°C are light shaded; the Gulf Stream boundary (24°C to 27°C) is unshaded, and two darker shades of grey are used for the 27°C to 31°C and the 31°C to 33°C. All of the unshaded areas within the less than 24°C water mass of the Slope Water are 22°C.

CALIBRATION OF NIMBUS II HRIR DATA

Figure 4 shows that portion of the Gulf Stream boundary defined by ship observations of 15-18 June 1966 and the sea surface temperatures contoured from the ART flight of 21 June 1966 that were used to calibrate the NIMBUS II HRIR data of 22 June 1966. Sea surface temperatures from the ship track and the ART data were compared with the respective HRIR grid-point data to determine an average bias between the radiation temperatures and the ground-truth data, and mean absolute errors were computed between the radiation temperatures and the ship and aircraft data. Because of the geographical uncertainty of the location of the NIMBUS II HRIR scan elements (up to 1° of latitude and longitude according to the NIMBUS II USER'S GUIDE) and of the time lapse between the ship observations and the data orbit, both the ship track and the aircraft flight track were shifted slightly to obtain the best agreement with the

radiometric determination of the Gulf Stream boundary. The ship data were shifted 1/2° westward, and the aircraft data were shifted 1° westward with respect to the HRIR coordinates to obtain the best fit of the data. The marked agreement between the ship data and the HRIR data demonstrate the persistence of this major Gulf Stream pattern over a period of several days.

Table 1 presents the results of the comparison of the ship and aircraft data with the NIMBUS II radiation temperature data. Surface temperature data from 64 BT casts, taken between 15 and 18 June 1966, were compared with the corresponding satellite grid-point data. Comparison of the average temperature values from the two sets of data showed that the satellite radiation temperatures were biased 3.6°C higher than the ship surface temperature data. Upon removal of the 3.6°C bias from the satellite data, there remained a mean absolute error of 1.5°C between the ship and the aircraft data.

Comparison of the satellite and the aircraft data showed the satellite data to be biased 2.4°C higher than the aircraft data. Removal of the bias from the satellite data results in a mean absolute error of 2.0°C between the satellite and aircraft data. One hundred and thirty-four one-minute (3nm) averages of the ART record were compared with the corresponding grid-point data values.

The primary sources of bias and mean absolute errors between the satellite radiation temperatures and the conventional sea surface temperatures are instrumental noise, atmospheric absorptions, computer averaging of the resolution elements into the grid-point values, extraneous reflections of solar radiation into the radiometer windows, and field contamination by subresolution element clouds. The instrumental system errors in the satellite radiation temperatures have been discussed by Warnecke, McMillin, and Allison (1968). The problem of removal of subresolution element clouds is being addressed by Meteorology International, Inc., in cooperation with FNWC, Monterey, under contract from Project FAMOS (Fleet Applications for Meteorological Observations from Satellite).

SST FIELD FROM SATELLITE DATA

Table 2 presents the summary data comparing the corrected satellite temperature field measurements with the aircraft and ship ground-truth data. It is seen that, within the clear-sky portion of the NIMBUS scan, the satellite data provide an adequate characterization of the temperature structure of the Gulf Stream boundary and of the surrounding water masses. The temperature gradient across the boundary, as determined from the satellite data, is approximately 5°C/11 kilometers between 71°W and 75°W.

SST ANALYSIS PRODUCTS

Figures 5, 6, and 7 present the SST analysis products for 22 June 1966 as prepared by FNWC, FWC (Norfolk), and NAVOCEANO, respectively. The Gulf Stream boundary, as defined by the ship data during 15-21 June, is superimposed on each of the figures to provide a frame of reference. All of the analysis products are based upon the standard ship reports of sea surface temperature received during a 3 1/2- to 7-day interval preceding the analysis time of 1200Z, 22 June 1966.

The FNWC analysis is produced from two adjacent 10 x 10 degree latitude-longitude fields derived from ZOOM analyses of 63 x 63 point grids, using ship data received during a 3 1/2-day interval. The FWC analysis is a manual subjective analysis of the input data field. The NAVOCEANO analysis was done by a developmental, large-scale numerical technique, using 1180 standard ship observations received during a 7-day interval.

The sea surface temperature gradients associated with the Gulf Stream boundary are much weaker in the standard analysis products than those determined from the satellite data and confirmed by the ship and flight data. The limitation of the standard products lies in the data density in the input data field. The grid-point density of the FNWC analysis field (approximately 10-mile spacing) is very close to that of the satellite HRIR grid-print map (approximately 6-mile spacing). The major difference is that there are not data entries at each of the FNWC grid points as is the case for the clear-sky portions of the grid-print map. Table 3 presents a comparison of the SST gradients associated with the Gulf Stream boundary as determined from the satellite and the FNWC, FWC, and NAVOCEANO analyses.

PLANS FOR FUTURE WORK

This study has demonstrated the potential of utilization of satellite SST data for depiction of major features of the ocean surface temperature structure. As the problems of instrument noise, geographic position error, atmospheric absorption, and cloud contamination are addressed, significant quantities of HRIR SST data will become available as data input for SST analyses.

The next step in this investigation will be, with the cooperation of FNWC, Monterey, to submit the corrected digitized HRIR grid-print data as the input data field for FNWC analysis of the SST pattern for 22 June 1966. It is expected that this test will determine the capability of the FNWC analysis program for characterization of the true SST field when provided with a dense input of satellite data.

REFERENCES

Fuglister, F. C. and A. D. Voorhis (1965). A New Method of Tracking the Gulf Stream, Limnology and Oceanography, 10 (Supplement: Readfield Anniversary Volume).

Warnecke, G., L. McMillin, and L. Allison (1968). Ocean Current and Sea Surface Temperature Observations from Meteorological Satellites, NASA Technical Report R-291.

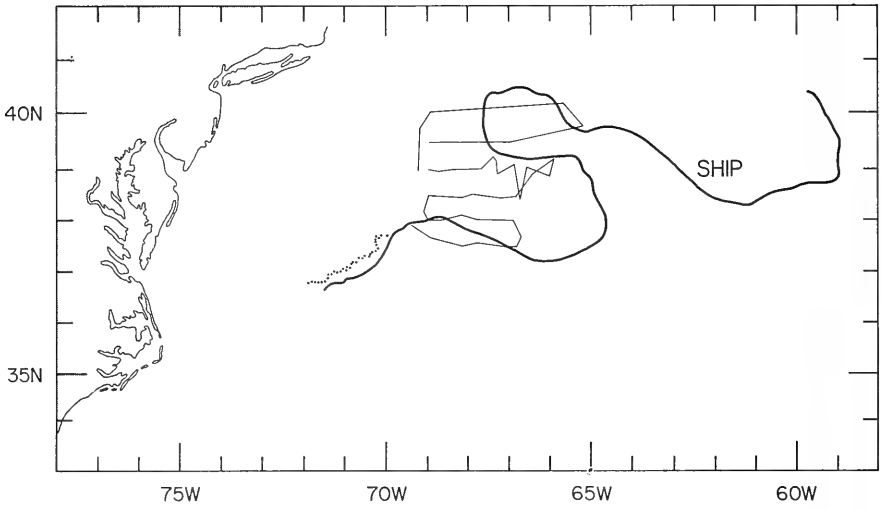

Figure 1

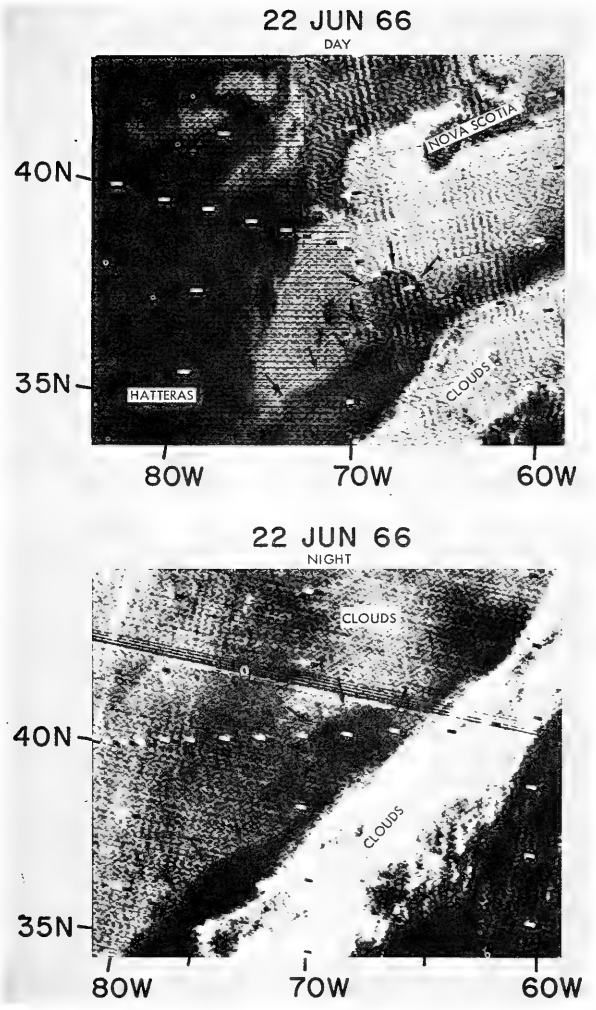
22 JUN 66
DAY
NOVA SCOTIA
40N
35N
HATTERAS
CLOUDS
80W
70W
60W
22 JUN 66
NIGHT
CLOUDS
40N
CLOUDS
35N
80W
70W
60W

FIGURE 2

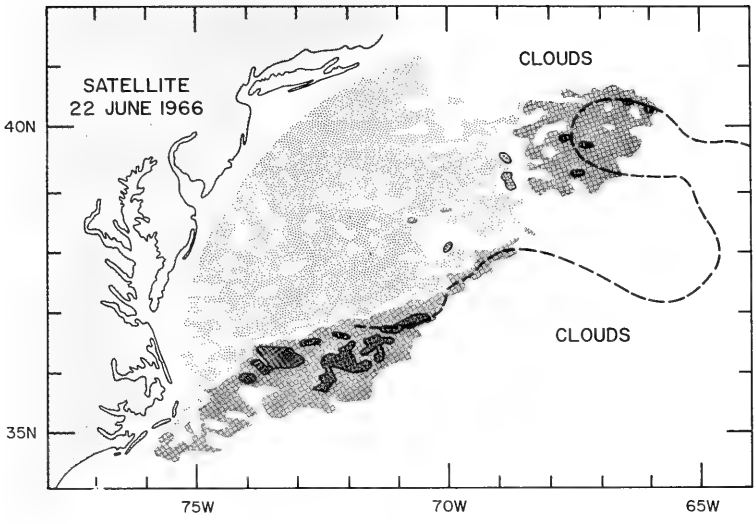

Figure 3.

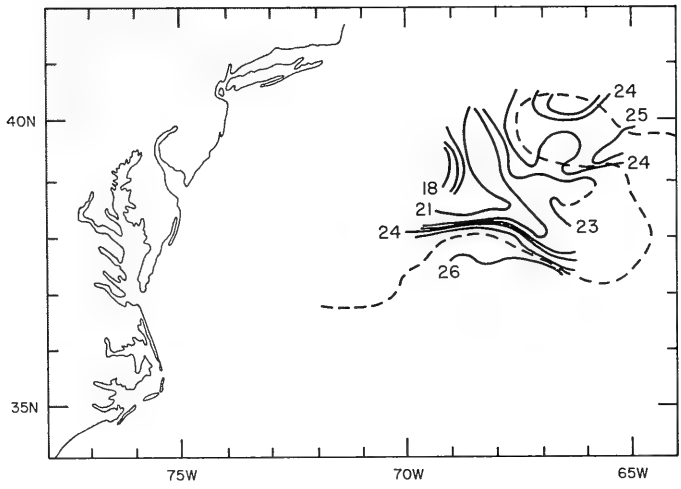

Figure 4.

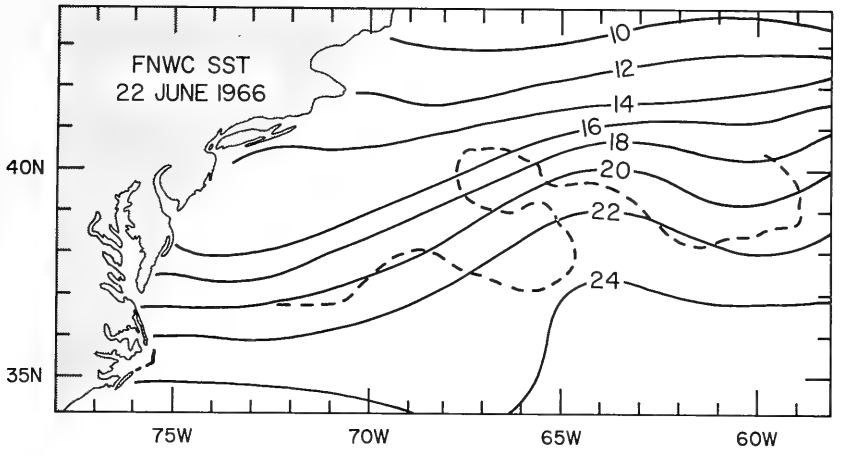

Figure 5.

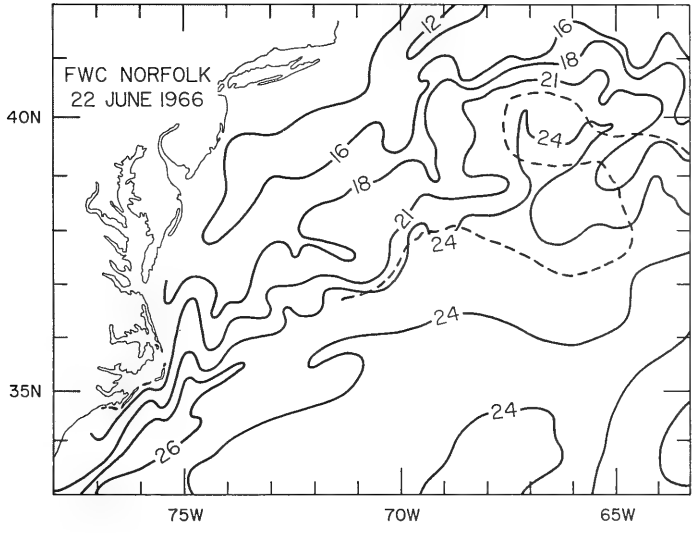

Figure 6.

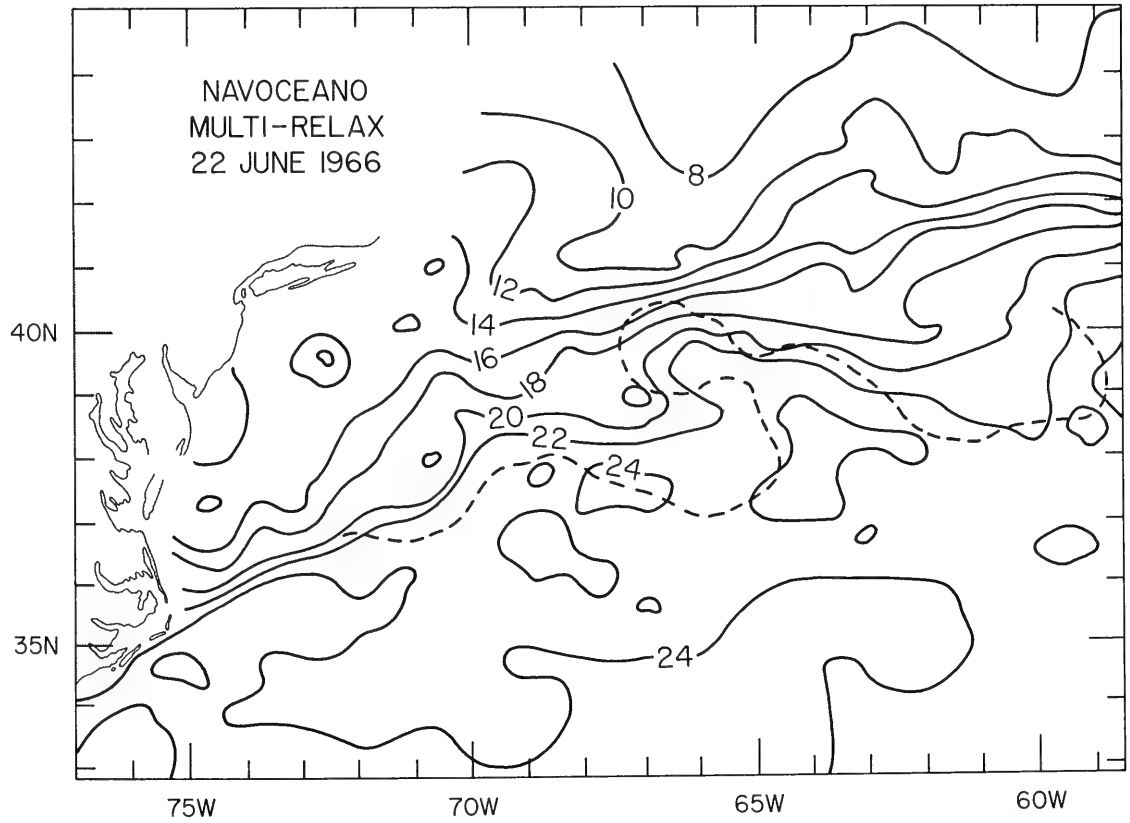
NAVOCEANO
MULTI-RELAX
22 JUNE 1966
8
10
12
14
16
18
20
22
24
24
40N
35N
75W
70W
65W
60W

FIGURE 7

TABLE 1

COMPARISON OF SHIP AND AIRCRAFT SST WITH NIMBUS II HRIR DATA, 22 JUNE 1966

Ship vs HRIR, 15-18 June 1966
64 points

Avg. Temp., Ship Data	23.5°C	Avg. Temp., ART Data	22.8°C
Avg. Temp., HRIR Data	27.1°C	Avg. Temp., HRIR Data	25.2°C
Temp. Bias	+ 3.6°C	Temp. Bias	2.4°C
Mean Absolute Error, Ship vs HRIR	3.94°C	Mean Absolute Error, ART vs HRIR	2.94°C
Mean Absolute Error, Ship vs HRIR (Bias subtracted from HRIR data)	1.5°C	Mean Absolute Error, ART vs HRIR (Bias subtracted from HRIR data)	2.0°C

TABLE 2

RANGE OF TEMPERATURE VALUES MEASURED ACROSS GULF STREAM

SLOPE WATER		
Dominant Temperature HRIR,	295°K - 297°K	(22°C - 24°C)
2.4°C Bias Removed		19.6°C - 21.6°C
ART Temperatures		18.1°C - 20.6°C
Ship SST		18°C
GULF STREAM BOUNDARY		
Radiation Temperature HRIR,	297°K - 300°K	(24°C - 27°C)
2.4°C Bias Removed		21.6°C - 24.6°C
ART Temperatures		20.1°C - 23.9°C
Ship SST		23°C - 24°C

TABLE 2 (continued)

GULF STREAM WATER

Radiation Temperature, HRIR, 2.4°C Bias Removed	300°K - 306°K	(27°C - 33°C) 24.6°C - 30.6°C
ART Temperatures		23.9°C - 26.4°C
Ship SST		25°C

TABLE 3

SST GRADIENT ASSOCIATED WITH GULF STREAM BOUNDARY

	ART	NIMBUS II HRIR	FNWC ZOOM ANALYSIS	FWC, NORFOLK	NAVOCEANO
1 min. avgs. - 21 June	3°C/4n.m. (.75°C/n.m.)	5°C/6n.m. (.85°C/n.m.)	4°C/60n.m. (.07°C/n.m.)	6°C/40n.m. (0.15°C/n.m.)	6°C/60n.m. (0.1°C/n.m.)
Max. gradient, Analog Trace 23 June	6°C/1/3n.m. (18°C/n.m.)				
	6°C/600m	5°C/11km	4°C/110km	6°C/70km	6°C/110km

TEMPERATURE FLUCTUATIONS ABOVE AN AIR-WATER INTERFACE

Noel E. J. Boston
Assistant Professor, Naval Postgraduate School

James R. Ramzy
Commander, United States Navy

Ernest T. Young, Jr.
Lieutenant Commander, United States Navy

Theodore Green, III
Assistant Professor, Naval Postgraduate School

ABSTRACT

Measurements of waves and temperature fluctuations as close as 2.5 cm. above the waves were made at a small lake in Seaside, California. Two fast response micro-bead thermistors were used. One was mounted on a styrofoam float and the other at a fixed height.

Data were collected on an Ampex CP-100 tape recorder using FM electronics at a tape speed of 1-7/8 ips.

The correlation between the fixed and float-mounted thermistor decreased as the height of the fixed thermistor increased. Larger temperature fluctuations were measured with the float-mounted thermistor than with the fixed thermistor. The temperature fluctuations measured by the fixed thermistor became smaller as its height was increased.

Signal analysis revealed only slight periodic components of temperature fluctuation associated with the wave action.

The large fluctuations measured by the float-mounted thermistor are believed to be caused by the vertical motion of the thermistor in a large vertical temperature gradient immediately above the sea surface. More detailed instrumentation is needed to confirm this hypothesis.

INTRODUCTION

The Department of Oceanography of the Naval Postgraduate School last year began studies in certain aspects of air/sea interaction. Specifically the studies are oriented towards achieving an understanding of the physical processes involving heat and momentum transfers very near, at, and just below the sea surface. The object of this research is to see if uninvolved parameterization of the temperature and velocity fields above and/or below the sea surface

can be made that will lead to better estimates of heat and momentum flux with a resultant improvement in the Naval environmental prediction programs.

Initial efforts have been towards building up an instrumentation capability in this field and testing sensor systems at an air-water interface. Because of the somewhat easier instrumentation problem, the temperature field has been first to be investigated. It also gives some information about the velocity field since the statistics of the near-passive, scalar temperature field can be expected to be similar in important ways to the statistics of the fluid-distorting velocity field.

This paper is a report of some of our first measurements of the temperature field over a wind-generated wave surface.

INSTRUMENTATION

The temperature measurements were made with micro-bead thermistors (VECO 41A401C) 0.005 in. in diameter. Their resistance at 25°C is 10,000 ohms. Their time constant in dry air was measured to be better than 0.1 sec. The thermistors were used as one arm of a DC operated Wheatstone bridge.

Waves were measured with a two-wire resistance wave gauge. The probe wires were Silbraze rods 1/16 of an inch in diameter and separated by 3/4 of an inch.

Mean wind speed was measured with a Casella cup anemometer. The data were collected on an Ampex CP 100 analog tape recorder at a speed of 1-7/8 ips using the FM record/reproduce system.

The sensors were mounted on a chassis made of pipe (Fig. 1). One thermistor was mounted on a styrofoam float shaped like a hemisphere. The float followed the vertical wave motion along a stretched wire through its center. A second thermistor was mounted on a steel rod at a fixed height.

The wave gauge was clamped to the frame so as to be as near as possible to the float and placed directly downstream of it.

The cup anemometer was bolted to the frame about 1 meter above the water surface.

FIELD PROGRAM

The measurements were made over Roberts Lake (Fig. 2) in Seaside, California. Roberts Lake is small - 1200 ft. long, 600 ft. wide and 6 ft. deep. However, it is convenient to the School, provides wind generated waves and illustrates some of the processes likely to be

encountered over large bodies of water. The measurement site was about 35 ft. from the shore in 4.5 ft. of water. Reeds along the shore absorbed incident waves. The wind fetch was about 200 ft. for each run analyzed. Data were collected at three wind speeds.

1. Calm to light winds to serve as a base condition with which to compare other measurements.

2. Light winds, 2 to 4 meters per second.

3. Moderate winds, 7 meters per second.

Unstable conditions existed, at least locally over the lake, for all runs up to the heights at which temperatures were measured. Conditions were most unstable for the calm case and became less unstable with increasing wind speed. Such conditions are not unusual at the time of the year (late October, early November) these measurements were made. Highest air temperatures occur in September and October and maximum insolation occurs in November.

RESULTS

1. Calm to light winds

The calm condition was interrupted at irregular intervals by gentle gusts with almost immediate small wave generation. Often appreciable temperature fluctuations accompanied the gusts. Temperature fluctuations in excess of $0.5^{o}C$ were observed with the float-mounted thermistor and occasionally (Fig. 3A) changes of $1^{o}C$ occurred in less than one second.

2. Light winds (October 30, 1968)

The mean wind speed during this run was 2.8 m/sec and the water temperature at a depth of 3 cm. was $17.7^{o}C$. The float-mounted thermistor was 2.5 cm. above the wave surface and the fixed thermistor 4.5 cm. above the highest wave crests and slightly behind the float-mounted thermistor. The significant wave height was about 4 cm.

The two most striking aspects observed were a.) the general agreement in the shape and phase of the two temperature records (Fig. 3B, Fig. 3C) and b.) the large temperature fluctuations measured by the float-mounted thermistor compared to those measured by the fixed thermistor. The magnitude of the temperature fluctuations is surprising. At one point there is a change of over $4^{o}C$ in less than a fifth of a second. Such fluctuations were not uncommon with the float-mounted thermistor but were not recorded by the fixed thermistor. A correlation between the temperature signals and the waves (Fig. 3D) is not obvious. At times there is a wave-like variation in the temperature signal such as at "A" and "B". But there are also sections

such as "C" and "D" where no apparent relation exists. And again there are sections such as "E" where there is a wave-like motion but double the frequency of the waves.

3. Moderate winds (November 12, 1968)

The results of this run confirm the impression of largest temperature fluctuations occurring near the wave surface.

For this run the wind was 6.6 m/sec; the water temperature at a depth of 6 cm. was 15.6°C and at 15 cm. was 15.7°C. The mean air temperature indicated by the float mounted thermistor was 12°C. It rode 3.5 cm. above the water surface.

The fixed thermistor was repositioned for the last half of this run. Initially it was 7 cm. above mean water level and indicated a mean temperature of 10.7°C. It was relocated 15.5 cm. above mean water level and registered a mean temperature of 10.3°C. These temperatures were checked in each case with a mercury thermometer.

Figure 4 shows a section for the latter part of the run with the fixed thermistor at 15.5 cm. Again the larger fluctuations are measured with the float-mounted rather than with the fixed thermistor but the general shape and phase agreement is not as strong as in run 2 though still present. The agreement was better, as might be expected, in the first half of this run. The comments made about wave-temperature signal agreement still stand.

These data suggest that there was a strong temperature gradient in the first few centimeters above the lake surface and possibly just below the lake surface. Reconstructing the data from the moderate wind run suggests the model shown in Figure 5. The closer the thermistor is to the surface, the larger the temperature gradient it is in and the larger the temperature fluctuations it will measure. The float-mounted thermistor measured the largest temperature fluctuations because it was being moved up and down in the temperature gradient by the waves. This being the case, one should expect a strong correlation between the temperature fluctuation and wave records which, as observations show, was not always present. The clue for the rather loose to zero correlation is given by the calm run. There are appreciable inhomogeneities in the air temperature which are advected past the sensors by the wind. Thus the temperature signal registered by the float-mounted thermistor is made up of the combination of advected temperature variations and temperature variations due to movement through the mean vertical temperature gradient.

From analyses made so far, wave and temperature fluctuation spectra provide inconclusive evidence regarding the validity of this model. There is a small peak in the October 30 (light winds) fixed-thermistor temperature spectrum exactly at the peak of the wave spectrum (Fig. 6).

Such a wave peak does not occur in either of the fixed-thermistor temperature spectra for the November 12 (moderate winds) data (Fig. 7). Only the temperature spectrum of the float-mounted thermistor data recorded during the first half of the November 12 run shows a peak at the frequency where the wave spectrum peaks (Table I).

The wave spectra are typical narrow-band wave spectra but are not completely analogous to ocean wave spectra. The wave energy contributing to the high frequency end of the wave spectrum is beginning to come from capillary waves.

In almost all cases there is at least a decade where the temperature fluctuation spectra follow the expected -5/3 power law. The fall-off from the -5/3 slope beyond 10 Hz is due to a combination of low pass filters and thermistor response.

CONCLUSIONS

These data indicate that there was a large temperature gradient near the lake surface and possibly just below the lake surface. Just how applicable these results are over the ocean remains to be seen, but certainly there are appreciable portions of the ocean where strong temperature gradients can exist: either cold air over warm water (such as was experienced in the Pacific Northwest in the winter of 1968) or warm air over cold water (such as off the California coast).

The heat flux is considered in general to be invariant with height. Heat flux estimates are often based on the wind velocity and air temperature at 10 m. and the sea surface temperature. This would appear to be insufficient since the heat flux according to these results is going to be determined in the first few centimeters above the surface. This being the case, any parameterization should include in some form the temperature gradient just above and just below the sea surface. The effect of waves on the transport of sensible heat would appear to be small.

The large temperature fluctuations were at first surprising. Extensive laboratory studies (Ramzy and Young, 1969) were made on the thermistors to test their response to velocity and humidity fluctuations and wetting. The linearity of the circuit was also rechecked. None of these features could account for the large fluctuations observed.

The data are being reworked so as to improve the spectra and clarify questions concerning the relation between the wave spectrum peak and the temperature spectra. Whether or not such a peak occurs in the spectrum derived from the fixed thermistor and how close it must be to the surface for the waves to influence its spectrum has some bearing on wave generation theories (Stewart, 1967).

ACKNOWLEDGMENTS

This research was supported by Naval Ordnance Systems Command Project ORDTASK ORD-03C-005/561-1/UR104-03-01.

REFERENCES

Ramzy, James R. and Ernest T. Young, Jr. (1968), "Investigations of Temperature Fluctuations near the Air-Sea Interface." Unpublished M.S. thesis, Naval Postgraduate School, Monterey, California, Dec. 1968.

Stewart, R. W. (1967), "Mechanics of the Air Sea Interface," Physics of Fluids, Supp.

TABLE 1

RUN	Sgn.Wave Ht. cm.	Ht.Float-Mount.Therm. above water sfc. cm.	Ht.Fixed Therm.above mean water level cm.	Wave peak in Temperature Spectrum	
				float	fixed
Calm	0	2.5	6.8	-	-
Light winds Oct.30/68	4	2.5	6.8	-	Yes
Moderate winds Nov.12/68	5	3.5	7.0	Yes	No
Moderate winds Nov.12/68	5	3.5	15.5	No	No

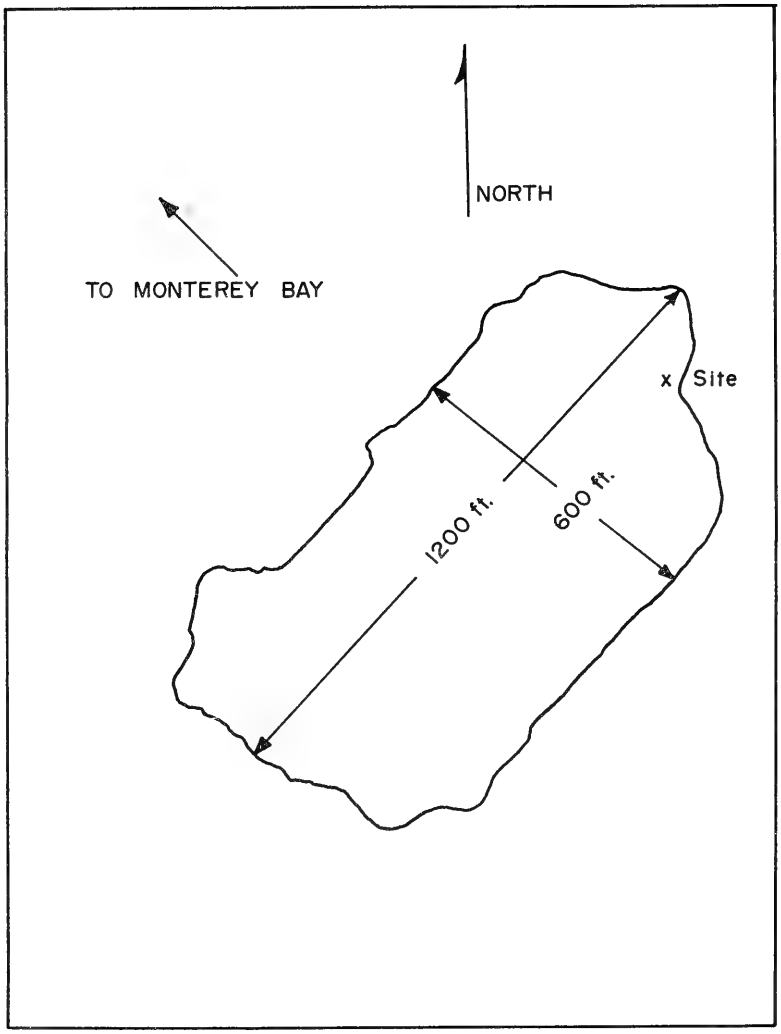

Figure 1. Roberts Lake

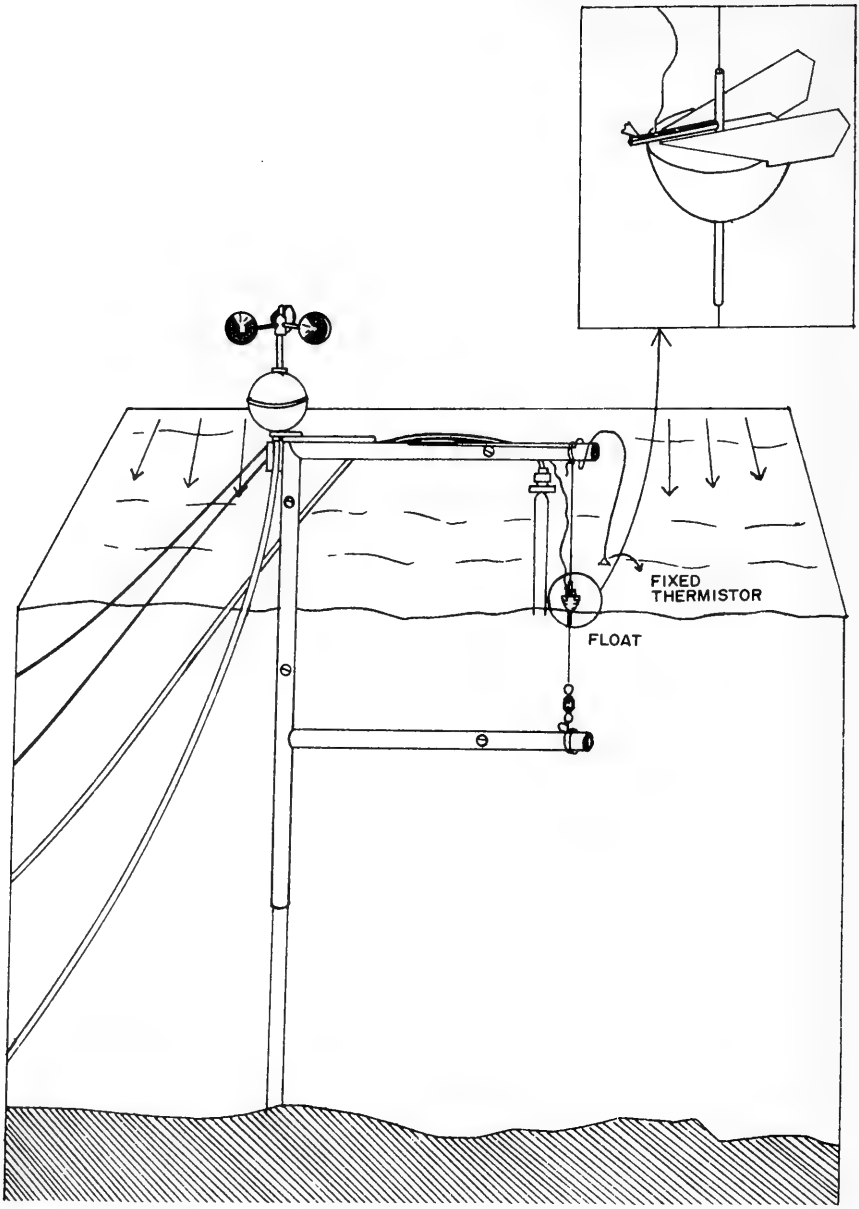

Figure 2. Arrangement of Sensors

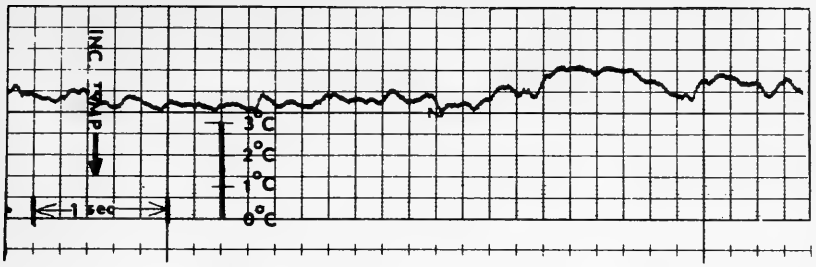

Figure 3A. Float-mounted Thermistor Record for Calm Conditions

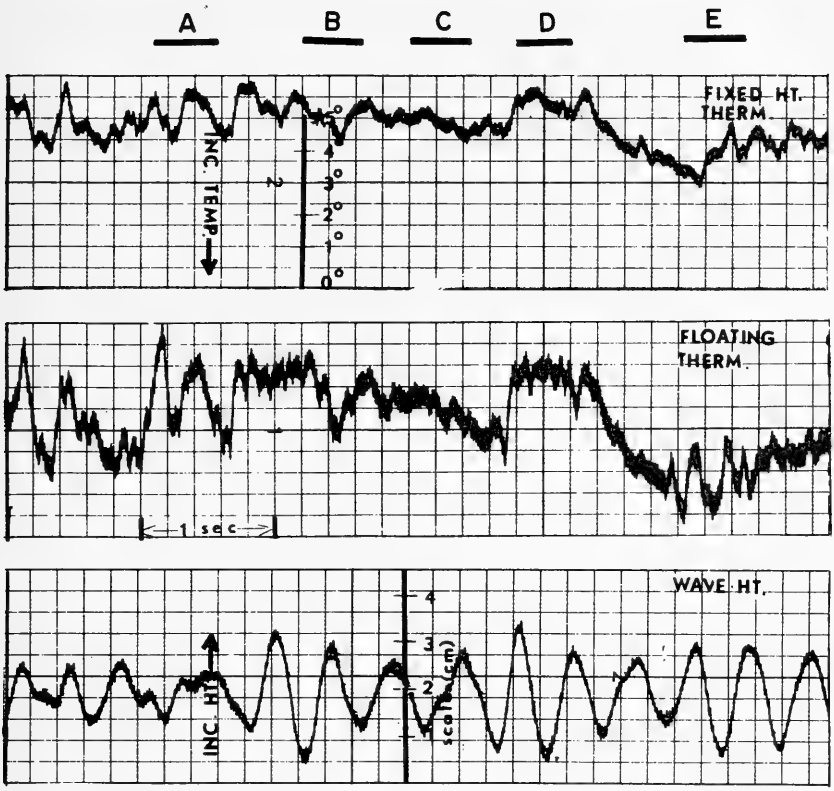

Figure 3B. Wave and Thermistor Records during Light Winds

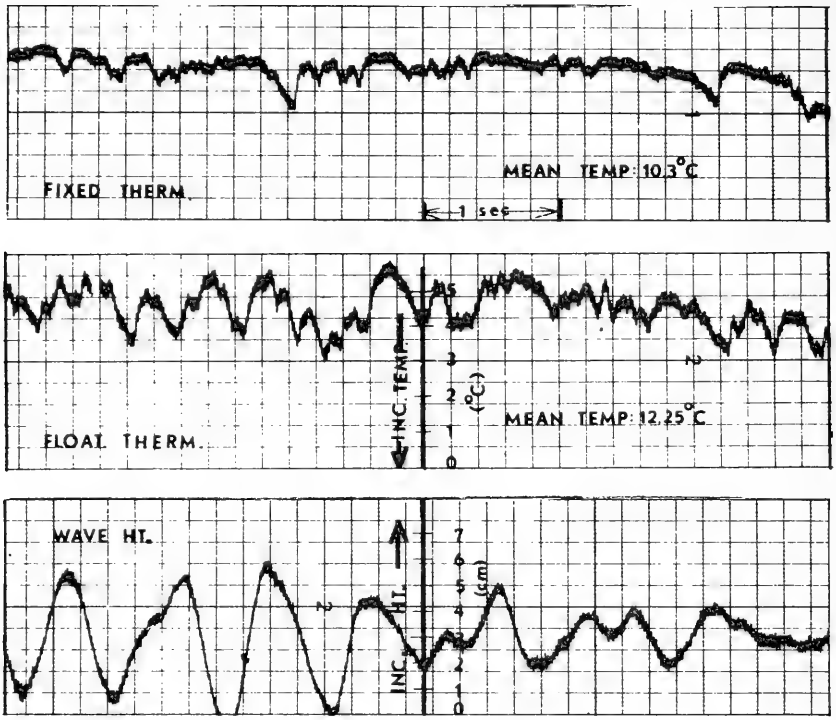

Figure 4. Wave and Thermistor Records during Moderate Winds

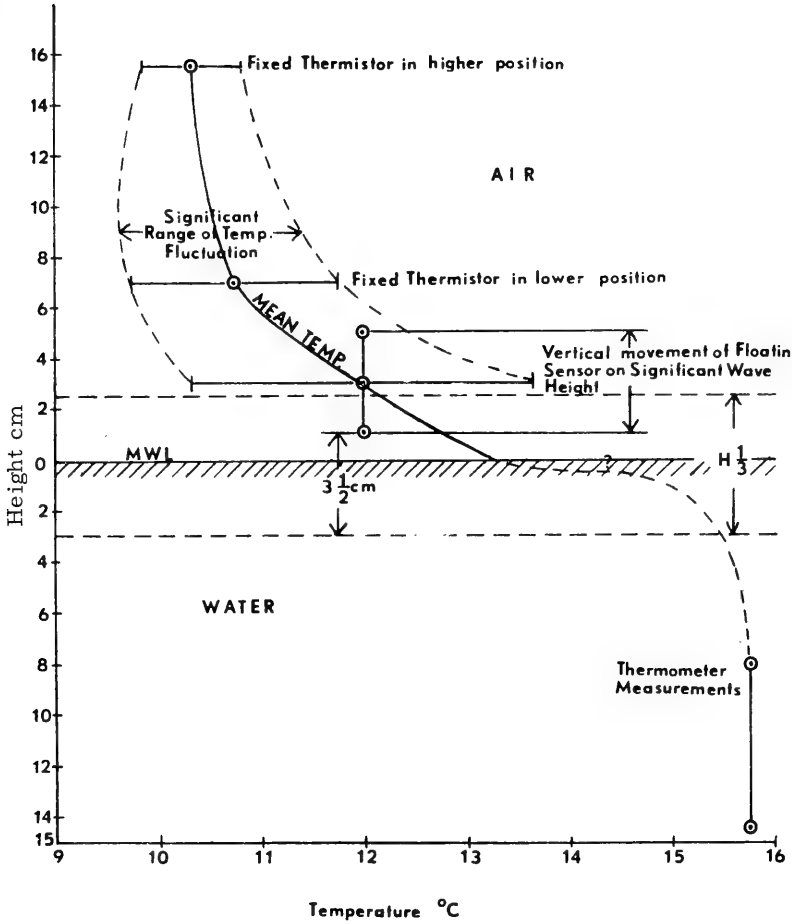

Figure 5. Temperature Profile Model

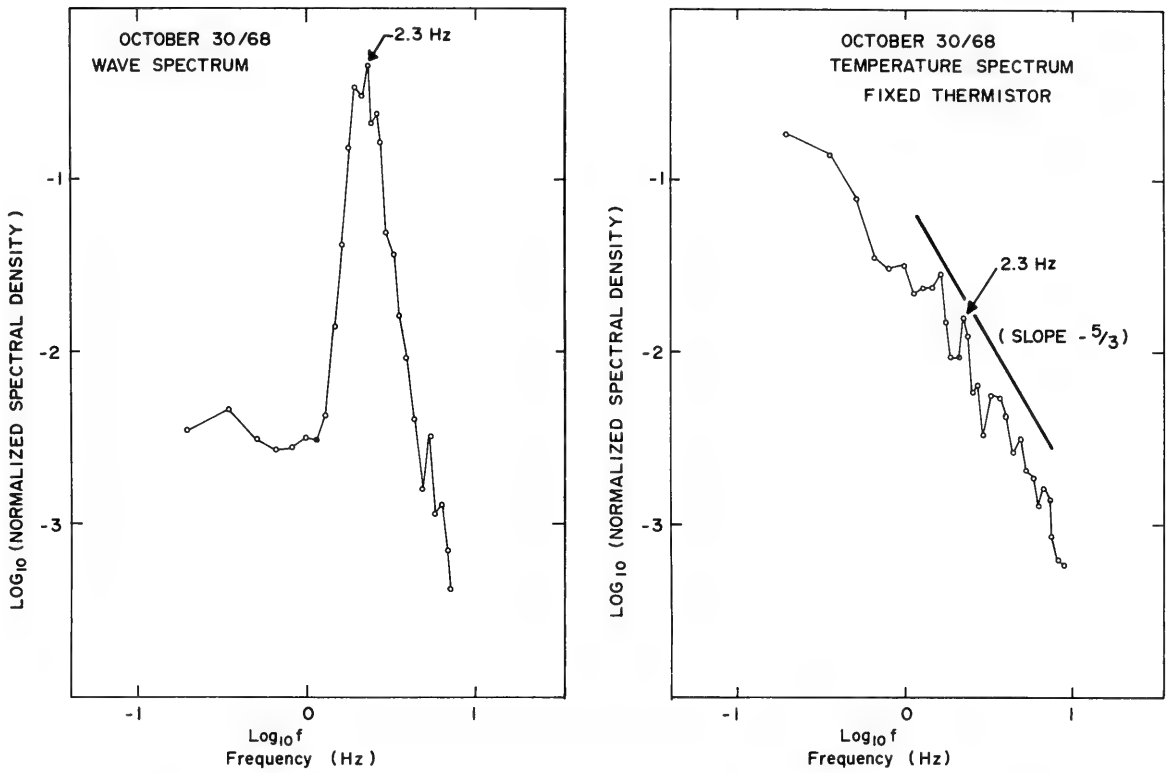

Figure 6. Wave and Fixed-Thermistor Spectra for Light Wind Condition

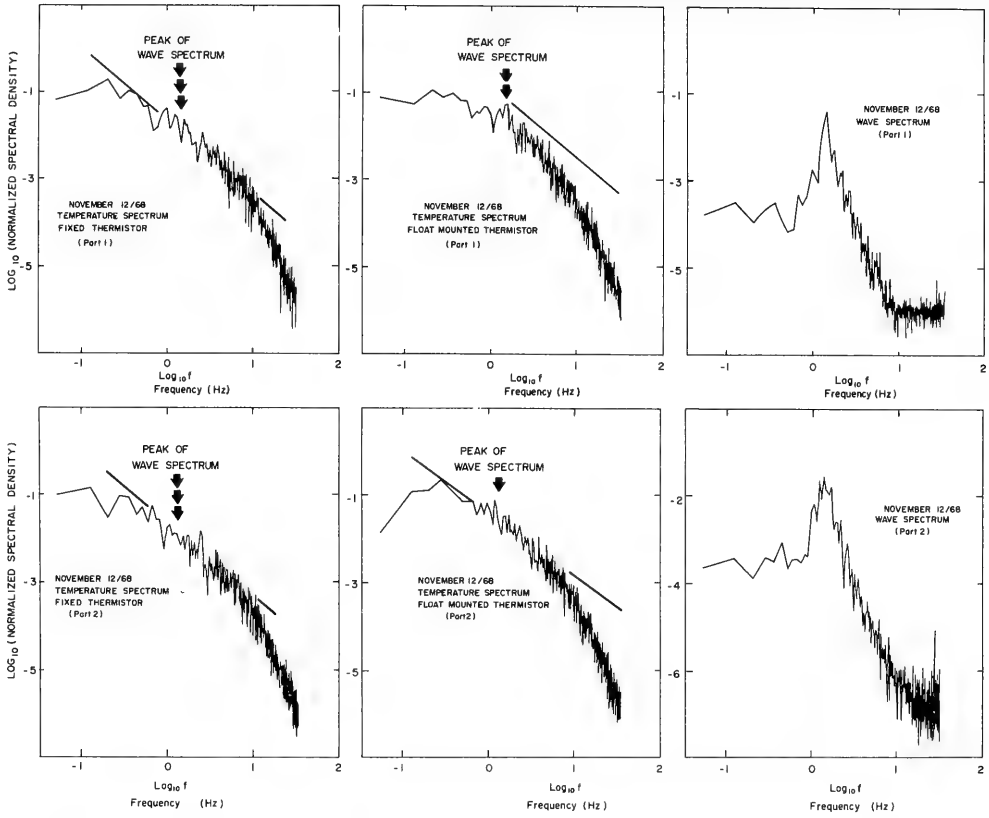

Figure 7. Wave and Temperature Spectra for Moderate Wind Condition

INTERNAL WAVES

L. H. Larsen, M. Rattray, Jr., W. Barbee, J. G. Dworski
Department of Oceanography, University of Washington

ABSTRACT

The interaction of tides and the continental shelf break is such that energy can be put into internal gravity waves. The amount of energy depends on the change in depth across the shelf break; larger amplitude and more confined internal waves occur when the depth change is large. A further dependence on the width of the shelf region is noted. The stability of the ocean is such that waves at the semidiurnal period and longer periods may be generated at most of the world's continental shelf breaks. Because, at the tidal frequencies, frictional damping is small, most of the internal-wave energy reaches the sea floor where it may be reflected upward. A beam in which the energy of the semidiurnal wave motion generated over the shelf break is concentrated may be reasonably expected to reach the sea floor some 25 to 75 km seaward of the shelf break.

Studies conducted at the University of Washington have provided an analytic model of the phenomenon and a laboratory demonstration, and have obtained data from the North Pacific. In this presentation a short film will be shown illustrating the generation of internal tides in a laboratory model, and the results of measurements taken in the North Pacific in September 1968 will be discussed.

Analytic studies that have been carried out by the authors will be set forth insofar as they provide insight into the properties of internal gravity waves. One feature of particular importance is the occurrence of a very complex modal structure over the shelf regions of the ocean.

INTRODUCTION

In a recent publication Rattray *et al.* (1969) discuss the generation of internal tides at the edges of the continental shelves by means of bathymetric coupling with the surface tides. In the model the ocean bathymetry is approximated by a shelf of uniform depth and given width and a deep ocean of uniform depth. At the break of the shelf the surface tide generates two internal wave systems: a standing internal wave system over the shelf and a propagating wave system seaward of the shelf break.

Internal waves have orthogonal group and phase velocities aligned so that the sum of the group and phase velocity vectors lies in a plane perpendicular to the gravitational field. The angle of phase velocity to the plane perpendicular to the gravitational field is

$$\frac{\sigma^2}{N^2} = \cos^2 \theta \qquad (1)$$

where N is the Brunt-Vaisälä frequency, σ is the wave frequency, and θ is the angle of the wave-number vector to the plane perpendicular to the gravitational field.

A beam of internal-wave energy represents a sum of waves of different wave numbers but identical frequencies that tend to cancel each other outside of a given region of space. Thus at one edge of the beam waves appear to form and pass through the beam cancelling each other at the opposite side of the beam; the energy flux is along the beam.

The seaward-propagating internal-wave system is roughly as wide as the depth of fluid above the continental shelf and propagates energy seaward and downward from the region of fluid above the shelf break. For the seaward-propagating internal-wave system, Fig. 1 shows the lines of constant phase, and thus the direction of energy flux for the internal-wave system. The phase of the wave increases in the direction of decreasing depth.

Such an internal-wave system when described by normal modes contains a large amount of energy in the high mode numbers. A great deal of vertical structure is found in the velocity and density fields and the wave signal is correlated not in the vertical but along the lines of constant phase. The slope of the cophasal lines, which depend on the stability of the ocean, is small, and the beam of wave energy meets the ocean floor some 30 to 50 km seaward of the continental shelf break.

The inviscid theory predicts that the wave beam would reflect from the ocean floor, then some distance further from the shelf reflect downward again from the surface. A problem with which we are concerned is the amount of energy that reaches the sea floor and is reflected upward. Knowledge of this permits determination of the distance from the shelf that the propagation of sound can be affected by baroclinic tidal oscillations.

Because each wave number is damped at a different rate, the viscous dissipation of the seaward-propagating wave system is complex. Furthermore, because the total system consists of waves of many different group velocities, a "Taylor hypothesis" based on a single group velocity may not be used to translate from a temporal analysis of the dissipation to a spatial analysis. We attempt here to discuss the problem of frictional modification of the beam by an analysis of the rate of energy flux by the wave system as a whole. Regions of space into which little energy is propagated would be expected to be affected rapidly by energy loss.

LeBlond (1966) considered a temporal analysis of the dissipation of internal wave energy. He found that waves of long wavelength are dissipated in time slower than waves of shorter wavelength, but under no reasonable circumstances would any of the normal modes that comprise

the internal tide beam propagate across an ocean basin. It was on the basis of this result that Rattray *et al.* assumed the internal wave generated at the continental shelf to be a progressive wave.

In October of 1968 we attempted to measure the internal tide system off the coast of Vancouver Island. Two vessels were used, each having a string of temperature sensors spanning the beam of wave motion. At this time the analysis of the resulting data has not been completed.

DIFFRACTION OF INTERNAL WAVES BY A KNIFE-EDGE BARRIER

Before looking at the Rattray model it is instructive to consider a simplified model. Consider an internal wave confined to a channel of a given depth. Then assume that a knife-edge barrier is inserted to extend from the bottom, partially blocking the channel. The region of fluid above the barrier will appear as a source region for the internal-wave motion existing in the lee of the barrier. If we wait long enough the transients should disappear and remaining will be signals of the frequency of the incident wave. The details are given by Larsen (1969) and we need not go into them here.

Now the energy flux of the wave system is given by the correlation of the pressure and velocity field. In Fig. 2 the magnitude and direction of energy flux are plotted at selected points. The most illuminating feature of this energy flux is its small magnitude in the central portion of the wave field. There exists an interaction of the pressure fields associated with each of the normal modes such that a cancellation of the energy flux occurs in the central portion of the beam. This is not a resonant interaction between modes, but a modification of the energy flux brought about by the presence of multiple modes.

The modification of the energy flux due to multiple modes may be illustrated by the following simple model. Consider a channel containing waves of the first two modes. In Fig. 3a we show the energy flux associated with a single mode. The energy flux for the first mode has a zero in the center of the channel and maximum at the channel boundaries. The energy flux associated with the second mode has a peak at the center as well as at the boundaries.

In Fig. 3b we show the energy flux for a combined system of the first two modes. The modes have identical amplitudes and phases. Because of the pressure field interaction the energy flux is no longer a simple sum of the energy fluxes of the individual modes. There does exist a vertical energy flux at some places. The energy flows along a sinusoidal curve with no net vertical flux of energy.

This has rather important consequences when we look at the dissipation. When we first began this study it was thought that frictional effects would erode the edges of the beam—the regions of high shear. However, there is a large flux of energy into these regions, hence the possibility of sustaining motion in the presence of strong dissipation. Recall that the shear is large during only portions of a cycle. In the central core, where the shears are minimal, there is little flux of energy. Thus, rather than be eroded at the edges alone, the beam of energy may be attacked by fluid friction more or less uniformly across the beam.

Progress has been made toward solving the spatial dissipation problem; however, it is not yet sufficiently far along that conclusions may be reached on how much energy of the internal tide system reaches the sea floors.

EXPERIMENTAL PROGRAM

In experiments where large amounts of data are collected, preanalysis, conditioning, and processing of the data can be difficult and time consuming. Data from our 1968 ocean experiment are still in the preanalysis stage, but since the steps to be taken in the processing and analysis are established, it is of interest to describe these operations.

Our experiment plan was to deploy sensors at two locations seaward of the continental shelf break—the sensor array from each vessel to span the predicted beam of internal waves. The model predicting the beam of wave energy was validated when the observed signals showed phase relationships in agreement with those predicted. The USCGC *Ivy* was stationed at the inshore position and USC&GSS *Oceanographer* at the offshore location.

The locations of the two sites and the deployment of the sensors are shown in Fig. 4. Temperature/time series were obtained at each of 30 depths at the inshore site, and at each of 10 depths at the offshore site. The time series were of about 10 days duration. The sampling interval was one minute in the inshore series, and one second in the offshore series. This made 30 series of about 13,000 temperatures and 10 series of nearly 900,000 temperatures to process. In addition to the temperature/time series at fixed depths, 200 STD casts were taken at intervals throughout the observation period. These casts were taken to provide the temperature/depth information necessary to transform temperature variations in the time series into depth variations.

The first stage of the data processing consists of rearranging the data and casting them into a format that allows for convenient manipulation and examination. The technique of delineating vertical excursions through the use of temperature variations depends on the fact that potential temperature is a conservative property. For this case, the vertical velocity of the fluid is given by

$$w = -\frac{(\partial\theta/\partial t)}{(\partial\theta/\partial z)}\ , \tag{2}$$

where θ is the potential temperature.

If a temperature/time series is taken digitally and the only temperature/depth information is from measurements taken at discrete depths, the usual practice is to determine vertical excursions as the following finite-difference integration of (2):

$$\zeta = -\frac{(\Delta\theta/\Delta t)}{(\Delta\theta/\Delta z)}\,\Delta t \tag{3}$$

The vertical temperature gradient is assumed constant in the neighborhood of the depth of interest. In the 1968 experiment, STD casts provided a monitor of the local temperature gradient, which is neither constant nor linear.

Obviously, to achieve an exact determination of vertical excursions, it would be necessary to sample continuously in time and depth; however, all we could do was to average the STD data and generate the excursion depth/time series by mapping the temperature measurements into the assumed temperature profile. Programs to handle this mapping of data are now on file at the University of Washington, Department of Oceanography.

The major difficulty in the analysis of our data is that they contain a large amount of ship-motion effects. We are currently using clipping and filtering techniques in an attempt to remove the ship-induced noise.

ACKNOWLEDGMENTS

This research has been sponsored by the National Science Foundation Grant GA-1417 and by the Office of Naval Research Contract Nonr-477(37), Project NR 083 012. The observations would not have been possible without the help of the U.S. Coast Guard and the U.S. Coast and Geodedic Survey, both of whom contributed ship time. This is Contribution 491 from the Department of Oceanography, University of Washington. The material discussed in this paper is unclassified.

REFERENCES

M. Rattray, Jr., Juraj G. Dworski, and Paavo E. Kovala, 1969. Generation of long internal waves at the continental slope. *Deep-Sea Research*, 16 (suppl.; in proof).

P. A. LeBlond, 1966. On the damping of internal waves in a continuously stratified ocean. *J. Fluid Mech.* 25:121-142.

L. H. Larsen, 1969. Internal waves incident upon a knife-edge barrier. *Deep-Sea Research*, 16:415-422.

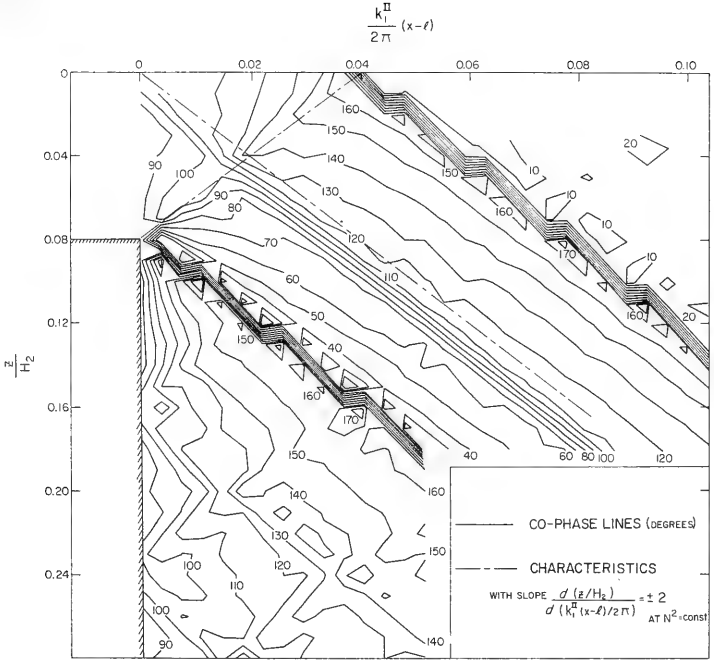

Figure 1.

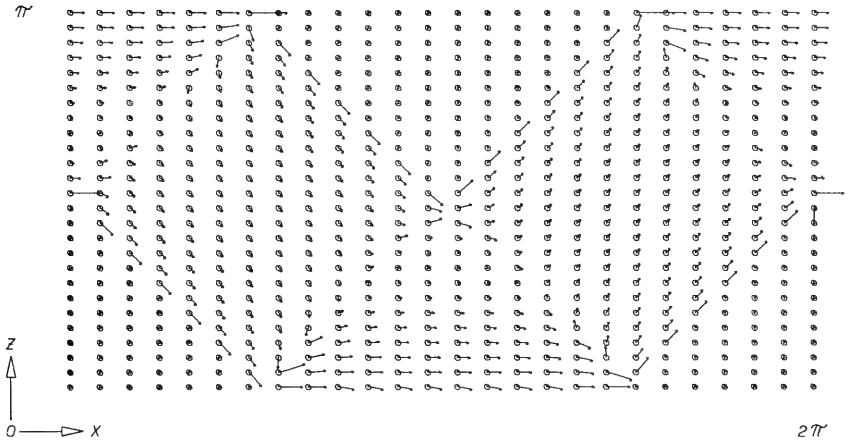

Figure 2.

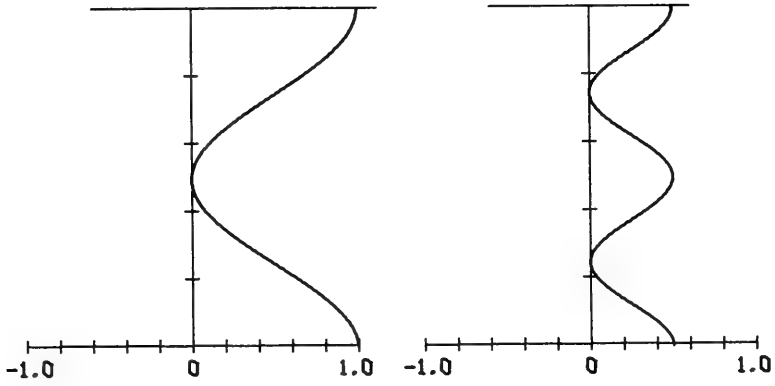

Figure 3a.

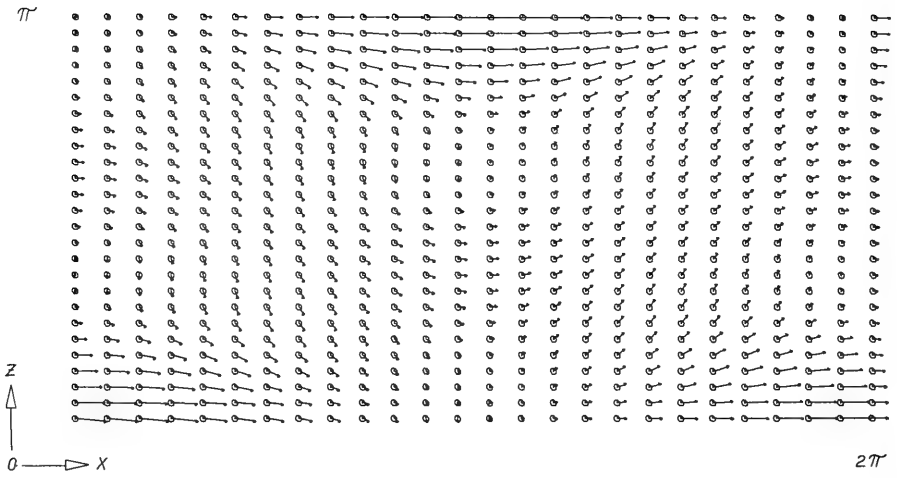

Figure 3b.

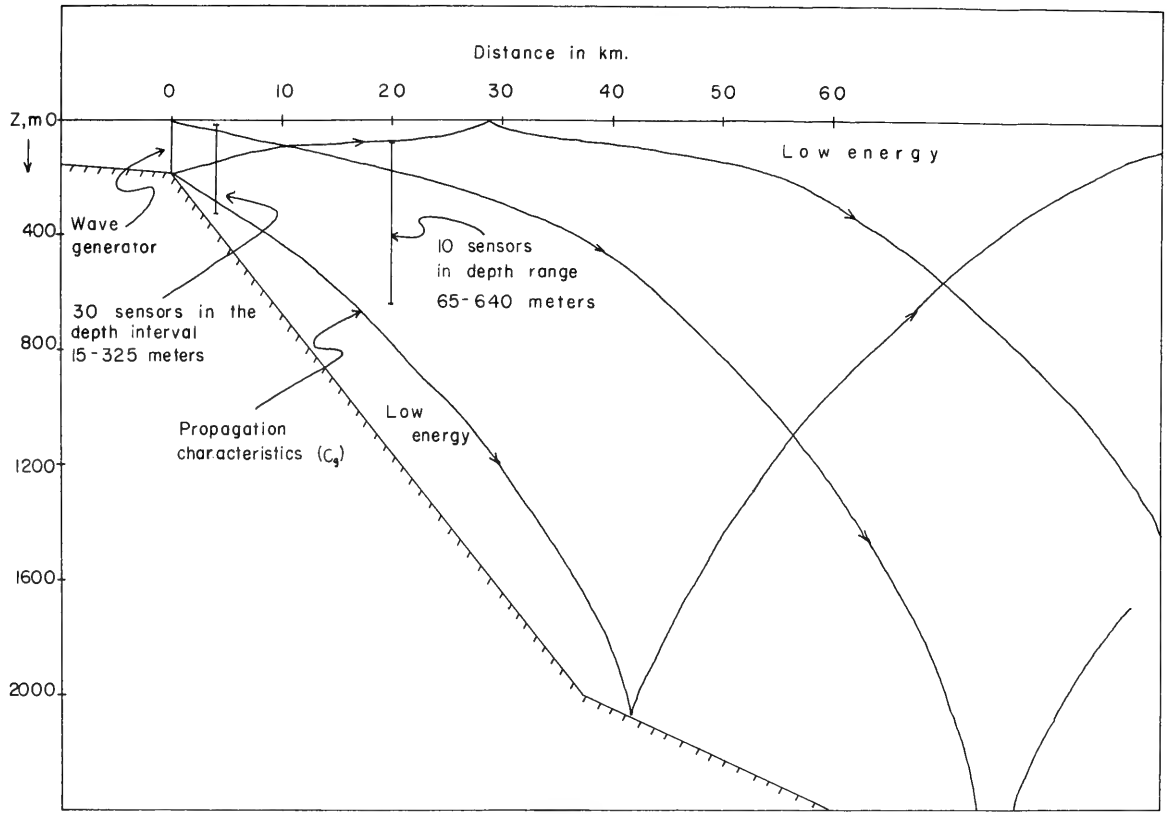
Distance in km.
0
10
20
30
40
50
60
Z,m
0
400
800
1200
1600
2000
Low energy
Wave generator
10 sensors in depth range 65-640 meters
30 sensors in the depth interval 15-325 meters
Low energy
Propagation characteristics (C_g)

Figure 4.

MASS TRANSPORT AND THERMAL UNDULATIONS CAUSED BY LARGE AND SMALL SCALE VARIABILITY IN THE STOKES' MASS TRANSPORT DUE TO RANDOM WAVES †

Hong Chin
Assistant Research Scientist
and
Willard J. Pierson, Jr.
Professor of Oceanography
New York University

The Stokes' mass transport is a well known second order effect for irrotational monochromatic periodic surface waves. It shows up most clearly in a Lagrangian analysis of wave motion to second order. However, when a continuous spectrum of frequencies and directions for surface waves is considered, this mass transport becomes variable at both the synoptic oceanographic scale and at temporal scales of five to twenty minutes. It is therefore possible to use the directional wave spectra obtained by both presently available and nearly completed wave forecasting models to compute mass transport current fields and possible thermocline undulations caused by this effect.

The currents prove to be comparable at times to those caused by Ekman theory, except that they grow and shrink in direct response to the waves that are present.

Second order nonlinear interactions produce difference frequencies and difference wave numbers that yield long period slow vertical and horizontal oscillations. Except for the shear at a region of strong density variation that occurs for internal waves, these motions have many features similar to internal wave motions and may easily be mistaken for them in a stratified fluid. Much of the apparent thermal unrest in the oceans may well be due to these second order wave effects, and, as such, a description of them is an easily obtained extension of present gravity wave forecasting models.

INTRODUCTION

Since the early work of G. G. Stokes in 1847, it has generally

---

†Contribution 79 of the Geophysical Sciences Laboratory, Department of Meteorology and Oceanography, New York University.

been recognized that a particle in an irrotational, progressive gravity wave motion will undergo a slow drift at the so-called Stokes' mass transport velocity. For a periodic wave in deep water, this velocity is in the direction of wave celerity and may be expressed as

$$\overline{U} = a^2 \omega k e^{-2kZ} \tag{1}$$

where a = wave amplitude
ω = angular frequency
k = wave number
Z = Eulerian depth

In a situation involving the actual sea surface, however, this expression is not directly applicable. The reason for this is, of course, quite obvious since the deep water sea surface cannot be approximated as a periodic motion. In order to derive reasonable estimates of wave-induced properties, one should generalize to at least a first order spectrum. A recent study by Chang (1969) has done precisely this for the mean component of Stokes' velocity. A spectral expression of the form

$$\overline{U} = 4 \int_0^\infty \frac{\omega^3}{g} e^{2(\omega^2/g)\delta} S_{1(x)}(\omega)\, d\omega \tag{2}*$$

where g = acceleration of gravity
δ = Lagrangian depth tag
$S_{1(x)}(\omega)$ = double-ended first order spectrum of the motion in the x-direction

was derived and shown to be applicable through the second order of the perturbed Lagrangian equations of motion. For the deep water case, it was shown that $S_{1(x)}(\omega)$ could be reasonably approximated by the first order spectrum of wave elevation in the z-direction (i.e., $S_{1(z)}(\omega)$). This allows an evaluation of $\overline{U}$ from eq. (2) since estimates of $S_{1(z)}(\omega)$ are, or soon will be, common products of present-day numerical wave forecasting models as described by Pierson, Tick and Baer (1966). In particular, estimates of the directional-frequency (d-f) spectrum, $\hat{S}(\omega, \theta)$, are especially useful in this context since a direction may be associated with the magnitude and thus result in a vector evaluation. Calculations of $\overline{U}$ fields involving $\hat{S}(\omega, \theta)$ have recently been completed on a CDC 1604 at the

*Note that eq. (1) is a special case of eq. (2)--namely that which occurs at the initial time ($z = -\delta$) in deep water ($kg = \omega^2$) if the x-motion is similar to the z-motion and purely sinusoidal ($a^2 = 4S_{1(x)}(\omega_o)$).

Data Processing and Computation Laboratory of New York University. The directional spectra and computational algorithm used for these calculations are discussed in the following section. The results of two surface drift fields are presented and discussed in the section on surface drift results. These prove to be of considerable significance not only because their magnitudes may at times be comparable to Ekman current velocities but because they apparently cannot be adequately explained by any of the classical pure wind-driven or thermohaline theories for ocean currents. In order to gain a deeper insight into the ramifications of these particle motions, a long-crested nonlinear model is considered. It is shown that under a series of not unreasonable assumptions, these motions may easily be mistaken for thermal undulations in a weakly stratified fluid.

CALCULATION OF THE MEAN STOKES' VELOCITY IN A SHORT-CRESTED RANDOM SEA

The directional spectra used for the calculation of $\overline{U}$ were essentially those described by Pierson and Tick (1964) and Coté et al. (1960) except for the recent inclusion of a modified Miles-Phillips growth mechanism by Inoue (1967). At each of 519 grid points of a Baer grid (Baer, 1962) in the North Atlantic, the directional spectrum can be thought of as 180 contributions to the total variance distributed among 15 frequency and 12 directional bands. Figure 1 is an attempt by the authors to represent schematically one of these spectra in three dimensions. The horizontal plane is a polar plot with angular frequency increasing radially outward from the central grid point and direction increasing clockwise from due north (0°). Each of the directional bands is a constant 30°. The frequency bandwidths are listed in Table I. Work in progress will double the number of angular bands. The vertical coordinate is a measure of variance in units of $(\text{ft})^2$. Within each d-f band, the estimate of variance, $E_{ij}(\omega, \theta)$, is assumed constant.

For completeness, this particular form of the spectrum for a fully developed wind sea may be expressed as

$$S(\omega, \theta) = \frac{\alpha g^2}{\omega^5} e^{-\beta(\omega_o/\omega)^4} [F(\omega, \theta)] \qquad (3)$$

where $\alpha = 8.1 \times 10^{-3}$

$\beta = 0.74$

$\omega_o = g/v_{19.5}$

$v_{19.5}$ = wind speed at 19.5 meters above the sea surface

and

$$F(\omega, \theta) = \frac{1}{\pi}[1 + (0.50 + 0.82e^{-(\omega/\omega_o)^4/4})\cos 2\theta + 0.32\, e^{-(\omega/\omega_o)^4/4} \cos 4\theta]$$

as an example, where θ = wind direction. $S(\omega, \theta)$ is defined for

$-\frac{\pi}{2} < \theta < \frac{\pi}{2}$ and zero otherwise (i.e. waves traveling against the mean local wind are not considered). The actual values of $\hat{S}(\omega, \theta)$ rarely coincide with this form because simple fully developed seas are not frequent in the North Atlantic.

The calculation of $\overline{U}$ now becomes a matter of applying eq. (2) to each d-f interval. The resulting magnitude is then assigned (as a first approximation) the centered direction of the band in which it is situated. By convention, the direction is taken as "from" the centered direction of the band--in the sense of Figure 1. When the procedure has been applied to all the d-f components in turn, a set of component vectors is produced. The vector sum is an approximation of the mean Stokes' velocity at the grid point. The magnitude evaluation is essentially all contained in a subroutine called UDRIFT. The logic behind it can be seen by examining eq. (2) in the form

$$\overline{U}_{ij} = 2\int_{\omega_j}^{\omega_{j+1}} \frac{\omega^3}{g} e^{2(\omega^2/g)\delta} \hat{S}_{ij}(\omega, \theta) d\omega \qquad (4)$$

$$i = 1, 2, \cdots, 12$$
$$j = 1, 2, \cdots, 15$$

where ω_{j+1} = upper limit of a particular frequency band
ω_j = lower limit of the same frequency band.

Since $\hat{S}_{ij}(\omega, \theta) = E_{ij}(\omega, \theta)/(\omega_{j+1} - \omega_j)$ and $E_{ij}(\omega, \theta)$ has previously been estimated as constant in the interval, $\hat{S}_{ij}(\omega, \theta)$ may be approximated as constant with respect to ω in the interval and taken out of the integral as a constant. For a specified δ, the remaining integral can then be seen to yield a constant. The product of these two quantities produces the desired component magnitude.

It should be noted that the right-hand side of eq. (2) has apparently been halved in the transition to eq. (4). This is to account for the fact that $S_{1(z)}(\omega)$ is a double-ended spectrum while $\hat{S}(\omega, \theta)$ is a single-ended estimate.

The results presented in the next section are confined to the free surface ($\delta = 0$) although, in principle, the computational procedure may be used for any acceptable* value of δ or to get a drift averaged over a range of depths. The basic effect of increasing depth (δ becoming more negative) is a function of the surface spectrum. That is, with increasing depth, the resultant vector will exhibit greater direction and magnitude persistence if the energy

*Longuet-Higgins (1960) has shown that a component of secondary vorticity is generated in a thin layer of thickness $(\nu T)^{\frac{1}{2}}$ adjacent to the surface and that this vorticity propagates into the interior of the fluid. These effects must be considered in future work.

in the low frequency bands is high. On the other hand, if the energy in the high frequency bands is large, the rapid energy decay with depth will allow the lower frequency bands to dominate with depth. In particular, if the lower frequency energy is in a different direction, the resultant will swing towards this direction with depth. In a situation where swell is running against a local wind sea at the surface, an indication of resultant direction reversal can be seen with increasing depth. Actually, these are simply consequences of the fact that long waves (low frequency) reach greater depths than short waves (high frequency).

SURFACE DRIFT RESULTS

Surface fields of mean Stokes' velocity have been computed for both 12Z, 27 February 1967 and 18Z, 4 March 1967. Figures 2 and 3 show the wind field at 19.5 meters above the sea surface and surface mass transport (or drift) velocity, respectively, for 4 March 1967. The 519 arrows indicate the direction of flow at each grid point and the isotach analysis indicates the speed distribution. The arrows on these figures show a general tendency of the current to flow in the wind direction. The current flow is mainly cyclonic under the intense low in the north (centered at approximately 62°N, 22°W) and roughly anticyclonic under the subtropical high situated further south (centered at approximately 35°N, 30°W). The isotach analyses clearly indicate the tendency for strong drift velocities to be situated in the vicinity of strong winds and weak or variable drift velocities to be situated near lesser winds.

In order to analyze these results, two conventional oceanographic statistics were employed. The first was a drift-speed to wind-speed ratio expressed as a percentage. The second was an angular measure of drift direction relative to the wind direction. If the current flowed to the right of the wind, the angle between the two vectors was taken as positive and if the current flowed to the left, the angle was taken as negative.

The amount of information derived from the first statistic proved to be only of limited significance. The reason for this, however, proved to be of considerable significance. If the ratio statistic were completely significant, this would imply a direct causal link between wind and waves. This, of course, is not true since there is a lag between wind changes and sea surface response. The isotach analyses in Figures 2 and 3 give an indication of the lag. A good example of this appears at grid point 276 (35.2°N, 25.2°W) in the 27 February analysis. In the hours prior to 12Z, brisk northerly winds raised appreciable energy in the high frequency bands. This, in turn, produced an appreciable Stokes' velocity. By 12Z, the wind had shifted to easterly and had decreased to about 1 knot. The spectrum, however, did not respond as rapidly and could still maintain a drift magnitude of 6.2 cm/sec. The computed ratio was then 12.22%, which is extremely high. Empirical studies usually set this ratio at

about 2 to 3%[Hughes (1956) estimated 2%; Smith (1968) estimated 3.4%].

It should be mentioned that empirically estimated ratios should be somewhat higher than those computed here partially because they contain not only the Stokes' mass transport effect, but also the Ekman drift and perhaps residual tidal and permanent current effects.

In regions of less wind variability such as the Trades, the statistic becomes more significant. A ratio on the order of less than one percent seems to be indicated.

In contrast with the first statistic, the direction statistic proved to be relatively easy to interpret. The results of the 4 March analysis are presented in Figure 4 in a histogram. The central peak in the distribution reinforces the idea of a wave-induced current apart from the Ekman mechanism since the peak is not to the right of the wind direction. Basically, the distribution reflects the tendency for wave energy to be situated in the general wind direction. The particle motions produced by these waves will then be in these directions. This may account for some of the variability found in conventional current measurements. In particular, the components in the wind direction would be especially susceptible to this explanation.

The bar on the far right in Figure 4 indicates an interesting feature. In this particular case, approximately 2% of the grid points showed a mean Stokes' drift against the wind.

THERMAL UNDULATIONS CAUSED BY STOKES' MASS TRANSPORT

Since the influence of surface waves reaches to a depth of approximately half their wavelength, it may be expected that particle motions are effective to considerable depths. In order to investigate this effect, a long-crested nonlinear Lagrangian model proposed by Pierson (1961) was used. Two of the solutions derived in this formulation were a set of second order equations for determining the Eulerian position (X,Z) of a fluid particle as a function of the Lagrangian tags α, δ, and time, t. If these equations are written in terms of 15 waves, they form

$$X(\alpha,\delta,t) = \alpha - \sum_{m=1}^{15} a_m e^{k_m\delta} \sin(k_m\alpha - \omega_m t)$$

$$- \sum_{m=1}^{14} \sum_{n=m+1}^{15} \frac{a_m a_n}{g}\left(\frac{\omega_m^3+\omega_n^2}{\omega_n-\omega_m}\right) e^{(k_n+k_m)\delta} \sin((k_n-k_m)\alpha-(\omega_n-\omega_m)t)$$

$$+ \sum_{m=1}^{14} \sum_{n=m+1}^{15} \frac{a_m a_n}{g}(\omega_n+\omega_m)\omega_n e^{(k_n-k_m)\delta} \sin((k_n-k_m)\alpha-(\omega_n-\omega_m)t)$$

$$+ \sum_{m=1}^{15} a_m^2 \omega_m k_m e^{2k_m\delta} t \qquad (5)$$

$$Z(\alpha,\delta,t) = \delta + \sum_{m=1}^{15} a_m e^{k_m \delta} \cos(k_m \alpha - \omega_m t)$$

$$+ \sum_{m=1}^{14} \sum_{n=m+1}^{15} \frac{a_m a_n}{g} (\omega_m^2 + \omega_m \omega_n + \omega_n^2) e^{(k_n + k_m)\delta} \cos((k_n - k_m)\alpha - (\omega_n - \omega_m)t)$$

$$- \sum_{m=1}^{14} \sum_{n=m+1}^{15} \frac{a_m a_n}{g} \omega_n (\omega_n + \omega_m) e^{(k_n - k_m)\delta} \cos((k_n - k_m)\alpha - (\omega_n - \omega_m)t) \quad (6)$$

The term that is linear in t in eq. (5) can be seen to be a summation of the Stokes' drift effect expressed in eq. (1). The double summation terms in both equations indicate the sum and difference interactions among the 15 waves. One of these terms dies out rapidly with depth. The other does not die out and produces long period, long wavelength, vertical and horizontal oscillations. In a random seaway, groups of high waves separated from other groups by areas where the waves are low produce locally strong Stokes' drifts over dimensions comparable to the size of the group. A meso-scale field of convergences and divergences is established which penetrates to considerable depth.

As an example of how this effect might manifest itself, consider a weakly stratified portion of ocean initially at rest. At this time, the Eulerian and Lagrangian positions are identical (i.e., $x = \alpha$, $z = \delta$, $t = 0$). Let the temperature distribution be such that every fluid particle at the same depth has the same temperature. If a wave motion is now added and time is set in motion, the particles will begin to move. At time scales on the order of five to twenty minutes, it is not unreasonable to assume that the subsurface fluid particles (say, below -40 meters) have been able to maintain their initial temperature. Therefore, the isotherm initially at some constant Eulerian depth will be moved both horizontally and vertically because of the motions of the fluid particles. The spectrum of grid point 13 (61.9°N, 10.1°W) of the 4 March case was used as a test to illustrate this effect. The ensemble of 15 waves with approximately the same centered frequencies, wave numbers and amplitudes given by the spectrum were substituted into eqs. (5) and (6) to produce a series of Eulerian positions for various values of α and δ in the vicinity of the Eulerian origin. The results of this calculation for $t = 15$ minutes are presented in Figure 5. The Stokes' velocity shear ($\partial \bar{U}/\partial \delta$) has purposely been masked so that only the vertical features are evident. The important feature to note here is in the vicinity of -40 to -70 meters. The levels that were originally at $z = -40$, -50, -60, and -70 meters have now been raised and exhibit a long wave oscillation due to the wave-induced particle motions. If they are assumed to be isotherms, then a shift in the thermal pattern is indicated. If one now imagines a ship situated

at x = 0 with a temperature probe at say, z = -50 meters, then the instrument would record undulations of temperature as the subsurface levels oscillated in response to the surface wave motions. Even if one considered the averaging that is usually applied to data, these effects need not necessarily average out since the wave conditions at any given point on the surface are continually changing. This effect may account for much of the apparent thermal unrest in the oceans.

REMARKS

The estimates of mean Stokes' velocity are, of course, only as good as the approximations and spectra that produced them. At the present time, it is still not possible to verify directly a directional spectrum. One can, however, verify the significant height and the frequency spectrum against actual observations of wave elevation as a function of time. Bunting and Moskowitz (1969) have provided the authors with an advance copy of significant height verification statistics for spectra similar to those used in the above calculations. The bias is on the order of -0.9 ft and the RMS deviation is about ±5.0 ft. These are well within the present state of the art.

It should be pointed out at this juncture that all the spectra used in the computations were not fully developed. For a fully developed local wind sea, the mean Stokes' velocity increases with wind speed as shown in Figure 6.

In order to compare the resultant drift magnitudes with Ekman magnitudes, the empirical equations of Durst and Thorade (as given by Neumann and Pierson, 1966) were applied to the 4 March wind field. The Durst magnitudes ranged from 0.3 to 20.7 cm/sec. The Thorade magnitudes ranged from 2.5 to 33.0 cm/sec. The drift magnitudes went from 0 to 19.0 cm/sec. Further examination shows that these values are not always proportionally related. At times, the drift may be comparable to or greater than the steady state Ekman velocity.

A convenient check on the magnitude of the drift was provided by comparing the long and short crested results. For instance, in the test calculation at δ = -40 meters, the long-crested model showed that the ensemble of particles had drifts ranging from 1.96 to 1.99 cm/sec with an average of 1.98 cm/sec. The short-crested model produced a mean velocity of 1.61 cm/sec. The latter should be expected to be lower than the former due to the effect of the short-crestedness.

The use of a ratio statistic in this context was found to be of only limited significance, especially in the westerlies. In those regions, one should resort to the spectral techniques to compute drift.

The work of Stokes showed that particles in an irrotational, progressive, gravity wave motion would undergo a slow drift. A description of this phenomenon now seems to be obtainable by a simple extension of present gravity wave forecasting models.

ACKNOWLEDGMENTS

The authors wish to acknowledge the assistance of Miss Catherine Vail in handling the data tapes and in aiding in the computations. This research was sponsored by the Office of Naval Research under Contract Nonr 285(57).

TABLE I

Frequency and direction bands for the spectral estimates used in calculating the Stokes' drift

Directional bands (degrees)	Centered directions (degrees)	Angular frequencies (rad/sec) From	To	Center
345- 15	360	0.226194	0.263893	0.244353
15- 45	30	0.263893	0.295309	0.279224
45- 75	60	0.295309	0.333008	0.314159
75-105	90	0.333008	0.364424	0.349093
105-135	120	0.364424	0.402123	0.383965
135-165	150	0.402123	0.433539	0.418899
165-195	180	0.433539	0.471238	0.453771
195-225	210	0.471238	0.502654	0.488706
225-255	240	0.502654	0.540353	0.523577
255-285	270	0.540353	0.609468	0.575979
285-315	300	0.609468	0.678583	0.645785
315-345	330	0.678583	0.785397	0.733059
		0.785397	0.892211	0.837548
		0.892211	1.029751	0.959945
		1.029751	∞	1.030441

REFERENCES

Baer, L. (1962): An experiment in numerical forecasting of deep water waves. LMSC-801296. Lockheed Missile and Space Co., Sunnyvale, Calif.

Bunting, D., and L. Moskowitz (1969): (Personal communication.)

Chang, M.S (1969): Mass transport in deep water long-crested random gravity waves. J. Geophys. Res., Vol. 74, No. 6, pp. 1515-1536.

Coté et al. (1960): The directional spectrum of a wind-generated sea as determined from data obtained by the Stereo Wave Observation Project. Meteor. Papers, Vol. 2, No. 6, New York University Press, New York.

Hughes, P. (1956): A determination of the relation between wind and sea-surface drift. Q. J. Roy. Meteor. Soc., 82, pp. 494-502.

Inoue, T. (1967): On the growth of the spectrum of a wind generated sea according to a modified Miles-Phillips mechanism and its application to wave forecasting. New York University, Geophysical Science Laboratory Tech. Report, TR-67-5.

Longuet-Higgins, M.S. (1960): Mass transport in the boundary layer at a free oscillating surface. J. Fluid Mechanics, 8, pp. 293-306.

Neumann, G., and W. J. Pierson, Jr. (1966): Principles of Physical Oceanography. Prentice-Hall, Inc., Englewood Cliffs, N. J., p. 210.

Pierson, W J. (1961): Models of random seas based on the Lagrangian equations of motion. Tech. Report under Contr. Nonr 285(03), College of Engineering, Research Division, New York University.

Pierson, W. J., and L. J. Tick (1964): Wave spectra hindcasts and forecasts and their potential uses in military oceanography. First U. S. Navy Symposium on Military Oceanography.

Pierson, W. J., L. J. Tick, and L. Baer (1966): Computer based procedures for preparing global wave forecasts and wind field analyses capable of using wind data obtained by a spacecraft. 6th Naval Hydrodynamics Sympos, Sept. 28-Oct. 4, 1966.

Smith, J. E. (1968): Torrey Canyon Pollution and Marine Life. Cambridge at the University Press, 196 pp.

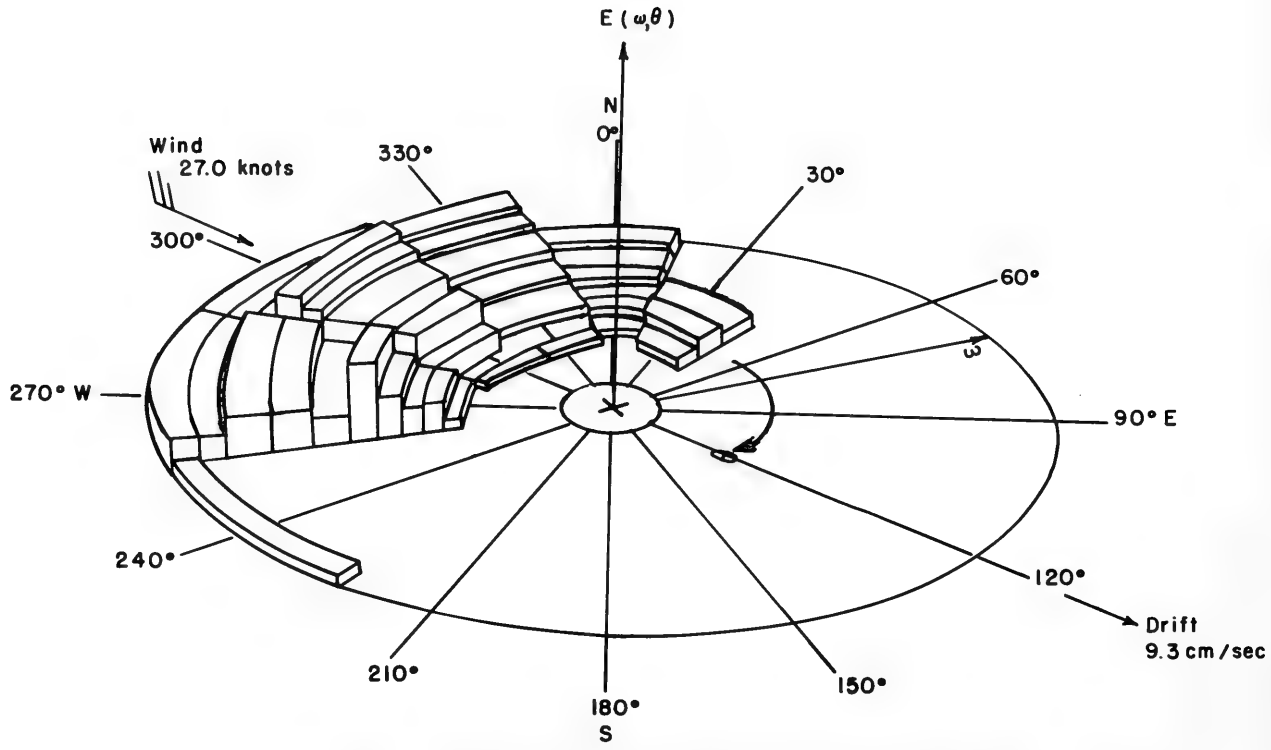

Figure 1. Schematic three-dimensional depiction of a directional spectrum

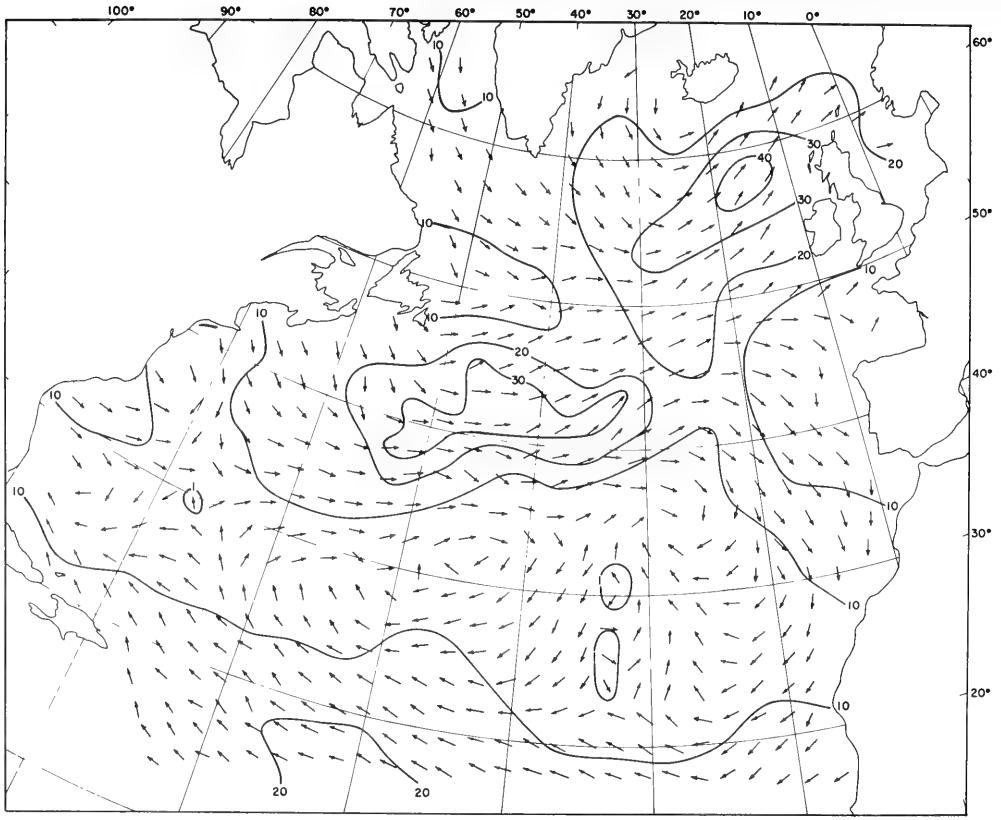

Figure 2. Wind field at 19.5 meters above the sea surface for 18Z, 4 March 1967.

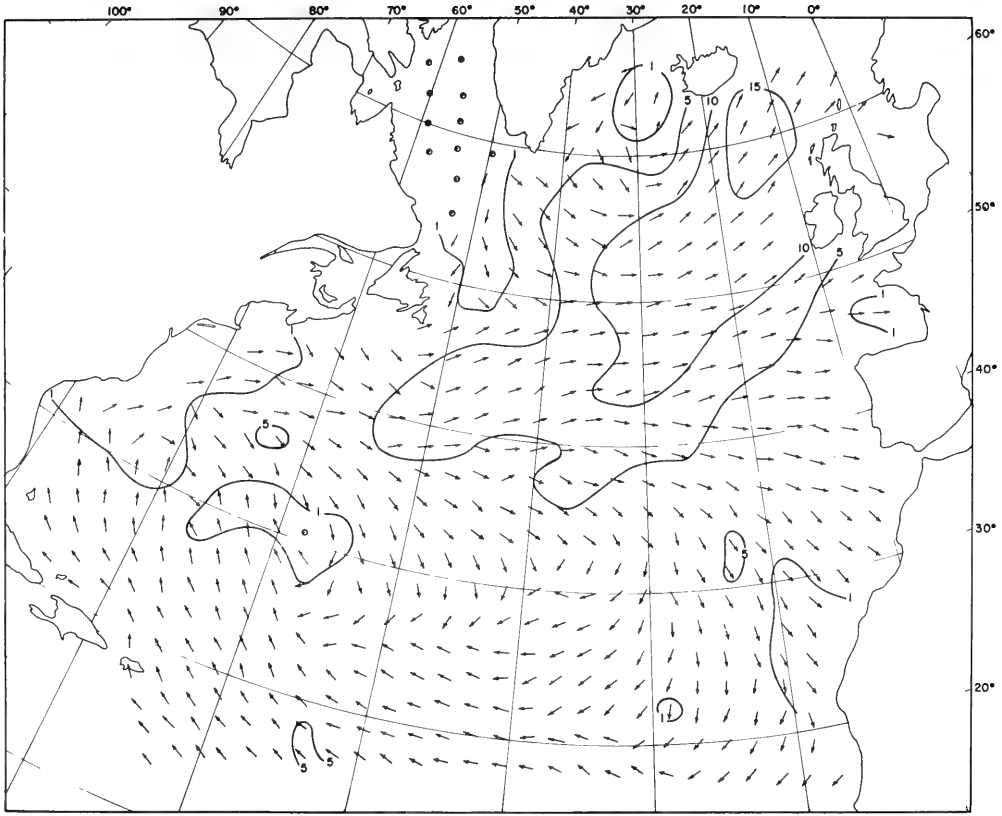

Figure 3. Surface field of mean Stokes' velocity for 18Z, 4 March 1967

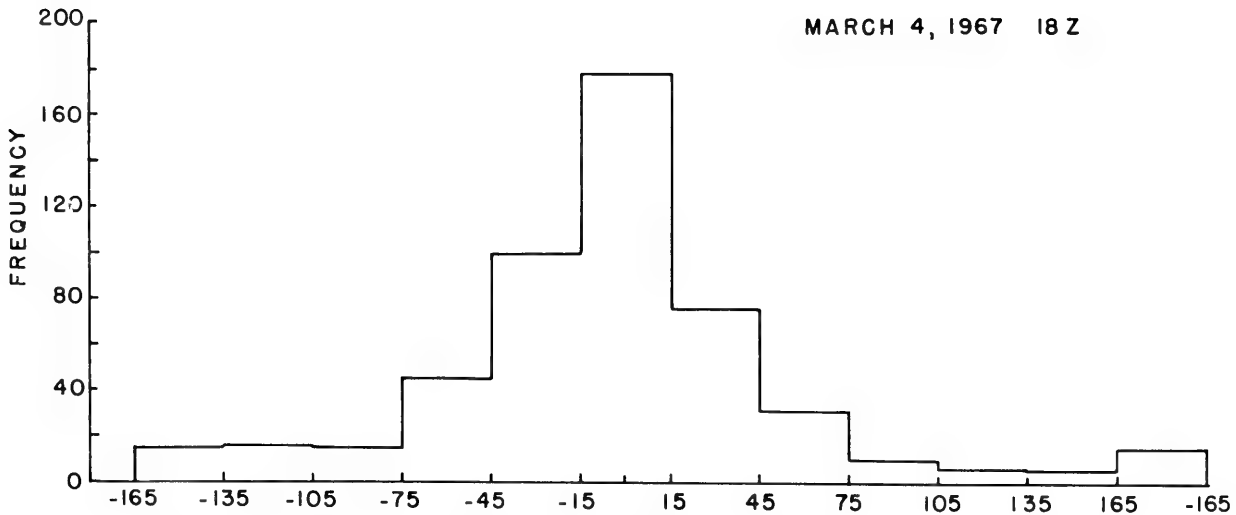

Figure 4. Histogram of drift direction relative to wind direction at zero degrees

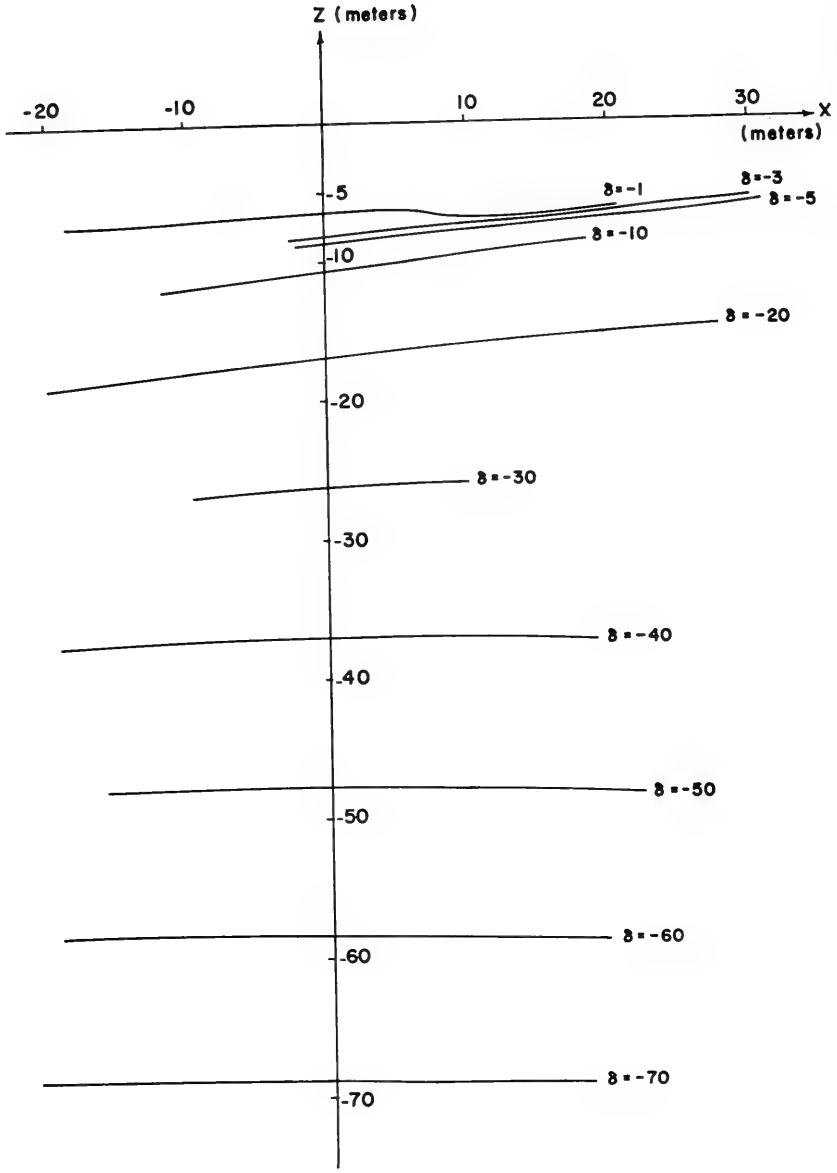

Figure 5. Schematic depiction of Lagrangian depth surfaces

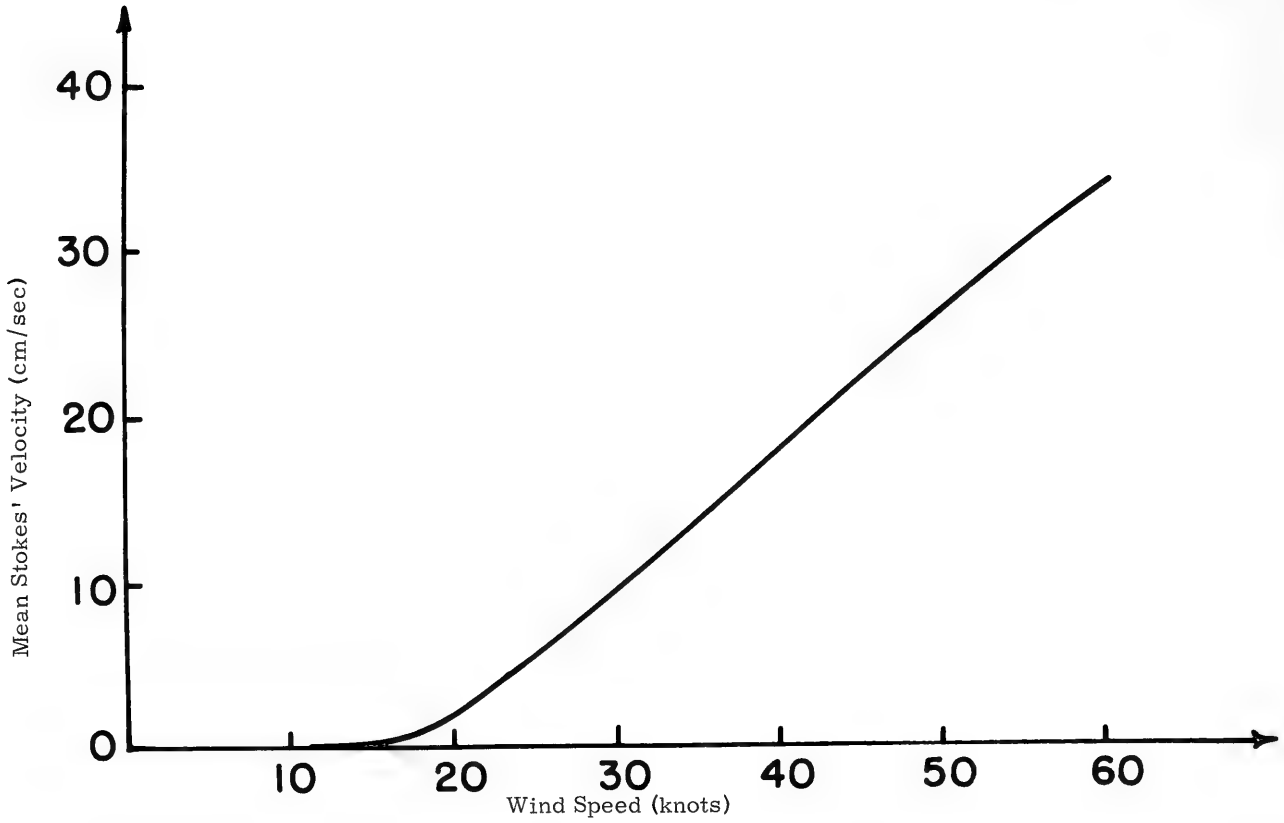

Figure 6. Variation of mean Stokes' velocity with wind speed for fully developed local wind seas

VARIABLENESS OF THE SOUND VELOCITY PROFILE ABOUT THE MID-ATLANTIC RIDGE AXIS

by
Eli Joel Katz
Associate Scientist
Woods Hole Oceanographic Institution
Woods Hole, Massachusetts, 02543

ABSTRACT

Mediterranean water, spreading across the North Atlantic Ocean, is shown to cause a disturbance to the acoustic medium in the vicinity of the Mid-Atlantic Ridge north of the Azores. In this region, the ridge crests are sufficiently shallow so as to impede the free movement of the intermediate waters. Warm and saline layers, nearly two hundred meters thick, were repeatedly observed in the lowering of continuous sampling sensors. These inversion layers are shown, by reconstruction, to result from local water movement across the ridge crest and are argued to be short lived and spatially confined. As a direct consequence, the observed depth of the sound-velocity minimum unpredictably fluctuated as much as five hundred meters within an area of two hundred miles square. The layers themselves result in secondary sound channels; the inversions of both temperature and salinity combining to produce inversions of four meters per second deep in the thermocline.

Introduction

Throughout most of the world's oceans the water column consists of a large bulk of cold, nearly isothermal water, topped by a warmer surface layer. As the velocity of propagation of sound in water increases with both depth (more precisely, pressure) and temperature, velocities are highest at either end of the column resulting in a widely spread sound channel in which sound can travel, practically speaking, for unlimited ranges. In general, the axis of the channel will be found at the bottom of the transition between the warmer and the colder water. The relative efficiency of the channel to propagate sound will be primarily related to the total temperature contrast between the two and the thicknesses of the intermediate and cold water layers. In the open ocean the parameters defining the sound channel, being products of the air-sea interchange and oceanic circulation, will normally vary slowly by season and over distances measured in hundreds of miles. Exceptions have to be explained in this same context.

To be discussed below is a collection of velocity profiles from a specific area which, while consistent with the broad description, had a variable behaviour at depths about the sound channel axis. The twofold cause of the variableness of the channel was the spreading of Mediterranean water and the effect of the Mid-Atlantic Ridge on the general circulation of the subsurface waters.

It is well known that the efflux of warm saline water from the Mediterranean Sea is the cause of a significant distortion to the sound velocity profile in a wide region about the Strait of Gibraltar. Penetrating the Atlantic water column above the sound channel axis, the warm saline water results in a distinctive double sound-channel profile whose variableness and geographic dependence is first being systematically investigated with observations like those of Piip (1968). To a lesser degree, the spreading of this water influences the shape of the velocity profile over an extensive zone of the Atlantic Ocean. Any process which disrupts the continuous diffusion of the Mediterranean Water's anomalous salinity will be reflected in the profiles of that region, and such is the case at the Mid-Atlantic Ridge, in at least one area. There, the ridge will be shown to mark a change in the sound velocity profile with a narrow transition containing unpredictable, but explainable, sound velocity structure.

During August and early September of 1968, continuous salinity and temperature profiles were obtained at seventeen stations to the north of the Azores. The lowerings straddled the ridge axis, and their positions relative to a coarse plot of the simultaneously obtained bathymetry are mapped in Figure 1. The depth of the sound channel axis from each lowering is noted. The two ridge crests enclosing the median valley are identifiable by the 2,000 meter line, including a lateral displacement at 43°N which is typical of the ridge. Crests are seen to reach within 1500 meters of the surface and, though not shown, some peaked at depths less than 1000 meters. Thus, the ridge intermittently rises above the level of the sound channel axis, a depth which itself is only poorly defined for this region.

The lowerings indicated that the movement of water at intermediate depths was neither stationary nor continuous on a broad front. Two lowerings which were repeated after two and three weeks and at locations within several miles of each other (nos. 40 and 49, nos. 36 and 44) had basically different velocity profiles. A sequence of three stations in 60 n.m. across the ridge axis, completed in 36 hours, led to equally diverse results. These three are shown in Figure 2 and one may note not only their differences, but also how unusual two of them are. No. 44 has almost no vertical velocity gradient for 500 meters about the

sound channel axis; No. 45 has two strong gradients in very restricted layers which define an inversion in the sound velocity of some four meters per second over 170 meters. These features are in the nature of distortions to the velocity profile, and it will next be suggested that they define a zone of transition between changes in the sound velocity profile across the ridge crest.

Geographic Classification of Sound Velocity Profiles

The velocity profiles in the immediate neighborhood of the ridge axis can be systematically divided into three groups. The four stations furthest from the axis can, more or less, be brought into the discussion, but they introduce differences due to their relative separation.

In Figure 3, two groupings of profiles are apparent in a superposition of seven lowerings. They are designated as east and west of the axis because that is their predominant geographical distribution, as seen in Figure 4. Two other stations which can be classified by their profiles are also included. The difference between the profiles of each group is the result of a relatively saline core of Mediterranean water (diffused to 35.5 o/oo from about 36.2 o/oo after the initial mixing at Gibraltar) which is present to the east and absent to the west. The velocity profiles diverge because the horizontal gradient in salinity across the ridge axis is balanced by an inverse temperature gradient, as the isopycnic surfaces tend to stay horizontal.

A third group of profiles is transitional between the main east and west groups, both in geography and in velocity profile. In Figure 5 they are compared at intermediate depths on an individual basis. The transitional profiles are of the two types described earlier, and they are separated accordingly. Though only one clear example of an iso-velocity layer at the channel axis is shown, No. 34 was in many ways similar. In the plot of their locations, Figure 4, the intermediate position of these transitional profiles is strongly suggested.

With only sound velocity information it would be difficult to offer any explanation for what has been presented. Examining the salinity data identified the source of the changes as a difference in the appearance of Mediterranean water to either side of the ridge axis. A comparison of temperature-salinity diagrams will suggest how transitional profiles are formed.

Inferred Dynamics of the Transition Zone

The temperature-salinity diagram has been the most useful technique of the oceanographer in inferring the circulation of ocean

water masses. Each water mass, as it enters the circulation pattern either by influx from another basin such as the Mediterranean water or by sinking from the surface at a particular site, can be unambiguously identified on a T-S plot and then traced until diffusion erodes its distinctiveness. Movement within the ocean is for the most part isentropic, and the Mediterranean water, originating from a warm saline sea, is traceable as a warm saline core spreading across the Atlantic Ocean.

The higher sound velocities at intermediate depths to the east of the ridge axis and the change in profile in a relatively short distance to the west indicate a rapid change in the properties of the core layer. Examination of the T-S plots for either side show this discontinuity clearly. If one next compares the T-S diagram of a transitional station there is a possibility, if excessive mixing has not already occurred, of dividing the water column into layers of known origin. One could thereby reconstruct the process by which a transition profile was formed. This was attempted for the lowerings of Figure 5.

Each reconstruction is somewhat different in detail and an example of one is shown in Figure 6. On the left-hand side of the figure, the T-S diagrams of two stations representing the east and west groups are compared, a data point being plotted every ten meters of water. The change in the salinity of the core layer from 35.5 o/oo to 35.3 o/oo was typical of the present observations and can be demonstrated as being generally valid from the data of this region contained in the NODC files. The iso-density lines of = 27.44 and 27.61 are indicated because it was at those densities that the discontinuities in the profiles (temperature, salinity and sound velocity) of the lowering to be reconstructed, No. 50, were observed.

On the right-hand side of Figure 6, two T-S diagrams are compared. The dots are data points from No. 50 (one every two meters), while the crosses define an artificial composition of the fresher (west) column, excluding the layer between the density limits, and that part of the saline layer of the east column which was between the density limits. The comparison is thought to be remarkably good; the temperature and salinity discontinuities across the upper interface are almost exactly reproduced. Lowering of Nos. 45 and 49 can be similarly reconstructed, and in this manner one group of transitional profiles can be inferred to have evolved from the penetration of a saline water layer into a fresher water column. A schematic of this interpretation is shown in Figure 7.

Stern (1967) has hypothesized that the lateral encounter of two water masses such as described here will result in the mutual penetration of each one into the other. The velocity profile (Figure 2) and the T-S diagram of No. 44 give some indication

that this column may be the result of the inverse penetration. Attempts to reconstruct such an occurrence, however, were unconvincing and the question is left open.

Instability of Transitional Profiles

The inversions in the velocity profiles may be assumed to dissipate rapidly, despite the fact that they were gravitationally stable. The upper interface of one intrusion is profiled in Figure 8 and is seen to be a sharp boundary between colder fresher water above and warmer more saline water below. In a series of tank experiments, Turner and Stommel (1964) and Turner (1965) investigated the mechanism and transfer rates across this class of interface. When the gravitational stability provided by the salinity was large compared to the inverse tendency to overturn associated with the temperature gradient considered alone, vertical transfer rates were low. Reducing the relative stability by considering smaller salinity differences caused the interface to undulate, with breaking waves providing an eddy mechanism for an accelerated transfer of both heat and salt to the upper layer. In the present observations the gravitational stability parameter was low (density differences due to salinity were only 50% greater than the opposing differences due to temperature) and large effective diffusion coefficients should be expected, at least in the early stages after penetration. Furthermore, the possibility of "salt-fingering" at the lower interface of the intrusion will tend to decrease the stability of the upper interface and enhance transfer rates there.

Summation and Possible Extension

It has been shown that the Mid-Atlantic Ridge marks a change in the sound velocity profile in the region studied. Although this change is not overly significant it was seen that, in the process of changing, unusual distortions occur in the region of the sound channel axis. The distorted profiles were not found to be permanently located, and it is supposed that their creation at any given time will depend on the local water movement at a depth of around 1,000 meters. The primary effect of the presence of the ridge is thought to be that it sufficiently controls these water movements so that a quasi-stationary transitional zone is established at the ridge axis.

Two types of transitional profiles were reported. One was characterized by an inversion layer above the sound channel axis, and it was shown how it may arise from the penetration of the local manifestation of Mediterranean water into a fresher water column. It was further suggested that the inversion layers would rapidly be eroded away by vertical mixing. The other type of

profile, which had a thick iso-velocity layer at the channel axis, may have been caused by a reverse penetration, but the point could not be demonstrated.

A final question to be asked is, "How widespread is this disturbance to the sound channel?" Shallow ridge crests and comparably saline core water can be found up and down the ridge, both north and south of the Azores, so that similar intrusions could occur. The proper approach to answer the question would be to investigate the salinity of the core layer across the ridge at various latitudes, but to do this from hydrocast data (samples typically spaced two hundred meters apart at the critical depths) is virtually impossible. As a substitute, until continuous salinity profiles are the rule, one can trace the salinity along an appropriate depth from a long section across the ridge. The salinity will vary with both diffusion and tilting of the isopycnal surfaces, but these should result in continuous changes with longitude, unless a phenomenon such as has been documented here is occurring. Depending then on the amount of scatter in the data due to temporal variations, some conjectures might be possible and two such plots are shown in Figure 9. The data is from the Atlantic Ocean Atlas (Fuglister, 1960) and a reference depth of 1,000 meters was selected because it was a frequent sample depth near the depth of maximum salinity. The plot at 40°N is essentially the same area as was studied here, and the expected discontinuity in salinity at the ridge axis is obviously present, agreeing even n magnitude with the data presented above. At 36°N, which runs just south of the Azores, there is some indication of a break at the Mid-Atlantic Ridge crest and a clear discontinuity at about the Azores-Gibraltar Lineament. The latter is deep (3,000 m) at this latitude but rises immediately to the northwest, where it becomes the Azores Platform. This type of evidence can be suggestive in locating other possible transition zones.

Acknowledgements:

The observations reported were made during the Mid-Atlantic Ridge survey of cruise No. 82 of R/V CHAIN. Data of this sort is very much a joint effort of the many hands on board, but I especially appreciated the presence of Joseph Phillips and Elizabeth Bunce who provided invaluable assistance by their knowledge of the topography of the ridge. Also making notabee contributions were William Rossow, who concluded the lowering program after I had left the cruise, and Mrs. Maxine Jones who programmed the date reduction.

The work was performed under contract Nonr-4029(00) with the Office of Naval Research.

Fuglister, F. C. (1960) Atlantic Ocean Atlas of temperature and salinity profiles and data from the International Geophysical Year of 1957-1958. Woods Hole Oceanographic Institution, 209 pp.

Piip, A. T. (1968) Precision sound velocity profiles in the ocean, Vol. IV. Tech. Rept. No. 6, CU-6-68, Lamont Geological Observatory, Columbia Univ., Palisades, New York, 78 pp.

Stern, M. E. (1967) Lateral mixing of water masses. Deep-Sea Res. 14, 747-753.

Turner, J. S. and H. Stommel (1964) A new case of convection in the presence of combined vertical salinity and temperature gradients. Proc. Nat. Acad. Sci. 52, 49-53.

Turner, J. S. (1965) The coupled turbulent transports of salt and heat across a sharp density interface. Int. J. Heat Mass Transfer 8, 759-767.

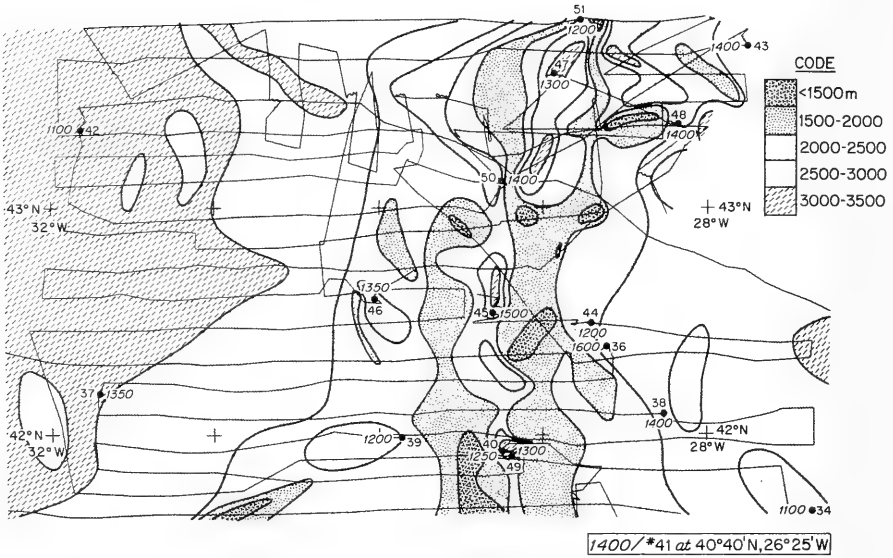

Figure 1.

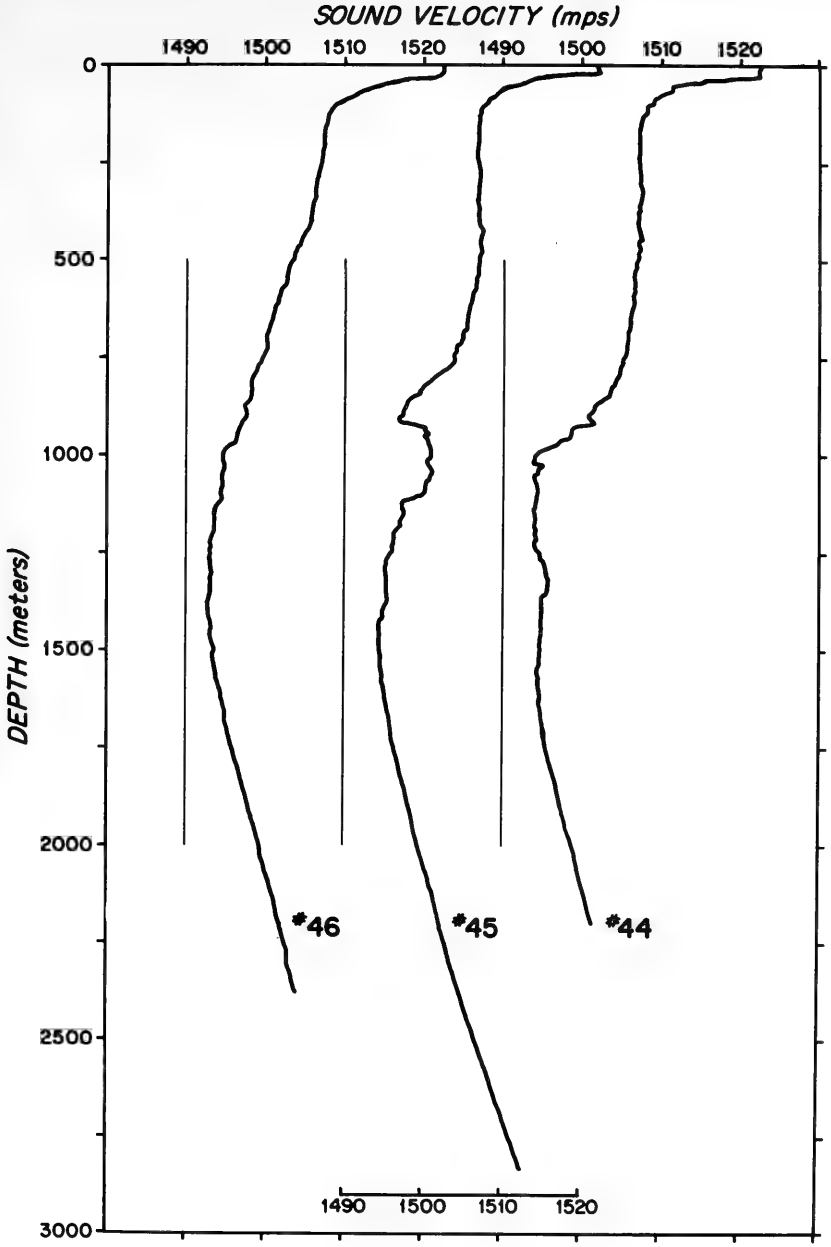
SOUND VELOCITY (mps)
1490
1500
1510
1520
1490
1500
1510
1520
0
500
1000
1500
2000
2500
3000
DEPTH (meters)
#46
#45
#44
1490
1500
1510
1520

Figure 2.

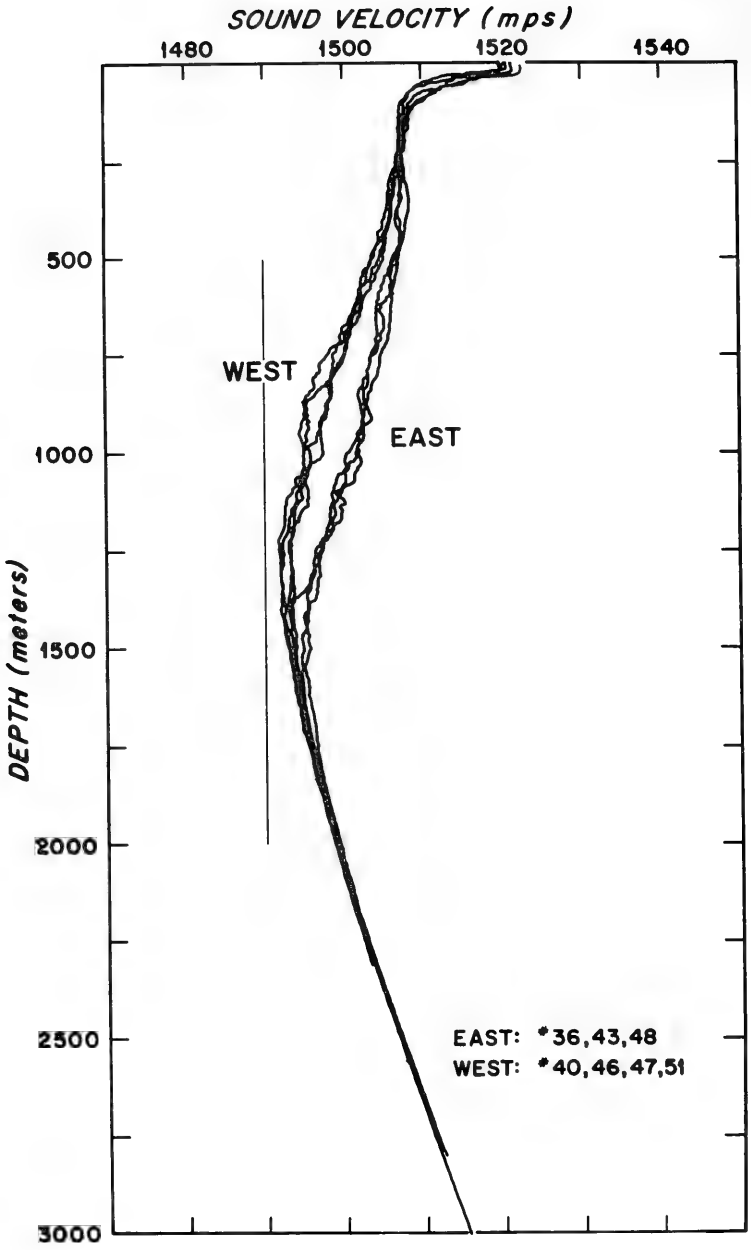
SOUND VELOCITY (mps)
1480
1500
1520
1540
500
1000
1500
2000
2500
3000
DEPTH (meters)
WEST
EAST
EAST: *36,43,48
WEST: *40,46,47,51

Figure 3.

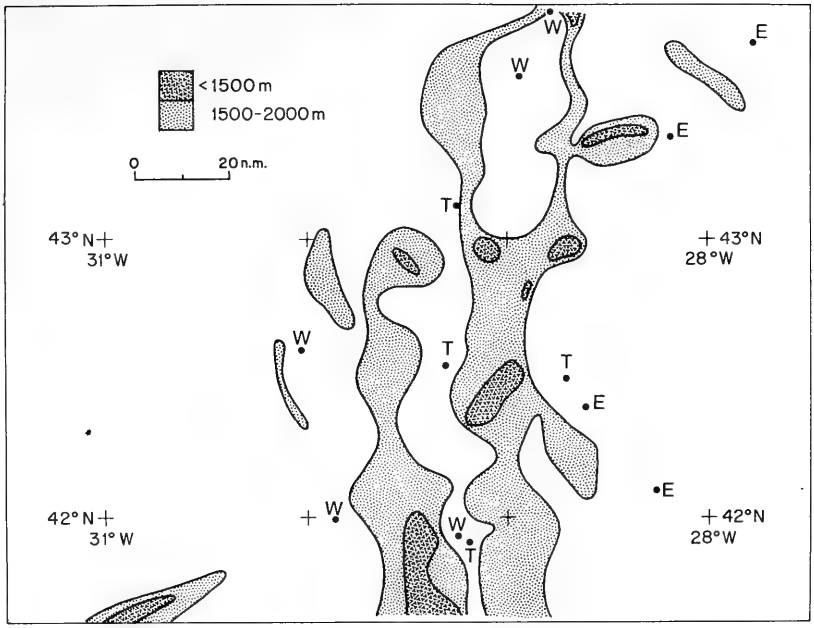

Figure 4.

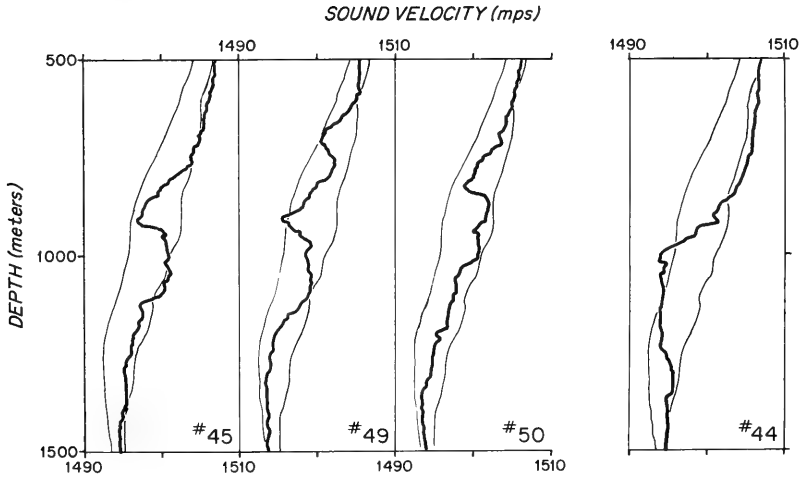

Figure 5

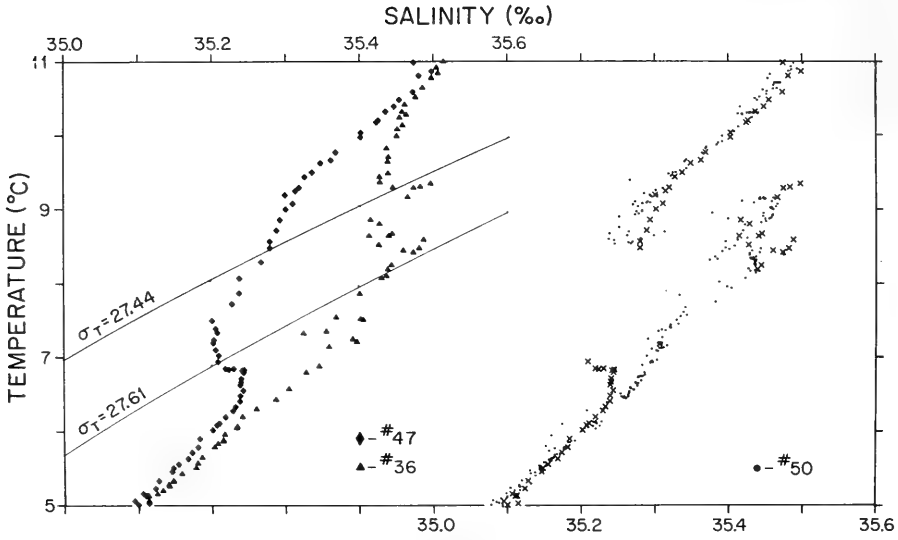

Figure 6

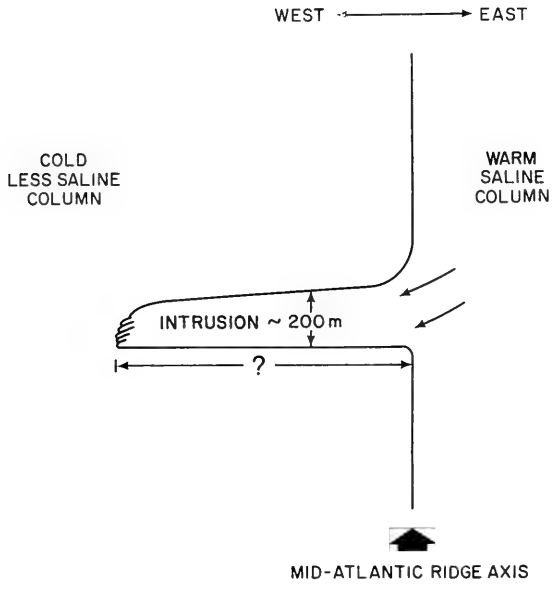

Figure 7

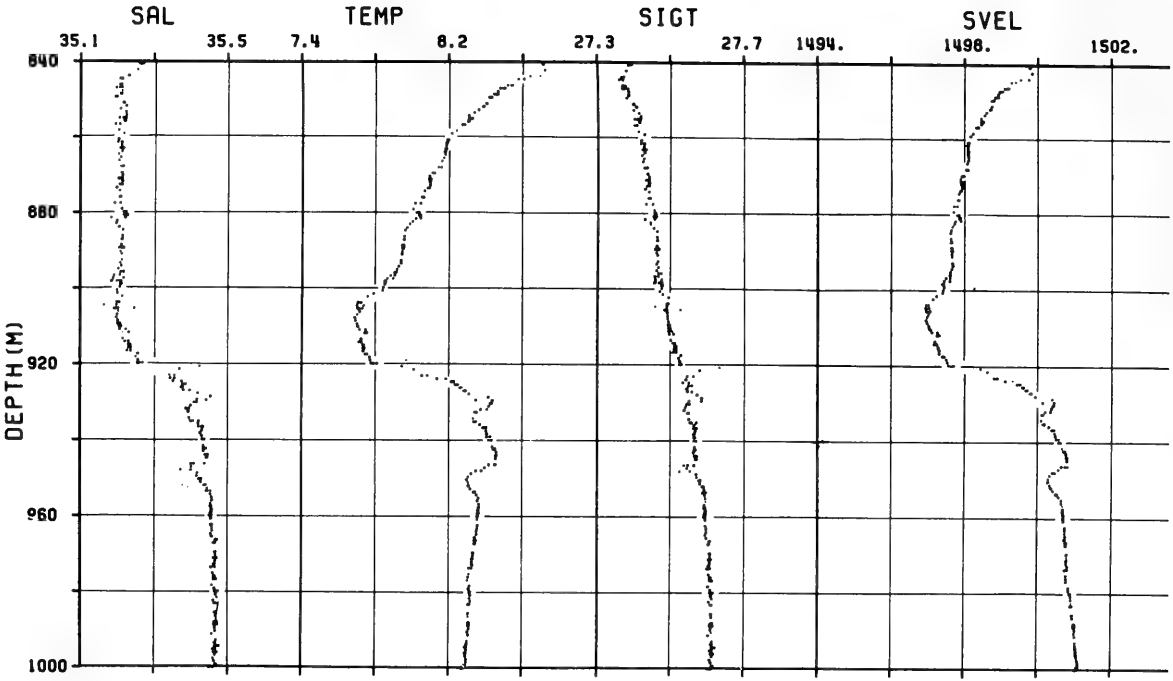
SAL
TEMP
SIGT
SVEL
35.1
35.5
7.4
8.2
27.3
27.7
1494.
1498.
1502.
840
880
920
960
1000
DEPTH (M)

Figure 8

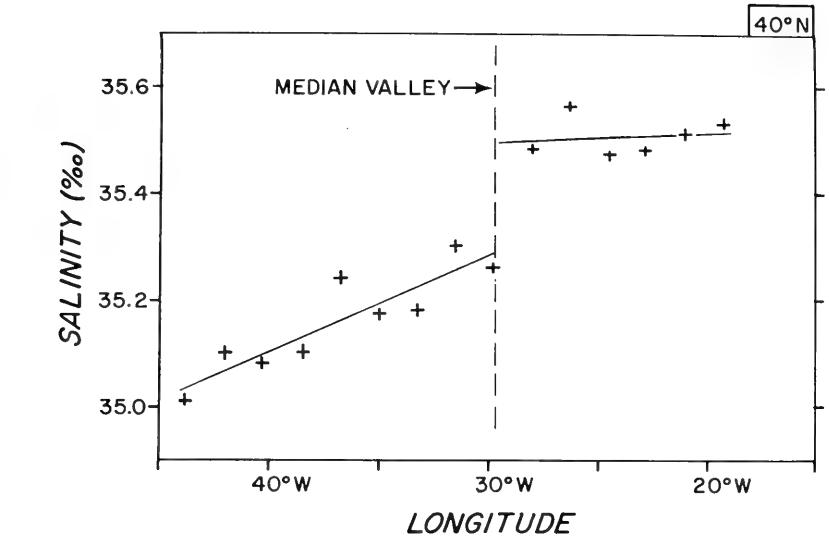
40°N
MEDIAN VALLEY
35.6
35.4
35.2
35.0
SALINITY (‰)
40°W
30°W
20°W
LONGITUDE

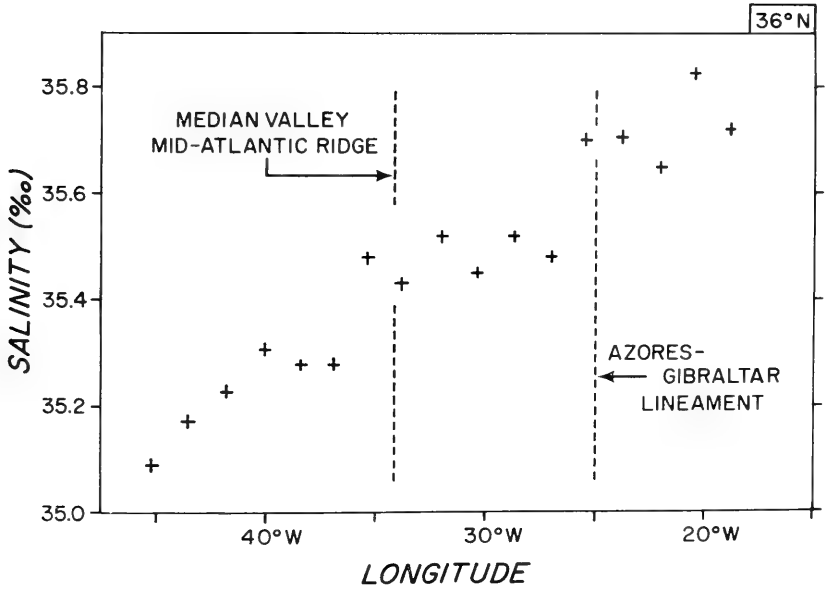
36°N
MEDIAN VALLEY
MID-ATLANTIC RIDGE
AZORES-
GIBRALTAR
LINEAMENT
35.8
35.6
35.4
35.2
35.0
SALINITY (‰)
40°W
30°W
20°W
LONGITUDE

Figure 9

THE HEAT OF MIXING OF SEAWATER

Donald N. Connors
Oceanography Branch Head
Naval Underwater Weapons Research and Engineering Station
Newport, R. I.

ABSTRACT

Experiments pertaining to the mixing of sea water were conducted using a simple copper calorimeter. The heat of mixing is determined from the change in temperature observed for the adiabatic mixing of two isothermal sea waters of different salinities. The temperature dependency of mixing sea waters with salinities of 10.2‰ and 60.5‰ was determined between 2° and 25°C. The observed change in temperature, as a function of temperature, can be expressed empirically as a quadratic:

$$\Delta T = -0.0736 + 3.11 \cdot 10^{-3} T - 4.72 \cdot 10^{-5} T^2$$

The salinity dependency of the heat of mixing was determined at 2°C using the salinity pairs 60.0/10.0, 54.6/15.0, 49.6/20.0, and 45.4/24.8‰. Within experimental error, a linear relationship exists between the partial specific enthalpy of sea salt and the salinity.

In recent years oceanographers have been using temperature measuring devices that can be read from 0.001C° to 0.0001C°. Mercury thermometers, by comparison, have a precision of about 0.01C°. This advance in the state of the art requires an evaluation of the assumption that temperature times mass is a conservative property of seawater for adiabatic mixing processes.

Adiabatic mixing in the ocean is usually discussed in terms of the temperature-salinity (T-S) diagram (Figure 1a). The assumption is made that when mixing water types A and B the resulting temperature and salinity lie on the straight line joining the two end members. In reality, for adiabatic mixing, the enthalpy (or heat content) is the thermodynamic property of interest, and one should employ a specific heat-content salinity diagram. The error incurred as a result of using a T-S diagram can be determined from a knowledge of the specific enthalpy of the waters mixed. An empirical equation for the enthalpy of seawater as a function of temperature and salinity can be determined from the heat capacity data of Cox and Smith (1959) and from a knowledge of the heat of mixing of seawater as a function of temperature.

Okubo (1951) has estimated the heat of mixing of seawater by using previously determined data on the heat of dilution for sodium chloride solutions at 25°C. Clark, Nabavian, and Bromley (1960) determined the heat of mixing of seawater at a salinity of 35‰ and a temperature of 29.4°C. By mixing 0.5 gm of 70‰ seawater with 0.5 gm of distilled water, they obtained a heat of mixing of -0.097±0.01 joules/gram. In both of these cases the data are insufficient for determining the thermodynamic properties of seawater as a function of temperature.

The preliminary results of a set of experiments for determining the temperature dependency of the heat of mixing of seawater are presented here. The calorimeter used (Figure 2) consisted of two copper cylinders, one inside the other and silver soldered to common end plates. The overall dimensions were 13.97 cm long by 11.43 cm in diameter. The inner cylinder had a series of holes running axially along the upper surface for filling and, upon inversion, for mixing. It was also offset from the axis of the outer cylinder to maximize thermal contact between the waters in the two cylinders. Located on the mid-point of the inner cylinder were two copper wells for positioning of thermistors. The two thermistors, wired in parallel, were calibrated at four or more temperatures between 0° and 28°C, using both ac and dc bridges. The plots of logarithm of resistance versus temperature were straight lines. Self-heating effects in the thermistors, as used, were found to be negligible.

The initial runs were made with an ac transformer bridge (Wayne Kerr High Precision Comparator, Model No. B821). An audio-oscillator (Hewlett-Packard, Model 201c) provided an excitation of 4 volts at 1 kHz. The output was monitored with a tuned amplifier and null detector (General Radio Co., Model No. 1232-A) and an oscilloscope (Hewlett-Packard, Model No. 120B). A 10 kilohm, 5-decade resistance box (Leads & Northrup) was used on the "standard" side of the bridge. Shielded and grounded leads

were used throughout. Early in the series of runs the ac bridge was abandoned in favor of a dc bridge. This bridge consisted of a Wheatstone bridge (Leeds & Northrup, Model No. 4735), a guarded dc null detector (Leeds & Northrup, Model No. 9834), and a regulated power supply (Lambda, Model No. LH 121 FM). The bridges could be read to 0.1 ohm and estimated to a few hundredths of an ohm.

In a typical run, approximately 300 ml of a high and a low salinity seawater were pipetted into the inner and outer cylinders, respectively. The high salinity seawater was covered with a thin layer of mineral oil to prevent water vapor transport with its concomitant salinity change and temperature gradient. The calorimeter was closed and cooled to a temperature slightly lower than the desired temperature of the run, and then placed into a dry, precooled, wide mouth Dewar flask. Styrofoam m inserts were used in the Dewar flask to fill up dead-air space and to prevent direct thermal contact between the calorimeter and the flask. The Dewar flask was sealed with a Styrofoam insulated plastic cover, and the whole assembly was clamped into a constant temperature water bath (Aminco, Model No. 4-8605) with a temperature control of ±0.02°C.

The temperature of the calorimeter was monitored by means of the ac or dc bridge described above. The temperature in the water bath was adjusted until the temperature in the calorimeter was relatively constant with time. The criterion used for equilibration was a rate-of-resistance change less than ±0.05 ohms/min. Equilibration time ranged from 1 to 24 hours. The two seawaters were mixed by inverting and rocking the Dewar flask/calorimeter assembly. The possibility of introducing heat during the mixing procedure was checked with 600 ml of distilled water in the calorimeter. No detectable change in temperature was observed.

The heat capacity of the Dewar flask/calorimeter assembly was determined by several methods. Initially, a known weight of water at a known temperature was introduced into the calorimeter. Since the initial and final temperatures as well as the heat capacity of the water were known, the heat capacity of the assembly could be calculated. After extensive modifications to the Dewar flask/calorimeter assembly, a second set of calibrations was carried out that more nearly reflected the experimental method used in the heat of mixing runs. Two sodium chloride solutions, 80.60‰ and 17.23‰ , were mixed at 25°C. From available data on the heat of dilution of sodium chloride solutions at 25°C (Harned and Owen, 1958) the theoretical temperature change was calculated. From this theoretical temperature change, the observed temperature change, and the weight and heat capacities of the solutions involved, the heat capacity of the Dewar flask/calorimeter was determined. This was assumed to be constant over the temperature range of the mixing experiments; i.e., from 1.93° to 25.3°C.

In an isothermal mixing experiment we would like to maximize the observed temperature change. This requires a maximum difference in the concentration of the waters to be mixed. The final concentration should be near c = 0.035 where c equals the grams of solute per gram of solution.

The maximum concentration we can use and still have seawater is approximately c = 0.070, since salts precipitate out of seawater with concentrations greater than this.

Harned and Owen (1958) have tabulated data on the relative partial heat content of sodium chloride at 25°C. (The relative partial heat content is the difference of the partial heat content of the salt at concentration c from that at infinite dilution.) The data are shown graphically in Figure 1b. Near infinite dilution, the relative partial heat content varies approximately as the square root of the concentration; whereas between 10‰ and 70‰ salinity, it varies linearly with the concentration. Since sea salt is more than 90% sodium chloride, the choice of seawaters to be mixed (at 25°C) was c = 0.01 and c = 0.06, for a final c of 0.035.

The low temperature concentration dependency of the heat of mixing was determined from a series of mixing experiments performed at 2°C. Ideally we would hope for a linear relationship between the partial specific heat content of sea salt $\bar{h}_s$ and the concentration c; i.e.,

$$\bar{h}_s = \bar{h}_1 + c\,\bar{h}_2 \tag{1}$$

where $\bar{h}_s = \left(\frac{\partial h}{\partial c}\right)_{T,\,P}$.

Since seawater can be regarded as a two component system made up of water and sea salt, the specific heat content at a temperature is:

$$h\,(T, c) = (1 - c)\,\bar{h}_w + c\bar{h}_s \,. \tag{2}$$

The concentration dependences of $\bar{h}_w$ and $\bar{h}_s$ can be related by the Gibbs-Duhem equation

$$c\,\frac{\partial \bar{h}_s}{\partial c} = -(1 - c)\,\frac{\partial \bar{h}_w}{\partial c} = c\bar{h}_2 \tag{3}$$

Assuming (1-c) ≈ 1 and integrating, we obtain

$$\bar{h}_w = \bar{h}_o - \frac{c^2\,\bar{h}_2}{2} \tag{4}$$

Substituting equations (1) and (4) into equation (2) and neglecting terms of order greater than 2, we obtain

$$h = (1 - c)\,\bar{h}_o + c\bar{h}_1 + \frac{c^2\,\bar{h}_2}{2} \tag{5}$$

The coefficients $\bar{h}_o$, $\bar{h}_1$ and $\bar{h}_2$ are functions of temperature; however, $\bar{h}_o$ will not be equal to the specific heat content of pure water since equation (1) is not valid for low concentrations. It is an empirical parameter which can be evaluated for the range of concentration where the linear approximation holds.

If 1-x gm of seawater of concentration c is mixed adiabatically with x gm of concentration $c + \Delta c$ (both at a temperature T), the temperature of the mixture T_f will differ from the temperature before mixing. The concentration of the mixture is $c + x\,\Delta c$, and its specific heat content is

$$h(T_f, c + x\Delta c) = (1-x\Delta c)\,\bar{h}_o(T,c) + x\Delta c\,\bar{h}_1(T) + x(2c\Delta c + \Delta c^2)\,\bar{h}_2(T)/2 \quad (7)$$

The specific heat content of the mixture at the original temperature T is:

$$h(T, c + x\Delta c) = (1-x\Delta c)\,\bar{h}_o(T,c) + x\Delta c\,\bar{h}_1(T) + (x\Delta c^2 + 2c\Delta c)\,\bar{h}_2(T)/2 \quad (8)$$

The change in temperature $T_f - T$ is therefore

$$T_f - T = \frac{h(T_f, c + x\Delta c) - h(T, c + x\Delta c)}{C_p} = + x(1-x)\,\Delta c^2\,\bar{h}_2(T)/2C_p \quad (9)$$

The temperature change on mixing two isothermal batches of seawater thus depends only on the value of the term $\bar{h}_2$ and is proportional to the square of the concentration difference.

The seawaters mixed were 60.0 with 10.0, 54.6 with 15.0, 49.6 with 20.0, and 45.4 with 24.8‰. They were made according to the formula and procedure of Kester, et al. (1967). The salinities were determined by the Mohr method of chloride titration; and, for the high salinity water, dilution and conductivity measurements were made. The silver nitrate solution used was standardized against I.A.P.O. standard seawater. The results are given in Table 1, and a plot of $\bar{h}_2$ versus $x(1-x)\Delta c^2$ is shown in Figure 3. Within an estimated experimental error of ±5%, Figure 3 indicates that the slope $\bar{h}_2$ of the linear equation for $\bar{h}_s$ is constant over the concentration range from 60‰ to 10‰.

The optimum salinities for determining the heat of mixing as a function of temperature are then 10‰ and 60‰. Therefore, a series of mixing experiments were carried out at various temperatures between 2° and 25.3°C on seawater of 10.2‰ and 60.5‰ salinity. The results are presented in Table 2 and are shown graphically in Figure 4.

The empirical equation for ΔT as a function of T is

$$\Delta T = -0.0736 + 3.11\cdot10^{-3}T - 4.72\cdot10^{-5}T^2. \quad (10)$$

Equation (10) can be substituted into equation (9) to obtain $\bar{h}_2$ as a function of temperature. Finally, $\bar{h}_o$ and $\bar{h}_1$ can be evaluated from heat capacity data to obtain an empirical equation for the enthalpy of seawater (equation 5) as a function of temperature and salinity.

ACKNOWLEDGEMENTS

The author wishes to thank Professor Peter K. Weyl of New York State University, Stony Brook, for his help and advice, and Mary McCann, of the Naval Underwater Weapons Research and Engineering Station, Newport, Rhode Island, for her assistance in carrying out some of the experimental work.

REFERENCES

Clark, R. L., K. J. Nabavian, and L. A. Bromley. (1960.) Heat of concentration and boiling point elevation of seawater. Adv. in Chem. Ser., 27:21-26.

Cox, R. A. and N. D. Smith. (1959.) The specific heat of seawater. Proc. Roy. Soc. London A 252, 51-62.

Harned, H. S. and B. B. Owen. (1958.) The physical chemistry of electrolyte solutions. Reinhold, N.Y. 3rd ed. 803 pp.

Kester, D. R., I. W. Duedall, D. N. Connors, and R. M. Pytkowicz. (1967) Preparation of artificial seawater. Limnol. Oceanog., 12:176-179.

Okubo, A. (1951) On the heat of mixing of seawater. Oceanographic Report (in Japanese, English abstract), 2, No. 1: 59-63.

Table 1. Concentration Dependency of the Partial Specific Enthalpy of Sea Salt.

Run #	Temp °C	$S‰_1$	$S‰_2$	ΔT C°	$\bar{h}_2$ J/gm
1	1.93	10.0	60.0	-0.067(0)	-860
2	1.90	10.0	60.0	-0.063(7)	-820
3	2.05	15.0	54.6	-0.041(1)	-840
4	2.02	15.0	54.6	-0.039(9)	-820
5	2.86	15.0	54.6	-0.040(6)	-830
6	2.00	20.0	49.6	-0.021(3)	-780
7	1.99	20.0	49.6	-0.022(1)	-810
8	2.08	24.8	45.4	-0.010(9)	-820
9	2.03	24.8	45.4	-0.010(5)	-790

$S‰_{final}$ = 35.0‰ to 35.4‰

Table 2. The Heat of Mixing 10.2‰ and 60.5‰ Salinity Seawater as a Function of Temperature

Run #	Temp. (°C)	$S‰_1$	$S‰_2$	$\Delta T(C°)$
1	25.3	10.2	60.5	-0.025(5)
2	24.6	"	"	-0.025(7)
3	21.4	"	"	-0.028(8)
4	20.0	"	"	-0.029(3)
5	15.0	"	"	-0.037(5)
6	14.2	"	"	-0.038(6)
7	9.15	"	"	-0.049(1)
8	3.10	"	"	-0.066(6)
9	2.75	"	"	-0.068(5)
10	2.00	"	"	-0.067(7)

$S‰_{final} = 35.8‰$

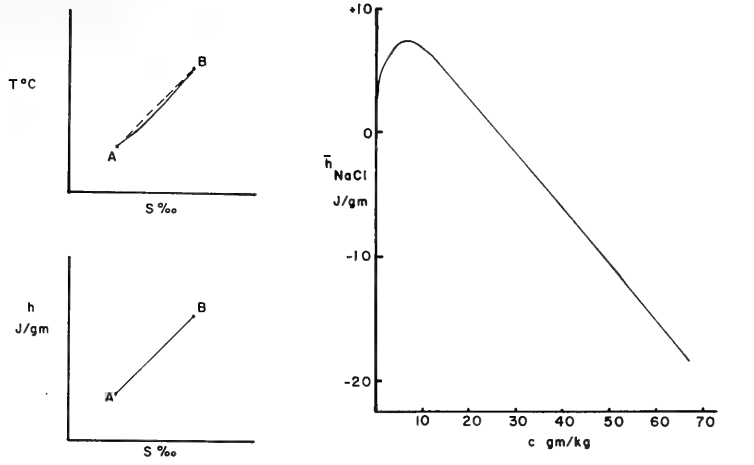

(a) Adiabatic mixing of seawater

(b) $\bar{h}_{NaCl}$ = Relative partial specific heat content of NaCl at 25°C

Figure 1.

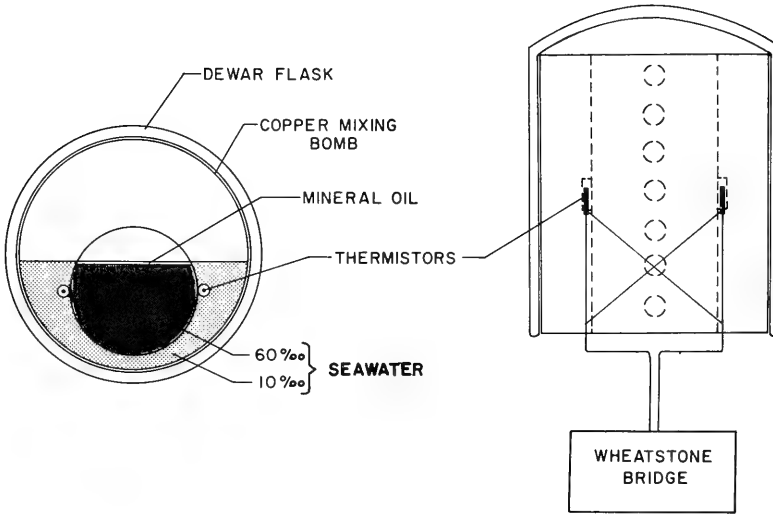

Figure 2.

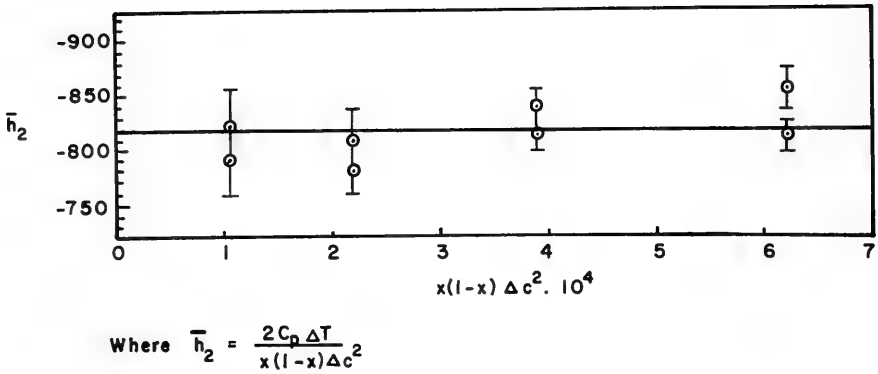

Figure 3.

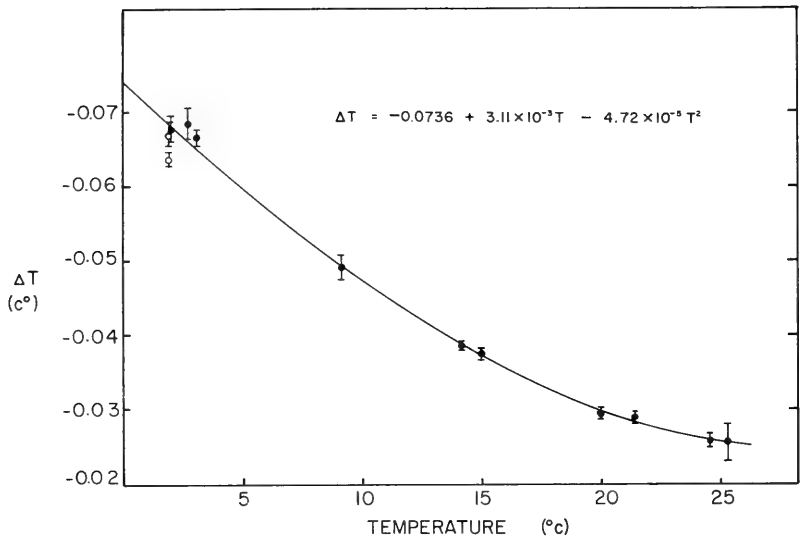

Figure 4.

SOUND SCATTERING LAYERS IN THE ARCTIC OCEAN OBSERVED FROM FLETCHER'S ICE ISLAND (T-3)

by
Kenneth Hunkins
Senior Research Associate
Lamont-Doherty Geological Observatory
of Columbia University
Palisades, N.Y., 10964

ABSTRACT

Continuous observations of sound scattering layers have been made in the Arctic Ocean from Fletcher's Ice Island (T-3) since 1963 with a 12 KHz sounder. A characteristic diffuse scattering layer between the depths of 25 and 200 m. was observed in the summers of 1963, 1964, 1965, and 1968, but not during the summers of 1966 and 1967. Since the ice island drifts continually, the measurements may indicate a spatial variation in this scattering layer which is superimposed on a seasonal cycle. The layer also varies diurnally, particularly at the time of the equinoxes when the maximum light contrast between day and night occurs.

Observations with a 100 KHz sounder in 1967 and 1968 showed that many individual scatterers are present in the upper layers even when no diffuse layer is observed at 12 KHz. The 100 KHz sounder was also able to resolve individual scatterers in the same layer which appeared cloud-like on the 12 KHz.

In addition the 100 KHz records show a persistent layer at a depth of about 50 m. This thin scattering layer coincides with the base of the homogeneous mixed layer. Tests are being made to determine whether this layer is caused by specular reflection from the density discontinuity or whether it is due to sound scattering from organisms or debris at that level.

Introduction

Sound returns from within the water column are often recorded with ships' depth sounders. These early returns arriving before the bottom echo are sound which has been either reflected or scattered by objects within the water. If the object is much larger than a wavelength, as for example a large fish, sound waves are specularly reflected. If the object is of the order of a wavelength or less in size, as may be the case for certain groups of plankton or for air bubbles, sound waves are scattered in all directions.

Both scattered and reflected arrivals appear on echo-sounder records made from a floating ice station in the Arctic Ocean (Hunkins, 1965). Scattering layers often appear at depths between 50 and 200 m in this ocean and often persist for several months. The arctic scattering layers have a diffuse, cloud-like appearance on echograms made with a 12 KHz sounder and sometimes occur as two or more layers (Fig. 1). One of the striking characteristics of the arctic scattering layer is its seasonal behavior. The layer generally appears only during the summer months, disappearing during the winter. This behavior is probably related to the special light conditions in the Arctic Ocean where the sun is above the horizon throughout the summer and below the horizon throughout the winter. The scattering layer, presumably biological in origin, responds to the predominantly seasonal light cycle.

Discrete reflected echoes from shallow depths are also noted on the echograms from T-3. These discrete echoes are frequently observed at shallow depths, even in the winter when no scattering layer is present. The discrete echoes often take a hyperbolic shape indicating relative movement between the ice station and the object.

The paper by Hunkins (1965) reported on the first two years of scattering layer observations at Fletcher's Ice Island, T-3. The same KHz Precision Echo Sounder has continued in operation almost without interruption at T-3 since it was first installed in June 1963. The system consists of a Gifft ESRTR-3 Sonar Transceiver, a UQN transducer, and a spark-type drum recorder. The repetition rate is once per second and the rate of chart advance is one cm per hour. The present paper describes the results of nearly six years of continuous monitoring from T-3 as it drifted under the influence of winds, currents, and pack ice pressure in the western Arctic Ocean. Since the data were taken from a single moving platform it is not possible to completely separate the temporal from the spatial variations of the layer. However, there is enough information to determine many of the layer's characteristics.

Variability in Time

The seasonal appearance and disappearance of the layer occurs suddenly and is easily determined from the records. The behavior of the arctic scattering layer as a function of time is shown in Figure 2 where its presence is indicated by the solid black bar. The layer was already present on June 19, 1963, when the echo-sounder began operation. It persisted, except for a short break, until August 24 of that year. The next year, 1964, it appeared in late June and persisted until early November, except for a short break in September. In 1965 it made only a short appearance in September and then disappeared for the following two years. No evidence of the arctic scattering layer was seen in 1966 and 1967, although the same sounder continued to operate in nearly the same

manner as previous years. There may be some question on the operation during the summer of 1966 as the transducer face became covered with ice at that time, which weakened its sensitivity. However, in the fall of 1966 the transducer was reestablished well below the ice and there can be no question that the layer was not present in 1967. After this long hiatus, the layer appeared again in late March 1968 and remained until October 27 with a long gap in late summer. Recent records just returned from T-3 show that the layer again reappeared on April 15, 1969.

For four seasons the layer has thus made a summer appearance and apparently is making a fifth appearance this year. It has appeared as early as March and disappeared as late as November. It has never been observed in December, January, or February. The lack of its appearance in 1966 may possibly be due to instrumental problems but the lack of appearance in 1967 is believed to be real. Since T-3 is drifting continually it is possible that the area of drift in 1966 and 1967 lacks the scattering layer and that this gap is explicable in terms of geographic distribution. This will be discussed further in the next section.

A diurnal variation in the scattering layer characteristics is also notable at certain times of the year. The best examples occur close to the autumnal equinox. Diurnal variations in solar radiation are most pronounced at the equinoxes, and the diurnal scattering behavior is very likely related to the light variations. Examples of this behavior are shown in Figure 3 for 1964 and in Figure 4 for 1965. The records are aligned so that recurring daily characteristics are evident. The scale is in terms of local sun time. In Figure 3 a distinctive layer between the depths of 40 and 100 m appears at about 1900 and disappears at about 0500. This dense layer is surmounted by a shallow layer of discrete echoes which may represent isolated specimens from the scattering layer or which may be predators feeding on it. This nighttime layer is centered generally about local midnight. In 1964, its duration was observed to increase fairly regularly each day from five hours on September 12 to 11 hours on September 29. During this same period the hours of darkness increased from approximately 8 to 13. There seems to be a direct correlation between the duration of the nighttime layer and the hours of darkness, with the layer appearing about one hour after sunset and disappearing about one hour before sunrise.

Variability in Space

T-3 is drifting in a circular current pattern (Figure 5). The ice moves clockwise about the gyre and completes one orbit in about five years. Between 1963 and 1969, T-3 covered slightly more than one revolution in an orbit with a diameter of about 800 km. The ice station was drifting in water depths of more than two km throughout the period. The presence of the scattering layer on

the drift track is indicated by the heavily thickened track line in Figure 5. The seasonal appearances of the scattering layer are all seen to be on the northern and eastern sides of the gyre. In 1966 and 1967 when the layer failed to appear, T-3 was drifting on the southern and western sides of the gyre. By the summer of 1968 the ice island was back in the same location it had been in 1963 when the layer was first discovered and, indeed, the layer reappeared in 1968. This suggests that the summer appearance of the layer has a definite geographic pattern which does not change from year to year. As T-3 drifts around the gyre the geographic pattern is superimposed on the seasonal pattern to give the observed behavior in time.

Observations With a 100 KHz Sounder

A high-frequency, narrow-beam echo sounder was installed at T-3 in March 1967 in an attempt to resolve individual scatterers within the layer. The instrument is a Ross model 200 A Fish Finder operating at 100 KHz. The sounding rate is 120 per minute with 250 watts of peak pulse power delivered to the transducer. The eight-element transducer has a beam angle of 5^{o} x 10^{o}. This sounder often resolves individual targets within the scattering layers. The short pulse length, rapid chart speed, high frequency and narrow beam all contribute to the increased resolution.

The most interesting finding with this sounder was a thin continuous scattering or reflecting layer at 50 m depths. This layer normally forms a thin straight line across the chart with a thickness of one or two meters. At times the line may thicken or thin slightly. At other times it may be deformed into undulations which probably represent internal wave motions (Fig. 7). There is generally a sharp increase in individual scatterers below this layer. This thin layer is never observed with the 12 KHz sounder. The records are not as continuous as they are for the 12 KHz sounder, but there does seem to be a tendency for the thin layer to disappear in late summer.

Water Structure and the Arctic Scattering Layers

The scattering layers are associated with characteristic features of the arctic water column. The distributions of temperature, salinity and sigma-t with depth which are shown in Figure 6 are typical of the entire area of the Arctic Ocean under discussion.

Four water masses are generally recognized: Arctic surface water, Pacific water, Atlantic water, and Arctic deep water. The surface water, with a temperature of about $-1.7^{o}C$ and salinity between 29 and $31^{o}/oo$, extends to a depth of 50 m. The profile in Figure 6 was taken in late winter when the surface water was well

mixed. In summer, melt-water runoff tends to stratify this layer and the sharp transition at 50 m disappears.

The Pacific water is characterized by a temperature maximum of -1.2 to -1.4°C at 75 m. The layer extends from 50 to 200 m. This water mass comes from the Pacific entering the Arctic Ocean through Bering Strait. Salinity increases with depth from about 30°/oo in this layer.

The Atlantic water is marked by a temperature maximum of 0.5° C at 500 m and extends from 200 to 900 m in depth. This water mass enters the Arctic Ocean near Spitsbergen and then spreads at depth throughout the Arctic Ocean. Below the Atlantic water, Arctic deep water extends to the bottom with nearly constant salinity and temperatures of -0.3 to -0.4°C.

The 12 KHz scattering layer occurring between depths of 50 and 200 m therefore coincides with the Pacific water mass. This is a region of high stability due to a sharp increase in salinity. In polar waters where temperature variations are small, density is primarily controlled by salinity.

The thin layer at 50 m recorded by the 100 KHz sounder coincides with the top of the Pacific water where the steepest gradient in water properties within the entire column is found. Detailed oceanographic profiles were made on several occasions to check the coincidence of this layer and the sharp change in water properties. The Nansen bottles were visible on the record and their position with respect to the layer could be determined exactly. The sampling interval between Nansen bottles was 2 m in the vicinity of the thin 50 m layer. In all cases there was agreement between depth of the scattering layer and the interface between the surface and Pacific waters. The increase in numbers of individual scatterers below this layer may be connected with the increased stability of the water column. Organisms could maintain their level more easily in the sharp density gradient below 50 m than in the homogeneous water above 50 m.

Origin of the Arctic Scattering Layers

The seasonal behavior of the 12 KHz scattering layer which shows considerable variation from year to year strongly suggests that it is caused by animals. The marked diurnal behavior which correlates with light conditions during the autumnal equinox also supports a biological cause. No known physical properties of the water vary as irregularly as this scattering layer. Attempts to capture the responsible animal have not been especially successful. The quick changes in the layer suggest a highly mobile animal which would be difficult to net.

Although the causative organisms have not been definitely identified, William Hansen (personal communication) has suggested that the Polar Cod Boreogadus saida is the most likely scatterer. This fish is one of the most common nektonic species of the high Arctic seas and has been caught at T-3 and at other ice stations. The fish's gas-filled swim bladder would presumably be the actual scattering agent. Annual migrations of these fish in large schools could account for the seasonal behavior of the scattering layer. The geographic distribution of the layer may be due to preferred migration routes and feeding areas, although there is no ready explanation for the particular geographic distribution observed.

The origin of the thin scattering layer observed at 50 m depth with the 100 KHz sounder is also obscure. This layer coincides so precisely with a sharp change in density that a physical cause cannot be ruled out immediately for this layer. It is possible that sound is reflected specularly from the density interface. The Ross echo sounder is now being calibrated to determine whether the layer can be accounted for simply as a reflection. The other possibility is that objects closely associated with this pycnocline scatter the sound. Planktonic material, living or dead, might tend to accumulate at this interface. Observations in other oceans have also shown scattering layers at pycnoclines (Weston, 1958). Weston found that plankton trapped in the interfacial layer were the scattering agent. Plankton tows at T-3 have shown a concentration of the pteropod Spiratella helicina (Limacina helicina) at a depth of 50 m in the Arctic Ocean and this may be the scatterer in the present case (William Hansen, personal communication). The calcareous shell of this planktonic mollusc would provide the contrast in acoustic impedance needed to scatter sound.

Whatever its cause, this thin layer observed with the 100 KHz instrument is clearly a good indication of the motions of the top of the Pacific water. The observed period of oscillation in Figure 7 is about 10 min. The Vaisala or stability period was $2\frac{1}{2}$ minutes at 53 m, increasing to 10 minutes at 100 m. These are upper limits for internal wave motions. The observed motions are thus within the internal wave range and would have a slow speed of propagation at this period.

Acknowledgements

I am indebted to all those from the Arctic group at Lamont-Doherty Geological Observatory who successfully maintained the echo sounders on T-3.

This work was supported by the Office of Naval Research and by the U.S. Naval Ordnance Laboratory under contract Nonr 266(82).

References

Hunkins, K., "The seasonal variation in the sound-scattering layer observed at Fletcher's Ice Island (T-3) with a 12 kc/s echo-sounder," Deep-Sea Research, 12, 879-881, 1965.

Hunkins, K., "The deep scattering layer in the Arctic Ocean," U.S. Navy Journal of Underwater Acoustics, 16, 323-330, 1966.

Weston, D.E., "Observations on a scattering layer at the thermocline," Deep-Sea Research, 5, 44-50, 1958.

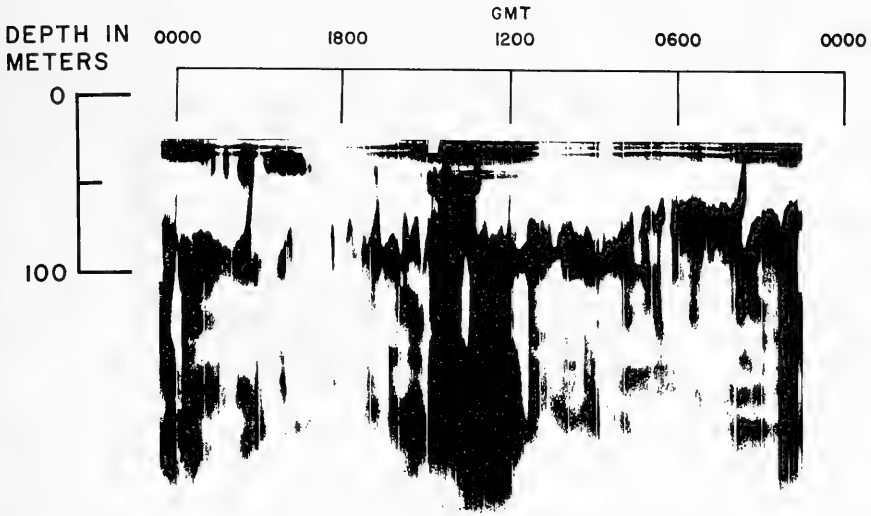

Figure 1.

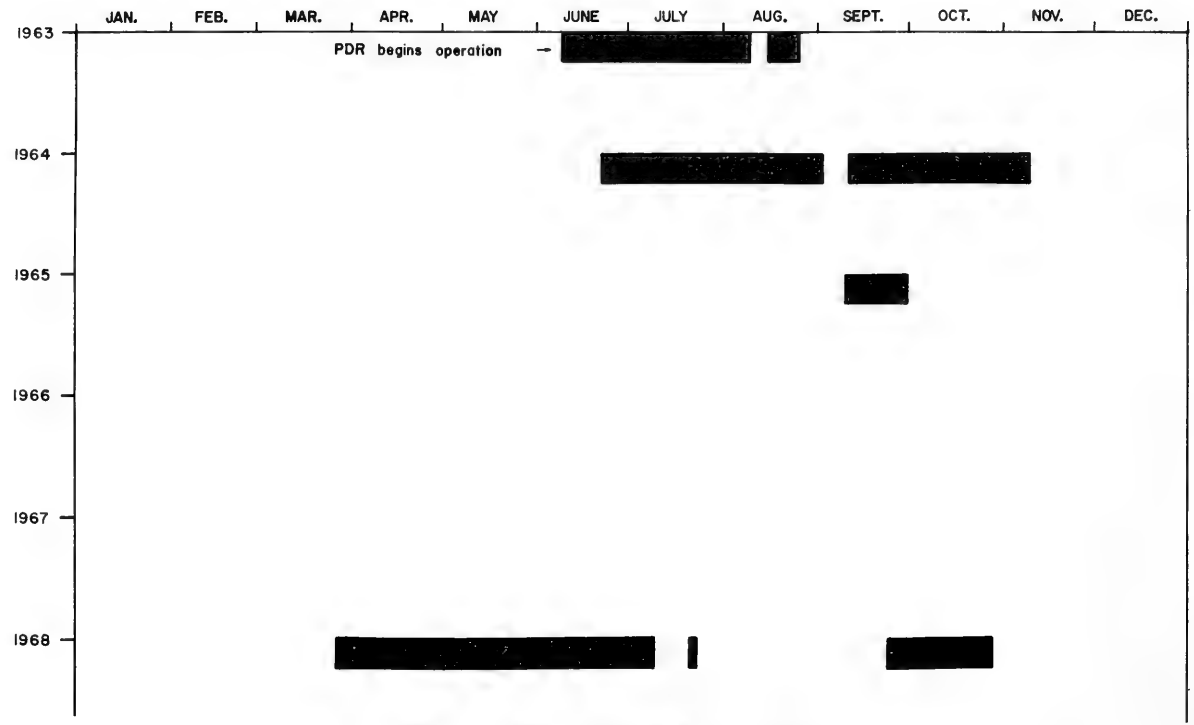
JAN.
FEB.
MAR.
APR.
MAY
JUNE
JULY
AUG.
SEPT.
OCT.
NOV.
DEC.
1963
PDR begins operation
1964
1965
1966
1967
1968
ARCTIC SOUND SCATTERING LAYER
observed from T-3 with 12kHz. sounder

Figure 2.

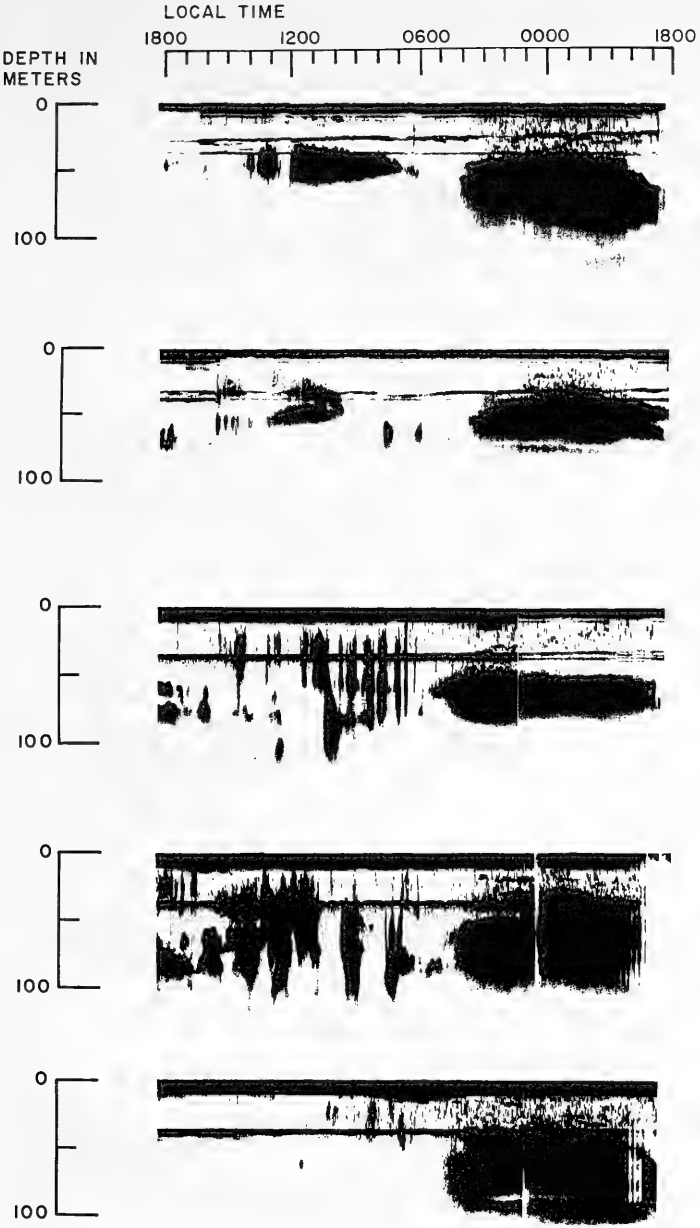
LOCAL TIME
1800
1200
0600
0000
1800
DEPTH IN METERS
0
100
0
100
0
100
0
100
0
100

Figure 3.

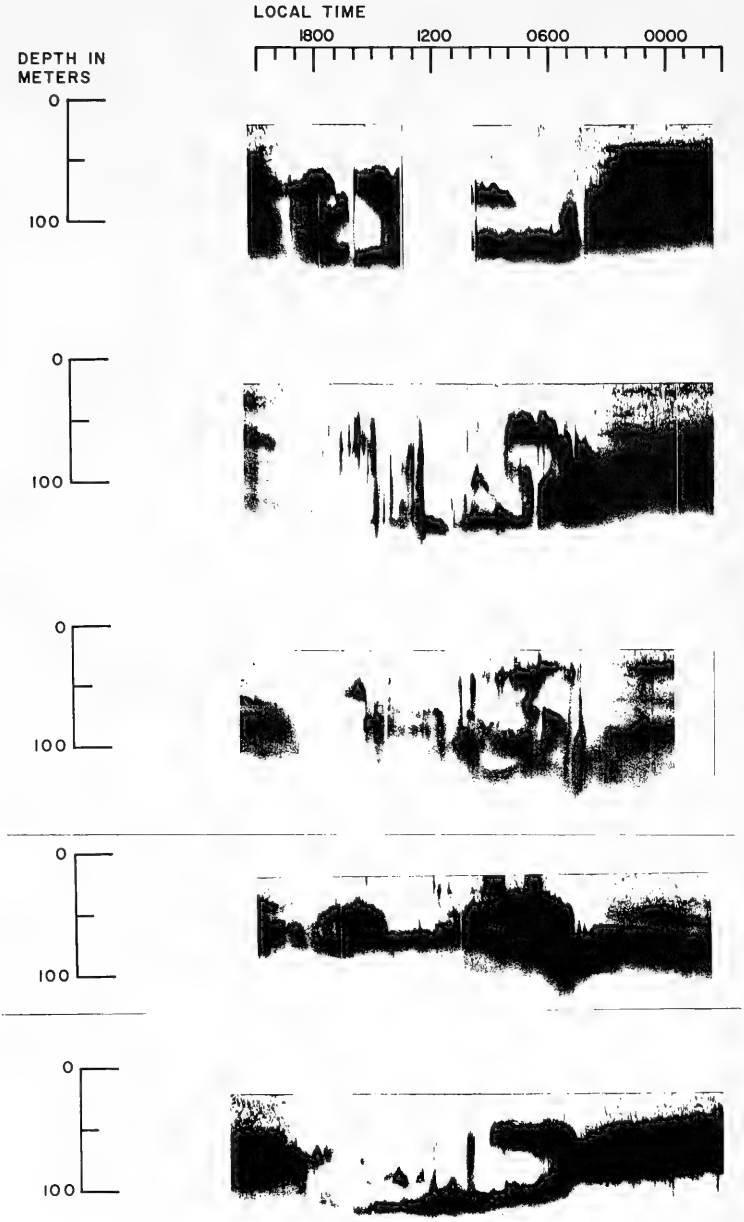
LOCAL TIME
1800
1200
0600
0000
DEPTH IN METERS
0
100
0
100
0
100
0
100
0
100

Figure 4.

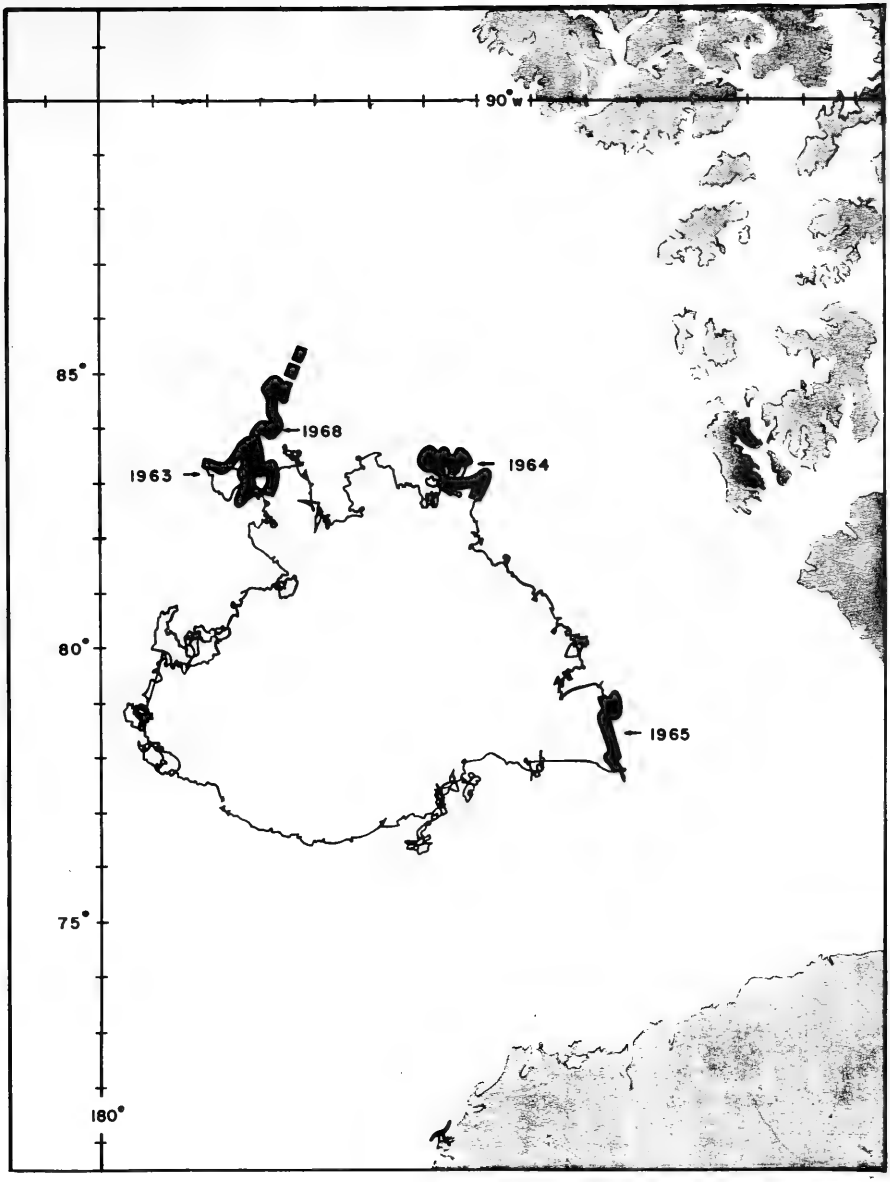

Positions of T-3 Scattering Layer Observations

Figure 5.

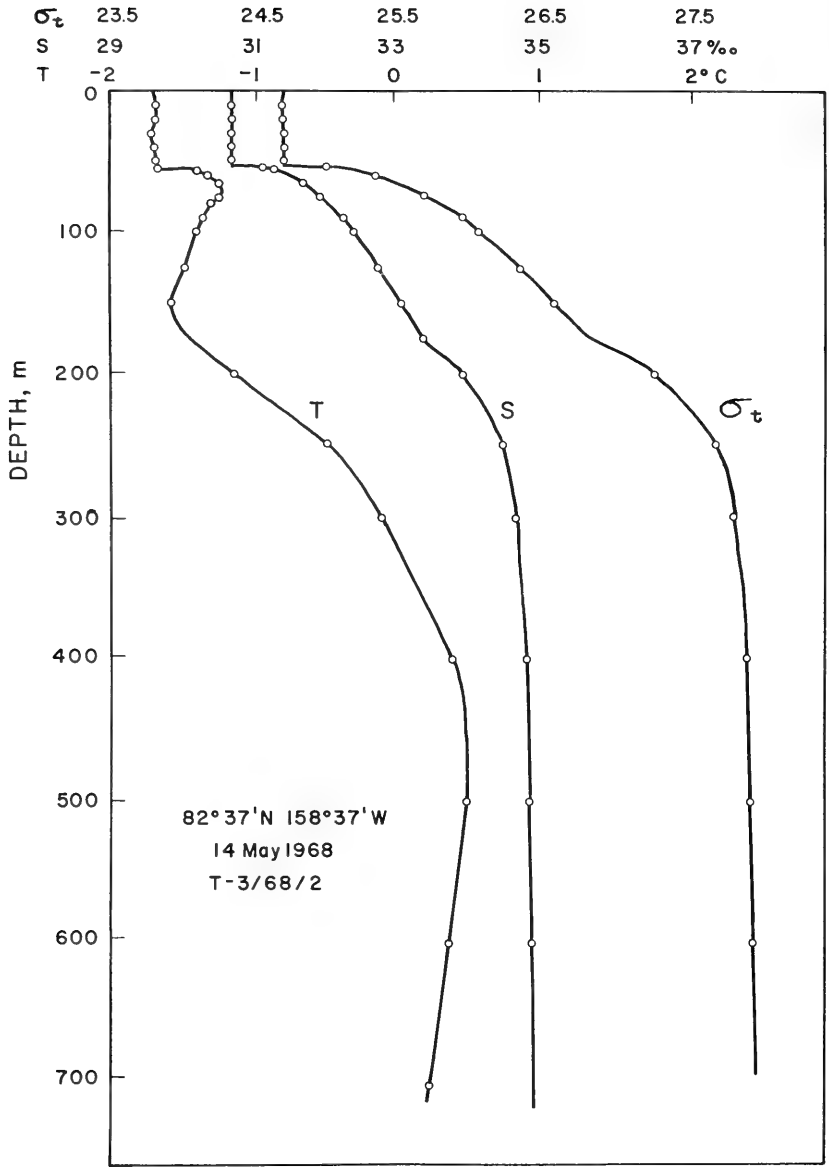
σt 23.5 24.5 25.5 26.5 27.5
S 29 31 33 35 37‰
T -2 -1 0 1 2° C
0
100
200
300
400
500
600
700
DEPTH, m
T
S
σt
82°37'N 158°37'W
14 May 1968
T-3/68/2

Figure 6.

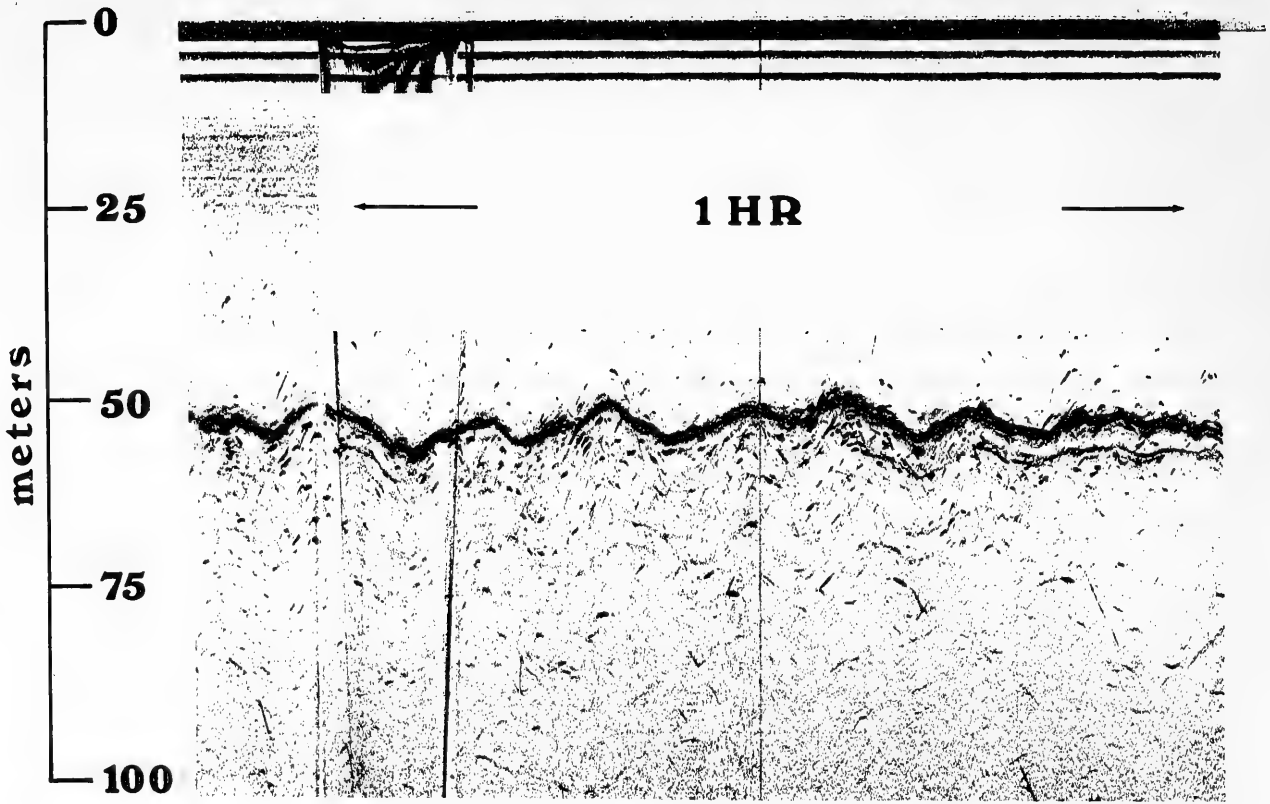

Figure 7.

PROBABILITY OF LOCATING A SUBMARINE WITHIN A STATED DISTANCE ON THE BASIS OF TWO DIRECTIONAL SENSORS

John E. Walsh*
Southern Methodist University

ABSTRACT

The general problem is to estimate the surface position under which a submarine is located. The information for this estimation is provided by two directional sensors whose locations are known. The observed directions, in combination with the sensor locations, are combined to yield the estimated position. The specific problem is to determine approximately the probability that the true submarine position is within a stated distance (on the ocean surface) of the estimated position. This article identifies the parameters involved and, in terms of these parameters, develops an approximate expression for the probability value.

Introduction.

The general problem is to estimate the surface position (on the ocean) under which a submarine is located. Here, all positions considered are on the ocean surface and, for brevity, the word "surface" is deleted in referring to positions or locations of the submarine or sensors.

The information for estimating the submarine position is provided by two directional sensors whose locations are known. That is, at a single fixed time, each sensor furnishes an observed direction (along the ocean surface) for the submarine location. These observed directions, in combination with the known locations of the sensors, yield an estimated location for the submarine at the time considered.

Let a circle with given radius be centered at the estimated submarine location. The specific problem is to determine approximately the probability that, at the time considered, the true submarine location is contained in this circle. This probability depends on the locations of the sensors, the radius of the circle, and on the probability distributions of the angular errors for the sensors. The purpose of this article is to identify the parameters involved and, in terms of these parameters, to develop an approximate expression for the probability that the circle contains the true (but unknown) location of the submarine.

Assumptions and Simplifications.

1. The ocean surface is considered to be flat (a geometric plane).

2. The submarine and the sensors can be represented as points.

3. The locations of the sensors are exactly known at the single time that is considered.

---

*Based on work done while the author was with Lockheed Aircraft Corporation and with System Development Corporation. Written in association with the Office of Naval Research Contract No. N00014-68-A-0515.

4. Time coordination is such that the angle readings for the location of the submarine position, as provided by the sensors, correspond to the observed submarine position at the time considered.

5. The observed directions furnished by the two sensors are statistically independent.

6. The observed direction provided by a sensor, at the time considered, has a normal (Gaussian) probability distribution with mean equal to the true direction of the submarine.

7. The sensors are positioned so that true submarine direction from any sensor is substantially different from the direction of the other sensor (with respect to this sensor).

8. The standard deviations of the angular probability distributions for the sensors are known and small (say, at most 0.03 radians). This combined with assumption 7, is considered to imply that second and higher order terms in angular errors (deviations from true direction) can be neglected in mathematical expressions.

Notation and Relationships.

For standardization purposes, and ease of analysis, one sensor is considered to be located at the origin of the (x,y) rectangular coordinate system that is used to represent the ocean surface. The second sensor is considered to be located at (D,0), where $D > 0$ is the distance between the sensors. Also, the submarine is considered to be located in the first quadrant. These standardizations do not represent any loss of generality for the type of analysis that is made.

The true location of the submarine is denoted by (A,B), while the position estimated on the basis of the directional observations is (X,Y). With respect to the first sensor, the true angular direction of the submarine is α_1 radians, while the observed angle $\alpha_1+\ell_1$ radians. For the second sensor, the true direction is α_2 radians, and the observed direction is $\alpha_2+\ell_2$ radians. Figure 1 contains a schematic diagram that illustrates the standardization and notation used.

Now, consider some relationships that occur for this situation. First, α_1 and α_2 are directly determined by A, B, and D. That is, $\tan \alpha_1 = B/A$ and $\tan \alpha_2 = B/(A-D)$, where A-D can be negative. Second,

$$X = D\{1 + \cot(\alpha_2 + \ell_2)/[\cot(\alpha_1 + \ell_1) - \cot(\alpha_2 + \ell_2)]\}$$

$$= D \cot(\alpha_1 + \ell_1)/[\cot(\alpha_1 + \ell_1) - \cot(\alpha_2 + \ell_2)]$$

$$Y = D/[\cot(\alpha_1 + \ell_1) - \cot(\alpha_2 + \ell_2)].$$

In addition, the following relations are useful in the derivations:

$$\cot(\alpha + \varepsilon) = (1 - \tan \alpha \tan \varepsilon)/(\tan \alpha + \tan \varepsilon),$$

and, for ε reasonably small (ε in radians), $\tan \varepsilon \doteq \varepsilon$, so that

$$\cot(\alpha + \varepsilon) \doteq (1 - \varepsilon \tan \alpha)/(\varepsilon + \tan \alpha) = [1 - \varepsilon(\tan \alpha + \cot \alpha)]/\tan \alpha ,$$

where α is not small.

Estimate of Submarine Position.

The method used to develop the approximation to the probability being sought consists in first approximating X and Y by linear functions of ℓ_1 and ℓ_2. The derivation of these linear functions (justified by assumptions 7 and 8) is given in detail

First, consider the linear expression for Y. Examination shows that $(Y/D)^{-1}$ approximately equals

$$[1 - \ell_1(\tan \alpha_1 + \cot \alpha_1)]/\tan \alpha_1 - [1 - \ell_2(\tan \alpha_2 + \cot \alpha_2)]/\tan \alpha_2$$

$$= \frac{\tan \alpha_2 - \tan \alpha_1}{\tan \alpha_1 \tan \alpha_2} \left\{ 1 - \ell_1 \left[\frac{(\tan \alpha_1 + \cot \alpha_1)\tan \alpha_2}{\tan \alpha_2 - \tan \alpha_1} \right] + \ell_2 \left[\frac{(\tan \alpha_2 + \cot \alpha_2)\tan \alpha_1}{\tan \alpha_2 - \tan \alpha_1} \right] \right\}.$$

Thus, Y approximately equals

$$\frac{D \tan \alpha_1 \tan \alpha_2}{\tan \alpha_2 - \tan \alpha_1} \left\{ 1 + \ell_1 \left[\frac{(\tan \alpha_1 + \cot \alpha_1)\tan \alpha_2}{\tan \alpha_2 - \tan \alpha_1} \right] - \ell_2 \left[\frac{(\tan \alpha_2 + \cot \alpha_2)\tan \alpha_1}{\tan \alpha_2 - \tan \alpha_1} \right] \right\}.$$

Hence, Y is approximately expressed in the form $a' + b'\ell_1 + c'\ell_2$, where a', b', and c' can be expressed as functions of A, B, D, on the basis of the derived relation. For example it is easily verified that $a' = B$.

Finally, consider the approximate linear expression for X. This can be developed through multiplication of the approximate expression for Y by the approximating linear expression (linear in ℓ_1) for $\cot(\alpha_1 + \ell_1)$. This yields

$$\frac{D \tan \alpha_2}{\tan \alpha_2 - \tan \alpha_1} \left\{ 1 + \ell_1 \left[\frac{1 + (\tan \alpha_1)^2}{\tan \alpha_2 - \tan \alpha_1} \right] - \ell_2 \left[\frac{(\tan \alpha_2 + \cot \alpha_2)\tan \alpha_1}{\tan \alpha_2 - \tan \alpha_1} \right] \right\}$$

as the approximate expression for X. Thus, X is expressed in the form $a + b\ell_1 + c\ell_2$, where it can be shown that $a = A$. Also b and c can be expressed as functions of A, B, D, that are determined by the derived expression.

Relation for Inclusion in Circle.

It is easily verified that the submarine location is contained in the circle of radius R centered at (X,Y) if and only if

$$(X - A)^2 + (Y - B)^2 \leq R^2 .$$

Stated in terms of the linear approximations to X and Y, this relation becomes

$$(1) \qquad (b\ell_1 + c\ell_2)^2 + (b'\ell_1 + c'\ell_2)^2 \leq R^2 ,$$

or equivalently

$$\sigma_1^2[b^2 + (b')^2](\ell_1/\sigma_1)^2 + 2\sigma_1\sigma_2(bc + b'c')(\ell_1/\sigma_1)(\ell_2/\sigma_2) + \sigma_2^2[c^2 + (c')^2](\ell_2/\sigma_2)^2 \leq R^2 ,$$

where σ_1 is the standard deviation of ℓ_1 , and σ_2 is the standard deviation of ℓ_2 . The problem is to evaluate the probability that this relation is satisfied.

The first step in this evaluation is to change, by linear transformations, from the random variables ℓ_1 , ℓ_2 to new random variables t_1 , t_2 . This is done so that t_1 and t_2 are standardized normal and independent. Also, so that relation (1) takes the form

$$v_1t_1^2 + v_2t_2^2 \leq R^2 .$$

In this form, existing methods are directly usable for approximately evaluating the probability that this relation holds.

Statement of Transformations.

The relation (1) can be expressed as

$$\sum_{i,j=1}^{2} A_{ij}(\ell_i/\sigma_i)(\ell_j/\sigma_j) \leq R^2 ,$$

where the matrix $||A_{ij}||$ equals

$$\begin{vmatrix} \sigma_1^2[b^2 + (b')^2] & \sigma_1\sigma_2(bc + b'c') \\ \sigma_1\sigma_2(bc + b'c') & \sigma_2^2[c^2 + (c')^2] \end{vmatrix} .$$

Let $||A^{ij}|| = ||A_{ij}||^{-1}$, and use $\lambda_1 \geq \lambda_2$ to denote the characteristic roots of $||A^{ij}||$. Since $A^{12} = A^{21}$, the values of λ_1 and λ_2 are the roots of

$$(A^{11} - \lambda)(A^{22} - \lambda) - (A_{12})^2 = 0 .$$

Specifically,

$$\lambda_1 = \frac{1}{2}\{A^{11} + A^{22} + [(A^{11} - A^{22})^2 + 4(A_{12})^2]^{1/2}\} ,$$

$$\lambda_2 = \frac{1}{2}\{A^{11} + A^{22} - [(A^{11} - A^{22})^2 + 4(A_{12})^2]^{1/2}\} ,$$

are values for λ_1 and λ_2 , where both values should be positive.

Let the y_{gi} be any set of four numbers (not all zero) satisfying the

four equations.

$$-\lambda_g y_{gi} + \sum_{j=1}^{2} A^{ij} y_{gj} = 0 , \qquad (i,g = 1,2) ,$$

(there are an infinite number of possible choices). Define the numbers C_{gi} by

$$C_{gi} = y_{gi} [\sum_{j=1}^{2} y_{gj}^2]^{-1/2} ,$$

and let

$$w_g = \sum_{i=1}^{2} C_{gi} (\ell_i/\sigma_i) .$$

Here, w_1 and w_2 are independent and $Ew_1 = Ew_2 = 0$. Then,

$$\sum_{i,j=1}^{2} A_{ij} (\ell_i/\sigma_i)(\ell_j/\sigma_j) = \sum_{g=1}^{2} w_g^2/\lambda_g .$$

It is easily verified that the variance $w_g/\sqrt{\lambda_g}$ is

$$v_g = \sum_{i=1}^{2} C_{gi}^2/\lambda_g , \qquad (g = 1,2) .$$

Let t_g equal $w_g/\sqrt{\lambda_g v_g}$. Then,

$$\sum_{i,j=1}^{2} A_{ij} (\ell_i/\sigma_i)(\ell_j/\sigma_j) = \sum_{g=1}^{2} v_g t_g^2 ,$$

where t_1 , t_2 are independent and standardized normal. Thus,

$$P(v_1 t_1^2 + v_2 t_2^2 \leq R^2) = P(v_2 t_1^2 + v_1 t_2^2 \leq R^2)$$

approximately equals the probability that the submarine position is within a distance R (on the ocean surface) from the estimated position (X,Y).

The procedure used to make these transformations is the method of principal components (for example, see ref. 1).

Evaluation of Probability.

Let $v = \min(v_1 , v_2)$ and $V = \max(v_1 , v_2)/v$. The probability to be approximately evaluated can be expressed in the form

$$P(t_1^2 + Vt_2^2 \leq R^2/v) .$$

One way of approximately evaluating probabilities of this form is by the method of ref. 2. Specifically, the cumulative distribution function of $t_1^2 + Vt_2^2$ can be expressed as

$$\sum_{w=0}^{\infty} H_w C_{2w+2}(x) ,$$

where $C_{2w+2}(x)$ is the cumulative distribution function for the continuous χ^2-distribution with $2w+2$ degrees of freedom. The H_w, which are non-negative numbers and satisfy $\sum_{w=0}^{\infty} H_w = 1$, are determined by the algebraic identity (in z)

$$V^{-1/2}[1 - (1 - 1/V)z]^{-1/2} \equiv \sum_{w=0}^{\infty} H_w z^w ,$$

for the expression that occurs for $|z|$ sufficiently small. Here,

$$[1 - (1 - 1/V)z]^{-1/2} = 1 + \frac{1}{2}(1 - 1/V)z + (3/8)(1 - 1/V)^2 z^2$$

$$+ (5/16)(1 - 1/V)^3 z^3 + (35/128)(1 - 1/V)^4 z^4 + \cdots$$

Thus,

$$H_0 = V^{-1/2} , \quad H_1 = \frac{1}{2}(1 - 1/V)V^{-1/2} , \quad H_2 = (3/8)(1 - 1/V)^2 V^{-1/2} ,$$

$$H_3 = (5/16)(1 - 1/V)^3 V^{-1/2} , \quad H_4 = (35/128)(1 - 1/V)^4 V^{-1/2} , \text{ etc.}$$

For practical applications, the inequalities ($W \geq 0$)

$$\sum_{w=0}^{W} H_w C_{w+2}(x) \leq \sum_{w=0}^{\infty} H_w C_{w+2}(x) \leq \sum_{w=0}^{W} H_w C_{w+2}(x) + [1 - \sum_{w=0}^{W} H_w]C_{2W+4}(x)$$

are helpful. Using these results,

$$\sum_{w=0}^{W} H_w C_{w+2}(R^2/v) \leq P(t_1^2 + Vt_2^2 \leq R^2/v) \leq \sum_{w=0}^{W} H_w C_{2w+2}(R^2/v)$$

$$+ [1 - \sum_{w=0}^{W} H_w]C_{2W+4}(R^2/v).$$

Ordinarily, the value of $P(t_1^2 + Vt_2^2 \leq R^2/v)$ can be approximated to reasonable accuracy without using a very large value for W.

REFERENCES

1. S. N. Roy, Some Aspects of Multivariate Analysis, John Wiley and Sons, 1957, Appendix.

2. Herbert Robbins and E. J. G. Pitman, "Application of the method of mixtures to quadratic forms in normal variates," Annals of Mathematical Statistics, Vol. 20 (1949), pp. 552-560.

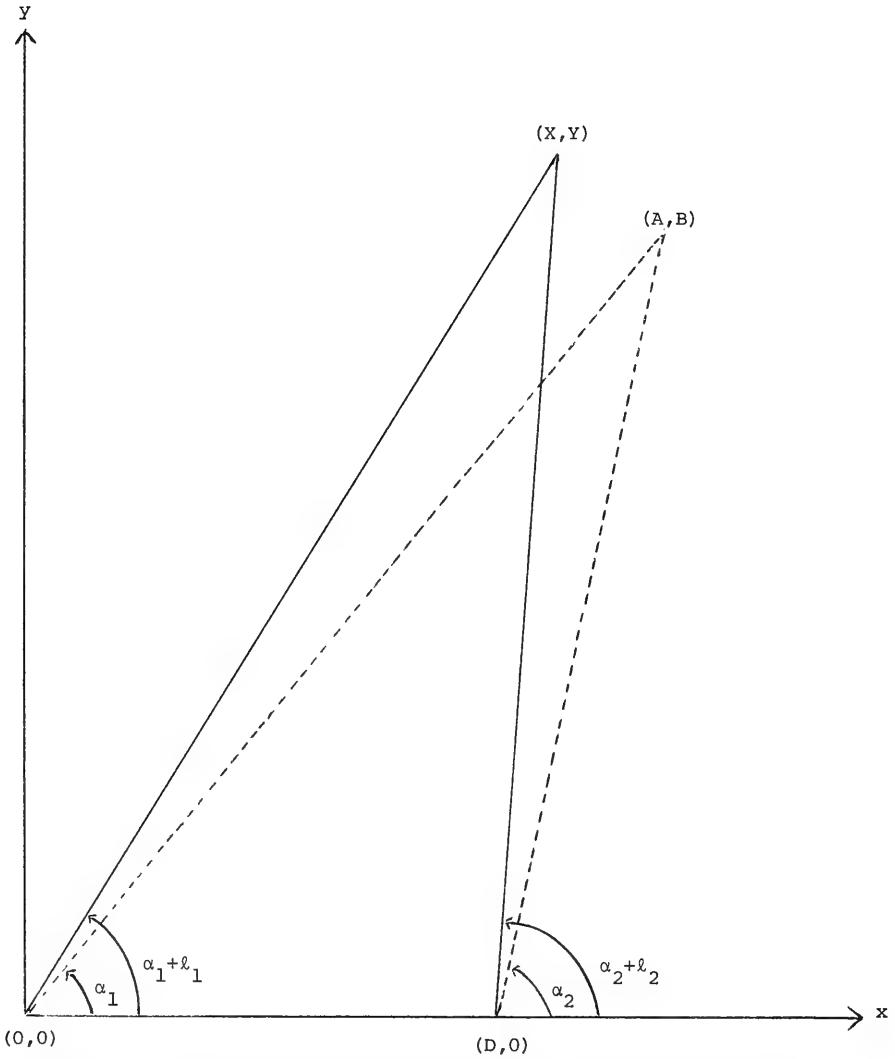

FIGURE 1. Schematic diagram for standardized representation and associated notation

THE SIGNIFICANCE OF TEMPERATURE STRATIFICATION IN THE ARCTIC

by

Stephen Neshyba, Victor T. Neal
Dept. of Oceanography, Oregon State University
Corvallis, Oregon

Warren Denner
U. S. Naval Postgraduate School
Monterey, California

Introduction

A number of measurements and studies of the fine structure of thermal and haline properties of the ocean have been published (Stommel and Fedorov, 1967; Gaul, 1968; Cooper and Stommel, 1968; Tait and Howe, 1968). The emerging picture of the ocean structure shows the vertical column separated into numerous layers, each more or less homogeneous, and each separated from adjacent layers by thin sheets characterized by large temperature and salinity gradients. Increasing use of continuous profile sensors has resulted in several observations of layering in the ocean. However, because of the difficulties involved in obtaining field measurements, laboratory studies are also important in providing an understanding of the processes involved.

Results of laboratory experiments on vertical thermal convection processes were published by Ostrach (1957) and by Globe and Dropkin (1959). The latter workers used dimensional analysis to arrive at a functional relationship between the Nusselt number, Nu, and the Rayleigh, Ra, and Prandtl numbers, Pr:

$$Nu = CRa^{m}Pr^{n}.$$

C is a coefficient determined empirically, and exponents m and n are also determined empirically. The Nusselt number is an indicator of how effectively heat is transferred by convection rather than conduction; when this number is equal to 1, convection does not exist. Dropkin and Somerscales (1965) performed similar experiments on a slanted cell and reported changes only in the value of the coefficient C. More recently, Prenger

(1968) performed a laboratory experiment with a two component system of immiscible fluids and obtained still different values for C, m, and n, indicating the need for the development of a suitable model relating the heat transfer through a multilayer system to that for a homogeneous system. These engineering studies did not include the salt flux as a factor. Laboratory studies reported by Turner (1965, 1967) included both salt and heat flux.

The criteria for formation of layers within an ocean structure are as yet unknown. However, it seems certain that velocity shear plays an important role (Woods, 1968).

Temperature and salinity gradients

The conditions that exist in the ocean have been classified by Turner and Stommel (1964) according to magnitude and sense of temperature and salinity gradients. They also discussed vertical convection processes associated with these gradients. We have indicated the four possible combinations of temperature and salinity gradients as Cases I, II, III and IV. One can illustrate the principal density on buoyancy fluxes associated with the four cases (Figure 1).

In Case I salinity increases with depth, while temperature decreases with depth, a stable situation. In order to produce homogeneity of temperature and salinity in Case I, an upward salt flux (F_S) and a downward heat flux (H) are required. The density flux ($d\rho_S$) associated with the salt flux and the density flux ($d\rho_H$) associated with the heat flux would both be upward.

Salinity and temperature both decrease with depth in Case II. These gradients can produce either a marginally stable or an unstable condition. Homogeneity of temperature and salinity could be produced by downward fluxes of both salt and heat. The salt density flux would be downward while the heat density flux would be upward.

Both salinity and temperature increase with depth in Case III. These gradients could produce either stability or instability. Vertical homogeneity of temperature and salinity in the column could be produced by upward fluxes of both salt and heat. In this case a downward heat density flux and an upward salt density flux would be required.

Case IV describes the condition when temperature increases with depth while salinity decreases with depth. These gradients would produce an unstable condition which would cause an upward flux of heat and a downward flux of salt. The density fluxes would both be downward.

Of the four cases described, Case IV is the only one that is always unstable. Therefore it cannot persist in the ocean and will not be further considered. Case I predominates beneath the central water masses of the ocean. Case II predominates within the central water masses. Case III is not common but is found in the Arctic above the core of Atlantic water (Coachman and Barnes, 1963).

Layering in Case I

Woods (1968) observed step structure in the thermocline of Maltese waters which have Case I conditions. He experimented with dye diffusion and concluded that shear induced instability in a local region led to a breakdown of the stable "sheet" or "offset" which separates two homogeneous layers. There is presumably high heat flux into the lower of the two layers after the break down occurs since the scale of interaction motion is suddenly driven into lower wave numbers by breaking of waves on the interface. However, Woods was able to follow a given layer for 40 miles.

Cooper and Stommel (1968) concluded that layers examined off Bermuda at 600 to 700 m (also Case I) have horizontal dimensions of 400 to 1000 meters. We have made one series of CTD casts from a drifting ship where Case I prevails off Oregon. We observed several layers or lenses at a depth of 1100 meters (Fig. 2). Ship drift during our series of casts was about 2 nautical miles. In order to apply the spasmodic mixing hypothesis discussed by Stommel and Fedorov (1967) to the data in Figure 2, one must account for the tapering of lens thickness to its lateral terminus. It seems likely that the lenses shown here are old, having spread under the influence of horizontal pressure gradients which remained after a spasmodic mixing of two layers. Since such a spreading motion includes a friction layer of some thickness at the upper and lower interfaces, the rate of spread would rapidly diminish when these friction layers merged; moreover, such a terminus would be distinguished in a temperature section as a point value within the large temperature gradient separating the parent layers as seen in Figure 2.

Layering in Case II

Laboratory studies by Turner (1967) have shown layering in Case II. He started his experiments with homogeneous layers in a vessel; warm, salty water was on top of colder fresh water. He sprayed a small amount of salt water on top. The salt fingering that resulted through the top did not penetrate the whole layer. Salt fingering also occurred simultaneously across the lower interface. In this marginally stable condition salt fingering transports both salt and heat downward. Once a salt column is created by a

a downward perturbation, lateral diffusion of heat from the descending column results in an increase in the negative buoyancy of the finger. Therefore it is able to overcome the stabilizing influence of the temperature gradient and continue its downward motion. Whether the process is self-limiting (i. e., whether convection cells thus generated are limited to a vertical length scale) is not known. However, a self-limiting situation must operate if layering is to occur due to the unstable density flux mixing both salt and heat downward.

Turner hypothesized that in the ocean some relation (as yet unknown) between the temperature gradient and the salt flux specifies the criteria for the formation of a new layer. There is observational evidence supporting his hypothesis. Tait and Howe (1968) measured very distinct layers under Case II conditions in a region of the Eastern Atlantic where warm, salty Mediterranean water overlies colder less salty water. Their data show extremely sharp interfaces in both salinity and temperature. The column is marginally stable at the outset and is maintained so by continuous horizontal advection of Mediterranean water which is the source of energy to resupply the energy lost by vertical molecular and convective diffusion processes.

Layering in Case III

Turner also experimented with Case III conditions. Using a dimensional argument, he showed that the ratio of turbulent transfer coefficients for salt and heat, K_S/K_T, is some function of the density difference (stability) ratio, $\beta \Delta S/\alpha \Delta T$, where β is the coefficient for density change due to salt, and α is the coefficient of volume expansion doe to temperature. For stability ratios between 2 and 7 the ratio of turbulent transfer coefficients decreases linearly. For the same stability ratio range the potential energy ratio is constant, within measurement error, at a mean value of about 0. 15.

Layering in the Arctic

In March 1969, we obtained a unique set of temperature profiles from the Arctic ice island, T-3. T-3 was then at 84° 34.1'N 128° 17'W where the water is about 2650 meters deep, a favorable location for the study of thermal microstructure. Previous reports of temperatures measured in that portion of the Arctic gave mean temperature drops of 0. 01° to 0. 02° C over a depth interval of about 200 meters, centered at the top of the relatively warm Atlantic water (Case III).

We used an expendable bathythermograph (XBT) system manufactured by General Motors. The XBT's were modified to reduce the fall rate from the normal fall rate of 20 ft/sec to about 7 ft/sec. Special amplifier circuits were added to the standard XBT deck electronics so we could obtain selectively expanded traces of the vertical temperature profile. We used the XBT's in three ways: (1) as modified free-fall units; (2) with the probe unit lowered at a nearly constant rate by hydrographic winch; and (3) with the probe repeatedly lowered and raised slowly by winch through a given depth interval with the electronics at high amplification (0.023° C/in width of chart paper).

A section of a typical profile taken by method (2) is shown in Fig. 3a. In the process of reproduction the trace has undergone some distortion, nevertheless the stair-step nature of the profile is evident. A section of a profile taken by method (3) is also shown in Fig. 3b, in this case covering that portion of the smaller scale profile shaded in the figure. The profiles obtained are much like stair steps in both traces.

Four aspects of the traces in Figures 3a and 3b are especially noteworthy. First, the temperature within each layer is extraordinarily homogeneous. For example, the layer 6.7 m thick, centered at 310 meters, shows less than 0.001° C variation. Second, the interface thickness is less than 20 cm based on the measured response time of the recorder and the winch speed. The lip at the end of each interface is recorder overshoot. Third, the magnitude of the temperature increment is remarkably constant over the profile section shown here with the most common temperature increment averaging about 0.027° C. However, there also appear to be some temperature increments of one-half the common average which we will refer to as half steps. One such increment is encircled in Figure 3. Fourth, below 350 meters where the temperature gradient is much smaller, the thickness of the layers is much larger. However, the thicker layers appear to be separated by several very small transition steps.

Our measurement plan on T-3 was largely devoted to time series profiling in the upper portion of the Atlantic water. Figure 4 shows one series of 22 XBT casts taken at 15 minute intervals using method (1). Also shown is the first of another series of XBT's begun about 18 hours after the completion of the first series. Since depth was not measured, the traces have been aligned along the specific discontinuity at approximately 250 meters.

Half steps about which the traces are aligned persisted unchanged in size for the duration of both series, about 24 hours. From 220 to 300 meters the steps are remarkably stable; the number of the steps remained constant and the dimensions of the steps remained nearly constant. We

conclude that the system is in quasi-steady state. The waviness of the lines connecting the same layers in the series (180 and 320 meters) is attributed to possible differences in fall rate of the XBT's as well as internal wave activity.

During the interval between series one and two, at least one new layer appeared in the profile. It is shown within the shaded section of Figure 4. This "new" layer seems to have formed from an interface zone much thicker than normal; it occurs within one of the zones showing considerable vertical fluctuations, indicating the possibility that it began with a mixing process initiated by internal wave activity. We do not know the extent of horizontal advection under the island; therefore, we cannot differentiate between the formation of a new layer and the relative advection of a new layer into the sampling area.

The half-steps which are shown in Figures 3a and 3b could be evidence of spasmodic mixing across an interface as suggested by Stommel and Fedorov (1967). The series of expanded profile sections displayed in Figure 5 contain several half-steps which show up in all profiles over the one-hour series. None of the half-steps exhibit any evidence of growth or decay. It is possible that our series of measurements "captured" the formation of a half-step (indicated in the shaded portion of Figure 4). We computed a mean turbulent diffusive heat flux for the T-3 profiles. Using a vertical eddy coefficient, A, of 1 cm^2/sec we obtained a flux of 2×10^{-5} g cal/cm^2. Using our heat flux calculation and the spasmodic model discussed by Stommel and Fedorov (1967) we calculated a cycle time of about 33 hours during which all interfaces should have been broken and reformed once. The profiles we measured are much too stable to fit the spasmodic model, but the stepped structure is virtually identical to such a model.

Arctic measurements taken from T-3 are significant for two reasons. First, T-3 is possibly the world's most stable sea-going platform. Second, both Case I and Case III stability structures occur under the ice. These structural classes are ones which must be investigated in situ before a complete understanding of layering phenomena is obtained.

The acoustic significance of layering in the Arctic.

It is also interesting to speculate on the significance of the Arctic step structure on the propagation of sound. The influence of the layering structure in the Arctic on sound propagation depends on the boundary gradients and the thickness of the layers, the frequency of the sound, and the number of layers. Since our measurements are only of temperature structure, the sound velocity and density contrasts cannot be specified with certainty. Therefore, the discussion in this section must be considered preliminary.

Sound velocity in the Arctic has previously been assumed to be a continuously increasing function of depth. Under these conditions all sound rays from a source undergo continuous upward refraction eventually reflecting from the water-ice interface leading to a surface sound channel axis. It is well established that low frequency sound propagates over long ranges with very little attenuation in sound channels. However, in the Arctic as the frequency increases the attenuation increases very rapidly, and is abnormally high compared to the open ocean attenuation above a hundred hertz (Urick, 1967). The high attenuation at higher frequencies has been attributed to scattering losses at the ice-water interface.

Up to the time of our measurements the existence of steps in the Arctic sound velocity structure had not been considered. Urick (1967) points out that the most significant effect of microstructure at short range and high frequency is the focusing and defocusing of the sound , whereas for long ranges and low frequencies forward scattering becomes the dominant process causing sound level fluctuations. However, these conclusions have been reached by considering the thermal microstructure in the sea to consist of patches more or less randomly distributed throughout the water column. Our measurements indicate that an important part of the microstructure, at least in the Arctic, consists of quasi-stable layers that may extend over large horizontal dimensions. Therefore, the influence of the microstructure in the Arctic might be quite different from its influence in open waters.

Another aspect of the step structure in the Arctic that differs from the lower latitude open oceans is that the steps are most prominent below the sound channel axis, whereas at lower latitudes the steps are above the sound channel axis. For a near surface source, many of the energy containing rays arrive at the depth of the stepped zone at near grazing angles.

The Rayleigh reflection coefficient of a single step is:

$$\alpha_r = \frac{\frac{\rho_2}{\rho_1} \operatorname{Sin}\theta_1 - \left[\frac{C_1}{C_2} - \operatorname{Cos}^2\theta\right]^{1/2}}{\frac{\rho_2}{\rho_1} \operatorname{Sin}\theta_1 + \left[\frac{C_1}{C_2} - \operatorname{Cos}^2\theta\right]^{1/2}}$$

where ρ_1 and ρ_2 are the densities and C_1/C_2 the sound velocity ratio across a finite discontinuity. θ is the angle of incidence. Density and sound velocity contracts across the layer boundaries cannot be calculated without knowing the salinity. High resultion salinity measurements are not available to go with our temperature measurements at this time. An estimate of the

density and sound velocity contrasts across a boundary can be made by assuming a one-to-one correspondence between salinity steps and temperature steps, that is, an equal number of temperature and salinity steps in a given depth interval. For the sake of calculation, take the 300-350 meter interval shown in Figure 3. There are eight temperature steps in this interval, averaging 0.027° C with average layer thickness of 6.25 meters. Assuming a linear salinity gradient of 2×10^{-3}‰/meter (Dunbar and Harding, 1968), eight salinity steps of 0.012 and 6.25 meter thickness would be required. Using a temperature step of 0.027° C and a salinity step of 0.012‰ in Wilson's equation to calculate the sound velocity contrast and Ekman's equation to compute the density contrast, the Rayleigh reflectivity can be computed for a single layer to be approximately 5×10^{-5} for normal incidence. While the reflectivity is small for normal incidence, it must approach unity at the critical angle (Brekhovskikh, 1960). However, the critical angle is very near zero for such small contrasts.

The acoustic significance of the step structure increases when we go from an isolated layer to many layers. Brekhovskikh treats the reflection of a sound wave from a multi-layered medium and the calculations should be made when better estimates of the sound velocity and density contrasts are possible. Some additional factors must be recognized for the multi-layered problem. First, the wavelength of the acoustic wave becomes important in determining the interference pattern. Secondly, the steps we measured do not appear as finite discontinuities. The boundary thickness appears to be about 20 cm. Officer (1958) shows that the reflection across a boundary of finite extent must depend on the wave length.

Thus, the significance of the layered structure in the Arctic is probably small for low frequency long-range propagation, but will increase as frequency increases. While the Rayleigh reflectivity at normal incidence is small, the reflectivity increases to unity as the grazing angle is approached. Certainly the multi-layered reflection problem must be considered as well as the finite thickness of the boundaries.

One of the chief aspects of the layering in the Arctic will be a redistribution of the energy from the continuous profile case. An interesting aspect to consider is the influence of the layers on the fluctuation of sound intensity between a fixed source and receiver. In the ice-free oceans, the intensity between a fixed source and receiver is observed to vary significantly with time due to the variability in the sea. Yet our measurements indicate that the layers in the Arctic are more stable than those in ice-free areas. Therefore, the induced variability should be less. Since we do not have a good picture of the internal wave structure in the Arctic, the significance of irregularities in the depth of a layer cannot be specified.

Acknowledgements

Supported by ONR 1286(10), Naval Ordinance Systems Command ORD-030-005/561-1URL) 104-03-01, and the Naval Arctic Research Laboratory.

REFERENCES

Brekhovskikh, L. M. (1960). Waves in layered media. Academic Press, New York, 561 p.

Coachman, L. K. and C. A. Barnes (1963). The movement of Atlantic water in the Arctic Ocean. Arctic 16(1): 8-16.

Cooper, J. W. and Stommel, H. (1968). Regularly spaced steps in the main thermocline near Bermuda. J. Geophys. Res. 73(18): 5849-5854.

Dropkin, D. and E. Somerscales (1965). Heat transfer by natural convection in liquids confined by two parallel plates which are inclined at various angles with respect to the horizontal. ASME J. Heat Transfer Series C, 87, (1): 77-84.

Dunbar, M. J. and G. Harding (1968). Arctic ocean water masses and plankton--a reappraisal of Arctic drifting stations. In Arctic Drifting Stations, Arctic Institute of North America, Washington, D. C. 315-326.

Gaul, R. D. (1968). Investigation of oceanic stratification, currents, and surface waves. Final Rpt. ONR Contract #N00014-67-C-0288, October 31, 1968.

Globe, Samuel and David Dropkin, (1959). Natural convection heat transfer in liquids confined by two horizontal plates and heated from below. J. Heat Transfer, 81: 24-28.

Officer, C. B. (1958). Introduction to the theory of sound transmission with application to the ocean. McGraw-Hill, New York, 284 p.

Ostrach, Simon (1957). Convection phenomena in fluids heated from below, Trans. Amer. Soc. Mech. Engrs., 79, (2).

Prenger, F. Coyne, Jr. (1968). Natural convection heat transfer between immiscible liquids. Master's thesis. Fort Collins, Colorado State University 32 pp.

Stommel, H. and Fedorov, K. N. (1967) Small scale structure in temperature and salinity near Timor and Mindanao. Tellus. 19: 306-325.

Tait, R. I. and Howe, M. R. (1968) Some observations of thermo-holine stratification in the deep ocean. Deep Sea Res. 15: 275-280.

Turner, J. S. (1965). The coupled transports of salt and heat across a sharp density interface. Int. J. Heat Mass Transfer, 8: 759-767.

Turner, J. S. (1967). Salt fingers across a density interface. Deep Sea Research 14: 599-611.

Turner, J. S. and H. Stommel (1964). A new case of convection in the presence of combined vertical salinity and temperature gradients. Proc. U. S. Nat. Acad. Sci. 52: 49-53.

Urick, R. J. (1967). Principles of Underwater Sound for Engineers. McGraw-Hill, New York. 342 pp.

Woods, J. D. (1968). An investigation of some physical processes associated with the vertical flow of heat through the upper ocean. The Meteorological Magazine 97(1148): 65-72.

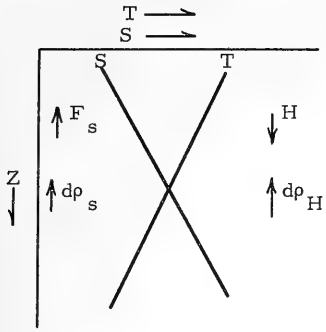

CASE I

1. Gravitationally stable
2. Mean density fluxes co-directional
3. Mixing dominated by velocity shear
4. Layering structure observed in all oceans, but generally is confused and irregular

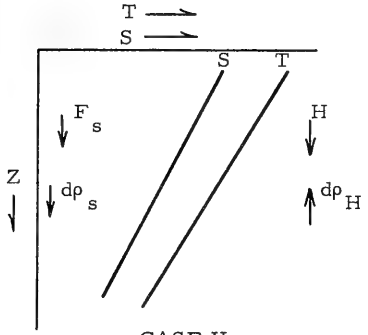

CASE II

1. Marginal gravitational $\begin{cases} \text{stability} \\ \text{instability} \end{cases}$
2. Mean density fluxes oppose
3. Salt fingering across interface
4. Strong layering observed in Eastern Atlantic; layer steps highly regular

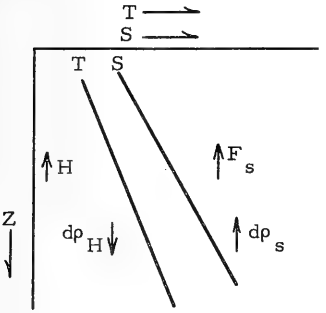

CASE III

1. Marginal gravitational $\begin{cases} \text{stability} \\ \text{instability} \end{cases}$
2. Mean density fluxes oppose
3. Thermal diffusion across interface, with strong vertical convection above and below interfaces
4. Strong layering observed in the Arctic Ocean

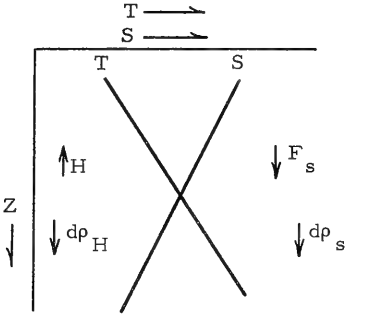

CASE IV

1. Gravitational instability
2. Mean density fluxes co-directional
3. Layering not observed

Figure 1. Four cases of possible temperature and salinity gradients. Cases II and III can be either marginally stable or unstable.

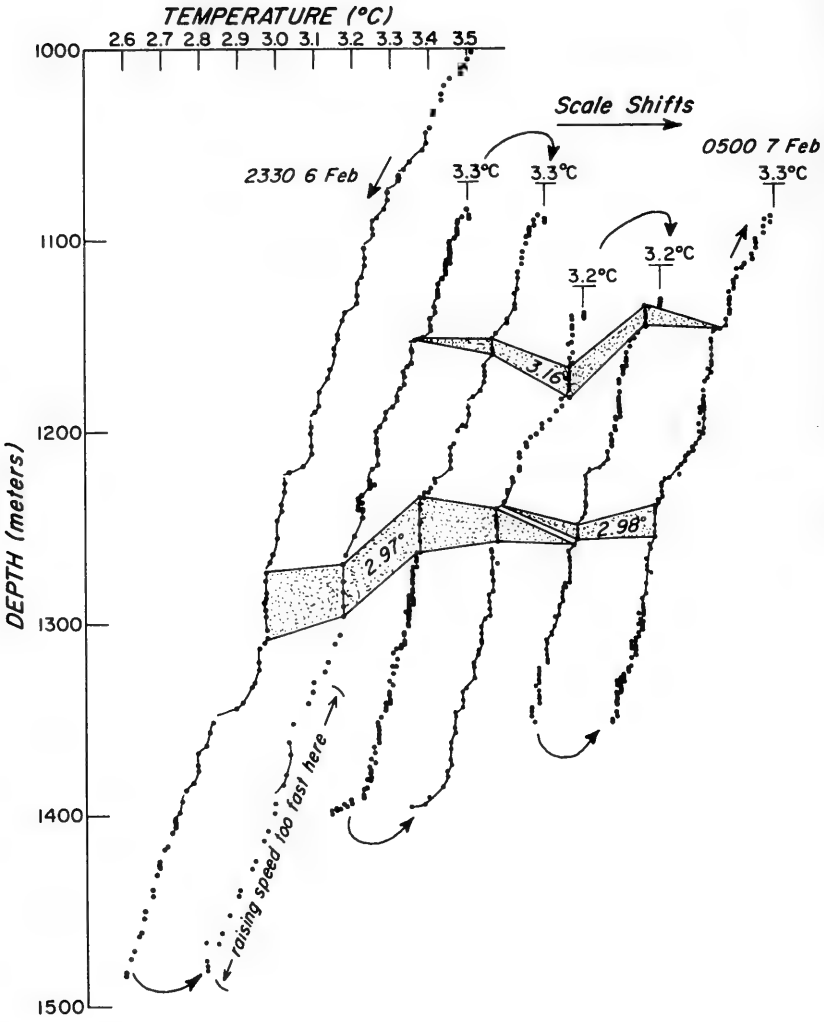

Figure 2. Successive temperature profiles made from drifting ship 45 miles off Newport, Oregon. Shaded lens of isothermal water are seen to terminate laterally in zones of high temperature gradient. Lateral drift during the series was two nautical miles.

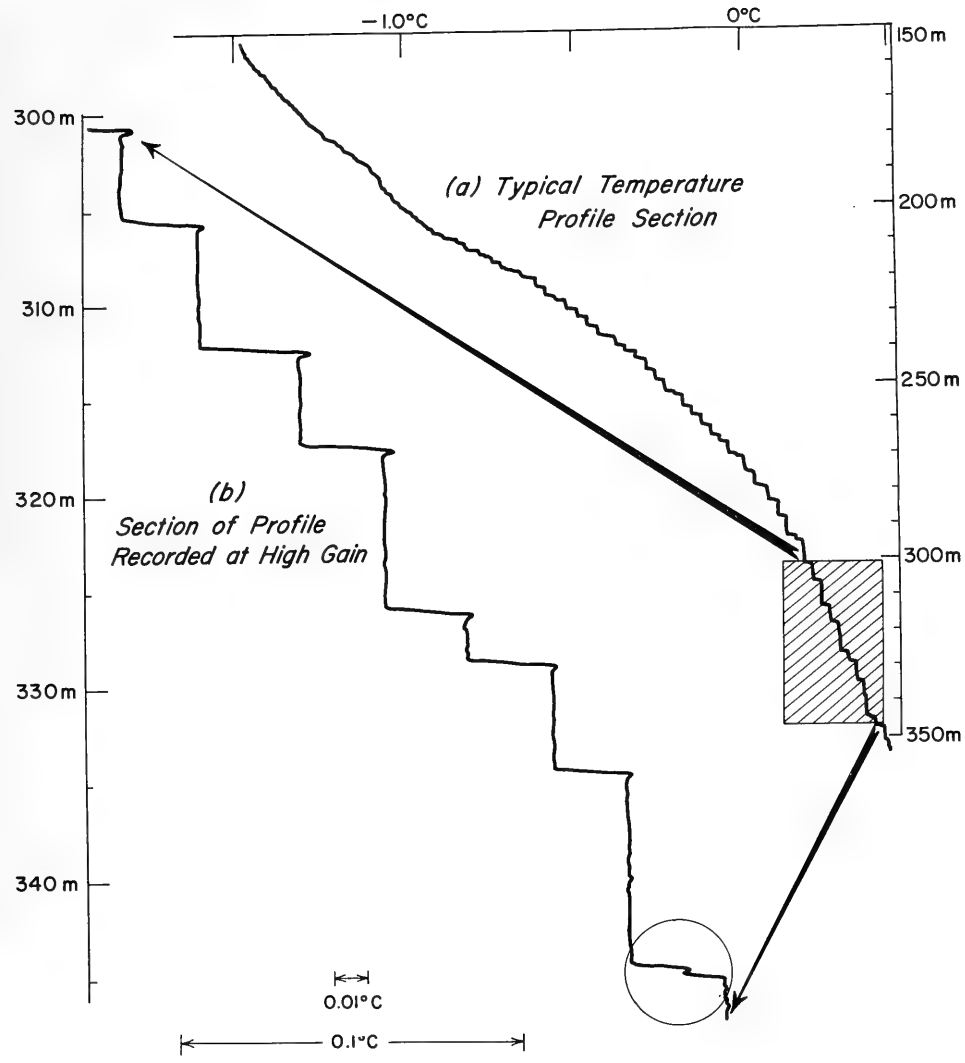

Figure 3. Vertical profile of temperature under T-3 (84°38'N, 128°21.6'W, 19 March 1969). Shaded section of profile (a) shown as observed in profile (b) to left.

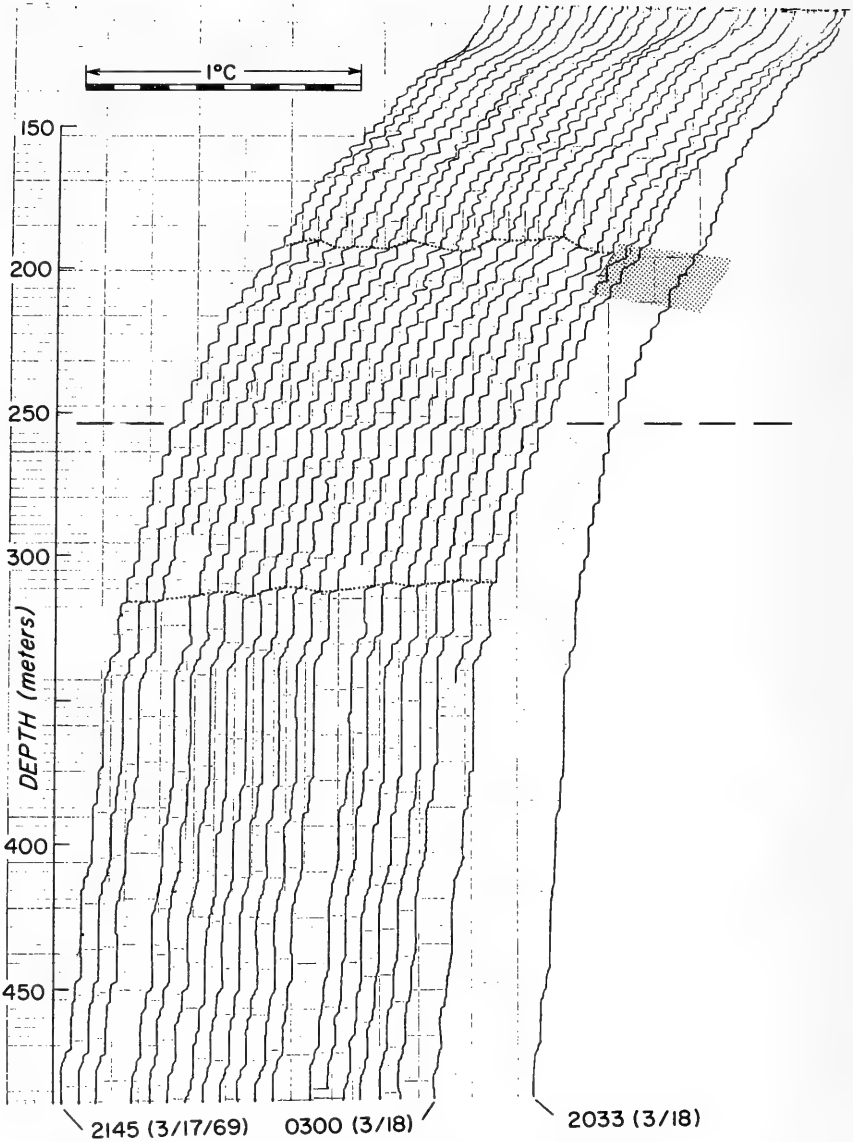

Figure 4. Time series with high amplification taken from T-3 in March 1969. Temperature increases from right to left. A "new layer" appears within the shaded section.

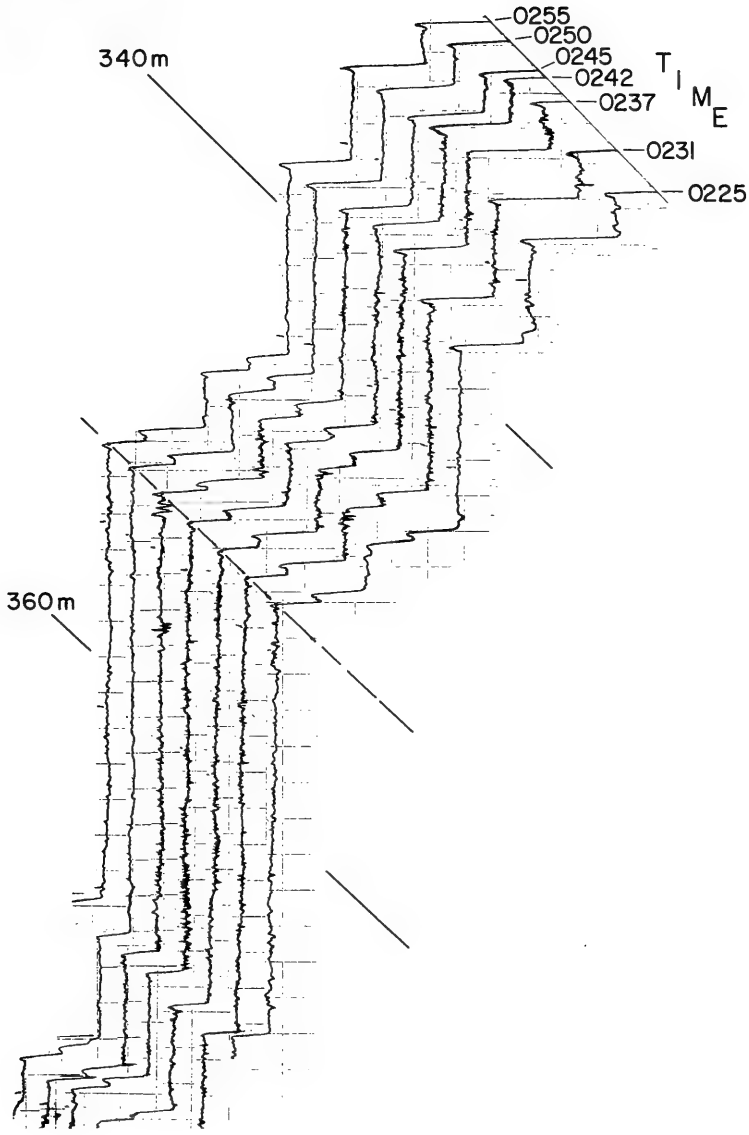

Figure 5. Time series taken from T-3 in March 1969. Temperature increases from right to left.

LIST OF ATTENDEES
6th U.S. NAVY SYMPOSIUM ON MILITARY OCEANOGRAPHY

ABO, Joe M.
U.S. Naval Torpedo Station

ALLEN, Dr. Royce H.
Naval Undersea R&D Center

ALLEN, William, Jr.
The Boeing Company

ALLNUTT, Ralph B.
Naval Ship R&D Center

ANDERSEN, Rolf
Naval Research Laboratory

ANDERSON, Dr. Ernest Robert
Naval Undersea R&D Center

ANDERSON, George Boine
Naval Undersea R&D Center

ANDERSON, CAPT Vernon F. (USN)
ASW Systems Project Office

ANNIS, Wilbert
Office of Naval Research

ANUNSON, Glenn A.
U.S. Naval Torpedo Station

ARNOLD, CAPT Henry A. (USN Ret)
United Aircraft Corp.

ARONSON, Frank
Naval Applied Science Lab.

ASA-DORIAN, Paul V.
Fleet Anti-Submarine Warfare Sch.

ATKINSON, CAPT Roy C. (USN)
Naval Oceanographic Office

AUGER, CAPT Thomas E. (USN)
ASW Systems Project Office

AUSTIN, George B., Jr.
Naval Ship R&D Laboratory

BAER, Dr. Ledolph
Lockheed-California Company

BALDWIN, David Arnold
U.S. Navy Electronics Lab. Ctr.

BALDWIN, Marvin M.
Naval Undersea R&D Center

BALL, James F.
Office of Naval Research

BALLARD, LT Robert D. (USNR)
Office of Naval Research

BANAUGH, Dr. Robert Peter
Boeing

BANKS, Russell Ewen
DRB/Defense Res. Establishment Atlantic Forces

BARBARY, Robert A.
The Sippican Corporation

BASS, Warren D.
Naval Facilities Engrng. Command

BASSETT, LCDR Charles Howard, Jr. (USN)
Fleet Weather Central Norfolk

BATES, Dr. Charles C.
U.S. Coast Guard

BAXTER, LT Peter C. (USN)
Patrol Squadron Thirty-One

BEARDSLEY, Asst. Prof. George F.
Oregon State University

BECK, Lloyd
Naval Undersea R&D Center

BENNETT, CAPT John E. (USN Ret)
Lockheed Ocean Laboratory

BENNETT, Dr. Ralph Decker
Martin Marietta Corporation

BLAKE, Dr. Francis Gilman
Chevron Oil Field Research Co.

BLEIL, Dr. David F.
Naval Ordnance Laboratory

BOCK, Prof. Arthur E.
U.S. Naval Academy

BOLST, LCDR Albert L. (USN)
Commander Anti-Submarine Warfare
Force, U.S. Atlantic Fleet

BOOSMAN, Jaap W.
Off. of the Oceanog. of the Navy

BOUDOV, Milton Harry
Commander Mine Force
U.S. Pacific Fleet

BOYER, CDR Walton R., Jr.
Advanced Res. Projects Agency
Off. of the Secretary of Defense

BRECKENRIDGE, Robert A.
Naval Civil Engineering Lab.

BRESLAU, Dr. Lloyd Robert
Applied Sciences Div., USCG

BRIDGES, Robert M.
Bendix Electrodynamics

BRIGHT, Hazel M.
U.S. Naval Oceanographic Office

BRISCOE, Dr. Melbourne G.
SACLANT ASW Research Centre

BRITTON, Dr. Max Edwin
Office of Naval Research

BROWN, Charles L., Jr.
Navy U/W Sound Laboratory

BROWN, Irwin M.
ASW Systems Project Office

BROWNYARD, Dr. Theodore L.
Naval Ordnance Systems Command

BRUNO, Anthony B.
Navy U/W Sound Laboratory

BUCK, Beaumont M.
AC Electronics

BUCKMASTER, CDR Albert T. (USN)
Staff Meteorologist
Commander in Chief Pacific

BURKHART, Marvin D.
Off. of the Oceanog. of the Navy

BURROUGHS, LT Lawrence D. (USN)
Fleet Weather Central Norfolk

BUSCHMANN, LCDR Virginia (USN)
Fleet Weather Central

BOWIN, Dr. Carl O.
Woods Hole Oceanographic Inst.

BALDWIN, LCDR J. A. (USN)
Off. of the Oceanog. of the Navy

BALINE, Russell E.
Navy U/W Sound Laboratory

BARAKOS, Dr. Peter A.
Navy U/W Sound Laboratory

BARBEE, CDR William D.
JORG, University of Washington

BARNES, Dr. Clifford Adrian
University of Washington

BASSETT, LCDR Charles G. (USN)
Fleet Numerical Weather Central

BEALOR, Jesse L., Jr.
Naval Ship R&D Laboratory

BECHELMAYR, LCDR Leroy R. (USN)
Fleet Numerical Weather Central

BECK, James A.
U.S. Naval Torpedo Station

BELLEW, Ira Thomas
Naval Air Development Center

BENNETT, Carl Melvin
Naval Ship R&D Laboratory

BENNETT, Charles Bruce
Naval Radiological Def. Lab.

BENNETT, Dr. Lee, Jr.
University of Washington

BEVING, LCDR D. U. (USN)
Off. of the Oceanog. of the Navy

BERMAN, Dr. Alan
Naval Research Laboratory

BIXBY, LCDR Harry L. (USN)
Anti-Submarine Warfare Force
Pacific

BOLLER, CAPT Jack Warren (USN)
Hq Naval Material Command
Oceanographer of the Navy

BOSTON, Noel E. J.
Naval Postgraduate School

BRIDGE, Richard Benedict
Naval Research Laboratory

BROWN, Louis B.
Naval Research Laboratory

BROWN, Prof. George A.
Univ. of Rhode Island

BUCHANAN, Chester Leroy
Naval Research Laboratory

BURGESS, CDR J. A. (USN)
U.S. Naval Torpedo Station

BUTERA, Anthony W.
Naval Applied Science Lab.

BYRNE, Prof. John Vincent
Oregon State University

CAGLE, Ben J.
Office of Naval Research

CALHOON, LCDR Theodore H. (USN)
Fleet Weather Central

CAMPBELL, Colin Lee
Fleet Weather Facility

CAMPBELL, Francis James
Naval Research Laboratory

CAMPBELL, James R.
Naval Undersea R&D Center

CAMPBELL, Walter Graham
Sippican Corporation

CANTWELL, Joseph R.
Sperry Rand Corporation

CARPENTER, Edward P.
Naval Undersea R&D Center

CARRIKER, A. Wendell
Naval Oceanographic Office

CARROLL, CAPT Kent J. (USN)
Office of Naval Research

CAULDWELL, F. Sherman
Naval Ship Engineering Ctr.

CERES, LCDR Robert L.
Naval Postgraduate School

CHAPMAN, Dr. Wilbert M.
U.S. Naval Oceanographic Office

CHARLTON, John D.
Bendix Corporation

CHASE, Thomas E.
Scripps Inst. of Oceanography

CHIN, CDR Donald (USN)
Naval Postgraduate School

CHRISTIAN, Ermine A.
Naval Ordnance Laboratory

CLARK, Paul, Jr.
ASW Systems Project Office

CLARK, RADM Robert N. S. (USN Ret)
NA Rockwell Corporation

CLIFTON, John
U.S. Navy U/W Sound Lab.

CLAUSNER, CDR Edward (USN)
Off. of the Oceanog. of the Navy

CLAUSEN, George N.
Bissett-Berman

CLEMENT, Stuart H.
Hayden, Stone, Inc.

COACHMAN, Dr. Lawrence K.
University of Washington

COHEN, Jeffrey
U.S. Navy U/W Sound Lab.

COOK, David N.
U.S. Naval Torpedo Station

COOK, Isidore
Naval Ship R&D Center

CONNORS, Dr. Donald Nason
Naval U/W Weapons Res. &
Engrng. Station

CORBEILLE, LCDR Reginald C. (USN)
Pacific Missile Range

COUPER, Butler K.
Naval Ship Systems Command

CRIMINALE, Dr. William O., Jr.
University of Washington

CRON, Benjamin F.
Navy U/W Sound Laboratory

CROTEAU, Rudolph E., Jr.
Navy U/W Sound Laboratory

DAHLEN, John M.
Mass. Institute of Technology

DAUGHERTY, F. M., Jr.
U.S. Naval Oceanographic Office

DAVIES, RADM Thomas D. (USN)
Hq Naval Material Command

DAVIES, CAPT James W.
Hq U.S. European Command

DAVIS, Robert D.
U.S. Naval Ship Engrng. Ctr.

DEACON, CDR W. III (USN)
U.S. Naval Torpedo Station

DENNER, Warren W.
Naval Postgraduate School

DERR, Iorwerth M.
U.S. Naval Civil Engrng. Lab.

DICKIE, CDR John W. (RNZN)
New Zealand Defence Staff

DiGIACOMO, Giulio
Naval Applied Science Lab.

DONALDSON, John G.
The Boeing Company

DOOLEY, LT John J. (USN)
Fleet Weather Central

DORMAN, CAPT Alvin E. (USN)
ASW Helo Program Coordinator
Chief of Naval Operations

DUKE, CDR Gus G. (USN Ret)
Northrop Ventura

DWORSKI, Juraj George
University of Washington

DUXBURY, Dr. Alyn Crandall
University of Washington

ECK, George F.
Naval Air Development Ctr.

EDGREN, LCDR Donald H. (USN)
Naval Weather Serv. Environ.
Detachment, Moffett Field

EDSALL, Thomas D.
U.S. Naval Oceanographic Office

EDVALSON, Fredrick M.
Naval Oceanographic Office

EDWARDS, Walter Lee
Naval Air Systems Command

EISENHUTH, Dr. Joseph J.
Ordnance Research Laboratory

ELLIOT, Dr. Joe O.
Naval Research Laboratory
Univ. of British Columbia

ELWOOD, Albert Andrew
Atlantic Undersea Test &
Evaluation Ctr.

EMMET, Robert T.
Naval Ship R&D Laboratory

ENGLISH, Dr. Thomas Saunders
University of Washington

EPPERT, Dr. Herbert C., Jr.
U.S. Naval Oceanographic Office

ERATH, Robert L.
Grumman Aircraft Engrng. Corp.

ERICKSON, John Walter
Commander Antisubmarine Warfare
Force, U.S. Atlantic Fleet

ERMENTROUT, John William
ITT Corporation

EWART, Dr. Terry E.
University of Washington

FARRELL, CDR John Roger
Naval Air Systems Command

FERRALL, RADM William E. (USN Ret)
Consultant, Boy Scouts of
America

FICK, CAPT Theodore R. (USN)
Naval Radiological Defense Lab.

FINLEN, LCDR James Rendell
Submarine Dev. Group I

FISCHER, Dr. Eugene C.
Naval Applied Science Lab.

FISHEL, Kenneth R.
Naval Undersea R&D Center

FITCH, Tom Lincoln
U.S. Naval Avionics Facility

FLETCHER, CDR Charles D.
Submarine Dve. Group I

FRANCESCHETTI, Alfred P.
Naval Ship Systems Command

FRY, John C.
Exec. Office of the President

FYE, Dr. Paul M.
Woods Hole Oceanog. Inst.

FRIEDMAN, Ben L.
Office of Naval Research

GAILLARD, Robert John
Texas Instruments Inc.

GALLAGHER, James J.
Navy U/W Sound Laboratory

GALLI, Lewis
Naval Research Laboratory

GANTON, John Herbert
Defence Research Bd. of Canada

GARDNER, Robert B.
Honeywell Marine Sys. Ctr.

GARNETT, CAPT Howard G. (USN)
Naval Torpedo Station

GAUVIN, Gerald R.
Scientific & Tech. Intelligence Ctr.

GEHMAN, CAPT Harold W. (USN)
Off. of the Oceanog. of the Navy

GETMAN, Charles F.
U.S. Naval Oceanographic Office

GENNARI, Jervis J.
Naval Research Laboratory

GEYER, Leo A.
Grumman Aircraft Engrng. Corp.

GILES, CDR Claude F. (USN)
Naval Postgraduate School

GILMORE, Jack G.
Naval Ship Systems Command

GILMORE, LCDR Kenneth D. (USN)
Naval Undersea R&D Center

GLENN, Morris Ferrell
U.S. Navy Oceangraphic Office

GOOD, Edwin M.
U.S. Navy Pacific Missile Range

GOODE, John W.
Explosives Corp. of America

GOODFELLOW, RADM A. Scott, Jr. (USN)
Asst. Oceanog. for Ocean Engrng. & Dev., Chief of Naval Material

GOODMAN, Dr. Ralph R.
Naval Research Laboratory

GORDON, Alexander R.
U.S. Naval Oceanographic Office

GORMAN, Dale R.
U.S. Naval Torpedo Station

GOTT, CDR Charles L. (USN)
Off. of the Oceanog. of the Navy

GOWEN, LT John A. (Royal Navy)
British Navy Staff

GRADE, Eugene E.
U.S. Naval Torpedo Station

GRAY, LT COL Gordon M. (USAF)
Off. of the Sec. of Defense
Advanced Res. Projects Agency

GRENFELL, VADM Elton W. (USN Ret)
General Motors/AC Research Labs.

HADAWAY, CAPT Richard B.
Lockheed Shipbldg. & Const. Co.

HAKKARINEN, William
U.S. Naval Weapons Quality
Assurance Office

HALL, LCDR Richard F. (USN Ret)
Tracor, Inc.

HALLADAY, CDR Norman E. (USN)
Naval Weather Serv. Environ.
Detachment, Whidbey Island

HALPER, David P.
Office of Naval Research

HAMMON, Willis Theodore
U.S. Naval Oceanographic Office

HANSSEN, George L.
U.S. Naval Oceanographic Office

HARD, Dr. Edward Wilhelm
Sun Oil Company

HARDING, CAPT Edwin T. (USN)
Naval Weather Serv. Command

HARLETT, LT John C. (USN)
Oregon State University

HARRISON, John H.
Naval Ship R&D Laboratory

HAUPT, Dr. Curtis Raymond
Naval Undersea R&D Center

HAUPT, CAPT Richard W. (USN)
Off. of the Oceanog. of the Navy

HAYNES, Eugene T.
The Boeing Company

HAYWARD, John L.
Sippican Corporation

HECKELMAN, A. Joseph
U.S. Naval Oceanographic Off.

HEIGES, LCDR John M.
Navy U/W Sound Laboratory

HEISKELL, Raymond H.
Naval Radiological Def. Lab.

HERMANSON, Joseph M.
The Boeing Company

HENDRIX, Prof. Charles N. G.
U.S. Naval Academy

HERSEY, Dr. J. B.
Office of Naval Research

HESSE, Mrs. Theodore S.
Fleet Numerical Weather Central

HILLER, Alexander John
Naval Research Laboratory

HIRES, Dr. Richard Ives
Stevens Institute of Tech.

HODGMAN, CAPT James A. (USCG)
Nat'l. Data Buoy Dev. Project Off.

HOGBEN, Herbert E.
British Navy Staff

HOGGE, Dr. Ernest A.
Naval Ship R&D Laboratory

HOLCOMBE, Troy Leon
U.S. Naval Oceanographic Office

HOLSTROM, Cecil C.
Naval Air Systems Command

HOFFMAN, Robert Terry
Quality Evaluation Laboratory

HOWARD, Walter W.
Naval Ship R&D Center

HOYT, Dr. Jack Wallace
Naval Undersea R&D Center

HUDOCK, LT Charles J. (USN)
Naval Weather Serv. Environ.
Detachment

HUETER, Dr. Theodor F.
Marine Sys. Ctr., Honeywell

HUGHES, LT Frank W. (USN)
University of Washington

HULSEMANN, Dr. Jobst
U.S. Naval Oceanographic Office

HUMASON, Harry W.
Naval Undersea R&D Center

HUNKINS, Dr. Kenneth L.
Lamont-Doherty Geological Obs.
Columbia University

HUSBY, David Michael
USCG Oceanographic Unit

HYMES, William H.
Oceanog. of the Navy Office

IGARASHI, Yoshiya
Naval Undersea R&D Center

IGELMAN, Kim Richard
Lockheed-California Co.

INGRAM, Carey
U.S. Naval Oceanographic Office

IRVING, LT Daniel R. (USCG)
13th Coast Guard District

LINDT, M. C.
U.S. Naval Torpedo Station

ISAAK, Dr. Robert D.
Honeywell Marine Systems

JAPP, RADM Joseph A. (USN Ret)
Stanley Associates

JACKSON, CAPT Leroy L., Jr.
(USN)
Atlantic Undersea Test &
Evaluation Ctr.

JAMES, CDR Joe Mitchell (USN)
Commander Operational Test &
Evaluation Force

JAQUES, Alvin T.
Naval Ordnance Laboratory

JEFFERS, CDR K. William (ESSA)
Coast & Geodetic Survey
Pacific Marine Center

JEFFERSON, Donald Earl
Naval Ordnance Laboratory

JENSEN, Edmond P.
Navy U/W Sound Laboratory

JOBST, William John
Naval Ordnance Sys. Command

JOHNSON, Edward W.
Chief of Naval Operations

JOHNSON, CDR John P. (USN)
Office of Naval Res.-Branch Off.

JONES, Donald O.
U.S. Naval Torpedo Station

JONES, Ronald E.
Naval Undersea R&D Center

JONES, Wilbert L., Jr.
Naval Research Laboratory

JUNG, Dr. Glenn H.
Naval Postgraduate School

KAHLBAU, Jerry Vaughn
Univ. of Texas at Austin

KAMMER, Charles George
U.S. Naval Oceanographic Office

KANABIS, William G.
Navy U/W Sound Laboratory

KANE, John J.
Office of Naval Research

KAUFMAN, Dr. Sidney
Shell Development Co.

KAULUM, Keith W.
Naval Radiological Def. Lab.

KATZ, Dr. Eli J.
Woods Hole Oceanog. Inst.

KAYE, Eric
Australian Naval Attache

KAYE, Kenneth William
U.S. Naval Oceanographic Office

KAZANOWSKA, LTjg, Maria (USNR)
Atlantic Undersea Test & Eval. Ctr.

KELLER, Karl H.
Naval Ship R&D Laboratory

KELLER, CAPT Robert M. (USN Ret)
Off. of the Oceanog. of the Navy

KELLEY, Dr. James C.
University of Washington

KELLEY, Terry Larimer
U.S. Naval Oceanographic Off.

KENIS, Paul Robert
Naval Undersea R&D Center

KINDLE, Dr. Earl C.
Navy Weather Research Facility

KING, Thomas A. J.
Strategic Sys. Project Off.

KIRK, LCDR Robert G. (USN)
Naval Weather Serv. Command

KLEINERMAN, Meinhard M.
U. S. Naval Ordnance Lab.

KOCH, LT Robert W. (USN)
Fleet Airborne Electronics
Training Unit, Atlantic

KOCHANSKI, Stephen
Naval Applied Science Lab.

KOEHR, LT James Elmer (USNR)
Fleet Weather Central Norfolk

KRAUTER, LCDR George E. (CEC, USN)
Naval Sch., Civil Engr. Corps
Officers

KUNIMUTSU, Reginald T.
Quality Evaluation Laboratory

KUNZ, D. A.
Naval Undersea R&D Center

KUPERMAN, William A.
Naval Research Laboratory

LAEVASTU, Dr. Taivo
Fleet Numerical Weather Central

LaFOND, Mrs. Katherine G.
Naval Undersea R&D Center

LaFOND, Dr. Eugene C.
Naval Undersea R&D Center

LANGILLE, CAPT J. E. (USN)
Naval Material Command Hq

LARSEN, Dr. Lawrence H.
University of Washington

LARSON, LCDR Charles D. (USN)
Naval Air Systems Command

LARSON, Siguard E.
Fleet Numerical Weather Central

LaVIOLETTE, Paul E.
Naval Oceanographic Office

LAW, Edgar Frederick
Naval Oceanographic Office

LEE, Owen Scott
Naval Undersea R&D Center

LeDEW, CDR Thomas A. (USN)
Staff, Commander in Chief
U.S. Pacific Fleet

LEIPPER, Dr. Dale F.
Naval Postgraduate School

LESSER, Marshall W.
Gen. Dynamics Electronics Div.

LEVINE, Sol
Anti-Submarine Warfare Sys. Project

LEWIS, Lloyd
Univ. of Rhode Island

LIBERATORE, Giacomo Leno
Naval Applied Science Lab.

LINCOLN, John Harvey
The Boeing Company

LINDBERGH, Jon Morrow
Ocean Systems, Inc.

LINNENBOM, Dr. Victor J.
Naval Research Laboratory

LITTRELL, Woodrow H.
Naval Undersea R&D Center

LIVINGSTON, James A.
Sylvania Electronic Systems
Western Div.

LOCKEE, CAPT Garette E. (USN)
Navy Program Planning

LOHNER, Richard C.
Naval Oceanographic Office

LOOSE, LT Ronald Russell
U.S. Navy Academy

LOUGHRIDGE, Dr. Michael S.
Naval Oceanographic Office

LOWENSTEIN, Dr. Carl D.
Univ. of Calif., Marine Physical Lab. of the Scripps Inst. of Oceanography

LUISTRO, James A.
Naval Ship R&D Center

LYON, Dr. Waldo K.
Naval Undersea R&D Center

MACANDER, Aleksander B.
Naval Applied Science Lab.

MACDONALD, Frank C.
Naval Research Laboratory

MACKEY, Harvey Andrew
Naval Ordnance Systems Command

MACOMBER, CAPT Mark M. (USN)
Naval Oceanographic Office

MacLEOD, CDR D. M. (RCN)
Canadian Def. Liaison Staff

MACLURE, Dr. Kenneth Cecil
Def. Res. Establishment Pacific

MacPHERSON, LCDR Hugh Alexander
(Canadian Armed Forces)
Weapons Div., Fleet Sch. Halifax

MADDEN, John G. W.
(Computing Devices of Canada, Ltd.)
Canadian Dept. of Def. Production

MAGNITZKY, A. Wayne
Chief of Naval Operations

MARTIN, Patrick
Naval Oceanographic Office

MARTIN, Dr. Seelye
University of Washington

MARTINEAU, Dr. Donald P.
ESSA

MASON, Curtis
Naval Ship Engrng. Center

MATHES, Robert Harris
Naval Research Laboratory

MATLACK, Donald Edwin
Naval Ordnance Laboratory

MAYER, Alan H.
Naval Air Sys. Command

MAYS, LT Michael E. (USN)
Navy Field Operational Intelligence Office

MESECAR, Asst. Prof. Roderick S.
Oregon State University

MILLER, CAPT Robert Nicholas (USN)
Naval War College

MILLIGAN, Donald Bristowe
Off. of the Oceanog. of the Navy

MILNE, Allen Ritchie
Def. Res. Board of Canada

MITTMAN, Sidney A.
Naval Applied Science Lab.

MOHR, Dr. John Luther
Univ. of Southern Calif.

MOLLOY, Arthur Eugene
Naval Undersea Warfare Ctr.

MOMIYAME, Thomas S.
Advanced Sys. Concepts Div.
Naval Air Systems Command

MOMMSEN, LT D. B., Jr. (USN)
Off. of the Oceanog. of the Navy

MONNEY, LCDR Neil T. (USN)
Off. of the Oceanog. of the Navy

MONTEATH, LCDR Gordon M. (USN)
Fleet Numerical Weather Central

MOONEY, CDR John B., Jr. (USN)
Chief of Naval Operations

MOONEY, A. Russell
Naval Oceanographic Office

MOOSE, Paul Henry
Honeywell Marine Sys. Ctr.

MORRIS, Mrs. Halcyon E.
Naval Undersea R&D Center

MORROW, Dr. Elman A.
Bureau of Naval Personnel

MORSE, CDR Richard M. (USCG)
Marine Sciences Div., Off. of Operations, USCG Hq

MOSELEY, Dr. William B.
U. S. Naval Research Laboratory

MUDIE, John D.
Univ. of Calif., Marine Physical Lab. of the Scripps Inst. of Oceanography

MUHLBAUM, Abraham M.
Naval Oceanographic Office

MUNSON, Dr. John C.
Naval Research Laboratory

MURDOCK, Lawrence C.
NEREUS Corporation
Northwestern Div.

MURPHY, Dr. Stanley R.
University of Washington

McCLEMENT, LT Charles C.
Naval Shore Elec. Engrng. Act.

McCLINTON, Arthur Thomas
Naval Research Laboratory

McCLOSKEY, LT Terry J. (USN)
Fleet Numerical Weather Central

McCOY. Donald R.
IBM Corporation

McDONALD, CAPT Carlton A. K.
Off. of Asst. Sec. of Navy (R&D)

McGILLICUDDY, CAPT Terry T. (USN)
Naval Applied Science Lab.

McGREGOR, Ronald K.
Off. of Naval Res., Arctic Program

McGUINNESS, William T.
Alpine Geophysical Associates

McKAY, William Clyde
Ocean Sci. & Engrng., Inc.

McLEAN, Max C.
ESSA-Coast & Geodetic Survey

McNITT, RADM Robert Waring
Naval Postgraduate School

NAGLER, Herbert
Naval Applied Science Lab.

NEES, Donald M.
Naval Torpedo Station

NELSON, Hilding Eugene
Naval Ship R&D Laboratory

NICKERSON, J. W.
Navy Weather Res. Facility

NORTHROP, Dr. John
Naval Undersea R&D Center

NOWATZKI, James A.
Bendix Electrodynamics Corp.

NUTANT, John Albert
Westinghouse Electric Corp.

NUTT, Harold V.
Naval Ship R&D Laboratory

NYGREN, RADM Harley D.
ESSA

NYSTROM, LCDR Robert Eric
Naval Ship R&D Laboratory

O'BRIEN, Douglas D.
Navy U/W Sound Laboratory

OLSON, Dr. Boyd E.
U.S. Naval Oceanographic Office

OLSON, Dr. Franklyn C. W.
Naval Ship R&D Laboratory

OLSON, CDR Fredrick G. (USN)
Commander Naval Air Force, U.S. Pacific Fleet

OLSON, LeRoy O.
University of Washington

O'NEAL, Henry A.
Office of Naval Research

O'NEILL, Robert, Jr.
Navy U/W Sound Laboratory

ORR, James F.
Navy U/W Sound Laboratory

OSBORN, Roger R.
Naval Oceanographic Office

O'TOOLE, CDR Kevin J. (USN)
Naval Postgraduate School

OWEN, Prof. Donald B.
Office of Naval Research

OWEN, RADM Thomas B. (USN)
Office of Naval Research

PANSHIN, Daniel A.
Oregon State University

PARKHURST, CAPT Robert D. (USCG)
Applied Sciences Div., CG Hq

PATTERSON, Robert Bruce
Naval Research Laboratory

PAQUETTE, Dr. Robert G.
General Motors/AC Electronics Def. Res. Lab.

PASZYC, Dr. Aleksy J.
Naval Civil Engrng. Laboratory

PAWLOWICZ, LT Edmund F. (CEC USNR)
Naval Civil Engrng. Laboratory

PEIRCE, Dr. Thomas Edwin
Naval Ordnance Sys. Command

PELOQUIN, Robert A.
Naval Oceanographic Office

PERSECHINO, Mario A.
Naval Research Laboratory

PETREE, LCDR Noel H., Jr. (USN)
Off. of the Special Asst. to the Jt. Chiefs of Staff for Environmental Services (SAES)

PHELPS, LCDR George T. (USN)
Oregon State University

PHILLIPS, Donald E.
Naval Ordnance Laboratory

PIERSON, Dr. Willard J., Jr.
New York University

PIIP, Ants Tonis
Navy Sofar Station
(Columbia U. Geophysical
Field Station)

POOR, CDR George McCoy
ESSA-Coast & Geodetic Survey

PYLE, Albin F.
Naval Air Sys. Command

QUADY, LCDR Emmett R. (USN Ret)
IBM-Federal Sys. Div.

QUINN, Dr. Thomas P.
Office of Naval Research

RATTRAY, Dr. Maurice, Jr.
University of Washington

REED, LCDR Robert G. (USN)
Def. Intelligence Agency
Mapping & Charting

REEVE, LCDR William F. (USN)
Naval Ship R&D Laboratory

REITZEL, Dr. John S.
Arthur D. Little, Inc.

RENDLER, Norbert J.
Naval Research Laboratory

RESTER, Gerald Franklin
Westinghouse Ocean Res. &
Engrng. Ctr.

RICH, Harry L.
Naval Ship R&D Center

RICHMOND, RADM Chester A., Jr.
(USCG)
Off. of R&D, USCG Hq

RIDLON, James B.
Naval Undersea R&D Center

RIFFENBURGH, Dr. Robert H.
Naval Undersea R&D Center

RINEY, Dr. Thomas D.
Systems, Science & Software

ROBINSON, CAPT Frederick G.
(USN)
SACLANT (NATO Staff)

ROCKWELL, Donald E., Jr.
Naval Ship R&D Laboratory

ROJAS, Richard R.
Naval Research Laboratory

ROPEK, John F.
Naval Ordnance Sys. Command

ROTH, LT Arthur (USN)
Naval Oceanographic Office

ROWELL, Dr. Charles F.
Naval Postgraduate School

RUEBSAMEN, CAPT Darrel D.
Off. of Supervisor of Salvage

RUMPF, Robert R.
Navy U/W Sound Laboratory

RUSSELL, John J.
Naval Undersea R&D Center

RYAN, Theodore V.
Pacific Oceanographic Res. Lab.
ESSA

SANDERS, Don Richard
Univ. of Texas at Austin

SANDS, Walter Casper
University of Washington

SARGENT, Dr. Marston C.
Office of Naval Research

SAVIT, Carl H.
Western Geophysical Co. of America

SAVITZ, Paul
Naval Air Dev. Center

SCHAUER, Dr. Heinrich M.
Naval Ship R&D Center

SCHEFER, Murray Harold
Naval Air Sys. Command

SCHIMKE, Gerald R.
Arthur D. Little, Inc.

SCHLOSSER, Arthur J.
Naval Undersea R&D Center

SCHRAMM, LCDR William G. (USN)
U.S. Naval Academy

SCHUERT, Edward A.
Naval Radiological Def. Lab.

SCHULKIN, Dr. Morris
Navy U/W Sound Laboratory

SCULL, David C.
Naval Oceanographic Office

SEELEY, Robert L.
U.S. Naval Underseas R&D Lab.

SEIDMAN, Louis
Naval Applied Science Lab.

SELVIDIO, James F.
Navy U/W Sound Laboratory

SEZACK, Stanley K.
Naval Applied Science Lab.

SHABELSKI, Joseph J.
Naval Ship R&D Center

SHAEFER, George V.
U.S. Naval Oceanographic Office

SHIRASAWA, Takeo H.
Naval Radiological Def. Lab.

SKYKIND, Dr. Edwin B.
Naval Research Laboratory

SIDES, ADM John H. (USN Ret)
Lockheed Aircraft Corp.

SISSON, CAPT Luther B. (USN)
Off. of the Oceanog. of the Navy

SKOP, Dr. Richard A.
Naval Research Laboratory

SLAVIN, Leon
Naval Ship Sys. Command

SLAVTCHEFF, Stephen
U.S. Navy U/W Sound Lab.

SMALL, Fred A.
Off. of the Oceanog. of the Navy

SMITH, Edward LaRay
Naval Undersea R&D Center

SMITH, Harold Derrell
Naval Undersea R&D Center

SMITH, James W.
Office of Naval Research

SNODGRASS, James Marion
Univ. of Calif, Scripps Inst. of Oceanography

SODERBERG, Emil F.
Navy U/W Sound Laboratory

SODERHOLM, Francis W.
Naval Air Sys. Command

SOLGA, J. Arthur
Naval Air Sys. Command

SOMERVELL, CAPT Willis L., Jr. (USN)
Navy Weather Res. Facility

SPIESS, Dr. Fred N.
Scripps Inst. of Oceanography

SPIGAI, LT Joseph John
Oregon State University

SPINA, John R.
Naval Ship R&D Center

STANDISH, CAPT Edwin Otin (USN Ret)
State of Wash., Dept. of Water Resources

STANLEY, RADM Emory D., Jr. (USN Ret)
Stanley Associates

STANLEY, Everett M.
Naval Ship R&D Laboratory

STEPHENS, Clark Wheeler
Naval Ship Sys. Command

STEVENS, Paul D.
Fleet Numerical Weather Central

STEVENS, Richard S.
Office of Naval Research

STEWART, Richard L.
Staff, Commander in Chief, U.S. Pacific Fleet

STINSON, James Oscar
Univ. of Texas at Austin

STOCKMAN, Richard R.
Honeywell Marine Systems Ctr.

STRANICK, LT Francis J. (USN)
Patrol Squadron Thirty

SUSSMAN, Bernard
Navy U/W Sound Laboratory

SUSSMAN, Harry
Navy U/W Sound Laboratory

SWEETLAND, Paul C.
Ordnance Research Laboratory

SYCK, LT James M. (USN)
Fleet Anti-Submarine Warfare Sch.

SYKES, CDR Lew (USN)
Naval Operation, Off. of the Chief

TABACK, Harold J.
Aerojet-General Corp.

TABER, Robert P.
Westinghouse Electric Corp.

TAMPA, Terry James
Naval Air Sys. Command

TAPAGER, James R. D.
Staff, Commander Anti-Submarine Warfare Force, Pacific

TATRO, LCDR Peter R. (USN)
Fleet Numerical Weather Central

TAYLOR, RADM Norman E. (ESSA)
Pacific Marine Ctr., ESSA

THOMAS, Charles Edmund
GE Company

THOMAS, Robert W.
Naval Oceanographic Office

THOMPSON, C. T.
Naval Torpedo Station

THOMPSON, Eugene H., Jr.
Singer-Gen. Precision, Inc.

THOMPSON, Dr. Warren C.
Naval Postgraduate School

TICKNER, Alvin J.
Naval Undersea R&D Center

TITCOMB, Forrest C.
Naval Research Laboratory

TOLBERT, William H.
Naval Ship R&D Laboratory

TREADWELL, CAPT Thurman K. (USN)
Naval Oceanographic Office

TROGOLO, Albert G.
Naval Oceanographic Office

TUCKER, Prof. Stevens P.
Naval Postgraduate School

TUCKER, LCDR Tracy C. (CEC, USN)
Naval Sch., Civil Engrng. Corps Officers

TUDOR, Sidney
Naval Applied Science Lab.

VADUS, Joseph Robert
Sperry Rand Corporation

VAN ATTA, William W.
Naval Oceanographic Office

VAN BIBBER, Vordaman H.
Naval Ship R&D Laboratory

VAN DE VELDE, Louis R.
IBM Corp.-Federal Sys. Ctr.

VANHAAGEN, Richard H.
Arthur D. Little, Inc.

VASTANO, Dr. Andrew C.
Woods Hole Oceanog. Inst.

VEIGELE, Dr. William J.
Kaman Nuclear

VINE, Allyn C.
Woods Hole Oceanog. Inst.

WAGEMAN, John M.
U.S. Naval Oceanographic Off.

WALLEN, Dr. I. Eugene
Off. of Oceanog. & Limnology
Smithsonian Institution

WALSH, Prof. John E.
Southern Methodist Univ.

WARNER, Jacob LaRue
Office of Naval Research

WATERS, RADM O. D. (USN)
Off. of the Oceanog. of the Navy

WATKINS, CDR Frank T., Jr. (USN)
Commander Submarine Dev. Group Two

WATSON, Alexander S.
(EMI Electronics Ltd.)
Canadian Dept. of Def. Production

WEISS, Benjamin Fred L.
Univ. of Texas at Austin

WENNEKENS, Dr. Pat M.
Office of Naval Research-SF

WERMTER, Raymond
Naval Ship R&D Center

WHEAT, CDR Newton L.
Def. Atomic Support Agency
Joint Task Force EIGHT

WHEELER, August E.
NA Rockwell Corp. Space Div.

WHITAKER, Walter E.
Navy U/W Sound Laboratory

WHITMARSH, David C.
Ordnance Research Lab.

WILCOX, Chester C.
COMASWFORPAC
Tactical Analysis Group

WILLENBRINK, CDR James F. (USN)
Off. of the Oceanog. of the Navy

WILLIAMS, Earl George
Naval Air Dev. Center

WINFREE, CDR H. D., Jr. (USN)
Office of Naval Research

WILSON, CDR William R.
Office of Naval Research

WOOD, Forrest Glenn
Naval Undersea R&D Center

WOODWORTH, William C.
Mellonics Systems Development

YACHNIS, Dr. Michael
Naval Facilities Engrng. Command

YOUNG, Charles, Jr.
Naval Ordnance Laboratory

YOUNG, Dr. George A.
Naval Ordnance Laboratory

ZENI, CAPT Levid E. (USN Ret)
Smithsonian Institution

ZETTEL, CAPT Ralph A. (USNR Ret)
Nat'l. Data Buoy Dev. Project Office